SYSTEMATICS, PHYLOGEOGRAPHY AND HISTORICAL BIOGEOGRAPHY OF EUSIROIDEA (CRUSTACEA, AMPHIPODA) FROM THE SOUTHERN OCEAN, WITH A SPECIAL FOCUS ON THE FAMILIES EPIMERIIDAE AND IPHIMEDIIDAE

MARIE VERHEYE

AOÛT 2017

Thèse présentée en vue de l'obtention du grade de docteur en sciences

Epimeria cf. *similis* sitting on a sponge, courtesy of NHK Antarctic Filming Expedition 2017

UNIVERSITÉ CATHOLIQUE DE LOUVAIN

Date of the public defense: August 28, 2017

The research presented in this thesis was conducted at the Royal Belgian Institute of Natural Sciences (RBINS), O.D. Taxonomy and Phylogeny (Brussels, Belgium) and the Université Catholique de Louvain-la-Neuve (UCL), Laboratoire de Biologie Marine (Louvain-la-Neuve, Belgium) and financially supported by a F.R.I.A. grant from the F.R.S.-FNRS (Fonds de la Recherche Scientifique).

Please refer to this work as:

Verheye, ML (2017) Systematics, phylogeography and historical biogeography of Eusiroidea (Crustacea, Amphipoda) from the Southern Ocean, with a special focus on the families Epimeriidae and Iphimediidae. PhD thesis, Université Catholique de Louvain-la-Neuve.

PROMOTERS

Dr. Cédric d'Udekem d'Acoz	(RBINS, Belgium)
Prof. Dr. Jérôme Mallefet	(UCL, Belgium)

READING COMMITTEE

Prof. Dr. Thierry Backeljau	(RBINS, Belgium)
Dr. Patrick Martin	(RBINS, Belgium)
Prof. Dr. Caroline Nieberding	(UCL, Belgium)

EXAMINATION COMMITTEE

Prof. Dr. Thierry Backeljau	(RBINS, Belgium)
Dr. Cédric d'Udekem d'Acoz	(RBINS, Belgium)
Prof. Dr. Michal Grabowski	(University of Lodz, Poland)
Prof. Dr. Jérôme Mallefet	(UCL, Belgium)
Prof. Dr. Caroline Nieberding	(UCL, Belgium)

ACKNOWLEDGEMENTS / REMERCIEMENTS

Commençons par le commencement: je voudrais remercier mon promoteur de l'UCL, Jérôme Mallefet pour m'avoir permis de faire, d'abord mon mémoire de Master, et ensuite ma thèse, en collaboration entre le labo de Biologie Marine de l'UCL et l'IRScNB. Si vous n'aviez pas proposé ce sujet de mémoire qui m'a tapé dans l'œil en 2010 et ne m'aviez pas ensuite encouragée à poursuivre dans cette voie, ce manuscrit ne serait pas. Merci donc d'avoir accepté de participer à ce projet et ce, malgré mon expatriation à l'IRScNB, qui rendait les visites au labo plus rares que je ne l'aurais souhaité. Mais lors de ces visites, j'ai beaucoup apprécié votre aide et votre enthousiasme communicatif, merci !

Un énorme merci également à Cédric, mon promoteur de l'IRScNB, qui m'aura suivi pendant ces nombreuses années, du mémoire au doctorat ! Tu t'es énormément impliqué dans ce projet, de sa conception aux révisions finales, toujours présent lorsque j'avais besoin d'aide. Merci de m'avoir tellement appris sur la taxonomie et morphologie des amphipodes, pour les heures de tri et d'identifications jusqu'à tomber de fatigue sur le *Polarstern,* pour les inombrables conseils et coups de main que tu m'auras donnés tout au long de cette thèse, pour les révisions détaillées et assidues de chacun de ses chapitres et enfin, des quelques centaines de pages de la version finale. Je me considère très chanceuse d'avoir eu un promoteur aussi disponible et passionné que toi! Aujourd'hui, ce projet touche à sa fin et je pense que c'est une page importante qui se tourne pour toi également. J'espère cependant de tout cœur encore de nombreuses discussions et collaborations futures !

A huge thank you to Thierry for reading, commenting and correcting every single chapter of this thesis. I learned a lot on tree thinking from our exchanges and enjoyed the discussions on species concepts and philosophical issues. It's always thrilling to talk with someone as passionated as you! I thank you deeply for your willingness to help even when you're already overloaded with work. And for the answers to my mails at 2 a.m., I felt less alone working at night! ;-) And finally, for your enthusiasm towards my work and words of encouragements, which really helped me to go on in 'close-to-burnout' moments.

I also deeply thank the remaining jury members for taking the time to read the complete manuscript and for improving its final version with constructive comments and corrections.

Merci aussi à Patrick pour m'avoir formée aux analyses phylogénétiques durant mon mémoire d'abord, et le début de ma thèse ensuite. Merci pour toute l'aide apportée lors de la rédaction du premier article, pour tes relectures, conseils et corrections. Merci enfin pour ta bonne humeur et tes nombreuses blagues — même si je ne les comprenais pas toujours ;-) — lorsque nous étions tous réunis au 7ème étage.

Thanks to all my colleagues from the Molecular lab on the 4th floor! Je voudrais remercier d'abord Zohra pour m'avoir formée aux techniques de séquençage durant mon mémoire ; formation qui m'aura également servi pour cette thèse. Merci pour ta gentillesse et ta disponibilité! I would like to deeply thank Zoltan (ex-JEMU), Gontran (JEMU) and Karin, who helped me with lab-related issues and were always of good advice.

Je remercie également mes collègues du MNHN: Marc Eléaume, Cyril Gallut, Laure Corbari et Paula Martin-Lefèvre pour l'accueil chaleureux lors de mes quelques visites au Muséum, pour votre aide précieuse sur place et par la suite, et pour le prêt de nombreux échantillons essentiels à la bonne réalisation de ce travail. A big thank you also to the great Invertebrates Collections' team from NIWA, New Zealand – Anne-Nina Lörz, Sadie Mills, Caroline Chin and Kareen Schnabel — for the warm welcome and for helping me out with the collections during the seven weeks of my stay.

Thank you to all the scientists and crew of the ANT-XXIX/3 *Polarstern* expedition, for contributing in making this such an unforgettable experience for me! I got heaps of great memories from these 2.5 months at sea — which are still making me nostalgic when I think about it — memories of incredibly beautiful landscapes and wildlife, but also of great people, some of whom I got the chance to see again after the cruise.

Heartful thanks to all the colleagues and friends who crossed my way during these Phd years, for longer-term — Vale, Nong, Séverine, Gontran, Christian, Dinarzarde, Tasnim, Silvia — or shorter periods — Arantza, Rylan, Oihana, Maud, Phuripong, Analia, Sophie. You punctuated my Phd years with happy lunches, afterwork drinks or dinners, big laughs, loads of runs around the 50tenaire, weekend trips and even great Hollidays! A big chapter of my life is now ending but you left me with so many great memories; this epic night of the birth of the 'panda gang' being just one amongst many others! Many of you had to go back to their home countries or sail off to new horizons, but it's always a blast to see some of you again in Belgium or else and I hope there'll be plenty more opportunities for reunions around Belgian beers or Thai dinners!

Une pensée toute spéciale pour ma Wiipii (Séverine), qui aura vécu avec moi toutes les épreuves du doctorat, du début à la fin. J'ai eu beaucoup de chance de t'avoir comme co-doctorante et amie

durant ces années ; parmi tous les collègues qui vont et viennent, tu auras été ma constante. Nous aurons partagé nos projets, passions et difficultés de doctorantes, mais aussi tellement de rires, des soirées bruxelloises, des expéditions dans d'autres villes belges et mêmes d'autres pays, des rencontres improbables (vive la confiture), et j'en passe. Merci pour ta bonne humeur inébranlable et tellement communicative, et aussi pour ce petit grain de folie qui a pimenté mes années de doctorat ! Et comme quelqu'un de très sage a dit un jour dans son speech d'après-défense « en fait, on a quand même passé des bons moments ! ». Je n'aurais pas trouvé de mots plus justes ;-)

Une thèse et un bébé étant deux jobs-à-plus-que-temps-plein, réussir à les cumuler n'est pas possible sans une équipe de choc. Je ne saurais donc jamais assez remercier la « team Cléo », sans qui tout ça n'aurait pas été possible. Enormes mercis d'abord à mes parents de m'avoir encouragée et soutenue pendant ces longues études, sans quoi je n'en serais pas là aujourd'hui. Et durant ces presque deux dernières années, merci de vous être si bien et si souvent occupés de votre petite fille, afin de me dégager du temps de travail et me permettre ainsi de terminer cette thèse. Un merci de plus à ma mère pour son aide précieuse dans la mise en page de ce manuscrit. Je remercie également de tout coeur mes beaux-parents qui sont venus tous les quelques mois de France, et ce pendant plusieurs semaines, faire du camping dans notre petit appartement afin de s'occuper de leur petite fille et de nous aider dans cette épreuve. Merci également à l'objet de toute cette attention, ma fille Cléo, pour m'avoir si spontanément rendu le sourire à chaque fois que la fatigue et le stress me l'enlevaient ; et pour me rappeler tous les jours que l'on peut s'émerveiller et être curieux de tout, ce qui est finalement à la base d'un travail de chercheur.

Et enfin, *last but not least*, merci à Mikael d'avoir été là pour Cléo et moi, d'avoir sacrifié toutes ses vacances, temps libres et de nombreuses heures de sommeil pour que je puisse terminer cette thèse et pour donner le meilleur à notre fille. Je sais que j'ai beaucoup de chance d'avoir à mes côtés quelqu'un qui est prêt à faire une croix sur lui-même pour sa famille, pendant si longtemps. Tu as autant de mérite que moi dans le résultat — ce manuscrit et une petite fille heureuse — je pense qu'on peut être fiers de nous! C'était une grande épreuve, mais si on l'a passée ensemble, on pourra encore accomplir des tas de choses merveilleuses et enrichissantes !

CONTENTS

GENERAL INTRODUCTION

1. CURRENT GEOGRAPHICAL CONTEXT

1.1. GEOGRAPHY

The Antarctic region is defined as the area contained within the Antarctic Circle, south of 66°33' S latitude. This limit for the South Pole corresponds to the angle between the axis of rotation of the earth and the plane of its orbit around the sun (Thomas et al., 2008).

Antarctica is a vast landmass of 14 million km^2 occupying the polar position. Separated from other landmasses by great distances (1000 km from the closest one, South America) and three deep-water basins of 4000–6000 m depth (the Atlantic-Indian Basin, the Indian-Antarctic basin and the Pacific-Antarctic Basin), it is the most isolated continent of the planet (Fig. 1) (David and Saucède, 2015; De Broyer and Jażdżewska, 2014; Knox, 2006).

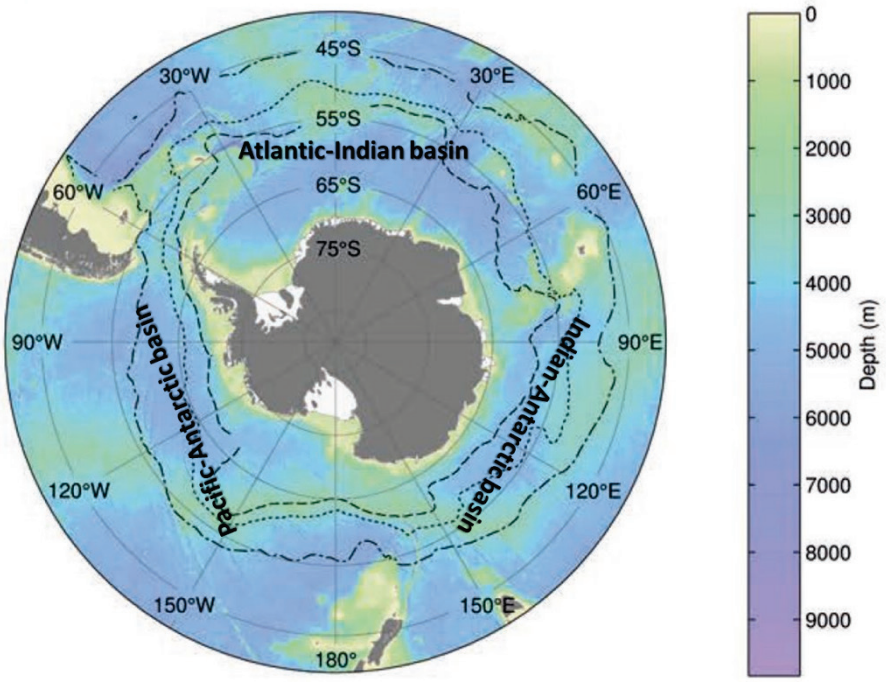

Figure 1. Bathymetric map of the Southern Ocean. The bathymetric data are derived from satellite altimetry and ship depth soundings (Smith and Sandwell, 1997). The dashed line indicates the southern extent of the Antarctic Circumpolar Current, the dotted line indicates the position of the Antarctic Polar Front and dash-dotted line indicates the position of the Sub-Antarctic Front [mean front positions are from Sokolov and Rintoul (2009)]. Figure modified from Post et al. (2014).

The political northern boundary of the Southern Ocean is at 60°S (Thomas et al., 2008). However, the Antarctic Polar Front (APF) [see section 1.3.] is of biogeographical significance, as it marks the northernmost extent of cold Antarctic surface water. This front is therefore considered by biologists and oceanographers as a hydrological northern boundary for the Southern Ocean (Fig. 1). Defined as such, this vast ocean covers nearly 35 million km^2 or 10 % of the earth's ocean surface (David and Saucède, 2015).

The Southern Ocean continental shelf covers 4.6 million km^2. Because of glacial erosion and the weight of the ice covering the coast, the Southern Ocean continental shelf is unusually deep, from 200 m to 1000 m depth, at places (Clarke and Johnston, 2003), which is two to four times deeper than other continental shelves (David and Saucède, 2015). The upper slope's lower limit reaches ca. 2500 m depth, whereas the lower slope has a maximum depth of around 3500 m (De Broyer and Jażdżewska, 2014).

1.2. CLIMATE AND SEASONALITY

Surface waters south of the APF are cold and of relatively constant temperature throughout the year, with averages of 1–2°C in winter and 3–5°C in summer. Closer to the continent, water temperatures range from -1.0°C to -1.9°C and many organisms live in close proximity to ice (Knox, 2006).

An extremely seasonal light regime characterizes this region, with permanent night in winter and constant daylight in summer. In addition, due to the low solar angle at high latitude, the predominance of cloudy weather conditions and the sea ice covering, the amount of daylight penetrating the water column and available for photosynthesis is very limited, even in summer (David and Saucède, 2015; Knox, 2006).

Dramatic seasonal changes in sea ice cover characterize the Southern Ocean. A layer of sea ice of approximately a meter thick extends over an area of about 4 million km^2 in late summer to 20 million km^2 in late winter (Fig. 2) (Cavalieri and Parkinson, 2008; Knox, 2006; Parkinson, 2014; Worby et al., 1996).

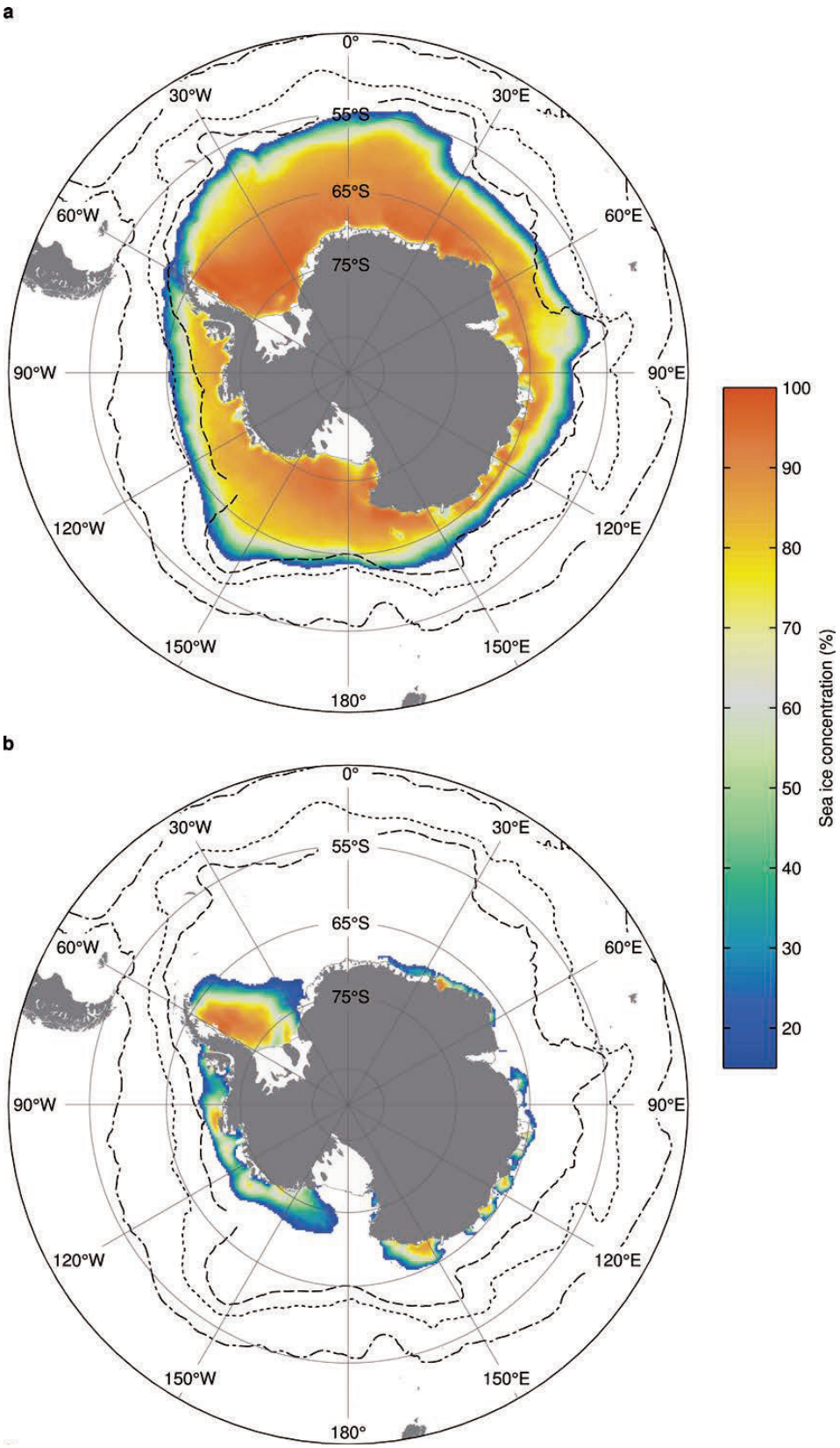

Figure 2. Mean Antarctic sea ice concentration in (a) September and (b) February. The dashed line shows the southern Antarctic Circumpolar Current Front, the dotted line the Polar Front and the dashed-dotted line the Sub-Antarctic Front [mean front positions are from Sokolov and Rintoul (2009)].

Following the seasonal variations in light regime, the phytoplankton biomass reaches its maximum around mid-December when the ice melts and then abruptly declines in February. As this ephemeral algal bloom feeds into the whole ecosystem, the Southern Ocean fauna is highly adapted to a seasonal food supply (Clarke, 1988).

1.3. Physical Oceanography

The **Antarctic Circumpolar Current (ACC)** is a wind-driven current flowing from west to east around Antarctica (Fig. 3). The ACC, being by far the largest current on earth, transports enormous amounts of water throughout the Atlantic, Pacific and Indian Ocean basins (Lagabrielle et al., 2009). This current strongly isolates Antarctica from lower latitudes warm water influences, thereby resulting in the "thermal isolation" of the Antarctic region (De Broyer and Jażdżewska, 2014; Exon et al., 2000).

South of the ACC, along the margin of the continent, at about 65°S, the wind drives the surface water to flow westward, thereby forming the **Antarctic Coastal Current** (or East Wind Drift) (Knox, 2006). This current makes two deep incursions into the Ross and Weddell Seas where it joins the gyres (spiral currents). The Antarctic Coastal Current is interrupted in West Antarctica, along the eastern side of the Peninsula (Fig. 3) (David and Saucède, 2015).

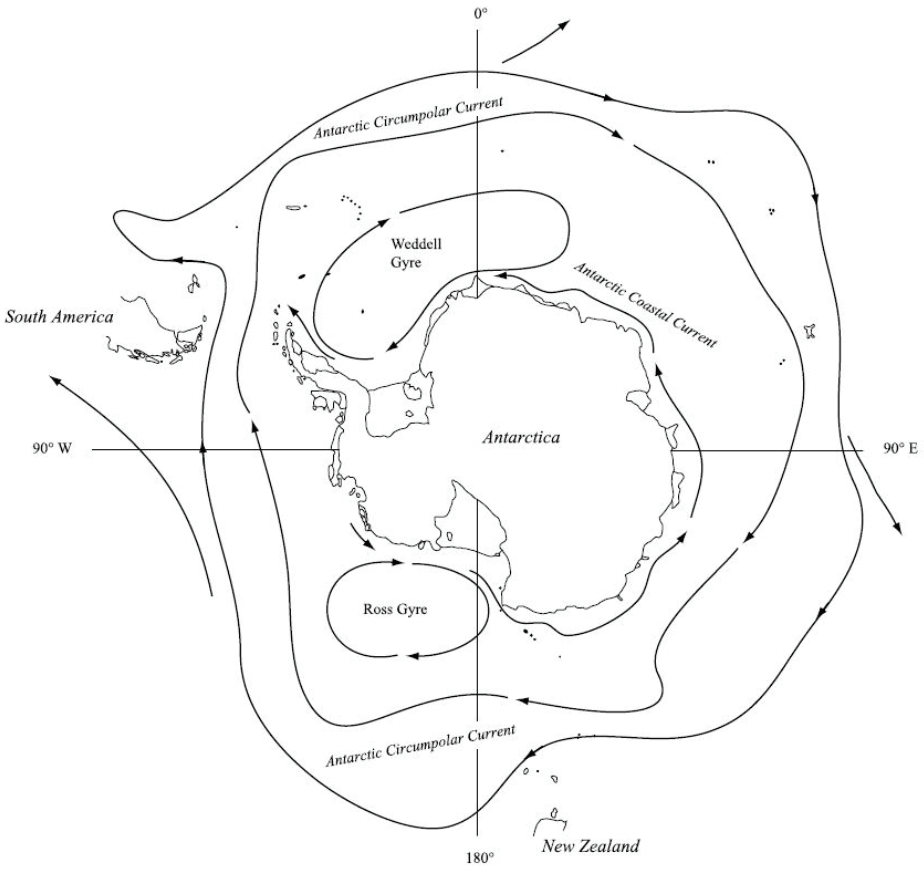

Figure 3. Map of the Southern Ocean showing the main surface currents. Figure from David and Saucède (2015).

Some major boundaries in near-surface hydrographic properties can be defined in ocean basins surrounding Antarctica, forming the polar frontal system [the fronts are indicated in black and bold in the text] (Post et al., 2014). These relatively narrow transitional zones separate regions with distinct vertical structures and physical, chemical and biological water mass properties [the water masses are indicated in grey and bold the text] (Whitworth, 1980).

Closest to the continent, the **Antarctic Slope Front** (or Antarctic Divergence) is a zone where the wind field produces Ekman divergence, resulting in the upwelling of the Circumpolar Deep Water. Part of this upwelled water goes south and sinks to the bottom around the continental margin into the very cold and salty (dense) northward-flowing Antarctic Bottom Water. The rest goes north forming the cold, low-salinity and high oxygen Antarctic Surface Water. This latter water mass meets the warmer (less dense) Sub-Antarctic Surface Water at the level of the **APF** (or Antarctic convergence) and sinks beneath it to form low salinity Intermediate Water (Fig. 4) (Gill and Bryan, 1971).

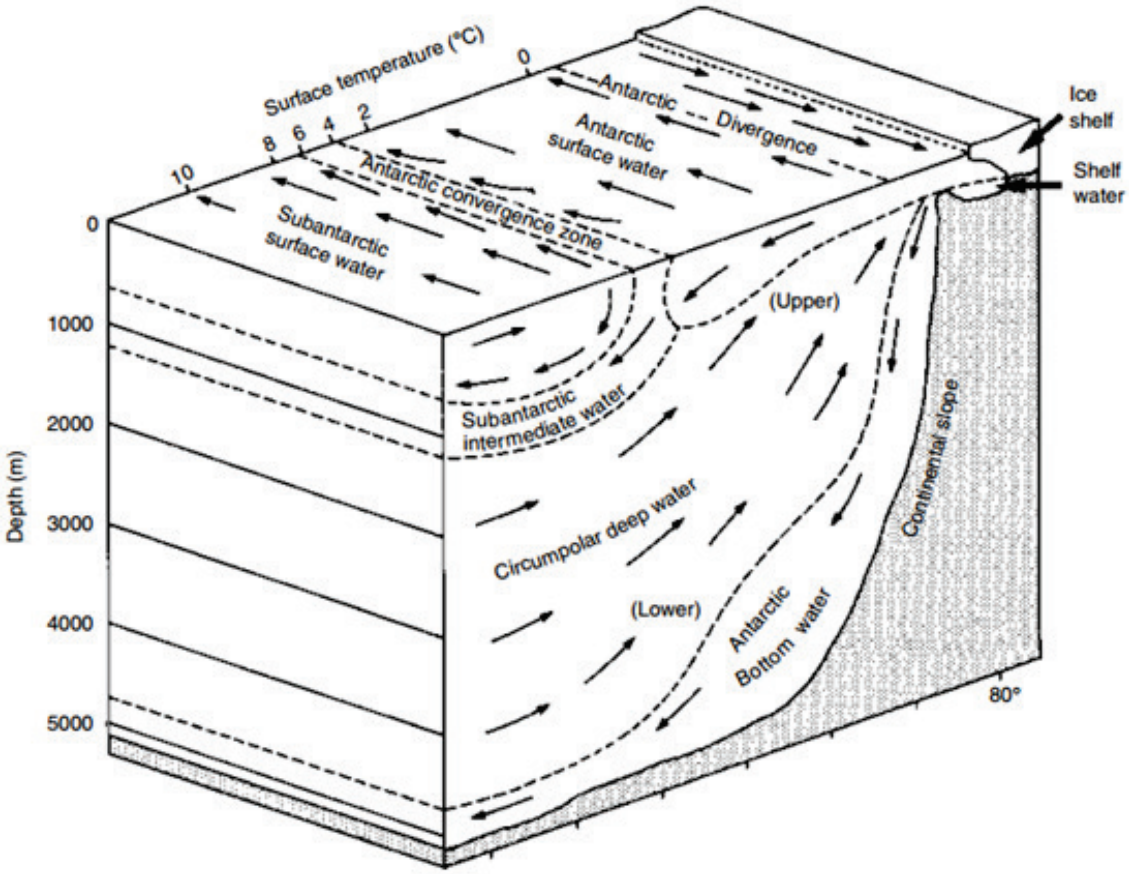

Figure 4. Schematic diagram of the meridional and zonal flow and water masses of the Southern Ocean. Figure from Knox (2006).

The APF is an important biogeographical boundary, as it marks a steep transition in sea-surface temperatures and salinity, but also in phytoplankton and zooplankton distributions (Deacon, 1982; Knox, 2006). This front divides the Southern Ocean into the sub-Antarctic region to the North and the Antarctic region to the South (Knox, 2006). The **Sub-Antarctic Front** separates Antarctic Intermediate Water to the south from northern surface waters and is also the northernmost continuous circumpolar front of the Southern Ocean (David and Saucède, 2015; Knox, 2006). To its North, the **Sub-Tropical Front** is the northern boundary of the sub-Antarctic zone (beyond that limit, the surface water temperature is above 10–12°C) and also marks the northern limit of the area affected by the ACC. Located between 30°S and 35°S, it is interrupted by Africa, Australia and South America (Fig. 5).

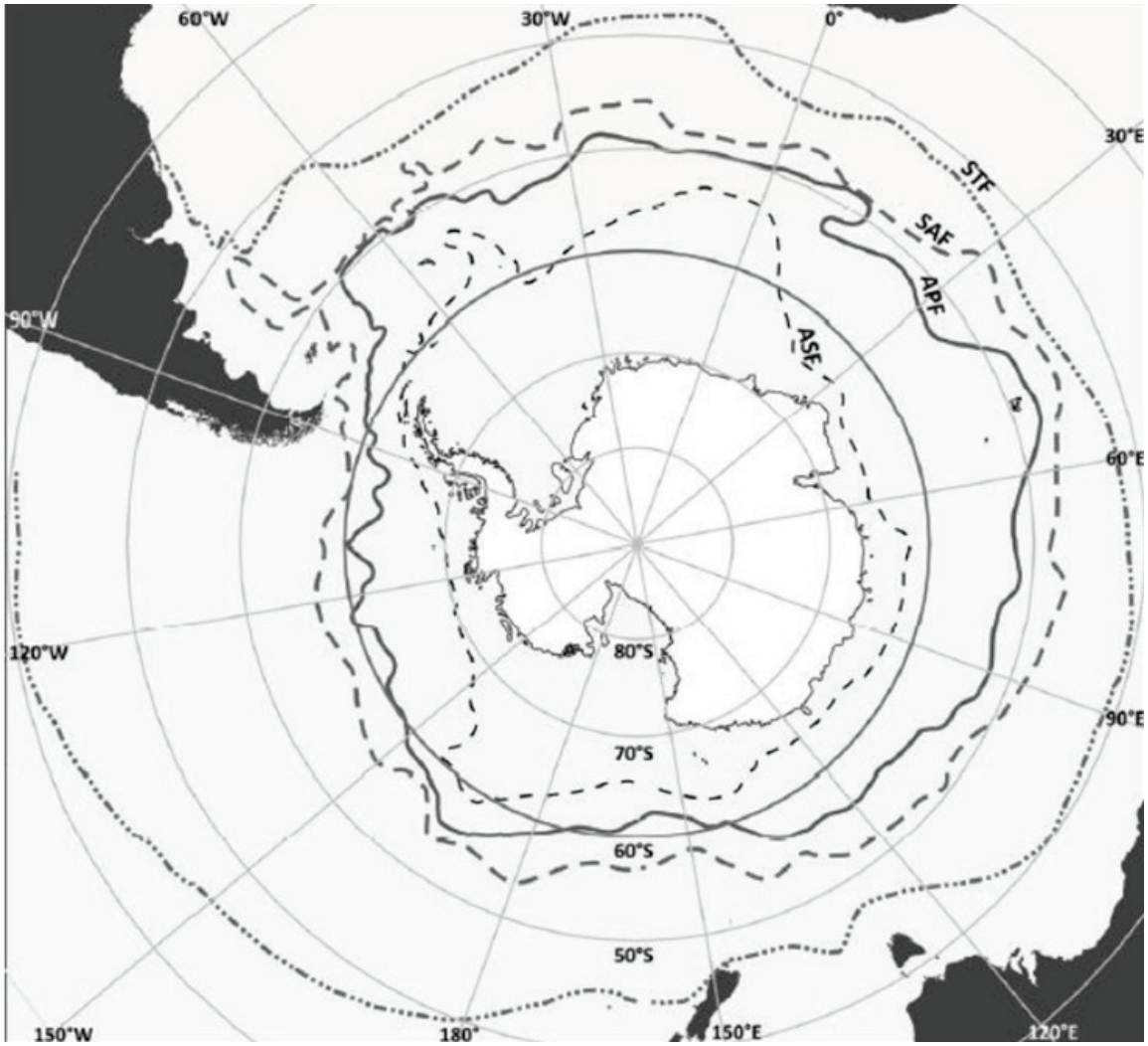

Figure 5. Polar frontal zone. ASF = Antarctic Slope Front (Antarctic Divergence). APF = Antarctic Polar Front (Antarctic Convergence). SAF = Sub-Antarctic Front. STF = Sub-Tropical Front. Figure from Flores (2009).

2. BIODIVERSITY

2.1. ANTARCTIC BENTHOS

The total number of described benthic species from the Southern Ocean exceeds 4100 (Clarke and Johnston, 2003). However, the true benthic diversity of the region is likely to be much higher, as the total macrofaunal diversity of the Antarctic shelf alone was estimated to exceed 15,000 species (Gutt et al., 2004). Moreover, the Southern Ocean deep-sea fauna is largely unknown (Brandt et al., 2007). Most of the Antarctic benthic fauna therefore likely remains to be described (Aronson et al., 2007).

While the species richness is comparable to that of some temperate or tropical non-reef areas (Clarke, 2008), in terms of composition, the Southern Ocean benthic fauna differs to that elsewhere in the world (Rogers, 2007). Some groups are particularly species rich compared to other oceans, while others are far less speciose (Fig. 6). Among the exceptionally diverse taxa are the pycnogonids, the ascidians and the peracarids (Aronson et al., 2007; Clarke and Johnston, 2003), while among the poorly represented taxa are the bivalves, decapod crustaceans and teleosts (Aronson et al., 2007).

Notably, there are virtually no brachyuran crabs, lobsters, sharks or rays in the Southern Ocean (Barnes et al., 2006). Skates are low in diversity and abundance and the teleostean fauna is largely composed of non-durophagous notothenioids and liparids (Clarke and Johnston, 1996; Clarke and Johnston, 2003; Eastman and Clarke, 1998).

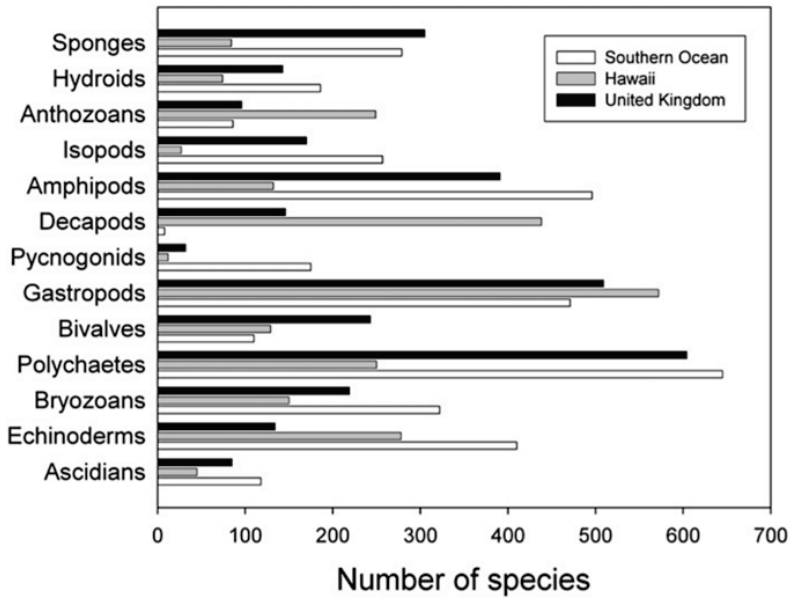

Figure 6. Comparison of species richness for selected marine benthic invertebrate groups from the Southern Ocean, Hawaii and north-west Europe. Non-Antarctic data come from Hayward and Ryland (1995), Eldredge and Miller (1994) and Howson and Picton (1997). Figure from Clarke (2008).

The peculiarity of Antarctic benthic communities, compared to other shelf ecosystems, is the dominance (in terms of biomass and seafloor coverage) of sessile suspension-feeders, living mostly on soft substrata (Dayton, 1990; Gili et al., 2006). In shallow Antarctic waters, assemblages are mostly composed of sponges, bryozoans, ascidians and cnidarians. They form complex three-dimensional structures, providing a microhabitat for a broad variety of associated fauna (Fig. 7) (Gili et al., 2006; Gutt, 2007). Among these non sessile organisms are mostly asteroids, pycnogonids, crinoids, peracarid crustaceans, holothurians, molluscs and sea urchins (Gutt and Schickan, 1998). This community type exists in patches all around the shelf at depths between 30 m and ca. 600 m (shelf break) (Gutt, 2007).

Another type of benthic community, dominated by deposit-feeders and infauna, is prevalent on the deeper shelf (> 350 m). This assemblage is mostly composed of mobile animals such as ophiuroids, polychaetes, peracarid crustaceans, and locally, molluscs (Fig. 8) (Gutt, 2007).

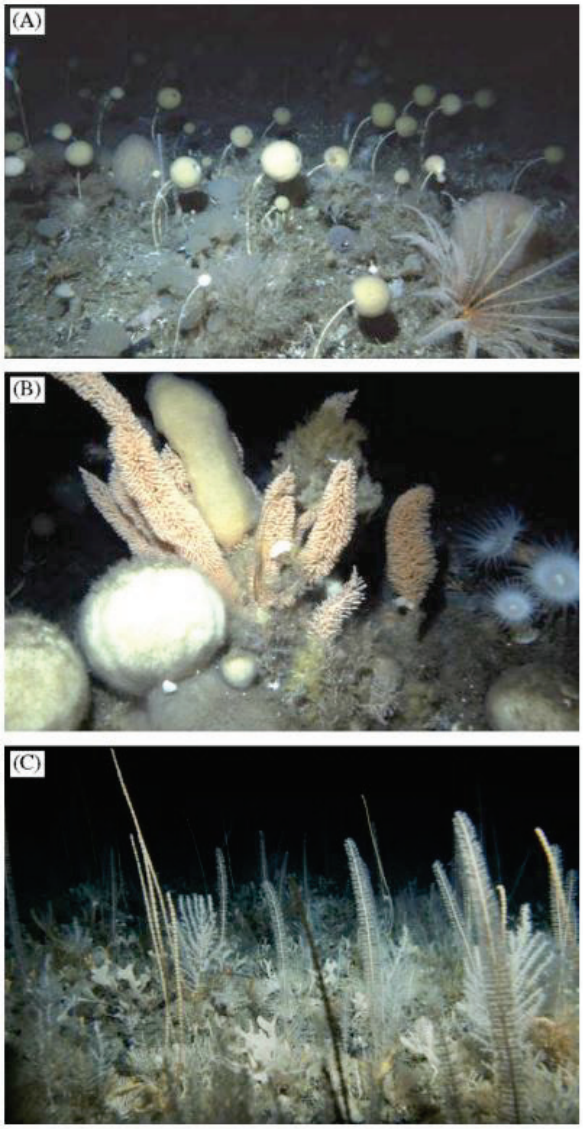

Figure 7. Highly diversified communities dominated by suspension-feeders. (A) Dense aggregation of sponges, crinoids, several soft bryozoans and a colonial ascidian. (B) Communities dominated by yellow-brown sponges and the pink bottle brush gorgonian with smaller colonies of primnoid corals and white anemones. (C) Communities dominated by bryozoans and gorgonians and white bottle brush colonies of bamboo coral. Pictures from Gili et al. (2006).

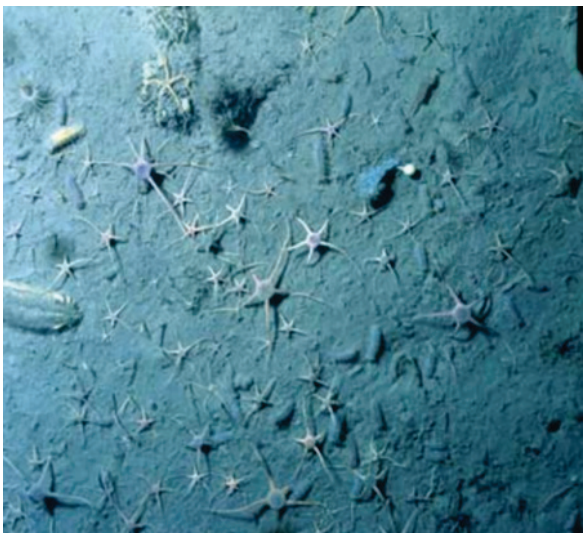

Figure 8. Community dominated by deposit-feeders, among which are holothurians, ophiuroids, polychaetes, and sparse sessile epifauna. Picture from Gutt (2007).

2.2. AMPHIPODS

2.2.1. ECOLOGY

With more than 853 described species, amphipods are among the most speciose macrobenthic organisms in Antarctic and Sub-Antarctic waters (De Broyer and Jażdżewska, 2014). Antarctic amphipods present a large diversity of trophic types, including specialist and generalist species, suspension-feeders, deposit-feeders, active predators, scavengers and micropredatory browsers (Dauby et al., 2001b). Six major amphipod habitats were identified on the Antarctic shelf: (1) the endobenthic habitat is the first centimeters of the sediment, inhabited by sedentary tube or "cell"-dwellers and burrowers; (2) the epibenthic habitat extends from the sediment surface to the top of the sessile organisms; (3) within the epibenthos, amphipods may occupy symbiotic or inquilinous microhabitats; (4) the hyperbenthic habitat, above the substrate, is colonized by benthopelagic to purely pelagic species and finally, (5) the cryopelagic habitat is the under surface of the sea ice (Fig. 9) (De Broyer et al., 2001). Amphipods are direct-developers or brooders. The female broods its embryo in an external ventral pouch or marsupium. The juveniles are fully developed and similar in appearance to the adults when released from the marsupium (Thiel, 1999).

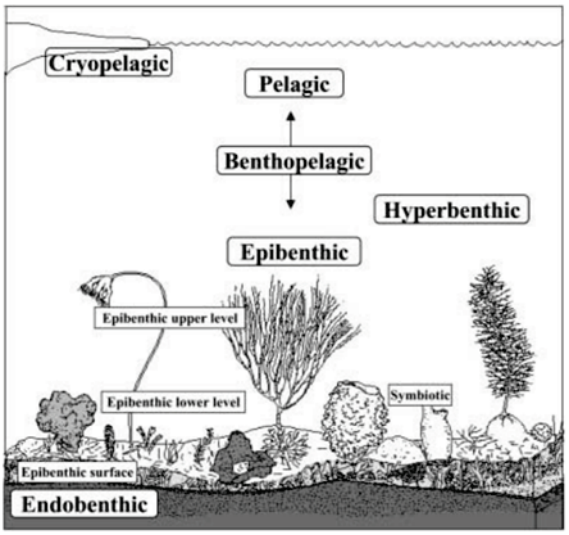

Figure 9. Scheme of the amphipod macrohabitats in the eastern Weddell Sea neritic zone. Figure from De Broyer et al. (2001)

2.2.2. MORPHOLOGY

The overall body plan is well-conserved among amphipods. The basic morphology of a typical gammaridean amphipod is outlined below. The description follows Bellan-Santini (1999), Coleman (2007) and Lincoln (1979) and all illustrations are from the latter author.

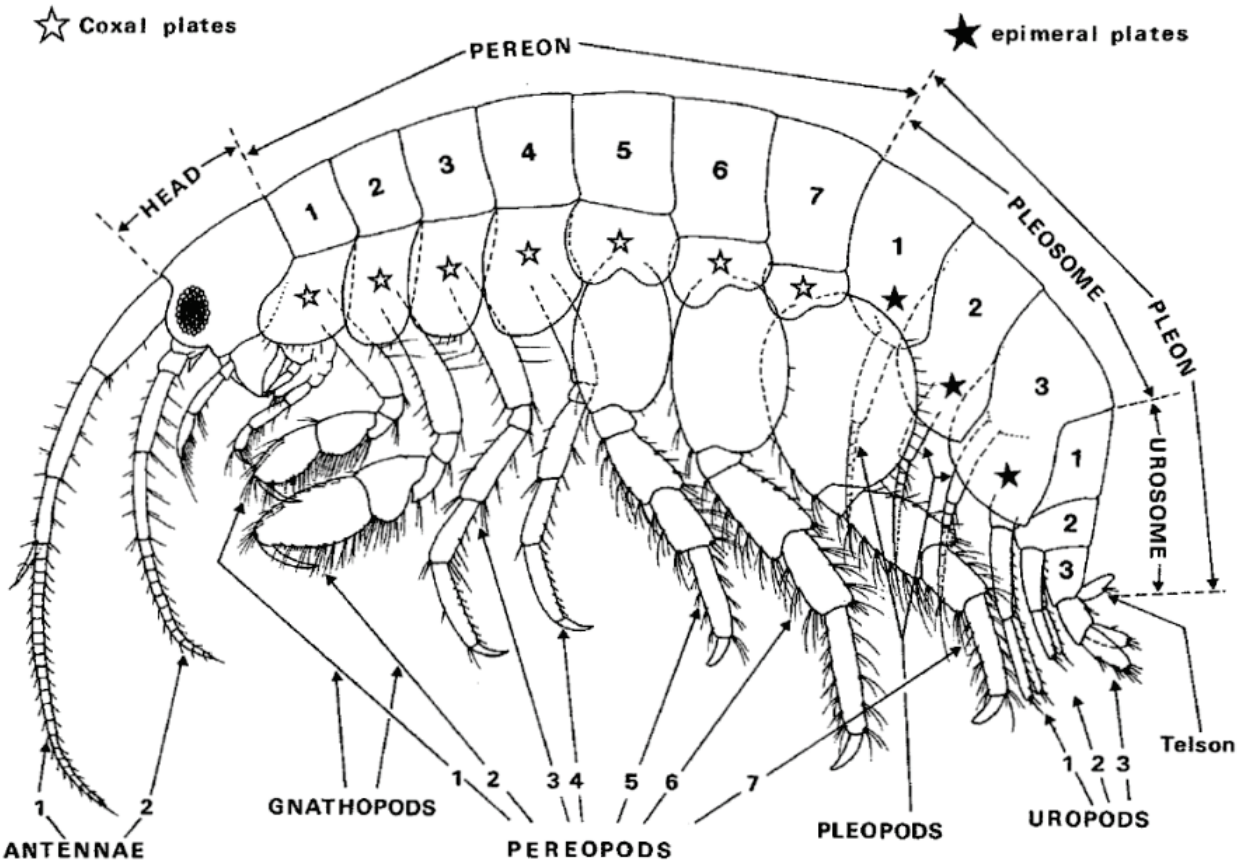

Figure 10. Basic morphology of a gammaridean amphipod.

The amphipod's body is laterally compressed. It is divided in: (1) the head (which is in fact a cephalothorax composed of the head and the first thoracopod fused together), (2) the thorax (or **pereon**) composed of 7 segments (or pereonites) and (3) the abdomen (or **pleon**) composed of 6 segments (or pleonites), namely the 3 segments of the **pleosome** (or pleosomites) and the 3 segments of the **urosome** (or urosomites) (Fig. 10).

The 7 pairs of appendages attached to the pereon are the **pereopods**. The first two pairs, mainly used for grasping food items, are the **gnathopods**. The first articles of the pereopods are fused to the body and expanded to form rather large side-plates or **coxae** (Fig. 10). **Gills** and **oostegites** (for females, forming the brood pouch or **marsupium**) are medial outgrowth of the coxae of some pereopods. The pereopods are composed of 6 free articles, proximally to distally: the basis, ischium, merus, carpus, propodus and dactylus (Fig. 11).

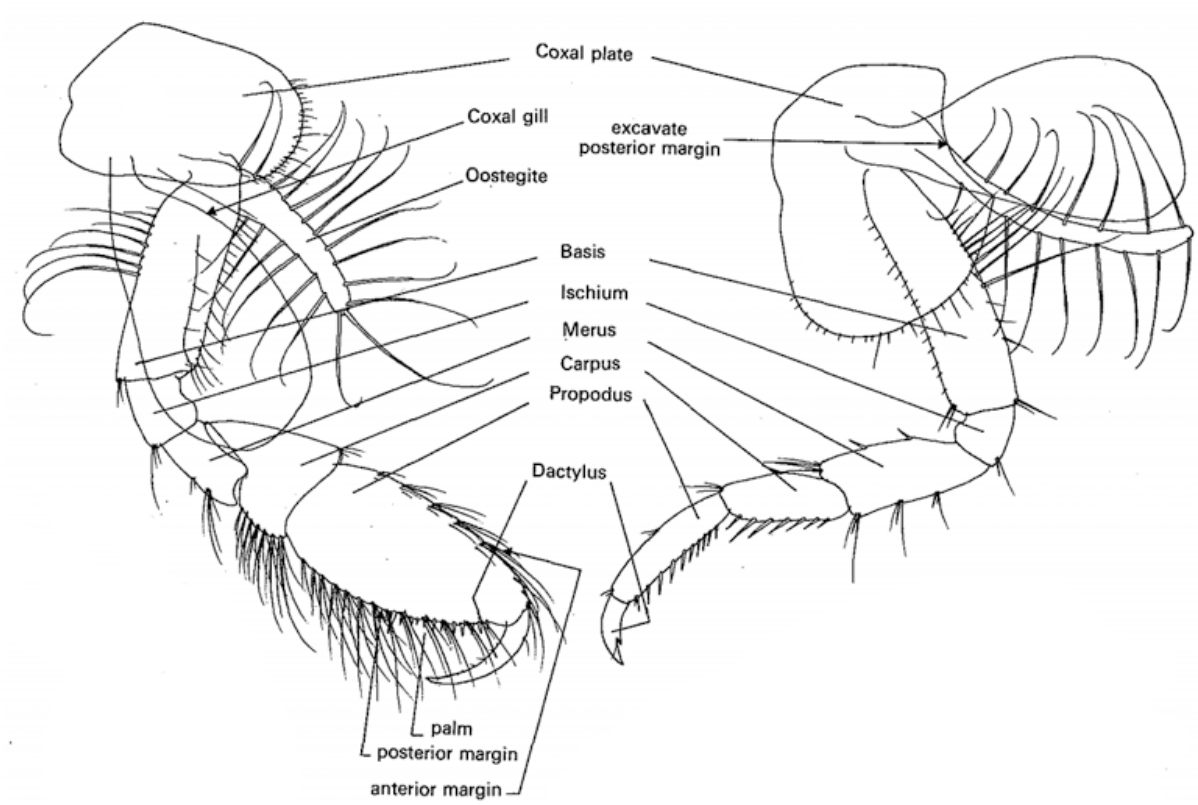

Figure 11. Appendages. Left: gnathopod 2; right: pereiopod 4.

The epimera (or **epimeral plates**) are laminar outgrowths of the pleosomites (Fig. 10). The three pairs of appendages attached to the pleon are the **pleopods**. The pleopods produce a posteriorly directed respiratory current to aerate the gills and in females, the marsupium. They also provide propulsion during swimming.

Each of these pleopods is composed of a stout basal article or peduncle and two multi-articulate rami bearing long lateral setae. The pleopod pairs are held together by small coupling hooks, on the inner margin of the peduncle (Fig. 12).

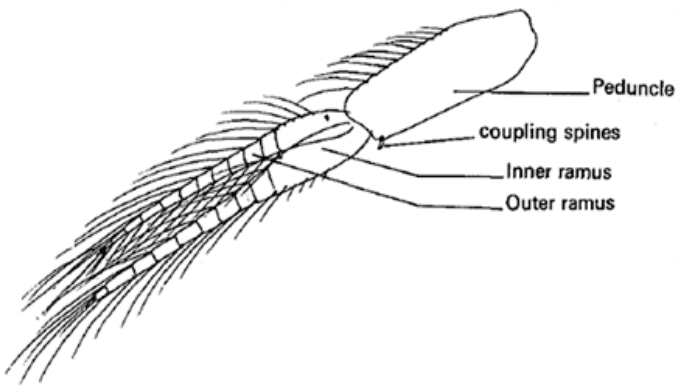

Figure 12. Appendages: pleopod 1.

The urosome bears 3 pairs of appendages called **uropods**. Their main function is to provide the amphipods with a purchase on the substratum, but they may also assist in swimming, burrowing and tube-dwelling. The uropods consist of an unarticulated peduncle and two rami, the inner and the outer (Fig. 13).

At the posterior end of the amphipod is the **telson**, which can be entire, cleft or notched medially (Fig. 13).

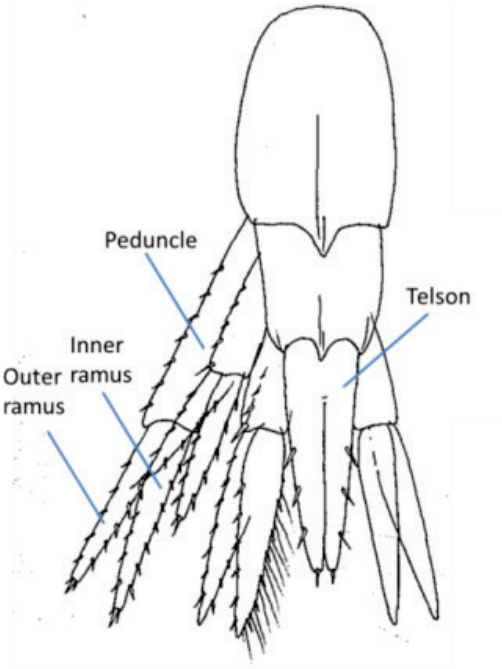

Figure 13. Urosome with the three pairs of uropods and telson.

In most gammaridean amphipods, the anterolateral margin of the head has a small rounded or angular process, the **lateral lobe** (or anterior head lobe). Below or behind the lateral lobe, the margin of the head, adjacent to the insertion of antenna 2, is often excavate and referred as the **post-antennal sinus** (or inferior antennal sinus). The eyes are sessile, compound, pigmented and most commonly, multifaceted. The head bears two pairs of antennae. **Antenna 1** has a peduncle of 3 articles and a flagellum. An **accessory flagellum** can be present at the basis of the flagellum, sometimes reduced to a small, inconspicuous scale. **Antenna 2** has a 5-articulated peduncle, article 1 and 2 being very small and sometimes partially fused, and a flagellum. The **rostrum** is a spine-like or triangular process on the anterodorsal margin of the head, between the bases of the first antennae (Fig. 14).

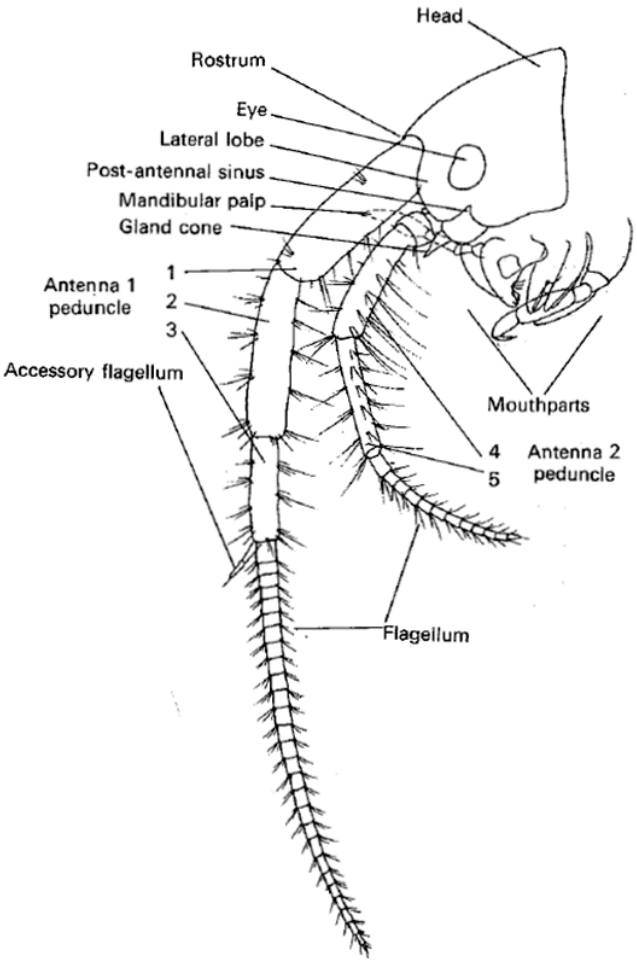

Figure 14. Head and antennae.

The mouthparts are located on the ventral side of the head. The anterior part, the **epistome**, bears a small plate, the upper lip or **labrum** (Fig. 15).

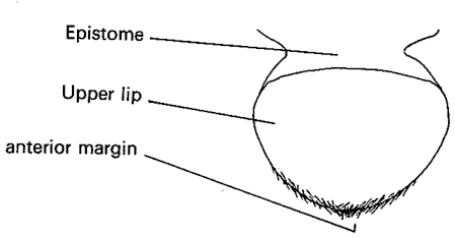

Figure 15. Mouthparts: upper lip or labrum

The **mandibles** are acting as jaws. They are typically composed of a distal cutting edge called **incisor**, and an articulated accessory cutting blade, the **lacinia mobilis** and a grinding process, the **molar**. Between the lacinia mobilis and the molar often lies a **setal row**. The mandible typically bears a 3-articulated **palp** (Fig. 16).

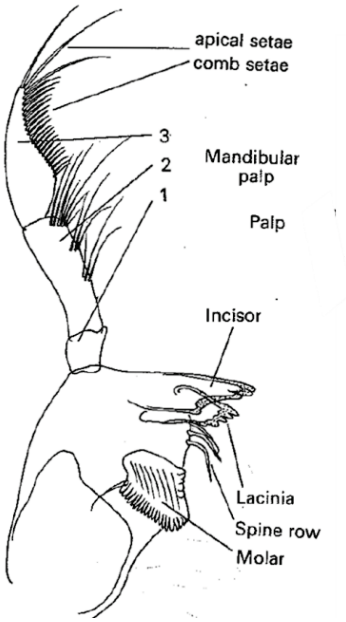

Figure 16. Mouthparts: mandible

The mandibles are followed by the lower lip or **labium**. The labium is bilobed, often with a pair of smaller inner lobes between the larger outer lobes (Fig. 17).

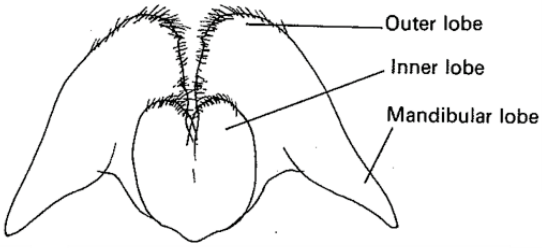

Figure 17. Mouthparts: lower lip or labium.

Posteriorly, **Maxilla 1** consists in an inner plate, borded with plumose setae, an outer plate with apical spine-like setae and a 1- or 2-articulated palp with a variable ornementation (Fig. 18).

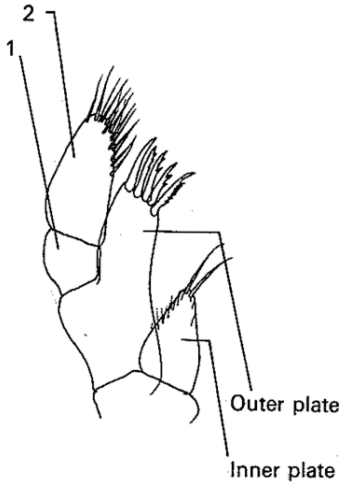

Figure 18. Mouthparts: maxilla 1.

Next in line is **Maxilla 2,** which is also composed of inner and outer plates, both bordered with setae distally and also medially for the inner plate (Fig. 19).

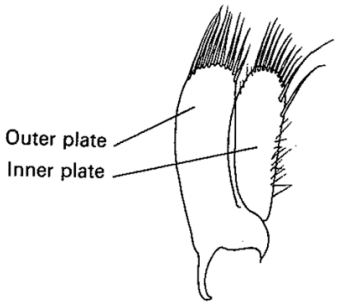

Figure 19. Mouthparts: maxilla 2

Finally, the posterior surface of the buccal mass is formed by the **maxilliped.** It is composed of a pair of inner and outer plates and of a 2 to 4-articulated palp, on both sides (Fig. 20).

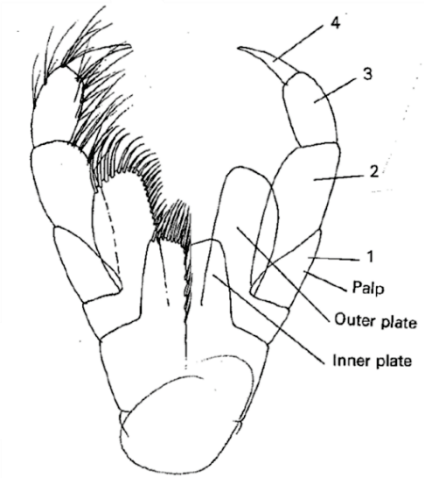

Figure 20. Mouthparts: maxilliped.

2.2.3. TAXONOMY

Traditionally, amphipods have been divided into three to five suborders: **Ingolfiellidea** Hansen, 1903; **Gammaridea** Latreille, 1802; **Hyperiidea** H. Milne Edwards, 1830; **Caprellidea** Leach, 1814 and **Corophiidea** Leach, 1814 (Barnard, 1969; Barnard and Karaman, 1984; Lincoln, 1979; Myers and Lowry, 2003; Stebbing, 1906). However, this classification is essentially phenetic and subsequent molecular studies revealed a hyperiid clade nested within Gammaridea and a caprellid clade nested within Corophiidea (Browne et al., 2007; Englisch, 2001; Ito et al., 2008). More recently, another morphologically-based higher classification of Amphipoda was suggested. The new suborder **Senticaudata** was erected on the basis of one alleged synapomorphy — the possession of apical, robust setae on the rami of uropods 1–2 — and includes most of the former Gammaridea, Corophiidea and Caprellidea (Lowry and Myers, 2013). However, regarding the incongruences between morphological and molecular phylogenies, the limits of amphipod suborders remain unclear.

Gammaridea contains the vast majority of amphipod families. Because of the great morphological disparity within the latter suborder and a probable prevalence of convergences, its taxonomy

remains highly controversial (Bousfield, 1978; Martin and Davis, 2001). In an attempt to break up this vast suborder into more manageable taxonomic units, Bousfield (1978) erected 20 amphipod superfamilies, among which is **Eusiroidea**. His classification into superfamilies was not retained by most subsequent authors (Table 1), because of the lack of a cladistics framework (Barnard and Barnard, 1983; Barnard and Karaman, 1975, 1991; Martin and Davis, 2001).

Seven families were originally included within Eusiroidea, viz. Pontogeneiidae Stebbing, 1906; Calliopiidae G.O. Sars, 1893; Eusiridae Stebbing, 1888; Gammarellidae Bousfield, 1977; Bateidae Stebbing, 1906; Amathillopsidae Heller, 1875 and Paramphithoidae Stebbing, 1906 (including the later erected Epimeriidae). Eusiroidea was not defined by demonstrated synapomorphies, but by a combination of morphological characters that holds more or less consistently across family members (Bousfield, 1978):

"Plesiomorphic, variously carinate or processiferous, rostrate, free-swimming and epibenthic amphipods, usually with moderately dimorphic terminal male stage; peduncles and flagella of antennae 1 and 2 bearing calceoli and less often brush setae; accessory flagellum small, vestigial, or lacking; eyes large, subrectangular; mouthparts more or less basic; upper lip without pronounced marginal notch; lower lip, inner lobes lacking or weakly developed; mandibular molar and palp usually strong; inner plates of maxilla 1 and 2 marginally setose, outer plate of maxilla 1 with 11 apical spine teeth; maxilliped plates and palp well developed, setose; coxal plates medium deep, 4th excavate; anterior peraeonal segments short, abdomen (especially pleon) segments large; coxae 5-7 posteriorly lobate; gnathopods 1 and 2 non- (or weakly) amplexing, subsimilar, usually weakly subchelate (gnathopod 1 vestigial in Bateidae), occasionally large and raptorial (Eusiridae); peraeopods 5-7 basically homopodous; brood plates large, broad; coxal gills simple, present on peraeopod 7; sternal gills occasionally present (some Pontogeneiidae); pleopods well developed, often powerful; uropods lanceolate, rami of 1 subequal, of 2 unequal; uropod 3, rami foliaceous, outer ramus 1-segmented; telson lobes distally separated, usually narrowly, apices with small notch and spine (seta), entire."

Consequently, the number of families included and their generic composition considerably changed throughout the years (Table 1). With 109 species in 27 genera, Eusiroidea *sensu* De Broyer et al. (2007) is the second most speciose superfamily (after the Lysianassoidea, 165 species) in Antarctic and sub-Antarctic waters (Fig. 21) (De Broyer and Jażdżewska, 2014).

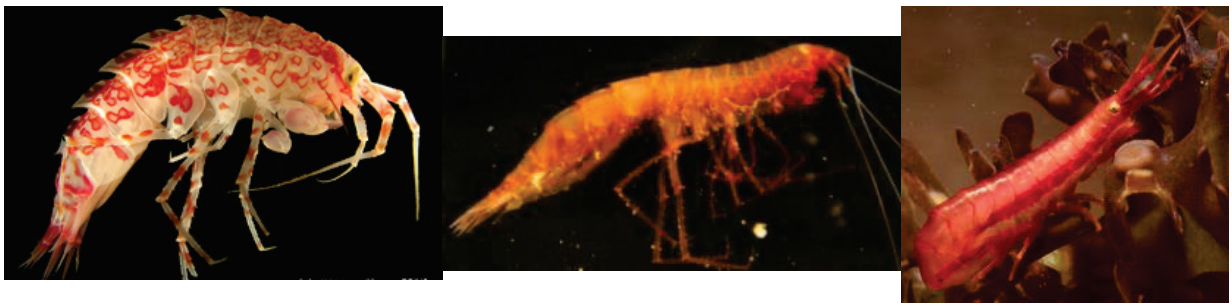

Figure 21. Examples of eusiroid amphipods. (A) *Eusirus perdentatus*, Eusiridae; (B) *Halirages cainae*, Calliopiidae and (C) *Gondogeneia redfearni*, Pontogeneiidae. Pictures from C. d'Udekem d'Acoz, C. De Broyer and G. Chapelle.

Stebbing, 1906 (S06)	Barnard, 1969 (B69)	Bousfield, 1978	Barnard & Karaman, 1991 (B&K91)	De Broyer *et al.*, 2007 (Antarctic taxa only)	Lowry & Myers, 2013 + WoRMS 2015
Suborder Gammaridea	***Suborder Gammaridea***	***Suborder Gammaridea***	***Suborder Gammaridea***	***Suborder Gammaridea***	***Suborder Gammaridea***
NO superfamilies defined	***NO superfamilies defined***	***Superfamily Eusiroidea***	***NO superfamilies defined***	***Superfamily Eusiroidea***	***Superfamily Eusiroidea***
Acanthonotozomatidae	***Acanthonotozomatidae***	***Amathillopsidae***	***Bateidae***	***Calliopiidae***	***Eusiridae***
• *Acanthonotozoma* • *Iphimedia* • *[Odius]* • *Panoploea* (=*Iphimedia*)	• *Acanthonotozoma* • *Acanthonotozomella* • *Acanthonotozomoides* • *Anchiphimedia* • *Bathypanoploea* • *Cypsiphimedia* (=*Iphimedia*) • *Echiniphimedia* • *Gnathiphimedia* • *Iphimedia* • *Iphimediella* • *Labriphimedia* • *Maoriphimedia* (=*Labriphimedia*) • *Maxilliphimedia* • *Panoploea* (=*Iphimedia*) • *Panoploeopsis* (= *Acanthonotozoma*) • *Paranchiphimedia* • *Parapanoploea* • *Pariphimedia* • *Pariphimediella* (= *Iphimediella*) • *Pseudiphimediella* • *[Odius]*	• *Cleonardo* • *Eusirella* • *Eusirogenes* • *Eusiropsis* • *Eusirus* • *Harcledo* • *Meteusiroides* • *Pareusirogenes* • *Rhachotropis* • *Triquetramana*
Bateidae	***Astyridae***	***Bateidae***	***Gammarellidae***	***Eusiridae***	***NO superfamilies defined***
• *Batea*	• *Astyra*	***Calliopiidae***	• *[Gammarellus]* • *[Weyprechtia]* • *Austroregia*	• *Cleonardo* • *Eusirella* • *Eusiroides* • *Eusirus* • *Rhachotropis*	***Acanthonotozomatidae***
Calliopiidae	***Bateidae***	***Eusiridae***	***Thurstonellidae*** (as Clarenciidae)	***Gammarellidae***	• *Acanthonotozoma*
• *Amphithopsis* • *Apherusa* • *Atylopsis* • *Bouvierella* • *Calliopius* • *Chosroes* • *[Cleippides]* • *Halirages* • *Haliragoides* • *Harpinioides* • *Laothoes* • *Leptamphopus* • *Oradarea* • *[Paracalliope]* • *Paraleptamphopus* • *Sancho* • *Schraderia* • *Stenopleura*	• *Batea* • *Carinobatea*	***[Gammarellidae]***	• *Thurstonella (as Clarencia)*	• *Austroregia* • *Chosroes*	***Acanthonotozomellidae***
Eusiridae	Genera of Bousfield, 1977	***Paramphithoidae***	***Eusiridae***	***Pontogeneiidae***	Genera of De Broyer *et al.* 2007
• *Cleonardo* • *Eusiroides* • *Eusirogenes*	***Paramphithoidae***	***Pontogeneiidae***	• *Abdia* • *Accedomoera* • *Antarctogeneia* • *Atyloella* • *Awacaris* • *Bathyschraderia* • *Calliopiurus* • *Dautzenbergia* • *Djerboa* • *Cleonardo* • *Cleonardopsis* • *Eusirella* • *Eusirogenes* • *Eusiroides* • *Eusiropsis* • *Eusirus* • *Gondogeneia* • *Harcledo*	• *Antarctogeneia* • *Atyloella* • *Bovallia* • *Djerboa* • *Eurymera* • *Gondogeneia* • *Liouvillea* • *Paramoera* • *Prostebbingia* • *Schraderia*	• *Amatiguakius*
	Pontogeneiidae	***Leucothoidea***			***Amathillopsidae***
		[Amphilochidae] ***[Anamixidae]*** ***[Colomastigiidae]*** ***[Cressidae]*** ***Laphystiopsidae*** ***[Leucothoidae]*** ***[Maxillipiidae]*** ***[Nihotungidae]*** ***[Pagetinidae]*** ***Pleustidae*** ***[Stenothoidae],*** ***[Thaumatelsonidae]***			Genera of De Broyer *et al.* 2007 Cleonardopsinae • *Cleonardopsis*
					Bateidae
					• *Batea*
					Diwidae
					• *Dikwa*
					Epimeriidae
					Genera of De Broyer *et al.* 2007

- *Eusiropsis*
- *Eusirus*
- *Rhachotropis*
- *Rozinante*

[Gammaridae]

- *[Gammarellus]*
- *[Weyprechtia]*

Lafystiidae

- *Lafystius*

Laphystiopsidae

- *Laphystiopsis*

Paramphithoidae

- *Actinacanthus*
- *Epimeria*
- *Paramphithoe*

Pleustidae

- *Dautzenbergia*
- *Mesopleustes*
- *Neopleustes*
- *Parapleustes*
- *Pleustes*
- *Stenopleustes*
- *Sympleustes*

Pontogeneiidae

- *Atyloides*
- *Bovallia*
- *Eurymera*
- *Paramoera*
- *Pontogeneia*
- *Prostebbingia* (as Stebbingia)
- *Zaramilla*

Tironidae

- *[Argissa]*
- *Astyra*

(= *Batea*)

Calliopiidae

- *Amphithopsis*
- *Apherusa*
- *Atylopsis*
- *Bouvierella*
- *Calliopiella*
- *Calliopius*
- *[Cleippides]*
- *Chosroes*
- *Haliragoides*
- *Halirages*
- *Harpinioides*
- *Laothoes*
- *Leptamphopus*
- *Metaleptamphopus*
- *Paraleptamphopus*
- *Oradarea*
- *Prolaphystius*
- *Regalia*
- *Sancho*
- *Stenopleura*
- *Stenopleuroides*
- *Thurstonella (as Clarencia)*

Eusiridae

- *Accedomoera*
- *Atyloella*
- *Bathyschraderia*
- *Dautzenbergia*
- *Djerboa*
- *Eusirus*
- *Cleonardo*
- *Cleonardopsis*
- *Eusirella*
- *Eusirogenes*
- *Eusiroides*
- *Eusiropsis*
- *Harcledo*
- *Harpinioidella*
- *Liouvillea*

Superfamily Pardaliscoidea

[Paradaliscidae]

Stilipedidae

[Hyperiopsidae]

Astyridae

[Vitjazianidae]

- *Liouvillea*
- *Lopyastis*
- *Manerogeneia*
- *Membrilopus*
- *Meteusiroides*
- *Nasaganeia*
- *Oligochinus*
- *Paramoerella*
- *Paracalliopiella*
- *Oligochinus*
- *Pareusirogenes*
- *Pontogeneoides*
- *Pseudomoera*
- *Pseudopontogeneia*
- *Relictomoera*
- *Rhachotropis*
- *Ronco*
- *Schraderia*
- *Sternomoera*
- *Tethygeneia*
- *Tylosapis*
- *Whangarusa*
- Former Calliopiidae *sensu* B69 (excl. *Cleippides, Prolaphystius, Thurstonella*)
- All the former Pontogeneiidae *sensu* S06

Iphimediidae

- *Acanthonotozomopsis*
- *Anisoiphimedia*
- *[Cleippides]*
- *[Curidia]*
- *Dikwa*
- *[Meraldia]*
- *Nodotergum*
- *[Postodius]*
- *Stegopanoploea*
- *[Ochlesis]* (former Ochlesidae)

NO superfamilies defined

Acanthonotozomellidae

- *Acanthonotozomella*
- *Acanthonotozomoides*

Amathillopsidae

Amathillopsinae
- *Amathillopsis*

Parepimeriinae
- *Parepimeria*

Astyridae

- *Astyra*
- *Eclysis*

Thurstonellidae (as Clarenciidae)

- *Thurstonella* (as *Clarencia*)

Dikwidae

- *Dikwa*

Epimeriidae

- *Actinacanthus*
- *Epimeria*
- *Epimeriella (=Epimeria)*
- *Metepimeria*
- *Uschakoviella*

Iphimediidae

- *Anchiphimedia*
- *Echiniphimedia*
- *Gnathiphimedia*
- *Iphimedia*
- *Iphimediella*
- *Labriphimedia*
- *Maxilliphimedia*
- *Nodotergum*
- *Paramphithoe*

Iphimediidae

Genera of De Broyer *et al.* 2007
- *Anisoiphimedia*
- *Coboldus*

Lafystiidae

- *Lafystius*
- *Paralafystius*
- *Protolafystius*

Laphystiopsidae

Genera of B&K91

[Ochlesidae]

- *[Antarctodius]*
- *[Cryptodius]*
- *[Curidia]*
- *[Gordonodius]*
- *[Meraldia]*
- *[Ochlesis]*
- *[Odius]*
- *[Postodius]*

Pleustidae

Full generic composition in Bousfield & Hendrycks (1994a, 1994b, 1995)
Hendrycks & Bousfield (2004)

Atylopsinae
- *Atylopsis*

Austropleustinae
- *Austropleustes*

Dactylopleustinae
Eosymtinae
Mesopleustinae
Neopleustinae
Parapleustinae
- *Incisocalliope*

Pleusirinae
Pleustinae
- *Pleustes*

- *[Bruzelia]*
- *[Pseudotiron]*
- *[Syrrhoe]*
- *[Syrrhoites]*
- *[Tiron]*

- *Meteusiroides*
- *Pareusirogenes*
- *Pontogeneiella*
- *Pontogeneoides*
- *Pseudomoera*
- *Pseudopontogeneia*
- *Rhachotropis*
- *Ronco*
- *Rozinante*
- *Schraderia*
- All the former Pontogeneiidae *sensu* S06

REM: in a note p. 481, Barnard (1969) proposes to amalgamate the Calliopiidae with the Eusiridae

Lafystiidae

- *Lafystius*

Laphystiopsidae

- *Laphystiopsis*
- *Prolaphystiopsis*
- *Prolaphystius*

[Ochlesiidae]

- *[Ochlesis]*

Paramphithoidae

- *Actinacanthus*
- *Amathillopsis*
- *Eclysis*
- *Epimeria*
- *Epimeriella (=Epimeria)*
- *Metepimeria*
- *Paramphithoe*
- *Parepimeria*
- *Pseudepimeria (=Epimeria)*
- *Uschakoviella*

- *[Ochlesodius]*
- All the former Acanthonotozoma-tidae *sensu* B69
- Former Paramphithoidae *sensu* B69 (excl. *Eclysis*)

Lafystiidae

- *Lafystius*

Laphystiopsidae

- *Laphystiopsis*
- *Prolaphystiopsis*
- *Prolaphystius*

Pleustidae

- *Arctopleustes*
- *Austropleustes*
- *Cleonardopsis*
- *Dactylopleustes*
- *Mesopleustes*
- *Neopleustes*
- *Parapleustes*
- *Pleusirus*
- *Pleustes*
- *Pleustomesus*
- *Pleustostenus*
- *Pleusymtes*
- *Stenopleustes*
- *Tepidopleustes*

Stilipedidae

- *Alexandrella*
- *Astyra*
- *Astyroides* (prev. *Alexandrella*)
- *Bathypanoploeae*
- *Eclysis*
- *Stilipes*

- *Paranchiphimedia*
- *Parapanoploea*
- *Pariphimedia*
- *Pseudiphimediella*
- *Stegopanoploea*

Laphystiopsidae

- *Prolaphystius*

[Ochlesidae]

- *[Antarctodius]*
- *[Curidia]*

Pleustidae

Atylopsinae
- *Atylopsis*

Austropleustinae
- *Austropleustes*

Mesopleustinae
- *Mesopleustes*

Pleusymtinae
- *Pleusymtes*

Stilipedidae

- *Alexandrella*
- *Bathypanoplea*
- *Stilipes*

Vicmusiidae

- *Acanthonotozomopsis*

Pleustoidinae
Pleusymtinae
Stenopleustinae

Stilipedidae

Alexandrellinae
- *Alexandrella*
- *Bathypanoploea*

Astyrinae
- *Astyra*
- *Astyroides*
- *Eclysis*

Stilipedinae
- *Stilipes*

Thurstonellidae

- *Thurstonella*

Suborder Senticaudata

Infraorder Hadziida

Superfamily Calliopioidea

Calliopiidae

Full generic composition in Lowry & Myers (2013)
- *Apherusa*
- *Calliopius*
- *[Cleippides]*
- *Halirages*
- *Oradarea*
- *[Weyprechtia]*

[Cheirocratidae]

[Hornelliidae]

Pontogeneiidae

Full generic composition in Lowry & Myers (2013)
- *Atyloella*
- *Bovallia*

	Pleustidae • *Austropleustes* • *Mesopleustes* • *Neopleustes* • *Parapleustes* • *Parepimeriella (=Parepimeria)* • *Pleustes* • *Pleusymtes* • *Stenopleustes* ***Stilipedidae*** • *Alexandrella* • *Stilipes*				• *Eurymera* • *Eusiroides* • *Gondogeneia* • *Liouvillea* • *Paramoera* • *Prostebbingia* • *Schraderia* **Infraorder Gammarida** ***Superfamily Gammaroidea*** ***[23 other families]*** ***Gammarellidae*** • *Austroregia* • *Chosroes* • *[Gammarellus]* • *Gondogeneia*

Table 1. Successive classifications of taxa included herein within Eusiroidea. Families and genera included in the phylogenetic analyses are respectively indicated in red and green. Genera excluded from Eusiroidea following the present study are put within brackets. Following abbreviations were used for the references: S06 = Stebbing (1906), B69 = Barnard (1969), B&K91 = Barnard & Karaman (1991), WoRMS = World Register of Marine Species (Barnard, 1969; Barnard and Karaman, 1991; Bousfield, 1977, 1978; Bousfield and Hendrycks, 1994a, b, 1995a).

The 18S rDNA phylogeny of Englisch (2001) — which includes only a few eusiroid species — shows a paraphyletic Eusiroidea. The clade that includes species of the families Calliopiidae, Eusiridae and Epimeriidae also includes species of the families Astyridae, Iphimediidae and Pleustidae, suggesting that additional families may need to be included in Eusiroidea in order to define a monophyletic superfamily grouping (Fig. 22).

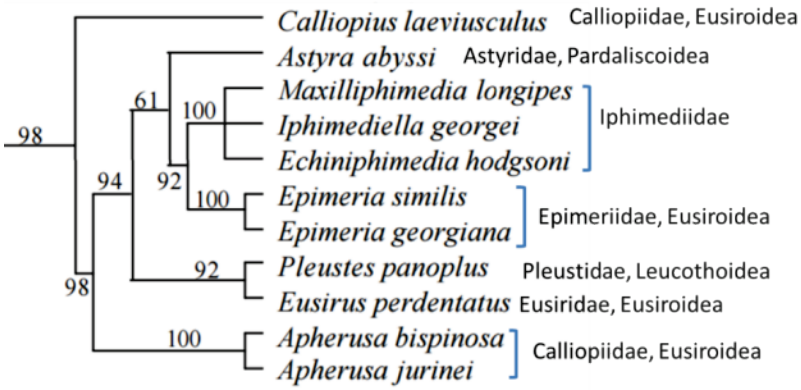

Figure 22. Clade extracted from Englisch (2001)'s Neighbor-Joining 18 rDNA phylogeny of Amphipoda, showing the paraphyly of the superfamily Eusiroidea. Family and superfamily (*sensu* Bousfield 1978) affiliations are indicated besides the species names. Iphimediidae were not classified in any superfamily. Bootstrap values (1000 replicates) are indicated above the nodes.

Eusiroidea is not valid in Lowry and Myers' (2013) classification of the Senticaudata, as part of the superfamily is not included in the new suborder. However, the latter classification did not take into account Englisch's molecular results.

2.2.4. FAMILY EPIMERIIDAE

The amphipod family Epimeriidae comprises a total of 64 species distributed in 5 genera, namely *Actinacanthus* Stebbing, 1888, *Epimeria* Costa in Hope, 1851, *Metepimeria* Schellenberg, 1931, *Paramphithoe* Bruzelius, 1859 and *Uschakoviella* Gurjanova, 1955 (Horton et al., 2013a). The vast majority of species belongs to the genus *Epimeria* (54 species), distributed in every world's oceans, but particularly diverse in the Southern Ocean (26 species). The other three genera with (sub-) Antarctic representatives, *Actinacanthus*, *Metepimeria* and *Uschakoviella*, are monotypic and rarely collected (Coleman, 2007). The seven *Paramphithoe* species all occur in the cold seas of the northern hemisphere (d'Udekem d'Acoz and Vader, 2004).

Epimeria species are mainly benthic, with only two recorded pelagic species, *E. macronyx* and *E. pelagica* (Birstein and Vinogradov, 1958; Walker, 1906). In the Southern Ocean, the genus mainly occurs on the continental shelf (< 1000 m), but several species also have a bathymetric range extending to slope depths (Coleman, 2007): *Epimeria puncticulata*, 1590 m; *Epimeria robusta,* 2000

m; *Epimeria rubrieques*, 1030 m and *Epimeria macronyx*, 1200 m. Outside of the Southern Ocean, epimeriids have generally lower bathymetric ranges, restricted to the continental shelf. Only two *Epimeria* species were found at abyssal depths: *Epimeria glaucosa* at 3710 m in New Zealand (Barnard, 1961) and *Epimeria abyssalis* at 5600 m in the Kuril-Kamchatka Trench (Shimomura and Tomikawa, 2016).

Antarctic *Epimeria* appears to typically inhabit the upper level of the epibenthic assemblages formed by sessile suspension-feeders. Species observed in aquaria were not substrate-selective, as they were found sitting on top of different kinds of sessile organisms or on the sediment surface. They usually stay motionless or walk slowly on the substrate, but can occasionally swim very fast (De Broyer et al., 2001). Regarding *Epimeria*'s trophic ecology, most studied species do not appear to be selective on their prey items. *Epimeria georgiana* would be a deposit-feeder (Dauby et al., 2001b; Graeve et al., 2001).

Epimeria macrodonta, E. robusta and E. rubrieques appear to be opportunistic feeders, coupling microbrowsing on colonial organisms, active capture of small living prey, microdetritivory and/or scavenging. *E. similis* would mainly feed on hydrozoans, although other various items were found in its gut (planktonic cells, sponges, polychaetes) (Fig. 23) (Dauby et al., 2001b; Nyssen et al., 2002). *E. walkeri* seems to be a predator of brittle star and an opportunistic scavenger (Dauby et al., 2001b).

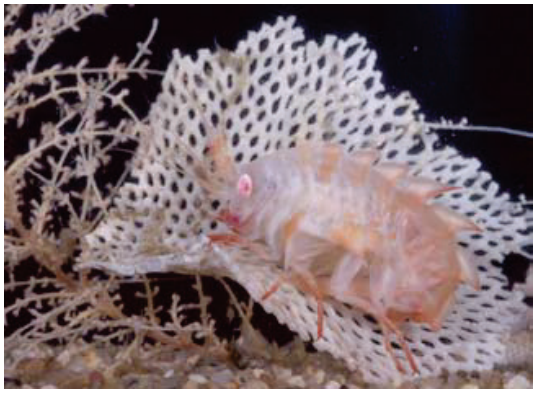

Figure 23. *Epimeria similis.* Picture from Nyssen (2005).

2.2.5. FAMILY IPHIMEDIIDAE

The amphipod family Iphimediidae comprises a total of 107 known species distributed in 15 genera, namely *Anchiphimedia* K.H. Barnard, 1930, *Anisoiphimedia* G. Karaman, 1980, *Coboldus* Krapp-Schickel, 1974, *Echiniphimedia* K.H. Barnard, 1930, *Gnathiphimedia* K.H. Barnard, 1930, *Iphimedia* Rathke, 1843, *Iphimediella* Chevreux, 1911, *Labriphimedia* K.H. Barnard, 1931, *Maxilliphimedia* K.H. Barnard, 1930, *Nodotergum* Bellan-Santini, 1972, *Paranchiphimedia* Ruffo, 1949, *Parapanoploea* Nicholls, 1938, *Pariphimedia* Chevreux, 1906, *Pseudiphimediella* Schellenberg, 1931 and *Stegopanoploea* Karaman, 1980. The family is distributed in every worlds' ocean, in cool-temperate

and tropical waters, and well-represented in the Southern Ocean, with 36 described species (Horton et al., 2013b).

Iphimediid species are strictly benthic and mainly occur on the continental shelf, from the coast to the shelf break, with only two Antarctic species also recorded from the upper slope (*Gnathiphimedia mandibularis*: 2000 m; *Echiniphimedia hodgsoni*: 1120 m) (Coleman, 2007). Iphimediids appear to typically inhabit the lower level of the **epibenthic** assemblages formed by sessile suspension-feeders. Iphimediid species observed in aquaria usually stay motionless or walk very slowly on the substrate, but were very rarely observed swimming (De Broyer et al., 2001). This family appears to be mostly composed of **micropredatory browsers**, specializing on a preferred food source. *Echiniphimedia hodgsoni* is the only amphipod species shown to feed almost exclusively on sponges (Fig. 24) (Amsler et al., 2009; Coleman, 1989b; Dauby et al., 2001b; Graeve et al., 2001; Nyssen et al., 2005). Similarly, other *Echiniphimedia* species presumably feed on sponges and/or use them as shelter (Dauby et al., 2001b), such as *Echiniphimedia echinata* (Nyssen, 2005) and *Echiniphimedia scotti* (De Broyer et al., 2001).

Figure 24. *Echiniphimedia hodgsoni* within a sponge. Picture by O. Coleman.

Gnathiphimedia mandibularis primarily feeds on bryozoans (Dauby et al., 2001b; Klages and Gutt, 1990) and crushes these hard items with its highly adapted mandibles (Fig. 25) (Coleman, 1989a).

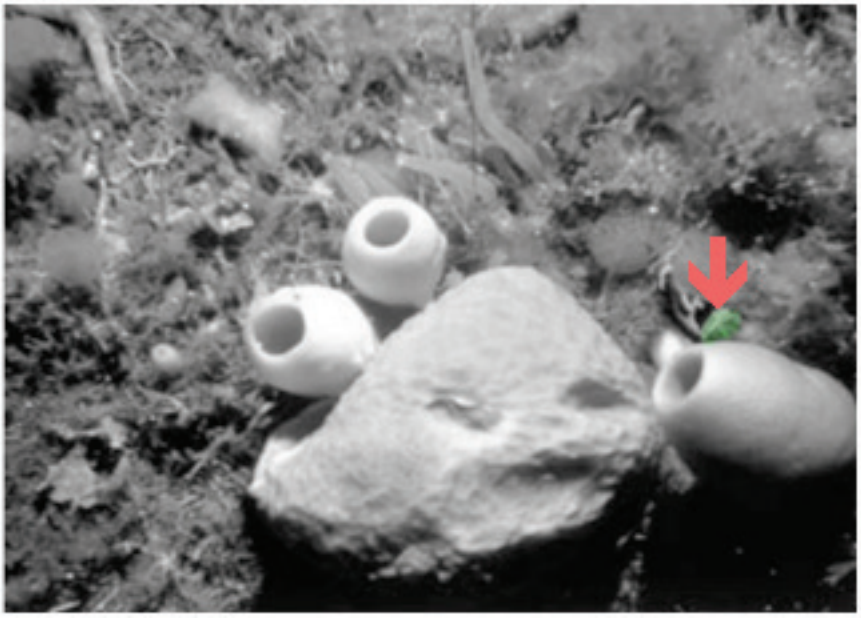

Figure 25. Typical habitat of *Gnathiphimedia mandibularis* (arrow), composed of bryozoan colonies and sponges. Picture from De Broyer et al. (2001); J. Gutt, A.W.I. (ANT VII/4, frame 262).

Maxilliphimedia longipes mainly feeds on cnidarian tissues (Dauby et al., 2001b), with its specialized mandibles, adapted to cut large fragments of soft food (Coleman, 1989b). *Iphimediella cyclogena* was found to feed primarily on holothurians, and occasionally polychaetes. The species was interpreted to be an opportunistic consumer, switching from scavenging holothurians to active predation on smaller organisms, following the availability of food (Nyssen et al., 2002). *Iphimediella bransfieldi* was caught in baited traps, designed to attract scavenger species, but this was interpreted as an accidental catch (De Broyer et al., 2004).

Curiously, iphimediids, which are common amphipods on the Antarctic shelf, are very rarely found in fishes' stomachs (Dauby et al., 2003). Their spinose and calcified body might offer some protection against heavy predation (Brandt, 1999).

2.3. Distribution patterns

The Antarctic benthic fauna is characterized by high degrees of **endemism**, generally around 50 % to 80 % of the species, depending on the group (Griffiths et al., 2009). Among amphipods, 66.6 % of benthic species are endemic to the high Antarctic region, whereas the endemism level reaches 83.6 % when the sub-Antarctic region is added (De Broyer and Jażdżewska, 2014).

The spatial distributions of benthic organisms are determined by their specific dispersal ability, which is itself constrained by their life history traits, but also by a number of important physical (geomorphology of the seafloor, depth, seabed temperature, sea-surface productivity, sea ice cover, degree of iceberg scouring, ocean currents and at a more local scale, substrate type) and biotic (predation, parasitism and starvation) environmental factors. The distances between suitable

habitats, steep environmental clines or geomorphic features can act as barriers to dispersal. Similar habitats will support different species assemblages when the distances between them are greater than the dispersal abilities of species (Douglass et al., 2014; Koubbi et al., 2014).

The study of the geographical structure of Southern Ocean biodiversity has led to the definition of distinct biogeographical regions, defined as homogeneous geographical areas in terms of environmental conditions and biodiversity, relative to adjacent areas. These bioregions are characterized by a certain degree of species endemism (David and Saucède, 2015). However, the defined bioregions vary for different taxonomic groups. While some groups do not exhibit any biogeographical split around the whole continent, others, such as amphipods, display a level of differentiation between **West** (Peninsula and Scotia Arc islands) and **East Antarctic bioregions** (continental circum-Antarctic area, excluding the Peninsula) (Fig. 26) (Griffiths et al., 2009; Koubbi et al., 2014; Rodríguez et al., 2007). The transitional area between East and West Antarctica, the eastern and southern Weddell Sea, has an ambiguous biogeographical affinity for amphipods. Whereas it is considered to be part of the East Antarctic bioregion for other groups (Fig. 26) (Pierrat et al., 2013; Zelaya, 2005), it shares significantly more amphipod species with the West Antarctic bioregion (De Broyer and Jażdżewska, 2014).

Sub-Antarctic islands are biogeographically distinct and have varying degrees of faunal similarities with high Antarctica, South America and other sub-Antarctic islands depending on the taxonomic group under study. The **Magellanic region** displays far more biogeographical affinities with Antarctica than any other non-Antarctic areas, such as New Zealand/Australia (Fig. 26) (Griffiths et al., 2009; Koubbi et al., 2014).

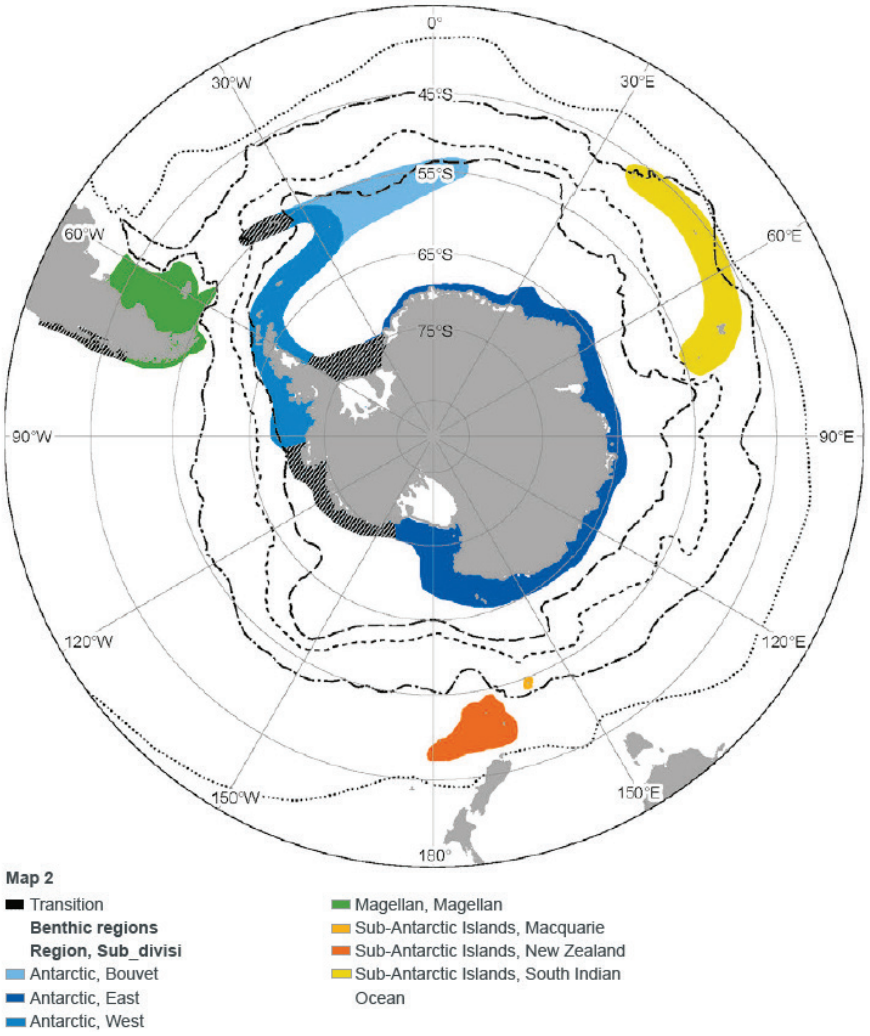

Figure 26. Summary of the general benthic biogeographical regions defined in the Southern Ocean. Figure from Koubbi et al. (2014).

The Antarctic benthic species were considered to be generally characterized by **circumpolar distributions** (Arntz et al., 1994; Arntz et al., 1997; Clarke and Crame, 1997). Notably, 22 % of all benthic and bentho-pelagic amphipod species are recorded as circum-Antarctic i.e. with a distributional range covering at least three widely separated localities around the continent (De Broyer and Jażdżewska, 2014). This generalized distributional pattern was inferred to result from the circumpolar current system — the ACC and the East-wind drift — transporting organisms around the continent (Hemery et al., 2012; Janosik et al., 2011; Leese et al., 2010; Riesgo et al., 2015), relatively uniform water temperatures and physical conditions (Arntz et al., 1994) and a continuous continental shelf (Griffiths et al., 2009).

However, whereas true circumpolarity has been confirmed by phylogeographical studies for several taxa (e.g. Arango et al., 2011; Havermans et al., 2013; Raupach et al., 2010), many others were shown to be composed of two or more regionally-restricted (pseudo)cryptic species (e.g. Havermans

et al., 2011; Havermans et al., 2013; Held, 2003; Held, 2014; Lörz et al., 2011). Therefore, the number of truly circumpolar species might be much lower than what is inferred from available distributional records.

3. HISTORICAL CONTEXT

3.1. GEOLOGICAL AND OCEANOGRAPHIC HISTORY OF ANTARCTICA

3.1.1. GONDWANA

200 Ma – Throughout the Mesozoic until ca. 160 Ma, Antarctica was the center of a vast landmass: the Gondwana supercontinent, which also comprised South America, Africa, Madagascar, India, Australia and New Zealand (Jokat et al., 2003).

The Antarctic continent is composed of different tectonic regions. East Antarctica is a single very large continental block, whereas West Antarctica is composed of numerous crustal blocks (Fig. 27) (Talarico and Kleinschmidt, 2009).

Figure 27. Reconstruction of Gondwana 200 Ma. Continents are indicated with coastlines and 2000 m isobaths. Tick marks are a 5° grid based on the present-day latitude and longitude for the continental fragments. AP, Antarctic Peninsula; CP, Campbell Plateau; CR, Chatham Rise; KN, Kenya; LHR, Lord Howe Rise; LM, Lebombo Monocline; MAD, Madagascar; MBL, Marie Byrd Land; MOZ, Mozambique; NNZ, North New Zealand; SL, Sri Lanka; SNZ, South New Zealand; SP, Shillong Plateau; TI, Thurston Island. Figure modified from Lawver et al. (1992).

3.1.2. Early Gondwana Break-up

160–130 Ma – In the late Jurassic, seafloor began to spread between East Gondwana (Antarctica, Australia, India and New Zealand) and West Gondwana (South America and Africa) (Lawver et al., 1992; Talarico and Kleinschmidt, 2009). By 130 Ma, the Weddell Sea would have become a substantial ocean basin (WB), connected to the Mozambique Basin (MB) and possibly the Somali Basin (SB) through a seaway between Africa and Madagascar (Lawver et al., 1992). Seafloor spreading began off the western margin of Australia and between Antarctica and India. India moved away from the Australia-Antarctica block in the interval 136–126 Ma (Fig. 28) (Gibbons et al., 2013).

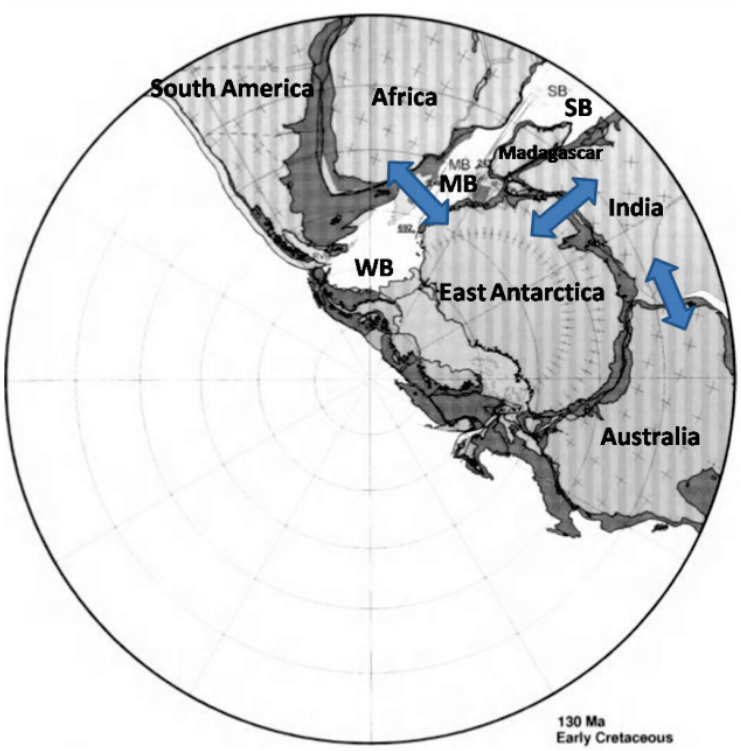

Figure 28. Paleogeographic reconstruction of Southern Gondwana at 130 Ma. The Weddell Basin continues to open. India starts to move away from the Australia-Antarctica block. WB = Weddell Basin; MB = Mozambique Basin; SB = Somali Basin. Figure modified from Lawver et al. (1992).

120–110 Ma – Antarctica positioned at southern polar latitudes. Madagascar, India and the southern Kerguelen Plateau had moved away from Antarctica, leaving a wide open seaway along that part of the present-day East Antarctic margin (Fig. 29) (Lawver et al., 1992).

Figure 29. Paleogeographic reconstruction of Southern Gondwana at 110 Ma. Madagascar, India and the southern Kerguelen Plateau have moved away from Antarctica. Figure modified from Lawver et al. (1992).

3.1.3. Opening of Tasmanian and Drake Passages

100–85 Ma – The northernmost Kerguelen Plateau had just cleared the Indian continental margin. From about 90 Ma, the gulf between Antarctica and Australia widened considerably, but Tasmania and the South Tasman Rise (STR) still blocked deep-water circulation (Lawver et al., 1992). At 85 Ma, New Zealand separated from Antarctica and Australia (Fig. 30) (Heads, 2016).

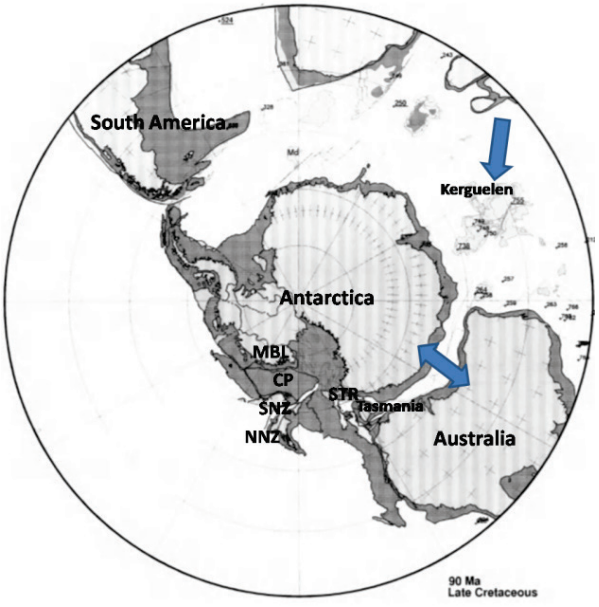

Figure 30. Paleogeographic reconstruction of Southern Gondwana at 90 Ma. The northernmost Kerguelen Plateau clears the Indian margin. Australia begins its motion away from Antarctica. NNZ = North New Zealand; SNZ = South New Zealand; STR = South Tasman Rise. Figure modified from Lawver et al. (1992).

80–40 Ma – A submarine trough between Tasmania and the South Tasman Rise (STR), the South Tasman Saddle, opened from 79 to 66 Ma. This developing seaway would, however, have remained a shallow to medium-deep passage between Australia and East Antarctica until at least early Eocene, as Tasmania and the STR still formed an effective barrier to deep-water circulation (Lawver et al., 2013). Australia initially moved very slowly northward. Rapid northward motion only started at about 45 Ma. The Antarctic Peninsula moved eastward with respect to the southern tip of South America (Fig. 31) (Lawver et al., 1992).

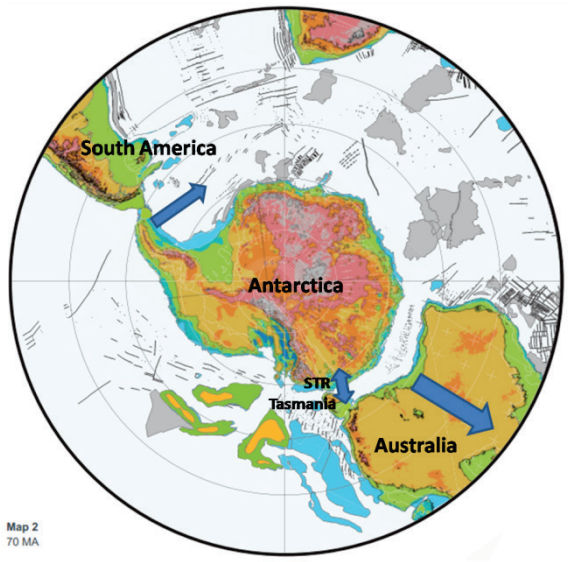

Figure 31. Paleogeographic reconstruction of Southern Gondwana at 70 Ma. Australia continues its motion away from Antarctica. STR = South Tasman Rise. Figure modified from Lawver et al. (2014).

40 Ma – The Drake Passage began to form, at least as a shallow water seaway (Lawver et al., 2014). Considerable controversy surrounds the timing of the opening of a deep-water passage between South America and Antarctica. However, it was inferred that at least a shallow water seaway was present by 40 Ma (Lawver et al., 2014; Scher and Martin, 2004). A shallow to intermediate-depth passage could even have existed as early as 50 Ma (Eagles et al., 2006; Livermore et al., 2005). It is debated whether the Drake Passage was a deep-water seaway by 40 Ma. If Terror Rise — shown as a fragment off the tip of Tierra del Fuego — was farther south than on Figure 32, it might have blocked deep-water circulation at that time (Fig. 32).

By 40 Ma, the South Tasman Saddle, between Tasmania and Antarctica, would have been at least a medium-depth seaway (maximum 3000 m deep, at places) of 200 km wide (Lawver et al., 2014). If the Oates Coast / George V shelf break was closer to the present East Antarctic shoreline, then a deep seaway may have existed as early as 40 Ma (Lawver et al., 2013). Continued volcanic activity by the Kerguelen hotspot (KP) at the western end of Broken Ridge (BR) at ~ 38 Ma would have blocked major circumpolar flow (Fig. 32) (Frey and Weis, 1995; Lawver et al., 2014).

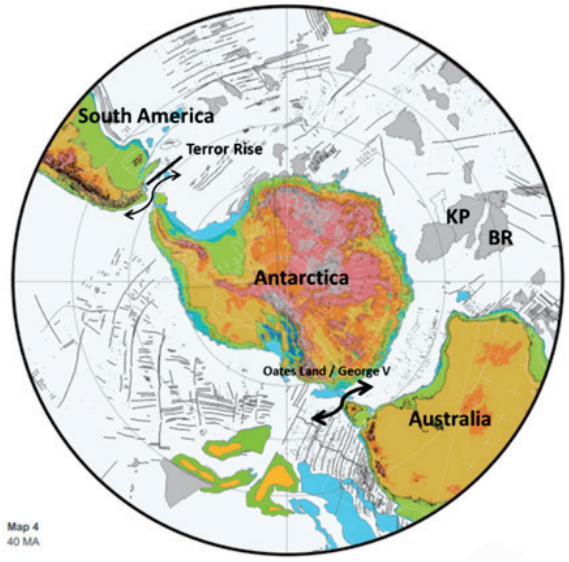

Figure 32. Paleogeographic reconstruction of Southern Gondwana at 40 Ma. The Drake Passage began to form as a shallow seaway between South America and Antarctica. The Tasmanian Gateway existed as a medium-depth seaway. KP = Kerguelen Plateau; BR = Broken Ridge. Figure modified from Lawver et al. (2014).

34–30 Ma – The Tasmanian Gateway deepened between 35.5 and 30.2 Ma (Stickley et al., 2004). Unrestricted opening deeper than 2000 m is dated at 33–32 Ma (Lawver and Gahagan, 2003). The Antarctic Peninsula had moved past the tip of southern South America (Lawver et al., 1992). The establishment of a deep-water seaway in the Drake Passage is generally dated in the interval 34–30 Ma by different authors (Lagabrielle et al., 2009; Latimer and Filippelli, 2002; Lawver and Gahagan, 2003; Livermore et al., 2005; Scher and Martin, 2004). An ancestral South Sandwich Arc would still form a barrier to circumpolar flow (Fig. 33) (Dalziel et al., 2013b). Geological records would, however, indicate that the opening of the Drake Passage was not monotonic. Following the onset of deep circulation, the Drake Passage would have experienced significant narrowing in the 29–22 Ma period (Brown et al., 2006; Lagabrielle et al., 2009).

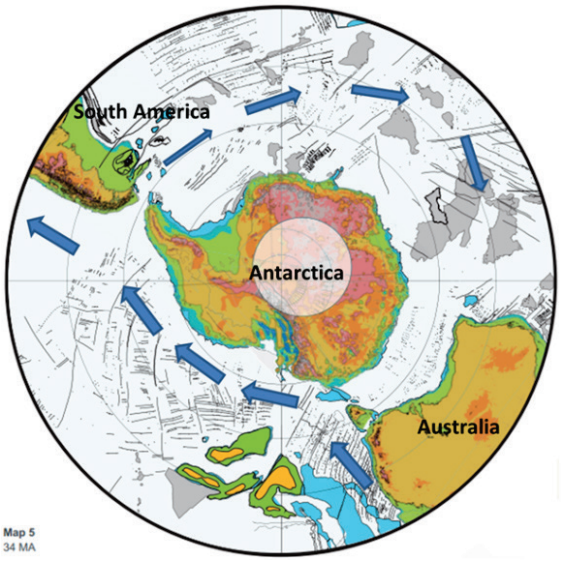

Figure 33. Paleogeographic reconstruction of Southern Gondwana at 34 Ma. Opening of Tasmanian Gateway to deep-water circulation. An ancestral South Sandwich Arc would still block deep-water circulation in the Drake Passage. Figure modified from Lawver et al. (2014).

3.1.4. Onset of the Antarctic Circumpolar Current

The opening of Drake Passage and Tasmanian Gateway enabled the formation of the ACC (Barker, 2001). As the opening of the Drake Passage is not well-constrained in time, the exact timing of the ACC's onset is as much debated (Barker et al., 2007). Some authors suggested that a shallower "proto-ACC" would have existed by 37–32 Ma (Diekmann et al., 2004; Diester-Haass and Zahn, 1996; Lagabrielle et al., 2009). The onset of an unrestricted deep passageway for the ACC was dated at different times in the interval 33–23 Ma (Diekmann et al., 2004; Florindo and Roberts, 2005; Latimer and Filippelli, 2002; Lawver and Gahagan, 2003; Lyle et al., 2007; Pfühl and McCave, 2005; Roberts et al., 2003a).

20 Ma – By this time, the ACC would have developed (Fig. 34) (Lawver and Gahagan, 2003; Lawver et al., 1992).

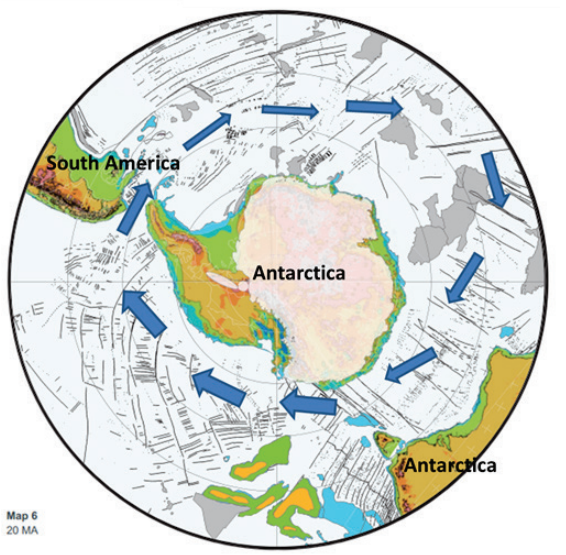

Figure 34. Paleogeographic reconstruction of Southern Gondwana at 20 Ma. The western Scotia Sea opened and the ACC developed. Figure modified from Lawver et al. (2014).

12 Ma – Alternatively, it was inferred that an ancestral South Sandwich Arc could have acted as a barrier to deep-water flow until ca. 12 Ma, supporting a mid-Miocene onset of the ACC (Dalziel et al., 2013a,b).

3.2. Climatic history of Antarctica

3.2.1. Antarctica in a Greenhouse

Antarctica has been located over southern polar latitudes since early Cretaceous (Lawver et al., 1992). However, in the mid-Cretaceous, summer temperatures were estimated to reach 20–24°C and low winter temperatures were just above freezing (Valdes et al., 1996). The climatic conditions in this region may have been remarkably diverse during this greenhouse period. While it is thought to have remained mostly ice-free, vegetated and with positive mean annual temperatures until the Eocene–Oligocene boundary, small- to medium-sized ephemeral ice sheets did occur in the interior of the continent during the late Cretaceous to the middle Eocene (Barrett, 1996; Florindo and Siegert, 2008; Miller et al., 2008a).

The early Eocene was marked by a warming event at ca. 48.5 Ma, known as the **Eocene Climatic Optimum** (Fig. 39). Following this latter peak warmth, high latitude surface water cooled across the early to middle Eocene boundary (ca. 48–49 Ma). This cooling would be linked to the closure of the early Cenozoic eastern Tethys, which previously discharged large amounts of very dense, warm and saline water into the Indian Ocean. This export ceased when Greater India collided with Eurasia and closed the seaway from 49 Ma (Lawver and Gahagan, 2003).

A second cooling phase occurred in the late Middle Eocene (ca. 44–41 Ma) (Miller et al., 2008a). However, despite the reversal of climatic trend, warming events still periodically affected the Eocene climate. The last of these events, the **Middle Eocene Climatic Optimum**, occurred at ca. 41.5 Ma with a temperature increase of up to 4°C (Fig. 39) (Bohaty and Zachos, 2003). From the beginning of the cooling trend, ice sheets progressively grew to culminate at the Eocene–Oligocene transition (Fig. 35) (Miller et al., 2008a).

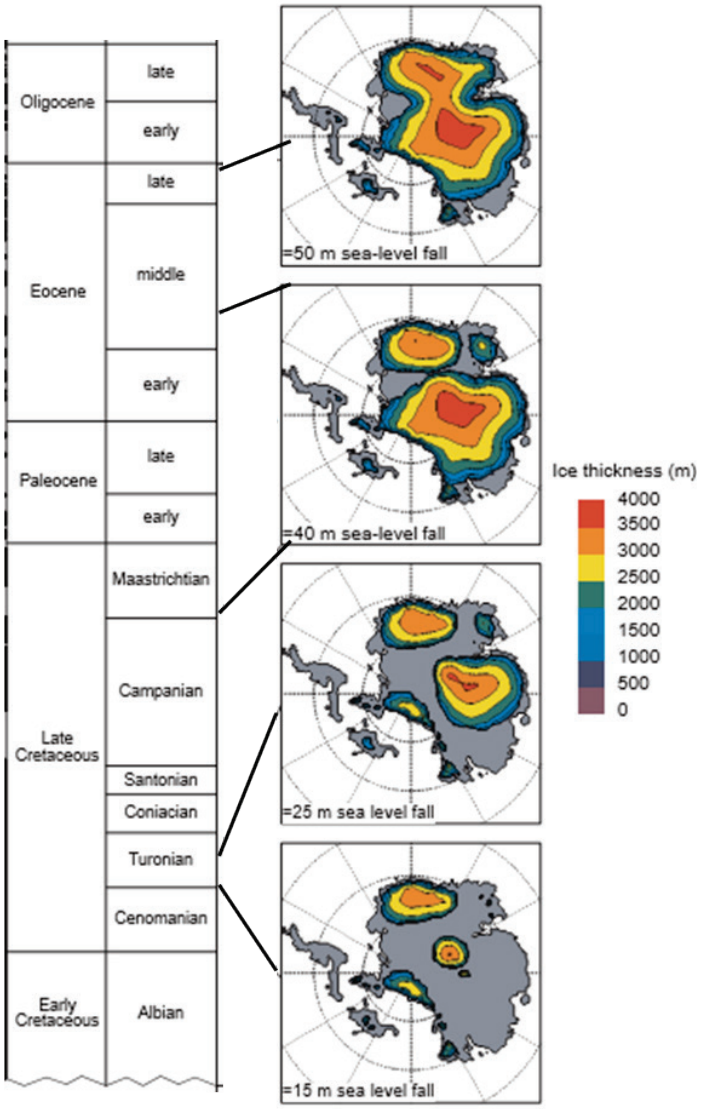

Figure 35. Maps are after DeConto and Pollard (2003a, b), showing the maximum sizes of ice sheets during peak glaciations for several intervals from the late Cretaceous to the Eocene–Oligocene boundary. Equivalent estimated sea-level change is indicated for each state. Figure modified from Miller et al. (2008b).

3.2.2. The Eocene–Oligocene Climate Transition

The first major glaciations took place at the Eocene–Oligocene boundary (Francis et al., 2008; Lear et al., 2000; Lear et al., 2004). Antarctica entered the Icehouse in the earliest Oligocene**.** This abrupt cooling at 33.55 Ma is known as the **Eocene–Oligocene Climate Transition** or Oi-1 glaciation event (Miller et al., 1991). The Antarctic ice sheet rapidly grew and reached about 80–100 percent of its present-day size (Fig. 36) (Sorlien et al., 2007; Wilson et al., 2013). In some places (e.g. Prydz Bay), ice extended to the shelf break for the first time (Hambrey et al., 1991).

This large ice sheet became a driver of climate change. The Antarctic region has been a source of deep-water to the world's oceans from the late Cretaceous. The Eocene–Oligocene boundary saw an intensification of this Antarctic Bottom Water [see section 1.3.] which, in turn, had a strong cold influence on the Antarctic coast (Kennett, 1977; Miller et al., 2008b).

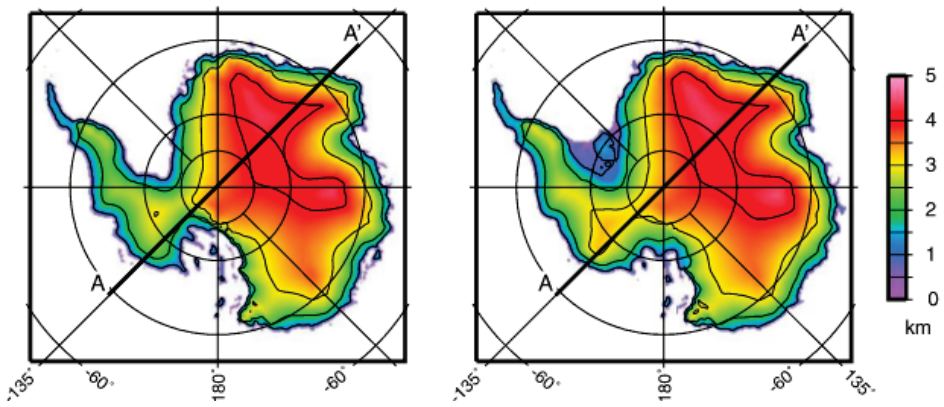

Figure 36. Modelled ice sheet at the Eocene–Oligocene boundary on minimum (left) and maximum (right) estimates of the topography. Color legend showing ice thickness. Figure from Wilson et al. (2013).

The Antarctic glaciation was originally hypothesized to have been mainly triggered by the opening of the Tasman or Australia–Antarctica Passage and the Drake Passage (Barker, 2001; Kennett, 1977; Kennett et al., 1975; Zachos et al., 1996). However, a decline in atmospheric CO_2 has also been proposed as a possible cause (DeConto and Pollard, 2003b; Lawver and Gahagan, 2003; Pearson and Palmer, 2000).

3.2.3. The Transition period

The Oligocene was presumably characterized by a gradual and steady cooling, which culminated in the early to mid-Miocene (Pekar and DeConto, 2006; Prebble et al., 2006; Roberts et al., 2003b). During glacial maxima of this period, the ice sheet would have advanced across the continental shelf (Fig. 37) (Gasson et al., 2016), reaching the shelf break at times in several areas, such as Prydz Bay, the Ross Sea and the Weddell Sea (Cochrane et al., 1995; Cooper et al., 1991).

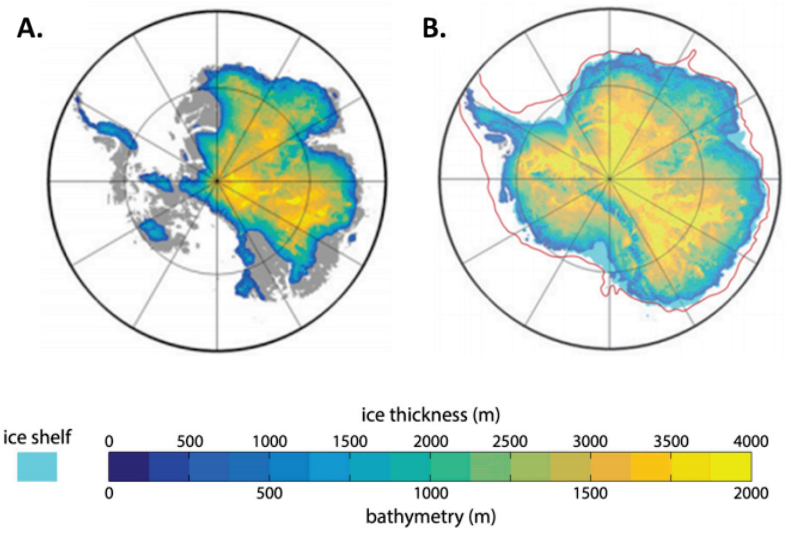

Figure 37. Ice sheet thickness simulated in response to different climate forcing, using an approximated mid-Miocene bedrock topography, atmospheric CO_2 and astronomical configurations inferred for the early to mid-Miocene timeframe. (A) Warmer interval simulation and (B) colder interval simulation. The red line shows the position of the shelf break. Figure modified from Gasson et al. (2016).

This period of large fluctuations in ice-sheet volume was followed by a prolonged warm period, called the the "**Mid-Miocene Climatic Optimum**" (MMCO) at ~17–15 Ma (Fig. 39) (Hauptvogel and Passchier, 2012; Lagabrielle et al., 2009). During the glacial periods, the ice sheet margin was located inland, with a maximum extent comparable to the present interglacial configuration (Hauptvogel and Passchier, 2012; Passchier et al., 2011).

3.2.4. The mid-Miocene Climate Transition

The MMCO was followed by long-term climatic deterioration toward colder icehouse conditions (Fielding et al., 2011). The **Middle Miocene Climate Transition** (MMCT), 14.2 to 13.8 Ma, was marked by a second rapid (< 0.5 My) Antarctic ice sheet growth (Shevenell et al., 2004). The ice sheet extended onto the shelf during glacial maxima, reaching the shelf break at least in some places (Chow and Bart, 2003; Cooper et al., 2008). Oceanographic changes were inferred to be responsible for the end of the warm period (Mackensen, 2004). The MMCT coincides with a re-widening of the Drake Passage and possible increase in ACC flows 14–15 Ma (Lagabrielle et al., 2009). In a scenario supporting a mid-Miocene onset of the ACC, the latter might have played a role in the subsequent cooling and intensification of Antarctic glaciations (Dalziel et al., 2013a,b). The early Miocene analogue of the Antarctic Bottom Water, the Southern Component Water, also intensified (Hamon et al., 2013; Lawver and Gahagan, 2003; Mackensen, 2004).

3.2.5. The Plio–Pleistocene Glacial Cycles

The amplitude of the glacial cycles progressively increased during the last 5 Ma (Fig. 39) (Naish et al., 2009). The modelling of the ice dynamics during this period suggests that the West Antarctic ice sheet extent would have varied from full glacial extent with grounding lines near the continental shelf break, to intermediate states similar to modern, and brief but dramatic retreats, leaving only small isolated ice caps on the West Antarctic islands. Such super-interglacials could have resulted in the (re)opening of a seaway between East and West Antarctica (Pollard and DeConto, 2009). In contrast, the East Antarctic ice sheet would have remained relatively stable (Naish et al., 2009).

While evidences of ice sheet advances on the shelf exist from the Eocene/Oligocene transition across the Plio-Pleistocene (Chow and Bart, 2003; McKay et al., 2012), a precise identification of the grounding line positions has not been possible for earlier glacial advances than the Last Glacial Maximum (LGM) of the Late Pleistocene (Convey et al., 2009). The ice sheets reached their maximum extent around 15,000 years ago and subsequently retreated to attain near-modern locations by 3,000 years ago (Fig. 38) (Denton and Hughes, 2002; Huybrechts, 2002; Pollard and DeConto, 2009). At the glacial maximum, grounded ice would have extended to the shelf break

around the whole continent (Fig. 38) (Anderson et al., 2002; Heroy and Anderson, 2005; Ó Cofaigh et al., 2005), except for outer shelf areas in (1) the western Ross sea (Licht et al., 1996; Ship et al., 1999), (2) Prydz Bay (Domack et al., 1998; O'Brien et al., 1999) and (3) George V Land (Beaman and Harris, 2003). However, the latter regions where either covered by floating ice shelves (Ross Sea and Prydz Bay) or heavily scoured (George V Land) (Beaman and Harris, 2003; Domack et al., 1998; Ship et al., 1999).

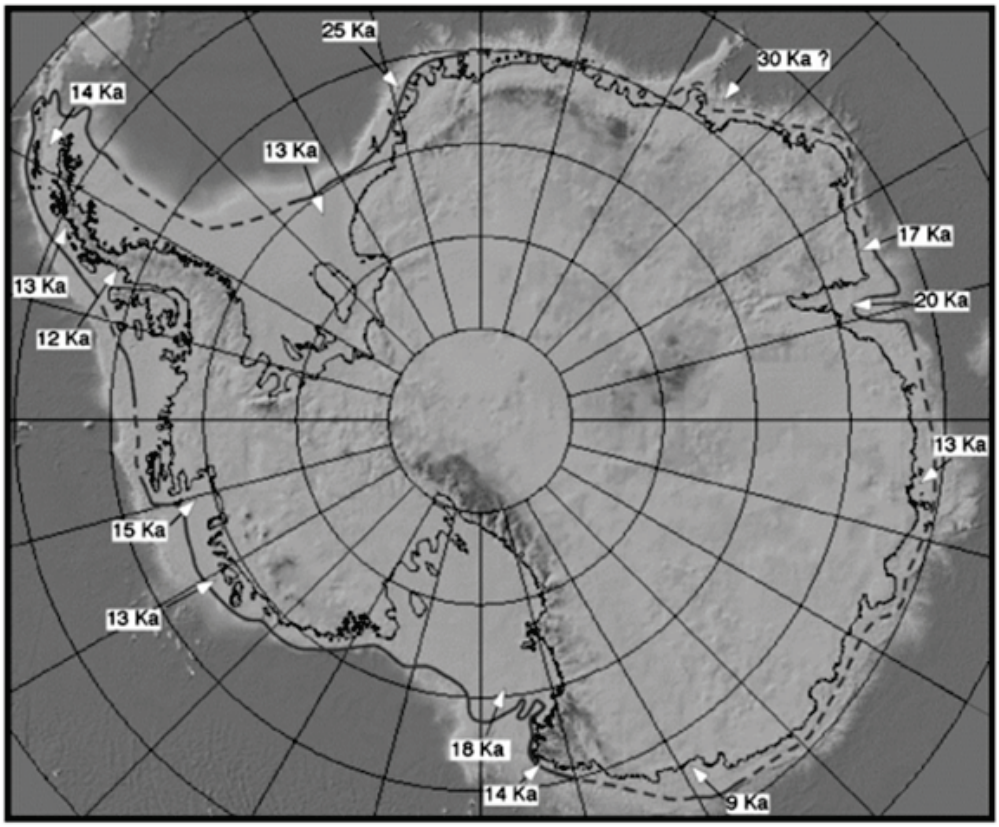

Figure 38. Marine geological reconstructions of grounding line positions of the Antarctic Ice Sheet at the LGM. The figure shows the oldest constraining ages for initial ice sheet retreat from the shelf. Figure from Anderson et al. (2002).

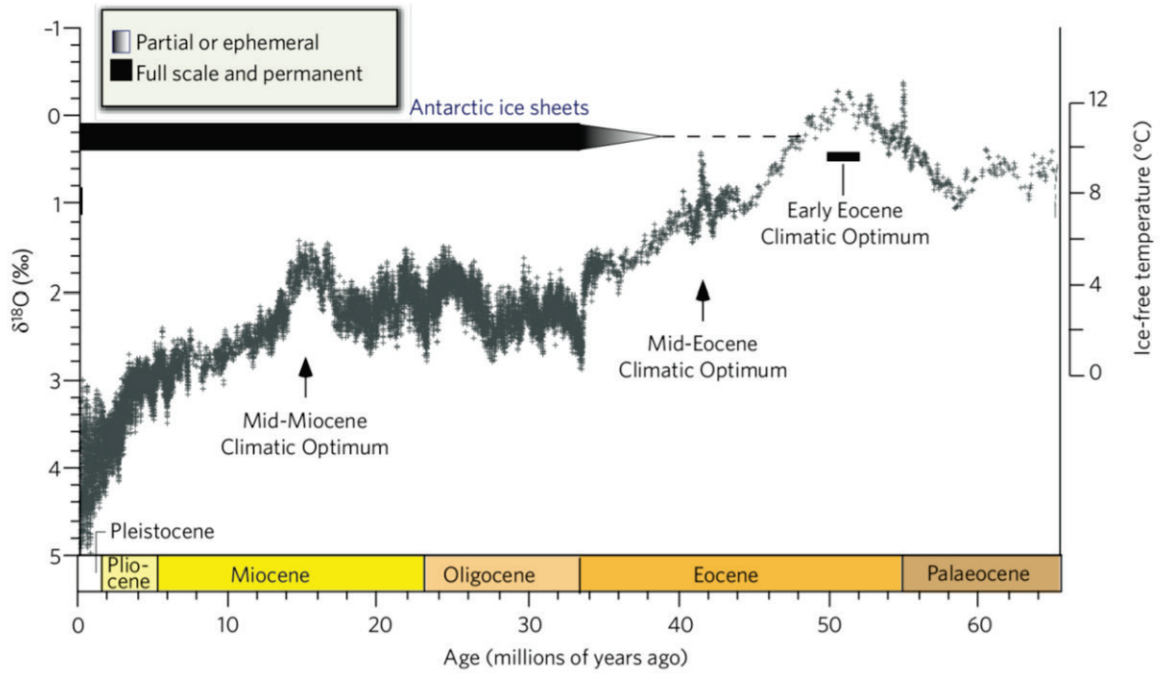

Figure 39. Temperature in the Southern Ocean during the Cenozoic inferred from the benthic foraminiferal $\delta^{18}O$ curve based on records from Deep Sea Drilling Project and Ocean Drilling Program sites [from Zachos et al. (2008)]. The figure shows the three major hyperthermals, followed by periods of intense cooling. Figure from Hauptvogel (2015).

4. Evolution in the Southern Ocean

The current biodiversity and distribution patterns of the Antarctic benthos result from the interactive effects of geological, climatic, oceanographic and biotic factors throughout the history of the Antarctic region (Allcock and Strugnell, 2012; Clarke and Crame, 2010; Crame, 1997; Crame, 1999; Griffiths et al., 2009).

The temperature variations and glacial advances led to the extinction of some lineages. Other lineages, however, would have been able to adapt *in situ* to decreasing temperature or increasing ice coverage (Clarke and Johnston, 2003). Part of the modern fauna did not originate in Antarctica, but descents from lower latitudes' colonizers. The Southern Ocean fauna therefore contains a mixture of lineages with different histories, some have evolved in the region for a long time, others are recent arrivals (Clarke and Crame, 1989).

4.1. *In situ* Evolution from Gondwanan ancestors – 160 to 34 Ma

Some components of the modern fauna possibly have ancestors dating back to the Late-Cretaceous – Early Cenozoic. At that time, the southern continents were separated by shallow cool-temperate waters extending from the southern tip of South America, through the western margin of Antarctica,

until eastern Australia (Stilwell et al., 2004) (Fig. 40). The observation of a similar and highly endemic molluscan paleofauna in the Late Cretaceous–Paleogene fossil record of these regions led to the assumption that it represented a single, broad and continuous biogeographical province, which was called the **Weddellian Province** (Zinsmeister, 1982). Following the final stages of Gondwana's break-up — the opening of the Drake and Tasmanian passages — the shelf regions of southern South America, Australia and Antarctica became progressively isolated, leading to the divergence of Antarctic lineages from their Late Gondwanan ancestors (e.g. Bargelloni et al., 2000; Lee et al., 2004; Near, 2004).

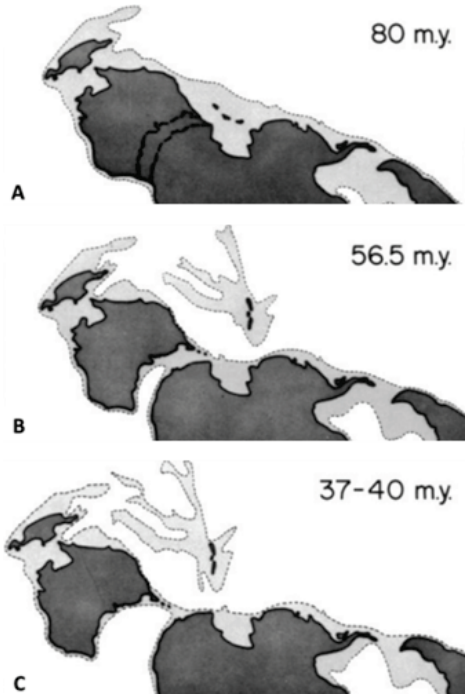

Figure 40. Changes in the paleogeography resulting from the final breakup of Gondwanaland. Shaded area represents inferred areas of shallow marine conditions. A. Late Cretaceous Weddelian Province. B. and C. Progressive drifting of Australia away from Antarctica in the Paleogene. Figure from Zinsmeister (1982).

4.2. Cretaceous-Paleogene mass extinction – 66 Ma

The last major global mass extinction event took place 66 Ma at the Cretaceous–Paleogene boundary. The eruption of the Deccan Traps volcanic province and the impact of the Chiccxulub meteorites are the two inferred causal events, which would have been both responsible for a significant global warming (Petersen et al., 2016). This extinction was presumably as rapid and severe in Antarctica as at lower latitudes (Witts et al., 2016). The total diversity of marine genera in the fossil record worldwide declined by nearly 50 % (Sepkoski, 1996). A large and permanent increase in origination rates occurred globally after the Cretaceous–Paleogene boundary, as a diversity-dependent effect in a depauperate environment (Krug et al., 2009; Miller and Sepkoski, 1988; Oleinik and Zinsmeister, 1996; Witts et al., 2016). Many new species and genera arose during the Paleocene, resulting in a highly distinctive fauna (Stilwell, 2003).

4.3. The cooling and the onset of continental glaciations – 49 to 34 Ma

While part of the shelf fauna would have been able to adapt *in situ* to cooler conditions, some groups were unable to cope with the temperature change (Brandt and Gutt, 2011; Clarke et al., 1992a). A major faunal turnover along this time period is observable in the fossil record, mostly from the La Meseta Formation at Seymour Island, off the Antarctic Peninsula (Aronson and Blake, 2001). The warm Middle Eocene fauna was progressively replaced by successively cooler faunal assemblages (Aronson and Blake, 2001; Boersma et al., 1987; Jadwiszczak, 2010; Keller et al., 1992; Stilwell and Zinsmeister, 1992).

Notably, the extinction of most durophagous predators (decapods crustaceans and fishes) caused a fundamental shift in the structure of marine benthic communities (Brandt and Gutt, 2011; Clarke et al., 1992a). A decrease in predation pressure and vacant ecological niches allowed other lineages to flourish. In absence of skeleton-crushing predation, dense populations of epifaunal suspension-feeding organisms, such as ophiuroids and crinoids were able to establish (Aronson et al., 1997). Other groups such as echinoderms, molluscs and bryozoans would have benefited from the reduced predation pressure as well. The main predators in such communities were slower moving invertebrates which do not crush hard-shelled preys, i.e. asteroids, ophiuroids, nemerteans, anthozoans, pycnogonids, isopods and shell-drilling gastropods (Aronson and Blake, 2001). It has been hypothesized, notably, that the extinction of many decapod crustaceans allowed the Peracarida to fill the free ecological niches (Brandt, 1999).

4.4. The onset of the ACC – ca. 33 to 23 Ma or 12 Ma (?)

As the ACC marks an extreme transition in temperatures, its onset was inferred to have driven vicariant events by creating a natural marine barrier to genetic exchange (Bargelloni et al., 2000; Barker et al., 2007; Lee et al., 2004).

4.5. The Glacial/Interglacial cycles – 14 Ma to present

After the MMCT, ice sheets repeatedly advanced on the shelf [see section 3.2.] (Chow and Bart, 2003; O'Brien et al., 2004; Pollard and DeConto, 2009). Even if the grounded ice did not reach the shelf break in some areas, ice scouring was probably too heavy for the subsistence of benthic communities (Thatje et al., 2005b). Mass-wasting processes such as slides, debris flows, turbidity currents and glaciogenic debris likely compromised survival on the continental slope as well (Fig. 41) (Gutt and Piepenburg, 2003). The permanent ice-cover over the shelf and slope also limited phytoplankton productivity, possibly causing starvation of benthic organisms (Thatje et al., 2005b).

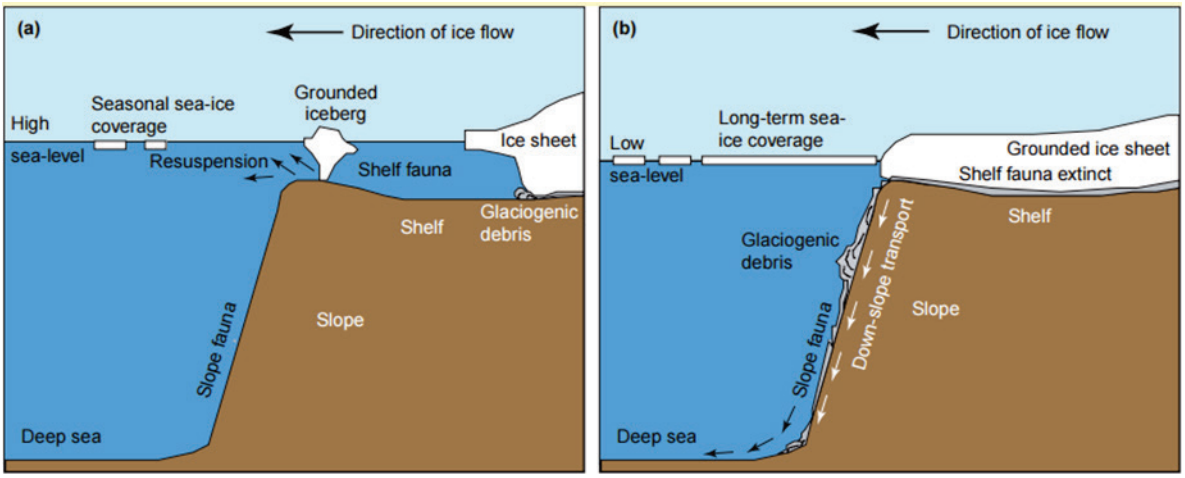

Figure 41. (a) During interglacials, sea-ice covers the Antarctic continental shelf only seasonally and the ice-sheet has retreated to the coast. (b) During glacials, grounded ice masses advance across the shelf, erasing the benthic shelf fauna. Outer shelf areas unaffected by grounded ice are covered by ice shelves or heavily scoured by icebergs. At the shelf edge, the grounded ice mass releases glaciogenic debris which flows down the slope, erasing the benthic fauna. Long-term sea ice coverage above the slope also results in low food supply. Figure from Thatje et al. (2005b).

However, the maximum ice extent might have occurred diachronously on the shelf, leaving isolated refugia, which change location during the glacial period (see Fig. 38) (Anderson et al., 2002). Only more dispersive pelagic organisms might however have been able to migrate from one shelter to another during diachronous onsets of glaciations. Scouring of the slope may have been localized (Clarke and Crame, 2010), as fast ice-streams could have stayed confined to specific channels (Ó Cofaigh et al., 2005). Furthermore, the ice did not advance to the shelf break in some areas during the LGM [see section 3.2.5.]. Therefore, part of the fauna might have survived *in situ* in ice-free shelf or slope refugia (Thatje et al., 2005b; Thatje et al., 2008). Additionally, eurybathic organisms might have been able to migrate to the circum-Antarctic deeper slope or deep-sea and subsequently re-colonize shelf areas (Thatje et al., 2005a; Thiel et al., 1996). Sub-Antarctic islands could also have acted as shallow-water refugia for more dispersive organisms (Poulin et al., 2002).

As the re-colonization process following a glacial period takes more time for less dispersive organisms, lacking a pelagic stage, populations underwent long periods of isolation in glacial refugia, possibly resulting in allopatric speciations before secondary contact (Held, 2003; Held and Wägele, 2005; Thatje et al., 2005b).

5. Dispersals in and out of the Antarctic shelf

As the APF marks a temperature cline of 3–4°C, most of the cold-adapted Antarctic fauna would not be able to establish viable population in warmer subpolar waters, on ecological timescales (Clarke et

al., 2005; Peck, 2002, 2005). Similarly, potential colonists that successfully cross the APF will not be able to establish in these colder waters. However, warmer water taxa might have colonized the Antarctic region during global warming phases, while colder water taxa could have dispersed northward during glacial maxima (Clarke et al., 1992a).

As the Antarctic shelf is well isolated from other oceans' shelves by great distances (> 850 km), deep seas (> 4000 m deep) and the strongest current on earth, the ACC (Clarke et al., 2005; Thornhill et al., 2008), the ability to disperse in and out of the shelf across the APF will mainly depend on life-history strategies (Thatje et al., 2005b).

5.1. Drifting of pelagic organisms (or life-stages) and passive rafting

The ACC is likely to be an important transportation vector between the sub-Antarctic islands (Fig. 42) (Leese et al., 2010; Nikula et al., 2010).

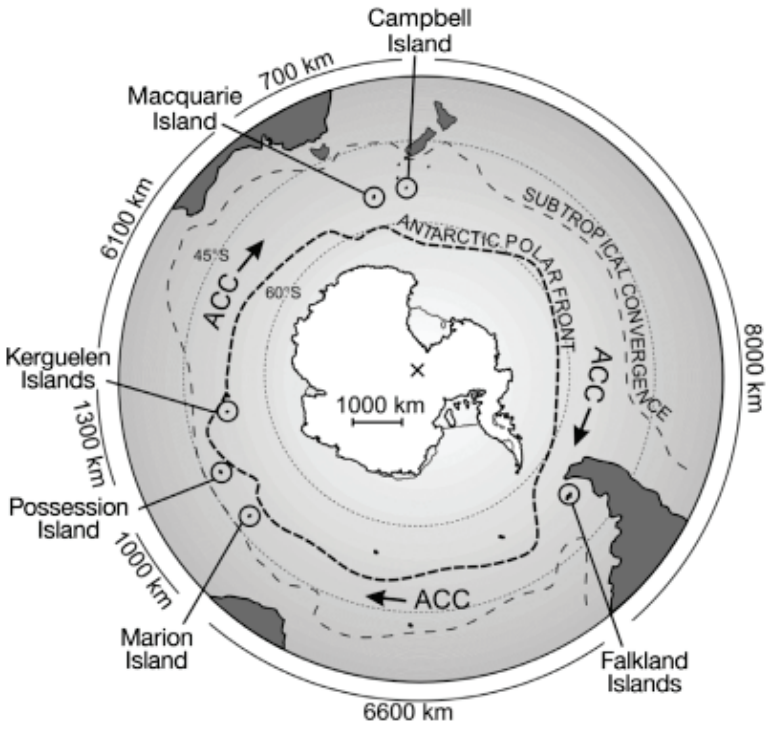

Figure 42. Polar-centric view of the Antarctic and sub-Antarctic regions, showing the sub-Antarctic islands. The ACC operates at and between the Sub-Tropical Convergence and the Antarctic Polar Front. Figure from Nikula et al. (2010).

Moreover, as the ACC is forced through the relatively narrow Drake Passage, numerous eddies are formed (Glorioso et al., 2005). Pelagic organisms might drift within these parcels of water transported out of the ACC, allowing a bidirectional transport: warm-core rings might carry sub-Antarctic plankton towards Antarctica and cold-core rings might transport Antarctic plankton to the north (Fig. 43) (Antezana, 1999; Clarke et al., 2005; Li et al., 2002; Nowlin and Klinck, 1986).

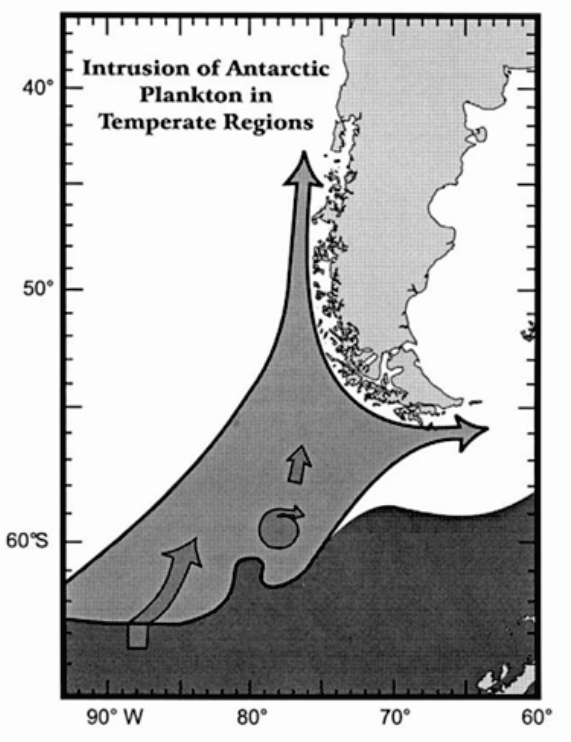

Figure 43. Eddies formed in the ACC and transported towards northern regions. Figure from Antezana (1999).

As pelagic species found in surface waters of the Southern Ocean are often also observed in deeper waters north of the Polar Front, another hypothesis is that they dispersed by sinking with the dense surface Antarctic water at the APF, through the Antarctic Intermediate water that extends northwards [see section 1.3.] (Antezana, 1999).

The eddies could be an important vector for transport of organisms with planktonic life stages, but they are unlikely to reach sufficient depth to directly transport benthic organisms (Clarke et al., 2005). Reports of benthic organisms with short-lived pelagic larvae or brooding young on both sides of the APF are much rarer (Clarke et al., 2005; Dell, 1972). However, in some cases, adults or eggs of such presumably poorly dispersive species appear to disperse over long distances and across the APF by passive mechanisms (Barnes et al., 2006; Helmuth et al., 1994; Leese et al., 2010; Waters, 2008). The *Macrocystis* kelp species are good colonizers and recent dispersal of northern hemisphere species to the Antarctic region were inferred (Coyer et al., 2001). The kelp *Durvillaea antarctica* has also a wide distribution comprising the sub-Antarctic and the Magellanic regions along with South Georgia in the Antarctic region (Fraser et al., 2009; Waters, 2008). These areas are indeed on the path of the ACC, which has been shown to carry a huge amount of detached *D. antarctica* at any one time (Smith, 2002), along with its associated epifauna, i.e. crustaceans, molluscs, annelids and echinoderms (Edgar and Burton, 2000; Nikula et al., 2010). Pumices and driftwood were shown to cross the APF as well, providing yet another possible mean of rafting (Barber et al., 1959; Coombs and Landis, 1966).

5.2. THROUGH THE DEEP-SEA

The APF does not appear to be a significant geographical barrier for the deep-sea fauna, whether with a planktonic life-stage or strictly benthic (Kaiser et al., 2013). Biogeographical affinities were inferred between the Antarctic deep-sea and both the adjacent Antarctic shelf and other oceans' deep waters. This would result from the development of the thermohaline circulation, which connects the Southern Ocean shallow and deep waters with the deep waters of the Atlantic, Indian and Pacific Oceans through an isothermal water column (Clarke et al., 2009; Rogers, 2000). Antarctic shelf organisms may disperse northward by "polar submergence" via the Antarctic Bottom Water, while deep-sea organisms may colonize the Antarctic shelf by "polar emergence" via the Circumpolar Deep Water [see section 1.3.] (Fig. 4). Moreover, with an average depth of 450 m and reaching > 1000 m at places, the Antarctic continental shelf is four times deeper than the shelf around other continents (Knox, 2006). This unusually deep shelf could facilitate faunal exchanges between shallow and deep-sea habitats (Clarke, 2003). With an average depth of 3000 m, the Drake Passage would be too deep to allow the dispersal of stenobathic shelf organisms along the benthos, over ecological timescales (e.g. Hunter and Halanych, 2008c; Shaw et al., 2004). However, historical submergences or emergences of benthic organisms (some of them lacking a pelagic stage) would have occurred over geological timescales (Berkman et al., 2004; Held, 2000; Strugnell et al., 2008).

5.3. ALONG THE SCOTIA ARC

It was inferred that an ancestral South Sandwich arc could have blocked deep-water flow in the Drake Passage area until ca. 12 Ma (Dalziel et al., 2013a, b). Under this scenario, dispersal between Antarctica and South America by stepping-stone might have been possible, even for organisms lacking a pelagic stage (Poulin et al., 2014).

OBJECTIVES AND OUTLINE

The overarching aim of this thesis is to contribute to the understanding of the evolutionary processes shaping the biodiversity and geographical distributions of benthic organisms on the Antarctic shelf. Such evolutionary processes — extinctions, dispersals and *in situ* diversifications — depend on past and present environmental factors such as the diversity in habitats, the tectonic configuration, the oceanography and the climatic conditions of the region. They also depend on the life history traits of the studied organisms, which condition their dispersal abilities and capacities to adapt to environmental changes, along their evolutionary history.

Biogeographical patterns emerge from the comparison of the geographical distribution of a taxon with other, related taxa. Therefore, each taxon must be properly defined as a monophyletic grouping and the evolutionary relationships between taxa must be traced back. To the latter purpose, molecular phylogenetics has proven to be a valuable tool. Moreover, DNA mutation rates provide a means for estimating timespans involved in this evolutionary process (i.e. place a timescale against the phylogenetic tree) in order to interpret it in relation to historical environmental events.

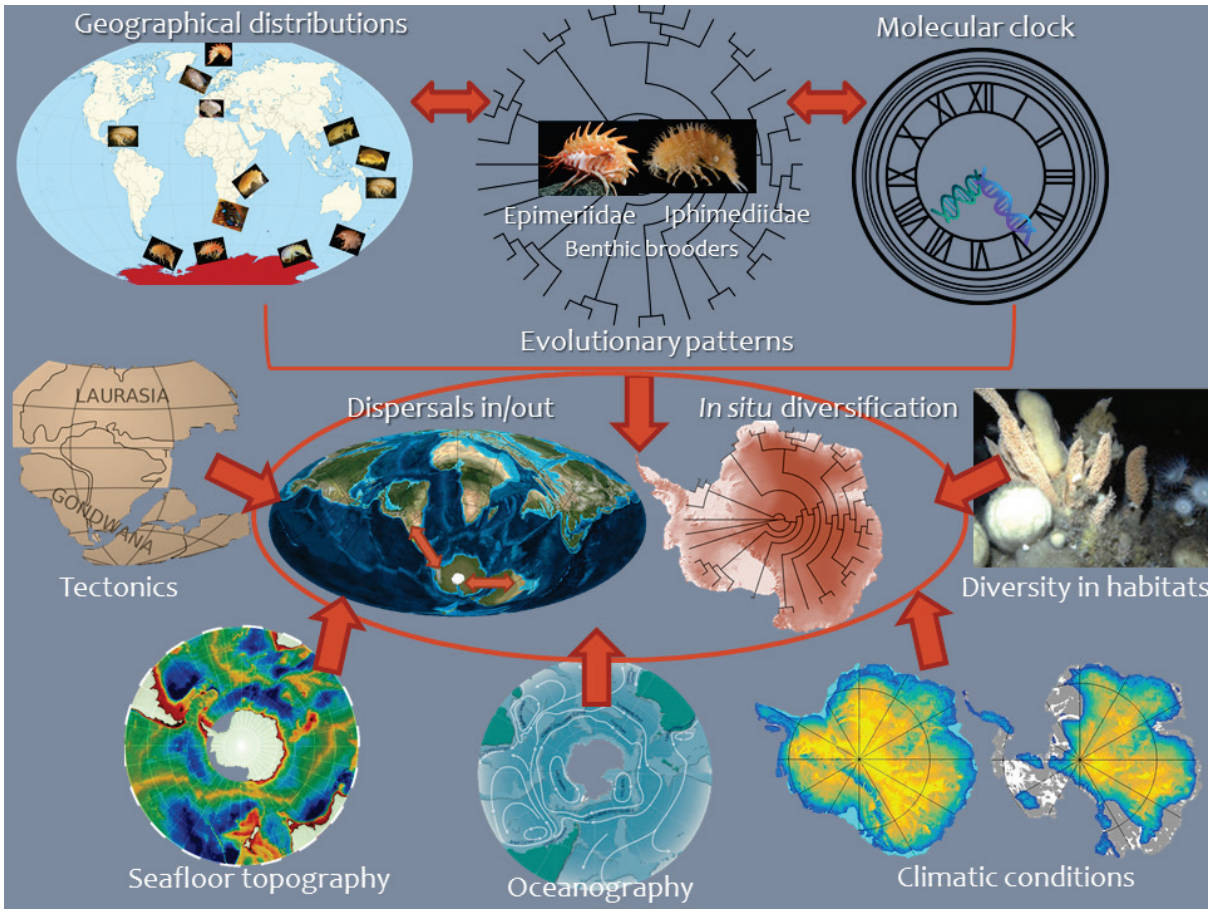

Figure 44. Graphical overview of the objectives of the thesis.

Epimeriiidae and Iphimediidae were chosen as model taxa for inferring biogeographical patterns because: (i) as these families are cosmopolitan, but diverse on the Antarctic shelf, the phylogenetic affinities between Antarctic and non-Antarctic representatives can be inferred and (ii) their morphology and life history traits suggest limited dispersal abilities, as they are benthic, brooders, large and heavily calcified amphipods; therefore, biogeographical patterns as revealed by the phylogeny are less likely to be blurred by frequent multidirectional dispersals.

To interpret evolutionary processes from the phylogenetic structure, the model taxon must be monophyletic group. Interpretations will be biased by missing informations if the taxon under study is in fact para- or polyphyletic. Therefore, an accurate taxonomic framework is an essential prerequisite to any biogeographical inference:

- A comprehensive molecular phylogenetic framework of the superfamily Eusiroidea — which presumably contains our model families, Epimeriidae and Iphimediidae — is therefore established, in order to explore the monophyly and evolutionary relationships of the Epimeriidae, Iphimediidae and related families — **CHAPTER 1.**

Phylogenies of the families Epimeriidae (represented by the most speciose genus *Epimeria*) and Iphimediidae are reconstructed and placed in their spatio-temporal context in order to infer biogeographical patterns:

- Species boundaries, diversity and distribution patterns are re-assessed in Antarctic Epimeriidae (including the description of many new species) — **CHAPTER 2 AND 3.**
- Detailed, time-calibrated, phylogenies of genus *Epimeria* and family Iphimediidae are reconstructed — **CHAPTERS 4 AND 5**.

CHAPTER 1: PHYLOGENETIC CONTEXT AND SYSTEMATICS OF EUSIROIDEA

The deeper phylogenetic relationships within Amphipoda are so poorly known that most taxonomic treatments simply list families alphabetically, without any classification (Barnard and Barnard, 1983; Barnard and Karaman, 1975; Martin and Davis, 2001). The 18S rDNA molecular phylogeny of Englisch (2001) offers the first evidence for the phylogenetic position of epimeriid and iphimediid species relative to other amphipod families. It shows a supported sister relationship between a few iphimediid and epimeriid species, the latter clade being included in a larger clade composed of species from the families Calliopiidae, Eusiridae (superfamily Eusiroidea), Pleustidae and Astyridae [see section 2.2.3.]. CHAPTER 1 expands on Englisch's (2001) results by including all available families

once assumed to belong to, or to be close to, Eusiroidea in a phylogeny reconstructed with 28S and 18S rDNA sequences. This provides the phylogenetic framework needed to explore the monophyly and phylogenetic position of Epimeriidae and Iphimediidae. Besides, this study has wider implications for the overall systematics of Eusiroidea, by providing new insights towards a phylogenetically meaningful delimitation of the superfamily and by exploring the monophyly and relationships between the composing families.

CHAPTER 2: ASSESSMENT OF SPECIES DIVERSITY AND GEOGRAPHICAL DISTRIBUTIONS WITHIN ANTARCTIC *EPIMERIA*

Large-scale biogeographical studies usually base their inferences on the recorded distributional ranges of morphospecies. However, these inferences may be biased if geographically widespread morphospecies are in fact complexes of local cryptic species. The discovery of such hidden diversity within a wide variety of Antarctic organisms has often led to reductions of species' distribution ranges and thereby to question the predominance of the long-standing circum-Antarctic paradigm. Many *Epimeria* species are reported with a circumpolar distribution. In CHAPTER 2, we use morphological descriptions combined with DNA-based methods to delimit putative species within Antarctic *Epimeria* and re-assess their geographical distributions.

CHAPTER 3: MORPHOLOGICAL DESCRIPTIONS OF ANTARCTIC *EPIMERIA* SPECIES: *EPIMERIA* SP. NOV. ROSS FROM THE ROSS SEA, AS AN EXAMPLE

The use of DNA-sequence data in addition to morphology for delimiting species is often not practically feasible in larger-scale biogeographical studies. The comparison of these two types of datasets can however help identifying taxonomically relevant versus highly convergent morphological characters, in order to assist in species identifications. Whereas truly cryptic species — relative to human's perception — do exist, overlooked species can often be readily set apart based on detailed morphological descriptions. CHAPTER 3 is a complement to a complete taxonomic revision of all the available Antarctic *Epimeria* material, in d'Udekem and Verheye (*in Press*) [which is not part of this thesis, due to its length]. The descriptions of these Antarctic *Epimeria* species are accompanied by data on their distributional ranges, which should provide additional informations on biogeographical patterns of the genus on the Antarctic shelf.

CHAPTER 4: ORIGIN, DISPERSAL AND DIVERSIFICATION OF ANTARCTIC *EPIMERIA*

In order to investigate the origin, dispersals in/out of the Antarctic shelf and *in situ* diversifications of the Antarctic *Epimeria* from CHAPTER 2, non-Antarctic *Epimeria*, along with taxa putatively related to *Epimeria*, were added to the extensive Antarctic sampling in CHAPTER 4. A molecular clock was applied to calibrate the phylogenetic tree in time, in order to relate divergence times and eventual variations in diversification rates to historical geological, oceanographic and/or climatic events.

CHAPTER 5: ORIGIN, DISPERSAL AND DIVERSIFICATION OF ANTARCTIC IPHIMEDIIDAE

The methods of CHAPTER 4 were also applied to Iphimediidae, in CHAPTER 5. A time-calibrated phylogeny comprising an extensive Antarctic sampling, along with non-Antarctic representatives of the family, was used to investigate the origin, dispersals in/out of the Antarctic shelf and *in situ* diversifications of Antarctic iphimediids, in relation to historical events. This enabled a comparison of historical biogeographical patterns between *Epimeria* (Epimeriidae) and Iphimediidae, which differ in their relative degree of eurybathy, endemism and trophic ecology.

CHAPTER 1

DNA ANALYSES REVEAL ABUNDANT HOMOPLASY IN TAXONOMICALLY IMPORTANT MORPHOLOGICAL CHARACTERS OF EUSIROIDEA (CRUSTACEA, AMPHIPODA)

Marie L. Verheye[1,2]

Patrick Martin[1]

Thierry Backeljau[1,3]

Cédric d'Udekem d'Acoz[1]

Published in: ***Zoologica Scripta*** **(2016) 45 (3)**

[1] Royal Belgian Institute of Natural Sciences, OD Taxonomy and Phylogeny, 29 rue Vautier, B-1000 Brussels, Belgium

[2] Catholic University of Louvain-la-Neuve, Department of Biology, Marine Biology Laboratory, 3 bte L7.06.04 Croix du Sud, B-1348 Louvain-la-Neuve, Belgium

[3] University of Antwerp, Evolutionary Ecology Group, 171 Groenenborgerlaan, 2020 Antwerp, Belgium

ABSTRACT

Eusiroidea is one of the 20 amphipod superfamilies that were erected to subdivide the very large and controversial suborder Gammaridea. Yet, the definition of the superfamily is not based on synapomorphies, but on a combination of diagnostic phenetic similarities that holds more or less consistently across families. Moreover, many of the characters used to define eusiroid families are suspected to show convergent evolution. The current classification of the Eusiroidea may therefore not reflect evolutionary relationships accurately. Here, we present a molecular phylogenetic re-analysis of the Eusiroidea based on a comparison of 18S and 28S rDNA sequences of 73 species, representing 47 genera and 16 families that potentially belong to the superfamily. The results suggest that at least species belonging to 14 of these traditional families would be part of a Eusiroidea clade, increasing by more than twofold the species and generic richness of the group. However, most of the eusiroid families surveyed do not appear monophyletic. Finally, the analyses show that several important morphological characteristics, traditionally used in eusiroid taxonomy, are homoplastic.

INTRODUCTION

Amphipoda (Crustacea; Malacostraca; Peracarida) is one of the most speciose crustacean orders, including more than 9100 species (Väinölä et al., 2008). Evolutionary radiations of amphipod lineages are well documented in various environments (Corrigan et al., 2014; Hou et al., 2011; Macdonald III et al., 2005) leading to great numbers of species, and high morphological and ecological diversity within the order. As a consequence of morphological convergence of unrelated lineages in similar environments, the identification of homologies for tracing phylogenies is very challenging (Barnard and Barnard, 1983; Barnard and Karaman, 1975; Bousfield, 1977). Deeper phylogenetic relationships within Amphipoda are so uncertain that several taxonomic treatments simply list families alphabetically (Barnard and Barnard, 1983; Barnard and Karaman, 1975; Martin and Davis, 2001).

Traditionally, amphipods have been divided into three to five suborders: Ingolfiellidea Hansen, 1903, Gammaridea Latreille, 1802, Hyperiidea H. Milne-Edwards, 1830, Caprellidea Leach, 1814 and Corophiidea Leach, 1814 (Barnard, 1969; Barnard and Karaman, 1984; Lincoln, 1979; Myers and Lowry, 2003; Stebbing, 1906). However, this classification is essentially phenetic (Bellan-Santini, 1999) and subsequent molecular studies revealed a hyperiid clade nested within Gammaridea and a caprellid clade nested within Corophiidea (Browne et al., 2007; Englisch, 2001; Ito et al., 2008).

Hence, the limits of amphipod suborders and their phylogenetic relationships remain unclear (Kim and Kim, 1993; Martin and Davis, 2001).

The superfamily Eusiroidea was erected, along with 19 others, in a general attempt to break up the vast suborder Gammaridea into more manageable taxonomic units (Bousfield, 1978). Seven families were included, viz.: Pontogeneiidae Stebbing, 1906, Calliopiidae G.O. Sars, 1893, Eusiridae Stebbing, 1888, Gammarellidae Bousfield, 1977, Bateidae Stebbing, 1906, Amathillopsidae Heller, 1875, and Paramphithoidae Stebbing, 1906. Subsequently, Bousfield and Hendrycks (1995b) also added the Gammaracanthidae Bousfield 1989 to the superfamily Eusiroidea. Yet, most other authors did not follow this classification in superfamilies (Barnard and Karaman, 1991; De Broyer and Jażdżewski, 1993; Martin and Davis, 2001). The superfamily Eusiroidea was used for the last time by De Broyer et al. (2007), but only for the families Calliopiidae G.O. Sars, 1893, Eusiridae Stebbing, 1888, Gammarellidae Bousfield, 1977 and Pontogeneiidae Stebbing, 1906. In the recent classification of the new suborder Senticaudata Lowry and Myers, 2013, the superfamily Eusiroidea *sensu* Bousfield (1978) or De Broyer et al. (2007) is not retained. The Senticaudata contains 95 gammaridean families sharing one alleged synapomorphy, the presence of robust apical setae on the rami of uropods 1–2. In this arrangement, Calliopiidae and Pontogeneiidae are considered as sister lineages in the new superfamily Calliopioidea, while Gammarellidae and Gammaracanthidae are classified in the superfamily Gammaroidea. All the remaining former eusiroid families are, however, not included within the Senticaudata (Lowry and Myers, 2013) [see Introduction section 2.2.3. Table 1 for details on successive classifications].

Many authors recognized the potential value of superfamily divisions to clarify the very confused systematics of the more inclusive taxonomic levels within the Amphipoda, but dismissed the current classification because of the lack of a cladistics framework (Barnard and Barnard, 1983; Barnard and Karaman, 1975, 1991; Martin and Davis, 2001). The classification of the Eusiroidea is still exclusively based on a combination of morphological diagnostic characters that holds more or less consistently across component family members, the most constant one being the general reduction of the accessory flagellum, and not on demonstrated synapomorphies. Eusiroid families are defined solely on one or few diagnostic characters, considered to be of primary taxonomic value, e.g. the shape of the telson is used to differentiate families in the Eusiridae-Pontogeneiidae-Calliopiidae complex (Bousfield, 1978). As the phylogenetic significance of these characters at more inclusive taxonomic levels is unknown, the present classification of the families within Eusiroidea may not reflect accurately evolutionary relationships.

Very little attention has been paid to studies of deeper (families and more inclusive taxa) molecular phylogenies within marine Gammaridea in its traditional sense. Yet, 18S rDNA phylogenies (Englisch, 2001) show a well-supported clade comprising Eusiridae, Calliopiidae, Astyridae, Iphimediidae, Epimeriidae, and Pleustidae, suggesting that (i) the Eusiroidea may comprise more families than hitherto was assumed, (ii) the family Calliopiidae is not monophyletic, and (iii) the gammarellid *Gammarellus homari* does not belong to the eusiroid clade. However, as this 18S study only treated a small number of potential eusiroid taxa, it provided little information on the composition of Eusiroidea and its internal relationships. Nevertheless, the incongruences between traditional classifications and the 18S data highlight the need for a systematics revision of Eusiroidea.

By analysing fragments of the 18S and 28S rDNA genes of 73 species, representing 47 genera of 16 families, this study aims (i) to explore the phylogenetic relationships of several families once assumed to belong, or to be close, to the Eusiroidea (see Table 1 for included families) in order to provide new insights towards a phylogenetically meaningful classification of the superfamily, (ii) to explore the monophyly of the eusiroid families and interfamilial relationships and (iii) to discuss the evolution of some important phenotypic characteristics, traditionally used in the taxonomy of this large amphipod group.

MATERIAL AND METHODS

TAXON SELECTION

The majority of the specimens used in this study were sampled during expeditions in the Southern Ocean: ANT-XXI/2, ANT-XXIV/2, ANT-XXVII/3, REVOLTA III and TAN802. Additional material was obtained by opportunistic collections from the Netherlands, the UK and Norway (including the Svalbard Archipelago). All specimens were preserved in 96–100% ethanol for DNA analysis. Vouchers are deposited at the Royal Belgian Institute of Natural Sciences (RBINS, Brussels, Belgium), the National Institute for Water and Atmospheric Research (NIWA, Wellington, New Zealand) and the Muséum National d'Histoire Naturelle (MNHN, Paris, France) (Table 1). Specimens were identified using primary taxonomic literature, yet eight specimens could not be identified to the species level. If possible, they have been assigned a working name indicating their similarity to described species. One specimen could not be identified to the genus level. It appears to represent a new, undescribed taxon, provisionally assigned to the family Acanthonotozomellidae.

A total of 73 putative eusiroid species were included in this study, representing 47 genera and 16 families. When possible, sequences were obtained from more than one individual per species (Table

1). The monophyly of the Eusiroidea was explored using 48 non-eusiroid sequences, mostly selected from the study of Englisch (2001). They include a wide range of genera, representing 34 amphipod families. *Nebalia* Leach, 1814 (Nebaliacea) and *Squilla empusa* Say, 1818 (Stomatopoda) were selected as outgroup taxa. The phylogeny of the superfamily Eusiroidea was further examined using up to 11 species and 7 genera per family of putative eusiroids, in order to explore the monophyly of these genera and families. Two and five lysianassoid species were used as outgroups for the 18S and 28S phylogenies, respectively.

DNA EXTRACTION, PCR AMPLIFICATION AND NUCLEOTIDE SEQUENCING

DNA was extracted from the pleopods and abdomen muscles using a NucleoSpin® Tissue kit (Macherey-Nagel, Hoerdt, France) following the manufacturer's protocol for animal tissues. The DNA was eluted in 100 µl of sterile distilled H_2O (RNase free) and stored at -20 °C.

Partial segments of 28S (~1400 bp) and 18S (~2200 bp) rDNA were amplified by PCR. Amplifications were performed in a 25 µl reaction mix, which contained 12.5 µl 5x HotStar HiFidelity PCR Buffer (incl. dNTPs), 4.5–9.5 µl RNase-free water, 1 µl of each primer and 1–6 µl of DNA extract.

The 28S rDNA fragment was amplified using the primers 28S-3311F (Witt et al., 2006) and 28R (Hou et al., 2007), modified as follows: 5'-GGGACTACCCGCTGAACTTAAGCAT-3' and 5'-GTCTTTCGCCCCTATGCCCAACTG-3'. PCR amplification settings for 28S rDNA consisted of an initial denaturation for 15 min at 95 °C, followed by 40 cycles of denaturation at 95 °C for 50 s, annealing at 50 °C for 50 s, extension at 72 °C for 50 s, and a final extension at 72 °C for 10 min. The 18S rDNA fragment was amplified using primers 18S-Universal/Reverse from Englisch (2001). The thermal cycling used for 18S was similar to that for 28S rDNA except that the annealing temperature was set to 55 °C and the extension time was increased from 50 s to 1 min 30 s.

PCR products were purified using ethanol/EDTA prior to sequencing. Forward and reverse strands were sequenced with fluorescent-labeled dideoxynucleotide terminators (BigDye v3.1, Applied Biosystems, Foster City, CA, USA) following the protocol of Sanger et al. (1977) and using an automated ABI 3130xl DNA analyzer (Applied Biosystems). The 28S fragment was sequenced using the PCR primers, whereas the 18S fragment was sequenced with primer pairs 18S-Universal/18S-1000R and 18S-1155F/18S-Reverse from Englisch (2001). All sequences have been deposited in GenBank (Table 1).

Family (Superfamily sensu Bousfield 1978)	Species	Collection			Voucher ID	Genbank accession number		Reference
		Locality	Latitude	Longitude		28S	18S	
Families included to test their potential belonging or sister relationship to Eusiroidea								
ACANTHONOTOZOMATIDAE	*Acanthonotozoma serratum*	Kvalsund, Norway	70°28.01'N	24°1.95'E	RBINS INV. 132629	KT808683	KT808777	This study
ACANTHONOTOZOMELLIDAE	*Acanthonotozomella trispinosa*	Larsen B, Antarctica	65°57.51'S	60°28.15'W	RBINS INV. 132673	KT808684	KT808770	This study
	Acanthonotozomoides oatesi	Shag Rocks (South Georgia, Antarctica)	53°23.94'S	42°40.10'W	RBINS INV. 132669	KT808686	KT808782	This study
	n. gen. n. sp.	Ride de Norfolk, Nouvelle-Calédonie	23°22.76′S	167°51.60′E	MNHN-2009-2497	KT808685	N/A	This study
AMATHILLOPSIDAE	*Amathillopsis charlottae*	Terre Adélie, Antarctica	66°38′ S	140°42′E	MNHN-IU-2009-2546	KT808689	KT808742	This study
	Parepimeria bidentata	Shag Rocks (South Georgia, Antarctica)	53°24.53'S	42°40.70'W	RBINS INV. 132640	KT808731	KT808761	This study
	Parepimeria crenulata	Bouvet Island, Antarctica	54°22.49'S	03°17.58'W	RBINS INV. 132664	KT808732	KT808760	This study
	Parepimeria minor	Eastern Weddell Sea, Antarctica	70°23.94'S	8°19.14'W	RBINS INV. 132672	KT808733	KT808762	This study
ASTYRIDAE (Pardaliscoidea)	*Astyra abyssi*	Vestfjorden, Norway	68°11.27'N	14°59.87'E	RBINS INV. 132658	KT808694	N/A	This study
	Astyra abyssi	Porsanger Hjellneset, Norway	70°30.60´N	25°33.42´E	None	N/A	DQ378000	Englisch (2001)
	Astyra antarctica	N/A	N/A	N/A	None	N/A	DQ377999	Englisch (2001)
CALLIOPIIDAE (Eusiroidea)	*Apherusa bispinosa*	Yerseke, Netherlands	51°29.58'N	4°2.92'E	RBINS INV. 132657	KT808691	N/A	This study
	Apherusa bispinosa	Helgoland, Germany	54°10.82'N	7°53.34'E	None	N/A	DQ378009	Englisch (2001)
	Apherusa glacialis	Northern Barents Sea	75°37.00′N	30°10.00′E	None	N/A	JF266612	Ki et al. (2011)
	Apherusa jurinei	Westkapelle, Netherlands	51°31.76'N	3°26.43'E	RBINS INV. 132654	KT808692	KT808767	This study
	Apherusa macrocephala	Grindøya, Norway	69°38.15'N	18°50.87'E	RBINS INV. 132633	KT808693	N/A	This study
	Calliopius laeviusculus	Bamburgh, United Kingdom	55°36.52'N	1°41.37'W	RBINS INV. 100191	KT808701	N/A	This study
	Cleippides quadricuspis	Kongsfjord, Spitsbergen	78° 57.13' N	7° 44.86' E	RBINS INV. 132935	KT808703	KT808779	This study
	Halirages cainae (holotype)	Norwegian Sea	69°04.00'N	012°28.00'E	ZMBN 87795	KT808719	N/A	This study
	Halirages fulvocinctus	Vestfjorden, Norway	68°11.27'N	14°59.87'E	RBINS INV. 132661	KT808720	N/A	This study
	Oradarea tricarinata	Eastern Weddell Sea, Antarctica	70°56.40'S	10°32.60'W	RBINS INV. 132662	KT808727	KT808749	This study
	Oradarea tridentata	Elephant Island, Antarctica	61°20.07'S	55°12.14'W	RBINS INV. 132674	KT808728	N/A	This study
	Oraradea megalops	Shag Rocks, Antarctica	53°24.53'S	42°40.70'W	RBINS INV. 132634	KT808696	KT808773	This study
	Paramoera sp.	Eastern Weddell Sea, Antarctica	70°23.94'S	8°19.14'W	RBINS INV. 132648	KT808729	KT808752	This study
	Weyprechtia pinguis	Kongsfjord, Spitsbergen	N/A	N/A	RBINS INV. 132665	KT808741	N/A	This study
DIKWIDAE	*Dikwa* n. sp.	Burdwood bank, Argentina	42°40.70'S	56°10.64'W	RBINS INV. 132666	KT808704	KT808771	This study
EPIMERIIDAE (prev. Paramphithoidae, Eusiroidea)	*Epimeria cornigera*	Vestfjorden, Norway	68°10.32'N	14°57.05'E	RBINS INV. 132630	KT808708	KT808753	This study
	Epimeria georgiana	Elephant Island, Antarctica	60°54.60´S	55°45.90´W	None	N/A	AF356546	Englisch (2001)

	Epimeria grandirostris	N/A	N/A	N/A	None	N/A	DQ378007	Englisch (2001)
	Epimeria loricata	Hinlopen, Spitsbergen	N/A	N/A	RBINS INV. 132637	KT808709	KT808764	This study
	Epimeria aff. *macrodonta*	Larsen B, Antarctica	65°57.51'S	60°28.15'W	RBINS INV. 132655	KT808710	KT808763	This study
	Epimeria similis	Elephant Island, Antarctica	60°54.60´S	55°45.90´W	None	N/A	DQ378006	Englisch (2001)
	Epimeria aff. *walkeri*	King George Island, Antarctica	62°18.21'S	58°39.90'W	RBINS INV. 132677	KT808711	N/A	This study
	Epimeria walkeri	N/A	N/A	N/A	None	N/A	DQ378005	Englisch (2001)
	Paramphithoe hystrix	Grindøya, Norway	69°38.15'N	18°50.87'E	RBINS INV. 132663	KT808730	N/A	This study
EUSIRIDAE (Eusiroidea)	*Eusiroides georgiana*	Shag Rocks, Antarctica	53°24.53'S	42°40.70'W	RBINS INV. 132638	KT808713	KT808784	This study
	Eusirus giganteus	King George Island, Antarctica	62°18.21'S	58°39.90'W	RBINS INV. 132621	KT808714	KT808766	This study
	Eusirus cf. *microps*	N/A	N/A	N/A	None	N/A	DQ378011	Englisch (2001)
	Eusirus perdentatus	King George Island, Antarctica	62°18.90´S	58°41.70`W	None	N/A	DQ378012	Englisch (2001)
	Rhachotropis antarctica	Eastern Weddell Sea, Antarctica	70°58.34'S	10°29.99'W	RBINS INV. 132649	KT808738	KT808757	This study
	Rhachotropis schellenbergi	Larsen A, Antarctica	64°54.84'S	60°36.63'W	RBINS INV. 132660	KT808739	KT808758	This study
GAMMARELLIDAE	*Austroregia regis*	N/A	N/A	N/A	RBINS INV. 132620	N/A	KT808775	This study
	Chosroes aff. *decoratus*	Shag Rocks, Antarctica	53°23.94'S	42°40.10'W	RBINS INV. 132635	KT808702	KT808774	This study
	Gammarellus angulosus	Westkapelle, Netherlands	51°31.76'N	3°26.43'E	RBINS INV. 132647	KT808715	KT808778	This study
	Gammarellus homari	Kleverberg, Baltic Sea	54°27.52'N	10°14.44'E	None	N/A	DQ378033	Englisch (2001)
IPHIMEDIDAE	*Anchiphimedia dorsalis*	King George Island, Antarctica	62°18.21'S	58°39.90'W	RBINS INV. 132625	KT808690	KT808747	This study
	Echiniphimedia echinata	King George Island, Antarctica	62°12.19'S	58°56.62'W	RBINS INV. 132652	KT808705	KT808743	This study
	Echiniphimedia gabrielae	Eastern Weddell Sea, Antarctica	70°50.64'S	10°36.11'W	RBINS INV. 132624	KT808706	KT808744	This study
	Echiniphimedia hodgsoni	Elephant Island, Antarctica	60°54.60´S	55°45.90´W	None	N/A	DQ378004	Englisch (2001)
	Echiniphimedia waegelei	Eastern Weddell Sea, Antarctica	70°50.64'S	10°36.11'W	RBINS INV. 132622	KT808707	N/A	This study
	Gnathiphimedia mandibularis	Western Ross Sea, Antarctica	76°36.14'S	176°48.12' W	NIWA 36653	KT808716	KT808748	This study
	Gnathiphimedia sexdentata	Eastern Weddell Sea, Antarctica	70°56.52'S	10°34.84'W	RBINS INV. 132644	KT808717	N/A	This study
	Gnathiphimedia sexdentata	Eastern Weddell Sea, Antarctica	70°50.64'S	10°36.11'W	RBINS INV. 132641	N/A	KT808746	This study
	Iphimediella cyclogena	Larsen A, Antarctica	64°55.58'S	60°33.37'W	RBINS INV. 132632	KT808722	KT808745	This study
	Iphimediella georgei	Drake Passage, Antarctica	61°18.60´S	57°1.70´W	None	N/A	DQ378002	Englisch (2001)
	Iphimediella margueritei	N/A	N/A	N/A	None	N/A	DQ378003	Englisch (2001)
	Maxilliphimedia longipes	Western Ross Sea, Antarctica	76°11.58'S	176°17.77' W	NIWA 36793	KT808724	N/A	This study
	Maxilliphimedia longipes	Elephant Island, Antarctica	60°54.60´S	55°45.90´W	None	N/A	AF356547	Englisch (2001)
	Pariphimedia integricauda	N/A	N/A	N/A	None	N/A	DQ378001	Englisch (2001)

OCHLESIDAE (Stegocephaloidea)	*Odius carinatus*	Kongsfjorden, Spitsbergen	N/A	N/A	RBINS INV. 132643	KT808726	N/A	This study
PLEUSTIDAE (Leucothoidea)	*Atylopsis* sp.	Elephant Island, Antarctica	61°20.07'S	55°12.14'W	RBINS INV. 132675	KT808695	KT808772	This study
	Austropleustes cuspidatus	Shag Rocks, Antarctica	53°24.53'S	42°40.70'W	RNINS INV. 132642	KT808698	KT808750	This study
	Incisocalliope aestuarius	Hoedekenskerke, Netherlands	51°25.48'N	3°54.78'E	RBINS INV. 132646	KT808721	N/A	This study
	Incisocalliope aestuarius	Hoedekenskerke, Netherlands	51°25.48'N	3°54.78'E	RBINS INV. 132646	N/A	KT808759	This study
	Neopleustes pulchellus	Hinlopen, Spitsbergen	N/A	N/A	RBINS INV. 132670	KT808725	KT808755	This study
	Pleustes panopla	Grindøya, Norway	69°38.15'N	18°50.87'E	RBINS INV. 132639	KT808734	KT808754	This study
PONTOGENEIIDAE (Eusiroidea)	*Atyoella tribinicuspidata*	Bouvet Island, Antarctica	54°30.14'S	3°13.50'E	RBINS INV. 132659	KT808697	KT808751	This study
	Bovallia gigantea	King George Island, Antarctica	62°13.28'S	58°53.21'W	RBINS INV. 132626	KT808700	N/A	This study
	Eurymera monticulosa	King George Island, Antarctica	62°13.28'S	58°53.21'W	RBINS INV. 132627	KT808712	KT808776	This study
	Gondogeneia sp.	Bouvet Island, Antarctica	54°30.14'S	3°13.50'E	RBINS INV. 132650	KT808718	N/A	This study
	Liouvillea sp. nov.	Eastern Weddell Sea, Antarctica	70°48.93'S	10°32.69'W	RBINS INV. 132671	KT808723	KT808765	This study
	Prostebbingia gracilis	Eastern Weddell Sea, Antarctica	70°51.13'S	10°36.11'W	RBINS INV. 132668	KT808735	KT808781	This study
	Prostebbingia longicornis	King George Island, Antarctica	62°13.28'S	58°53.21W	RBINS INV. 132628	KT808736	N/A	This study
	Prostebbingia serrata	Eastern Weddell Sea, Antarctica	70°56.40'S	10°32.60'W	RBINS INV. 132631	KT808737	KT808780	This study
	Schraderia gracilis	Eastern Weddell Sea, Antarctica	70°58.34'S	10°29.99'W	RBINS INV. 132636	KT808740	KT808756	This study
STILIPEDIDAE (Pardaliscoidea)	*Alexandrella* aff. *dentata*	Larsen A, Antarctica	64°54.75'S	60°39.01'W	RBINS INV. 132653	KT808688	KT808769	This study
	Bathypanoploea schellenbergi	Eastern Weddell Sea, Antarctica	70°23.94'S	8°19.14'W	RBINS INV. 132623	KT808699	KT808768	This study
THURSTONELLIDAE	*Thurstonella chelata*	Eastern Weddell Sea, Antarctica	70°23.94'S	8° 19.14'W	RBINS INV. 132651	N/A	KT808785	This study
VICMUSIIDAE	*Acanthonotozomopsis pushkini*	Shag Rocks, Antarctica	53°24.53'S	42°40.70'W	RBINS INV. 132656	KT808687	KT808783	This study

Families included to test the monophyly of Eusiroidea

AMPELISCIDAE (Ampeliscoidea)	*Byblis gaimardi*	Porsanger Anskarholmen, Norway	70°21.44´N	25°15.19´E	None	N/A	AY826964	Englisch (2001)
AMPHILOCHIDAE (Leucothoidea)	*Amphilochius tenuimanus*	Vargsund Bekkarfjordneset, Norway	71°18.08´N	23°21.40´E	None	N/A	DQ378029	Englisch (2001)
ATYLIDAE (Dexaminoidea)	*Atylus swammerdami*	Kattegat, Baltic Sea	56°57.12'N	11°18.03'E	None	N/A	DQ378031	Englisch (2001)
BATHYPOREIIDAE	*Bathyporeia sardoa*	N/A	N/A	N/A	None	N/A	DQ377996	Englisch (2001)
CAPRELLIDAE (Caprelloidea)	*Caprella linearis*	Baltic Sea	58°28.01´N	11°11.70´E	None	N/A	DQ378039	Englisch (2001)
	Pseudoprotella phasma	Baltic Sea	58°28.01´N	11°11.70´E	None	N/A	DQ378041	Englisch (2001)
COLOMASTIGIDAE (Leucothoidea)	*Colomastix fissilingua*	N/A	N/A	N/A	None	N/A	DQ378032	Englisch (2001)

CRANGONYCTIDAE (Crangonyctoidea)	*Bactrurus pseudomucronatus*	Oregon Co., Missouri, USA	36°48.90'N	91°10.85'W	None	N/A	AF202985	Englisch (2001)
CYAMIDAE (Cyamoidea)	*Cyamus balaenopterae*	Antarctic ocean (body of minke whale)	N/A	N/A	None	N/A	AB520635	Ito et al. 2011
EURYTHENEIDAE (Lysianassoidea)	*Eurythenes gryllus*	King George Island, Antarctica	62°17.60´S	57°59.80´W	None	N/A	AY826967	Englisch (2001)
	Eurythenes n. sp.	Argentine basin, Argentina	35°56'S	48°54'W	N/A	JX887110	N/A	Havermans et al. (2013)
GAMMARACANTHIDAE	*Gammaracanthus lacustris*	Savonranta munic, Finland	62°07.80'N	29°22.8'E	SLOCHN141	N/A	JF966191	Hou et al. (2011)
	Gammaracanthus loricatus	Spitsbergen	70°24.00'N	21°00.60'E	SLOCHN171	N/A	JF966192	Hou et al. (2011)
GAMMARIDAE (Gammaroidea)	*Echinogammarus obtusatus*	Great Cumbrae, Scotland	55°45.90'N	4°55.54'W	None	N/A	AF419224	Englisch (2001)
	Gammarus duebeni	Great Cumbrae, Scotland	55°45.90'N	4°55.54'W	None	N/A	AF356545	Englisch (2001)
HAUSTORIIDAE (Pontoporeioidea)	*Haustorius arenarius*	Great Cumbrae, Scotland	55°45.90'N	4°55.54'W	None	N/A	AY826950	Englisch (2001)
HYPERIIDAE (Phronimoidea)	*Hyperia galba*	Great Cumbrae, Scotland	N/A	N/A	None	N/A	DQ378046	Englisch (2001)
INGOLFIELLIDAE	*Ingolfiella tabularis*	N/A	N/A	N/A	None	N/A	DQ378054	Englisch (2001)
ISCHYROCERIDAE (Corophioidea)	*Jassa falcata*	Baltic Sea	58°28.01´N	11°11.70´E	None	N/A	DQ378017	Englisch (2001)
LEUCOTHOIDAE (Leucothoidea**)**	*Leucothoe spinicarpa*	N/A	N/A	N/A	None	N/A	DQ378025	Englisch (2001)
LILJEBORGIIDAE (Liljeborgioidea**)**	*Idunella picta*	Ile Callot, Brittany, France	48°41.38'N	3°55.20'W	RBINS INV. 132656	N/A	KT808786	This study
	Sextonia longirostris	Le Dossen, Brittany, France	48°42.17'N	4°03.98'W	RBINS INV. 132327	N/A	KT808787	This study
	Liljeborgia fissicornis	Vargsund Bekkarfjordneset, Norway	71°18.08´N	23°21.40´E	None	N/A	AY826959	Englisch (2001)
LYSIANASSIDAE (Lysianassoidea**)**	*Orchomenella acanthurus*	Weddell Sea, Antarctica	70°56'S	10°31'W	N/A	GU109223	N/A	Havermans et al. (2010)
	Orchomenyx macronyx	Joinville Island, Antarctica	62°33'S	55°41'W	N/A	GU109202	N/A	Havermans et al. (2010)
	Pseudorchomene coatsi	Scotia Sea, Antarctica	61°44'S	60'45°W	N/A	GU109213	N/A	Havermans et al. (2010)
MEGALUROPIDAE	*Megaluropus longimerus*	Curacao, Carribean Sea	12°10.98'N	69°2.57'W	None	N/A	DQ378035	Englisch (2001)
MELITIDAE (Hadzioidea)	*Maera inaequipes*	Roses Gulf, Spain	42°11.39'N	3°10.60'E	None	N/A	AF419229	Englisch (2001)
	Melita dentata	N/A	N/A	N/A	None	N/A	DQ378014	Englisch (2001)
	Paraceradocus gibber	Elephant Island, Antarctica	61°05.40´S	55°56.40´W	None	N/A	AF419232	Englisch (2001)
MELPHIDIPPIDAE (Melphidippoidea)	*Melphidippa antarctica*	N/A	N/A	N/A	None	N/A	DQ377998	Englisch (2001)
NIPHARGIDAE (Crangonyctoidea)	*Niphargus kochianus*	N/A	N/A	N/A	None	N/A	AF419221	Englisch (2001)
OEDICEROTIDAE	*Arrhis phyllonyx*	Porsanger Anskarholmen, Norway	70°21.45´N	25°15.13´E	None	N/A	AF419235	Englisch (2001)
	Bathymedon obtusifrons	Porsanger Osterbotn, Norway	70°07.11´N	25°10.65´E	None	N/A	AF419236	Englisch (2001)
	Monoculodes packardi	N/A	N/A	N/A	None	N/A	DQ378015	Englisch (2001)
PHOXOCEPHALIDAE (Phoxocephaloidea**)**	*Fuegophoxus abjectus*	South Shetland Islands, Antarctica	61°46.50´S	57°30.20´W	None	N/A	AY826972	Englisch (2001)
PODOCERIDAE	*Podocerus septemcarinatus*	N/A	N/A	N/A	None	N/A	DQ378021	Englisch (2001)

(Corophioidea**)**								
PRONOIDAE	*Eupronoe minuta*	Atlantic Ocean	30°08.4´N	28°34.8´W	None	N/A	DQ378052	Englisch (2001)
SALENTINELLIDAE (Liljeborgioidea**)**	*Salentinella angelieri*	N/A	N/A	N/A	None	N/A	DQ378037	Englisch (2001)
STEGOCEPHALIDAE (Stegocephaloidea**)**	*Stegocephalus inflatus*	Porsanger Langcy, Norway	70°26.71´N	25°22.24´E	None	N/A	AY826970	Englisch (2001)
STENOTHOIDAE (Leucothoidea**)**	*Antatelson walkeri*	Elephant Island, Antarctica	61°13.70´S	55°58.10´W	None	N/A	AY826961	Englisch (2001)
SYNOPIIDAE (Synopioidea**)**	*Syrrhoe psychrophila*	N/A	N/A	N/A	None	N/A	DQ378030	Englisch (2001)
TALITRIDAE (Talitroidea**)**	*Orchestia mediterranea*	Great Cumbrae, Scotland	55°45.90'N	4°55.54'W	None	N/A	AY826952	Englisch (2001)
	Talitrus saltator	Great Cumbrae, Scotland	55°45.90'N	4°55.54'W	None	N/A	AY826955	Englisch (2001)
URISTIDAE **(**Lysianassoidea**)**	*Abyssorchomene chevreuxi*	Antarctic Peninsula	65°17'S	51°35'W	N/A	GU109197	N/A	Havermans et al. (2010)
	Uristes murrayi	N/A	N/A	N/A	None	N/A	AY826965	Englisch (2001)
	Crangonyx forbesi	St. Louis Co., Missouri, USA	38°36.95'N	90°42.06'W	None	N/A	AF202980	Englisch (2001)
UROTHOIDAE (Phoxocephaloidea)	*Urothoe brevicornis*	Great Cumbrae, Scotland	55°45.90'N	4°55.54'W	None	N/A	AY826973	Englisch (2001)
Non-amphipod outgroup								
NEBALIIDAE (Nebaliacea, Leptostraca)	*Nebalia* sp.	N/A	N/A	N/A	None	N/A	L81945	Spears & Abele (1997)
SQUILLIDAE (Squilloidea, Stomatopoda)	*Squilla empusa*	N/A	N/A	N/A	None	N/A	L81946	Spears & Abele (1997)

Table 1. Details of the specimens used in this study including collection locality, voucher information and GenBank accession numbers. New sequences are marked by accession numbers in bold. “N/A” (not available) indicates unobtainable sequence data. The classification of the selected specimens followed De Broyer et al. (2007) for Southern Ocean species and Costello et al. (2001) for most European species.

The sequence chromatograms were checked, and forward and reverse sequence fragments were assembled using Codoncode Aligner 3.7.1. (CodonCode Corporation, available from http://www.codoncode.com/aligner/).

ALIGNMENTS

Sequences were aligned with MAFFT v.7 (Katoh and Standley, 2013) (available from http://mafft.cbrc.jp/alignment/server/), on three separate datasets (two 18S and one 28S alignments), using the structural alignment strategy Q-INS-i under default settings. As some regions of the ribosomal sequences were too divergent to be confidently aligned, the software program ALISCORE v.2.0. (Misof and Misof, 2009) was used to identify poorly aligned regions for removal with ALICUT v.2.3, prior to further analysis.

An Incongruence Length Difference (ILD) test (Farris et al., 1995) was implemented using Paup*4.0b10 (Swofford, 2003) in order to test for congruence between the 28S- and 18S-based phylogenies.

SUBSTITUTION SATURATION

Substitutional saturation in the 28S and 18S data was assessed using saturation plots and Xia's test (Xia et al., 2003) as implemented in DAMBE5 (Xia, 2013). Maximum composite likelihood (MCL) distances were plotted against uncorrected pairwise distances, separately for transitional and transversional substitutions. In the absence of saturation, these plots should reveal a linear increment of corrected in relation to uncorrected distance, with the number of transitions being higher than the number of transversions. Once substitution saturation is achieved, the plot should reach a plateau and transversions will eventually outnumber transitions. Numbers of substitutions and corrected sequences divergences were obtained using MEGA6 (Tamura et al., 2013) and plotted in Microsoft Excel 2007. ML model parameters were derived by the same method as for phylogenetic analyses (see below).

Xia's test was applied on each dataset, by analyzing unambiguous sites only. Iss is the index of substitution saturation. Iss. c is the critical Iss value at which saturation occurs and the sequences will begin to fail to recover the true tree, assuming a symmetrical topology (Iss. cSym) or an asymmetrical topology (Iss. cAsym). Xia's test (Xia et al., 2003) calculates if Iss is significantly lower than the Iss.c calculated for the same sequences.

PHYLOGENETIC ANALYSES

For each dataset, phylogenetic trees were inferred using Bayesian (BI) and Maximum Likelihood (ML) methods. The best-fit models of DNA substitution were selected using the Akaike Information Criterion (AIC), the Bayesian Information Criterion (BIC) and under a decision theoretic framework (DT), as implemented in JMODELTEST 2 (Darriba et al., 2012).

BI trees were reconstructed using MRBAYES 3.2 (Ronquist and Huelsenbeck, 2003). BI analysis of 18S and 28S alignments of putative eusiroid sequences, included two runs of 10^7 generations. Trees were sampled every 1000 generations using four Markov chains, and default heating values. Convergence was assessed by the standard deviation of split-frequencies (< 0.01) and by examining the trace plots of log-likelihood scores in TRACER 1.6 (Rambaut and Drummond, 2005). The first 10 % trees were discarded as burn-in, while the remaining trees were used to construct a 50 % majority rule consensus tree and estimate the posterior probabilities (PP). For the BI analysis of the larger alignment of available amphipod 18S sequences, 3 x 10^7 generations were needed to reach convergence. Other settings used were identical to preceding analyses. Nodes with PP ≥ 0.95 were considered as strongly supported.

ML trees were estimated using GARLI 2.0 (Zwickl, 2006). For each dataset, two separate ML searches were run independently from different stepwise-reconstructed trees. The best scoring tree across runs was considered for further analyses. Confidence levels of branches were estimated by 1000 bootstrap replicates. Nodes with bootstrap values (BV) ≥ 70 were considered as strongly supported.

Sources of significant rate heterogeneity were localized in the 18S phylogeny of Amphipoda by applying the branch length test (BLT) of Takezaki et al. (1995) with the LINTREE program (1995, available from http://www.personal.psu.edu/nxm2/ software.htm). The BLT aims to detect whether the branch length of a lineage is significantly different from the average branch length across the tree, that is if this lineage evolves significantly faster or slower (Takezaki et al., 1995). δ is the difference of the root-to-tip distance of each sequence from the average of all sequences under the root. For this test, a neighbour-joining tree was constructed with the Tamura-Nei model of DNA substitution and γ correction (the most similar option to the general time reversible model with site-specific rates of nucleotide substitution, not found in LINTREE). The value of γ was estimated by ML for the Tamura-Nei plus γ model in MEGA6.

RESULTS

ALIGNMENTS

Two separate datasets were used to reconstruct a phylogeny of Eusiroidea: (i) the 28S Eusiroidea dataset includes 59 sequences of putative eusiroids obtained in this study and five sequences of lysianassoid outgroup species retrieved from Genbank and (ii) the 18S Eusiroidea dataset includes 44 sequences of putative eusiroids obtained in this study, 16 additional sequences of putative eusiroids and 2 sequences of lysianassoid outgroup species retrieved from Genbank. Forty sequences were obtained from the same specimen for the 28S and 18S genes, whereas 6 sequences were obtained from different specimens of the same species for either gene. A third larger dataset was used to infer a general phylogeny of Amphipoda: the 18S Amphipoda dataset includes thirty-seven 18S sequences of putative eusiroids together with 43 sequences of supposedly non-eusiroid species (41 retrieved from GenBank), and two non-amphipod outgroup species.

Unaligned sequences were 1193–1669 bp and 2023–2596 bp long, for 28S and 18S respectively. After removal of the non-conserved positions with Aliscore, the alignment lengths for the phylogenies of Eusiroidea were 1315 bp, with 982 variable sites for 28S and 2169 bp, with 1267 variable sites, for 18S. The final 18S alignment used for the general phylogeny of Amphipoda, was 1898 bp long, with 1233 variable sites.

When all available putative eusiroid sequences were taken into account, uncorrected sequence divergence values averaged 15.9 % for 18S (range: 0.2 % – 30.8 %) and 31.6 % for 28S (range: 0.3 % – 43.7 %).

SUBSTITUTION SATURATION AND RATE HETEROGENEITY

Saturation plots revealed saturation of nucleotide substitution for both rDNA genes beyond GTR distances beyond 15 % for both rDNA genes (Fig. 1). It is more pronounced in the 28S dataset (R^2 = 0.75 for transitional substitutions) (Fig. 1A), than for the 18S sequences (R^2= 0.91 for transitional substitutions) of putative eusiroids (Fig. 1B). The sequences are, however, expected to remain phylogenetically informative below these divergence levels. Xia's test result is that the null hypothesis of no effect of substitutional saturation is not rejected for each random subsets of 4, 8, 16 and 32 rDNA sequences.

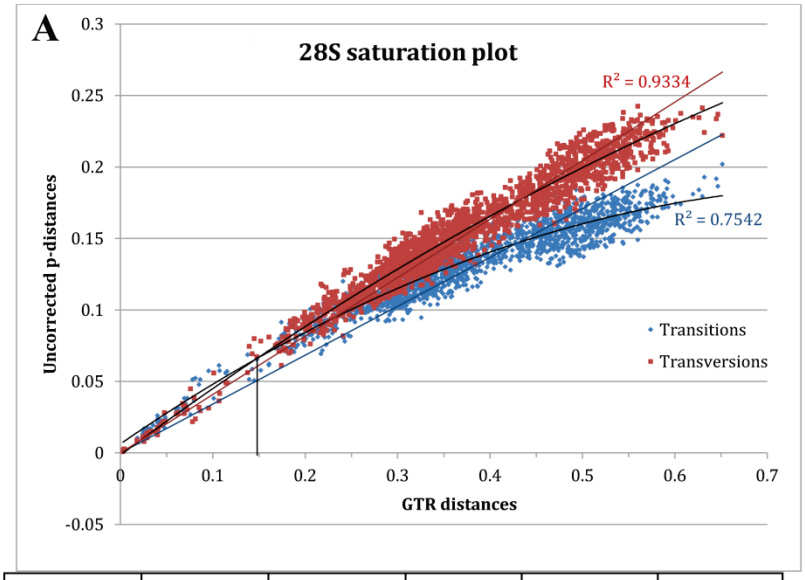

Num. OTU	Iss	Iss. cSym	P	Iss. cAsym	P
4	0.347	0.811	0.000	0.780	0.000
8	0.340	0.775	0.000	0.666	0.000
16	0.345	0.756	0.000	0.550	0.000
32	0.352	0.730	0.000	0.410	0.006

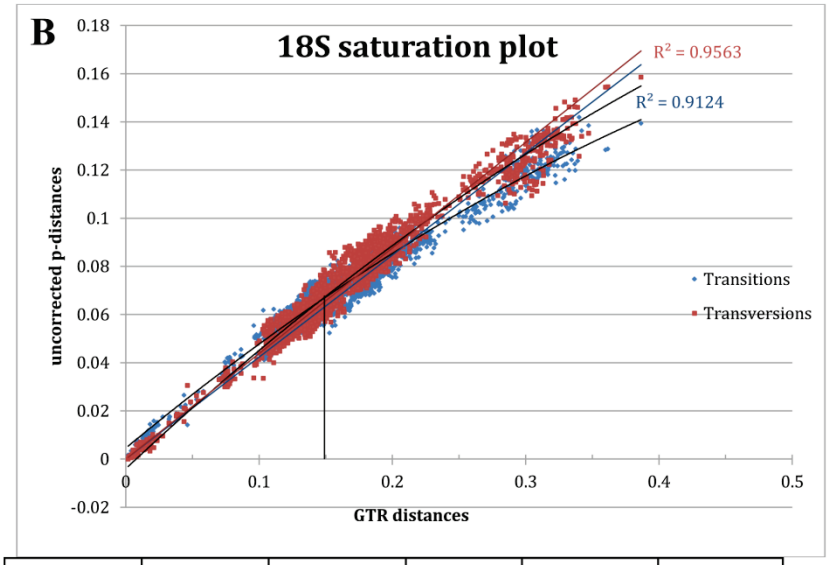

Num. OTU	Iss	Iss. cSym	P	Iss. cAsym	P
4	0.190	0.833	0.000	0.802	0.000
8	0.186	0.808	0.000	0.707	0.000
16	0.189	0.791	0.000	0.607	0.000
32	0.198	0.773	0.000	0.488	0.000

Figure 1. Substitution saturation scatter plots with results of Xia's tests for (A) 28S and (B) 18S datasets. The graphs represent the increase in GTR distances corrected for multiple nucleotide substitutions versus the increase in p-distances between pairs of sequences, considering transitions only (in blue) and transversions only (in red); R^2 values shows the fit of the relationship to a linear regression model. Polynomial trendlines are shown in black. In the absence of saturation, these plots should reveal a linear increment of corrected in relation to uncorrected distance, with the number of transitions being higher than the number of transversions. Once substitution saturation is achieved, the plot should reach a plateau and transversions will eventually outnumber transitions.

The BLT indicates that rate heterogeneity is present in the 18S phylogeny of Amphipoda. Four putative eusiroid sequences i.e. *Acanthonotozomopsis pushkini* (δ[1] = 0.12), *Acanthonotozomoides oatesi* (δ = 0.08), *Eusiroides georgiana* (δ = 0.1), and *Thurstonella chelata* (δ = 0.12) and nine putative non-eusiroid sequences show a higher substitution rate than average, producing exceptionally long tree branches (Fig. 2). The 28S sequences also show an elevated substitution rates for *A. pushkini* (δ = 0.11), but not in *A. oatesi* and *E. georgiana* (there are no 28S data for *T. chelata*). Furthermore, the 28S sequences of *Prostebbingia gracilis, P. serrata, P. longicornis, Eurymera monticulosa* and *Bovallia gigantea* show even higher substitution rates (δ values of 0.26, 0.26, 0.45, 0.43 and 0.61, respectively), but not so in the 18S of the *Prostebbingia* species and no 18S data is available for *B. gigantea* (Fig. 3).

18S PHYLOGENETIC ANALYSIS OF THE AMPHIPODA (FIG. 2)

The 18S topologies obtained by ML and BI analyses differ, but the incongruences are only observed for unsupported nodes. Most of the putative eusiroid taxa are included in a well-supported clade (clade A in Fig. 2; PP = 1.00, BV = 98), along with eight supposedly non-eusiroid species, viz. three oedicerotids (*Arrhis phyllonyx*, *Monoculodes packardi* and *Bathymedon obtusifrons*), two hyperiids (*Eupronoe minuta* and *Hyperia galba*), a leucothoid (*Leucothoe spinicarpa*), an amphilochid (*Amphilochus tenuimanus*) and a colomastigid (*Colomastix fissilingua*). Within clade A, the vast majority of putative eusiroid taxa form another clade in both analyses, although not supported by PP or BV (Clade B in Fig. 2). Clade B includes taxa from the putative eusiroid families Calliopiidae, Eusiridae, Gammarellidae, Pontogeneiidae, Iphimediidae, Epimeriidae, Amathillopsidae, Acanthonotozomatidae, Acanthonotozomellidae, Dikwidae, Pleustidae, Stilipedidae and Astyridae.

Two putative eusiroid genera, viz. *Gammarellus* (Gammarellidae) and *Cleippides* (Calliopiidae) do not belong to clade A, but their phylogenetic relationship with clade A is unresolved. One putative eusiroid species *Odius carinatus* (Ochlesidae) is not present in the 18S phylogeny but is nested within the outgroup of lysianassoid species in the 28S tree (Fig. 3A).

The putative eusiroid species *A. oatesi, A. pushkini, T. chelata* and *E. georgiana* are part of clade A but not of clade B (branches in red on Fig. 2). However, they involve long branches and as such their position might be spurious and result from a long branch attraction to the eight supposedly non-eusiroid species in clade A (marked in grey in Fig. 2). When these 12 long-branched taxa of clade A are excluded from the analysis, the support of clade B is maximal (1.00, 100).

[1] δ is the difference of the root-to-tip distance of the sequence of interest from the average of all sequences under the root, as calculated in LINTREE.

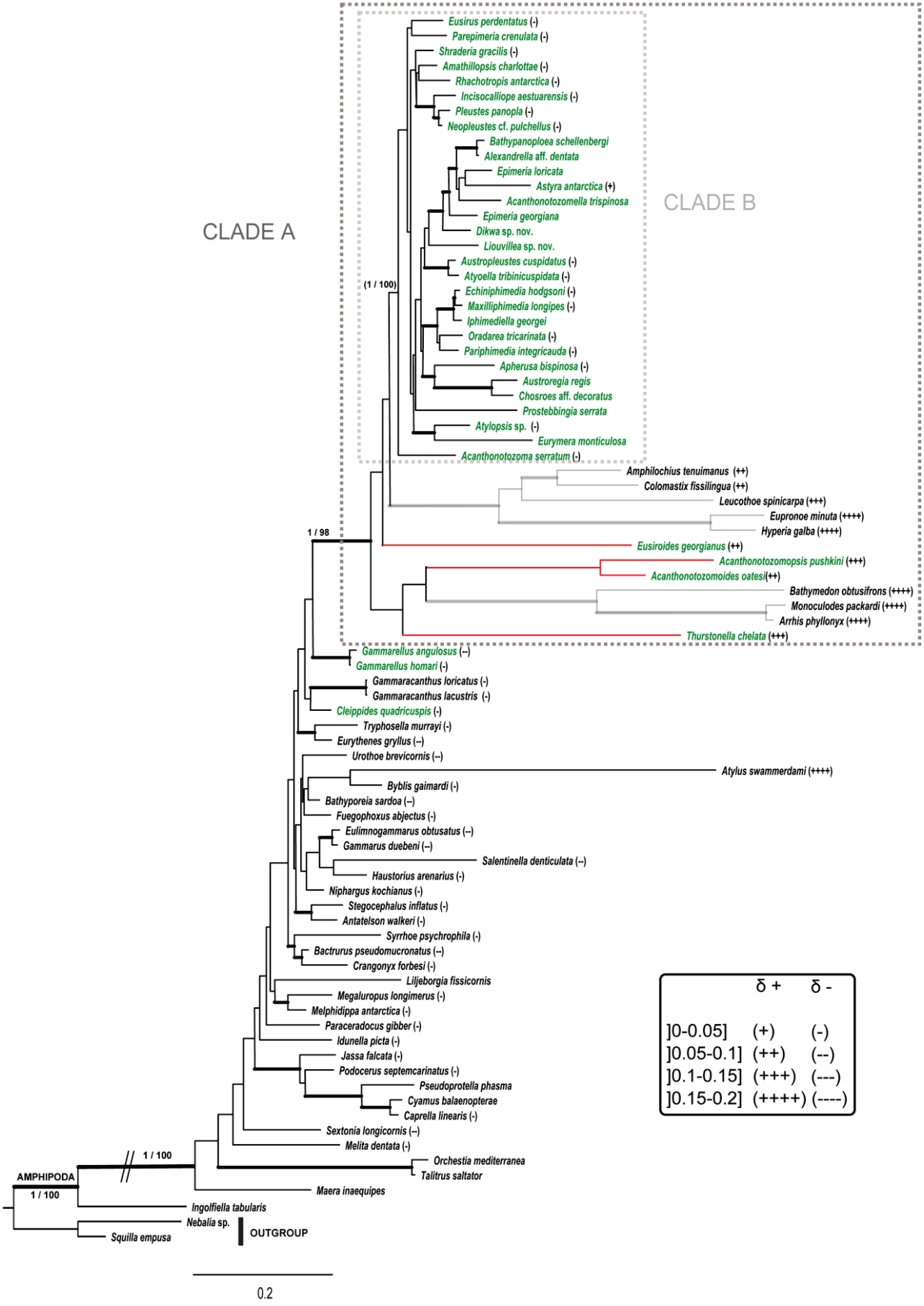
CLADE A
CLADE B
Eusirus perdentatus (-)
Parepimeria crenulata (-)
Shraderia gracilis (-)
Amathillopsis charlottae (-)
Rhachotropis antarctica (-)
Incisocalliope aestuarensis (-)
Pleustes panopla (-)
Neopleustes cf. pulchellus (-)
Bathypanoploea schellenbergi
Alexandrella aff. dentata
Epimeria loricata
Astyra antarctica (+)
Acanthonotozomella trispinosa
Epimeria georgiana
Dikwa sp. nov.
Liouvillea sp. nov.
Austropleustes cuspidatus (-)
Atyoella tribinicuspidata (-)
(1 / 100)
Echiniphimedia hodgsoni (-)
Maxilliphimedia longipes (-)
Iphimediella georgei
Oradarea tricarinata (-)
Pariphimedia integricauda (-)
Apherusa bispinosa (-)
Austroregia regis
Chosroes aff. decoratus
Prostebbingia serrata
Atylopsis sp. (-)
Eurymera monticulosa
Acanthonotozoma serratum (-)
Amphilochius tenuimanus (++)
Colomastix fissilingua (++)
Leucothoe spinicarpa (+++)
Eupronoe minuta (++++)
Hyperia galba (++++)
1 / 98
Eusiroides georgianus (++)
Acanthonotozomopsis pushkini (+++)
Acanthonotozomoides oatesi(++)
Bathymedon obtusifrons (++++)
Monoculodes packardi (++++)
Arrhis phyllonyx (++++)
Thurstonella chelata (+++)
Gammarellus angulosus (--)
Gammarellus homari (-)
Gammaracanthus loricatus (-)
Gammaracanthus lacustris (-)
Cleippides quadricuspis (-)
Tryphosella murrayi (-)
Eurythenes gryllus (--)
Urothoe brevicornis (--)
Atylus swammerdami (++++)
Byblis gaimardi (-)
Bathyporeia sardoa (--)
Fuegophoxus abjectus (-)
Eulimnogammarus obtusatus (--)
Gammarus duebeni (--)
Salentinella denticulata (--)
Haustorius arenarius (-)
Niphargus kochianus (-)
Stegocephalus inflatus (-)
Antatelson walkeri (-)
Syrrhoe psychrophila (-)
Bactrurus pseudomucronatus (--)
Crangonyx forbesi (-)
Liljeborgia fissicornis
Megaluropus longimerus (-)
Melphidippa antarctica (-)
Paraceradocus gibber (-)
Idunella picta (-)
Jassa falcata (-)
Podocerus septemcarinatus (-)
Pseudoprotella phasma
Cyamus balaenopterae
Caprella linearis (-)
Sextonia longicornis (--)
Melita dentata (-)
1 / 100
Orchestia mediterranea
Talitrus saltator
AMPHIPODA
1 / 100
Maera inaequipes
Ingolfiella tabularis
Nebalia sp.
Squilla empusa
OUTGROUP
0.2
δ +
δ -
]0-0.05] (+) (-)
]0.05-0.1] (++) (--)
]0.1-0.15] (+++) (---)
]0.15-0.2] (++++) (----)

Figure 2. Phylogenetic tree obtained by maximum likelihood analysis of the 18S rDNA sequences. Bootstrap values (1000 pseudoreplicates) and Bayesian posterior probabilities are indicated above the nodes of interest. Branches supported by BV > 70 and PP > 0.95 are indicated by thick lines. Candidate eusiroid species are shown in green. Branches that are significantly longer (+) or shorter (-) than average according to the BLT test are marked aside the taxa names. δ is the difference of the root-to-tip distance of each sequence from the average of all sequences under the root. Long branches leading to the *a priori* non eusiroid taxa are shown in grey, whereas long branches leading to the potential eusiroid taxa are shown in red. Support values of clade B indicated within brackets were obtained after the removal of the eight long branches (in red and grey).

PHYLOGENETIC ANALYSES OF THE EUSIROIDEA (FIG. 3).

Although the ILD test rejected the null hypothesis of congruence between the 28S and 18S Eusiroidea trees ($P = 0.01$), the conflicting nodes were never supported by BV and very few had a PP > 0.95. Nevertheless, both dataset were run separately because concatenation did not improve support values, and the datasets on their own comprised more species than the concatenated dataset.

For both gene trees, there is no disagreement between the BI and ML topologies with respect to well-supported relationships.

Based on nodes supported by high PP (> 0.95) and BV values (> 70), the families Pleustidae, Calliopiidae, Pontogeneiidae, Gammarellidae and Epimeriidae appear polyphyletic (Fig. 3). The family Acanthonotozomellidae is polyphyletic only with high PP but no BV support. The family Eusiridae is monophyletic with high support in the 28S tree, but is polyphyletic in the 18S BI tree (not ML). The only monophyletic family consistently recovered with high support in both 18S and 28S trees is the Stilipedidae. The Iphimediidae are monophyletic with high support in the 28S phylogeny, whereas the family presents an unsupported polyphyly in the 18S tree.

Five clades with multiple genera were consistently recovered with high support on both 28S and 18S gene trees and by the two different methods (Fig. 3). These clades may vary in species composition between the two gene trees, because of differences in sequencing success. Three additional clades were consistently recovered on the 28S trees only, and one on the 18S trees only.

Clade 1 comprises the northern pleustid genera *Neopleustes*, *Pleustes* and *Incisocalliope*.

Clade 2 includes species of the calliopiid genera *Calliopius*, *Apherusa* and *Halirages* and the epimeriid *Paramphithoe hystrix.* In the 28S phylogeny, *Calliopius laevisculus* is sister to the other members of the clade. The genus *Apherusa* appears paraphyletic and so does *Halirages*, though with no support. Clade 2 is also recovered on the 18S phylogeny (1.00, 100), but only sequences of *Apherusa* sp. were obtained.

Clade 3 includes the genus *Epimeria* and the families Stilipedidae (*Bathypanoploea* and *Alexandrella*), Acanthonotozomellidae (*Acanthonotozomoides* and *Acanthonotozomella*), Vicmusiidae (*Acanthonotozomopsis*), Dikwidae (*Dikwa*) and Astyridae (*Astyra*). The non-monophyly of Acanthonotozomellidae is supported by the BI 18S tree and by ML and BI of both datasets, if one considers the maximally supported sister relationship between the long-branched *Acanthonotozomoides oatesi* and *Acanthonotozomopsis pushkini* as reliable. The genus *Epimeria* is not monophyletic, since the Antarctic *Epimeria* species are the sister taxon of the Stilipedidae, though only supported by BI of 18S.

Clade 4 comprises three species, representing the genera *Paramoera* (Pontogeneiidae), *Austropleustes* and *Atyloella* (Pleustidae).

Clade 5 includes one species of *Atylopsis* and *Oradarea macrocephala*. The genus *Oradarea* appears non-monophyletic.

Two additional clades, each including only one genus, were consistently recovered with maximal support in both gene trees (the monophyletic genus *Parepimeria* and two species of the polyphyletic genus *Prostebbingia*).

Because the taxon sampling or node support was not identical in the 18S and 28S analyses, four clades were detected that occurred only in one of the two datasets.

Clade 6 comprises the family Eusiridae in the 28S phylogeny. Yet, in the 18S trees, *E. georgiana* is not included in this clade, but appears as sister taxon to *E. monticulosa* with a high PP, but not with BV. However, as *E. georgiana* presents an exceptionally long branch in the 18S phylogeny, this grouping might result from long branch attraction.

Clade 7 comprises *Liouvillea* sp. nov., *Oradarea* spp. and the family Iphimediidae (genera *Iphimediella*, *Gnathiphimedia*, *Echiniphimedia*, *Maxilliphimedia* and *Anchiphimedia*) in the 28S phylogeny. In the 18S tree, the clade comprising *Oradarea* spp. and the iphimediids is well-supported, but the position of *Liouvillea* sp. nov. is unsupported.

The grouping of clades 3, 4 and 7 is supported on the 28S phylogeny, but the relationships among these clades are less reliable.

Clade 8 in the 28S phylogeny consists of three pontogeneiid species, with *Bovallia gigantea* as sister taxon to a clade of *P. longicornis* and *E. monticulosa*. However, as the 28S sequences of these three species appear to show extensive rate acceleration, this sister relationship might be a long branch attraction artefact. The genus *Prostebbingia* appears non-monophyletic.

Clade 9 in the 18S phylogeny includes *Chosroes* aff. *decoratus* and *Austroregia regis*.

The phylogenetic relationships between these nine clades are mostly unresolved.

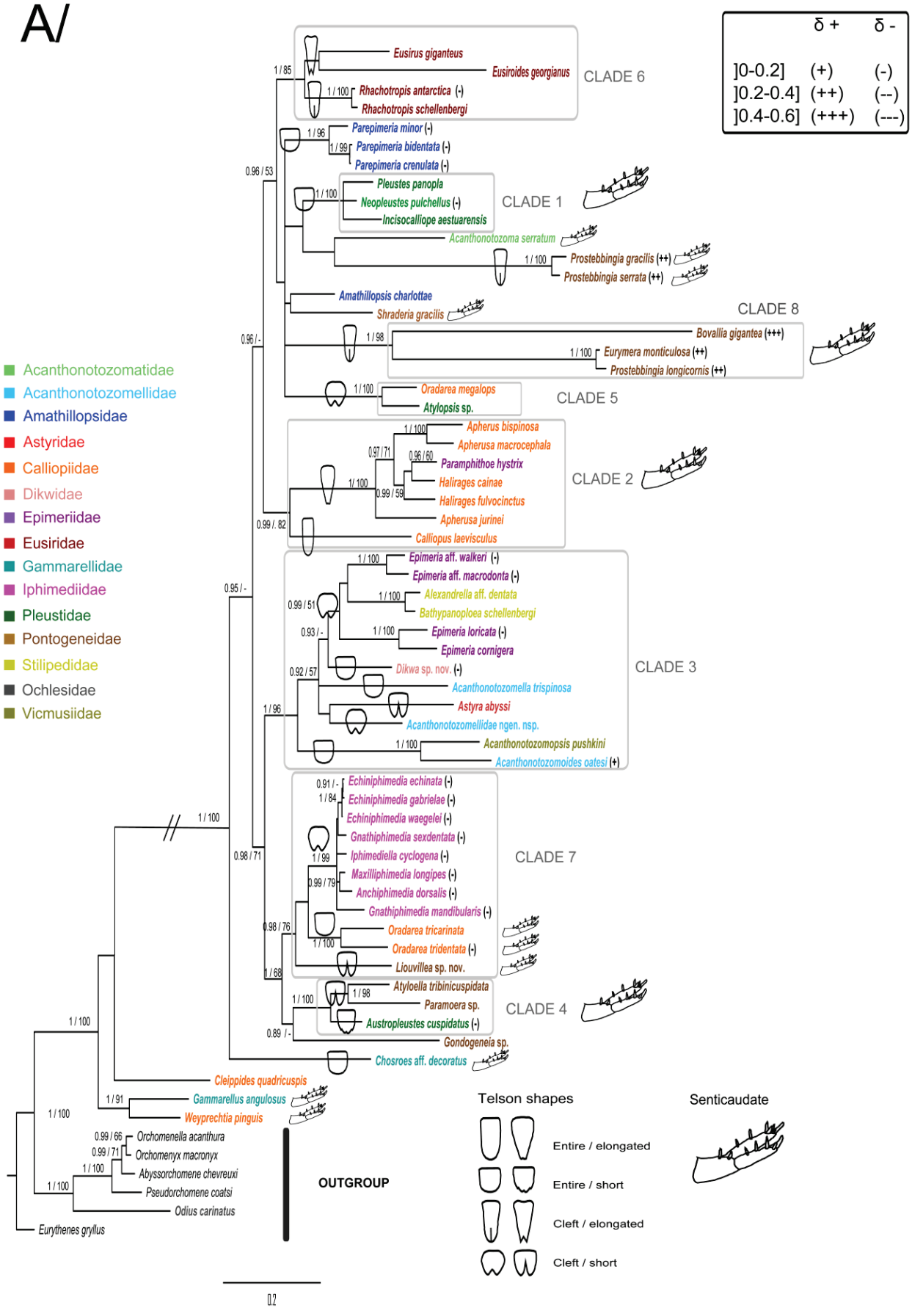
A/
δ +
δ -
]0-0.2] (+) (-)
]0.2-0.4] (++) (--)
]0.4-0.6] (+++) (---)
Acanthonotozomatidae
Acanthonotozomellidae
Amathillopsidae
Astyridae
Calliopiidae
Dikwidae
Epimeriidae
Eusiridae
Gammarellidae
Iphimediidae
Pleustidae
Pontogeneidae
Stilipedidae
Ochlesidae
Vicmusiidae
Eusirus giganteus
Eusiroides georgianus
Rhachotropis antarctica (-)
Rhachotropis schellenbergi
CLADE 6
Parepimeria minor (-)
Parepimeria bidentata (-)
Parepimeria crenulata (-)
Pleustes panopla
Neopleustes pulchellus (-)
Incisocalliope aestuarensis
CLADE 1
Acanthonotozoma serratum
Prostebbingia gracilis (++)
Prostebbingia serrata (++)
Amathillopsis charlottae
Shraderia gracilis
CLADE 8
Bovallia gigantea (+++)
Eurymera monticulosa (++)
Prostebbingia longicornis (++)
Oradarea megalops
Atylopsis sp.
CLADE 5
Apherus bispinosa
Apherusa macrocephala
Paramphithoe hystrix
Halirages cainae
Halirages fulvocinctus
Apherusa jurinei
Calliopus laevisculus
CLADE 2
Epimeria aff. walkeri (-)
Epimeria aff. macrodonta (-)
Alexandrella aff. dentata
Bathypanoploea schellenbergi
Epimeria loricata (-)
Epimeria cornigera
Dikwa sp. nov. (-)
Acanthonotozomella trispinosa
Astyra abyssi
Acanthonotozomellidae ngen. nsp.
Acanthonotozomopsis pushkini
Acanthonotozomoides oatesi (+)
CLADE 3
Echiniphimedia echinata (-)
Echiniphimedia gabrielae (-)
Echiniphimedia waegelei (-)
Gnathiphimedia sexdentata (-)
Iphimediella cyclogena (-)
Maxilliphimedia longipes (-)
Anchiphimedia dorsalis (-)
Gnathiphimedia mandibularis (-)
Oradarea tricarinata
Oradarea tridentata (-)
Liouvillea sp. nov.
CLADE 7
Atyloella tribinicuspidata
Paramoera sp.
Austropleustes cuspidatus (-)
CLADE 4
Gondogeneia sp.
Chosroes aff. decoratus
Cleippides quadricuspis
Gammarellus angulosus
Weyprechtia pinguis
Orchomenella acanthura
Orchomenyx macronyx
Abyssorchomene chevreuxi
Pseudorchomene coatsi
Odius carinatus
Eurythenes gryllus
OUTGROUP
0.2
Telson shapes
Entire / elongated
Entire / short
Cleft / elongated
Cleft / short
Senticaudate

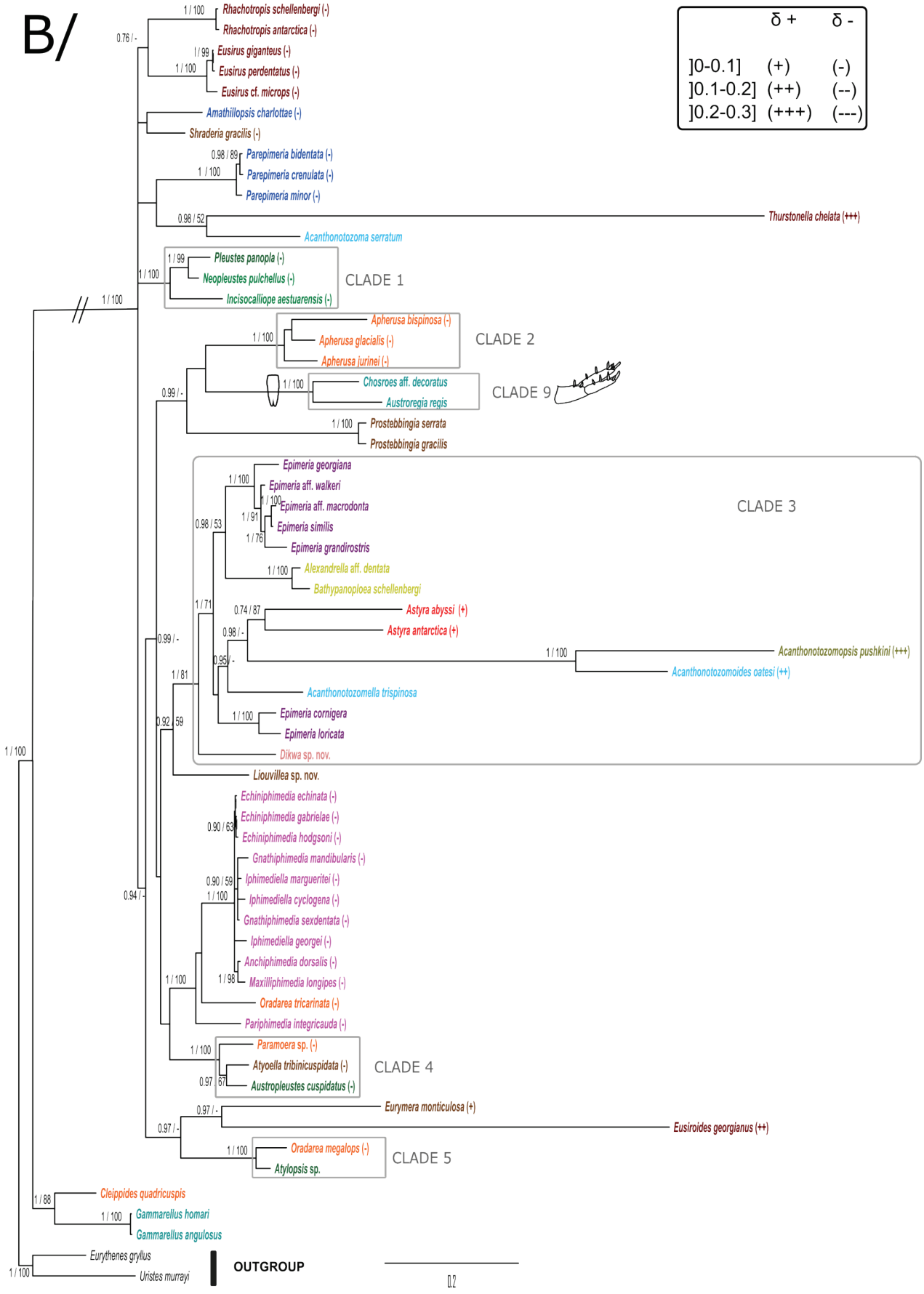
B/
δ +
δ -
]0-0.1] (+) (-)
]0.1-0.2] (++) (--)
]0.2-0.3] (+++) (---)
Rhachotropis schellenbergi (-)
Rhachotropis antarctica (-)
Eusirus giganteus (-)
Eusirus perdentatus (-)
Eusirus cf. microps (-)
Amathillopsis charlottae (-)
Shraderia gracilis (-)
Parepimeria bidentata (-)
Parepimeria crenulata (-)
Parepimeria minor (-)
Thurstonella chelata (+++)
Acanthonotozoma serratum
Pleustes panopla (-)
Neopleustes pulchellus (-)
Incisocalliope aestuarensis (-)
CLADE 1
Apherusa bispinosa (-)
Apherusa glacialis (-)
Apherusa jurinei (-)
CLADE 2
Chosroes aff. decoratus
Austroregia regis
CLADE 9
Prostebbingia serrata
Prostebbingia gracilis
Epimeria georgiana
Epimeria aff. walkeri
Epimeria aff. macrodonta
Epimeria similis
Epimeria grandirostris
CLADE 3
Alexandrella aff. dentata
Bathypanoploea schellenbergi
Astyra abyssi (+)
Astyra antarctica (+)
Acanthonotozomopsis pushkini (+++)
Acanthonotozomoides oatesi (++)
Acanthonotozomella trispinosa
Epimeria cornigera
Epimeria loricata
Dikwa sp. nov.
Liouvillea sp. nov.
Echiniphimedia echinata (-)
Echiniphimedia gabrielae (-)
Echiniphimedia hodgsoni (-)
Gnathiphimedia mandibularis (-)
Iphimediella margueritei (-)
Iphimediella cyclogena (-)
Gnathiphimedia sexdentata (-)
Iphimediella georgei (-)
Anchiphimedia dorsalis (-)
Maxilliphimedia longipes (-)
Oradarea tricarinata (-)
Pariphimedia integricauda (-)
Paramoera sp. (-)
Atyoella tribinicuspidata (-)
Austropleustes cuspidatus (-)
CLADE 4
Eurymera monticulosa (+)
Eusiroides georgianus (++)
Oradarea megalops (-)
Atylopsis sp.
CLADE 5
Cleippides quadricuspis
Gammarellus homari
Gammarellus angulosus
Eurythenes gryllus
Uristes murrayi
OUTGROUP
0.2

Figure 3. Phylogenetic trees obtained by Bayesian analyses of DNA sequences based on (A) 28S and (B) 18S rDNA genes. Support values were indicated above the nodes with Bayesian posterior probabilities > 0.9 and/or bootstrap values > 70 (1000 pseudoreplicates). Branches that are significantly longer (+) or shorter (-) than average according to the BLT test are marked aside the taxon names. δ is the difference of the root-to-tip distance of each sequence from the average of all sequences under the root. Nine clades are delimited on the phylogenies because they were consistently recovered with high PP (> 0.95) and BV (> 70) on BI and ML trees. Both genes recover clades 1–5. Sequence names are highlighted using a colour code indicating their affiliation to the traditional families listed on the side. Telsonic shapes and the senticaudate character are represented by symbols besides the corresponding lineage.

DISCUSSION

CAVEATS OF RDNA SEQUENCE DATA

Several well-known problems of rDNA based phylogeny inference (Abouheif et al., 1998) may have affected our results. The amount of phylogenetic information supporting the deeper nodes is reduced by saturation in both gene trees, and more strongly so for the 28S gene (Fig. 1). The substantial branch length differences detected in 18S and 28S phylogenies can also bias topologies and nodes support. Particularly, the 18S sequences of some lineages showed considerable rate acceleration (Fig. 3B).

Evidences of rate acceleration have been found in the rRNA genes of a wide variety of eukaryotic taxa (Friedrich and Tautz, 1997; Omilian and Taylor, 2001; Philippe and Germot, 2000). Long branches resulting from such faster evolving lineages have been shown to introduce biases in phylogenetic inferences, including those based on ML (Anderson and Swofford, 2004; Kück et al., 2012; Parks and Goldman, 2014) and Bayesian Inference (Kolaczkowski and Thornton, 2009; Susko, 2015). LBA problems arise when the probability that close relatives share identical character states due to common ancestry is exceeded by the probability that more distantly related and rapidly evolving taxa share states due to parallelism (Anderson and Swofford, 2004; Bergsten, 2005; Wägele and Mayer, 2007).

A simulation-based study showed that the incorporation of secondary structure information improves the alignment of rDNA sequences. Notably, the effect of increasing branch lengths is less pronounced in alignments based on structure-aided methods. MAFFT structural algorithms (Q-ins and X-ins) also performed significantly better than other methods (RNASALSA, MXS-CARNA). However, this improvement vanished in tree reconstructions, probably because of ambiguously aligned positions. Exclusion of these positions with Aliscore restores the significant superiority of structure-aided methods (Letsch et al., 2010).

In order to further address these analytical problems in future studies of this group, additional taxa should be sampled to break up long branches and additional genes should be used to increase the phylogenetic content of the dataset (Bergsten, 2005).

THE DELIMITATION OF THE SUPERFAMILY EUSIROIDEA

As the support of clade B becomes maximal when the 12 long-branched taxa of clade A are removed from the analysis, the lack of support of clade B on Fig. 2 is assumed to be an artefact caused by long branch attractions. Therefore, clade B is interpreted as being well-supported. It includes species of both traditional and putative eusiroid families, viz. Calliopiidae (excluding *Cleippides*), Eusiridae (excluding *Eusiroides*), Gammarellidae (excluding *Gammarellus*), Pontogeneiidae, Astyridae, Iphimedidae, Epimeriidae, Pleustidae, Acanthonotozomatidae, Acanthonotozomellidae (excluding *Acanthonotozomoides*), Dikwidae, Stilipedidae and Amathillopsidae.

As the 18S sequences of *E. georgiana*, *A. oatesi*, *A. pushkini and T. chelata* yield long branches caused by greatly accelerated evolution (z-values[2] of 5.29, 4.92, 5.75 and 5.26, respectively), their position with respect to clade B cannot be resolved on the basis of the present 18S dataset. However, *A. pushkini* do not present significantly longer branches in the 28S tree, whereas it is slightly longer for *A. oatesi*, just above the 1 % significance level (z-values of 2.37 and 2.44, respectively). The phylogenetic relationships of these species in the 28S tree are thus probably less prone to long branch attraction artefacts than in the 18S phylogeny. In the 28S tree (Fig. 3A). *A. oatesi* (Acanthonotozomellidae) and *A. pushkini* (Vicmusiidae) are part of clade 3 with high support, with species of Acanthonotozomellidae, Epimeriidae, Dikwidae, Stilipedidae and Astyridae. All these families share a number of putative synapomorphies (see below).

Eusiroides georgiana does not present a significantly longer branch in the 28S tree. It is part of clade 6, along with all the species of the family Eusiridae. Until very recently, *Eusiroides* has been traditionally classified in the family Eusiridae (Barnard and Karaman, 1991; Bousfield, 1978; Bousfield and Hendrycks, 1995b; De Broyer and Jażdżewski, 1993; De Broyer et al., 2007), whereas it is currently classified in the Pontogeneiidae (Lowry and Myers, 2013). The morphological characters used to define the family Eusiridae are possible synapomorphies for clade 6 (see below) (Fig. 2A).

A provisional diagnosis of the superfamily Eusiroidea, including species belonging to 14 of the traditional families studied herein, i.e. Acanthonotozomatidae, Acanthonotozomellidae, Amathillopsidae, Astyridae, Calliopiidae (excluding *Cleippides*), Dikwidae, Eusiridae, Epimeridae, Gammarellidae s.l. (excluding *Gammarellus*), Iphimediidae, Pleustidae, Pontogeneiidae, Stilipedidae and Vicmusiidae is presented in Appendix S1. Convergent evolution of many of the traits used to

diagnose the superfamily and the lack of supported deep relationships in the phylogeny of Amphipoda make it difficult to identify synapomorphies defining the group. However, the following character states are considered as putative synapomorphies of the Eusiroidea: (i) the antennae are not sexually dimorphic in size, (ii) the antennae have many flagellar articles, (iii) the peduncle is neither shortened (e.g. Lysianassoidea, Stegocephalidae), nor strongly elongated (e.g. Ampeliscidae, many Stenothoidae, Melphidippidae), (iv) the accessory flagellum is absent or 1-articulated (v) the gnathopods are generally subsimilar and never strongly sexually dimorphic, (vi) the rami of uropod 3 are lanceolate, much longer than the peduncle, elongated but not filiform, with a one-segmented outer ramus subequal or shorter than the inner ramus.

As the phylogenetic position of the eight long-branched putative non-eusiroid species of the taxa Amphilochidae, Colomastigidae, Hyperiidea, Leucothoidae and Oedicerotidae is unresolved in the 18S phylogeny, they will be excluded from the diagnosis of Eusiroidea until new data suggest otherwise. Although they have a reduced accessory flagellum, they do not possess most of the remaining putative synapomorphies of Eusiroidea : (i) the antennae are usually sexually dimorphic in size (Amphilochidae, Hyperiidea, Oedicerotidae), (ii) the flagella of the antennae are reduced to a few articles (Leucothoidae, Amphilochidae, Colomastigidae, some hyperiids), (iii) the peduncles of the antennae are often elongated (Oedicerotidae, Leucothoidae, Colomastigidae), inflated (some leucothoids and colomastigids) or shortened (Hyperiidea), (iv) the gnathopods are usually dissimilar (all), and sexually dimorphic (Leucothoidae, Colomastigidae) and (v) uropod 3 has an elongated peduncle, longer than the rami (Leucothoidae, Amphilochidae, Hyperiidea, some oedicerotids), or only slightly shorter (some oedicerotids) (see Appendix S2 for all phenetic differences).

Some species that were formerly treated as (putative) eusiroids are not part of clade B. *Gammarellus* spp., *Cleippides quadricuspis* and *Weyprechtia pinguis* were traditionally placed in the Eusiroidea, respectively in the families Gammarellidae, Calliopiidae, and in both of these families successively. In our 18S analyses, *Gammarellus* spp. and *C. quadricuspis* are positioned outside clade A (Fig. 2). On the 28S tree, *W. pinguis* is sister to *Gammarellus angulosus* with high support. As the relationships of *Gammarellus* spp. and *C. quadricuspis* with clade A and therefore clade B (if we consider that the relationships involving the long branches are unreliable) are unsupported, they will be provisionally excluded from the Eusiroidea. The accessory flagellum of *Gammarellus* spp. and *Weyprechtia* spp. is always well-developed. The antennae of *Gammarellus* spp. are sexually dimorphic in size (unknown for *Weyprechtia*). In both genera, the inner ramus of uropod 3 is shorter than the outer. *C. quadricuspis*, however, presents all the putative synapomorphic characters of Eusiroidea.

Odius carinatus (Ochlesidae) was suggested to be part of the iphimedioid clade of Lowry and Myers (2000) which comprises the other armored families Iphimediidae, Epimeriidae, Acanthonotozomellidae, Dikwidae, Vicmusiidae and Amathillopsidae. However, in the 28S tree, the species appears nested within the lysianassoid outgroup with maximal support (Fig. 3A). Although *O. carinatus* does not have an accessory flagellum, its antennae are very short with few flagellar articles, the gnathopods are very dissimilar and the outer ramus of uropod 3 is not much longer than the peduncle. Some genera of Ochlesidae are also strongly sexually dimorphic (Coleman and Lowry, 2006). The family Ochlesidae shares some possible synapomorphies with the lysianassoids: the short and stout antenna with enlarged peduncular article, the large and deep-plated coxa, the markedly dissimilar gnathopods and the reduced inner plate of the maxilla 1.

STATUS OF EUSIROID FAMILIES

The problem of morphological convergences affects the interpretation of taxa within the Eusiroidea (Barnard, 1969; Barnard and Karaman, 1991). Moreover, eusiroid families were often defined by morphological characters presenting continuous variation so that their limits were highly debatable. Therefore, the families included here in the Eusiroidea were long considered as a large complex of poorly defined families (Barnard, 1964), with frequent transfers of genera from one family to another. The monophyly of the eusiroid families and evolutionary relationships are here discussed in the context of some morphological characteristics that were traditionally used in the taxonomy of this taxon.

TELSON SHAPE. The traditional eusiroid families Calliopiidae, Eusiridae, Gammarellidae and Pontogeneiidae were defined almost exclusively on the shape of the telson. Calliopiids are defined by their entire telson. The validity of the family Gammarellidae was questioned by some authors, who asserted that gammarellids were simply calliopiids (in the sense that they have an entire telson) with a well-developed accessory flagellum (Barnard and Barnard, 1983; Barnard and Karaman, 1991). The Eusiridae have a telson that is either markedly cleft or only notched and that is always distinctively elongated. The definition of pontogeneiids similarly relies almost exclusively on the cleft telson (Barnard, 1969).

However, the familial boundaries have changed repeatedly throughout the history of classification of the superfamily, as some authors questioned the taxonomic value of the telson (Barnard, 1969; Barnard and Karaman, 1991). These eusiroid families were later resurrected (Bousfield and Hendrycks, 1995b) and kept separated in subsequent schemes (De Broyer et al., 2007; Lowry and Myers, 2013).

The present phylogenetic analyses suggest that the families Calliopiidae and Pontogeneiidae are not monophyletic (Fig. 3). Hence, the telsonic character states entire / cleft are homoplasious. Within clades 3, 4 and 7 both states occur and within clades 3, 6, and 7 the cleft state varies from only notched apically to deeply cleft. Some lineages, however, have retained an entire (e.g. the pleustids of clade 1, the calliopiids + *P. hystrix* of clade 2), weakly notched (e.g. the iphimediids, the gammarellids of clade 9) or deeply cleft (e.g. the pontogeneiids of clade 8) telson throughout their evolution. This character state could have a phylogenetic significance at some less inclusive taxonomic levels, but as it is highly homoplasious, it should be used with caution to characterize taxonomic groupings. On the other hand, the telsonic character state short / elongated could be a synapomorphy of some of the defined clades and/or at more inclusive taxonomic levels. The larger clade composed of clades 3, 4 and 7 presents a short telson, as it is also the case for the pleustids of clade 1 and the two species of clade 5. The eusirids of clade 6, the calliopiids + *P. hystrix* of clade 2, the pontogeneids of clade 8 (Fig. 3A) and the gammarellids of clade 9 (Fig. 3B) present an elongated shape of the telson.

CALCEOLI TYPES. The antennae of eusiroids are commonly calceoliferous in both sexes. Calceoli are microscopic external surface structures of unknown function and varying shapes and arrangement on the antennae of about 10 % of the known gammaridean species. There are three types of calceoli within the Eusiroidea: (i) The “pontogeneiid type 4” has a concave, from crescent-shaped to cup-shaped, proximal element partially overlapping with a large strongly banded distal element, (ii) The “eusirid type 5” has a cup-shaped proximal element well-separated from the distal element, which carries a series of discrete crescentic plates, (iii) The “gammarellid type 6” has a second cup-shaped element between the basic proximal and distal elements (Lincoln and Hurley, 1981).

The Gammarellidae were synonymised with the Calliopiidae, because of their entire telson (Bousfield, 1983). Yet, Barnard (1989) revived the family using calceolus morphology and arrangement as synapomorphy. He grouped the genera *Gammarellus*, *Chosroes*, *Gondogeneia* and *Austroregia* based on the type 6 calceolus (gammarellid type) (Barnard, 1989). Later, two types of calceoli were observed on the antennae of *G. angulosus*: small gammarellid-type 6 and large pontogeneiid-type 4 (Steele and Steele, 1993). But, the genus *Gammarellus* is excluded from the Eusiroidea in our analyses (Fig. 3). Nevertheless, the gammarellids *A. regis* and *Chosroes* aff. *decoratus* form a well-supported clade (clade 9) within the Eusiroidea in the 18S tree (Fig. 3B). These genera do not possess accessory flagella, but were classified in Gammarellidae because of the type 6 calceoli.

The families Iphimediidae, Epimeridae, Acanthonotozomellidae, Stilipedidae, and Astyridae (clade 3 and the iphimediid lineage of clade 7) and the northern Pleustidae lineage were recorded as not calceoliferous (Lincoln and Hurley, 1981). A synapomorphy of clade 6 might be the eusirid-type 5 calceoli (Fig. 3A) — this state was recorded in *Rhachotropis* and *Eusirus* species, but is not verified for *E. georgiana*. Finally, the pontogeneiid-type 4 calceoli have been observed in *C. laevisculus*, *Apherusa* and *Halirages* species. This state might be a synapomorphy of clade 2, with only *P. hystrix* which would have lost the calceoli. Additional data are, however, needed to clarify the evolution of the calceoli within the Eusiroidea.

EUSIRIDAE AND CARNIVORY-ASSOCIATED CHARACTERS. Following the restricted definition of Eusiridae of Bousfield & Hendrycks (1995), the family appears monophyletic in the 28S tree (clade 6 in Fig. 3A). The external placement of *E. georgiana* on the 18S phylogeny may be due to LBA (Fig. 3B).

The family Eusiridae can be defined on the basis of several synapomorphies associated with carnivory. Although ecological data are only available for some species (Dauby et al., 2001b; Krapp et al., 2008), it seems that Eusiridae prey on various benthic invertebrates or small fast moving crustaceans in the water column. As such, they have large subsimilar raptorial gnathopods, with a lobate carpus and an enlarged propodus, allowing to rapidly capture preys. This character state appeared convergently in other eusiroid clades: clade 1 (*Pleustes panoplus*), clade 2 (*C. laevisculus*) and clade 8 (*B. gigantea*). The mouthparts of Eusiridae are also typically modified in relation to carnivory (well-developed molar, strong and dentate incisor and dentate left lacinia on the mandible; strong maxillipedal palp). However, these mouthpart characters are homoplasious within Eusiroidea. The abdominal segments, pleopods and tailfan of Eusiridae are typically large and strongly developed, allowing rapid propulsion and change in direction. Deep-water Eusiridae have in addition slender, long-dactylate peraeopods allowing to stand on soft bottoms, awaiting prey (Bousfield and Hendrycks, 1995b). The elongated and cleft telson in this family could also be an adaptation to pelagic or epibenthic life style (Bousfield and Shih, 1994). All the characters linked to the mode of nutrition or life style are very likely to appear convergently under similar selection pressures and have been demonstrated to be highly homoplasious within Amphipoda (Browne et al., 2007; Corrigan et al., 2014; Havermans et al., 2011; Serejo, 2004).

PLEUSTIDAE AND THE SHAPE OF THE LABIUM. Pleustidae share many character states with Eusiridae, similar mouthparts and gnathopods presumably specialized in relation to carnivory and raptorial feeding behavior. They have a deeper-plated body shape than most other Eusiroidea, and their body is often toothed or carinated (Bousfield and Hendrycks, 1994b). Pleustidae are recognized as a distinct family because they show several typical alleged synapomorphies: (i) the special shape of

the labium with its inner, wide lobes and its outer lobes that are tilted inward (Barnard and Karaman, 1991), (ii) the variously notched labrum, with subequal to asymmetrical lobes, and (iii) the plate-like telson with a ventral keel (Bousfield and Hendrycks, 1994b).

The three northern Pleustidae species of the genera *Neopleustes*, *Pleustes* and *Incisocalliope*, form a well-supported clade (clade 1, Fig. 3) in the 28S tree. *Austropleustes cuspidatus*, is not part of this clade and appears more closely related to Calliopiidae and Pontogeneiidae species (*Atyloella tribinicuspidata* and *Paramoera* sp.). *Austropleustes* is the only pleustid genus found exclusively in the Southern Ocean, while the family is essentially holarctic. The two species of the genus (*A. cuspidatus* and *A. simplex*) possess the typical pleustid mouthparts and keeled telson, while they depart from the "pleustid type" in several other aspects: their gnathopods are quite feeble, weakly subchelate, with elongated and subequal carpus and propodus, their coxae are short and their telson is notched or weakly cleft (Barnard, 1931, 1932). The position of *A. cuspidatus* in the trees suggests that the three pleustid characters (see above) are homoplasious.

THE IPHIMEDIOID COMPLEX AND THE ARMORED BODY FORM. The following families share an armored body, i.e. a body that is strongly calcified and/or often bears dorsal and lateral teeth and carinae: Acanthonotozomatidae, Amathillopsidae, Astyridae, Stilipedidae, Epimeriidae, Iphimediidae, Odiidae, Acanthonotozomellidae and Dikwidae. They have been historically treated together as a group of morphologically similar, yet often ill-defined, families with unknown phylogenetic relationships (Coleman and Barnard, 1991). Consequently, their classification has often changed over time. They have been successively merged in an extended concept of the family Iphimediidae (Barnard and Karaman, 1991) and rediagnosed as separate families (Coleman and Barnard, 1991). All these families, except for the Stilipedidae and Astyridae, were later reorganized into three families (Epimeriidae, Iphimediidae and Odiidae), which together formed the superfamily Iphimedioidea (Lowry and Myers, 2000). Yet, this classification was not generally accepted because the processiferous morphology was suspected to appear convergently (Macdonald III et al., 2005; Sherbakov et al., 1999; Sherbakov et al., 1998). Therefore, these nine families were kept separated in subsequent classifications (Coleman, 2007; De Broyer and Jażdżewski, 1993), with two changes: the Odiidae were synonymized with the Ochlesidae (Berge et al., 1999) and *Acanthonotozomopsis* was transferred to the Vicmusiidae (Just, 1990).

Our analyses show that the families Acanthonotozomellidae, Astyridae, Epimeriidae, Dikwidae, Stilipedidae and Vicmusiidae form the well-supported clade 3 (Fig. 3). All families of clade 3 share some putative synapomorphies: (1) odd-numbered dorsal processes (except for *Acanthonotozomopsis*), usually associated with an enhanced calcification of the tegument; (2)

general tendency towards acumination of the first four coxae; (3) processes on the peduncular articles of the antennae; (4) bases of pereiopods 5–7 with posterior lobes or processes and/ or posteriorly concave (except for *Acanthonotozomopsis*); (5) maxilla 1 bearing a strong palp with an elongated or enlarged article 2 (greatly enlarged in Stilipedidae); and (6) notched, sometimes asymmetric labrum. *Acanthonotozomopsis pushkini* has a very modified morphology. This latter species does not possess dorsal processes, but laterally divided pereonal and pleonal tergites, which is an autapomorphy (Just, 1990).

The monophyletic family Iphimediidae is not part of clade 3 and appears more closely related to amphipods with a smooth or weakly toothed body (calliopiids, pontogeneiids and the austral pleustid *Austropleustes*), and especially the *Oradarea* species (Clades 4 and 7, Fig. 3). Nevertheless, Iphimediidae share many of the morphological features related to the "armored morphology" with the families of clade 3: a strong calcification of the integument and a processiferous body (although the dorsal processes of Iphimediidae are paired), processes on the peduncular articles of the antennae; and the tendency towards acumination of the first coxae and of the bases of pereiopods 5–7.

The Amathillopsidae do not belong to clade 3 and the phylogenetic relationships between *Parepimeria* and *Amathillopsis*, as well as with other eusiroids, are mostly unresolved. These two genera were associated with the iphimedioid complex mainly because they possess dorsal teeth (both paired and odd-numbered) and acuminated anterior coxae.

Acanthonotozoma serratum (Acanthonotozomatidae) is neither part of clade 3 and phylogenetic affinities with other eusiroid taxa are mostly unresolved. The most processiferous species of the genus *Acanthonotozoma* possess many of the morphological features related to the "armored morphology": the (odd-numbered) dorsal processes, the deep and acuminate coxae 1–4, the frequent presence of posterior cusps on the bases of pereiopods 5–7 and rarely weak processes on the peduncles of antennae.

As stated before, DNA data indicate that *Odius carinatus* (Ochlesidae) is not part of Eusiroidea, but is nested within a lysianassoid clade. Ochlesidae have been misleadingly associated with the armored eusiroids, mostly because of phenetic similarities with the Dikwidae: their head is similarly telescoped into pereonite 1, the inner plate of the first maxilla is reduced and the palm of the first gnathopod is similar (Berge et al., 1999). Ochlesidae are generally not very processiferous amphipods, with usually no or weak dorsal projections. Some *Curidia*, *Ochlesodius*, *Meraldia* and

Ochlesis spp. have processes on the peduncular articles on the antennae and on the bases of pereiopods 5–7 (Coleman and Lowry, 2006).

Hence, overall, these DNA data indicate that the character states associated with an "armored" body (i.e. dorsal projections, strong calcification of the integument, processes on the peduncles of the antennae, acumination of the coxae and the bases of the pereiopods 5–7), are homoplasious. The armored form could be adaptive and may appear convergently under predation pressure (Moore, 1981). The processiferous amphipods are hypothetically less palatable for predators, as the spines prick in their mouth and digestive tracks. Moreover, the highly calcified teguments could be more difficult to digest. Finally, in some cases, the hedgehog-like morphology may also act as a camouflage for commensal amphipods on sponges, such as *Echiniphimedia hodgsoni* (Coleman, 1989b) or *Paramphithoe hystrix* (Oshel and Steele, 1985).

THE SENTICAUDATE CHARACTER. The taxa forming the clades 1, 2, 4, 8 and 9 present the "senticaudate" character state i.e. apical spines (or "robust setae") on the rami of uropods 1–2 (Lowry and Myers, 2013) (Fig. 3). It is also observed in species of clade 7 (*Oradarea* and *Liouvillea*) and in some species of uncertain position in our trees (*Schraderia gracilis*, the *Prostebbingia* clade and *Acanthonozoma serratum*). According to these results, this character state would appear or disappear convergently, but could have a phylogenetic significance at less inclusive levels than the suborder.

CONCLUSIONS

Using two rDNA gene sequences, this study reconstructed a phylogeny of the superfamily Eusiroidea. Phylogenetic uncertainties prevented a supported delimitation of the superfamily. However, our results suggest that at least species of 14 traditional families would be included in a Eusiroidea clade, increasing by more than twofold the species and generic richness of Eusiroidea sensu De Broyer (2007). Hence, the Eusiroidea would be one of the most speciose amphipod superfamilies. The monophyly of most of the putative and traditional eusiroid families is refuted herein (except for Iphimediidae), including the Calliopiidae, Pontogeneiidae, Eusiridae, Gammarellidae, and Pleustidae, whereas there is insufficient evidence to assess the monophyly of the remaining families. Most of the morphological characters, traditionally used in the classification of the Eusiroidea, appear to be highly homoplasious (e.g. the shape of the telson, the processiferous/armored morphology). Several taxa that were previously classified as eusiroids are excluded from the superfamily: *Gammarellus angulosus* (Gammarellidae), *Cleippides quadricuspis* (Calliopiidae), *Weyprechtia pinguis* (Calliopiidae) and *Odius carinatus* (Ochlesidae). These results

indicate that an extensive reassessment of eusiroid families and phylogenetic relationships is essential before a comprehensive classification of the superfamily can be established. Ultimately, increased taxon sampling and the inclusion of additional DNA data in future molecular studies are necessary to reconstruct a robust phylogeny of Eusiroidea.

ACKNOWLEDGEMENTS

The first author has a PhD fellowship from F.R.I.A. (F.N.R.S., Belgium). The last author was supported by an “Action 1” research project (contract number MO/36/022) and two successive complementary “Additional Scientist” contract, funded by BELSPO. We thank the Alfred Wegener Institute for Polar and Marine Research, Bremerhaven for the invitation to participate in the expeditions ANT-XXI/2, ANT-XXIV/2 and ANT-XXVII/3 and the crew of the *RV Polarstern* for their professional help during the cruises. We are indebted to Anne-Nina Lörz (National Institute for Water and Atmospheric Research, New Zealand) for providing specimens collected during the IPY-CAML expedition in 2008 undertaken by the National Institute for Water and Atmospheric Research. We thank Laure Corbari from the Museum national d’Histoire naturelle, Paris, for providing specimens collected during the REVOLTA 3 (2012) expedition in Terre Adélie and Bathus 3 (1993) in New Caledonia. Thanks also to David Barnes from the British Antarctic Survey (BAS) for providing specimens from the BIOPEARL I expedition of 2006 and to Dirk Schories (Meeresforschung, MGS, Forschungszentrum, Jülich GmbH) for providing shallow-water species from King George Island. We are grateful to Zohra Elouaazizi, Karin Breugelmans, Gontran Sonet and Zoltan Nagy (all RBINS) for helpful advices.

CHAPTER 2

LOOKING BENEATH THE TIP OF THE ICEBERG: DIVERSIFICATION OF THE GENUS *EPIMERIA* ON THE ANTARCTIC SHELF (CRUSTACEA, AMPHIPODA)

Marie L. Verheye[1,2]

Thierry Backeljau[1,3]

Cédric d'Udekem d'Acoz[1]

Published in: ***Polar Biology*** **(2016) 39 (5):925–945**

[1] Royal Belgian Institute of Natural Sciences, OD Taxonomy and Phylogeny, 29 rue Vautier, B-1000 Brussels, Belgium

[2] Catholic University of Louvain-la-Neuve, Department of Biology, Marine Biology Laboratory, 3 bte L7.06.04 Croix du Sud, B-1348 Louvain-la-Neuve, Belgium

[3] University of Antwerp, Evolutionary Ecology Group, 171 Groenenborgerlaan, 2020 Antwerp, Belgium

ABSTRACT

The amphipod genus *Epimeria* is very speciose in Antarctic waters. Although their brooding biology, massive and heavily calcified body predict low dispersal capabilities, many *Epimeria* species are documented to have circum-Antarctic distributions. However, these distribution records are inevitably dependent on the morphological species definition. Yet, recent DNA evidence suggests that some of these *Epimeria* species may be complexes of species with restricted distributions. Mitochondrial COI and nuclear 28S rDNA sequence data were used to infer evolutionary relationships among 16 nominal *Epimeria* species from the Antarctic Peninsula, the eastern Weddell Sea and the Adélie Coast. Based on this phylogenetic framework, we used morphology and the DNA-based methods GMYC, bPTP and BPP to investigate species boundaries, in order to revise the diversity and distribution patterns within the genus. Most of the studied species appeared to be complexes of pseudocryptic species, presenting small and previously overlooked morphological differences. Altogether, 25 lineages were identified as putative new species, increasing twofold the actual number of Antarctic *Epimeria* species. Whereas most of the species may be geographically restricted to one of the three studied regions, some still have very wide distribution ranges, hence suggesting a potential for large-scale dispersal.

INTRODUCTION

As a consequence of its distinctive oceanographic and tectonic history, the Southern Ocean underwent prolonged isolation, which resulted in high levels of endemism of its biota. Several major taxa (e.g. pycnogonids, polychaetes, ascidians and peracarid crustaceans) are also unusually speciose compared to non-Antarctic marine ecosystems (Kaiser et al., 2013). Moreover, the Antarctic shelf biodiversity is probably still grossly underestimated, since in the last decade, a plethora of molecular studies detected cryptic species complexes in a wide variety of organisms, such as polychaetes (Schüller, 2011), nemerteans (Mahon et al., 2008; Thornhill et al., 2008), molluscs (Allcock et al., 2011; Linse et al., 2007), arthropods (e.g. Arango et al., 2011; Baird et al., 2011; Raupach et al., 2007) and echinoderms (Hemery et al., 2012; Janosik and Halanych, 2010). Various physical factors, such as glacial cycles, bathymetry, oceanography, geomorphology or habitat may contribute to these patterns of previously undetected biodiversity (Rogers, 2007). As a result, the Southern Ocean paradigm of a largely connected circum-Antarctic fauna is often challenged, when putatively circum-Antarctic species show geographic population genetic structuring and/or local cryptic taxonomic diversity (Riesgo et al., 2015).

However, the delimitation of species remains challenging for systematics. The features that are generally used as indicative of isolation or common ancestry (e.g. geographic distributions, ecological differentiation, DNA sequence divergence, morphological differences) are often difficult to interpret objectively. For instance, proponents of the biological species concept (BSC) have to decide which degree of morphological or molecular divergence reflects intrinsic reproductive isolation (Fujita et al., 2012). A variety of statistical methods have recently been proposed to detect independently evolving lineages (putative species) by fitting models of historical diversification to DNA sequence data, e.g. GMYC (Pons et al., 2006), spedeSTEM (Ence and Carstens, 2011), BPP (Yang and Rannala, 2010), PTB (Zhang et al., 2013). However, it remains difficult to decide which may be the most suitable method to use on empirical data. Therefore, it is recommended to use several methods and look for consistencies (Carstens et al., 2013; Miralles and Vences, 2013; Satler et al., 2013). Such DNA-based species delimitation methods could play an important role within an integrative taxonomic framework that relies on multiple and complementary data types (Dayrat, 2005; Padial et al., 2010; Schlick-Steiner et al., 2010; Sites and Marshall, 2004), by reducing investigator-driven biases, hence stabilizing taxonomic inferences (Fujita et al., 2012).

With a total of 54 described species, *Epimeria* Costa, 1851 is a globally distributed genus of marine amphipods that is particularly diverse in the Southern Ocean (26 species). Being large (20 to 70 mm) and common amphipods, epimeriids have attracted substantial attention in systematic studies of Antarctic amphipods. Coleman (2007) published a synopsis, compiling short descriptions of the 25 species of Antarctic Epimeriidae Boeck, 1871 known at that time: one species of *Actinacanthus* (Stebbing, 1883), 18 species of *Epimeria*, four species of *Epimeriella* Walker, 1906 [a genus subsequently synonymized with *Epimeria* (Lörz et al., 2009)], one species of *Metepimeria* Schellenberg, 1931, and one species of *Uschakoviella* Gurjanova, 1955. Four additional species of *Epimeria* were subsequently described (Lörz, 2009; Lörz et al., 2007, 2009, 2011).

Based on distribution records from the Antarctic Peninsula, the eastern Weddell Sea, the Ross Sea and the Adélie Coast, at least 10 *Epimeria* species [*Epimeria georgiana* Schellenberg, 1931*, E. grandirostris* (Chevreux, 1912), *E. inermis* Walker, 1903, *E. macrodonta* Walker, 1906, *E. puncticulata* K.H. Barnard, 1930, *E. macronyx* (Walker, 1906)*, E. robusta* K.H. Barnard, 1930*, E. walkeri* K.H. Barnard, 1930*, E. scabrosa* (K.H. Barnard, 1930) and *E. similis* Chevreux, 1912] were believed to have a circum-Antarctic distribution (Coleman, 2007; De Broyer et al., 2007). However, molecular evidence suggests that several of these nominal species may in fact represent complexes of distinct species with restricted distributions: (1) *Epimeria schiaparelli* Lörz, Maas, Linse & Fenwick, 2007 was described from the Ross Sea and may have been confounded in the past with the morphologically

similar *Epimeria similis* (Lörz et al., 2007). (2) The COI phylogeny of Lörz et al. (2009) showed that *Epimeria robusta*, which was first described as a widely distributed species (Coleman, 1994) in fact includes two morphologically similar, yet distinct species: *Epimeria robustoides* Lörz & Coleman, 2009 was described from the Weddell Sea, whereas the type specimen of *E. robusta* comes from the Ross Sea. (3) Uncorrected COI p-distances of 5 % separated *Epimeria walkeri* from the Ross Sea and the Weddell Sea, which exceeds the intraspecific threshold sequence divergence of < 2.5 % observed in other *Epimeria* species. The morphology of these specimens was, however, not examined (Lörz et al., 2009). (4) *Epimeria georgiana* may also represent a complex of several species, since a COI phylogeny revealed four clades separated by 2.49–22.46 % K2P distances: three in the Scotia Arc area and one in the eastern Weddell Sea. This latter clade shows conspicuous morphological differences with the original description of *E. georgiana*, and was therefore recently described as *Epimeria angelikae* Lörz & Linse, 2011.

Aforementioned studies were carried out on a limited geographical scale and focused on one or a few *Epimeria* taxa. Therefore, extending the geographic and taxonomic scope of *Epimeria* studies is likely to reveal even more (overlooked) taxonomic diversity. Hence, in the present study, we implement the first phylogenetic analysis of the genus, based on 16 of the 26 known Antarctic *Epimeria* species and covering three main regions on the Antarctic shelf (Antarctic Peninsula area, eastern Weddell Sea and Adélie Coast). Phylogenies were inferred using nuclear and mitochondrial DNA sequence data in order to further examine the genetic structure and distribution patterns of Antarctic *Epimeria*. Our aims were to (1) infer phylogenetic relationships of Antarctic *Epimeria* species, to assess the monophyly of morphological species *sensu* Coleman (2007), (2) use recent DNA sequence-based species delimitation methods and morphological data to determine whether nominal species may involve complexes of different species, and (3) determine whether *Epimeria* species have circum-Antarctic or geographically-restricted distributions.

MATERIAL AND METHODS

TAXON SAMPLING

Samples were collected during several expeditions of the *R.V. Polarstern*: ANT-XXIX/3 in the Drake Passage, Bransfield Strait and the eastern coast of the Antarctic Peninsula, ANT-XXIV/2 and ANT-XXVII/3 in the eastern Weddell Sea. Additional specimens were sampled from the Adélie Coast during the CEAMARC and REVOLTA expeditions (Table 1). All specimens were preserved in 96 % ethanol for DNA analysis. Vouchers are deposited at the Royal Belgian Institute of Natural Sciences

(RBINS, Brussels, Belgium) and the Muséum national d'Histoire naturelle (MNHN, Paris, France) (Table 1).

METHODOLOGY

The monophyly of species and eventual cryptic lineages within the species were assessed as follows: (1) Specimens were preliminary identified to species or species complexes using the handbook of Coleman (2007). Specimens belonging to species complexes were labeled "aff" as a reference to the morphologically most similar described species. Specimens with characters that did not comply with existing species descriptions were tentatively interpreted as representing undescribed, new species and were therefore provisionally assigned the label "sp. nov.". (2) Phylogenetic trees were reconstructed with the separated and concatenated DNA sequence datasets (28S rDNA and COI). (3) Clades were assigned MOTU names (e.g. MA1 for *Epimeria* aff. *macrodonta* MOTU 1). (4) The species status of these MOTUs was evaluated using three different species delimitation methods. In parallel, the morphology of the specimens was thoroughly re-examined [see d'Udekem d'Acoz and Verheye (*In Press*) for details of morphological analyses]. (5) A MOTU was identified as a putative species if most DNA-based methods and morphology gave congruent results regarding its delimitation. Incongruences between the mitochondrial and nuclear loci were discussed.

DNA SEQUENCING

DNA was extracted from the pleopods and abdomen muscles using a NucleoSpin® Tissue kit (Macherey-Nagel) following the manufacturer's protocol for animal tissues. The DNA was eluted in 100 µl of sterile distilled H_2O (RNase free), and stored at -20°C.

Because of differing properties of mitochondrial and nuclear genes (e.g. rates of evolution, inheritance pathway, ploidy), phylogenetic conflicts can arise between the inferred gene trees (Toews and Brelsford, 2012). In order to reduce the risk of erroneously interpreting artefactual relationships, the mitochondrial cytochrome c oxidase subunit I (COI) and nuclear 28S rDNA genes were used in combination. Partial segments of COI (~550 bp) and 28S (~1400 bp) genes were amplified by PCR. Amplifications were performed in a 25-µl reaction mix, which contained 0.15 µl Taq DNA Polymerase (5 U μl^{-1}; Quiagen, Antwerp, Belgium), 2.5 µl 10x CoralLoad PCR Buffer (Quiagen, Antwerp, Belgium), 2.5 µl dNTPs mix (250 µM of each), 11–16 µl RNase-free water, 1.25 µl of each primer (2 µM), and 1–6 µl of DNA extract. In order to increase the yield of COI amplifications, 0.25 µl of Bovine Serum Albumin (BSA Acetylated, 10 mg ml^{-1}; Biolabs, Ipswich, MA, USA) was added to the reaction.

Specimens ID code	Species with clade id code	Locality	Expedition	Station	Latitude	Longitude	Voucher ID	Genbank accession number	
								COI	28S
	EPIMERIIDAE								
A20	*Epimeria* aff. *macrodonta* MA1	Peninsula, Larsen B	ANT-XXVII/3	248-2	65°57.51'S	60°28.15'W	RBINS INV.132655	KU870817	KU759589
I7	*Epimeria* aff. *macrodonta* MA1	Peninsula, Larsen B	ANT-XXVII/3	248-2	65°57.51'S	60°28.15'W	RBINS INV.132975	KU870851	KU759628
I6	*Epimeria* aff. *macrodonta* MA1	Peninsula, Larsen A	ANT-XXVII/3	228-3	64°54.96'S	60°31.97'W	RBINS INV.132661	KU870850	KU759627
ANT34	*Epimeria* aff. *macrodonta* MA1	Peninsula, Dundee Island	ANT-XXIX/3	185-3	63°51.34'S	55°41.11'W	RBINS INV.122941	KU870821	KU759593
K4	*Epimeria* aff. *macrodonta* MA2	Adélie Coast	REVOLTA I	007b (sample 249)	66°38.42'S	139°49.72'E	MNHN-IU-2009-2570	KU870872	KU759652
K5	*Epimeria* aff. *macrodonta* MA2	Adélie Coast	REVOLTA III	REVO_064 (collect ID: REVO_481)	66°36.37'S	140°05.07'E	MNHN-IU-2009-2563	KU870876	KU759657
M10	*Epimeria* aff. *macrodonta* MA2	Adélie Coast	REVOLTA II	REVO_162	66°41.12'S	139°56.69'E	MNHN-2014-7325	KU870878	KU759661
M11	*Epimeria* aff. *macrodonta* MA2	Adélie Coast	REVOLTA II	REVO_191	66°40.12'S	139°55.93'E	MNHN-IU-2014-4296	NA	KU759662
I19	*Epimeria* aff. *macrodonta* MA3	Peninsula, Dundee Island	ANT-XXIX/3	164-4	63°37.28'S	56°09.11'W	RBINS INV.132974	KU870844	KU759621
K36	*Epimeria* aff. *macrodonta* MA3	Peninsula, North of Joinville Island	ANT-XXIX/3	116-9	62°33.79'S	56°27.81'W	RBINS INV.122929B	KU870868	KU759648
K35	*Epimeria* aff. *macrodonta* MA3	Peninsula, North of Joinville Island	ANT-XXIX/3	116-9	62°33.79'S	56°27.81'W	RBINS INV.122929A	NA	KU759647
ANT35	*Epimeria* aff. *macrodonta* MA3	Peninsula, Erebus and Terror Gulf	ANT-XXIX/3	162-7	63°58.78'S	56°46.24'W	RBINS INV.122940	NA	KU759594
I17	*Epimeria* aff. *macrodonta* MA4	Bransfield Strait East	ANT-XXIX/3	193-8	62°43.73'S	57°29.04'W	RBINS INV.132660	NA	KU759619
N1	*Epimeria* aff. *macrodonta* MA4	Bransfield Strait East	ANT-XXIX/3	193-8	62°43.73'S	57°29.04'W	RBINS INV.132973	NA	KU759677
I12	*Epimeria* aff. *similis* SI1	Eastern Weddell Sea	ANT-XXVII/3	300-1	70°50,48'S	10°35,28'W	RBINS, INV.132664	NA	KU759614
K31	*Epimeria* aff. *similis* SI2	Bransfield Strait Central	ANT-XXIX/3	217-6	62°53.45‘S	58°13.06‘W	RBINS INV.122931A	KU870865	KU759644
K32	*Epimeria* aff. *similis* SI2	Bransfield Strait Central	ANT-XXIX/3	217-6	62°53.45‘S	58°13.06‘W	RBINS INV.122935	KU870866	KU759645
K6	*Epimeria* aff. *similis* SI3	Adélie Coast	REVOLTA III	Collect ID REVO_449	66°38.00'S	140°42.00'E	MNHN-IU-2009-2532	NA	KU759658
M7	*Epimeria* aff. *similis* SI3	Adélie Coast	CEAMARC	62EV303 (sample CEAMARC 1421)	66°10.57'S	143°20.75'E	MNHN-IU-2014-7321	NA	KU759674
M8	*Epimeria* aff. *similis* SI3	Adélie Coast	CEAMARC	50AEV220 (sample CEAMARC 1384)	66°45.14'S	145°20.07'E	MNHN-IU-2014-4333	NA	KU759675

M9	*Epimeria* aff. *similis* SI3	Adélie Coast	CEAMARC	31EV268 (sample CEAMARC 1643)	66°45.14'S	145°20.07'E	MNHN-IU-2014-4322	NA	KU759676
M5	*Epimeria* aff. *similis* SI3	Adélie Coast	CEAMARC	30EV66 (sample CEAMARC 300)	65°59.83'S	143°38.99'E	MNHN-IU-2014-4340	NA	KU759672
K7	*Epimeria* aff. *similis* SI3	Adélie Coast	REVOLTA III	Collect ID REVO 449	66°38.00'S	140°42.00'E	MNHN-IU-2009-2539	NA	KU759659
P36	*Epimeria similis* SI4	Bransfield Strait East	ANT-XXIX/3	193-8	62°43.73'S	57°29.04'W	RBINS INV.122956A	NA	KU759680
P38	*Epimeria similis* SI4	Bransfield Strait Central	ANT-XXIX/3	217-6	62°53.45'S	58°13.06'W	RINBS INV.122922B	NA	KU759682
ANT37	*Epimeria* aff. *similis* SI5	Bransfield Strait East	ANT-XXIX/3	196-8	62°47.80'S	57°05.35'W	RBINS INV.122942	KU870823	KU759596
I13	*Epimeria* aff. *similis* SI5	Bransfield Strait East	ANT-XXIX/3	193-8	62°43.73'S	57°29.04'W	RBINS INV.132976	KU870839	KU759615
I9	*Epimeria* aff. *similis* SI5	East ern Weddell Sea	ANT-XXVII/3	265-2	70°47.34'S	10°40.39'W	RBINS INV.132665	KU870853	KU759630
P41	*Epimeria* aff. *similis* SI5	East ern Weddell Sea	ANT-XXIV/2	48-1	70°23.94'S	08°19.14'W	RBINS INV.132977	KU870895	KU759684
K39	*Epimeria* aff. *similis* SI5	Bransfield Strait Central	ANT-XXIX/3	217-6	62°53.45'S	58°13.06'W	RBINS INV.122922A	KU870871	KU759651
ANT36	*Epimeria* aff. *similis* SI5	Bransfield Strait East	ANT-XXIX/3	193-9	62°43.50'S	57°27.92'W	RBINS INV.132666	KU870822	KU759595
M6	*Epimeria* aff. *similis* SI5	Adélie Coast	CEAMARC	51AEV215	66°44.86'S	145°26.66'W	MNHN:IU-2014:7324	KU870889	KU759673
I16	*Epimeria* sp. nov. 1 SP1	Eastern Weddell Sea	ANT XXVII/3	263-6	70°38.66'S	10°28.16' W	RBINS INV.132667	KU870842	KU759618
K44	*Epimeria* sp. nov. 2 SP2	Eastern Weddell Sea	ANT-XXIV/2	17-11	70°05.13'S	03°23.50'W	RBINS INV.132663	KU870875	KU759656
ANT48	*Epimeria* aff. *puncticulata* PUN1	Bransfield Strait	ANT-XXIX/3	197-6	62°45.05'S	57°26.68'W	RBINS INV.122947	NA	KU759607
K42	*Epimeria* aff. *puncticulata* PUN1	Peninsula, Dundee Island	ANT-XXIX/3	164-5	63°36.84'S	56°10.28'W	RBINS INV.122934	NA	KU759655
I2	*Epimeria* aff. *puncticulata* PUN2	Peninsula, Larsen B	ANT-XXVII/3	248-2	65°57.51'S	60° 28.15'W	RBINS INV.132651	KU870845	KU759622
K33	*Epimeria* aff. *puncticulata* PUN3	Adélie Coast	REVOLTA III	REVO_084 (Collect ID REVO_477)	66°39.28'S	139°55.85'E	MNHN-IU-2009-2578	KU870867	KU759646
M4	*Epimeria* aff. *puncticulata* PUN4	Adélie Coast	CEAMARC	65EV322 (sample CEAMARC 2072)	65°48.48'S	143°03.76'E	MNHN-IU-2014-4288	KU870888	KU759671
M3	*Epimeria* aff. *puncticulata* PUN4	Adélie Coast	CEAMARC	65EV322 (sample CEAMARC 2072)	65°48.48'S	143°03.76'E	MNHN-IU-2014-4288	NA	KU759670
A6	*Epimeria* aff. *walkeri* WA1	King George Island	ANT-XXVII/3	222-5	62°18.21'S	58° 39.90'W	RBINS INV.132667	KU870819	KU759591
Ex169	*Epimeria* aff. *walkeri* WA1	Eastern Weddell Sea	ANT-XXVII/3	288-3	70° 56.40'S	10° 32.60'W	Specimen missing	KU870836	KU759610
ANT42	*Epimeria* aff. *walkeri* WA1	Bransfield Strait Central	ANT-XXIX/3	217-7	62° 53.64'S	58° 12.52'W	RBINS INV.122944	KU870828	KU759601
K40	*Epimeria* aff. *walkeri* WA2	Bransfield Strait East	ANT-XXIX/3	197-5	62° 44.73'S	57° 26.79'W	RBINS INV.122932	KU870873	KU759653

ANT43	*Epimeria* aff. *walkeri* WA3	Drake Passage West	ANT-XXIX/3	234-5	62°17.36'S	61°12.06'W	RBINS INV.122949	KU870829	KU759602
I15	*Epimeria* aff. *walkeri* WA3	Peninsula, South of Joinville Island	ANT-XXIX/3	188-5	63°50.92‘ S	55° 37.66‘W	RBINS INV.132656	KU870841	KU759617
I4	*Epimeria* aff. *walkeri* WA3	Elephant Island	JR144	E1-EBS-SUPRA	61°20.76'S	55°12.14'W	RBINS INV.132959	KU870848	KU759625
M12	*Epimeria* aff. *walkeri* WA4	Adélie Coast	CEAMARC	50AEV220 (sample CEAMARC 1384)	66°45.14'S	145°20.07'E	MNHN-IU-2014-4331	KU870879	KU759663
M13	*Epimeria* aff. *walkeri* WA4	Adélie Coast	CEAMARC	71EV447 (sample CEAMARC 2724)	66°23.99'S	140°32.35'E	MNHN-IU-2014-4336	KU870880	KU759664
ANT38	*Epimeria macronyx* MX1	Drake passage West	ANT-XXIX/3	238-1	62°22.65'S	61°17.63'W	RBINS INV.122943	KU870824	KU759597
ANT39	*Epimeria macronyx* MX1	Drake passage West	ANT-XXIX/3	238-1	62°22.65'S	61°17.63'W	RBINS INV.122943	KU870825	KU759598
M19	*Epimeria macronyx* MX2	Adélie Coast	CEAMARC	51AEV215 (sample CEAMARC 1317)	66°44.86'S	145°26.66'E	MNHN-IU-2014-4276	KU870885	KU759668
ANT41	*Epimeria* aff. *georgiana* GE1	Bransfield Strait East	ANT-XXIX/3	197-5	62° 44.73'S	57°26.79'W	RBINS INV.122867	KU870827	KU759600
I14	*Epimeria* aff. *georgiana* GE1	Drake passage West	ANT-XXIX/3	234-5	62°17.36'S	61°12.06'W	RBINS INV.132970	KU870840	KU759616
I20	*Epimeria* aff. *georgiana* GE1	Peninsula, Dundee Island	ANT-XXIX/3	185-4	63°51.53'S	55°40.74'W	RBINS INV.132971	KU870846	KU759623
K21	*Epimeria* aff. *georgiana* GE1	Bransfield Strait West	ANT-XXIX/3	224-3	63°00.53'S	58°35.67'W	RBINS INV.122926	KU870855	KU759633
K22	*Epimeria* aff. *georgiana* GE1	Bransfield Strait West	ANT-XXIX/3	224-3	63°00.53'S	58°35.67'W	RBINS INV.122924	KU870856	KU759634
K23	*Epimeria* aff. *georgiana* GE1	Peninsula, East of Joinville Island	ANT-XXIX/3	160-3	63°10.57'S	54°06.66'W	RBINS INV.122930A	KU870857	KU759635
K24	*Epimeria* aff. *georgiana* GE1	Peninsula, East of Joinville Island	ANT-XXIX/3	160-3	63°10.57'S	54°06.66'W	RBINS INV. 122933	KU870858	KU759636
K26	*Epimeria* aff. *georgiana* GE1	Peninsula, South of Joinville Island	ANT-XXIX/3	249-2	63°51.34'S	55°41.11'W	RBINS INV.122921A	KU870860	KU759638
K27	*Epimeria* aff. *georgiana* GE1	Peninsula, North of Joinville Island	ANT-XXIX/3	116-9	62°33.79'S	56°27.81'W	RBINS INV.122920	KU870861	KU759639
K28	*Epimeria* aff. *georgiana* GE1	Peninsula, North of Joinville Island	ANT-XXIX/3	116-9	62°33.79'S	56°27.81'W	RBINS INV.122920	KU870862	KU759640
K29	*Epimeria* aff. *georgiana* GE1	Peninsula, Dundee Island	ANT-XXIX/3	164-4	63°37.28'S	56°09.11'W	RBINS INV.122923	KU870863	KU759641
K30	*Epimeria* aff. *georgiana* GE1	Peninsula, Dundee Island	ANT-XXIX/3	164-4	63°37.28'S	56°09.11'W	RBINS INV.122925	KU870864	KU759643
P35	*Epimeria* aff. *georgiana* GE1	Peninsula, South of Joinville Island	ANT-XXIX/3	185-3	63°51.34'S	55°41.11'W	RBINS INV.122921B	KU870893	KU759679
P37	*Epimeria* aff. *georgiana* GE1	Peninsula, South of Joinville Island	ANT-XXIX/3	185-3	63°51.34'S	55°41.11'W	RBINS INV.122921C	KU870894	KU759681
I10	*Epimeria* aff. *georgiana* GE2	South Orkney Islands	ANT-XXIX/3	217-6	61°09.62'S	44°02.37'W	RBINS INV.132658	KU870838	KU759612

K25	*Epimeria* aff. *georgiana* GE3	Drake Passage East	ANT-XXIX/3	249-2	62°53.45'S	58°13.06'W	RBINS INV.122936	KU870859	KU759637
M16	*Epimeria* aff. *georgiana* GE4	Adélie Coast	CEAMARC	67AEV326 (sample CEAMARC 2173)	65°43.12'S	143°03.61'E	MNHN-IU-2014-4344	KU870882	KU759665
M17	*Epimeria angelikae* GE5	Adélie Coast	CEAMARC	86EEV518 (sample CEAMARC 3410)	65°28.85'S	139°24.18'E	MNHN-IU-2014-4278	KU870883	KU759666
M18	*Epimeria angelikae* GE5	Adélie Coast	CEAMARC	32AEV400 (sample CEAMARC 2271)	65°52.74'S	144°10.92'E	MNHN-IU-2014-4281	KU870884	KU759667
M24	*Epimeria rimicarinata* RI	Prydz Bay	MD42	22	66°55.75'S	74°04.19'E	MNHN-IU-2014-4265	KU870887	NA
I5	*Epimeria rubrieques* RU	Eastern Weddell Sea	ANT-XXVII/3	265-2	70°47.34'S	10° 40.39'W	RBINS, INV.132668	KU870849	KU759626
K41	*Epimeria rubrieques* RU	Eastern Weddell Sea	ANT-XXIV/2	48-1	70°23.94'S	08°19.14'W	RBINS INV.132643	KU870874	KU759654
ANT44	*Epimeria inermis* IN1	Bransfield Strait West	ANT-XXIX/3	227-2	62°55.83'S	58°41.09'W	RBINS INV.122948	KU870830	KU759603
ANT45	*Epimeria inermis* IN1	Bransfield Strait West	ANT-XXIX/3	224-3	63°00.53‘S	58°35.67'W	RBINS INV.122945	KU870831	KU759604
I18	*Epimeria inermis* IN1	Bransfield Strait Central	ANT-XXIX/3	199-4	62°57.22'S	58°14.60'W	RBINS INV.132953	KU870843	KU759620
I11	*Epimeria inermis* IN2	Eastern Weddell Sea	ANT-XXVII/3	281-1	70°48.93'S	10° 32.69'W	RBINS INV.132655	NA	KU759613
K2	*Epimeria inermis* IN2	Adélie Coast	REVOLTA III	REVO_032 (Collect ID REVO_509)	66°39.31'S	140°01.63'E	MNHN-IU-2009-2531	NA	KU759632
K3	*Epimeria inermis* IN2	Adélie Coast	REVOLTA I	REVO_020b (sample 143)	66°40.50'S	139°55.07'E	MNHN-IU-2009-2569	NA	KU759642
M1	*Epimeria inermis* IN2	Adélie Coast	CEAMARC	42EV167 (sample CEAMARC 971)	66°53.36'S	142°38.90'E	MNHN-IU-2014-4272	KU870877	KU759660
M2	*Epimeria inermis* IN2	Adélie Coast	CEAMARC	71EV447 (sample CEAMARC 2724)	66°23.99'S	140°32.35'E	MNHN-IU-2014-4338	KU870886	KU759669
I3	*Epimeria inermis* IN3	Eastern Weddell Sea	ANT-XXIV/2	48-1	70°23.94'S	8°19.14'W	RBINS INV. 132654	KU870847	KU759624
ANT33	*Epimeria* aff. *robustoides* RO1	Bransfield Strait East	ANT-XXIX/3	196-8	62°47.80'S	57°05.35'W	RBINS INV.122937A	KU870820	KU759592
ANT40	*Epimeria* aff. *robustoides* RO1	Bransfield Strait West	ANT-XXIX/3	227-2	62°55.83'S	58°41.09'W	RBINS INV.122939	KU870826	KU759599
K37	*Epimeria* aff. *robustoides* RO1	Bransfield Strait Central	ANT-XXIX/3	217-6	62°53.45'S	58°13.06'W	RBINS INV.122927	KU870869	KU759649
K38	*Epimeria* aff. *robustoides* RO1	Bransfield Strait Central	ANT-XXIX/3	217-6	62°53.45'S	58°13.06'W	RBINS INV.122928	KU870870	KU759650
Ex114	*Epimeria robustoides* RO2	Eastern Weddell Sea	ANT-XXVII/3	265-2	70°47.34'S	10°40.39'W	RBINS-INV.122894	KU870834	KU759608
I8	*Epimeria robustoides* RO2	Eastern Weddell Sea	ANT-XXIV/2	48-1	70°23.94'S	8°19.14'W	RBINS INV.132969	KU870852	KU759629
K1	*Epimeria robusta* RO3	Adélie Coast	REVOLTA 1	REVO-043	66°38.46'S	140°01.84'E	MNHN-IU-2009-2571	KU870854	KU759631
ANT46	*Epimeria grandirostris* GR1	Peninsula, Dundee Island	ANT-XXIX/3	185-3	63°51.34'S	55°41.11'W	RBINS INV.122946	KU870832	KU759605

ANT47	*Epimeria grandirostris* GR1	Bransfield Strait East	ANT-XXIX/3	197-6	62°45.05'S	57°26.68'W	RBINS INV.122950	KU870833	KU759606
P40	*Epimeria* aff. *grandirostris* GR2	Adélie Coast	CEAMARC	36EV297 (sample CEAMARC 3978)	66°20.33'S	143°41.13'E	MNHN-IU-2014-4327	NA	KU759683
M14	*Epimeria* aff. *pulchra* PUL1	Adélie Coast	CEAMARC	28EV53 (sample "CEAMARC V3 st. 158")	65°59.78'S	143°02.95'E	MNHN-IU-2014-4284	KU870881	NA
N7	*Epimeria oxicarinata* OX	Elephant Island	ANT-XXIII/8	605-5	60°52.37'S	55°29.80'W	RBINS INV.122468	KU870891	NA
N8	*Epimeria oxicarinata* OX	Elephant Island	ANT-XXIII/8	605-3	61°20.33'S	55°31.53'W	RBINS INV.122483	KU870892	NA
I1	*Epimeria annabellae*	East ern Weddell Sea	ANT-XXVII/3	281-1	70° 50.56'S	10°36.20'W	RBINS INV.132652	KU870897	KU759611
N2	*Epimeria annabellae*	Eastern Weddell Sea	ANT-XXIII/8	603-5	70°30.99'S	08°48.08'W	RBINS INV.122476	KU870890	KU759678
	IPHIMEDIIDAE								
Ex154	*Gnathiphimedia sexdentata*	Eastern Weddell Sea	ANT-XXVII/3	286-1	70°50.64'S	10° 36.11'W	RBINS INV.132752	KU870835	KU759609

Table 1. Sampling details for the sequenced *Epimeria* specimens (sample location, voucher number and GenBank accession number). Underlined species names indicate described species.

The COI fragment was amplified using the primers Cp-COIF3 (Pilar Cabezas et al., 2013) and COI2R (Otto and Wilson, 2001). The thermal cycling used for the COI was as follows: initial 4-min denaturation at 94°C, followed by 40 cycles of 45 s at 94°C, 1 min at 51°C and 1 min at 72°C. The amplification ended with a final extension step at 72°C for 10 min.

The 28S rDNA fragment was amplified using the primers 28S-3311F (Witt et al., 2006) and 28R (Hou et al., 2007), modified as follows: 5'-GGGACTACCCGCTGAACTTAAGCAT-3' and 5'-GTCTTTCGCCCCTATGCCCAACTG-3'. PCR amplification settings for 28S rDNA consisted of an initial denaturation for 3 min at 94 °C, followed by 40 cycles of denaturation at 94°C for 40 s, annealing at 45°C for 40 s, extension at 72°C for 90 s, and a final extension at 72°C for 10 min.

The PCR products were visualized under blue light on 1.2 % agarose gel stained with SYBR Safe (ThermoFisher Scientific,Waltham, MA, USA), with a comigrating 200-bp ladder molecular-weight marker to confirm their correct amplification. Prior to sequencing, PCR products were purified using Exonuclease I (20 U μl^{-1}) and FastAP^{TM} Thermosensitive alkaline phosphatase (1 U μl^{-1}) (ThermoFisher Scientific, Waltham, MA, USA), following the manufacturer's protocol. Forward and reverse strands were sequenced with fluorescent-labeled dideoxynucleotide terminators (BigDye v.3.1; Applied Biosystems, Foster City, CA, USA) following the protocol of Sanger et al. (1997) and using an automated ABI 3130xl DNA analyzer (Applied Biosystems, Foster City, CA, USA). Both fragments were sequenced using the PCR primers.

PHYLOGENETIC ANALYSES

Sequence chromatograms were checked, and forward and reverse sequence fragments were assembled using *Codoncode Aligner* v.3.7.1. (CodonCode Corporation, available from http://www.codoncode.com/aligner/). All sequences have been deposited in GenBank (Table 1).

28S sequences were aligned with MAFFT v.7 (Katoh and Standley, 2013) (available from http://mafft.cbrc.jp/alignment/server/), using the structural alignment strategy Q-INS-i under default settings. As some regions of the 28S sequences were too divergent to be confidently aligned, the software program Aliscore v.2.0. (Misof and Misof, 2009) was used to identify poorly aligned regions for removal with Alicut v.2.3, prior to further analysis. CLUSTALW was used to align the COI sequences in MEGA6 (Tamura et al., 2013). In order to prevent inclusion of pseudogenes in the analyses, amino acid translations of the COI sequences were checked for stop codons. Uncorrected COI p-distances were calculated with MEGA6 and GTR+G+I distances were estimated by Maximum Likelihood (ML) with Paup*4.0b10 (Swofford, 2003), using the parameter values estimated by ML

during the phylogenetic reconstruction with GARLI v2.0 (see below) (gamma shape parameter: 0.65, proportion of invariable sites: 0.43) (Tamura et al., 2013).

The best-fit models of DNA substitution were selected using the Akaike Information Criterion (AIC), the Bayesian Information Criterion (BIC) and under a Decision Theoretic framework (DT), as implemented in jModelTest v.2 (Darriba et al., 2012) for the 28S alignment, and using the BIC separately on the three codon positions of the COI gene in PartitionFinder (Lanfear et al., 2012).

Bayesian inference (BI) and ML methods were used to reconstruct phylogenetic trees based on the separate datasets and on a dataset concatenated with SequenceMatrix (Vaidya et al., 2011).

BI trees were reconstructed using MrBayes v.3.2 (Ronquist and Huelsenbeck, 2003). BI analysis of COI and 28S alignments included two runs of 10^7 generations. Trees were sampled every 1000 generations using four Markov chains, and default heating values. Convergence was assessed by the standard deviation of split-frequencies (< 0.01) and by examining the trace plots of log-likelihood scores in Tracer 1.6 (Rambaut and Drummond, 2005). The first 10 % trees were discarded as burn-in, while the remaining trees were used to construct a 50 % majority rule consensus tree and estimate the posterior probabilities (PP). Nodes with PP ≥ 0.95 were considered as significantly supported.

ML trees were estimated using GARLI v.2.0 (Zwickl, 2006). For each dataset, two separate ML searches were run independently from different stepwise reconstructed trees. The best scoring tree across runs was considered for further analyses. Confidence levels of branches were estimated by 1000 bootstrap replicates. Nodes with bootstrap values (BV) ≥ 70 were considered as significantly supported.

DATA CONGRUENCE

An Incongruence Length Difference (ILD) test (Farris et al., 1995) was implemented using Paup*4.0b10, using 1000 heuristic search repetitions, in order to test for congruence between the COI- and 28S-based phylogenies. However, as ILD tests the overall topology, it may be prone to rejecting congruence between partitions even though the conflicting signal is restricted to a limited number of nodes or taxa (Hipp et al., 2004; Struck et al., 2006). Previous investigations suggested that this incongruence test is too conservative, and should only be used as a measure of heterogeneity between gene partitions rather than a measure of combinability (Barker and Lutzoni, 2002; Darlu and Lecointre, 2002; Dolphin et al., 2000; Yoder et al., 2001). Therefore, we used the partition addition bootstrap alteration (PABA) approach to identify more precisely which nodes are causing the incongruence (Struck et al., 2006). The alteration (δ) of bootstrap value at a given node

is examined when an additional data partition is added. The rationale behind the method is that addition of congruent, or incongruent, data will cause bootstrap support for the node of interest to increase or decrease, respectively. TreSpEx (Struck, 2014) was used to summarize the bootstrap support of every bipartitions across the different datasets, in order to calculate δ.

DISCOVERY-BASED SPECIES DELIMITATION

We used two types of discovery-based methods of species delimitation, which do not require *a priori* assignments of individual to putative species. Firstly, we used the Bayesian implementation of the Poisson Tree Processes model (bPTP) (Zhang et al., 2013). This method estimates the mean expected number of substitutions per site between two branching events, using the branch length information of a phylogeny. It implements two independent classes of Poisson processes (for intra- and inter-specific branching events). The assumption is that the number of substitutions between species is significantly higher than the number of substitutions within species, resulting in two different branch length classes. For each possible species delimitation, the Poisson processes are fitted to the two branch length classes. In the Bayesian implementation, a Markov Chain Monte Carlo (MCMC) sampler is used to produce PP of these species delimitations. PP ≥ 0.95 was considered as a significant support for the species. The analyses were conducted on the web server for bPTP (available at http://species.h-its.org/ptp/) using the BI topology, with 500,000 generations, thinning set to 100 and burnin at 10 %.

Secondly, we used the General Mixed Yule Coalescent (GMYC) model (Fujisawa and Barraclough, 2013; Pons et al., 2006). This method models speciation via a pure birth process and within-species branching events as neutral coalescent processes. It identifies the transition points between inter- and intraspecies branching rates on a time-calibrated ultrametric tree by maximizing the likelihood score of the model. All lineages leading from the root to the transition point are then considered as different species. We built an ultrametric tree in BEAST v.1.8.0 required to run the GMYC algorithm. Identical sequences (haplotypes) were pruned to a single copy before implementation, because zero-length terminal branches hamper the likelihood estimation (Fujisawa and Barraclough, 2013; Monaghan et al., 2009). The phylogenetic analysis was performed under a relaxed exponential clock set to an evolutionary rate of 1.0 (i.e. no attempt to estimate divergence time) and a speciation: Yule Process Tree Model, using a random starting tree. Analyses were run for 1×10^8 (28S dataset) and 2×10^7 (COI dataset) MCMC generations, sampled every 1000th generations, and the first 10 % of the samples were discarded as burn-in. Tracer v.1.6 (Rambaut and Drummond, 2005) was used to check for minimum Effective Sample Sizes (ESS) of 200 and visually inspect stationarity and convergence by plotting likelihood values. The resulting trees were summarized into a target maximum clade

credibility tree using TreeAnnotator v.1.8.0. The GMYC analysis was carried out in R v3.0.1 using the splits (Ezard et al., 2009) and ape (Paradis et al., 2004) packages under the single-threshold method and excluding the outgroup (Fujisawa and Barraclough, 2013). The AIC-based support values for the species clusters were calculated, in order to account for delineation uncertainty (Powell, 2012).

VALIDATION–BASED SPECIES DELIMITATION

We used Bayesian species delimitation as implemented in Bayesian Phylogenetics and Phylogeography (BPP) (Rannala and Yang, 2013; Yang and Rannala, 2010). This method relies on the multispecies coalescent prior to accommodate for uncertainties in the gene trees (incomplete lineage sorting). The analysis A11 implemented in the new version of the program BPP v3.1 (Yang, 2015; Yang and Rannala, 2014) jointly infers species delimitation and species phylogeny. An MCMC proposal based on the nearest-neighbor interchange algorithm is used to change the species tree topology, eliminating the need for a user-specified guide tree. A reversible-jump MCMC algorithm successively splits or joins nodes on the proposed species trees, generating the posterior probabilities for different collapsed subtrees. PP ≥ 0.95 was considered as a significant support. A gamma prior G θ (α, β) with mean α/β is used on the population size parameter (θ). The age of the root in the species tree (τ_0) is assigned a gamma prior G τ_0 (α, β), whereas the other divergence parameters are assigned the Dirichlet prior (Yang and Rannala, 2010). We performed analyses separately for the four lineages that were inferred from the phylogenetic analyses, viz: *E. macrodonta-similis-puncticulata-annabellae* Coleman, 1994, *E. walkeri-macronyx*, *E. georgiana-rubrieques* De Broyer & Klages, 1991-*rimicarinata* Watling & Holman, 1980-*inermis-robustoides* Lörz & Coleman, 2009 and *E. grandirostris-pulchra* Coleman, 1990-*oxicarinata* Coleman, 1990*,* to increase computational efficiency. The putative species recovered by bPTP and GMYC analyses were used for the *a priori* assignment of individuals to populations.

Analyses were run for 5 x 10^5 MCMC generations with a sampling interval of five and a burn-in period of 1 x 10^4 generations. Each rooted tree was assigned equal prior probability. We introduced a heredity multiplier of 0.25 for mtDNA, to account for the difference in effective population sizes for mtDNA and nDNA data. While the average rate for all loci is fixed at 1, the rates among loci were assumed to be generated from a Dirichlet distribution D (3.0). A small value of this parameter is appropriate when the rates are variable among loci. The sensitivity of the posterior estimates to G θ (α, β) and G τ_0 (α, β) was tested by changing the parameters in the priors using A00 in BPP v.3.1 (Yang, 2015). Diffuse priors were used, as we do not have prior knowledge on the values of θ and τ_0. After initial trials, we selected gamma priors of G θ (2, 1000) and G τ_0 (2, 100) for the *E. walkeri-macronyx* dataset, of G θ (2, 200) and G τ_0 (2, 40) for the *E. georgiana-rubrieques-rimicarinata-*

inermis-robustoides dataset and G θ (2, 2000), G τ_0 (2, 40) for the *E. macrodonta-similis-puncticulata-annabellae* dataset and G θ (2, 40) and G τ_0 (2, 100) for the *E. grandirostris-pulchra-oxicarinata* dataset. Each analysis was run twice using different seeds and both speciation algorithm 0 with the default prior value e = 2 and algorithm 1 with the default prior values a = 2 and m = 1. When the chain mixes well, the results should be the same between multiple runs using the two algorithms. In order to deal with potential prior misspecification, we also tested three additional prior schemes, according to an approach suggested by Leaché and Fujita (2010): (1) large ancestral population sizes and deep divergences: G θ (1, 10) and G τ_0 (1, 10), (2) small ancestral population sizes and shallow divergences: G θ (2, 2000) and G τ_0 (2, 2000) and (3) large ancestral populations sizes and shallow divergences: G θ (1, 10) and G τ_0 (2, 2000).

RESULTS

TAXON SAMPLING AND MOLECULAR DATA

We obtained 79 COI and 97 28S sequences of Antarctic *Epimeria* specimens. The aligned COI fragment was 555 bp long, with 250 variable sites. The 28S alignment was 1603 bp long (after removal of ambiguous regions with Aliscore), with 567 variable sites. The combined dataset contained 2158 bp.

Interspecific GTR+G+I distances between *Epimeria* species within each species complexes are provided in Table 2.

	MA1	MA2	MA3	SI2	SI5	SP1	SP2
MA1	**0**	0.012	0.067	0.112	0.152	0.183	0.132
MA2	0.012	**0**	0.1	0.17	0.227	0.32	0.235
MA3	0.064	0.074	**0**	0.18	0.21	0.29	0.21
SI2	0.104	0.108	0.11	**0**	0.183	0.25	0.2
SI5	0.137	0.131	0.125	0.11	**0.003**	0.202	0.242
SP1	0.162	0.158	0.149	0.149	0.12	-	0.32
SP2	0.119	0.126	0.115	0.115	0.13	0.156	-

	PUN2	PUN3	PUN4
PUN2	-	0.17	0.37
PUN3	0.102	-	0.31
PUN4	0.158	0.143	-

	WA1	WA2	WA3	WA4
WA1	**0.002**	0.08	0.167	0.123
WA2	0.062	-	0.173	0.17
WA3	0.105	0.108	**0.001**	0.147
WA4	0.081	0.099	0.091	**0**

	GE1	GE2	GE3	GE4	GE5	RIM	RUB
GE1	**0.002**	0.055	0.06	0.305	0.295	0.166	0.161
GE2	0.046	-	0.04	0.33	0.31	0.17	0.165
GE3	0.05	0.038	-	0.3	0.28	0.12	0.17
GE4	0.145	0.15	0.142	-	0.28	0.26	0.25
GE5	0.144	0.15	0.144	0.14	**0**	0.33	0.295
RIM	0.103	0.103	0.08	0.134	0.154	-	0.23
RUB	0.102	0.105	0.108	0.134	0.147	0.13	**0.004**

	RO1	RO2	RO3
RO1	**0.001**	0.11	0.29
RO2	0.081	**0**	0.26
RO3	0.14	0.134	-

	GR1	PU1	OX
GR1	**0.005**	0.115	0.147
PU1	0.07	-	0.13
OX	0.097	0.086	**0.002**

Table 2. Intraclade mean uncorrected COI distances in bold on the diagonal. ML estimations of GTR+G+I mean COI interclade distances above the diagonal and p-uncorrected distance below.

PHYLOGENETIC TREES

The best model of nucleotide substitution inferred by jModelTest (28S) and Partitionfinder (COI) was GTR+G+I for both genes, and was used in all BI and ML analyses.

The ILD test rejected the null hypothesis of congruence between the 28S and COI trees (*p=0.001*). The PABA approach revealed several cases of strongly supported (BV ≥ 70, PP ≥ 0.95) conflict between the two gene trees within MOTUs (Fig.1). The separate analysis of 28S and morphology strongly supports MA1 (94, 0.97). Conversely, the separate analysis of COI strongly supports a sister relationship between 2 taxa in MA1 (ANT34, I6) and MA2 (75, 0.97). Therefore, the BV of MA1 decreases by 40.3 when the datasets are combined. SI5 is strongly supported in the COI gene tree (100, 1.00) and by morphology, whereas the 28S phylogeny strongly supports the grouping of all taxa in SI5 except taxon M6 (100, 1.00). The BV of SI5 is slightly decreased (-1.4) when the datasets are combined. The separate analysis of 28S strongly supports IN2 (72, 0.99), whereas one taxon in IN2 (I3) is sister to a strongly supported clade (100, 1.0) comprising all the remaining IN taxa in the COI gene tree. Therefore, the BV of IN2 is diminished by 71.6 when the datasets are combined. No morphological variability was observed within IN. Except for these strong localized incongruences within MOTUs, the remaining nodes that were discordant among the separate analyses were unsupported (or by PP only). Moreover, several incongruences in the phylogenetic relationships between MOTUs were also identified by PABA, within the complexes *walkeri*, *puncticulata* and *macrodonta-similis.* The only strongly supported conflict is in the sister relationship between MA1-MA2 and MA3 (82, 1.00) in the COI phylogeny. This node shows a great decrease in bootstrap

support (-75.6) when the 28S data is added, as it is not present in the 28S gene tree. The taxa involved in strongly supported conflicts within MOTUs between the gene trees (ANT34, I6, M6, I3) were removed from the concatenated and species delimitation analyses (Fig. 1). In order to get an overview of the total evidence, a concatenated analysis was performed (Fig. 2).

All phylogenetic analyses (based on the separated and concatenated datasets) supported the monophyly of most formerly recognized species and species complexes (clades B, C, D and F in Fig. 2, *Epimeria* aff. *robustoides* and *E.* aff. *grandirostris*), except for *E.* aff. *macrodonta, E.* aff. *similis* and *E.* aff. *georgiana,* which were polyphyletic. *E.* aff. *macrodonta* and *E.* aff. *similis* form a clade with two undescribed species (*E.* sp. nov.1 and *E.* sp. nov.2) (clade A), *E.* aff. *georgiana* forms a clade with *E. rubrieques* and *E. rimicarinata* (clade E). *E. robusta* and *E.* aff. *robustoides* are united within clade G. *E.* aff. *pulchra*, *E.* aff. *grandirostris* and *E. oxicarinata* together form clade H. Three more inclusive clades were consistently recovered by all methods and loci: (1) *E.* aff. *similis, E.* aff. *macrodonta, E.* sp. nov.1*, E.* sp. nov.2 and *E*. aff. *puncticulata*; (2) *E.* aff. *walkeri* and *E. macronyx*; and (3) *E*. aff. *robustoides, E. robusta, E.* aff. *georgiana, E. rubrieques, E. rimicarinata* and *E. inermis.*

SPECIES DELIMITATION

All the ESS values obtained from the BEAST analyses for both genes were above 200. The topologies of the resulting ultrametric trees, used as input for the GMYC analyses, were the same than the topologies of the BI trees obtained with MrBayes.

The GMYC analysis of the COI phylogeny returned 30 ML entities ("species") excluding the outgroup (confidence interval 28–33). The log-likelihood ratio test suggested that this model was a better fit for the data than the single-species model (likelihood ratio = 9.6*, p = 0.008*). The bPTP analysis of the COI Bayesian phylogeny gave a total of 30 putative species as well. The results of bPTP are mostly consistent with the GMYC analysis, and incongruent delimitations are supported by PP (bPTP) or AIC-based support values (GMYC) < 0.7 (Fig. 2).

The GMYC analysis of the 28S phylogeny couldn't reject the null hypothesis of a single species (likelihood ratio = 0.58, *p = 0.75*). The bPTP analysis of the 28S Bayesian tree returned 27 putative species (Fig. 2).

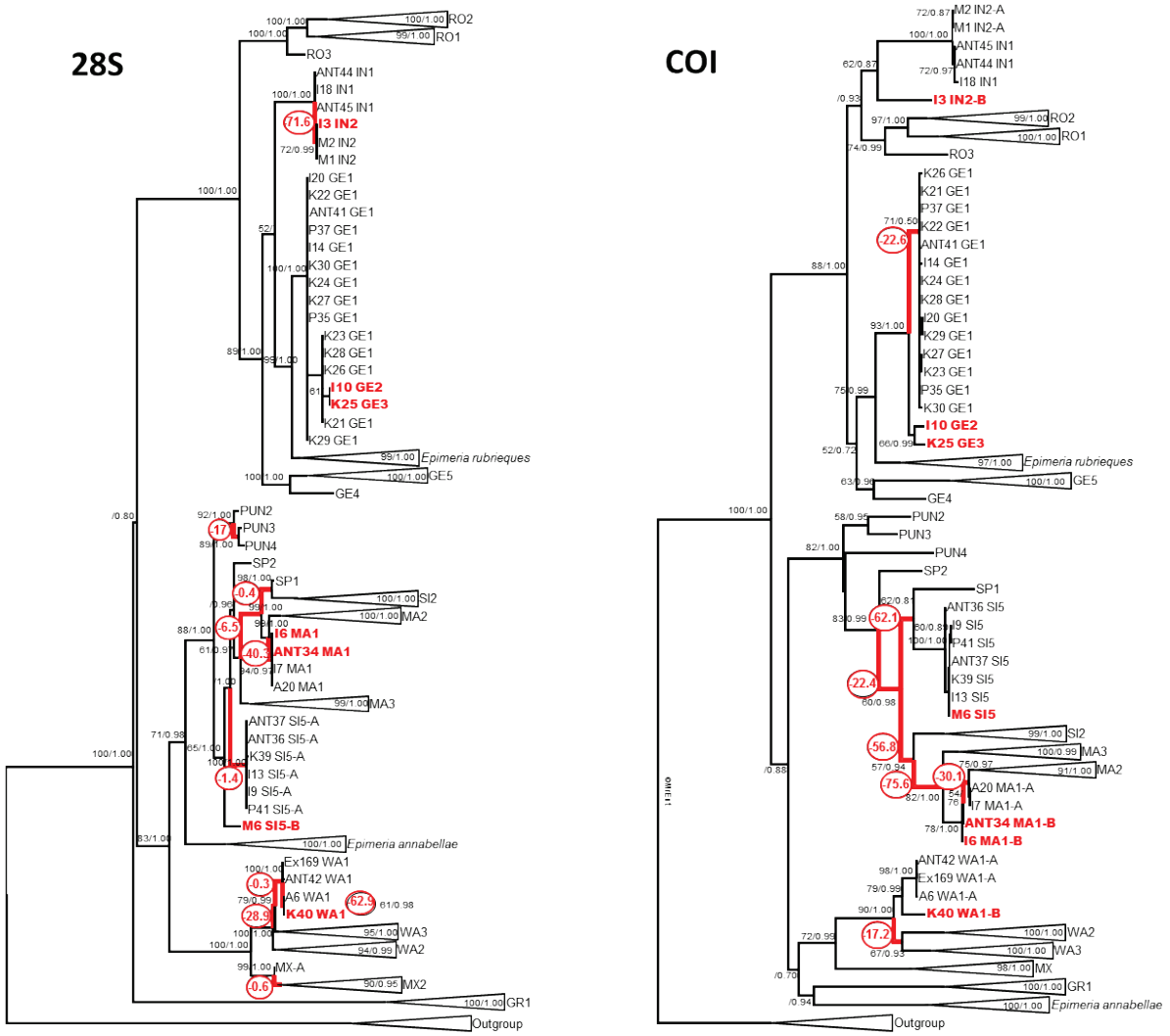

Figure 1. Phylogenetic trees obtained by Maximum Likelihood analysis of the separate COI and 28S datasets. Bootstrap values (1000 replicates) ≥ 50 and posterior probabilities ≥ 0.5 (from the Bayesian analysis) are indicated above the nodes. Sequences are named with the sequence identifiers and the MOTUs codes. MOTUs that did not show incongruences between the two gene trees were collapsed. Taxa with discordant positions in the two gene trees are indicated in red. Red thick lines indicate incongruent nodes identified by PABA. Encircled numbers represent the alteration in bootstrap support (δ) of these incongruent nodes when the other dataset is added to the analysis.

The BPP method, based on the two loci, recovered the largest number of putative species (37 in total) (Fig. 2). The use of different prior schemes did not have significant effects on species delimitations. The number of delimited species was generally lower with the θ G (1, 10) and τ_0 G (1, 10) scheme, but in these few cases, different species delimitations were not supported by PP.

CLADE A – *MACRODONTA-SIMILIS* COMPLEX

All 11 MOTUs within clade A, four in the *macrodonta* complex, five in the *similis* complex and two other new species, were identified as putative species by most methods. Only GMYC applied on the COI dataset lumped MA1 and MA2 into one species (AIC-based support: 0.81). For four of these clades, three in the *similis* complex and one in the *macrodonta* complex, only the 28S gene could be sequenced (Fig. 2).

There were consistent morphological differences between the 11 MOTUs (MA1-4, SI1-5, SP1 and SP2). Main morphological differences between all clades are observed in (1) the shape of the mid-dorsal tooth on pereonite 3, (2) the shape of the mid-dorsal teeth on pereonites 4–6, (3) the shape of the mid-dorsal teeth on pereonite 7–pleonite 3, (4) the shape of coxa 4 and (5) the orientation and shape of the lateral tooth (when present) of coxa 4. Unique (or rare) distinguishing character states, representing putative autapomorphies, can be identified for all clades, and particularly for SP1 and SP2 [details are presented in Appendix S3A].

CLADE B – *PUNCTICULATA* COMPLEX

The four MOTUs within the *puncticulata* complex were delimited as putative species by most methods. Only bPTP applied on the 28S phylogeny consider PUN3 and PUN4 as a single species, but this species delineation is unsupported (Fig. 2).

Different combinations of morphological character states are found for each of the four MOTUs (PUN1-4). These four morphospecies mainly differ in the shape of coxa 4 (ventral corner and proportions). Moreover, species-specific character states (putative autapomorphies) were observed for each of the four putative species [details are presented in Appendix S3B].

CLADE C – *WALKERI* COMPLEX

The four MOTUs within the *walkeri* complex were identified as putative species by all methods except bPTP applied on the 28S phylogeny. The latter analysis returns a single species for the whole *walkeri* group, but the PP support for this delimitation is not significant (Fig. 2).

Phenotypic differences were observed between the four MOTUs (WA1-4). They mainly differ in (1) the shape of the rostrum in dorsal view (length and width), (2) the shape of coxa 4 (although it is very similar for WA1 and WA4), (3) the posterodistal corners of the basis of p6 and (4) the posterodistal corner of the basis of p7. The smaller eyes of WA4 could be an autapomorphy for this lineage [details are presented in Appendix S3C].

CLADE D – *EPIMERIA MACRONYX*

All methods identify *E. macronyx* as a single species (Fig. 2) and no phenotypic differences are observed between the two MOTUs, MX1 and MX2.

CLADE E – GEORGIANA-RIMICARINATA-RUBRIEQUES COMPLEX

Most methods delimit all seven MOTUs within clade E as putative species, five in the *georgiana* complex, *E. rubrieques* and *E. rimicarinata*. Only the bPTP applied on the 28S phylogeny identify the *georgiana* clades GE1-3 as a single species, although the PP of this species delimitation is not significant (Fig. 2).

Combinations of distinctive morphological characteristics were found for each of the seven MOTUs (GE1-5, RI, RU). Main differences are observed in: (1) the shape of the rostrum (curvature, width and length), (2) the number and the degree of lateral compression of the mid-dorsal carinae (except for *E. rimicarinata* and *E. rubrieques,* which have respectively tridimensionally sculpted carinae and huge styliform mid-dorsal teeth), (3) the shape of the coxa 4 and of its carina (on the posteroventral area), (4) the shape of the posterior projection of coxa 5, and (5) the angle of the posterodistal notch of the basis of pereiopod 7 [details are presented in Appendix S3D].

CLADE F – *EPIMERIA INERMIS*

GMYC (COI) and BPP analyses divide *E. inermis* into two distinct species (IN1-2), whereas bPTP analyses retain a single species (Fig. 2).

No phenotypic differences were observed between the two MOTUs, IN1 and IN2.

CLADE G – *ROBUSTOIDES-ROBUSTA* COMPLEX

The discovery methods applied on the COI tree and BPP divide *E. robustoides* into two putative species (RO1 and 2), whereas bPTP applied on the 28S phylogeny further divides RO2 into two putative species. *E. robusta* is identified as a distinct species by all methods (Fig. 2).

There are morphological differences between the three MOTUs (RO1-3) in: (1) the shape of the mid-dorsal projections on the pleonites (no projections on pleonites 1–2 for *E. robusta*), (2) the sharpness of the posterodistal corner of the basis of pereipods 5–7 and (3) the concavity of the dorsolateral margins of urosomite 3. Moreover, each of these morphotypes also presents unique character states [details are presented in Appendix S3E].

CLADE H – *GRANDIROSTRIS-PULCHRA-OXICARINATA* COMPLEX

All methods identify four putative species within clade H, two in the *grandirostris* complex, *E*. aff. *pulchra* and *E. oxicarinata* (Fig. 2).

Morphological differences are observed between these four clades (GR1-2, PUL1 and OX). They mainly vary in: (1) the shape and relative sizes of the dorsal projections, (2) the shape of coxa 4, (3) the shape of coxa 5, and (4) the median angle on the posterior border of the basis of pereiopod 7. Moreover, character states specific to some of these clades (putative autapomorphies) were observed [details are presented in Appendix S3F].

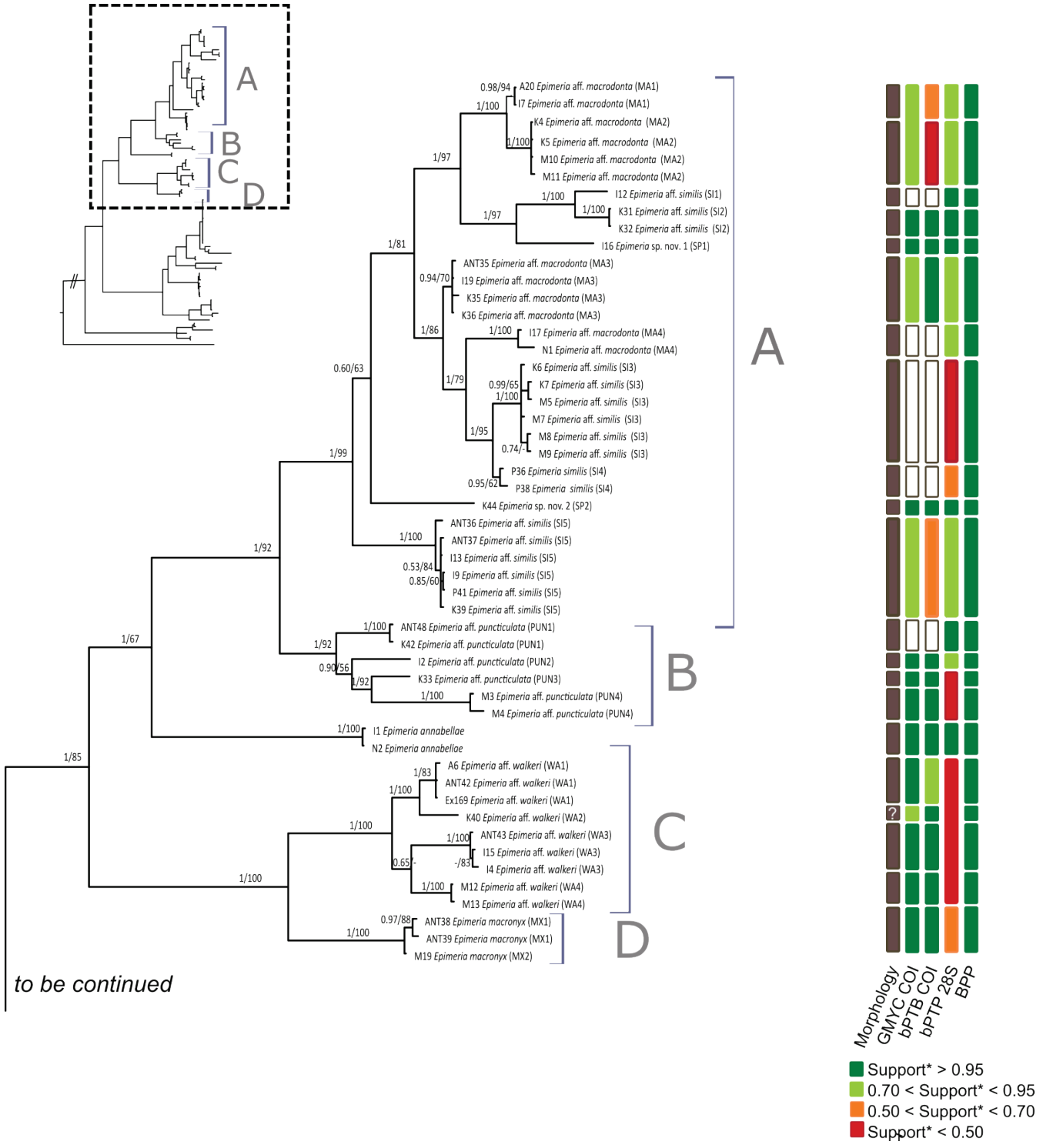
A
B
C
D
0.98/94 A20 Epimeria aff. macrodonta (MA1)
1/100 I7 Epimeria aff. macrodonta (MA1)
K4 Epimeria aff. macrodonta (MA2)
1/100 K5 Epimeria aff. macrodonta (MA2)
M10 Epimeria aff. macrodonta (MA2)
M11 Epimeria aff. macrodonta (MA2)
1/97
1/100 I12 Epimeria aff. similis (SI1)
1/100 K31 Epimeria aff. similis (SI2)
1/97 K32 Epimeria aff. similis (SI2)
I16 Epimeria sp. nov. 1 (SP1)
1/81
ANT35 Epimeria aff. macrodonta (MA3)
0.94/70 I19 Epimeria aff. macrodonta (MA3)
K35 Epimeria aff. macrodonta (MA3)
K36 Epimeria aff. macrodonta (MA3)
1/86
1/100 I17 Epimeria aff. macrodonta (MA4)
N1 Epimeria aff. macrodonta (MA4)
0.60/63
K6 Epimeria aff. similis (SI3)
1/79
0.99/65 K7 Epimeria aff. similis (SI3)
1/100 M5 Epimeria aff. similis (SI3)
M7 Epimeria aff. similis (SI3)
1/95
M8 Epimeria aff. similis (SI3)
0.74/- M9 Epimeria aff. similis (SI3)
1/99
P36 Epimeria similis (SI4)
0.95/62 P38 Epimeria similis (SI4)
K44 Epimeria sp. nov. 2 (SP2)
ANT36 Epimeria aff. similis (SI5)
1/100 ANT37 Epimeria aff. similis (SI5)
1/92
I13 Epimeria aff. similis (SI5)
0.53/84
0.85/60 I9 Epimeria aff. similis (SI5)
P41 Epimeria aff. similis (SI5)
K39 Epimeria aff. similis (SI5)
1/100 ANT48 Epimeria aff. puncticulata (PUN1)
1/92 K42 Epimeria aff. puncticulata (PUN1)
1/67
0.90/56 I2 Epimeria aff. puncticulata (PUN2)
1/92 K33 Epimeria aff. puncticulata (PUN3)
1/100 M3 Epimeria aff. puncticulata (PUN4)
M4 Epimeria aff. puncticulata (PUN4)
1/100 I1 Epimeria annabellae
N2 Epimeria annabellae
1/85
1/83 A6 Epimeria aff. walkeri (WA1)
1/100 ANT42 Epimeria aff. walkeri (WA1)
Ex169 Epimeria aff. walkeri (WA1)
K40 Epimeria aff. walkeri (WA2)
1/100
1/100 ANT43 Epimeria aff. walkeri (WA3)
0.65 I15 Epimeria aff. walkeri (WA3)
-/83 I4 Epimeria aff. walkeri (WA3)
1/100
1/100 M12 Epimeria aff. walkeri (WA4)
M13 Epimeria aff. walkeri (WA4)
0.97/88 ANT38 Epimeria macronyx (MX1)
1/100 ANT39 Epimeria macronyx (MX1)
M19 Epimeria macronyx (MX2)
to be continued
?
Morphology
GMYC COI
bPTB COI
bPTP 28S
BPP
Support* > 0.95
0.70 < Support* < 0.95
0.50 < Support* < 0.70
Support* < 0.50

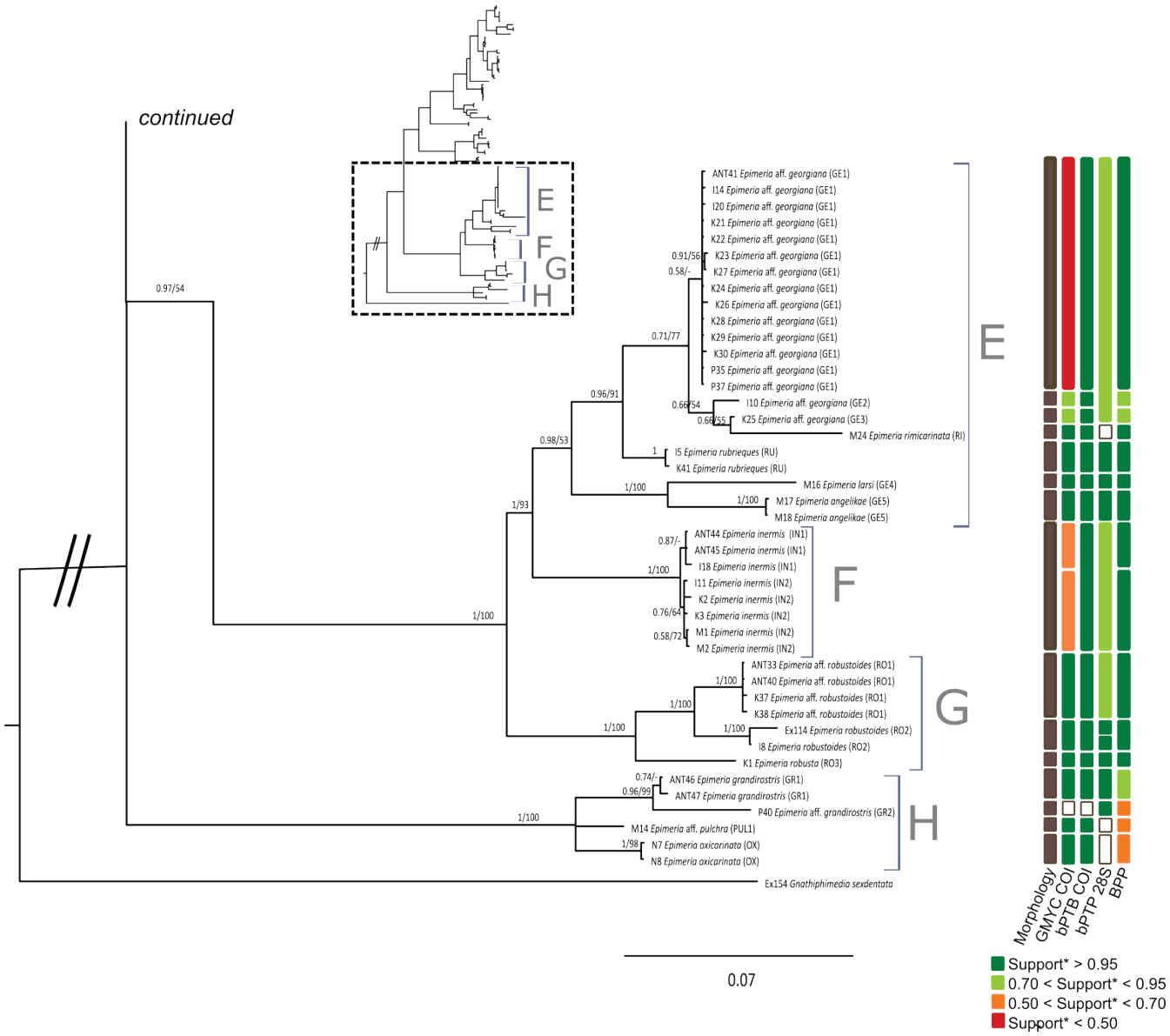

Figure 2. Phylogenetic tree obtained by Bayesian analysis of the concatenated COI and 28S sequences. Bayesian PP and BV (1000 replicates) from the ML analysis are indicated above the nodes of interest. Bootstrap values inferior to 50 are not indicated. Sequences are named according to the corresponding species complex (aff.) or the described species, followed by the MOTU code. Species delimitation results inferred by morphology and DNA-based methods (GMYC, bPTP and BPP), applied separately to the two gene trees (COI, 28S) or based on both loci for BPP, are indicated besides the concatenated tree. *Boxes are coloured according to the posterior probability (bPTP and BPP analyses) or the AIC-based GMYC support values (GMYC) of the inferred delimitation.

DISCUSSION

MITO-NUCLEAR DISCORDANCE

When comparing nuclear versus mtDNA-based phylogenetic trees, some relationships are conflicting at the species-level (Fig. 1). A weak phylogenetic signal may result in poor phylogenetic resolution or inaccurate gene trees. If a gene is evolving too slowly relative to the rate of speciation or a too small fragment of that gene is analyzed, the obtained data may provide too few informative characters to robustly recover the underlying gene tree (Funk and Omland, 2003). Therefore, incongruence restricted to unsupported nodes is likely due to phylogenetic estimation errors. The discordant positions of GE1-2-3 in the gene trees (Fig. 1) are likely due to such errors, as the relationships between these MOTUs on the nuclear phylogeny are unsupported. GE2 and GE3 also present morphological differences with each other and GE1 (see Appendix S3D), which does appear to fall into GE1's morphological variability, therefore supporting their external position from GE1 in the COI gene tree. Phylogenetic biases might also be responsible for the position of K40 (WA2) within WA1 in the nuclear gene tree (Fig. 1). However, as the specimen is an incomplete juvenile, the observed morphological differences with WA1 have to be interpreted with caution (see Appendix S3C). As mitochondrial sequences are evolving faster, they are less prone to lacking phylogenetic signal at the species-level (Funk and Omland, 2003), unless they are saturated, which is not the case of the present data (Fig. 3). Hence, the (unsupported by PP) lumping of several otherwise well-delimitated MOTUs by a method based on the 28S gene only (PUN 3-4, WA1-2-3-4; Fig. 2) might be due to the insufficient variability of the 28S gene fragment studied.

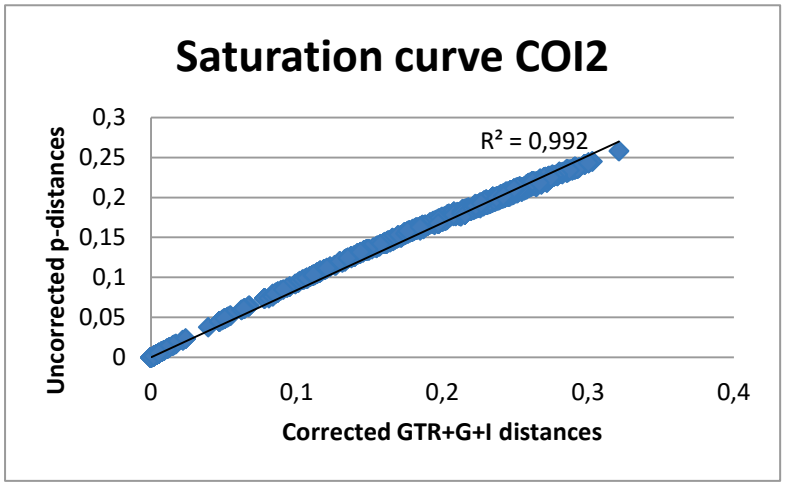

Figure 3. Substitution saturation scatter plot for the COI dataset. The graph represents the increase in GTR+I+G distances (estimated by ML), corrected for multiple nucleotide substitutions, versus the increase in p-distances between pairs of sequences. R^2 value shows the fit of the relationship to a linear regression model. In the absence of saturation, the plot should reveal a linear increment of corrected in relation to uncorrected distance. Once substitution saturation is achieved, the plot should reach a plateau.

Some conflicts also receive strong support (positions of M6, I3, ANT34 and I7; Fig. 1). This type of incongruence may reveal conflicting evolutionary histories among genes, inherent to the different properties of mitochondrial and nuclear markers (Funk and Omland, 2003; Som, 2015; Toews and Brelsford, 2012). However, as these strongly supported incongruences only concern a few taxa, a more comprehensive taxonomic sampling would be needed to rule out the possibility of a contamination of the samples with neighboring DNA and reveal eventual cases of incomplete lineage sorting, introgressive hybridization and/or gene duplications.

PSEUDOCRYPTIC DIVERSITY WITHIN ANTARCTIC *EPIMERIA*

Similarly to the ever increasing number of DNA studies presenting evidence of cryptic diversity in a wide variety of organisms in the Southern Ocean (Allcock et al., 2011; Held, 2003; Held and Wägele, 2005; Krabbe et al., 2010; Linse et al., 2007), Antarctic *Epimeria* is here shown to be much more speciose than was previously assumed. Altogether, these results confirm that the Antarctic shelf diversity is likely to be grossly underestimated. In the case of *Epimeria,* different species of a complex appear to present small and previously overlooked morphological differences, rather than being truly cryptic.

Overall, the different molecular species delimitation methods and morphology yielded very consistent results, except for the GMYC method applied on the 28S phylogeny which failed to identify the breaking point between speciation and coalescent events. The most likely explanation for this non-significant outcome is the sparse sampling within the clades. The intraspecific variation might therefore not be sufficient in this case to detect the transition between inter- and intraspecific branching patterns (Fujisawa and Barraclough, 2013; Pons et al., 2006).

A total of 25 *Epimeria* lineages were identified as putative new species by morphology and DNA sequence-based methods. Within the *macrodonta* complex (type locality of *E. macrodonta*: Ross Sea), four putative new species (MA1-4), were delineated. Some of them occur in neighboring stations on the eastern side of the Antarctic Peninsula (MA1, MA3) and the Bransfield Strait (MA3, MA4), whereas MA2 is recorded from the Adélie Coast only (Fig.4; map 1). As MA4 was only sequenced for the 28S gene, a more variable marker would be needed to confirm the single species delimitation. However, as the two sequenced specimens are also morphologically similar, MA4 will be provisionally considered as a putative species. Two morphotypes were observed within MA2, although all specimens of this clade present the same COI and 28S haplotypes. Hence, morphological species delimitation within MA2 could be misleading because of the observed intraspecific variation in the shape and presence/absence of a small middorsal tooth. One well-delineated species of the

similis complex from the Bransfield Strait (SI4) corresponds to the original description of *E. similis* (type locality: King George Island). Additionally, four putative new species, two of them occurring in sympatry with *E. similis* in the Bransfield Strait (SI2 and SI5), one found only in the eastern Weddell Sea (SI1) and one on the Adélie Coast (SI3), were revealed in our analyses. Only one of these new species (SI5) has a wider distribution, as it also occurs in the eastern Weddell Sea (Fig. 4; map 1). Since only 28S data was available for the delimitation of SI3 and SI4, additional evidence from more variable markers is needed to confirm the single-species delimitation for each of these clades. But as no morphological variability was found within the clades, they will be provisionally considered as putative species. Four new species were delineated within the *puncticulata* complex, one living on the tip of the Antarctic Peninsula (PUN1), one in Larsen B (PUN2) and two on the Adélie Coast (PUN3 and 4) (Fig.4; map 2). PUN1 is only delimited on the basis of 28S, but as we could not detect morphological discrepancies, the clade is here provisionally considered as a putative species. Four new species were delimitated in the *walkeri* complex as well, two occurring in the Bransfield Strait (WA1 and WA2), one in the Drake Passage (including Elephant Island) and the northeastern side of the Antarctic Peninsula (WA3) and one on Adélie Coast only (WA4). Only one of these new species (WA1) has a wider distribution, occurring also in the eastern Weddell Sea (Fig. 4; map 3). One well-delineated species of the *georgiana* complex from the Adélie Coast (GE5) corresponds to the description of *E. angelikae* (type locality: eastern Weddell Sea) (Lörz et al., 2011). An additional well-delineated new species from the *georgiana* complex from the Adélie Coast (GE4) corresponds to the description of *E. larsi* Lörz, 2009. Similarly to the study of Lörz et al. (2011), we found three *georgiana* clades in the Scotia arc area, which were here identified as putative new species: two in the Drake Passage (GE1, GE3), while GE1 is also found in the Bransfield Strait and northeastern Peninsula, and one on the plateau of the South Orkney Islands (GE2) (Fig. 4; map 5). Two species were delimited within the *E. inermis* clade by the GMYC analysis (COI) and BPP, whereas the bPTP analyses of both gene trees identified a single species. As no morphological discrepancies were found between the two clades, a conservative approach will be adopted in considering *E. inermis* as a single species. One clearly delineated species of the complex *robusta-robustoides* from the Adélie Coast (RO3) was recognized as the nominal species *E. robusta* (type locality: Ross Sea), whereas RO2 from the eastern Weddell Sea is morphologically assigned to *E. robustoides* (type locality: eastern Weddell Sea). The results suggest that *E.* aff*. robustoides* from the Bransfield Strait (RO1) is a distinct new species within the *robusta-robustoides* complex (Fig. 4; map 7). *E. grandirostris* may be a complex of species as well, since specimens from the Bransfield Strait and the northeastern Antarctic Peninsula (GR1) were assigned to the nominal species (type locality: Marguerite Bay), whereas a new species from the Adélie Coast (GR2) was delimited by the present study (Fig. 4; map 8). The single

specimen of *E.* aff. *pulchra* (PUL1) from the Adélie Coast differs morphologically from *E. pulchra* (type locality: South Orkney Islands), but molecular data from the type specimen of *E. pulchra* would be needed to confirm that PUL1 represents a distinct new species.

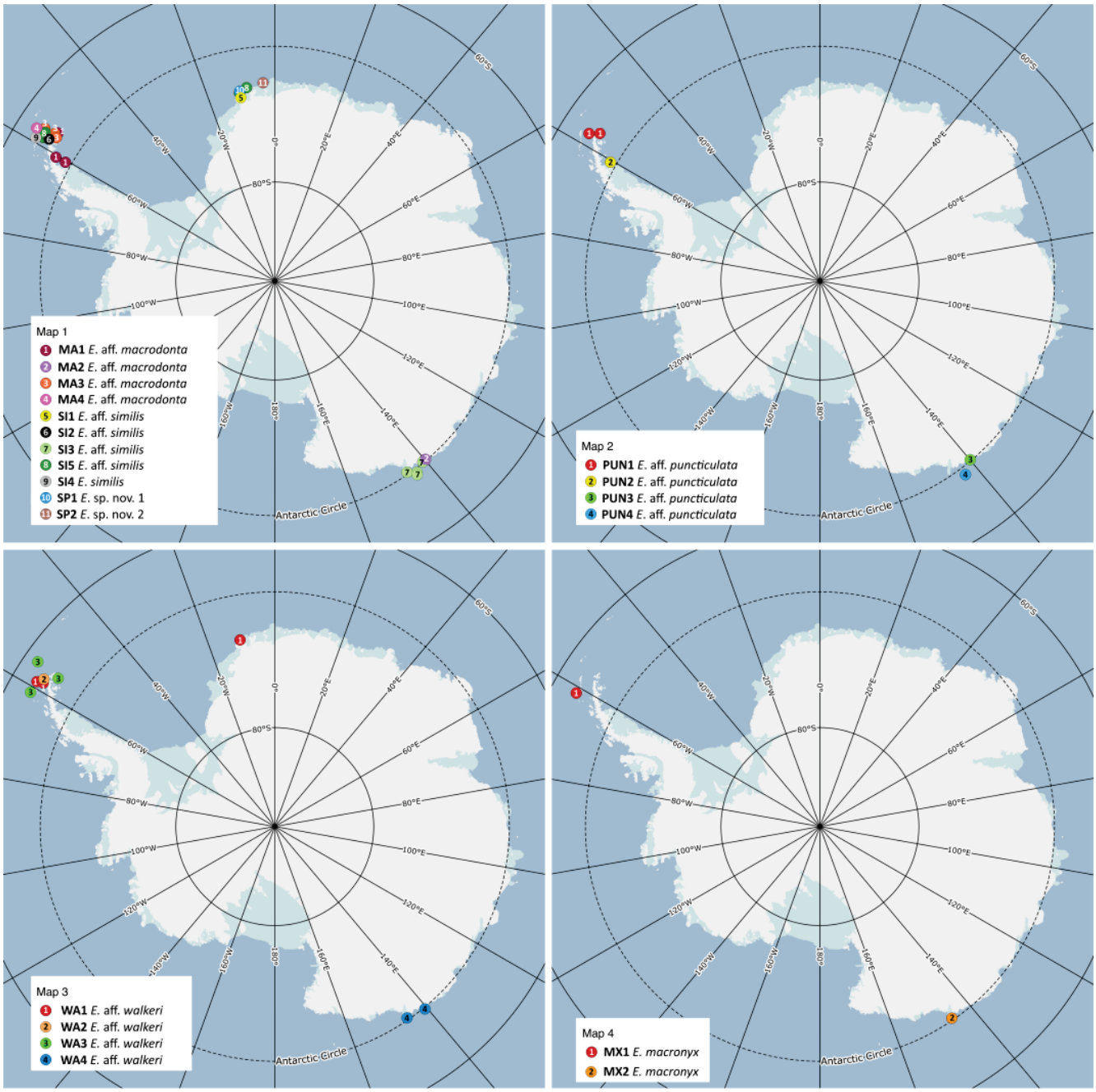

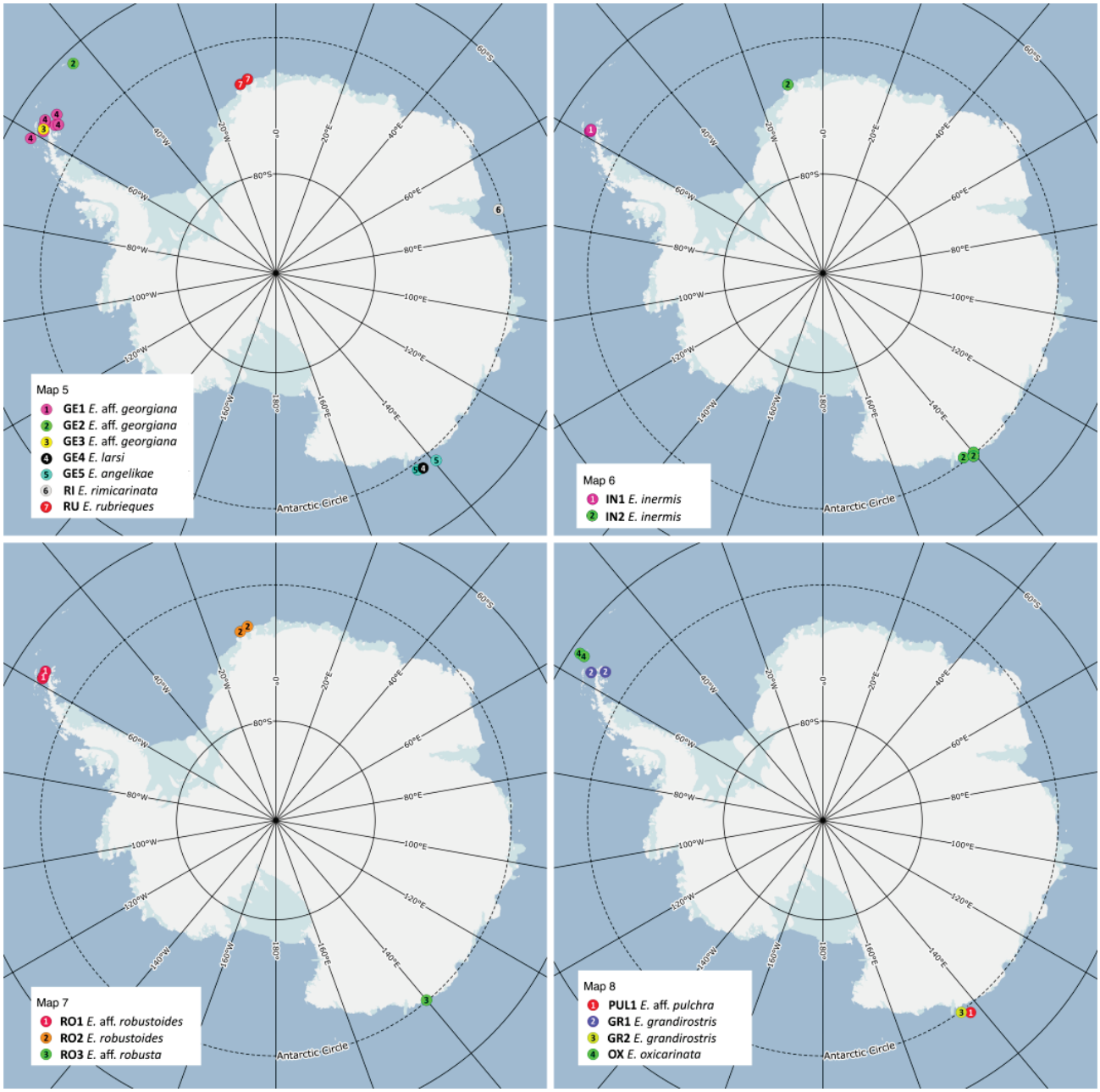

Figure 4. Distribution maps of the sequenced specimens. Each map (1–8) indicates distribution records for species belonging to clades A–H. Species are named according to the corresponding species complex (aff.) or the described species.

Evolution of *Epimeria* on the Antarctic shelf

The identification of the factors underlying Southern Ocean benthic biodiversity is not straightforward, as diversification processes are likely influenced by numerous biotic and abiotic factors, such as biological interactions, ice-mediated processes, sediment structure, topography and water masses (Kaiser et al., 2013). Among these factors, the glaciation process that affected the region over the last 34 million years has been pointed out as a major driver for taxonomic diversification (e.g. Allcock and Strugnell, 2012; Thatje et al., 2005b; Wilson et al., 2009). Assuming

the global molecular clock of 0.018 substitutions/site/My (mean COI rate per lineage), that was estimated for the Ponto-Caspian amphipod *Pontogammarus maeoticus* (Nahavandi et al., 2013), and considering the lowest COI corrected pairwise distance of 4 % (GE2-GE3) and the highest distance of 37 % (PUN2-PUN4) (Table 2), we roughly estimate that divergence times between the species within the complexes range between 10.28 and 1.11 Mya. This is in agreement with main allopatric speciation events within the genus occurring during Plio-Pleistocene glacial cycles (Clarke et al., 1992b).

During glacial periods, the ice sheet expanded across the continental shelf, erasing shelf benthos and even affecting the slope by mass-wasting processes. In some cases, migrations to the deep-sea might have permitted limited survival during glacial periods, and this process has been invoked to explain the eurybathy of some Antarctic benthic organisms (Allcock and Strugnell, 2012; Arango et al., 2011; Brey et al., 1996; Havermans et al., 2011). *Epimeria* species occur mainly on the shelf and no case of very wide eurybathy has been reported to date. Records of Antarctic deep water (below 1000 m) *Epimeria* species are scarce. However, *Epimeria* sp. nov. 2, nested within the shelf species of the *macrodonta-similis* complex on our tree, was collected at 1724–2091 m. Similarly, *E. larsi* (GE4) was collected at 1957–2154 m depth and is nested within shelf species of clade E. A similar case was also observed before within *Epimeria*: a new species collected at 2157 m depth is nested within shelf species (closely related to *E. georgiana* and *E. rubrieques*) in the COI phylogeny of Lörz et al. (2009). This indicates that polar submergences and/or emergences occurred during the evolutionary history of the genus, possibly following the oscillations of shelf ice extension. Connections between the Antarctic shelf and the deep-sea are also facilitated by the exceptionally deep continental shelf (on average four times deeper than in other continents) coupled with submerging Antarctic bottom water and emerging circumpolar deep water (Clarke and Crame, 1989; Menzies et al., 1979; Strugnell et al., 2011; Zinsmeister, 1984; Zinsmeister and Feldmann, 1984).

The presence of many closely related cryptic species around the Antarctic continent, mainly at shelf and slope depths is better explained by a scenario of continental shelf refugia (Pearse et al., 2008). Because of a diachronous formation of the ice-sheet around the continent, all areas might not have been glaciated at the same time (Anderson et al., 2002; Mackintosh et al., 2014; Stolldorf et al., 2012). There is also evidence for the presence of ice-free polynyas on the continental shelf edge, during the last glacial maximum (Smith et al., 2010; Thatje et al., 2008). Small populations isolated in these refugia may have gone through bottlenecks and diverged from each other by genetic drift. If there is an ecological cline within a refugium, selection might also lead to rapid fixation of alleles in these small populations and ecological speciation might occur (Allcock and Strugnell, 2012). A more

comprehensive sampling with respect to geographical scale and number of specimens per species is needed to detect eventual molecular evidence of bottlenecks (reduced haplotypic diversity) and subsequent demographic expansion (Allcock and Strugnell, 2012). However, adequate sample sizes are difficult to attain for such population-level studies, given the high number of (pseudo)cryptic species, the patchiness of these amphipods' distributions and the sporadic nature of sampling in the Southern Ocean.

GEOGRAPHIC PATTERNS

Speciation on the Antarctic shelf appears to be less dependent on the dispersal abilities of the organisms than it was previously inferred from the observed high occurrence of cryptic species in direct-developers (Allcock et al., 2011; Allcock and Strugnell, 2012; Hemery et al., 2012; Mahon et al., 2008; O'Loughlin et al., 2011; Pearse et al., 2008; Wilson et al., 2009), as it appears to be relatively common in organisms with a planktotrophic larval stage as well (Hemery et al., 2012; Janosik et al., 2011; Wilson et al., 2007). But the extent of contemporary species distributions is directly related to the species' mobility and the effectiveness of the physical barriers to surmount (e.g. currents, geographical distance and deep stretches). Hence, mobile species (with a pelagic or passively drifting adult and/or larval stage) are expected to present larger distribution ranges (Leese et al., 2010).

Epimeria species are brooders, mainly benthic, usually massive and heavily calcified amphipods, and therefore, are not expected to be highly dispersive. Most of the species delimited here appear to be geographically restricted to one of the three Antarctic regions studied (Antarctic Peninsula, eastern Weddell Sea and Adélie Coast). Two species, however, are present on both sides of the Weddell Sea (SI5 and WA1) (> 2000 km) (Fig. 4; maps 1 and 3), and do not exhibit partitioning of COI diversity among the two regions. Populations of some species are separated by even greater geographical distances. For example, the same COI haplotype of *E. macronyx* was collected in the Drake Passage area and the Adélie Coast (> 6000 km) (Fig. 4; map 4). This species is the only recorded pelagic Antarctic epimeriid (De Broyer et al., 2007), and hence, is potentially more dispersive. *Epimeria inermis,* assuming that it is a single species, occurs in the three studied regions (Fig. 4; map 6). The COI corrected distance (GTR+G+I) between the haplotypes from the Scotia Arc area and the Adélie Coast is 1.3 %. As the single specimen from the eastern Weddell Sea was only sequenced for the 28S gene, it is possible that the more variable COI gene would show some differentiation with the haplotypes from the Adélie Coast as well. Under a two-species scenario, the two 28S lineages (Antarctic Peninsula/eastern Weddell Sea + Adélie Coast) could represent recently diverged cryptic species. *Epimeria angelikae* (GE5) from this study was collected on the Adélie Coast (Fig. 4; map 5),

whereas the type specimen of this species was collected in the eastern Weddell Sea (~7000 km). Sequence data from this type specimen are however needed to confirm that GE5 is not a cryptic new species.

Altogether, our results imply that, in contrast to previous hypotheses (Lörz et al., 2009), at least some *Epimeria* species would be able to migrate over greater distances than expected. Counterintuitively, large-scale genetic exchanges appear to be common in Antarctic benthic brooders (e.g. Arango et al., 2011; Linse et al., 2007; O'Loughlin et al., 2011; Wilson et al., 2009), and very widespread distributions were revealed by molecular methods in other benthic amphipods (Baird et al., 2011; Havermans et al., 2011). These results reflect the existence of past or present connectivity sufficient to impede divergence processes, even at the scale of thousands of kilometers. Evidence for long-distance dispersal in *Epimeria* species remains, however, limited to very few species, bearing in mind that the true absence of these species from other areas cannot be confirmed without an extremely comprehensive sampling program. As the 1.3 % COI corrected distance found between the remote haplotypes of *E. inermis* (Antarctic Peninsula/Adélie Coast) is much higher than any other intraspecific distances (Table 2), genetic exchanges occurring over such distances would possibly be relatively rare, episodic events. Passive transport of rafting adults has been suggested as a means of dispersal for brooders (Baird et al., 2011; Dietz et al., 2015; Dömel et al., 2015; Hunter and Halanych, 2008; Krabbe et al., 2010; Leese et al., 2010; Wilson et al., 2009). The epifaunal propensity of *Epimeria* species (De Broyer et al., 2001) could provide opportunities for passive transport via fragmented sessile organisms, dislodged by anchor ice. Individuals could then be carried by ocean currents to other geographic localities. The clockwise Antarctic Circumpolar Current is the most prominent current in the Southern Ocean, and is hypothesized to have a homogenizing effect on the populations (Hemery et al., 2012; Janosik et al., 2011; Leese et al., 2010; Riesgo et al., 2015). However, a counter-clock current (East-wind drift), closer to the continent, would be more likely to aid long-distance dispersal of *Epimeria* species in these shelf locations (e.g. in the cases of *E. macronyx* and *E. inermis*), and the Weddell gyre could be responsible for the lack of differentiation between populations from the eastern and western sides of the Weddell Sea (SI5 and WA1) (Thatje, 2012).

CONCLUSION

Recent species delimitation methods combined with morphological evidence suggested that most of the studied nominal species of the amphipod genus *Epimeria* are in fact complexes of pseudocryptic species. A total of 25 putatively new species were inferred, which would increase by twofold the

actual number of Antarctic *Epimeria* species. An extension of the geographic coverage of the Antarctic shelf and increased sampling effort are likely to reveal even further undetected diversity within the genus. Along with the numerous studies accounting for cryptic species complexes in a wide variety of organisms (e.g. Allcock et al., 2011; Arango et al., 2011; Janosik and Halanych, 2010; Linse et al., 2007; Raupach and Wägele, 2006; Wilson et al., 2009), this is striking evidence of the great underestimation of Antarctic shelf biodiversity. Overlooked biodiversity often comes with overestimations of the actual species' geographic ranges (Held and Wägele, 2005; Krabbe et al., 2010; Wilson et al., 2009). Our results also challenge the previous assumption of circum-Antarctic distributions of many *Epimeria* species, as most of the species appear to be geographically restricted to one of the three studied regions. However, despite their brooding biology and massive morphology, a few species demonstrate widespread distributions (some over 6000 km), suggesting a potential for large-scale dispersal. The distinctive oceanography and climatic history of the Southern Ocean are likely to be the main drivers for the diversification and distribution patterns within the region (Kaiser et al., 2013). The present results, along with similar studies of other Antarctic benthic species, will contribute to the understanding of speciation and migration processes that led to the observed biodiversity on the Southern Ocean shelf.

ACKNOWLEDGEMENTS

The first author has a PhD fellowship from F.R.I.A. (F.N.R.S., Belgium). The last author was funded by the Digit 3 program of BELSPO. We thank the Alfred-Wegener-Institut, Helmholtz-Zentrumfür Polar- und Meeresforschung (AWI) and the captain, crew and chief scientists of various *RV Polarstern* expeditions for their efficiency, as well as present and past colleagues of the staff of the Royal Belgian Institute of Natural Sciences (RBINS), especially Henri Robert and Charlotte Havermans, for collecting specimens on board. Laure Corbari, on behalf of the Muséum national d'Histoire naturelle (MNHN), Paris, is acknowledged for giving us access to the biological material of the research program REVOLTA 1124, supported by the Institut polaire français Paul Émile Victor (IPEV), and the CAML-CEAMARC cruise of *RV Aurora Australis* (IPY project n°53), supported by the Australian Antarctic Division, the Japanese Science Foundation and the IPEV (project ICOTA). This publication is registered as CAML (Census of Antarctic Marine Life) publication No. 164 and contribution No. 210 to ANDEEP. Many thanks to Anton Van de Putte (RBINS) for kindly providing distribution maps. We are also grateful to Zohra Elouaazizi, Karin Breugelmans, Gontran Sonet and Zoltan Nagy (all RBINS) for helpful methodological advices.

CHAPTER 3

EPIMERIA SP. NOV. ROSS*, A NEW CRESTED AMPHIPOD FROM THE ROSS SEA, WITH NOTES ON ITS AFFINITIES (CRUSTACEA, AMPHIPODA, EUSIROIDEA, EPIMERIIDAE)

Marie L. Verheye[1,2]

Anne-Nina Lörz [3]

Cédric d'Udekem d'Acoz[1]

*The name of the new species is not communicated before publication, in order to avoid nomenclatural issues.

Submitted

[1] Royal Belgian Institute of Natural Sciences, OD Taxonomy and Phylogeny, 29 rue Vautier, B-1000 Brussels, Belgium

[2] Catholic University of Louvain-la-Neuve, Department of Biology, Marine Biology Laboratory, 3 bte L7.06.04 Croix du Sud, B-1348 Louvain-la-Neuve, Belgium

[3] Zoologisches Museum Hamburg, Centrum für Naturkunde (CeNak), Martin-Luther-King-Platz 3, 20146 Hamburg, Germany

ABSTRACT

A new crested amphipod, *Epimeria* sp. nov. Ross, is described after specimens collected in the western Ross Sea, Southern Ocean, at 151–409 m depth. This increases the number of *Epimeria* species known from the Ross Sea to eleven. This new species, which belongs to the *macrodonta* species complex, is very similar to *Epimeria reoproi* Lörz & Coleman, 2001, *E*. sp. aff. *reoproi* sensu d'Udekem d'Acoz & Robert, 2008 and *E. vaderi* Coleman, 1998, the latter three species being known only from the Antarctic Peninsula and South Shetland Islands. *Epimeria* sp. nov. Ross can be distinguished from them by the following combination of characters: flexed rostrum, narrow coxa 3, long ventral tooth on coxa 4 and non-duplicate lateral tooth on pleonites 1–2. The phylogenetic relationships between *E.* sp. nov. Ross and other *Epimeria* of the *macrodonta* species complex are briefly outlined based on a phylogenetic analysis of 28S rDNA fragments.

INTRODUCTION

The genus *Epimeria* includes some of the largest and most eye-catching amphipod species from the icy waters surrounding the Antarctic continent, where they exhibit a high morphological diversity (Rauschert and Arntz, 2015). As Antarctic *Epimeria* is monophyletic and particularly diverse, this clade has been qualified as a species flock (Lecointre et al., 2013; Lörz and Held, 2004). The taxonomy of the genus has been extensively studied. It was first revised by Coleman (2007). Lörz, (2009) and Lörz et al. (2007, 2009, 2011) subsequently described several new species.

However, molecular and morphological analyses suggested the existence of numerous previously overlooked species (Lörz et al., 2011; Verheye et al., 2016a). In the light of these new data, Antarctic *Epimeria* were revised for a second time by d'Udekem d'Acoz & Verheye (*in Press*). No less than 28 new species are described in the latter monograph. However, because of the high occurrence of morphologically similar species within *Epimeria* and the sporadic nature of sampling in the Southern Ocean, additional species likely remain to be discovered. The present paper supports this assumption, by presenting yet another new *Epimeria* species from the Ross Sea.

MATERIAL AND METHODS

Specimens studied herein have been collected during several expeditions to the Ross Sea. First, the New Zealand expeditions BIOROSS and IPY in 2004 and 2008 deployed four different gear types to collect benthic invertebrates from the *RV Tangaroa*: Van Veen grabs, Agassiz trawls, an epibenthic

sled and a rock dredge. Amphipods were sorted from collections immediately (often alive), fixed in 98 % ethanol and transferred to 70 % ethanol about four months later. Secondly, the Italian expedition XIX in 2004 deployed an Agassiz Trawl to collect benthic samples from the *RV Italica*. The preservation data are missing, but these specimens were presumably fixed in 98 % ethanol.

Specimens were examined and dissected using a Leica MZ9.5 stereomicroscope and drawn using a camera lucida attachment. Small appendages (mouthparts, uropods, telson) were drawn using a Nikon compound microscope fitted with a camera lucida. The body lengths of specimens examined were measured by tracing individual's mid-trunk lengths (tip of the rostrum to end of telson) using a camera lucida, measuring this curved length and then converting this to actual animal body length by correcting for magnification. All illustrations were inked electronically using a Wacom Board and applying the method described by Coleman (2003, 2009).

Type material is held in the National Institute of Water and Atmospheric Research Invertebrate Collection at Wellington (NIWA), New Zealand; the Zoological Museum Genova, Italy and the Zoological Museum Hamburg, Germany.

28 rDNA sequences from other specimens of the *macrodonta* complex were obtained from Verheye *et al*. (2016a). The laboratory protocol used for sequencing therefore follows Verheye *et al*. (2016a). Sequence chromatograms were checked and forward and reverse sequence fragments were assembled using *Codon Code Aligner* v.3.7.1. Sequences were aligned with MAFFT v.7 (Katoh and Standley, 2013) (available from http://mafft.cbrc.jp/alignment/server/), using the structural alignment strategy Q-INS-i under default settings. The best-fit models of DNA substitution was selected using the Akaike Information Criterion (AIC), the Bayesian Information Criterion (BIC) and under a Decision Theoretic framework (DT), as implemented in jModelTest v.2 (Darriba et al., 2012). A Bayesian tree was reconstructed using MrBayes v.3.2 (Ronquist and Huelsenbeck, 2003). BI analysis of the 28S alignment included two runs of 10^7 generations. Trees were sampled every 1000 generations using four Markov chains, and default heating values. Convergence was assessed by the standard deviation of split frequencies (< 0.01) and by examining the trace plots of log-likelihood scores in Tracer 1.6 (Rambaut and Drummond, 2005). The first 10 % trees were discarded as burn-in, while the remaining trees were used to construct a 50 % majority rule consensus tree and estimate the posterior probabilities (PP). Nodes with PP ≥ 0.95 were considered as significantly supported.

MORPHOLOGICAL SYSTEMATICS

Order AMPHIPODA Latreille, 1816

Superfamily EUSIROIDEA Stebbing, 1888

Family EPIMERIIDAE Boeck, 1871

Genus *Epimeria* Costa in Hope, 1851

***Epimeria* sp. nov. Ross (Figs 1–5)**

Epimeria sp. 1.—d'Udekem d'Acoz & Verheye *in press*: key and note.

TYPE MATERIAL

MNA4450, holotype, ovigerous female, 34.5 mm, XIX Expedition/Hout3 bis, *RV Italica*, 17 February 2004, 258 m, 72°17.45’ S 170°26.40’ E

NIWA20976, paratype 1, female, 30.2 mm, TAN0402/188, *RV Tangaroa*, 27 February 2004, 286–280 m, 71°33.00' S 171°06.60’ E

NIWA20953, paratype 2, male, 30.6 mm, TAN0402/22, *RV Tangaroa*, 9 February 2004, 151–180 m, 71°48.00’ S 170°56.40’ E

NIWA42762, paratype 3, female, 46 mm, TAN0802/17, *RV Tangaroa*, 9 February 2008, 321 m, 73°07.20’ S 174°19.20’ E

NIWA20965, paratype 4, male, 35.5 mm, TAN0402/39, *RV Tangaroa*, 10 February 2004, 251–253 m, 71°45.00’ S 171°08.40’ E

MNA8688, paratype 5, female, 47 mm, XIX Expedition/Hout3 bis, *RV Italica*, 17 February 2004, 258 m, 72°17.45’ S 170°26.40’ E

ZMH K-46194, paratype 6, female, 33.5 mm, TAN0402/39, *RV Tangaroa*, 10 February 2004, 251–253 m, 71°45.00’ S 171°08.40’ E

NIWA20952, paratype 7, male, 52.1 mm, TAN0402/17, *RV Tangaroa*, 5 February 2004, 403–409 m, 71°44.40’ S 171°39.00’ E

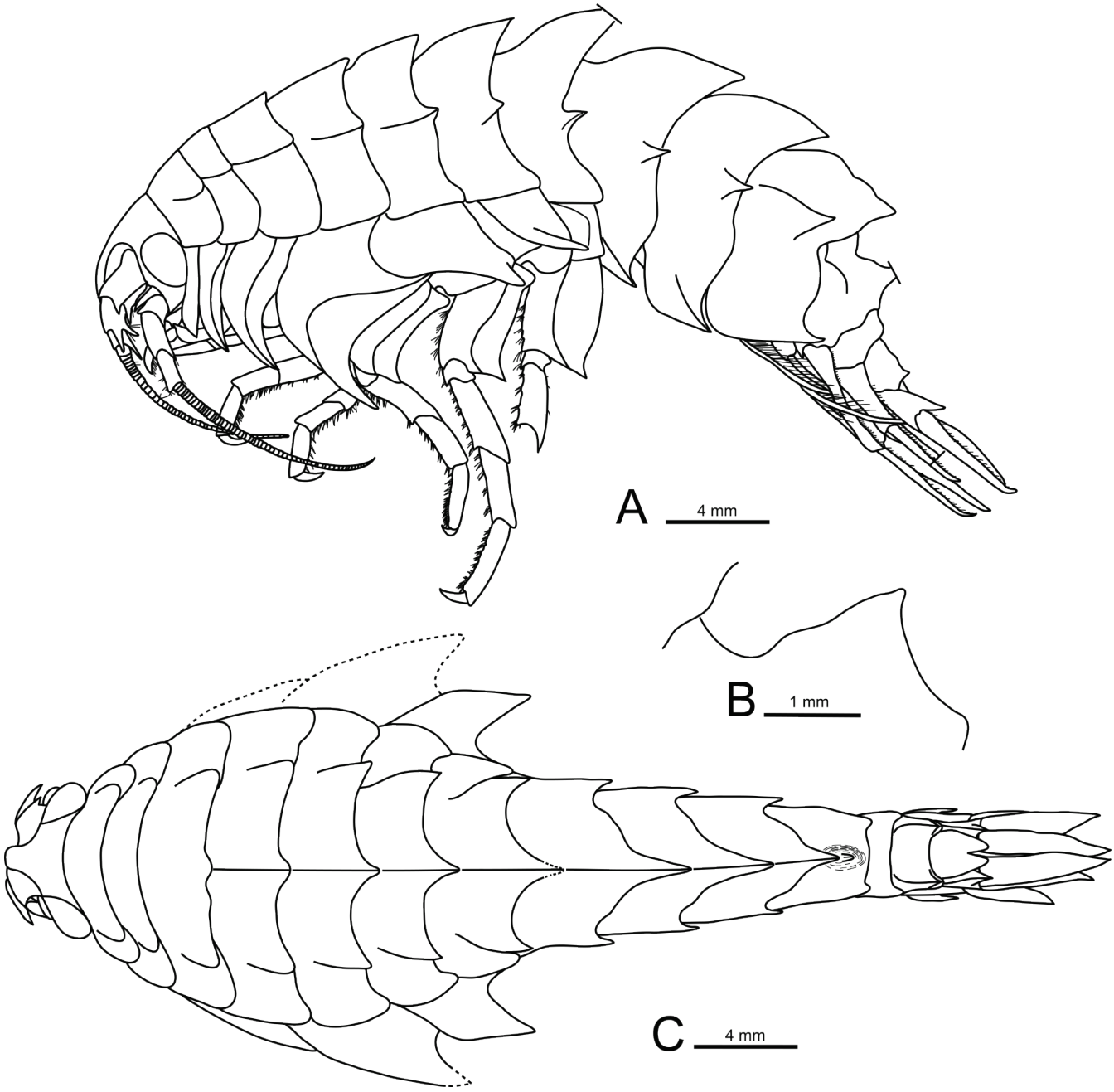

Figure 1. *Epimeria* **sp. nov**. **Ross.** A, C, Holotype, 34.5 mm, MNA4450; B, Paratype 5, 47 mm, MNA8688; A, lateral habitus; B, dorsal process of urosomite 2; C, dorsal habitus.

ETYMOLOGY

Epimeria sp. nov. Ross is dedicated to the daughter of the first author, who was born during the preparation of this manuscript. The name is a noun in apposition.

DESCRIPTION

Head: rostrum as long as head, overreaching distal margin of the first article of antenna 1; eye oval, 0.4 x head height.

Pereonites: pereonite 1 subequal in length to head (excluding rostrum), pereonite 2 c. 0.7 x length of pereonite 1, pereonites 1 and 2 lacking mid-dorsal process, bearing apically rounded weak carinate lateral projection; pereonites 3–7 with size-increasing, low mid-dorsal tooth (that of pereionite 2 nearly reduced to a bump); pereonites 3 to 5 bearing mid-lateral carinate projection (apically rounded in pereonite 3–4, apically acute or subacute in pereonite 5); pereonites 6 and 7 with sharp mid-lateral tooth.

Pleosome: pleonites 1–3 with low mid-dorsal tooth (anteriorly regularly rounded) and mid-lateral tooth. Mid-dorsal tooth of pleonite 3 with very weak median notch (and with trace of a second notch on distal 0.2). Epimeral plates 1–3 anteroventral angle rounded, posteroventral angle produced into a strong tooth.

Urosome: urosomite 1 with sharp triangular mid-dorsal tooth; urosomite 2 shortest, dorsolaterally smooth; urosomite 3 middorsally smooth, dorsolateral angle produced into a small triangular tooth.

Antenna 1: article 1 of peduncle about 2 x as long as article 2, 3 x as long as article 3, with distolateral tooth not reaching mid of article 2 (teeth excluded), with distomedial tooth reaching about mid of article 2 (teeth excluded), with major ventral tooth almost reaching half of article 2 (teeth excluded) and a second (half the length) ventral tooth more medially. Article 2 of peduncle about 2 x as long as article 3, with lateral and medial tooth overreaching corpus of article 3 and reaching mid of ventral tooth of article 3; with two subequal ventral teeth (parallel and very close to each other) and slightly overreaching corpus of article 3. Article 3 with ventral tooth about as long as corpus of article. Accessory flagellum scale like, reaching distal end of first flagellar article; primary flagellum with 44 articles.

Antenna 2: article 4 of peduncle slightly longer than article 5, with distolateral denticle; flagellum with 66 articles.

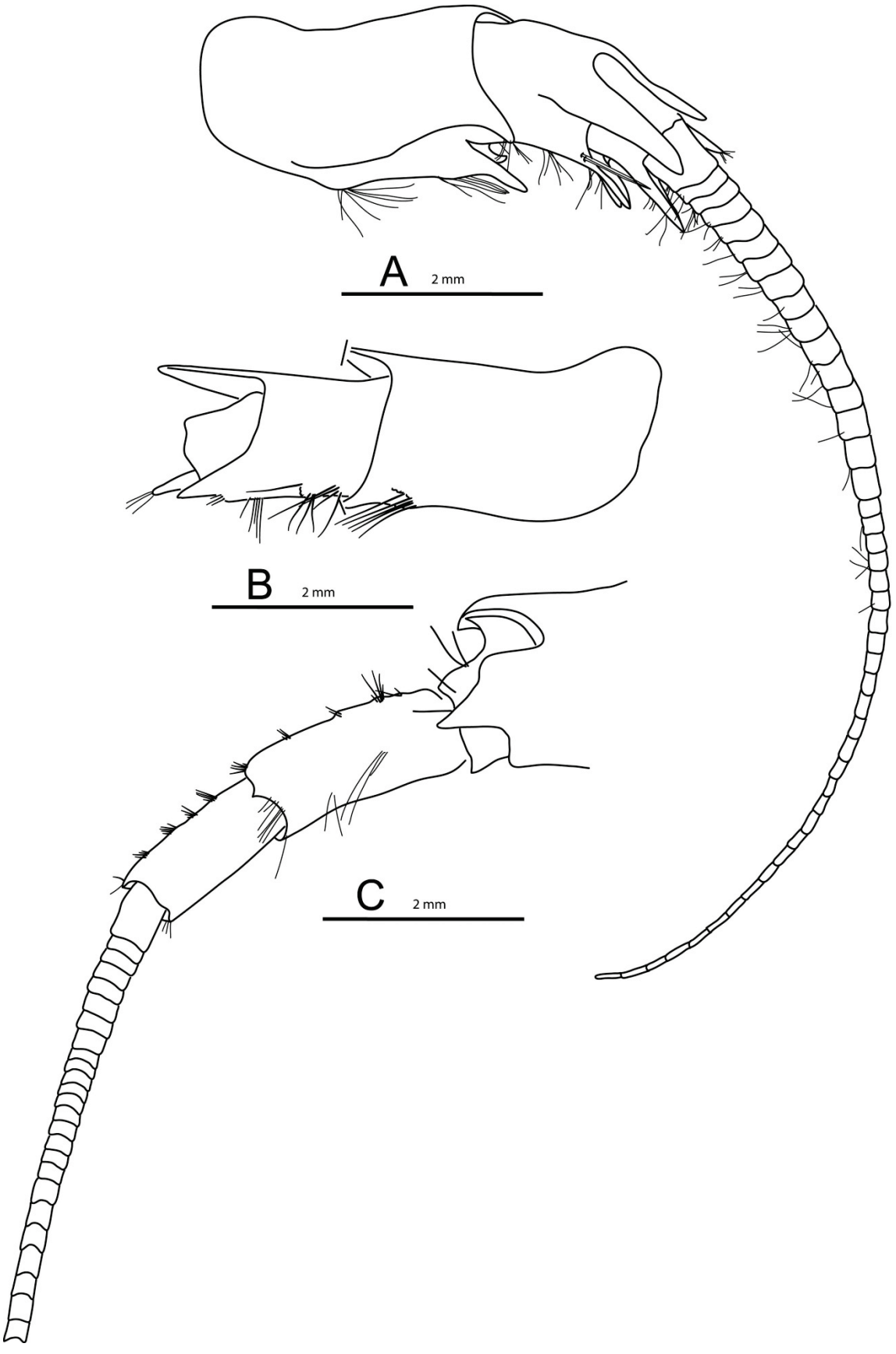

Figure 2. *Epimeria* **sp. nov. Ross.** Holotype 34.5 mm, MNA4450. A, right antenna 1; B, peduncle antenna 1; C, antenna 2.

Labrum: with very short distal hair-like setae at both sides of terminal notch.

Hypopharynx: lobes broad, distally and medially covered with hair-like setae, lateral process narrow, rounded.

Mandible: incisor with 4 blunt teeth, molar produced and triturative; palp article 1 non-setose, article 2 setose medially, article 3 densely setose medially, with 4 long setae distally.

Maxilla 1: inner plate subtriangular, obliquely convex inner margin with 14 stout plumose setae; outer plate distal margin oblique, with 11 lobate robust setae; palp exceeding outer plate, palp article 1 short, article 2 curved medially with 7 robust setae distomedially and 5 slender setae behind them.

Maxilla 2: with long, slender setae distally on lateral and medial plates.

Maxilliped: outer plate broadly rounded distally, reaching mid length of second article of maxillipedal palp; inner plate with row of long setae medially and anteriorly; palp medial margin strongly setose, propodus with groups of long setae reaching distal end of dactylus (two groups of setae forming transverse rows).

Gnathopod 1: coxa long, slender, anterior margin with slight angular discontinuity at distal 0.2, distally pointed, longitudinal mid lateral ridge well developed; basis linear, slender, both margins with slender setae; merus slightly longer than ischium, anterior margin very short, distal margin oblique, posterodistal angle acute, setose; carpus slightly expanding at distal end, posterior margin strongly setose, anterodistal margin with group of long setae; propodus margins convex, posterior margin and palm lined with robust setae, palm oblique; dactylus slender, slightly curved, posterior margin minutely serrated.

Gnathopod 2: coxa 2 wider and longer than coxa 1, with lateral ridge, pointed; basis linear; ischium and merus similar to gnathopod 1; carpus linear and more elongate than in gnathopod 1, strongly setose posterior margin; propodus very similar to that of gnathopod 1 but slightly more elongate; dactylus similar to that of gnathopod 1.

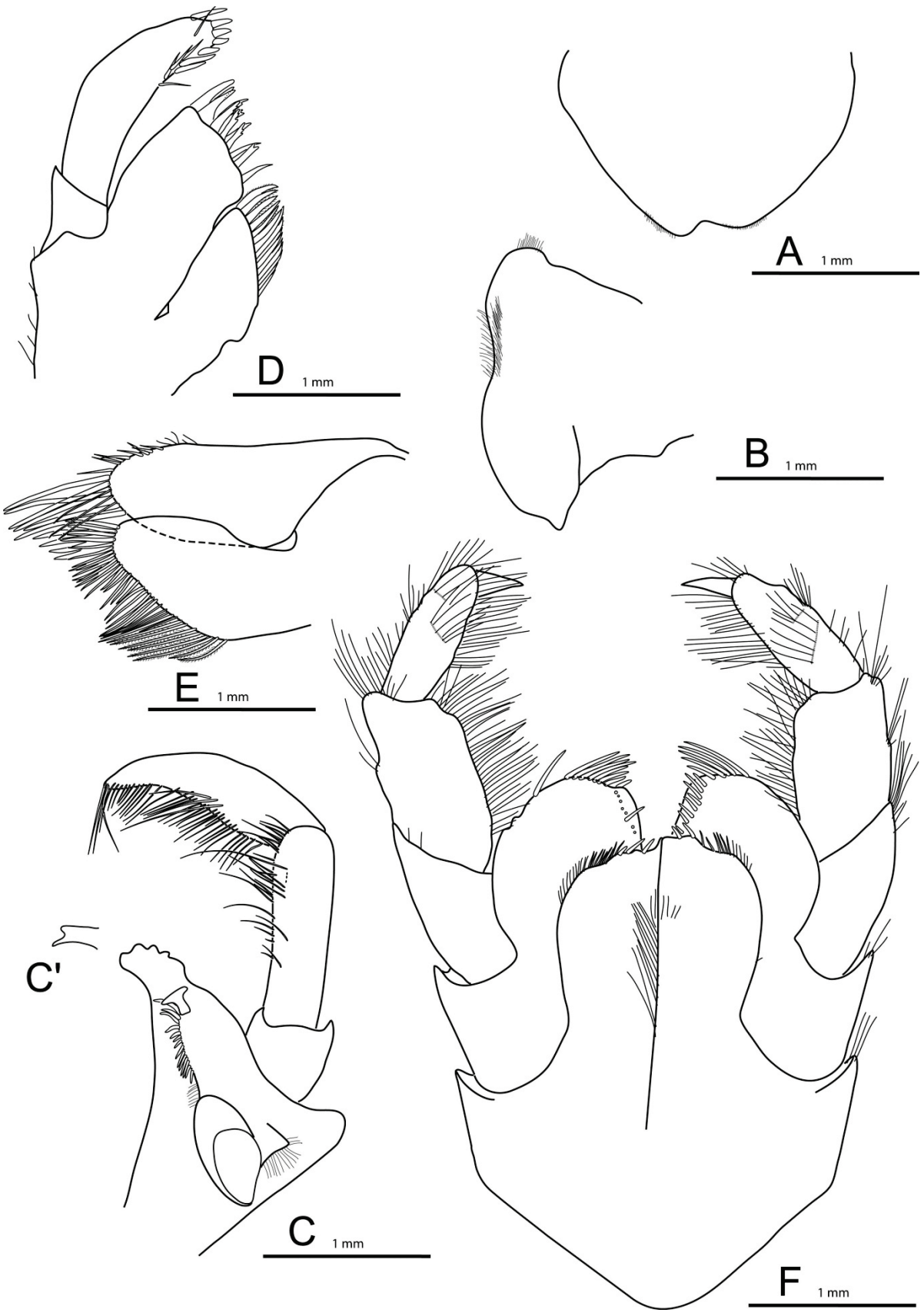

Figure 3. *Epimeria* **sp. nov. Ross**. Holotype 34.5 mm, MNA4450. A, labrum; B, hypopharynx; C, left mandible; D, right maxilla 1; E, left maxilla 2; F, maxilliped.

Pereopod 3: coxa 3 longer than coxa 2, with midlateral ridge, pointed; basis linear, slender setae on anterior and posterior margin; merus, carpus and propodus very robust; merus and carpus slightly expanded distally; carpus 0.6 length of merus; propodus 0.8 length of merus; carpus, merus and propodus with robust setae on posterior margin, anteriorly nearly naked except robust seta on anterodistal corner; dactylus stout, without setae and curved.

Pereopod 4: coxa 4. Anterodorsal border nearly straight and of normal length; anteroventral border nearly straight (inconspicuously convex) and of normal length; a low and long curve forms a very gradual transition between the anterodorsal and anteroventral borders; ventral tooth long, slender, apically acute and oriented backwards; lateral carina without tooth or angularity, not projecting laterally, carina very distant from margin of coxa at its deepest point; basis to dactylus as for pereopod 3.

Pereopod 5: coxa with posterodistal corner strongly produced, drawn out to pointed wing in dorsal view; basis anterior margin straight, setose, posterior margin slightly expanded proximally, with posterodistal corner produced into and acutely triangular tooth, with ridge along entire length of basis; ischium anterodistal margin pointed; merus, carpus and propodus very robust; merus with posterior margin produced; carpus about as long as merus, with anterior margin setose; dactylus stout, curved.

Pereopod 6: coxa with carinate, lateral tooth, forming a triangular wing in dorsal view; posteroventral corner broadly rounded; basis to dactylus as for pereopod 5.

Pereopod 7: coxa subrectangular, with low lateral carina, with posterodistal corner bluntly angular; basis larger than of pereopod 6, posteriorly weakly sigmoid, with posterodistal corner produced into a small tooth; ischium to dactylus as for pereopod 5 and 6.

Pleopods: pleopods 1–3 with two rami each; inner and outer rami subequal, twice as long as peduncle.

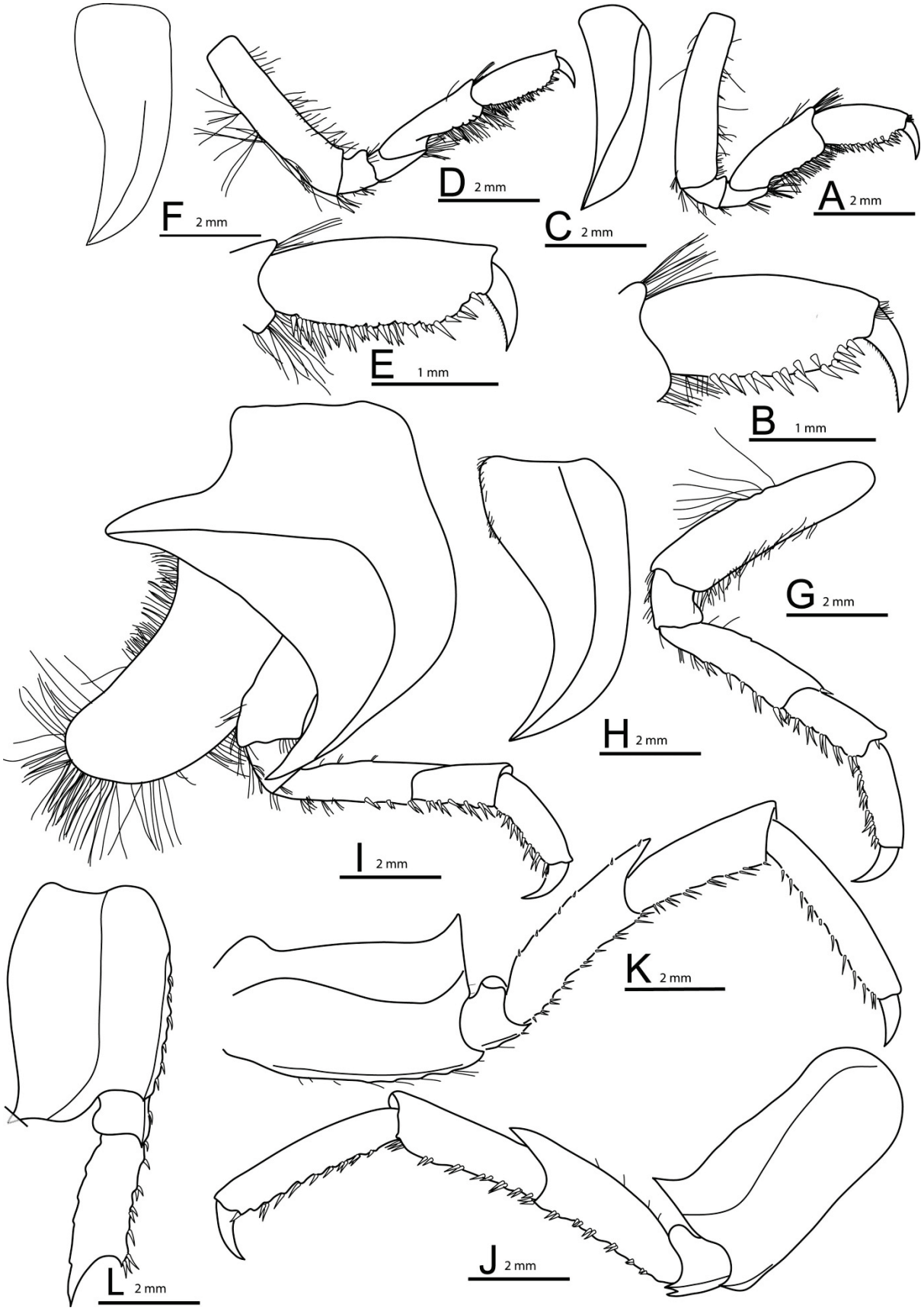

Figure 4. *Epimeria* **sp. nov. Ross**. Holotype 34.5 mm, MNA4450. A, right gnathopod 1; B, palm of right gnathopod 1; C, right coxa 1; D, right gnathopod 2; E, palm of right gnathopod 2; F, right coxa 2; G, right pereopod 3; H, right coxa 3; I, right pereopod 4; J, right pereopod 5; K, left pereopod 6; L, right pereopod 7.

Uropod 1: peduncle slightly longer than rami; rami subequal in length, margins with short robust setae.

Uropod 2: peduncle naked, 0.9 x length of outer ramus; inner ramus 1.3 x outer ramus; both rami outer and inner margin short robust setae.

Uropod 3: peduncle short, half length of outer ramus, peduncle mid dorsal ridge, drawn out in 3 pointed processes; inner margin of both rami with sparse robust setae.

Telson: 1.2 longer than wide, with narrow V-shaped cleft third of length, lobes triangular.

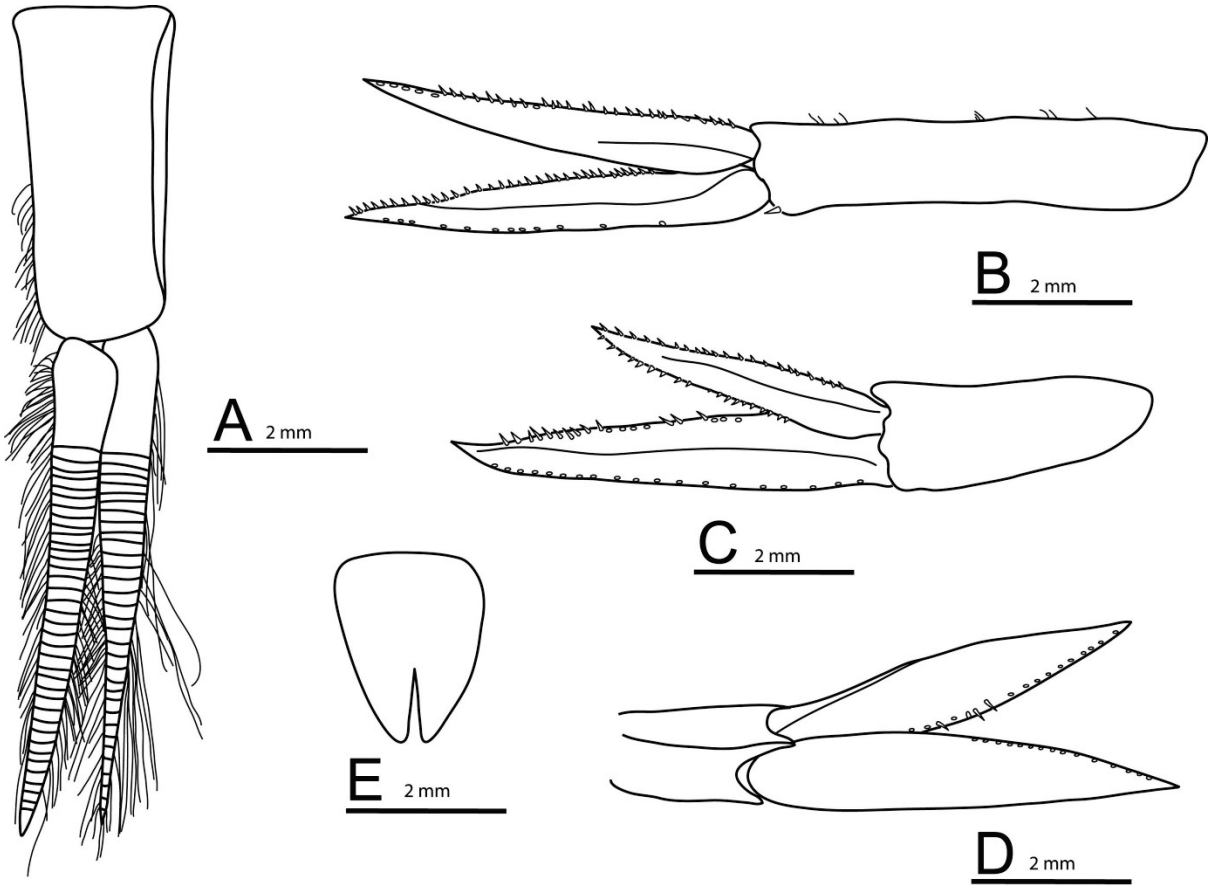

Figure 5. *Epimeria* **sp. nov**. **Ross.** Holotype 34.5 mm, MNA4450. A, right pleopod 1; B, left uropod 1; C, left uropod 2; D, right uropod 3; E, telson.

VARIATION

In dorsal view, males with pereon thinner than in females.

BODY LENGTH

Up to 52 mm.

DISTRIBUTION

Southern Ocean: western Ross Sea, 151–409 m.

TAXONOMIC REMARKS

E. sp. nov. Ross belongs to a morphologically homogeneous *Epimeria* species complex from the Southern Ocean that also includes *E. macrodonta* Walker, 1906, *E. reoproi* Lörz & Coleman, 2001, *E. schiaparelli* Lörz, Maas, Linse & Fenwick, 2007, *E. similis* Chevreux, 1912, *E. vaderi* Coleman, 1998 and 12 new species to be described by d'Udekem d'Acoz & Verheye (*in Press*). *Epimeria* sp. nov. Ross is included as *Epimeria* sp. 1 in the key to the *macrodonta* species complex of the latter monograph. In all species of this complex, several pereon body segments and all pleosome segments bear a sharp, acute-tiped, dorsolaterally strongly flattened carinated tooth, arching posteriorly. In previous molecular phylogenies, all studied species were shown to form a clade (Lörz et al., 2007; Verheye et al., 2016a).

The *macrodonta* complex can be divided into two clear-cut phenotypic groups. The group 1 includes those with a pair of small teeth pointing upwards on urosomite 2. The group 2 includes those which have no such teeth. *Epimeria* sp. nov. Ross belongs to that group 2. The group 2 includes species with 3 morphotypes of coxa 4 as seen in dorsal view: (A) those with the lateral carina presenting a tooth projecting laterally; (B) those with the lateral carina presenting an obtuse angle (but no real tooth) visible in dorsal view and (C) those with the carina looking perfectly smooth or with a low rounded (not angular) protrusion in dorsal view. *Epimeria* sp. nov. Ross belong to that category 2C, along with *Epimeria reoproi* Lörz & Coleman, 2001, "*Epimeria reoproi* sensu Rauschert and Arntz (2015)", "*Epimeria* aff. *reoproi* sensu d'Udekem D'Acoz and Robert (2008)" and *Epimeria vaderi* Coleman, 1998. "*Epimeria reoproi* sensu Rauschert and Arntz (2015)" and "*Epimeria* aff. *reoproi* sensu d'Udekem d'Acoz and Robert (2008)" will be described as new species by d'Udekem d'Acoz and Verheye (*in Press*). The first one is a deep-sea species found below 2000 m, and it departs from all species of the *macrodonta*-clade by the shape of the dorsal projection of its urosomite 1, which points backwards instead of upwards.

E. sp. nov. Ross is compared in Table 1 to the three morphologically most similar species, *E. reoproi*, *E*. aff. *reoproi* sensu d'Udekem d'Acoz and Robert (2008) and *E. vaderi*.

	***Epimeria* sp. nov. Ross**	***Epimeria vaderi***	***Epimeria reoproi***	***Epimeria* aff. *reoproi***
Rostrum	flexed	nearly straight	flexed	nearly straight
Coxa 1 ventrally	pointed	pointed	rounded	pointed
Coxa 3	narrow	wide	wide	narrow
Coxa 4 excavation	deeply excavate	not deeply excavate	deeply excavate	deeply excavate
Coxa 4 ventral tooth	long	short	long	short
Coxae 5–6 in dorsal view	with large tooth projecting laterally	with small tooth not projecting laterally	presumably with large tooth projecting laterally	with large tooth projecting laterally
Dorsal carinae starting	on pereonite 3	on pereonite 4	on pereonite 6	on pereonite 4
Mid-dorsal tooth of pereonite 7, pleonites 1–2	regularly rounded profile	regularly rounded profile	regularly rounded profile	very angulate profile
Dorsolateral teeth On pleonite 1	single tooth	two teeth	single tooth	two teeth
Dorsolateral teeth On pleonite 2	single tooth	two teeth	single tooth	single tooth

Table 1. Morphological differences between *Epimeria* sp. nov. Ross, *E. vaderi* Coleman, 1998, *E. reoproi* Lörz & Coleman, 2001 and *Epimeria* aff. *reoproi* sensu d'Udekem & Robert, 2008.

PHYLOGENETIC TREE

A Bayesian tree of 34 specimens from the *macrodonta* complex was reconstructed based on a 1120 bp alignment (substitution model: GTR + I + G). *E.* sp. nov. Ross is shown to be nested within the clade composed of *E. similis* and 9 new species, morphologically similar to *E. similis* and *E. macrodonta* (Verheye et al., 2016a).

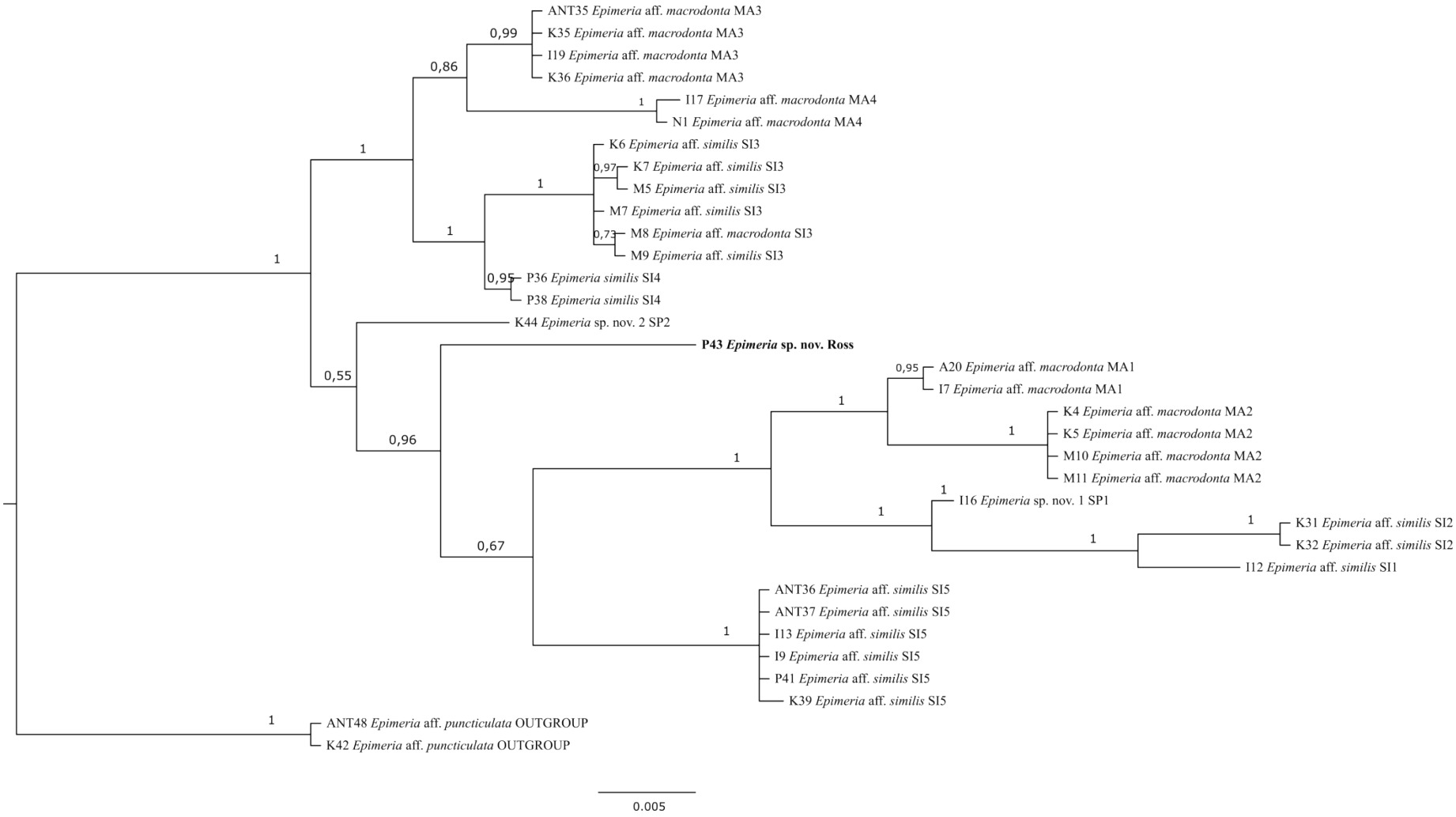

Figure 6. Bayesian tree of the *macrodonta* complex reconstructed with 28S rDNA fragments. Posterior probabilities are indicated above the nodes. MOTUs names (putative species) from Verheye *et al.* (2016a) are indicated besides the names.

DISCUSSION

The discovery of *Epimeria* sp. nov. Ross increases the number of *Epimeria* species from the Ross Sea to 11. It is shown to be part of a "*macrodonta* clade", along with *E. similis* and 9 new species morphologically similar to *E. similis* and *E. macrodonta* (to be described in d'Udekem d'Acoz and Verheye, *in Press*). *E. schiaparelli* and *E. reoproi* were also shown to be part of a clade including *E. macrodonta* and *E. similis* (Lörz and Held, 2004; Lörz et al., 2007). As *E*. *vaderi* and *E*. aff. *reoproi* are the morphologically most similar species to *E.* sp. nov. Ross, the latter species are assumed to belong to this "*macrodonta* complex" as well.

Although *Epimeria* sp. nov. Ross is here recorded from the western Ross Sea, the morphologically most similar species, *Epimeria vaderi*, *Epimeria reoproi* and *Epimeria* aff. *reoproi* have so far only been found in the Peninsular/South Shetlands area. However, large sections of the Ross Sea remain undersampled, such as the eastern area and the deep-sea (below 2000 m; Lörz et al., 2007). Therefore, further sampling might reveal additional diversity within this complex. The discovery of *Epimeria* — which can be identified by clear-cut morphological characters — further exemplifies the underestimation of species diversity within one of the best studied Antarctic amphipod genera.

ACKNOWLEDGMENTS

The first author has a Ph.D. fellowship from F.R.I.A. (F.N.R.S., Belgium). We appreciate the kind help of the NIWA Invertebrate Collection staff, Wellington, New Zealand with loan of the material. We also thank Stefano Schiaparelli (University of Genova, Italy) for giving us access to the material of the *RV Italica* XIX expedition to the Ross Sea.

CHAPTER 4

LOCKED IN THE ICEHOUSE: EVOLUTION OF AN ENDEMIC *EPIMERIA* (AMPHIPODA, CRUSTACEA) SPECIES FLOCK ON THE ANTARCTIC SHELF

Marie L. Verheye[1,2]

Thierry Backeljau[1,3]

Cédric d'Udekem d'Acoz[1]

Published in: ***Molecular phylogenetics and Evolution*** **(2017): 114, 14–33.**

[1] Royal Belgian Institute of Natural Sciences, OD Taxonomy and Phylogeny, 29 rue Vautier, B-1000 Brussels, Belgium

[2] Catholic University of Louvain-la-Neuve, Department of Biology, Marine Biology Laboratory, 3 bte L7.06.04 Croix du Sud, B-1348 Louvain-la-Neuve, Belgium

[3] University of Antwerp, Evolutionary Ecology Group, 171 Groenenborgerlaan, 2020 Antwerp, Belgium

ABSTRACT

The Antarctic shelf's marine biodiversity has been greatly influenced by the climatic and glacial history of the region. Extreme temperature changes led to the extinction of some lineages, while others adapted and flourished. The amphipod genus *Epimeria* is an example of the latter, being particularly diverse in the Antarctic region. By reconstructing a time-calibrated phylogeny based on mitochondrial (COI) and nuclear (28S and H3) markers and including *Epimeria* species from all oceans, this study provides a temporal and geographical framework for the evolution of Antarctic *Epimeria*. The monophyly of this genus is not supported by Bayesian Inference, as Antarctic and non-Antarctic *Epimeria* form two distinct well-supported clades, with Antarctic *Epimeria* being a sister clade to two stilipedid species. The monophyly of Antarctic *Epimeria* suggests that this clade evolved in isolation since its origin. While the precise timing of this origin remains unclear, it is inferred that the Antarctic lineage arose from a late Gondwanan ancestor and hence did not colonize the Antarctic region after the continent broke apart from the other fragments of Gondwanaland. The initial diversification of the clade occurred 38.04 Ma (95 % HPD [48.46 Ma; 28.36 Ma]) in a cooling environment. Adaptation to cold waters, along with the extinction of cold-intolerant taxa and resulting ecological opportunities, likely led to the successful diversification of *Epimeria* on the Antarctic shelf. However, there was neither evidence of a rapid lineage diversification early in the clade's history, nor of any shifts in diversification rates induced by glacial cycles. This suggests that a high turnover rate on the repeatedly scoured Antarctic shelf could have masked potential signals of diversification bursts.

INTRODUCTION

The Southern Ocean is traditionally viewed as an isolated ecosystem where the marine fauna has essentially evolved *in situ* (Clarke and Crame, 1989; Dell, 1972; Knox and Lowry, 1977; Lipps and Hickman, 1982). The eastward flowing Antarctic Circumpolar Current (ACC), encircling Antarctica since the Oligocene, is the most powerful sea current on earth. The Antarctic Polar Front (APF), one of the ACC's jets, marks a sharp change in surface water temperatures and impedes north-south exchange of water. Therefore, it appears to be an important barrier to dispersal (Angel, 1997; Clarke et al., 2005; Dell, 1972). The high degree of species-level endemism of the Antarctic marine fauna is a signature of this long history in isolation (Arntz et al., 1997; Clarke and Crame, 1997; Clarke and Johnston, 2003). Some Antarctic lineages are descendants of Gondwanan ancestors, which arose by vicariance when the supercontinent progressively broke apart (e.g. Brandt, 1992; Clarke and

Johnston, 1996; Waters et al., 2007; Williams et al., 2003). While the APF has been shown to be a permeable barrier for a variety of pelagic and deep-sea organisms (Antezana, 1999; Bargelloni et al., 2000; Brandt et al., 2007; Hodgson et al., 1997; Page and Linse, 2002; Pawlowski et al., 2007; Thatje and Fuentes, 2003), the Drake Passage is too deep to allow the dispersal of stenobathic shelf organisms along the benthos (e.g. Hunter and Halanych, 2008; Shaw et al., 2004). However, some benthic taxa lacking a pelagic stage would be able to cross the front by drifting on macroalgae or floating debris (Barber et al., 1959; Coombs and Landis, 1966; Fraser et al., 2009; Helmuth et al., 1994; Waters, 2008). Historical cases of polar emergences — colonizations of the Antarctic shelf from the depths — or submergences — dispersals from the shelf towards the depths — were also inferred for some strictly benthic organisms (Held, 2000; Strugnell et al., 2008). Such movements may be facilitated by the formation of cold and dense water near the continent which sinks northward at a layer below 4000 m depth to become the "Antarctic Bottom Water", thereby forming an isothermal water column between the shelf and the deep-sea (Knox and Lowry, 1977). The Southern Ocean fauna would therefore contain a mixture of lineages with different histories, some would have evolved *in situ* since before Antarctica existed, others would be more recent colonizers (Clarke and Crame, 1989).

All along its geological history, the Antarctic region has faced profound climatic changes, which deeply impacted Southern Ocean marine biodiversity (Clarke and Crame, 1997). The fossil record indicates major changes in the nature of the marine fauna along the cooling trend, which began across the early to middle Eocene boundary (ca. 48–49 Ma). While many taxa went extinct, the availability of previously occupied benthic niches provided ecological opportunities for surviving lineages (Aronson et al., 2007; Brandt, 1999). Ecological opportunity has been inferred to drive initial rapid lineage diversification (Condamine et al., 2013; Losos and Mahler, 2010; Yoder, 2010). As lineages rapidly fill unoccupied niches and available habitats run out, the rate of diversification would consequently decrease (Freckleton and Harvey, 2006; Rabosky and Lovette, 2008; Schluter, 2000; Walker and Valentine, 1984). Alternatively, the simultaneous formation of multiple geographical barriers can be responsible for a burst of allopatric speciation (Rundell and Price, 2009). Hence, by providing ecological opportunities or causing allopatric speciation, several main events in Antarctica's climatic history could have impacted species' origination rates. For instance, the gradual extinction of decapods, possibly beginning with the cooling trend which started in the early Eocene (Thatje et al., 2005b), likely triggered the radiation of the peracarids (Aronson et al., 2007). The Eocene–Oligocene boundary (34 Ma) was marked by a sudden drop in temperatures, the first continent-wide glaciations (Lear et al., 2000, 2004), the opening of the Tasmanian and Drake passages (Barker, 2001; De Broyer and Jażdżewska, 2014; Exon et al., 2000; Stickley et al., 2004) and

the formation of the ACC (Lawver and Gahagan, 2003; Lyle et al., 2007; Pfühl and McCave, 2005). The resulting thermal and geographical isolation of the Antarctic region is presumed to have promoted vicariant speciations in Southern Ocean taxa. Since the Mid-Miocene Climate Transition (MMCT; ~14 Ma), the ice-shelf grounding line periodically extended to the outer shelf break, at least in some places during glacial maxima. These glacial cycles, which intensified in the Late Pliocene-Pleistocene period (Lewis et al., 2008; McKay et al., 2012; Pollard and DeConto, 2009) were inferred to act as a "diversity pump" on the Southern Ocean continental shelf (Clarke and Crame, 1989, 2010; Clarke et al., 1992b). The isolation of populations in ice-free refugia during glacial advances would have resulted in allopatric speciations of less dispersive organisms (Thatje et al., 2005b).

The Antarctic component of the amphipod genus *Epimeria* Costa, 1851 was put forward as an example of an Antarctic species flock, i.e. a highly diverse clade of species that originated and diversified in the Antarctic region (Lecointre et al., 2013). However, the assumption of monophyly was based on a previous COI phylogeny of *Epimeria*, comprising 17 Antarctic species, but only two non-Antarctic (New Zealand) species (Lörz et al., 2009). Yet, the genus is cosmopolitan, but particularly well represented in the Southern Ocean, with 26 described species out of a total of 54 worldwide (Coleman, 2007; Lörz, 2009; Lörz et al., 2007, 2009, 2011). Moreover, a recent study of COI and 28S sequence data identified 24 lineages as putative new Antarctic species, showing that the species richness of this genus on the shelf is still greatly underestimated (Verheye et al., 2016a). *Epimeria* contains a mixture of regionally-restricted and (almost) circum-Antarctic species (Verheye et al., 2016a; d'Udekem d'Acoz and Verheye, *in Press*), but no species are found on both sides of the APF. Their mostly benthic (only two pelagic species are known) and brooding ecology, coupled with limited eurybathy, would prevent such long-distance dispersal across deep passages, on ecological timescales (d'Udekem d'Acoz and Verheye, *in Press*). In the COI phylogeny of Lörz and Held (2004), comprising six Antarctic and no extralimital species, ages of 15.7 and 34.9 Ma were inferred for the last common ancestor of Antarctic *Epimeria*, using respectively a COI rate of evolution estimated for cirripeds and for alpheid shrimps, and assuming a strict molecular clock. The authors concluded that Southern Ocean *Epimeria* evolved *in situ* when Antarctica was already isolated from the other fragments of Gondwana (Lörz and Held, 2004). The cosmopolitan distribution of *Epimeria,* coupled with a low dispersal potential, makes it a good model to study the connection between the Antarctic shelf and the other oceans, the origin of this component of the shelf benthos and its *in situ* diversification patterns.

Inferences on the historical biogeography of the *Epimeria* Antarctic shelf species are not possible without a robust phylogeny, based on an extensive sampling of both Antarctic and non-Antarctic

species. Therefore, we reconstructed a phylogeny of *Epimeria* using three gene fragments (COI, 28S and H3) and including 12 out of the 26 described Antarctic *Epimeria* species as well as 24 putative new Antarctic *Epimeria* species. The non-Antarctic material is composed of 21 *Epimeria* species collected in every other world's oceans. In order to explore the monophyly and systematics of *Epimeria*, we included representatives of other families which form a clade with *Epimeria*, viz. Acanthonotozomellidae, Dikwidae, Stilipedidae and Vicmusiidae (Verheye et al., 2016b). Then, we used a relaxed molecular clock to date the phylogenetic tree and considered the geographical distribution of the specimens to address the following issues: 1. Does the Antarctic component of *Epimeria* form a single clade or does the phylogeny provide evidence of historical dispersal events in and/or out of the shelf (which would make this Antarctic component non-monophyletic)? 2. When and where did the Antarctic component originate, i.e. is it a Gondwanan relict or a more recent colonizer? 3. Does the historical diversification pattern of Antarctic *Epimeria* bear signatures of an early diversification burst or of shifts in diversification rates which might be associated with climatic events (e.g. glacial cycles)?

MATERIAL AND METHODS

TAXON SAMPLING

We included data of 12 out of the 26 described species of Antarctic *Epimeria*, as well as the 24 putative new Antarctic species of Verheye et al. (2016a), i.e. a total of 36 out of 50 known species (72.5 %). Non-Antarctic *Epimeria* included one species from continental Norway (*Epimeria cornigera*), one from the Svalbard Archipelago (*Epimeria loricata*), one from Mexico (*Epimeria morronei*) and 16 putative new species, viz. 14 from the Melanesian subregion (Indonesia, Papua New Guinea, New Caledonia, Solomon, Vanuatu and Fiji islands), one from Taiwan and one from Mozambique. Species from other families that were shown to be related to *Epimeria* in Verheye et al. (2016b) (i.e. *Acanthonotozomoides oatesi* and Acanthonotozomellidae n. gen. n. sp. [Acanthonotozomellidae], *Dikwa andresi* [Dikwidae], *Astyra abyssi*, *Bathypanoploea schellenbergi* and *Alexandrella dentata* [Stilipedidae] and *Acanthonotozomopsis pushkini* [Vicmusiidae]) were included as well, in order to explore the monophyly of the genus. Three iphimediid species were used as outgroup. All specimens used in this study are listed in Table 1.

Samples were collected during several expeditions of the *R.V. Polarstern* in the Southern Ocean: ANT-XXIV/2, ANTXXIII/8, ANT-XXVII/3 and ANT-XXIX/3 in the Drake Passage, Bransfield Strait, eastern coast of the Antarctic Peninsula and eastern Weddell Sea. Additional specimens were sampled from

the Adélie Coast during the CEAMARC and REVOLTA I, II, III expeditions and in Prydz Bay during the MD42 (SIBEX) expedition of the *R.V. Marion Dufresne*. One specimen was sampled during the JR144 expedition with the RRS James Clark Ross near Elephant Island. Non-Antarctic specimens were sampled during BIOPAPUA, Papua Niugini (Papua New Guinea), KARUBAR (Indonesia), EXBODI, NORFOLK2, BATHUS3 (New Caledonia), SOLOMON2 and 3 (Solomon Islands), MUSORSTOM8, SANTO (Vanuatu), FIDJI (Fiji Islands), Taiwan 2000 (Taiwan) and MAINBAZA (Mozambique) expeditions. Additional material was obtained by opportunistic collections from Mexico and Norway (including the Svalbard archipelago) (Table 1).

All specimens were preserved in 96–100 % ethanol for DNA analysis. Vouchers are deposited at the Royal Belgian Institute of Natural Sciences (RBINS, Brussels, Belgium) and the Muséum national d'Histoire naturelle (MNHN, Paris, France). For voucher collection ID numbers, see Table 1.

DNA SEQUENCING

DNA was extracted from the pleopods and abdomen muscles using a NucleoSpin® Tissue kit (Macherey-Nagel) following the manufacturer's protocol for animal tissues. The DNA was eluted in 100 µl of sterile distilled H_2O (RNase free) and stored at -20 °C.

Partial segments of the mitochondrial cytochrome c oxidase subunit I (COI) (~550 bp), nuclear 28S rDNA (~1400 bp) and Histone 3 (H3) (~360 bp) were amplified by PCR. Amplifications were performed in a 25 µl reaction mix, which contained 0.15 µl Taq DNA Polymerase (5 U μl^{-1}; Qiagen, Antwerpen, Belgium), 2.5 µl 10x CoralLoad PCR Buffer (Qiagen, Antwerpen, Belgium), 2.5 µl dNTPs mix (250 µM of each), 11–16 µl RNase-free water, 1.25 µl of each primer (2 µM), and 1–6 µl of DNA extract. The COI fragment was amplified using the primers Cp-COIF3 (Pilar Cabezas et al., 2013) and COI2R (Otto and Wilson, 2001). The thermal cycling used for the COI amplification followed Pilar Cabezas et al. (2013), except for the annealing temperature set at 51°C. The 28S rDNA fragment was amplified using the primers 28S-3311F (Witt et al., 2006) and 28R (Hou et al., 2007), modified as follows: 5'-GGGACTACCCGCTGAACTTAAGCAT-3' and 5'-GTCTTTCGCCCCTATGCCCAACTG-3'. PCR amplification settings for 28S rDNA consisted of an initial denaturation for 3 min at 94 °C, followed by 40 cycles of denaturation at 94 °C for 40 s, annealing at 45 °C for 40 s, extension at 72 °C for 90 s, and a final extension at 72 °C for 10 min. The H3 fragment was amplified using the primers H_3aF and H_3aR (Colgan et al., 1998). PCR amplification settings were as in Colgan et al. (1998), with an annealing temperature of 54–60°C.

Specimens id code	Species	Locality	Latitude	Longitude	Voucher ID	Genbank accession number		
						COI	28S	H3
EPIMERIIDAE								
A20	*Epimeria* aff. *macrodonta* MA1	Peninsula, Larsen B	65° 57.51' S	60° 28.15' W	RBINS INV.132655	KU870817	KU759589	**KY825815**
I7	*Epimeria* aff. *macrodonta* MA1	Peninsula, Larsen B	65° 57.51' S	60° 28.15' W	RBINS INV.132975	KU870851	KU759628	**KY825863**
K4	*Epimeria* aff. *macrodonta* MA2	Adélie Coast	66° 38.42' S	139° 49.72’ E	MNHN-IU-2009-2570	KU870872	KU759652	**KY825893**
K5	*Epimeria* aff. *macrodonta* MA2	Adélie Coast	66° 36.37' S	140° 05.07' E	MNHN-IU-2009-2563	KU870876	KU759657	**KY825898**
M10	*Epimeria* aff. *macrodonta* MA2	Adélie Coast	66° 41.12' S	139° 56.69' E	MNHN-IU-2014-4299	KU870878	KU759661	**KY825921**
M11	*Epimeria* aff. *macrodonta* MA2	Adélie Coast	66° 40.12' S	139° 55.93' E	MNHN-IU-2014-4296	N/A	KU759662	**KY825922**
I19	*Epimeria* aff. *macrodonta* MA3	Peninsula, Dundee Island	63° 37.29‘ S	56° 09.11‘ W	RBINS INV.132974	KU870844	KU759621	**KY825858**
K36	*Epimeria* aff. *macrodonta* MA3	Peninsula, North of Joinville Island	62° 33.79‘ S	56° 27.81‘ W	RBINS INV.122929B	KU87086	KU759648	**KY825889**
K35	*Epimeria* aff. *macrodonta* MA3	Peninsula, North of Joinville Island	62° 33.79‘ S	56° 27.81‘ W	RBINS INV.122929A	N/A	KU759647	**KY825888**
ANT35	*Epimeria* aff. *macrodonta* MA3	Peninsula, Erebus and Terror Gulf	63° 58.78‘ S	56° 46.24‘ W	RBINS INV.122940	N/A	KU759594	**KY825820**
I17	*Epimeria* aff. *macrodonta* MA4	Bransfield Strait East	62° 43.73‘ S	57° 29.04‘ W	RBINS INV.132660	N/A	KU759619	**KY825856**
N1	*Epimeria* aff. *macrodonta* MA4	Bransfield Strait East	62° 43.73‘ S	57° 29.04‘ W	RBINS INV.132973	N/A	KU759677	**KY825920**
I12	*Epimeria* aff. *similis* SI1	Eastern Weddell Sea	70° 50.48' S	10° 35.28' W	RBINS INV.132664	N/A	KU759614	**KY825851**
K31	*Epimeria* aff. *similis* SI2	Bransfield Strait Central	62° 53.45‘ S	58° 13.06‘ W	RBINS INV.122931A	KU870865	KU759644	**KY825885**
K32	*Epimeria* aff. *similis* SI2	Bransfield Strait Central	62° 53.45‘ S	58° 13.06‘ W	RBINS INV.122935	KU870866	KU759645	**KY825886**
K6	*Epimeria* aff. *similis* SI3	Adélie Coast	66° 38.00' S	140° 42.00' E	MNHN-IU-2009-2532	N/A	KU759658	**KY825899**
M7	*Epimeria* aff. *similis* SI3	Adélie Coast	66° 10.57' S	143° 20.75' E	MNHN-IU-2014-4342	N/A	KU759674	**KY825936**
M8	*Epimeria* aff. *similis* SI3	Adélie Coast	66° 45.14' S	145° 20.07' E	MNHN-IU-2014-4333	N/A	KU759675	**KY825937**

M9	*Epimeria* aff. *similis* SI3	Adélie Coast	66° 45.14' S	145° 20.07' E	MNHN-IU-2014-4322	N/A	KU759676	**KY825938**
M5	*Epimeria* aff. *similis* SI3	Adélie Coast	65° 59.83' S	143° 38.99' E	MNHN-IU-2014-4340	N/A	KU759672	**KY825934**
K7	*Epimeria* aff. *similis* SI3	Adélie Coast	66° 38.00' S	140° 42.00' E	MNHN-IU-2009-2539	N/A	KU759659	**KY825900**
P36	*Epimeria similis* SI4	Bransfield Strait East	62° 43.73‘ S	57° 29.04‘ W	RBINS INV.122956A	N/A	KU759680	**KY825935**
P38	*Epimeria similis* SI4	Bransfield Strait Central	62° 53.45‘ S	58° 13.06‘ W	RINBS INV.122922B	N/A	KU759682	**KY825953**
ANT37	*Epimeria* aff. *similis* SI5	Bransfield Strait East	62° 47.80‘ S	57° 05.35‘ W	RBINS INV.122942	KU870823	KU759596	**KY825822**
I13	*Epimeria* aff. *similis* SI5	Bransfield Strait East	62° 43.73‘ S	57° 29.04‘ W	RBINS INV.132976	KU870839	KU759615	**KY825852**
I9	*Epimeria* aff. *similis* SI5	Eastern Weddell Sea	70° 47.34' S	10° 40.39' W	RBINS INV.132665	KU870853	KU759630	**KY825865**
P41	*Epimeria* aff. *similis* SI5	Eastern Weddell Sea	70° 23.94' S	08° 19.14' W	RBINS INV.132977	KU870895	KU759684	**KY825955**
K39	*Epimeria* aff. *similis* SI5	Bransfield Strait Central	62° 53.45‘ S	58° 13.06‘ W	RBINS INV.122922A	KU870871	KU759651	**KY825892**
ANT36	*Epimeria* aff. *similis* SI5	Bransfield Strait East	62° 43.50‘ S	57° 27.92‘ W	RBINS INV.132666	KU870822	KU759595	**KY825821**
I16	*Epimeria* sp. nov. 1 SP1	Eastern Weddell Sea	70° 38.66' S	10° 28.16' W	RBINS INV.132667	KU870842	KU759618	**KY825855**
K44	*Epimeria* sp. nov. 2 SP2	Eastern Weddell Sea	70° 05.13' S	03° 23.50' W	RBINS INV.132663	KU870875	KU759656	**KY825897**
ANT48	*Epimeria* aff. *puncticulata* PUN1	Bransfield Strait	62° 45.05‘ S	57° 26.68‘ W	RBINS INV.122947	N/A	KU759607	**KY825832**
K42	*Epimeria* aff. *puncticulata* PUN1	Peninsula, Dundee Island	63°36.84' S	56° 10.28' W	RBINS INV.122934	N/A	KU759655	**KY825896**
I2	*Epimeria* aff. *puncticulata* PUN2	Peninsula, Larsen B	65° 57.51' S	60° 28.15' W	RBINS INV.132651	KU870845	KU759622	**KY825859**
K33	*Epimeria* aff. *puncticulata* PUN3	Adélie Coast	66° 39.3' S	139° 55.8' E	MNHN-IU-2009-2578	KU870867	KU759646	**KY825887**
M4	*Epimeria* aff. *puncticulata* PUN4	Adélie Coast	65° 48.48' S	143° 03.76' E	MNHN-IU-2014-4288	KU870888	KU759671	**KY825933**
M3	*Epimeria* aff. *puncticulata* PUN4	Adélie Coast	65° 48.48' S	143° 03.76' E	MNHN-IU-2014-4288	N/A	KU759670	**KY825932**
A6	*Epimeria walkeri* WA1	King George Island	62° 18.21' S	58° 39.90' W	RBINS INV.132667	KU870819	KU759591	**KY825818**
Ex169	*Epimeria walkeri* WA1	Eastern Weddell Sea	70° 56.40' S	10° 32.60' W	Specimen missing	KU870836	KU759610	**KY825842**
ANT42	*Epimeria walkeri* WA1	Bransfield Strait Central	62° 53.64‘ S	58° 12.52‘ W	RBINS INV.122944	KU870828	KU759601	**KY825826**
K40	*Epimeria* aff. *walkeri* WA2	Bransfield Strait East	62° 44.73‘ S	57° 26.79‘ W	RBINS INV.122932	KU870873	KU759653	**KY825894**
ANT43	*Epimeria* aff. *walkeri* WA3	Drake Passage West	62° 17.36‘ S	61° 12.06‘ W	RBINS INV.122949	KU870829	KU759602	**KY825827**

I15	*Epimeria* aff. *walkeri* WA3	Peninsula, South of Joinville Island	63° 50.92‘ S	55° 37.66‘ W	RBINS INV.132656	KU870841	KU759617	**KY825854**
I4	*Epimeria* aff. *walkeri* WA3	Elephant Island	61° 20.76' S	55° 12.14' W	RBINS INV.132959	KU870848	KU759625	**KY825861**
M12	*Epimeria* aff. *walkeri* WA4	Adélie Coast	66° 45.14' S	145° 20.07' E	MNHN-IU-2014-4331	KU870879	KU759663	**KY825923**
M13	*Epimeria* aff. *walkeri* WA4	Adélie Coast	66° 23.99' S	140° 32.35' E	MNHN-IU-2014-4336	KU870880	KU759664	**KY825924**
ANT38	*Epimeria macronyx* MX1	Drake Passage West	62° 22.65‘ S	61° 17.63‘ W	RBINS INV.122943	KU870824	KU759597	**KY907661**
ANT39	*Epimeria macronyx* MX1	Drake Passage West	62° 22.65‘ S	61° 17.63‘ W	RBINS INV.122943	KU870825	KU759598	**KY825823**
M19	*Epimeria macronyx* MX2	Adélie Coast	66° 44.86' S	145° 26.66' E	MNHN-IU-2014-4276	KU870885	KU759668	**KY825930**
ANT41	*Epimeria* aff. *georgiana* GE1	Bransfield Strait East	62° 44.73‘ S	57° 26.79‘ W	RBINS INV.122867	KU870827	KU759600	**KY825825**
I14	*Epimeria* aff. *georgiana* GE1	Drake Passage West	62° 17.36‘ S	61° 12.06‘ W	RBINS INV.132970	KU870840	KU759616	**KY825853**
I20	*Epimeria* aff. *georgiana* GE1	Peninsula, Dundee Island	63° 51.53‘ S	55° 40.74‘ W	RBINS INV.132971	KU870846	KU759623	**KY825860**
K21	*Epimeria* aff. *georgiana* GE1	Bransfield Strait West	63° 00.53‘ S	58° 35.67‘ W	RBINS INV.122926	KU870855	KU759633	**KY825874**
K22	*Epimeria* aff. *georgiana* GE1	Bransfield Strait West	63° 00.53‘ S	58° 35.67‘ W	RBINS INV.122924	KU870856	KU759634	**KY825875**
K23	*Epimeria* aff. *georgiana* GE1	Peninsula, East of Joinville Island	63° 10.57‘ S	54° 06.66‘ W	RBINS INV.122930A	KU870857	KU759635	**KY825876**
K24	*Epimeria* aff. *georgiana* GE1	Peninsula, East of Joinville Island	63° 10.57‘ S	54° 06.66‘ W	RBINS INV. 122933	KU870858	KU759636	**KY825877**
K26	*Epimeria* aff. *georgiana* GE1	Peninsula, South of Joinville Island	61° 56.05‘ S	60° 05.56‘ W	RBINS INV.122921A	KU870860	KU759638	**KY825879**
K27	*Epimeria* aff. *georgiana* GE1	Peninsula, North of Joinville Island	62° 33.79‘ S	56° 27.81‘ W	RBINS INV.122920	KU870861	KU759639	**KY825880**
K28	*Epimeria* aff. *georgiana* GE1	Peninsula, North of Joinville Island	62° 33.79‘ S	56° 27.81‘ W	RBINS INV.122920	KU870862	KU759640	**KY825881**
K29	*Epimeria* aff. *georgiana* GE1	Peninsula, Dundee Island	63° 37.28‘ S	56° 09.11‘ W	RBINS INV.122923	KU870863	KU759641	**KY825882**
K30	*Epimeria* aff. *georgiana* GE1	Peninsula, Dundee Island	63° 37.28‘ S	56° 09.11‘ W	RBINS INV.122925	KU870864	KU759643	**KY825884**
P35	*Epimeria* aff. *georgiana* GE1	Peninsula, South of Joinville Island	63° 51.34‘ S	55° 41.11‘ W	RBINS INV.122921B	KU870893	KU759679	**KY825927**
P37	*Epimeria* aff. *georgiana* GE1	Peninsula, South of Joinville Island	63° 51.34‘ S	55° 41.11‘ W	RBINS INV.122921C	KU870894	KU759681	**KY825952**
I10	*Epimeria* aff. *georgiana* GE2	South Orkney Islands	62° 53.45‘ S	58° 13.06‘ W	RBINS INV.132658	KU870838	KU759612	**KY825849**

K25	*Epimeria* aff. *georgiana* GE3	Drake Passage East	61° 56.05‘ S	60° 05.56‘ W	RBINS INV.122936	KU870859	KU759637	**KY825878**
M16	*Epimeria* aff. *georgiana* GE4	Adélie Coast	65° 43.12' S	143° 03.61' E	MNHN-IU-2014-4344	KU870882	KU759665	**KY825926**
M17	*Epimeria angelikae* GE5	Adélie Coast	65° 28.85' S	139° 24.18' E	MNHN-IU-2014-4278	KU870883	KU759666	**KY825928**
M18	*Epimeria angelikae* GE5	Adélie Coast	65° 52.74' S	144° 10.92' E	MNHN-IU-2014-4281	KU870884	KU759667	**KY825929**
M24	*Epimeria rimicarinata* RI	Prydz Bay	66° 55.75' S	74° 04.19' E	MNHN-IU-2014-4265	KU870887	N/A	N/A
I5	*Epimeria rubrieques* RU	Eastern Weddell Sea	70° 47.34' S	10° 40.39' W	RBINS, INV.132668	KU870849	KU759626	**KY825862**
K41	*Epimeria rubrieques* RU	Eastern Weddell Sea	70° 23.94' S	08° 19.14' W	RBINS INV.132643	KU870874	KU759654	**KY825895**
ANT44	*Epimeria inermis* IN1	Bransfield Strait West	62° 55.83‘ S	58° 41.09‘ W	RBINS INV.122948	KU870830	KU759603	**KY825828**
ANT45	*Epimeria inermis* IN1	Bransfield Strait West	63° 00.53‘ S	58° 35.67‘ W	RBINS INV.122945	KU870831	KU759604	**KY825829**
I18	*Epimeria inermis* IN1	Bransfield Strait Central	62° 57.22‘ S	58° 14.60‘ W	RBINS INV.132953	KU870843	KU759620	**KY825857**
I11	*Epimeria inermis* IN2	Eastern Weddell Sea	70° 48.93' S	10° 32.69' W	RBINS INV.132655	N/A	KU759613	**KY825850**
K2	*Epimeria inermis* IN2	Adélie Coast	66° 39.30' S	140° 01.60' E	MNHN-IU-2009-2531	N/A	KU759632	**KY825873**
K3	*Epimeria inermis* IN2	Adélie Coast	66° 40.50' S	139° 55.20' E	MNHN-IU-2009-2569	N/A	KU759642	**KY825883**
M1	*Epimeria inermis* IN2	Adélie Coast	66° 53.36' S	142° 38.90' E	MNHN-IU-2014-4272	KU870877	KU759660	**KY825919**
M2	*Epimeria inermis* IN2	Adélie Coast	66° 23.99' S	140° 32.35' E	MNHN-IU-2014-4338	KU870886	KU759669	**KY825931**
ANT33	*Epimeria* aff. *robustoides* RO1	Bransfield Strait East	62° 47.80‘ S	57° 05.35‘ W	RBINS INV.122937A	KU870820	KU759592	**KY825819**
ANT40	*Epimeria* aff. *robustoides* RO1	Bransfield Strait West	62° 55.83‘ S	58° 41.09‘ W	RBINS INV.122939	KU870826	KU759599	**KY825824**
K37	*Epimeria* aff. *robustoides* RO1	Bransfield Strait Central	62° 55.83‘ S	58° 41.09‘ W	RBINS INV.122927	KU870869	KU759649	**KY825890**
K38	*Epimeria* aff. *robustoides* RO1	Bransfield Strait Central	62° 55.83‘ S	58° 41.09‘ W	RBINS INV.122928	KU870870	KU759650	**KY825891**
Ex114	*Epimeria robustoides* RO2	Eastern Weddell Sea	70° 47.34' S	10° 40.39' W	RBINS-INV.122894	KU870834	KU759608	**KY825840**
I8	*Epimeria robustoides* RO2	Eastern Weddell Sea	70° 23.94' S	08° 19.14' W	RBINS INV.132969	KU870852	KU759629	**KY825864**
K1	*Epimeria robusta* RO3	Adélie Coast	66° 38.40' S	140° 01.80' E	MNHN-IU-2009-2571	KU870854	KU759631	**KY825866**
ANT46	*Epimeria grandirostris* GR1	Peninsula, Dundee Island	63° 51.34‘ S	55° 41.11‘ W	RBINS INV.122946	KU870832	KU759605	**KY825830**
ANT47	*Epimeria grandirostris* GR1	Bransfield Strait East	62° 45.05‘ S	57° 26.68‘ W	RBINS INV.122950	KU870833	KU759606	**KY825831**
P40	*Epimeria* aff. *grandirostris* GR2	Adélie Coast	66° 20.33' S	143° 41.13' E	MNHN-IU-2014-4327	N/A	KU759683	**KY825954**

M14	*Epimeria* aff. *pulchra* PUL1	Adélie Coast	65° 59.78' S	143° 02.95' E	MNHN-IU-2014-4284	KU870881	N/A	**KY825925**
N7	*Epimeria oxicarinata* OX	Elephant Island	61°20.27' S	55° 30.92' W	RBINS INV.122468	KU870891	N/A	**KY825949**
N8	*Epimeria oxicarinata* OX	Elephant Island	61° 20.33' S	55° 31.53' W	RBINS INV.122483	KU870892	N/A	N/A
I1	*Epimeria annabellae* AN	Eastern Weddell Sea	70° 48.93' S	10° 32.69' W	RBINS INV.132652	KU870837	KU759611	**KY825848**
N2	*Epimeria annabellae* AN	Eastern Weddell Sea	70° 30.99' S	08° 48.08' W	RBINS INV.122476	KU870890	KU759678	**KY825948**
L16	*Epimeria* sp. 1	Indonesia	05° 14.00' S	133° 00.00’ E	MNHN-IU-2009-2493	**KY907637**	N/A	**KY825908**
MP10	*Epimeria* sp. 1	Indonesia	05° 15.00 S	133° 01.00' E	MNHN-IU-2009-2491	**KY907648**	**KY907501**	**KY825939**
L6	*Epimeria* sp. 2	Papua New Guinea, Bismarck Sea, Dogreto Bay	03° 18.00' S	143° 00.00' E	MNHN-IU-2013-1583	**KY907643**	**KY907496**	**KY825915**
L7	*Epimeria* sp. 2	Papua New Guinea, Brokenwater Bay	03° 52.64’ S	144° 40.60‘ E	MNHN-IU-2013-11797	**KY907645**	**KY907497**	**KY825916**
K10	*Epimeria* sp. 3	Papua New Guinea	09° 06.00' S	152° 19.00' E	MNHN-IU-2009-2487	N/A	**KY907483**	**KY825867**
K11	*Epimeria* sp. 4	Papua New Guinea	04° 16.00' S	152° 18.00' E	MNHN-IU-2009-2486	**KY907627**	N/A	**KY825868**
L13	*Epimeria* sp. 4	Papua New Guinea, Solomon Sea, South East of Tuam Island	06° 04.25’ S	148° 10.42’ E	MNHN-IU-2013-18091	**KY907635**	**KY907488**	**KY825905**
K13	*Epimeria* sp. 5	Taiwan	24° 08.70’ N	122° 09.90’ E	MNHN-IU-2009-2520	**KY907629**	N/A	**KY825870**
K14	*Epimeria* sp. 5	Taiwan	24° 08.70’ N	122° 09.90’ E	MNHN-IU-2009-252	**KY907630**	**KY907484**	**KY825871**
L9	*Epimeria* sp. 6	New Caledonia	22° 23.40’ S	167° 21.60’ E	MNHN-IU-2013-1666	**KY907644**	**KY907499**	**KY825918**
L10	*Epimeria* sp. 6	New Caledonia	22° 21.80’ S	167° 20.80’ E	MNHN-IU-2011-6489	**KY907634**	**KY907486**	**KY825903**
L12	*Epimeria* sp. 7	Solomon Islands	07° 42.00' S	157° 43.00' E	MNHN-IU-2009-2504	N/A	**KY907487**	**KY825904**
MP8	*Epimeria* sp. 8	Indonesia	05° 46.00’ S	132° 10.00’ E	MNHN-IU-2009-2495	**KY907657**	N/A	**KY825946**
K12	*Epimeria* sp. 9	Vanuatu	16° 02.14' S	166° 38.39' E	MNHN-IU-2009-2514	**KY907628**	N/A	**KY825869**
K8	*Epimeria* sp. 10	Fiji Islands	17° 16.00' S	179° 35.00' W	MNHN-IU-2009-2517	**KY907632**	N/A	**KY825901**
K15	*Epimeria* sp. 11	New Caledonia	23° 54.00' S	167° 42.00' E	MNHN-IU-2007-2501	**KY907631**	N/A	**KY825872**
L1	*Epimeria* sp. 12	Papua New Guinea, Bismarck sea, West Kairiru Island	03° 21.00' S	143° 26.00' E	MNHN-IU-2013-18106	**KY907633**	**KY907485**	**KY825902**
L2	*Epimeria* sp. 12	Papua New Guinea, Woodlark Islands	09° 09.00' S	152° 18.00' E	MNHN-IU-2014-3478	**KY907640**	**KY907493**	**KY825911**
L3	*Epimeria* sp. 12	Papua New Guinea, Woodlark Islands	09° 07.00' S	152° 14.00' E	MNHN-IU-2014-4270	**KY907642**	N/A	**KY825914**
MP1	*Epimeria* sp. 12	Papua New Guinea	09° 09.00' S	152° 18.00' E	MNHN-IU-2009-2481	**KY907647**	**KY907500**	N/A

MP2	*Epimeria* sp. 12	Papua New Guinea	09° 09.00' S	152° 18.00' E	MNHN-IU-2009-2482	**KY907652**	**KY907503**	**KY825941**
MP4	*Epimeria* sp. 13	Indonesia	05° 15.00’ S	132° 59.00’ E	MNHN-IU-2009-2496	**KY907653**	N/A	**KY825943**
L14	*Epimeria* sp. 20	Solomon Islands	08° 24.40’ S	159° 22.55’ E	MNHN-IU-2009-2506	**KY907636**	**KY907489**	**KY825906**
L15	*Epimeria* sp. 14	Solomon Islands	08° 24.40’ S	159° 22.55’ E	MNHN-IU-2009-3479	**KY907649**	**KY907490**	**KY825907**
MP12	*Epimeria* sp. 14	Solomon Islands	08° 24.40’ S	159° 22.55’ E	MNHN-IU-2009-2511	**KY907650**	N/A	**KY825940**
MP5	*Epimeria* sp. 15	Solomon Islands	08° 19.60’ S	160° 01.95’ E	MNHN-IU-2009-2513	**KY907654**	**KY907505**	**KY825956**
L21	*Epimeria* sp. 16	Solomon Islands	09° 55.00’ S	161° 33.00’ E	MNHN-IU-2014-4315	N/A	**KY907495**	**KY825913**
MP9	*Epimeria* sp. 17	Solomon Islands	08° 19.60’ S	159° 22.55’ E	MNHN-IU-2009-2507	**KY907658**	N/A	**KY825947**
MP3	*Epimeria* sp. 18	Papua New Guinea	05° 40.00' S	154° 29.00' E	MNHN-IU-2011-2345	N/A	**KY907504**	**KY825942**
H3	*Epimeria loricata*	Svalbard, Erik Eriksenstrait	N/A	N/A	RBINS INV. 132637	**KY907625**	KT808709	**KY825846**
H4	*Epimeria loricata*	Svalbard, Hinlopen	N/A	N/A	RBINS INV. 138044	**KY907626**	**KY907482**	**KY825847**
L18	*Epimeria morronei*	Mexico, Pacific	23° 09.91’ N	115° 51.00’ W	None	**KY907638**	**KY907491**	**KY825909**
L19	*Epimeria morronei*	Mexico, Pacific	29° 20.90’ N	115° 51.00’ W	None	**KY907639**	**KY907492**	**KY825910**
L20	*Epimeria morronei*	Mexico, Pacific	30° 48.40’ N	116° 47.80’ W	None	**KY907641**	**KY907494**	**KY825912**
L8	*Epimeria* sp. 19	Mozambique	24° 22.29’ S	35° 41.86’ E	MNHN-IU-2009-22	**KY907646**	**KY907498**	**KY825917**
MP6	*Epimeria* sp. 19	Mozambique, Vizconde de Eza	24° 02.06’ S	35° 40.66’ E	MNHN-IU-2009-2527	**KY907655**	N/A	N/A
MP7	*Epimeria* sp. 19	Mozambique, Visconde de Eza	24° 05.28’ S	35° 41.73’ E	MNHN-IU-2009-2525	**KY907656**	**KY907506**	**KY825945**
NOR13	*Epimeria cornigera*	Norway	68° 11.27' N	14° 59.87' E	RBINS INV. 138043	**KY907659**	**KY907507**	**KY825950**
NOR15	*Epimeria cornigera*	Norway	N/A	N/A	RBINS INV. 132630	**KY907660**	KT808708	**KY825951**
ACANTHONOTOZOMELLIDAE								
B12	*Acanthonotozomoides oatesi*	Sub-Antarctic, Shag Rocks	53° 24.81' S	42° 40.03' W	RBINS INV. 132669	**KY907616**	KT808686	**KY825834**
F6	*Acanthonotozomoides oatesi*	Sub-Antarctic, Shag Rocks	53° 23.94' S	42° 40.10' W	RBINS INV. 138046	**KY907622**	**KY907480**	**KY825843**
G9	*Acanthonotozomoides oatesi*	Sub-Antarctic, Shag Rocks	53° 24.53' S	42° 40.70' W	RBINS INV. 138045	**KY907624**	**KY907481**	**KY825845**
MP19	Acanthonotozomellidae n. gen. n. sp.	New Caledonia	23° 43.00' S	168° 02.00' E	MNHN-IU-2009-2499	**KY907651**	**KY907502**	N/A
G4	Acanthonotozomellidae n. gen. n. sp.	New Caledonia	23° 22.76' S	167° 51.60' E	MNHN-IU-2009-2497	**KY907623**	KT808685	**KY825844**
E16	*Acanthonotozomella trispinosa*	Antarctica, Larsen B	65° 57.51' S	60° 28.15' W	RBINS INV. 132673	**KY907618**	KT808684	**KY825836**
DIKWIDAE								
B10	*Dikwa andresi*	Sub-Antarctic, Burdwood Bank	54° 34.04' S	56° 10.64' W	RBINS INV. 132666	**KY907614**	**KY907478**	**KY825833**
B11	*Dikwa andresi*	Sub-Antarctic, Burdwood Bank	54° 34.04' S	56° 10.64' W	RBINS INV. 132666	**KY907615**	KT808704	N/A

STILIPEDIDAE								
A5	*Bathypanoploea schellenbergi*	Antarctica, Eastern Weddell Sea	70° 23.94' S	08° 19.14' W	RBINS INV. 132623	**KY907613**	KT808699	**KY825817**
E3	*Alexandrella dentata*	Antarctica, Eastern Weddell Sea	70° 56.52' S	10° 34.84' W	RBINS INV. 132653	**KY907619**	**KY907479**	**KY825837**
E4	*Alexandrella dentata*	Antarctica, Larsen A	64° 54.75' S	60° 39.01' W	RBINS INV. 132653	**KY907621**	KT808688	**KY825839**
B20	*Astyra abyssi*	Norway, Vestfjorden	68° 11.27' N	14° 59.87' E	RBINS INV. 132658	**KY907617**	KT808694	**KY825835**
VICMUSIIDAE								
E30	*Acanthonotozomopsis pushkini*	Sub-Antarctic, Shag Rocks	53° 24.53' S	42° 40.70' W	RBINS INV. 132656	**KY907620**	KT808687	**KY825838**
OUTGROUP								
Ex154	*Gnathiphimedia sexdentata*	Eastern Weddell Sea	70° 50.64' S	10° 36.11' W	RBINS INV.132752	KU870835	KU759609	**KY825841**
A4	*Anchiphimedia dorsalis*	Antarctica, King George Island	62° 18.21' S	58° 39.90' W	RBINS INV. 132625	**KY907612**	KT808690	**KY825816**
A2	*Iphimediella cyclogena*	Antarctica, Larsen A	64° 55.58' S	60° 33.37' W	RBINS INV. 132632	**KY907611**	KT808722	**KY825814**

Table 1. Sampling details for the sequenced *Epimeria* specimens including sample location, geographical coordinates, voucher number and GenBank accession number. "N/A" (not available) indicates unobtainable data. GenBank accession numbers of sequences obtained in this study were indicated in bold.

The PCR products were visualized under blue light on 1.2 % agarose gel stained with SYBR Safe (ThermoFisherScientific, Waltham, MA, USA), with a comigrating 200-bp ladder molecular-weight marker to confirm their correct amplification. Prior to sequencing, PCR products were purified using Exonuclease I (20 U μl^{-1}) and FastAP^{TM} Thermosensitive alkaline phosphatase (1 U μl^{-1}) (ThermoFisher Scientific, Waltham, MA, USA), following the manufacturer's protocol. Forward and reverse strands were sequenced with fluorescent-labeled dideoxynucleotide terminators (BigDye v.3.1; Applied Biosystems, Foster City, CA, USA) following the protocol of Sanger et al. (1977) and using an automated ABI 3130xl DNA analyzer (Applied Biosystems, Foster City, CA, USA). Both fragments were sequenced using the PCR primers.

PHYLOGENETIC ANALYSES

Sequence chromatograms were checked, and forward and reverse sequence fragments were assembled using Codoncode Aligner v.3.7.1. (CodonCode Corporation; http://www.codoncode.com/aligner/). All sequences have been deposited in GenBank (Table 1).

28S sequences were aligned with MAFFT v.7 (Katoh and Standley, 2013) (http://mafft.cbrc.jp/alignment/server/), using the structural alignment strategy Q-INS-i under default settings. As some regions of the 28S sequences were too divergent to be confidently aligned, the software program Aliscore v.2.0. (Misof and Misof, 2009) was used to identify poorly aligned regions for removal with Alicut v.2.3, prior to further analysis. CLUSTALW was used to align the COI and H3 sequences in MEGA6 (Tamura et al., 2013). In order to prevent inclusion of pseudogenes in the analyses, amino acid translations of both fragments were checked for stop codons.

In order to evaluate the congruence between genes and reconstruction methods, preliminary phylogenetic trees were inferred using Bayesian inference (BI) on the separate datasets. The Incongruence Length Difference (ILD) test (Farris et al., 1995) was implemented using Paup*4.0b10 (Swofford, 2003). BI and Maximum Likelihood (ML) were then used to reconstruct phylogenetic relationships based on a dataset concatenated with SequenceMatrix (Vaidya et al., 2011).

The best-fit models of DNA substitution were selected using the Bayesian Information Criterion (BIC) on the concatenated dataset partitioned by gene and by codon position (for COI and H3), in PartitionFinder (Lanfear et al., 2012). This model selection procedure was performed both by assuming a single set of underlying branch lengths for the tree and independent set of branch lengths for each partition and the best scheme was selected based on the BIC value.

BI trees were reconstructed using MrBayes v.3.2 (Ronquist and Huelsenbeck, 2003) on the CIPRES portal (Miller et al., 2010). BI analysis of each alignment included two runs of 10^7 generations. Trees were sampled every 1000 generations using four Markov chains, and default heating values. Convergence was assessed by the standard deviation of split-frequencies (< 0.01) and by examining the trace plots of log-likelihood scores in Tracer 1.6 (Rambaut and Drummond, 2005). The first 10 % trees were discarded as burn-in, while the remaining trees were used to construct a 50 % majority rule consensus tree and estimate the posterior probabilities (PP). Nodes with posterior probabilities (PP) ≥ 0.95 were considered as significantly supported.

ML trees were estimated using GARLI v.2.0 (Zwickl, 2006). For each dataset, 10 separate ML searches were run independently from different stepwise-reconstructed trees. The best scoring tree across runs was considered for further analyses. Confidence levels of branches were estimated by 1000 bootstrap replicates. Nodes with bootstrap values (BV) ≥ 70 were considered meaningful.

ESTIMATION OF DIVERGENCE TIMES

As intraspecific variation may lead to the overestimation of divergence times (Ho et al., 2008), the time-calibrated reconstruction was based on a reduced multimarker dataset. For the Antarctic *Epimeria* clade, one individual per Molecular Taxonomic Unit (MOTU) identified as a putative species by Verheye et al. (2016a) was retained. For other sequences, one individual per clade corresponding to a morphospecies was selected.

BEAST2 (Bouckaert et al., 2014) on the CIPRES portal (Miller et al., 2010) was used to estimate divergence times under a Bayesian approach. A Bayesian Model Averaging method was implemented in BEAST2 with the bModelTest package (Bouckaert and Drummond, 2015) in order to estimate a phylogeny averaged over site models, and not to rely on a likelihood-based method to determine the site model. During the Bayesian analysis, Markov Chain Monte-Carlo (MCMC) proposals switch between substitution models and estimate the posterior support for gamma-distributed rate heterogeneity, proportion of invariable sites and unequal base frequencies.

We simultaneously inferred the posterior distribution of trees and estimated divergence times assuming a relaxed clock model of evolution, allowing substitution rates to vary among branches. Both uncorrelated lognormal (UCLD) and exponential (UCED) models of rate change were implemented. In order to assess the pertinence of a relaxed estimation, the coefficients of variation of the clock rates were checked in Tracer v.1.6 (Rambaut et al., 2014). The coefficient of variation is the standard deviation of the clock rate distribution divided by its mean, and is used to assess the clock-likeness of the data. Values closer to zero indicate that the data are more clock-like. Therefore,

values < 0.1 are generally considered low enough to justify the use of a strict molecular clock (Drummond and Bouckaert, 2015). To identify the best relaxed clock model, the marginal likelihoods of the competing models were estimated and summarized via the path-sampling method (Lartillot and Philippe, 2006), implemented in the MODEL_SELECTION package in BEAST2. Both Yule and Birth-death speciation processes were used as tree priors in combination with the UCLD clock model, and a path-sampling method was again used to select for the best tree model. All the path-sampling analyses were run for 100 steps of 2 x 10^6 generations each. The log Bayes Factors (BF) were calculated as follows: $\log_e BF(M_0, M_1) = \log_e P(X|M_0) - \log_e P(X|M_1)$, where $\log_e P(X|M_i)$ is the marginal $\log_e$-likelihood estimate for the model M_i. The strength of support for a given model was based on the interpretation of BF suggested by (Kass and Raftery, 1995). Values of 2 $\log_e$ BF between 0 and 2 were interpreted as no evidence for the alternative model M_1 over the null model M_0. When 2 $\log_e$ BF values were above 2, the alternative model M_1 was supported over the null model M_0, and values over 10 were interpreted as a very strong support for the alternative model.

Likely due to their thin cuticle, peracarid crustaceans do not fossilize well (e.g. Briggs and Kear, 1994; Briggs and Wilby, 1996; Taylor, 1972). Their fossil record is very incomplete and therefore of limited utility for molecular dating. The aquatic fossil amphipods known (Coleman, 2004; Coleman and Myers, 2000; Coleman and Ruffo, 2002; Coleman, 2006; Jażdżewski et al., 2014; Jażdżewski and Kulicka, 2000a, 2002; Jażdżewski and Kupryjanowicz, 2010; Weitschat et al., 2002) are all from freshwater taxa, phylogenetically distant from *Epimeria* (Verheye et al. 2016b). Moreover, the detailed phylogenetic placement of these fossils could generally not be determined, due to their relatively poor preservation (e.g. Coleman, 2004; Coleman and Myers, 2000; Coleman and Ruffo, 2002; Jażdżewski and Kulicka, 2000b). Similarly, there is no unambiguous biogeographical event that could be used to calibrate the tree. We therefore used priors on rates of COI, 28S and H3 evolution based on rates inferred in previous studies. The prior rate of COI was set as a normal distribution with a mean of 0.018 substitutions/site/My and a standard deviation (SD) of 0.0043. This rate was previously inferred for *Pontogammarus* amphipods (Nahavandi et al., 2013). A normal prior with a mean of 0.003 substitutions/site/My and SD of 0.0007 was used for the 28S gene, a rate inferred for the *Gammarus balcanicus* complex (Mamos et al., 2016). Rates of H3 evolution are, to our knowledge, not available for amphipods. Therefore, the prior rate of H3 was set as a normal distribution with a mean of 0.0019 and SD of 0.0004, a rate inferred for freshwater crabs (Klaus et al., 2010).

Two independent runs were performed with 200 million generations and a sampling frequency of 20000 generations. The first 1000 trees were discarded as burn-in and the results of the two runs

were combined using the LogCombiner v1.7.5. Convergence was assessed by trace plots in Tracer v.1.6. and the effective sampling size for all parameters was more than 200 (Rambaut et al., 2014). The maximum clade credibility tree showing the mean nodal height was generated by TreeAnnotator v1.8.0. The final analyses were also run without data to ensure that the prior settings will not bias the results.

RATE AND MODE OF DIVERSIFICATION

The reduced dataset (one individual per species or putative species) was also used for diversification rates analyses because intraspecific polymorphisms can induce a false increase in diversification rates in the most recent history. All the diversification rate analyses were based on the Antarctic *Epimeria* clade. Incomplete taxonomic sampling can result in spurious declines in diversification rates over time (Pybus and Harvey, 2000). Our phylogeny comprises 72.5 % of the known (putative) species. However, as Verheye et al. (2016a) discovered at least 24 new *Epimeria* species from the Peninsula, eastern Weddell Sea and Adélie Coast, it is likely that similar studies of material from e.g. the Ross, Amundsen and Bellingshausen Seas will reveal an even higher diversity within the genus. Therefore, the methods used herein to examine diversification patterns tested the effect of different levels of taxonomic sampling on the results: sampling proportions of 72 %, 50 % and 10 % were considered.

A mean semilogarithmic lineage through time (LTT) plot was constructed using the R package Ape to visualize the temporal pattern of lineage diversification. A straight line is expected under constant diversification rate. A departure from this straight line in the distant past may indicate a diversification rate change: (1) a concave plot either indicates a decelerating diversification rate or incomplete taxon sampling, (2) a convex plot may indicate accelerating diversification or a non-zero background extinction rate. The command sim.bd.taxa.age from the R package TreeSim (Stadler, 2011) was used to simulate 100 trees under Pure Birth (PB) and Birth-Death (BD), with speciation and extinction rates estimated with bd.shift.optim from the R package TreePar (Stadler, 2011). Both functions were used assuming a sampling fraction of 72 %. The LTT plot of the empirical phylogeny was compared to the 95 % confidence intervals of the expected pattern under PB and BD, to detect eventual deviations from the null hypothesis of constant rates.

In order to account for incomplete taxonomic sampling in methods that do not include a correction for missing species, we used the CorSim function from the R package TreeSim to simulate the missing splits on the empirical phylogeny (Cusimano et al., 2012). Missing speciation events were simulated 200 times under the assumption that evolution followed a constant BD model. Simulated

branching times are added to the empirical branching times to obtain 200 completed (semi-empirical) datasets. Speciation and extinction rates used for the simulation were those estimated under BD with the bd.shifts.optim function of the TreePar package. Missing taxa were assumed to be located randomly across the tree, as both deep and shallower nodes are likely missing from the phylogeny. Three semi-empirical datasets were obtained for 72 %, 50 % and 10 % sampling.

The γ statistic was calculated on the semi-empirical datasets, using the GamStat function of the R package LASER (Rabosky, 2006a). This statistic tests for departure from a constant-rate pure birth model. Negative γ values indicate a prevalence of nodes closer to the root than expected under a Pure Birth process, therefore suggesting a decreasing rate of diversification through time. Positive γ values indicate either an increasing rate or non-zero extinction rate (Pybus and Harvey 2000).

We compared the fit of the branching times to various models of lineage accumulation, using the Akaike Information Criterion (AIC), for the three semi-empirical datasets. AIC is calculated as $-2\iota + 2k$, where ι is the log-likelihood value and k is the number of free parameters of the model (Burnham and Anderson, 2002). All model-fitting analyses were conducted with the R packages LASER (Rabosky, 2006a) and TreePar (Stadler, 2011). The constant-rate models included PB (constant speciation rate λ and no extinction) and BD (constant speciation rate λ and extinction rate μ). Two density-dependent models were included, which assume that the diversification rate decreases as the lineage population reaches some threshold density. The density-dependent linear (DDL) model assumes that λ decreases linearly and there is no extinction. The density-dependent exponential (DDX) model assumes that λ decreases exponentially and there is no extinction (Rabosky and Lovette, 2008). λ and μ may also change through time in response to external factors. Therefore, we included Yule-2-rate (Rabosky, 2006b) and Birth-death-shift (BDS) (Stadler, 2011) models in order to test whether and when discrete shifts in diversification rate occurred during the clade's history. In between shifts, these models simplify to the constant-rate PB or BD. The mean and SD of the –Log Likelihood value, models' parameters and AIC scores were computed for each of the semi-empirical datasets. In order to compare the relative fit of the models, the 95 % confidence interval of the AIC values was computed. The difference in AIC (dAIC) between each model and the best-fitting model (with the lowest AIC) was computed. Minimal and maximal dAIC were calculated considering the AIC values comprised in the 95 % confidence intervals. The amount of statistical confidence for each model is represented by the Akaike weights (wAIC).

In order to test rate-variable models that allow for increasing or decreasing rates of speciation, extinctions and declining diversity, we also used the method of (Morlon et al., 2011), implemented in the R package RPANDA. The fit of the following models was compared using the AIC: (1) Bcst:

constant speciation rate, no extinction (PB); (2) Bvar: exponential variation of speciation rate, no extinction; (3) BvarDcst: exponential variation of speciation rate, constant extinction; (4) BcstDcst: constant speciation and extinction rates (BD); (5) BcstDvar : constant speciation and exponential variation in extinction rate; and (6) BvarDvar: exponential variation in both speciation and extinction rates. These models were tested assuming sampling fractions of 0.1, 0.5 and 0.72.

The BAMM (Bayesian Analysis of Macroevolutionary Mixtures) 2.4.0 (Rabosky, 2014) software was used to explore eventual shifts in regimes across the branches of a phylogenetic tree, a regime being a constant or time-varying process of speciation and extinction. These heterogeneous mixtures of macroevolutionary rate regimes are sampled with reversible-jump MCMC. Priors were estimated using the setBAMMpriors command. MCMC chains were run for 10 million generations, and sampled every thousand generations. We checked for convergence of the MCMC chains and ESS (at least more than 200) using the R package coda (Plummer et al., 2006). The first 10 % of samples were discarded as burn-in. The R package BAMMtools (Rabosky et al., 2014) was used to calculate the BF and the 95 % credibility set for the shift configurations and to plot diversification rates through time (Rabosky, 2014). BAMM analyses were computed assuming different levels of taxon sampling: 10, 50 and 72 %.

RESULTS

DATA OVERVIEW

We obtained 132 COI, 139 28S and 159 H3 sequences of *Epimeria* species and related taxa, and three iphimediid sequences used as outgroup. The aligned COI sequences contained 613 bp, with 379 variable sites (among ingroup taxa). The 28S alignment was 1797 bp long (after removal of ambiguous regions with Aliscore), with 1154 variable sites. The length of the H3 alignment was 369 bp, with 119 variable sites. The datasets were concatenated, resulting in an alignment of 2779 bp. The best models and partitioning scheme suggested by PartitionFinder are indicated in Table 2. A single set of underlying branch lengths was assumed for the tree.

Subset Partitions	Best Model
28S	GTR + I + G
COI_pos1	SYM + I + G
COI_pos2	GTR + I + G
COI_pos3	GTR + I + G
H3_pos1, H3_pos2	JC + I
H3_pos3	GTR + G

Table 2. Best partitioning scheme and models of DNA substitution, inferred by PartitionFinder.

PHYLOGENETIC ANALYSES

CONGRUENCE BETWEEN GENE TREES AND METHODS – The ILD test rejected the null hypothesis of congruence between all tree comparisons (*p = 0.001*). Upon examination of the tree topologies, incongruences between the three gene trees affected mostly unsupported nodes. Only one supported phylogenetic relationship within the Papuasian clade of *Epimeria* sp. 3 differs between the COI and 28S gene trees. As this unique incongruence does not affect the conclusions of this study, the datasets were concatenated. Differences between the topologies of the two reconstruction methods (ML and BI) were minimal. In all cases, these ambiguities affected only unsupported nodes.

EPIMERIA AND RELATED TAXA – The Antarctic component of *Epimeria* is monophyletic with maximal support. All non-Antarctic *Epimeria* species also form a strongly supported clade (PP = 1.00, BV = 92). However, the monophyly of *Epimeria* is not supported by BI, as Antarctic *Epimeria* species form a sister clade to two stilipedid species (PP = 0.99), while this sister relationship remains unresolved by ML (BV = 68). Deeper relationships between the Antarctic and non-Antarctic *Epimeria* clades, *Astyra abyssi*, the Acanthonotozomellid species and *Acanthonotozomopsis pushkini* are not supported. *Acanthonotozomoides oatesi* and *A. pushkini* form a maximally-supported clade (Fig. 1).

ANTARCTIC *EPIMERIA* CLADE – The molecular systematics of the Antarctic *Epimeria* clade has been studied in detail in Verheye et al. (2016a) and the morphological taxonomy in d'Udekem d'Acoz and Verheye (*in Press*).

NON-ANTARCTIC *EPIMERIA* CLADE – Twenty monophyletic morphospecies representing putatively new species are observed among Indo-Pacific *Epimeria* (Fig. 1). An indepth systematics study of these non-Antarctic *Epimeria* species is out of the scope of this paper and should be dealt with elsewhere.

Figure 1. Bayesian phylogenetic tree of the concatenated dataset (COI, 28S, H3). Posterior probabilities are indicated above the nodes and Bootstrap values (> 50) from the Maximum Likelihood analysis below the nodes. MOTUs names (putative species) from Verheye et al. (2016a) are indicated for Antarctic *Epimeria* specimens.

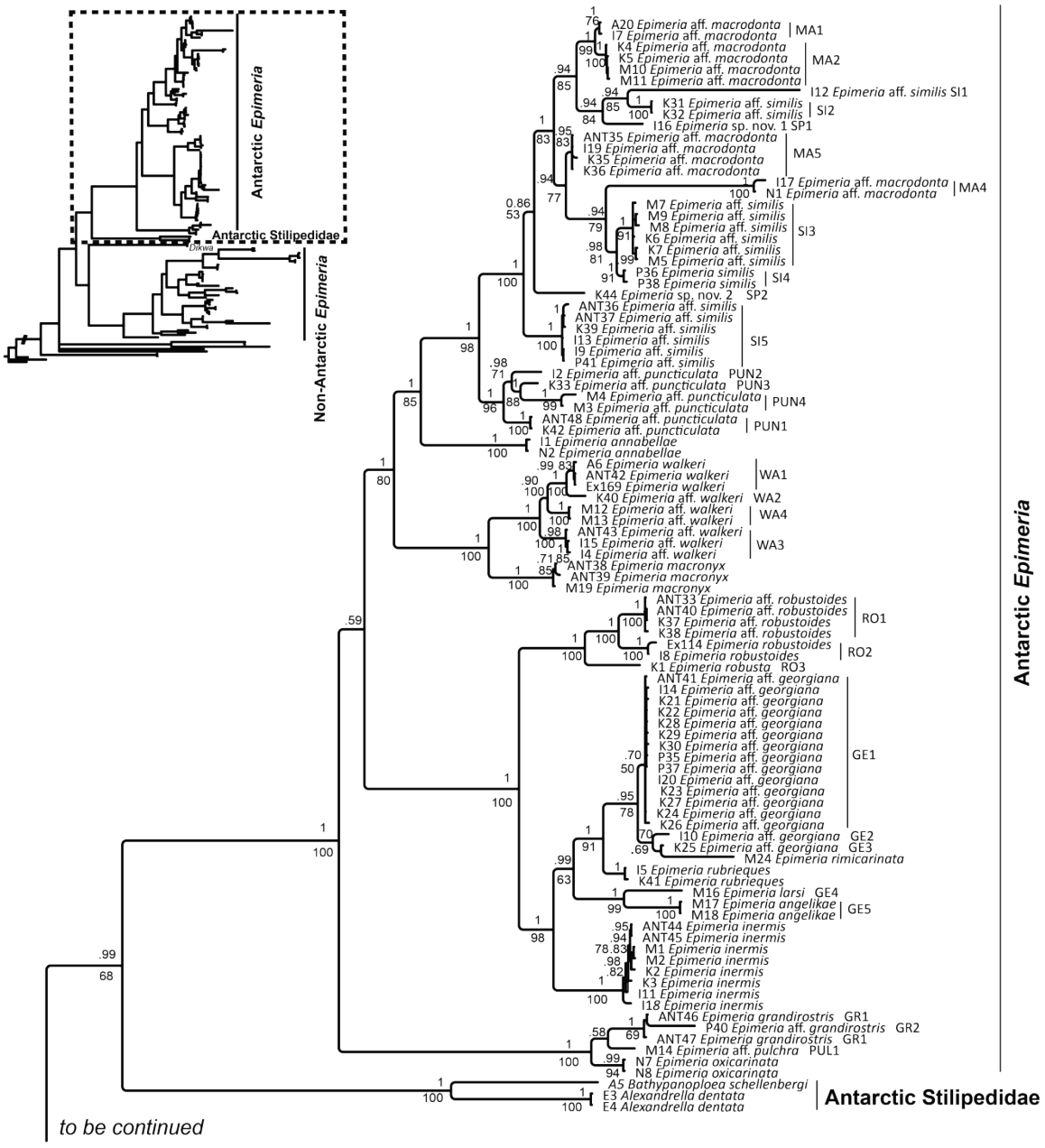
Antarctic Epimeria
Antarctic Stilipedidae
Non-Antarctic Epimeria
A20 Epimeria aff. macrodonta | MA1
I7 Epimeria aff. macrodonta
K4 Epimeria aff. macrodonta
K5 Epimeria aff. macrodonta | MA2
M10 Epimeria aff. macrodonta
M11 Epimeria aff. macrodonta
I12 Epimeria aff. similis SI1
K31 Epimeria aff. similis | SI2
K32 Epimeria aff. similis
I16 Epimeria sp. nov. 1 SP1
ANT35 Epimeria aff. macrodonta
I19 Epimeria aff. macrodonta | MA5
K35 Epimeria aff. macrodonta
K36 Epimeria aff. macrodonta
I17 Epimeria aff. macrodonta | MA4
N1 Epimeria aff. macrodonta
M7 Epimeria aff. similis
M9 Epimeria aff. similis
M8 Epimeria aff. similis | SI3
K6 Epimeria aff. similis
K7 Epimeria aff. similis
M5 Epimeria aff. similis
P36 Epimeria similis
P38 Epimeria similis | SI4
K44 Epimeria sp. nov. 2 SP2
ANT36 Epimeria aff. similis
ANT37 Epimeria aff. similis
K39 Epimeria aff. similis
I13 Epimeria aff. similis | SI5
I9 Epimeria aff. similis
P41 Epimeria aff. similis
I2 Epimeria aff. puncticulata PUN2
K33 Epimeria aff. puncticulata PUN3
M4 Epimeria aff. puncticulata
M3 Epimeria aff. puncticulata | PUN4
ANT48 Epimeria aff. puncticulata
K42 Epimeria aff. puncticulata | PUN1
I1 Epimeria annabellae
N2 Epimeria annabellae
A6 Epimeria walkeri
ANT42 Epimeria walkeri | WA1
Ex169 Epimeria walkeri
K40 Epimeria aff. walkeri WA2
M12 Epimeria aff. walkeri | WA4
M13 Epimeria aff. walkeri
ANT43 Epimeria aff. walkeri
I15 Epimeria aff. walkeri | WA3
I4 Epimeria aff. walkeri
ANT38 Epimeria macronyx
ANT39 Epimeria macronyx
M19 Epimeria macronyx
ANT33 Epimeria aff. robustoides
ANT40 Epimeria aff. robustoides
K37 Epimeria aff. robustoides | RO1
K38 Epimeria aff. robustoides
Ex114 Epimeria robustoides
I8 Epimeria robustoides | RO2
K1 Epimeria robusta RO3
ANT41 Epimeria aff. georgiana
I14 Epimeria aff. georgiana
K21 Epimeria aff. georgiana
K22 Epimeria aff. georgiana
K28 Epimeria aff. georgiana
K29 Epimeria aff. georgiana
K30 Epimeria aff. georgiana
P35 Epimeria aff. georgiana | GE1
P37 Epimeria aff. georgiana
I20 Epimeria aff. georgiana
K23 Epimeria aff. georgiana
K27 Epimeria aff. georgiana
K24 Epimeria aff. georgiana
K26 Epimeria aff. georgiana
I10 Epimeria aff. georgiana GE2
K25 Epimeria aff. georgiana GE3
M24 Epimeria rimicarinata
I5 Epimeria rubrieques
K41 Epimeria rubrieques
M16 Epimeria larsi GE4
M17 Epimeria angelikae | GE5
M18 Epimeria angelikae
ANT44 Epimeria inermis
ANT45 Epimeria inermis
M1 Epimeria inermis
M2 Epimeria inermis
K2 Epimeria inermis
K3 Epimeria inermis
I11 Epimeria inermis
I18 Epimeria inermis
ANT46 Epimeria grandirostris GR1
P40 Epimeria aff. grandirostris GR2
ANT47 Epimeria grandirostris GR1
M14 Epimeria aff. pulchra PUL1
N7 Epimeria oxicarinata
N8 Epimeria oxicarinata
A5 Bathypanoploea schellenbergi
E3 Alexandrella dentata
E4 Alexandrella dentata
Antarctic Stilipedidae
to be continued


Eastern
Weddell
Sea
Antarctic
Peninsula
Adélie Coast

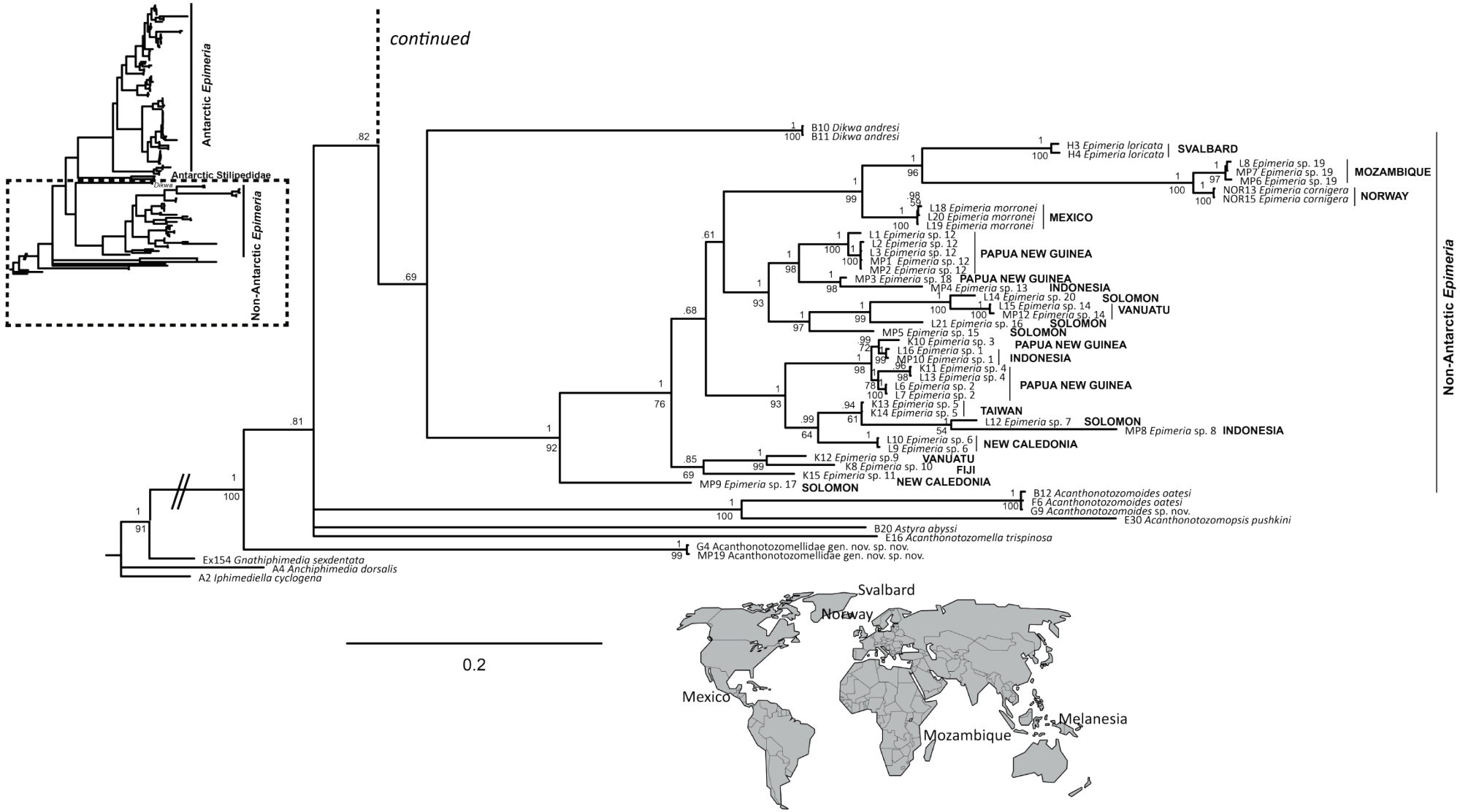
Antarctic Epimeria
Antarctic Stilipedidae
Dikwa
Non-Antarctic Epimeria
continued
.82
.69
.81
.68
.61
1
100
1
91
1
76
1
92
1
93
1
97
1
98
1
99
1
96
1
100
1
99
.98
.59
1
100
1
100
1
100
1
98
1
93
1
100
1
99
.99
.72
1
99
.96
.98
1
78
1
100
.94
61
.99
64
1
54
.85
99
1
69
1
100
1
100
1
99
B10 Dikwa andresi
B11 Dikwa andresi
H3 Epimeria loricata
H4 Epimeria loricata
SVALBARD
L8 Epimeria sp. 19
MP7 Epimeria sp. 19
MP6 Epimeria sp. 19
MOZAMBIQUE
NOR13 Epimeria cornigera
NOR15 Epimeria cornigera
NORWAY
L18 Epimeria morronei
L20 Epimeria morronei
L19 Epimeria morronei
MEXICO
L1 Epimeria sp. 12
L2 Epimeria sp. 12
L3 Epimeria sp. 12
MP1 Epimeria sp. 12
MP2 Epimeria sp. 12
PAPUA NEW GUINEA
MP3 Epimeria sp. 18
PAPUA NEW GUINEA
MP4 Epimeria sp. 13
INDONESIA
L14 Epimeria sp. 20
SOLOMON
L15 Epimeria sp. 14
MP12 Epimeria sp. 14
VANUATU
L21 Epimeria sp. 16
SOLOMON
MP5 Epimeria sp. 15
SOLOMON
K10 Epimeria sp. 3
PAPUA NEW GUINEA
L16 Epimeria sp. 1
MP10 Epimeria sp. 1
INDONESIA
K11 Epimeria sp. 4
L13 Epimeria sp. 4
L6 Epimeria sp. 2
L7 Epimeria sp. 2
PAPUA NEW GUINEA
K13 Epimeria sp. 5
K14 Epimeria sp. 5
TAIWAN
L12 Epimeria sp. 7
SOLOMON
MP8 Epimeria sp. 8
INDONESIA
L10 Epimeria sp. 6
L9 Epimeria sp. 6
NEW CALEDONIA
K12 Epimeria sp.9
VANUATU
K8 Epimeria sp. 10
FIJI
K15 Epimeria sp. 11
NEW CALEDONIA
MP9 Epimeria sp. 17
SOLOMON
B12 Acanthonotozomoides oatesi
F6 Acanthonotozomoides oatesi
G9 Acanthonotozomoides sp. nov.
E30 Acanthonotozomopsis pushkini
B20 Astyra abyssi
E16 Acanthonotozomella trispinosa
G4 Acanthonotozomellidae gen. nov. sp. nov.
MP19 Acanthonotozomellidae gen. nov. sp. nov.
Ex154 Gnathiphimedia sexdentata
A4 Anchiphimedia dorsalis
A2 Iphimediella cyclogena
Non-Antarctic Epimeria
0.2
Svalbard
Norway
Mexico
Mozambique
Melanesia

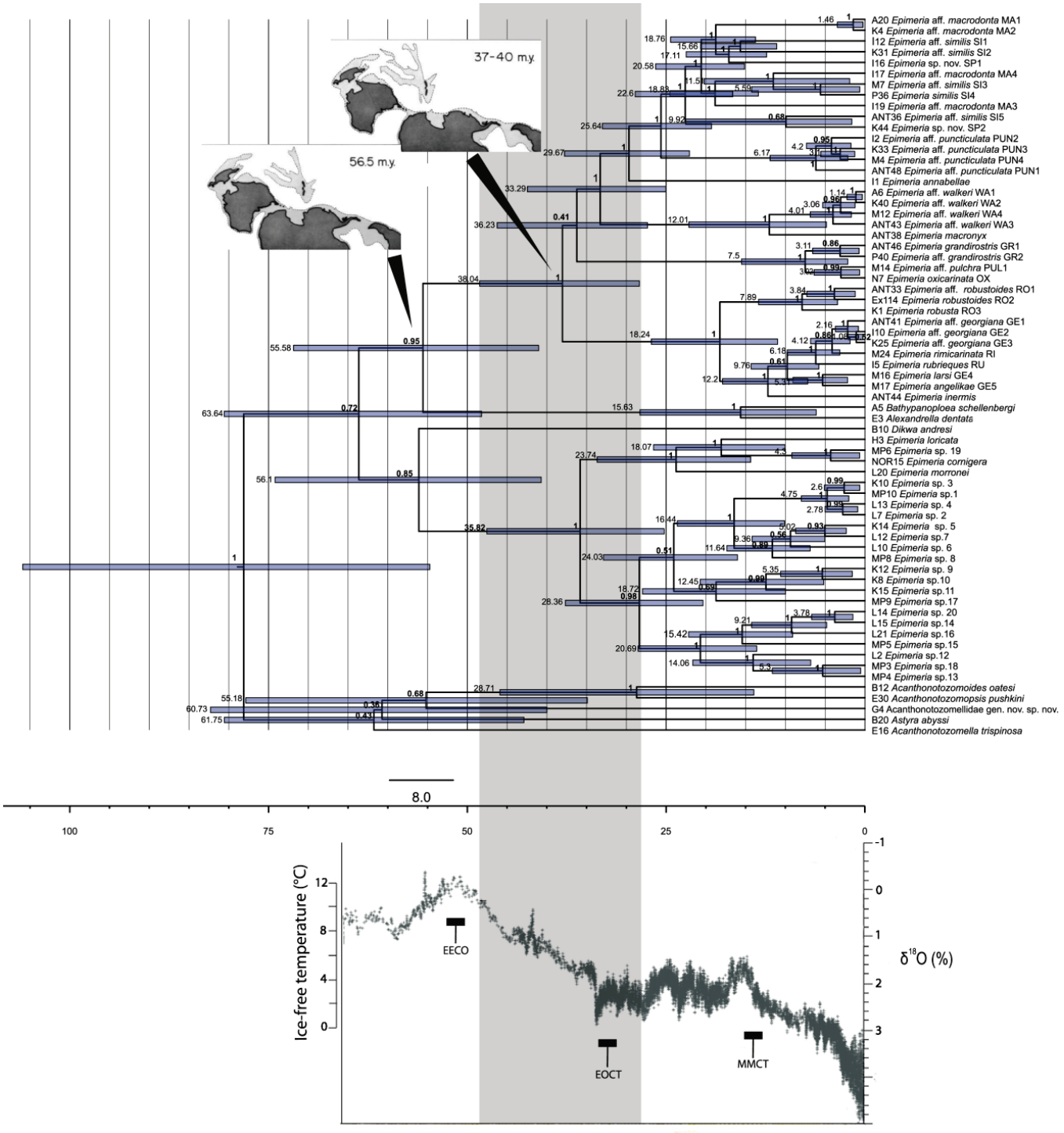

Figure 2. Maximum clade credibility chronophylogenetic tree from the BEAST analysis of the concatenated dataset. Blue bars on the tree indicate 95 % confidence intervals for estimated node ages. Mean node ages are indicated in front of the bars. Posterior probabilities are indicated above the nodes. The grey shaded area is the 95 % confidence interval of the initial diversification of the Antarctic *Epimeria* clade. The paleogeographic figures [from Zinsmeister (1982)] on the tree show the Late Gondwana's breakup. Shaded area on these figures represent inferred areas of shallow marine conditions. The graph below [modified from Zachos et al. (2008)] shows the paleotemperatures over the past 65 million years, inferred from the benthic foraminiferal $\delta^{18}O$ curve, which is based on records from Deep Sea Drilling Project and Ocean Drilling Program sites. EECO = Early Eocene Climate Optimum; EOCT = Eocene-Oligocene Climate Transition; MMCT = Middle Miocene Climate Transition.

DIVERGENCE TIMES

The coefficients of variation were much higher than 0.1 for the three genes (COI: 1.1, 28S: 0.961, H3: 0.963), indicating that the sequences analyzed did not evolve at a constant rate along the branches. Therefore, we proceeded to use a relaxed molecular clock. Results of the path-sampling analysis and calculation of the BF are presented in Table 3. The UCED relaxed clock was strongly favored over the UCLD model. The BF strongly supports the Birth-Death over the Yule model (Table 3).

	MLE	**2 lnBF**
UCED	-36461	10278
UCLD	-41600	-
Birth-Death	-35922	34
Yule	-35939	-

Table 3. Marginal likelihood estimation (MLE) values recovered by path-sampling. Bayes Factors (2 lnBF) were estimated from the MLE to compare two relaxed clock models (UCED and UCLD) and two tree models (Yule and Birth-Death).

Bayesian posterior divergence times recovered by BEAST under an exponential relaxed clock model and Birth-Death tree model were consistent across the two runs. A mean age of 55.58 Ma (95 % HPD: 71.85–41.02 Ma) was estimated for the most recent common ancestor (MRCA) of the clade comprising the stilipedids and Antarctic *Epimeria*. The MRCA of the Antarctic *Epimeria* clade was given a mean age of 38.04 Ma (95 % HPD: 48.46–28.36 Ma). The MRCA of the non-Antarctic *Epimeria* clade was dated at 35.81 Ma (95 % HPD: 47.54–25.24 Ma), which separates into a Melanesian and an American-European-African lineage (Fig. 2).

RATES OF DIVERSIFICATION

Based on the γ statistic, we found no evidence of a decelerating lineage accumulation rate towards present time in the origination pattern of the Antarctic *Epimeria* clade. When incomplete sampling is taken into account, assuming 72 % or 50 % sampling, the γ values are positive, but the null hypothesis of constant rate of speciation is not rejected ($p > 0.01$). When a 10 % sampling is assumed, the γ value is significantly positive ($p < 0.01$), indicating either an increasing rate of speciation, or non-zero extinction (Table 4).

Dataset	γ	*p-value* (2-tailed)
Semi-emp 10 %	11.02 (0.8)	0 (0)*
Semi-emp 50 %	1.419 (0.6)	0.14 (0.18)
Semi-emp 72 %	0.37 (0.47)	0.63 (0.21)
Empirical	-0.27	0.79

Table 4. Results of the CR test applied on the empirical and semi-empirical datasets.

No evident deviation from the null hypotheses of constant-rate models (BD or PB) is visible on the LTT plots (Fig. 3).

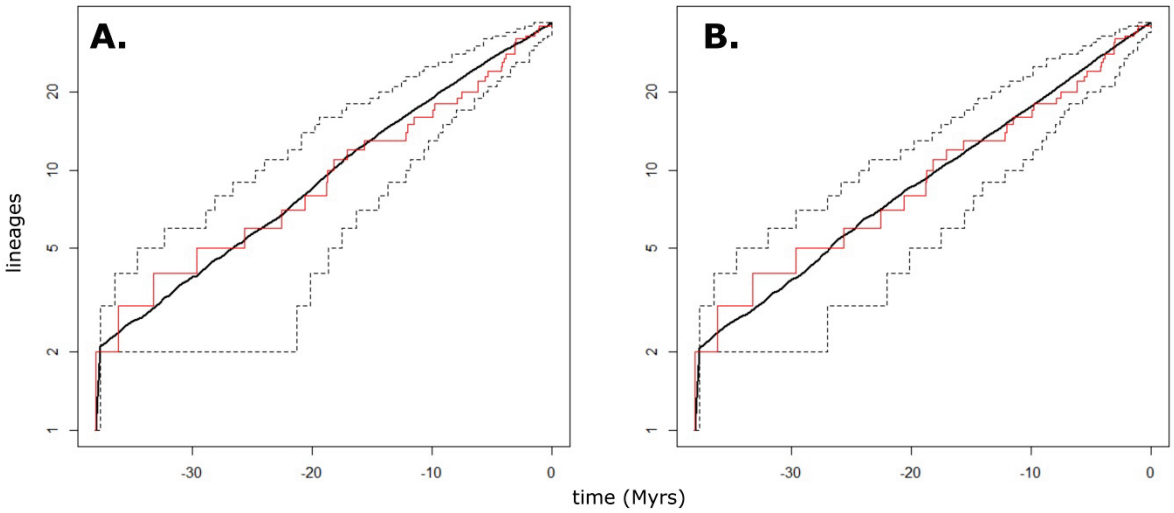

Figure 3. Lineage diversification through time plot of the Antarctic *Epimeria* clade, generated with the dated tree from the BEAST analysis (in red). Dotted lines represent the 95 % confidence interval of lineage diversification simulated 100 times under PB (A) and BD (B) models, with λ = 0.09 (PB) and with λ = 0.09 and μ = 0.02 (BD), and assuming a sampling fraction of 0.72.

The BDL analyses indicate PB as the best supported model of lineage diversification, closely followed by Yule2rate.The estimated probability that PB is the best model for our data among the evaluated models (wAIC) is only 31 %, which demonstrates that the method does not strongly support one model over the others. Table 5 shows the results for the best-scoring models only and Appendix S4 for all models evaluated. When incomplete sampling is taken into account, PB is the best model for the 72 % semi-empirical dataset (wAIC = 33 %), Yule2rate is the best model for the 50 % semi-empirical dataset (wAIC = 27 %) and BD is the best model for the 10 % semi-empirical dataset (wAIC = 62 %) (Appendix S4).

Models	LH	shift times	λ	AIC	dAIC	wAIC
PB	**-28.47**	**-**	**0.078**	**58.94**	**0.00**	**0.31**
Yule2rate	-26.62	2.09	0.088 0.027	59.24	0.30	0.27

Table 5. Parameter estimates and comparison of the fit of different lineage diversification models to the empirical dataset. Results are shown for the two best-scoring models. LH is the log-likelihood value of the model. The shift times (Ma) are indicated for the models implying discrete shifts in diversification rates. λ is the speciation rate. For each model, the Akaike Information criterion (AIC) was computed. The best-fitting model with the lowest AIC score is indicated in bold. dAIc is the difference between the AIC score of the evaluated model and the AIC score of the best-fitting model. wAIC are the Akaike weights.

The evaluation of Morlon et al.'s (2011) models of lineage diversification with RPANDA yielded the following results. When a 0.72 sampling fraction was assumed, Bcst (PB) was the best fit among the evaluated models (wAIC = 0.45), followed by Bvar (wAIC = 0.22), which implies an increasing speciation rate and no extinction. The Bvar model (again implying an increasing speciation rate and no extinction), was the best-fitting model when assuming a sampling fraction of 0.5. However, the latter had almost the same probability than Bcst (PB) of being the best fit among the evaluated models (wAIC = 0.32 and 0.30, respectively). For the 0.1 sampling fraction, Bvar (with an increasing speciation rate and no extinction) was also the best-fitting model with a wAIC of 0.54. Table 6 shows the results for the best-scoring models only and Appendix S5 for all models evaluated.

Dataset	Model	AIC	dAIC	wAIC	λ	α
Sampling 72 %	Bcst	243.44	0.00	0.45	0.093	-
	Bvar	244.88	1.44	0.22	0.11	-0.015
Sampling 50 %	Bcst	244.34	0.16	0.30	0.11	-
	Bvar	244.18	0.00	0.32	0.14	-0.03
Sampling 10 %	Bvar	242.72	0.00	0.54	0.37	-0.07

Table 6. Parameter estimates and comparison of the fit of Morlon et al.'s (2011) lineage diversification models with RPANDA. Results are shown for the best-scoring model and the second best fit whenever the wAIC of the best-scoring model was < 0.5. For each model, the Akaike Information criterion (AIC) was computed. The best-fitting model with the lowest AIC score is indicated in shaded grey. dAIC is the difference between the AIC score of the evaluated model and the AIC score of the best-fitting model. wAIC are the Akaike weights. λ is the speciation rate and α is the parameter controlling the exponential variation of the speciation rate with time.

For all considered sampling fractions (0.72, 0.5 and 0.1), the maximum posterior probability (MAP) shift configuration returned by BAMM — which is the distinct shift configuration with the highest posterior probability — is a single macroevolutionary regime across the whole tree and, i.e. no discrete rate shift. This is also the only regime contained in the 95 % credible shift set. Bayes Factor analyses also favour a model with no rate shifts, for all sampling scheme (Table 7). The rate through time plots show a constant diversification rate for the 0.72 sampling scheme, while it is increasing for the 0.1 and 0.5 sampling schemes (Fig. 4). However, the current version of BAMM assumes that all regimes are time-variable. In order to investigate the rate variation observed for the 0.1 and 0.5 sampling schemes, we computed the 95 % Higher Posterior Density (HPD) interval of the post-burnin samples of the lambda shift parameter. This parameter is the standard deviation of the normal distribution of speciation rates. A value of zero therefore indicates rate constancy. As the 95 % HPD of the lambda shift parameter includes 0 in both cases (95 % HPD for 10 % sampling [-0.005, 0.057] and for 50 % sampling [-0.022; 0.057]), there is no evidence for a variable speciation rate.

	Sampling	1 shift	2 shifts	3 shifts
0 shift	10 %	21.522	137.203	-
	50 %	9.729	60.878	213.075
	72 %	7.495	32.676	95.057

Table 7. Matrix of pairwise Bayes Factors (BF), where the BF is the ratio of marginal likelihoods between two models, Mi and Mj. Numerator models are given as rows and denominator models as columns. BF > 3 is considered positive support for Mi, while > 20 is a strong support (Kass and Raftery, 1995).

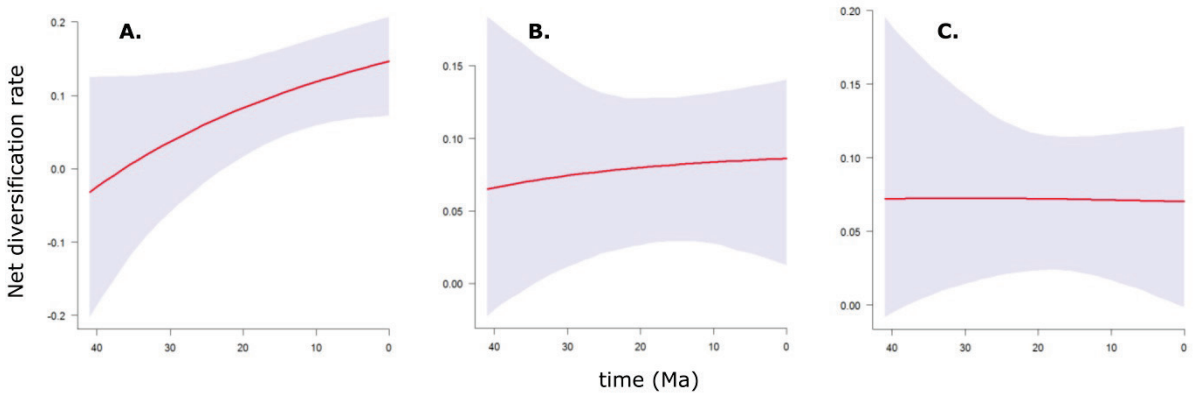

Figure 4. Net diversification rate through time inferred with BAMM for the Antarctic Epimeria clade, assuming sampling fractions of A. 0.1 B. 0.5 and C. 0.72.The shaded grey area represents the 95 % credible interval on the rate values.

DISCUSSION

SYSTEMATICS OF *EPIMERIA*

The monophyly of *Epimeria* was not supported by BI, as two species of Stilipedidae from the subfamily Alexandrellinae (*Bathypanoploea schellenbergi* and *Alexandrella dentata*) are sister to the Antarctic *Epimeria* clade (PP = 0.99). This relationship is however not supported by ML (BV = 68), and should therefore be verified with additional data (Fig. 1). The systematics of *Epimeria* should therefore be revised, as the genus may potentially include (at least part of) the Stilipedidae. This latter family was divided into three subfamilies: Astyrinae, Stilipedinae and Alexandrellinae (Holman and Watling, 1983). However, Stilipedidae is not monophyletic, as *Astyra abyssi* (from the subfamily Astyrinae) is not sister to Alexandrellinae neither in the present study nor in a previous phylogeny of Eusiroidea (Verheye et al. 2016b). Since the systematics of Stilipedidae remains unclear, we will consider here only the Alexandrellinae as a potential sister clade to the Antarctic *Epimeria*. However, as this relationship is supported by low BV (68) and PP have been shown to lead to higher type I error rates (Cummings et al., 2003; Erixon et al., 2003), the support of this node should be verified with additionnal data before making any taxonomic changes. The main differences between *Epimeria* auctorum and *Alexandrella* reside in the mouthpart morphology. Several possible autapomorphies indeed characterize *Alexandrella*: (1) the mandibular molar is absent, (2) the palp of the maxilla 1 is expanded, (3) the inner and outer plates of the maxilla 2 are expanded and (4) the outer plate of the maxilliped is greatly expanded (Holman and Watling, 1983). Moreover, the non-ommatidian eyes in Alexandrellinae could be indicative of a deep-sea ancestor (Warrant and Locket, 2004). If the Alexandrellinae are indeed nested within *Epimeria*, a shift of trophic niche and/or bathymetric range of their ancestor could have led to these morphological modifications.

ISOLATION OF ANTARCTIC *EPIMERIA* OR HISTORICAL DISPERSALS?

As Antarctic *Epimeria* species are monophyletic and the origin of this Antarctic clade is estimated to be older or contemporaneous to the geographical isolation of Antarctica, it is hypothesized that *Epimeria* did not disperse in/out of the shelf throughout its evolutionary history. However, to further test the monophyly of this Antarctic component, it would be interesting to include the single Magellanic (*Metepimeria acanthurus*) and sub-Antarctic (*Epimeria ashleyi,* from the Macquarie Ridge) *Epimeria* species in the phylogenetic tree.

The Antarctic shelf is well isolated from the other ocean's shelves by large distances (> 850 km), deep seas and the most powerful current on earth, the ACC (Clarke et al., 2005; Orsi et al., 2005).

Moreover, beyond the APF, surface water temperatures rise by 3–4 °C. Because of their limited tolerance to such temperature change, many Antarctic marine invertebrates would not be able to establish on the other side of the APF (Peck, 2002). *Epimeria* is presumably cold-adapted, as outside the Antarctic region, it is mainly found at bathyal depths. Temperature is therefore likely to be an important isolating factor for the Antarctic *Epimeria* clade. However, historical movements of stenothermal taxa in and out of the Antarctic shelf could have been possible during periods of climatic changes (Clarke et al., 1992b). A variety of pelagic organisms (or organisms with a pelagic life stage) were reported to cross the APF, supposedly by means of eddies, i.e. water masses transported out of the ACC (Antezana, 1999; Clarke et al., 2005; Li et al., 2002) or by the Antarctic Intermediate water that extends northwards (Antezana, 1999). As such currents do not reach the ocean floor (Clarke et al., 2005), benthic taxa lacking a pelagic larval stage can only disperse through the deep-sea. Historical events of such polar emergences (i.e. colonization of the shelf by deep-sea fauna) and submergences (i.e. colonization of the deep-sea by shelf fauna) did occur in the evolutionary history of some strictly benthic taxa (Held, 2000; Raupach et al., 2007; Strugnell et al., 2011; Strugnell et al., 2008). Such movement is indeed facilitated by the thermohaline circulation, which connects the Southern Ocean shelf with the deep waters of the other world's oceans through an isothermal water column, and by the unusually deep Antarctic shelf (reaching > 1000 m at places) (Clarke, 2003; Clarke et al., 2009; Rogers, 2000). Polar submergences occurred in the Antarctic *Epimeria* clade history: whereas the vast majority of Antarctic *Epimeria* species are found on the shelf and upper slope (< 1200 m), two species (*Epimeria larsi* and *Epimeria* sp. 2) nested within shelf clades have bathymetric distributions restricted to slope depths (around 2000 m). However, the Drake Passage has an average depth of 3400 m (Smith and Sandwell, 1997). The bathymetric distributions of *Epimeria* species worldwide suggest that this might be too deep for most *Epimeria* to disperse in and/or out of the Antarctic region along the benthos, which would explain the evolutionary isolation of the Antarctic clade. However, two species were sampled in the abyssal plain: *Epimeria glaucosa* was found at 3710 m around New Zealand (Barnard, 1961) and *Epimeria abyssalis* at around 5600 m in the Kuril-Kamchatka Trench (Shimomura and Tomikawa, 2016). Additional deep-sea sampling and inclusion of abyssal species in phylogenetic analyses might reveal undetected historical dispersal of *Epimeria* through the deep-sea.

ORIGIN AND HISTORICAL BIOGEOGRAPHY OF ANTARCTIC *EPIMERIA*

The first hypothesis aiming at determining the temporal and geographical origin of Antarctic *Epimeria* was presented by Lörz and Held (2004). Ages of between 34.9 and 15.7 Ma were inferred for the MRCA of *Epimeria*, based on COI distances and rates estimated for cirripeds (3.1 %/Myr) and

for alpheid shrimps (2.4 %/Myr), and assuming a strict molecular clock. Applying a relaxed clock model on a combined dataset (COI, 28S and H3), we obtained a mean COI rate estimate of 1.6 %/Myr and an age of 38.04 Ma (95 % HPD [48.46 Ma; 28.36 Ma]) for the MRCA of the Antarctic *Epimeria* clade. As the 95 % HPD interval spans an older period than the age estimation of Lörz and Held (2004), the assumption that this clade originated when Antarctica was already isolated from the other fragments of Gondwana is equivocal (Fig. 2).

From the Late Cretaceous to the early Cenozoic, Antarctica, South America, Australia and New Zealand were connected in an area of cool temperate shallow seas known as the Weddelian Province (Woodburne and Zinsmeister, 1984; Zinsmeister, 1979; Zinsmeister, 1984). The South Tasman Saddle, a submarine trough between Tasmania and the South Tasman Rise, existed as a shallow to medium-depth seaway in the late Paleocene to early Eocene. If the Antarctic George V and Oates Coast shelf breaks were closer to the present shoreline at that time, it is possible that a deep seaway between Australia and East Antarctica existed as early as 40 Ma. Otherwise, a deepwater passage only developed after the late Eocene (Lawver et al., 2013; Lawver et al., 2014). It has indeed been inferred that the Tasmanian gateway deepened in the period 35.5 to 30.2 Ma (Stickley et al., 2004) and was open to unrestricted deepwater circulation at 32 Ma (Lawver and Gahagan, 2003). An early opening of the Drake Passage to shallow water was suggested to have taken place in the Middle to Late Eocene (50–41 Ma) (Eagles et al., 2006; Livermore et al., 2005; Scher and Martin, 2004). This was followed by a progressive widening and deepening to intermediate depth at 37 Ma, while the deepwater passage is usually dated in the interval 34–30 Ma (Lagabrielle et al., 2009; Latimer and Filippelli, 2002; Lawver and Gahagan, 2003; Livermore et al., 2005; Scher and Martin, 2004) (Fig. 2). The opening of the Tasmanian and Drake passages were inferred as important vicariant events, promoting speciation in other Antarctic benthic shelf species (Göbbeler and Klussmann-Kolb, 2010; Lee et al., 2004; Matschiner et al., 2011; Near, 2004).

It cannot be inferred from the current data whether the Antarctic *Epimeria* clade originated in the Weddelian Province or by vicariance when the continent separated from the other Gondwanan fragments. The divergence from its stilipedid sister clade (*Bathypanoploea schellenbergi* and *Alexandrella dentata*) occurred 55.58 Ma (95 % HPD [71.85; 41.02 Ma]), in the Weddelian Province (Fig. 2). However, the inclusion of additional non-Antarctic samples — especially from historically connected and geographically closer regions such as South America, Australia and the sub-Antarctic islands — may help to identify the sister lineage of the Antarctic *Epimeria* clade and shed light on its biogeographic origin. The endemicity of the Antarctic *Epimeria* clade would suggest that it originated *in situ* when the region was already isolated. In the case that this isolation was not yet geographical,

it was suggested that a latitudinal gradient in seasonality might have promoted an early Cenozoic divergence of the polar fauna (Crame, 2013).

In any way, the initial diversification of the Antarctic *Epimeria* lineage would have occurred in a cooling environment. Following the early Eocene Climatic Optimum (EECO), high latitude surface water began to cool across the early to middle Eocene boundary (49–48 Ma) (Lawver and Gahagan, 2003). A second cooling phase occurred in the late Middle Eocene 44–41 Ma. From the beginning of this cooling trend, the ice sheets progressively grew to culminate at the Eocene–Oligocene boundary (Miller et al., 2008a). The transition to an icehouse climate in the earliest Oligocene, known as the Eocene–Oligocene Climate Transition (EOCT), was marked by an abrupt cooling at 33.55 Ma (Miller et al., 1991) and the first continent-wide glaciations (Hambrey et al., 1991; Sorlien et al., 2007; Wilson et al., 2013). Most of the species complexes identified in Verheye et al. (2016a) diversified after the MMCT, (~14 Ma), a period marking the beginning of repeated ice sheet advances over the shelf and retreats inshore (Shevenell et al., 2004). Globally, these results suggest that the Antarctic *Epimeria* clade's diversification would be related to cold waters (Fig. 2). Many modern Antarctic lineages likely arose in the time period spanning this transition from Eocene cool-temperate climate to Oligocene polar climate, as the fossil record indicates a fundamental shift in the structure of benthic communities. The extinction of many durophagous (skeleton-crushing) predator taxa — decapods, teleost and cartilaginous fishes — decreased the predation pressure, which allowed the establishment of dense populations of erect sessile suspension feeders (Aronson et al., 2007). These organisms constitute a food source for many amphipods, which are predatory food specialists (e.g. Coleman, 1989b; Coleman, 1991; Klages and Gutt, 1990). Moreover, sessile suspension-feeders form dense assemblages which provide a three-dimensionally structured habitat for an errant fauna of mostly slow-moving invertebrates, such as amphipods (Arntz et al., 2005; Aronson and Blake, 2001; Clarke et al., 2004; Clarke and Crame, 2010). In summary, the adaptation of *Epimeria* to a cold environment, coupled with the extinction of cold-intolerant taxa and resulting abundant available niche-space likely led to their successful diversification on the Antarctic shelf.

The divergence between a clade entirely composed of Melanesian species and a clade that includes European, African and South-American species occurred 35.81 Ma 95 % HPD [47.54 Ma; 25.24 Ma] (Fig. 2). The Indo-Pacific islands were likely not colonized by *Epimeria* species from the Weddelian Province or Australia, but rather from south-eastern continental Asia. Indeed, at the time of origin of this Melanesian clade, the South East Asian gateway that connects the Indian and Pacific oceans was widely opened, likely forming an efficient barrier to dispersion between Australia and the Indo-Pacific region (Hall et al., 2011).

No early diversification burst was detected in the phylogenetic pattern of the Antarctic *Epimeria* clade, nor any shift in diversification rates associated with glacial cycles. The Antarctic *Epimeria* clade has survived through multiple mass extinction events associated with the cooling of the continent and the glacial cycles. The fossil record indeed indicates many biotic turnovers induced by climate change (Beu, 2009; Crame et al., 2014; Hara, 2001). Furthermore, it was shown that following the MMCT, the ice sheet extended to the outer shelf during glacial maxima, at least in some places, thereby erasing shelf habitats and their associated biota (e.g. Chow and Bart, 2003; Hambrey and McKelvey, 2000; Passchier et al., 2003).

Despite the evidence for repeated extinctions of the Antarctic shelf biota, the extinction rate estimates given by the different methods used herein are unrealistically close to zero. Extinction rate estimates from phylogenies of extant taxa were often shown to be unreliable (Nee, 2006; Purvis, 2008; Rabosky, 2010; Rabosky and Lovette, 2008; Ricklefs, 2007). In the present case, the phylogeny may simply lack sufficient information to accurately estimate extinction rates or infer diversity dynamics (Liow et al., 2010; Morlon et al., 2011; Quental and Marshall, 2009; Rabosky, 2010).

Mass extinctions are believed to promote adaptive radiations, manifested by a subsequent sharp increase in the rate of diversification (Benton and Emerson, 2007; Condamine et al., 2013; McInnes et al., 2011). These “rebounds” would be followed by a diversity-dependent decrease in diversification rates. However, if repeated mass extinctions occurred, the signals of older pulses of diversification tend to be eroded by subsequent extinctions (Phillimore and Price, 2008; Rabosky and Lovette, 2008; Ricklefs and Jønsson, 2014; Weir, 2006). Because of the presumed high turnover rate in the evolutionary history of the Antarctic *Epimeria* clade, even a large early diversification burst could be undetectable (McInnes et al., 2011; Quental and Marshall, 2009; Rabosky and Lovette, 2008). However, without a fossil record, we cannot determine whether this turnover rate was sufficiently high compared to the initial speciation rate to erode an early burst signature (Quental and Marshall, 2009).

If the history of environmental disturbances is responsible for the lack of an early burst signature, then we can expect similar patterns in other benthic shelf taxa. The paucity of branching events between the Oligocene and MMCT in the notothenioid fishes' phylogeny was interpreted as unobserved extinction, possibly eroding the signature of an explosive early radiation. However, the latter study also provided evidence of evolutionary radiations for several younger subclades, coinciding with the MMCT climate change event (Near et al., 2012).

The relatively low number of tips in our phylogeny might decrease the statistical power of the tests to detect lineage-specific shifts. It has been shown that a reduced taxon sampling compromises the detection of discrete rate shifts and slowdowns in diversification (Laurent et al., 2015). This could also explain the inability of the model-selection analyses to discriminate between different equally fitting models. When the true diversity of the clade is better known, diversification analyses repeated on a thoroughly sampled phylogeny might reveal unobserved diversification regime changes.

Finally, in order to detect an early burst of diversification, the clade must also be close to its equilibrium diversity (McInnes et al., 2011; Quental and Marshall, 2010). Yet, the Antarctic *Epimeria* clade may still be in the earliest stage of a logistic growth following the Last Glacial Maximum. The exponential growth of diversity that would be observed in such case (Liow et al., 2010; Quental and Marshall, 2010) is consistent with our results of either constant or increasing rates of speciation. Assuming that the dynamics of the Antarctic *Epimeria* clade is governed by diversity-dependent diversification, there is, however, no way of determining in which stage of its diversification trajectory this clade actually stands (Quental and Marshall, 2010).

CONCLUSIONS

By including species from all the world's oceans and by applying a relaxed clock model to date the phylogeny, this study provides the first spatiotemporal framework for the evolution of Antarctic *Epimeria*. Although the precise timing of origin of the Antarctic clade is still debatable, our data suggest that this lineage originated *in situ* — in the Late Gondwanan Weddellian Province or by vicariance when the plates broke apart — and does not result from a colonization event after the geographical isolation of the continent. The initial diversification of the clade occurred in a cooling environment, which suggests that the adaptation of this genus to cold waters, along with the extinction of cold-intolerant taxa and resulting availability of habitats, would have led to their successful radiation on the Antarctic shelf. The Antarctic *Epimeria* clade appears to have evolved in complete isolation from the other world's oceans, as our data do not provide any evidence of dispersal in and/or out of the shelf since the isolation of Antarctica. Sampling of additional non-Antarctic *Epimeria*, especially from historically connected regions (South America, Australia and New Zealand), could help identify the sister lineage of the Antarctic clade and clarify its biogeographical origin.

ACKNOWLEDGEMENTS

This work was supported by a Ph.D. fellowship from F.R.I.A. (F.N.R.S., Belgium). The last author was funded by the Digit 3 program of BELSPO. We thank the Alfred-Wegener-Institut, Helmholtz-Zentrumfür Polar- und Meeresforschung (AWI) and the captain, crew and chief scientists of various *R.V. Polarstern* expeditions for their efficiency, as well as present and past colleagues of the staff of the Royal Belgian Institute of Natural Sciences (RBINS), especially Henri Robert and Charlotte Havermans, for collecting specimens on board. The travel expenses of the first and last authors during ANT-XXIX/3 were funded by the Fonds Léopold III. The research program led by Guillaume Lecointre, REVOLTA 1124, supported by the Institut polaire français Paul Emile Victor (IPEV) and the Muséum national d'Histoire naturelle (MNHN), and the CAML-CEAMARC cruise of RSV Aurora Australis (IPY project no. 53), supported by the Australian Antarctic Division, the Japanese Science Foundation and the IPEV (project ICOTA), are acknowledged for providing extensive Antarctic material. The Melanesian specimens used in this study were collected during various deep-sea cruises, conducted respectively by MNHN and Institut de Recherche pour le Développement (IRD) as part of the Tropical Deep-Sea Benthos programme (http://expeditions.mnhn.fr/program/tropicaldeep-seabenthos). Funders and sponsors include the French Ministry of Foreign Affairs, the Total Foundation, Prince Albert II of Monaco Foundation, Stavros Niarchos Foundation, and Richard Lounsbery Foundation. We thank Laure Corbari (MNHN) for giving us access to this material. This publication is registered as CAML (Census of Antarctic Marine Life) publication No. 164 and contribution No. 215 to ANDEEP. We are also grateful to Zohra Elouaazizi (RBINS), Karin Breugelmans (RBINS) and Gontran Sonet (RBINS- JEMU) for helpful methodological advices. TB contributed to this manuscript on behalf of the "Joint Experimental Molecular Unit" (RBINS-JEMU) and the FWO Research Community W0.009.11N "Belgian Network for DNA Barcoding" (BeBoL).

CHAPTER 5

ANTARCTICA AS AN EVOLUTIONARY INCUBATOR? ORIGIN AND DIVERSIFICATION DYNAMICS OF IPHIMEDIIDAE (AMPHIPODA, CRUSTACEA) FROM THE ANTARCTIC SHELF

Marie L. Verheye[1,2]

Thierry Backeljau[1,3]

Mélodie Locrel[2]

Cédric d'Udekem d'Acoz[1]

Unpublished chapter

[1] Royal Belgian Institute of Natural Sciences, OD Taxonomy and Phylogeny, 29 rue Vautier, B-1000 Brussels, Belgium

[2] Catholic University of Louvain-la-Neuve, Department of Biology, Marine Biology Laboratory, 3 bte L7.06.04 Croix du Sud, B-1348 Louvain-la-Neuve, Belgium

[3] University of Antwerp, Evolutionary Ecology Group, 171 Groenenborgerlaan, 2020 Antwerp, Belgium

ABSTRACT

The physical isolation of the Antarctic shelf and extreme life conditions contribute to its high degree of endemism. The Antarctic shelf fauna would, however, be composed of Gondwanan descendants, but also of more recent colonizers. The peculiar Antarctic climatic history might have provided environmental prerequisites to the radiation of some lineages, some of which might afterwards have colonized ocean shelves elsewhere. Iphimediidae are cosmopolitan amphipods that are well-represented on the Antarctic shelf. Despite their brooding ecology and presumably limited mobility, some species are distributed in the Antarctic as well as sub-Antarctic regions. By reconstructing a time-calibrated molecular phylogeny of Antarctic, sub-Antarctic and northern iphimediid species, this study investigates the origin, propensity towards dispersal in/out of the shelf and *in situ* diversification patterns of (sub-)Antarctic Iphimediidae. All analyses support the monophyly of the studied Antarctic and sub-Antarctic iphimediids, which together appear as sister clade to the non-Antarctic iphimediids. Whereas the precise timing of origin of (sub-)Antarctic iphimediids remains ambiguous, their inferred divergence times and monophyly suggest that adaptation to harsh polar conditions and/or tectonic vicariance might have promoted the divergence of a late Gondwanan/early Antarctic iphimediid lineage. The initial diversification of the clade occurred during the progressive transition to an Icehouse climate (35.14 [46.41; 25.22] Ma) and would therefore be related to cold waters. Subsequently, a diversification burst within one or two subclades might have occurred after the mid-Miocene Climate Transition. Furthermore, the data suggest at least one historical dispersal event from the high Antarctic to sub-Antarctic islands, after the geographical isolation of Antarctica. However, Antarctic iphimediids do not appear to have dispersed further north than sub-Antarctic islands and Tierra del Fuego at any point of their evolutionary history.

INTRODUCTION

The Antarctic shelf is isolated from the other ocean's shelves by great distances (> 850 km), deep-water basins (> 4000 m) and the most powerful current on earth, the Antarctic Circumpolar Current (ACC) (Clarke et al., 2005; Thornhill et al., 2008). Moreover, the Antarctic Polar Front (APF), one of the ACC's jets, marks a sharp change in water temperatures (3–4 °C). The extreme seasonality in light regime and ice coverage drives huge variations in primary production which feeds into the whole benthic ecosystem (Clarke, 1988; Clarke and Leakey, 1996). The physical isolation of the Antarctic shelf and extreme life conditions contribute to its biological distinctiveness by preventing

organisms which are poorly adapted and/or with low dispersal abilities to cross the APF and establish viable populations in the Antarctic region (Crame, 2013; Peck, 2002; Peck, 2005). This apparent isolation raised the question of the origin of the Antarctic shelf fauna (Clarke et al., 2005; Clarke and Crame, 1989; Knox and Lowry, 1977). It was previously believed that most of the modern fauna evolved *in situ* since before Antarctica separated from other fragments of Gondwana (Baker et al., 2006; Bargelloni et al., 2000; Beu, 2009; Clarke et al., 2005; Near, 2004; Patarnello et al., 1996; Zinsmeister, 1982). The APF is, however, a permeable barrier for a variety of pelagic (Antezana, 1999; Bargelloni et al., 2000; Page and Linse, 2002; Thatje and Fuentes, 2003) and benthic organisms lacking a pelagic stage (Held, 2000; Strugnell et al., 2008). The ACC, encircling Antarctica, transports huge amounts of water throughout the surrounding Oceans (Rintoul et al., 2001), thereby acting as a "highway" for pelagic organisms and floating macroalgae with their associated epifauna (Edgar and Burton, 2000; Nikula et al., 2010; Smith, 2002), between sub-Antarctic islands (Barnes et al., 2006; Fraser et al., 2009; Helmuth et al., 1994; Leese et al., 2010; Waters, 2008). The numerous eddies in the Drake Passage area, i.e. parcels of water transported out of the ACC, might allow a bidirectional transport in and out of the Antarctic region (Antezana, 1999; Clarke et al., 2005; Glorioso et al., 2005). The Antarctic shelf is also connected to the other oceans' deep waters through an isothermal water column — which is part of the thermohaline circulation system (Clarke et al., 2009; Rogers, 2000) — providing yet another mean of dispersal (e.g. Díaz et al., 2011; Göbbeler and Klussmann-Kolb, 2010; Held, 2000; Raupach et al., 2009; Schüller, 2011; Strugnell et al., 2008). All in all, the modern Antarctic marine fauna is a mixture of Gondwanan remnants and more recent colonizers (Clarke and Crame, 1989).

The taxonomic composition of the Antarctic marine fauna differs from that elsewhere in the world (Rogers, 2007). While some groups are relatively poorly represented (e.g. gastropods, bivalves, teleosts) to virtually absent (e.g. decapods) compared to other oceans, others are particularly species-rich (e.g. pycnogonids, ascidians and peracarids) (Aronson et al., 2007; Clarke and Johnston, 2003). Among these exceptionally diverse taxa, some have been qualified as "species flocks", i.e. bursts of closely-related endemic species which are ecologically diverse and numerous, relative to adjacent areas (Lecointre et al., 2013). Such bursts in lineage diversification might arise from ecological opportunity generated by the colonization of new areas, the extinction of competitors, or the development of key innovations (Gavrilets and Losos, 2009; Glor, 2010; Losos, 2010; Schluter, 2000; Yoder, 2010). Notably, a "rebound" of diversification can occur in the aftermath of a mass extinction event (Condamine et al., 2013; Erwin, 2001, 2008). Alternatively, the simultaneous formation of multiple geographical barriers can be responsible for a burst of allopatric speciation (Rundell and Price, 2009). The peculiar climatic history of the Antarctic region might have repeatedly

created such environmental prerequisites to the radiation of lineages. Antarctica has been located over southern polar latitudes since Early Cretaceous (Lawver et al., 1992), but was however characterized by a warm to cool temperate climate until the early to middle Eocene boundary (ca. 48–49 Ma), which marks the beginning of the cooling trend (Francis et al., 2008; Lawver and Gahagan, 2003). An abrupt drop in temperatures led to the onset of the first continental glaciations at the Eocene–Oligocene boundary (ca. 34 Ma). The fossil record bears evidences of a fundamental faunal turnover during this cooling period (Aronson et al., 2009; Berkman et al., 2004; Beu, 2009; Stilwell and Zinsmeister, 1992). The durophagous predators (fishes and decapods) — which are largely responsible for structuring marine food webs at lower latitudes — went mostly extinct, causing a shift in the structure of Antarctic benthic communities (Aronson et al., 2007, 2009). Under decreased predation pressure, dense assemblages of epifaunal suspension feeders could establish, providing a three-dimensionally structured habitat for an errant fauna of slow-moving invertebrates e.g. ophiuroids, asteroids, echinoids, pycnogonids, isopods, amphipods and nemerteans (Arntz et al., 2005; Aronson and Blake, 2001; Aronson et al., 2007; Clarke et al., 2004; Clarke and Crame, 2010; Gili et al., 2006). Following the Mid-Miocene Climate Transition (MMCT; ca. 14 Ma), interglacial periods alternated with glacial periods during which the continental shelf was repeatedly scoured over large sections by the ice sheets, sometimes advancing to the outer shelf edge (Pollard and DeConto, 2009; Tripati et al., 2009). The near-shore benthic fauna was therefore periodically erased (Thatje et al., 2005b; Thatje et al., 2008). Moreover, the isolation of populations in ice-free refugia during glacial advances would have resulted in allopatric speciation of low dispersal organisms (Thatje et al., 2005b).

The amphipod family Iphimediidae is a good model taxon for the study of the Antarctic shelf benthos' historical biogeography and diversification, as it is distributed in every world's ocean (107 species in total) and well-represented on the Antarctic shelf (36 species). Moreover, the family is composed of brooding, strictly benthic and mostly shallow-water shelf species. These life history traits would in theory limit long-distance dispersal across deep passages. However, a few species occur on both sides of the APF, in the high Antarctic region, as well as in sub-Antarctic islands and the Magellanic area (Coleman, 2007). This raised the question of the origin of Antarctic iphimediids and their ability to disperse in and/or out of the shelf. Based on a cladogram reconstructed with 6 morphological characters, Watling and Thurston (1989) inferred that the iphimediid lineage likely originated on the Antarctic shelf from Gondwanan ancestors and suggested that the cooling of Antarctic waters promoted its diversification. In the COI phylogeny of Lörz and Held (2004), comprising eight Antarctic species, ages of 34.4 and 71.7 Ma were inferred for the last common ancestor of these Antarctic iphimediids, using respectively a COI rate of evolution estimated for

cirripeds and for alpheid shrimps, and assuming a strict molecular clock. These estimates are equivoqual regarding the Antarctic origin of iphimediids, as the openings of the last land bridges between Antarctica and other fragments of Gondwana (South America and Australia) to deepwater are dated in the interval 40–30 Ma (Lagabrielle et al., 2009; Latimer and Filippelli, 2002; Lawver and Gahagan, 2003; Lawver et al., 2013, 2014; Livermore et al., 2005; Scher and Martin, 2004; Stickley et al., 2004). Moreover, Watling and Thurston (1989) inferred that iphimediids dispersed out of the Antarctic region and subsequently radiated throughout the world's oceans, as their cladogram shows genera with an entirely or nearly exclusively non-Antarctic distribution (*Labriphimedia*, *Coboldus* and *Iphimedia*) nested within strictly high Antarctic genera. This led to the assumption that the Antarctic shelf might act as an "evolutionary incubator", supplying colonizing taxa to the world's ocean after a radiation phase within Antarctic waters (Brandt, 1999; Briggs, 2003; Watling and Thurston, 1989).

An evaluation of these preliminary inferences on the historical biogeography of Iphimediidae requires a robust phylogeny of the family based on an extensive Antarctic sampling, along with non-Antarctic representatives. We therefore reconstructed a phylogeny of Iphimediidae using three gene fragments (COI, 28S and H3) and including 27 out of the 36 described Antarctic iphimediid species. The non-Antarctic material is composed of 7 *Iphimedia* species collected in Europe, South Africa and Melanesia. We used a relaxed molecular clock to date the phylogenetic tree and considered the geographical distribution of the specimens in order to address the following questions: (1) When and where did Antarctic iphimediids originate? (2) Did iphimediids disperse in and/or out of Antarctica after its physical isolation from other Gondwanan land masses? (3) Does the historical diversification pattern of Antarctic iphimediids bear signatures of diversification bursts, e.g. in its early history and/or associated with climatic events?

MATERIAL AND METHODS

TAXON SAMPLING

We included 27 out of the 36 described Iphimediidae species from the Antarctic region (south of the Polar Front), along with 6 species tentatively identified as undescribed. Specimens from potentially undescribed species were named with "aff." as a reference to the morphologically most similar described species or "sp. nov." when no such similarities were observed. Non-Antarctic iphimediids included one species from Norway (*Iphimedia obesa*), two from France (*I. nexa* and *I.* aff. *nexa*), one

from Italy (*I.* aff. *obesa*), one from South Africa (*I. gibba*) and two from Vanuatu (*I.* cf. *damawan* and *I.* cf. *beeslayae*).

Antarctic samples were collected during several expeditions of the *R.V. Polarstern*: ANT-XXIII/8, ANT-XXIV/2, ANT-XXVII/3 and ANT-XXIX/3 in the Drake Passage, Bransfield Strait, eastern coast of the Antarctic Peninsula and eastern Weddell Sea. Additional specimens were sampled from the Adélie Coast on board of *R.V. Astrolabe* during the CEAMARC and REVOLTA expeditions. Specimens from the Ross Sea were collected during TAN0402 and TAN0802 expeditions of *R.V. Tangaroa*. Non-Antarctic specimens were collected during the SANTO expedition in Vanuatu, with the *R.V. Johan Ruud* in Norway and by opportunistic sampling in France, Italy and South Africa (Table 1).

All specimens were preserved in 96–100 % ethanol for DNA analysis. Vouchers are deposited at the Royal Belgian Institute of Natural Sciences (RBINS, Brussels, Belgium), the Muséum national d'Histoire naturelle (MNHN, Paris, France) and the National Institute of Water and Atmospheric Research (NIWA, Wellington, New Zealand).

DNA SEQUENCING

DNA was extracted from the pleopods and abdomen muscles using a NucleoSpin® Tissue kit (Macherey-Nagel) following the manufacturer's protocol for animal tissues. The DNA was eluted in 100 µl of sterile distilled H_2O (RNase free) and stored at -20 °C.

Partial segments of the mitochondrial cytochrome c oxidase subunit I (COI) (~550 bp), nuclear 28S rDNA (~1400 bp) and Histone 3 (H3) (~360 bp) were amplified by PCR. Amplifications were performed in a 25 µl reaction mix, which contained 0.15 µl Taq DNA Polymerase (5 U μl^{-1}; Quiagen, Antwerp, Belgium), 2.5 µl 10x CoralLoad PCR Buffer (Quiagen, Antwerp, Belgium), 2.5 µl dNTPs mix (250 µM of each), 11–16 µl RNase-free water, 1.25 µl of each primer (2 µM), and 1–6 µl of DNA extract.

The COI mtDNA fragment was amplified using the primers Cp-COIF3 (Pilar Cabezas et al., 2013) and COI2R (Otto and Wilson, 2001). The thermal cycling used for the COI amplification followed Pilar Cabezas et al. (2013), except for the annealing temperature set at 51 °C. The 28S rDNA fragment was amplified using the primers 28S-3311F (Witt et al., 2006) and 28R (Hou et al., 2007), modified as follows: 5'-GGGACTACCCGCTGAACTTAAGCAT-3' and 5'-GTCTTTCGCCCCTATGCCCAACTG-3'. PCR amplification settings for 28S rDNA consisted of an initial denaturation for 3 min at 94 °C, followed by 40 cycles of denaturation at 94 °C for 40 s, annealing at 45 °C for 40 s, extension at 72 °C for 90 s, and a final extension at 72 °C for 10 min.

Specimens id code	Species	Locality	Expedition	Station	Latitude	Longitude
IPHIMEDIIDAE						
A4	*Anchiphimedia dorsalis*	King George Island	ANT-XXVII/3	222-5	62° 18.21' S	58° 39.90' W
C1	*Anchiphimedia dorsalis*	Ross Sea	TAN0402	195	71° 37.32' S	170° 55.38' E
C2	*Anchiphimedia dorsalis*	Ross Sea	TAN0402	33	71° 45.28’ S	171° 25.02’ E
J7	*Anchiphimedia dorsalis*	Adélie Land	CEAMARC	16A/ 467	66° 20.30’ S	140° 01.75’ E
J8	*Anchiphimedia dorsalis*	Adélie Land	CEAMARC	8/126	66° 33.86' S	142° 23.23’ E
N18	*Anchiphimedia dorsalis*	Eastern Weddell Sea	ANT-XXIV/2	48	70° 23.94’ S	08° 19.14’ W
N19	*Anchiphimedia dorsalis*	Eastern Weddell Sea	ANT-XXIV/2	48	70° 23.94’ S	08° 19.14’ W
P9	*Anchiphimedia dorsalis*	Elephant Island	ANT-XXIII/8	609-6	61° 08.58' S	54° 31.86' W
A14	*Echiniphimedia echinata*	King George Island	Dirk Schories KGI Exp. 2011	20110204-02	62° 13.28’ S	58° 53.21’ W
A15	*Echiniphimedia echinata*	King George Island	Dirk Schories KGI Exp. 2011	20110204-02	62° 13.28’ S	58° 53.21’ W
ANT9	*Echiniphimedia echinata*	Bransfield Strait East	ANT-XXIX/3	197-5	62° 44.73‘ S	57° 26.79‘ W
J14	*Echiniphimedia echinata*	Adélie Land	CEAMARC	11/424	66° 33.71’ S	141° 15.71’ E
O5	*Echiniphimedia echinata*	Larsen A	ANT-XXVII/3	228-4	64° 55.58’ S	60° 33.37’ W
O6	*Echiniphimedia echinata*	Weddell, Erebus and Terror Gulf	ANT-XXIX/3	162-7	63° 58.78‘ S	56° 46.24‘ W
P22	*Echiniphimedia echinata*	Bransfield Strait, Nord of Joinville	ANT-XXIX/3	116-4	62° 33.79‘ S	56° 27.16‘ W
ANT28	*Echiniphimedia* aff. *echinata*	Drake Passage East	ANT-XXIX/3	246-3	62° 00.23‘ S	60° 03.81‘ W
Ex151	*Echiniphimedia* aff. *echinata*	Eastern Weddell Sea	ANT-XXVII/3	286-1	70° 50.64’ S	10° 36.11’ W
J13	*Echiniphimedia* aff. *echinata*	Adélie Land	CEAMARC	9/117	66° 32.08’ S	141° 58.96’ E
P23	*Echiniphimedia* aff. *echinata*	Bransfield Strait central	ANT-XXIX/3	217-6	62° 53.45‘ S	58° 13.06‘ W

P31	*Echiniphimedia* aff. *echinata*	Bransfield Strait, Nord of Joinville Island	ANT-XXIX/3	116-9	62° 33.79‘ S	56° 27.81‘ W
O3	*Echiniphimedia barnardi*	Eastern Weddell Sea	ANT-XXIV/2	48	70° 23.94’ S	08° 19.14’ W
O4	*Echiniphimedia barnardi*	Eastern Weddell Sea	ANT-XXIV/2	48	70° 23.94’ S	08° 19.14’ W
ANT8	*Echiniphimedia gabrielae*	Bransfield Strait East	ANT-XXIX/3	193-8	62° 43.73‘ S	57° 29.04‘ W
ANT1	*Echiniphimedia hodgsoni*	Bransfield Strait central	ANT-XXIX/3	199-4	62° 57.22‘ S	58° 14.60‘ W
ANT2	*Echiniphimedia hodgsoni*	Bransfield Strait East	ANT-XXIX/3	197-5	62° 44.73‘ S	57° 26.79‘ W
ANT25	*Echiniphimedia hodgsoni*	Bransfield Strait West	ANT-XXIX/3	224-3	63° 00.53‘ S	58° 35.67‘ W
C41	*Echiniphimedia hodgsoni*	Ross Sea	TAN0802	46	74° 44.20’ S	167° 03.67’ E
C42	*Echiniphimedia hodgsoni*	Ross Sea	TAN0802	100	76° 12.12’ S	176° 14.88’ E
J20	*Echiniphimedia hodgsoni*	Adélie Land	REVOLTA I	REVO 002	66° 39.80' S	139° 59.40' E
J9	*Echiniphimedia hodgsoni*	Adélie Land	CEAMARC	34/288	66° 19.28’ S	144° 18.53’ E
N13	*Echiniphimedia hodgsoni*	Eastern Weddell Sea	ANT-XXIV/2	48	70° 23.94’ S	08° 19.14’ W
N14	*Echiniphimedia hodgsoni*	Eastern Weddell Sea	ANT-XXIV/2	48	70° 23.94’ S	08° 19.14’ W
N15	*Echiniphimedia hodgsoni*	Weddell, Erebus and Terror gulf	ANT-XXIX/3	162-7	63° 58.78‘ S	56° 46.24‘ W
N16	*Echiniphimedia hodgsoni*	Larsen A	ANT-XXVII/3	231-3	64° 54.79’ S	60° 30.80’ W
O40	*Echiniphimedia hodgsoni*	Elephant Island	ANT-XXIII/8	654-6	61° 22.80’S	56° 03.84’ W
P25	*Echiniphimedia hodgsoni*	Dundee Island	ANT-XXIX/3	164-4	63° 37.28‘ S	56° 09.11‘ W
P16	*Echiniphimedia imparidentata*	Adélie Land	REVOLTA II	REVO 048/REVO 220	66° 38.00' S	140° 01.40' E
P17	*Echiniphimedia imparidentata*	Adélie Land	REVOLTA II	REVO 048/REVO 220	66° 38.00' S	140° 01.40' E
ANT10	*Echiniphimedia scotti*	Tip Peninsula, south of Dundee Island	ANT-XXIX/3	185-4	63° 51.53‘ S	55° 40.74‘ W
N12	*Echiniphimedia scotti*	Eastern Weddell Sea	ANT-XXI/2	276	71° 06.44’ S	11° 27.76’ W
ANT27	*Echiniphimedia waegelei*	Bransfield Strait central	ANT-XXIX/3	217-6	62° 53.45‘ S	58° 13.06‘ W
ANT6	*Echiniphimedia waegelei*	Bransfield Strait central	ANT-XXIX/3	199-4	62° 57.22‘ S	58° 14.60‘ W
ANT7	*Echiniphimedia waegelei*	Bransfield Strait East	ANT-XXIX/3	193-9	62° 43.50‘ S	57° 27.92‘ W

C12	*Echiniphimedia waegelei*	Ross Sea	TAN0802	100	76° 12.12' S	176° 14.88' E
C13	*Echiniphimedia waegelei*	Ross Sea	TAN0402	126	71° 18.55’ S	170° 27.02’ E
H10	*Echiniphimedia waegelei*	Adélie Land	CEAMARC	12/431	66° 33.59’ S	140° 47.83’ W
H9	*Echiniphimedia waegelei*	Adélie Land	CEAMARC	12/431	66° 33.59’ S	140° 47.83’ E
J19	*Echiniphimedia waegelei*	Adélie Land	CEAMARC	32/400	66° 32.08’ S	141° 58.96’ E
A7	*Gnathiphimedia barnardi*	Bouvet Island	ANT-XXVII/3	312-3	54° 30.14' S	03° 13.50' E
A8	*Gnathiphimedia barnardi*	Bouvet Island	ANT-XXVII/3	312-3	54° 30.14’ S	03° 13.50’ E
O18	*Gnathiphimedia barnardi*	Bouvet Island	ANT-XXVII/3	312-3	54° 30.14’ S	03° 13.50’ E
O21	*Gnathiphimedia barnardi*	Bouvet Island	ANT-XXVII/3	312-3	54° 30.14’ S	03° 13.50’ E
C4	*Gnathiphimedia mandibularis*	Ross Sea	TAN0802	31	74° 35.43’ S	170° 16.54’ E
C5	*Gnathiphimedia mandibularis*	Ross Sea	TAN0802	84	76° 36.14’ S	176° 48.12’ E
C6	*Gnathiphimedia mandibularis*	Ross Sea	TAN0402	108	71° 16.31’ S	170° 35.98’ E
J6	*Gnathiphimedia mandibularis*	Adélie Land	CEAMARC	9/117	66° 32.09’ S	141° 58.96’ E
ANT16	*Gnathiphimedia sexdentata*	Tip Peninsula, south of Dundee Island	ANT-XXIX/3	185-4	63° 51.53‘ S	55° 40.74‘ W
ANT29	*Gnathiphimedia sexdentata*	Bransfield Strait West	ANT-XXIX/3	227-2	62° 55.83‘ S	58° 41.09‘ W
C27	*Gnathiphimedia sexdentata*	Ross Sea	TAN0802	100	76° 12.12’ S	176° 14.88’ E
J4	*Gnathiphimedia sexdentata*	Adélie Land	CEAMARC	11/429	66° 33.82’ S	141° 15.34’ E
O14	*Gnathiphimedia sexdentata*	South Orkney Island	JR 144	PB-EBS-4-5	60° 49.18’ S	46° 29.06’ W
O15	*Gnathiphimedia sexdentata*	Bransfield Strait, Joinville Nord	ANT-XXIX/3	116-6	62° 33.80' S	56° 23.86' W
O16	*Gnathiphimedia sexdentata*	Larsen B	ANT-XXVII/3	248-2	65° 57.51’ S	60° 28.15’ W
O17	*Gnathiphimedia sexdentata*	Larsen B	ANT-XXVII/3	248-2	65° 57.51’ S	60° 28.15’ W
O24	*Gnathiphimedia sexdentata*	Larsen B	ANT-XXVII/3	248-2	65° 57.51’ S	60° 28.15’ W
P32	*Gnathiphimedia sexdentata*	Adélie Land	REVOLTA IV	REVO 047/ REVO 804	66° 37.99’ S	139° 54.89’ E
P33	*Gnathiphimedia sexdentata*	Adélie Land	REVOLTA IV	REVO 008/REVO 785	66° 40.16’ S	139° 51.46’ E
ANT20	*Gnathiphimedia watlingi*	Tip Peninsula, south of Dundee	ANT-XXIX/3	185-4	63° 51.53‘ S	55° 40.74‘ W

		Island				
O1	*Iphimedia imparilabia*	South of Falkland Islands	ANT-XXVII/3	208-5	54° 32.81’ S	56° 10.00’ W
N21	*Iphimediella bransfieldi*	Eastern Weddell Sea	ANT-XXI/2	132	70° 56.42’ S	10° 31.61’ W
P20	*Iphimediella bransfieldi*	Adélie Land	CEAMARC	20/490	66° 00.98’ S	140° 00.03’ E
A2	*Iphimediella cyclogena*	Larsen A	ANT-XXVII/3	228-4	64° 55.58' S	60° 33.37' W
ANT30	*Iphimediella cyclogena*	Tip Peninsula, south of Dundee Island	ANT-XXIX/3	185-3	63° 51.34‘ S	55° 41.11‘ W
ANT5	*Iphimediella cyclogena*	Bransfield Strait East	ANT-XXIX/3	197-5	62° 44.73‘ S	57° 26.79‘ W
C18	*Iphimediella cyclogena*	Ross Sea	TAN0402	186	71° 30.72’ S	171° 25.51’ E
C19	*Iphimediella cyclogena*	Ross Sea	TAN0402	94	71° 31.80’ S	170°06.66’ E
C35	*Iphimediella cyclogena*	Ross Sea	TAN0402	108	71° 16.31’ S	170° 35.98’ E
C36	*Iphimediella cyclogena*	Ross Sea	TAN0402	108	71° 16.31’ S	170° 35.98’ E
N22	*Iphimediella cyclogena*	Larsen C	ANT-XXVII/3	239-3	66° 11.89’ S	60° 09.75’ W
N23	*Iphimediella cyclogena*	Eastern Weddell Sea	ANT-XXVII/3	265-2	70° 47.34’ S	10° 40.39’ W
O33	*Iphimediella cyclogena*	Larsen B	ANT-XXVII/3	248-2	65° 57.51’ S	60° 28.15’ W
O9	*Iphimediella cyclogena*	Eastern Weddell Sea	ANT-XXIV/2	48	70° 23.94’ S	08° 19.14’ W
P14	*Iphimediella cyclogena*	Bransfield Strait, Nord of Joinville	ANT-XXIX/3	116-9	62° 33.79‘ S	56° 27.81‘ W
C24	*Iphimediella georgei*	Ross Sea	TAN0802	157	72° 01.41’ S	173° 10.82’ E
C26	*Iphimediella georgei*	Ross Sea	TAN0402	152	71° 59.68’ S	172° 08.05’ E
J12	*Iphimediella* aff. *georgei*	Adélie Land	CEAMARC	66/324	65° 45.94’ S	142° 55.17’ E
ANT13	*Iphimediella margueritei*	Bransfield Strait East	ANT-XXIX/3	197-6	62° 45.05‘ S	57° 26.68‘ W
J15	*Iphimediella margueritei*	Adélie Land	CEAMARC	11/424	66° 33.71’ S	141° 15.71’ E
O38	*Iphimediella margueritei*	King George Island	CHILI	20110208-10	62° 13.28’ S	58° 53.21’ W
P5	*Iphimediella margueritei*	Elephant Island	ANT-XXIII/8	654-6	61° 22.80' S	56° 03.84' W
C15	*Iphimediella microdentata*	Ross Sea	TAN0802	100	76° 12.12’ S	176° 14.88’ E
C16	*Iphimediella microdentata*	Ross Sea	TAN0802	81	76° 35.64’ S	176° 49.68’ E

H13	*Iphimediella microdentata*	Adélie Land	CEAMARC	13 A/465	66° 08.89’ S	140° 38.99’ W
H14	*Iphimediella microdentata*	Adélie Land	CEAMARC	28/163	66° 00.15’ S	142° 57.12’ W
J5	*Iphimediella microdentata*	Adélie Land	CEAMARC	14/460	66° 19.98’ S	140° 39.13’ E
O7	*Iphimediella microdentata*	Eastern Weddell Sea	ANT-XXVII/3	275-3	70° 56.01’ S	10° 29.28’ W
O8	*Iphimediella microdentata*	Eastern Weddell Sea	ANT-XXVII/3	281-1	70° 48.93’ S	10° 32.69’ W
O13	*Iphimediella acuticoxa*	Bouvet Island	ANT-XXVII/3	312-3	54° 30.14’ S	03° 13.50’ E
ANT18	*Iphimediella paracuticoxa*	Bransfield Strait East	ANT-XXIX/3	197-6	62° 45.05‘ S	57° 26.68‘ W
O12	*Iphimediella paracuticoxa*	Elephant Island	JR144	E1-EBS-4	61° 20.76’ S	55° 12.14’ W
ANT3	*Iphimediella rigida*	Bransfield Strait central	ANT-XXIX/3	199-4	62° 57.22‘ S	58° 14.60‘ W
ANT4	*Iphimediella rigida*	Bransfield Strait East	ANT-XXIX/3	193-8	62° 43.73‘ S	57° 29.04‘ W
C21	*Iphimediella rigida*	Ross Sea	TAN0802	31	74° 35.43’ S	170° 16.54’ E
C22	*Iphimediella rigida*	Ross Sea	TAN0802	17	73° 07.47’ S	174° 19.23’ E
N17	*Iphimediella rigida*	Weddell, Erebus and Terror gulf	ANT-XXIX/3	162-7	63° 58.78‘ S	56° 46.24‘ W
O10	*Iphimediella rigida*	Dundee Island	ANT-XXIX/3	164-4	63° 37.28‘ S	56° 09.11‘ W
O11	*Iphimediella rigida*	Dundee Island	ANT-XXIX/3	164-4	63° 37.28‘ S	56° 09.11‘ W
P3	*Iphimediella rigida*	Eastern Weddell SeaN20	ANT-XXIII/8	603-8	70° 30.99' S	08° 48.08' W
P15	*Iphimediella rigida*	Bransfield Strait, Nord of Joinville	ANT-XXIX/3	116-4	62° 33.79‘ S	56° 27.16‘ W
H17	*Iphimediella ruffoi*	Adélie Land	CEAMARC	11/429	66° 33.82’ S	141° 15.34’ W
H18	*Iphimediella ruffoi*	Adélie Land	REVOLTA III	REVO 032/ REVO 509	66° 39.30' S	140° 01.60' E
ANT15	*Iphimediella* aff. *ruffoi*	Bransfield Strait, Nord of Joinville	ANT-XXIX/3	116-9	62° 33.79‘ S	56° 27.81‘ W
N20	*Iphimediella* aff. *ruffoi*	Eastern Weddell Sea	ANT-XXIV/2	48	70° 23.94’ S	08° 19.14’ W
O2	*Iphimediella serrata*	Eastern Weddell Sea	ANT-XXVII/3	275-3	70° 56.01’ S	10° 29.28’ W
P8	*Iphimediella serrata*	Joinville Island	ANT-XXIII/8	689-5	62° 27.20' S	55° 25.93' W
P26	*Iphimediella* sp. nov. 1	Eastern Weddell Sea	ANT-XXIV/2	48	70° 23.94' S	08° 19.14' W
Q20	*Iphimediella* sp. nov. 1	Eastern Weddell Sea	ANT-XXIV/2	17 11	70° 05.13' S	03° 23.50' W
Q21	*Iphimediella* sp. nov. 1	Eastern Weddell Sea	ANT-XXIV/2	17 11	70° 05.13' S	03° 23.50' W
P29	*Iphimediella* sp. nov. 2	Eastern Weddell Sea	ANT-XXIV/2	48	70° 23.94' S	08° 19.14' W
N24	*Iphimediella* sp. nov. 3	Eastern Weddell Sea	ANT-XXIV/2	48	70° 23.94’ S	08° 19.14’ W
P28	*Iphimediella* sp. nov. 3	Eastern Weddell Sea	ANT-XXIV/2	48	70° 23.94' S	08° 19.14' W

C44	*Labriphimedia pulchridentata*	Macquarie Ridge	TAN0802	93	55° 21.20’ S	158° 26.21’ E
P18	*Labriphimedia* aff. *pulchridentata*	Adélie Land	CEAMARC	86/518	65° 28.85’ S	139° 24.18’ E
P19	*Labriphimedia* aff. *pulchridentata*	Adélie Land	CEAMARC	86/518	65° 28.85’ S	139° 24.18’ E
ANT11	*Maxilliphimedia longipes*	Bransfield Strait central	ANT-XXIX/3	204-2	62° 56.07‘ S	57° 58.14‘ W
ANT12	*Maxilliphimedia longipes*	Bransfield Strait East	ANT-XXIX/3	197-5	62° 44.73‘ S	57° 26.79‘ W
C7	*Maxilliphimedia longipes*	Ross Sea	TAN0802	17	73° 07.47’ S	174° 19.23’ E
C8	*Maxilliphimedia longipes*	Ross Sea	TAN0802	94	71° 31.79’ S	170° 06.65’ E
J1	*Maxilliphimedia longipes*	Adélie Land	CEAMARC	54/393	65° 54.74’ S	143° 58.01’ E
J2	*Maxilliphimedia longipes*	Adélie Land	CEAMARC	79/544	65° 42.41’ S	140° 35.84’ E
O34	*Maxilliphimedia longipes*	South Shetland Islands	ANT-XXIII/8	680-5	62° 23.37’ S	61° 25.58’ W
P7	*Maxilliphimedia longipes*	Elephant Island	ANT-XXIII/8	605-5	61° 20.27' S	55° 30.92' W
O19	*Parapanoploea longirostris*	Eastern Weddell Sea	ANT-XXVII/3	308-1	70° 51.30’ S	10° 35.35’ W
O22	*Parapanoploea longirostris*	Eastern Weddell Sea	ANT-XXIV/2	48	70° 23.94’ S	08° 19.14’ W
O23	*Parapanoploea longirostris*	Eastern Weddell Sea	ANT-XXIV/2	48	70° 23.94’ S	08° 19.14’ W
O35	*Pariphimedia integricauda*	King George Island	Dirk Schories KGI Exp. 2011	20110205-12	62° 12.09’ S	58° 57.61’ W
O36	*Pariphimedia integricauda*	King George Island	Dirk Schories KGI Exp. 2011	20110201-30	62° 12.09’ S	58° 57.61’ W
J17	*Stegopanoploea joubini*	Adélie Land	REVOLTA III	REVO 449	66° 38.00' S	140° 42.00' E
J18	*Stegopanoploea joubini*	Adélie Land	CEAMARC	11/424	66° 33.71’ S	141° 15.71’ E
O28	*Stegopanoploea joubini*	Eastern Weddell Sea	ANT-XXIV/2	48	70° 23.94’ S	08° 19.14’ W
O29	*Stegopanoploea joubini*	Eastern Weddell Sea	ANT-XXIV/2	48	70° 23.94’ S	08° 19.14’ W
O30	*Stegopanoploea joubini*	Larsen B	ANT-XXVII/3	248-2	65° 57.51’ S	60° 28.15’ W
ANT22	*Stegopanoploea* aff. *joubini*	Tip Peninsula, south of Dundee Island	ANT-XXIX/3	185-4	63° 51.53‘ S	55° 40.74‘ W
ANT17	*Stegopanoploea* aff. *joubini*	Dundee Island	ANT-XXIX/3	164-4	63° 37.28‘ S	56° 09.11‘ W
O39	*Stegopanoploea* aff. *joubini*	King George Island	Dirk Schories KGI Exp. 2011	20110128-18	62° 12.58’ S	58° 55.55’ W
P1	*Stegopanoploea* aff. *joubini*	Joinville Island	ANT-XXIII/8	689-5	62° 27.20’ S	55° 25.93’ W
Q16	*Iphimedia* cf. *beeslayae*	Vanuatu	SANTO	EP34	15° 33.24’ S	167° 12.90’ E
Q18	*Iphimedia* cf. *damawan*	Vanuatu	SANTO	EP39	15° 33.56’ S	167° 16.46’ E
Q1	*Iphimedia gibba*	South Africa, Roman Rock, False	NA	NA	34° 10.51’ S	18° 27.36’ E

		Bay				
Q10	*Iphimedia nexa*	France, Saint Lunaire	NA	NA	48° 38.55’ N	02° 06.60’ W
Q8	*Iphimedia nexa*	France, Saint Enogat	NA	NA	48° 38.43’ N	02 °04.28’ W
Q9	*Iphimedia* aff. *nexa*	France, Saint Lunaire	NA	NA	48° 38.55’ N	02° 06.60’ W
Q3	*Iphimedia obesa*	Norway, Grindøya	J. Ruud	730-02	69° 38.23' N	18° 52.81' E
Q4	*Iphimedia obesa*	Norway, Grindøya	J. Ruud	734-02	69° 52.04’ N	18° 52.82’ E
Q5	*Iphimedia obesa*	Norway, Kvalsund	J. Ruud	734-02	69° 52.04’ N	18° 52.82’ E
Q6	*Iphimedia obesa*	Norway, Kvalsund	J. Ruud	734-02	69° 52.04’ N	18° 52.82’ E
Q7	*Iphimedia* aff. *obesa*	Italy, Giglio	NA	V1.2001	NA	NA
PLEUSTIDAE (outgroup)						
O20	*Austropleustes* sp.	Shag Rocks	ANT-XXVII/3	211-6	53° 23.94' S	42° 40.10' W

Table 1. Sampling details for the sequenced iphimediid specimens including expedition name, station, location and geographical coordinates. “NA” (not available) indicates unobtainable data.

The H3 fragment was amplified using the primers HisH3f and HisH3r (Corrigan et al., 2014). PCR amplification settings were as in Corrigan et al. (2014) except for the annealing temperature set to 48 °C.

The PCR products were visualized under blue light on 1.2 % agarose gel stained with SYBR Safe (ThermoFisher Scientific, Waltham, MA, USA), with a comigrating 200-bp ladder molecular-weight marker to confirm their correct amplification. Prior to sequencing, PCR products were purified using Exonuclease I (20 U μl^{-1}) and FastAP Thermosensitive alkaline phosphatase (1 U μl^{-1}) (ThermoFisher Scientific, Waltham, MA, USA), following the manufacturer's protocol. Forward and reverse strands were sequenced with fluorescent-labeled dideoxynucleotide terminators (BigDye v.3.1; Applied Biosystems, Foster City, CA, USA) following the protocol of Sanger et al. (1977) and using an automated ABI 3130xl DNA analyzer (Applied Biosystems, Foster City, CA, USA). Both fragments were sequenced using the PCR primers.

PHYLOGENETIC ANALYSES

Sequence chromatograms were checked, and forward and reverse sequence fragments were assembled using Codoncode Aligner v.3.7.1. (CodonCode Corporation, available from http://www.codoncode.com/aligner/). All sequences have been deposited in GenBank (Table 1).

28S sequences were aligned with MAFFT v.7 (Katoh and Standley, 2013) (available from http://mafft.cbrc.jp/alignment/server/), using the structural alignment strategy Q-INS-i under default settings. As some regions of the 28S sequences were too divergent to be confidently aligned, the software program Aliscore v.2.0. (Misof and Misof, 2009) was used to identify poorly aligned regions for removal with Alicut v.2.3, prior to further analysis. CLUSTALW was used to align the COI and H3 sequences in MEGA6 (Tamura et al., 2013). In order to prevent inclusion of pseudogenes in the analyses, amino acid translations of the both fragments were checked for stop codons.

Preliminary phylogenetic trees were first inferred using Bayesian Inference (BI) on the individual gene datasets, in order to check for congruence between gene trees. Two different datasets were then constructed by concatenation with SequenceMatrix (Vaidya et al., 2011): (1) a combined 28S and H3 sequences dataset, referred to as the "nuclear dataset" and (2) a combined 28S, H3 and COI dataset with a more limited taxon sampling — as fewer COI sequences were obtained than nuclear sequences — referred to as the "total evidence dataset". BI and Maximum Likelihood (MI) were used to reconstruct phylogenetic relationships.

The best-fit models of DNA substitution were selected using the Bayesian Information Criterion (BIC) on the total evidence dataset partitioned by gene and by codon position (for COI and H3) in PartitionFinder (Lanfear et al., 2012).

BI trees were reconstructed using MrBayes v.3.2 (Ronquist and Huelsenbeck, 2003) on the CIPRES portal (Miller et al., 2010). BI analysis of all datasets included two runs of 10^7 generations. Trees were sampled every 1000 generations using four Markov chains, and default heating values. Convergence was assessed by the standard deviation of split-frequencies (< 0.01) and by examining the trace plots of log-likelihood scores in Tracer 1.6 (Rambaut and Drummond, 2005). The first 10 % trees were discarded as burn-in, while the remaining trees were used to construct a 50 % majority rule consensus tree and estimate the posterior probabilities (PP). Nodes with posterior probabilities (PP) ≥ 0.95 were considered as significantly supported.

ML trees of concatenated datasets were estimated using GARLI v.2.0 (Zwickl, 2006) on the CIPRES portal (Miller et al., 2010). For each dataset, 10 separate ML searches were run independently from different stepwise-reconstructed trees. The best scoring tree across runs was considered for further analyses. Confidence levels of branches were estimated by 1000 bootstrap replicates. Nodes with bootstrap values (BV) ≥ 70 were considered as well-supported.

DELIMITING PUTATIVE SPECIES

METHODOLOGY

Cryptic and pseudocryptic species are common within Antarctic Amphipoda (Baird et al., 2011; Havermans et al., 2011; Verheye, 2011; Verheye et al., *in Press*). A reliable delimitation of species within Iphimediidae would require additional data and is out of the scope of this paper. As unrecognized intraspecific variation may bias the results of divergence time and diversification rate analyses (Ho et al., 2008), we aimed to delimit a minimal number of putative species for further analyses. A potential failure to recognize cryptic species is less problematic than oversplitting, as it can be accounted for by testing the effect of different levels of incomplete taxon sampling on the results.

The following approach was used to define putative species. Specimens were first identified by morphology using the handbook of Coleman (2007). Whenever characters did not comply with existing species descriptions, specimens were tentatively interpreted as new species, and labelled as "sp. nov." or "aff" (referring to the morphologically most similar nominal species). Based on the COI and 28S trees and genetic distances, the putative species status of clades was evaluated using three

different species delimitation methods (see below). However, the results suggested that the 28S gene evolves too slowly relative to the rate of speciation: 28S-based species delimitation methods lumped together morphologically well-defined and generally accepted species. We therefore did not rely on the 28S-based species delimitation results, but rather used the nuclear data to ensure that COI clades were also monophyletic in the 28S gene tree, i.e. to investigate the possibility of introgression or incomplete lineage sorting (Funk and Omland, 2003). Supported COI clades were considered as putative species when (1) all species delimitation methods or at least the most conservative one (in case of incongruence) identify this clade as a putative species and (2) specimens of this clade form a supported 28S clade and/or (3) the specimens of this clade are morphologically undistinguishable.

TREE-BASED SPECIES DELIMITATION

We used two different tree-based species delimitation methods. Firstly, we used the Bayesian implementation of the Poisson Tree Processes model (bPTP) (Zhang et al., 2013). This method estimates the mean expected number of substitutions per site between two branching events, using the branch length information of a phylogeny. It implements two independent classes of Poisson processes (for intra- and interspecific branching events). The assumption is that the number of substitutions between species is significantly higher than the number of substitutions within species, resulting in two different branch length classes. For each possible species delimitation, the Poisson processes are fitted to the two branch length classes. In the Bayesian implementation, a Markov Chain Monte Carlo (MCMC) sampler is used to produce PP of these species delimitations. PP ≥ 0.95 was considered as a significant support for the species. The analyses were conducted on the web server for bPTP (available at http://species.h-its.org/ptp/) using the BI topology, with 500,000 generations, thinning set to 100 and burnin at 10 %.

Secondly, we used the General Mixed Yule Coalescent (GMYC) model (Fujisawa and Barraclough, 2013; Pons et al., 2006). This method models speciation via a pure birth process and within-species branching events as neutral coalescent processes. It identifies the transition points between inter- and intraspecies branching rates on a time-calibrated ultrametric tree by maximizing the likelihood score of the model. All lineages leading from the root to the transition point are then considered as different species. We used an ultrametric tree reconstructed with BEAST v.2.4, required to run the GMYC algorithm. Identical sequences (haplotypes) were pruned to a single copy before implementation, because zero-length terminal branches hamper the likelihood estimation (Fujisawa and Barraclough, 2013; Monaghan et al., 2009). The phylogenetic analysis was performed under a relaxed lognormal clock set to an evolutionary rate of 1.0 (i.e. no attempt to estimate divergence

time) and a speciation Yule Tree Model, using a random starting tree. Analyses were run for 1 x 10^8 MCMC generations, sampled every 1000th generations, and the first 10 % of the samples were discarded as burn-in. Tracer v1.6 (Rambaut and Drummond, 2005) was used to check for minimum effective sample size (ESS) of 200 and visually inspect stationarity and convergence by plotting likelihood values. The resulting trees were summarized into a target maximum clade credibility tree using TreeAnnotator v1.8.0. The GMYC analysis was carried out in R v3.0.1 using the Splits (Ezard et al., 2009) and Ape (Paradis et al., 2004) packages under the single-threshold method and excluding the outgroup (Fujisawa and Barraclough, 2013). The AIC-based support values for the species clusters were calculated, in order to account for delineation uncertainty (Powell, 2012).

DISTANCE-BASED SPECIES DELIMITATION

The Automatic Barcode Gap Discovery (ABGD) method aims to identify the "barcode gap" which separates intraspecific and interspecific genetic distances, even when the two distributions overlap. The pairwise genetic distances are first ranked from smallest to largest. A local slope function is computed for a given window size to detect peaks of slope values, the significantly highest peak being the barcoding gap. A Primary Partition is defined based on this barcoding gap. The procedure is then recursively repeated on each group of the Primary Partition to obtain Secondary Partitions until no further gaps can be detected (Puillandre et al., 2012). The analysis was performed on the ABGD webserver at http://wwwabi.snv.jussieu.fr/public/abgd. Tamura-Nei distances were computed with MEGA6 (Tamura et al., 2013). The latter model was the best-fit for the COI dataset among the models available in MEGA, according to the results of the model selection analysis with JmodelTest v.0.1.1. As the genus *Echiniphimedia* was lumped together as one candidate species when ABGD was applied on the whole dataset, this genus was analyzed separately from the remaining iphimediid taxa. The X (proxy for the minimum gap width) was set to 1.0, as above these values, only one group was recovered in each case. The remaining parameters were set to default (Pmin = 0.001, Pmax = 0.100, Steps = 10, Number of bins = 20). In order to limit oversplitting, the putative species detected using the largest P value (maximal prior intraspecific distance) were considered. ABGD was not performed on the 28S dataset, as each potential species was represented by one or very few haplotypes and ABGD performs poorly when the number of sequences per species is too small (Puillandre et al., 2012).

ESTIMATION OF DIVERGENCE TIMES

As intraspecific variation may lead to the overestimation of divergence times (Ho et al., 2008), the time-calibrated reconstruction was based on a reduced multimarker dataset. One individual per

putative Antarctic species was retained. For the non-Antarctic specimens, one individual per morphospecies was selected.

BEAST2 (Bouckaert et al., 2014) on the CIPRES portal (Miller et al., 2010) was used to estimate divergence times under a Bayesian approach. A Bayesian Model Averaging method was implemented in BEAST2 with the bModelTest package (Bouckaert and Drummond, 2015) in order to estimate a phylogeny averaged over site models, and not to rely on a likelihood-based method to determine the site model. During the Bayesian analysis, MCMC proposals switch between substitution models and estimate the posterior support for gamma-distributed rate heterogeneity, proportion of invariable sites and unequal base frequencies.

We simultaneously inferred the posterior distribution of trees and estimated divergence times assuming a relaxed molecular clock, allowing substitution rates to vary among branches. Both uncorrelated lognormal (UCLN) and exponential (UCED) models of rate change were implemented. In order to assess the pertinence of a relaxed estimation, the coefficients of variation of the clock rates were checked in Tracer v.1.6 (Rambaut et al., 2014). The coefficient of variation is the standard deviation of the clock rate distribution divided by its mean, and is used to assess the clock-likeness of the data. Values closer to zero indicate that the data are more clock-like. Therefore, values < 0.1 are generally considered low enough to justify the use of a strict molecular clock (Drummond and Bouckaert, 2015). To identify the best relaxed clock model, the marginal likelihoods of the competing models were estimated and summarized via the path-sampling method (Lartillot and Philippe, 2006), implemented in the MODEL_SELECTION package in BEAST2. Both Yule and Birth-Death speciation processes were used as tree priors in combination with the UCLN clock model, and a path-sampling method was again used to select for the best model. All the path-sampling analyses were run for 100 steps of 2 x 10^6 generations each. The log Bayes Factors were calculated as follows: $\log_e BF(M_0, M_1) = \log_e P(X|M_0) - \log_e P(X|M_1)$ where $\log_e P(X|M_i)$ is the marginal $\log_e$-likelihood estimate for the model Mi. The strength of support for a given model was based on the interpretation of BF suggested by (Kass and Raftery, 1995). Values of 2 $\log_e$ BF between 0 and 3 were interpreted as no evidence for the alternative model M_1 over the null model M_0. When 2 $\log_e$ BF values were above 3, the alternative model M1 was supported over the null model M0, and values over 20 were interpreted as a very strong support for the alternative model.

Peracarid crustaceans do not fossilize well (e.g. Briggs and Kear, 1994; Briggs and Wilby, 1996; Taylor, 1972), so that their fossil record is very incomplete and therefore of limited utility for divergence time dating. The only known aquatic amphipod fossils are from freshwater taxa from the families Niphargidae (Coleman and Myers, 2000; Coleman and Ruffo, 2002; Jażdżewski and

Kupryjanowicz, 2010), Crangonyctidae (Coleman, 2006; Jażdżewski et al., 2014), Gammaridae (Coleman, 2004; Coleman and Myers, 2000; Coleman, 2006; Jażdżewski et al., 2014; Jażdżewski and Kulicka, 2000a, 2002) and Corophiidae (Weitschat et al., 2002) preserved in Baltic amber. These families are phylogenetically distant from *Epimeria* (Verheye et al., 2016b). Moreover, because of their poor preservation, the phylogenetic position of these fossils can generally not be determined accurately (e.g. Coleman, 2004; Coleman and Myers, 2000; Coleman and Ruffo, 2002; Jażdżewski and Kulicka, 2000b). As no unambiguous biogeographic event could be used to calibrate the tree either, we used priors on rates of COI, 28S and H3 evolution based on rates inferred in previous studies. The prior rate of COI was set as a normal distribution with a mean of 0.018 substitutions/site/My and a standard deviation (SD) of 0.0043. This rate was previously inferred for *Pontogammarus* amphipods (Nahavandi et al., 2013). A normal prior with a mean of 0.003 substitutions/site/My and SD of 0.0007 was used for the 28S gene, a rate inferred for the *Gammarus balcanicus* complex (Mamos et al., 2016). Rates of H3 evolution are, to our knowledge, not available for amphipods. Therefore, the prior rate of H3 was set as a normal distribution with a mean of 0.0019 and SD of 0.0004, a rate inferred from freshwater crabs (Klaus et al., 2010).

The MCMC analyses were run for 300 million generations, with a sampling frequency of 30 000 generations. The first 1000 trees were discarded as burn-in. Convergence was assessed by trace plots in Tracer v.1.6. and the effective sampling size for all parameters was more than 200 (Rambaut et al., 2014). The maximum clade credibility tree showing the mean nodal height was generated by TreeAnnotator v1.8.0. The final analyses were also run without data to ensure the prior settings will not bias the results.

RATE AND MODE OF DIVERSIFICATION

The reduced dataset (one individual per species) was also used for diversification rates analyses because intraspecific polymorphisms can induce a false increase in diversification rates in the most recent history. All the diversification rate analyses were based on the Antarctic iphimediid clade. Incomplete taxonomic sampling can result in spurious declines in diversification rates over time (Pybus and Harvey, 2000). The analyzed Antarctic iphimediid clade comprises 79.5 % of the known (putative) species. However, as a conservative approach was used for the delimitation of putative species, (pseudo)cryptic species might have been overlooked. Moreover, Antarctic regions not sampled for this study (e.g. the Amundsen and Bellingshausen Seas) likely host additional undescribed species. Therefore, the methods used herein to examine diversification patterns tested the effect of different levels of taxonomic sampling on the results: sampling fractions of 79.5 %, 50.0 % and 10.0 % were considered.

A mean semilogarithmic lineage through time (LTT) plot was constructed using the R package Ape to visualize the temporal pattern of lineage diversification. A straight line is expected under constant diversification rate. A departure from this straight line in the distant past may indicate a diversification rate change: (1) a concave plot either indicates a decelerating diversification rate or incomplete taxon sampling, (2) a convex plot may indicate accelerating diversification or a non-zero background extinction rate. The command sim.bd.taxa.age from the R package TreeSim (Stadler, 2011) was used to simulate 100 trees under Pure Birth (PB) and Birth-Death (BD), with speciation and extinction rates estimated with bd.shift.optim from the R package TreePar (Stadler, 2011). Both functions were used assuming a sampling fraction of 79.5, 50.0 and 10.0 %. The LTT plot of the empirical phylogeny was compared to the 95 % confidence intervals of the expected pattern under PB and BD, to detect eventual deviations from the null hypothesis of constant rates.

In order to account for incomplete sampling in methods that do not include a correction for missing species, we used the CorSim function from the R package TreeSim to simulate the missing splits on the empirical phylogeny (Cusimano et al., 2012). Missing speciation events were simulated 200 times under the assumption that evolution followed a constant BD model. Simulated branching times are added to the empirical branching times to obtain 200 completed (semi-empirical) datasets. Speciation and extinction rates used for the simulation were those estimated under BD with the bd.shifts.optim function of the TreePar package. Missing taxa were assumed to be located randomly across the tree, as both deep and shallower nodes are likely missing from the phylogeny. Three semi-empirical datasets were obtained for 79.5 %, 50.0 % and 10.0 % sampling fractions. Besides, 200 trees with the number of taxa corresponding to the total number of species in the genus (assuming the three sampling fractions tested) were simulated separately under constant speciation and extinction. This simulation was performed using the function sim.bd.taxa.age of the R package TreeSim (Stadler, 2011). This completely simulated dataset is referred to as a null distribution dataset.

The γ statistic was calculated on the semi-empirical datasets, using the GamStat function of the R package LASER (Rabosky, 2006a). This statistic tests for departure from a constant-rate PB model. Negative γ values indicate a prevalence of nodes closer to the root than expected under a PB process, therefore suggesting a decreasing rate of diversification through time. Positive γ values indicate either an increasing rate or non-zero extinction rate (Pybus and Harvey, 2000).

We compared the fit of the branching times to various models of lineage accumulation, using the Akaike Information Criterion (AIC), for the three semi-empirical datasets. AIC is calculated as $-2\iota + 2k$, where ι is the log-likelihood value and k is the number of free parameters of the model (Burnham

and Anderson, 2002). All model-fitting analyses were conducted with the R packages LASER (Rabosky, 2006a) and TreePar (Stadler, 2011). The constant-rate models included PB (constant speciation rate λ and no extinction) and BD (constant speciation rate λ and extinction rate μ). Two density-dependent models were included, which assume that the diversification rate decreases as the lineage population reaches some threshold density. The density-dependent linear (DDL) model assumes that λ decreases linearly and there is no extinction. The density-dependent exponential (DDX) model assumes that λ decreases exponentially and there is no extinction (Rabosky and Lovette, 2008). λ and μ may also change through time in response to external factors. Therefore, we included Yule-n-rate (Rabosky, 2006b) and Birth-Death-shift (BDS) (Stadler, 2011) models in order to test whether and when discrete shifts in diversification rate occurred during the clade's history. In between shifts, these models simplify to respectively the constant-rate PB or BD. The use of the Cusimano *et al*.'s (2012) method to account for incomplete taxon sampling was shown to result in a small proportion of outlier λ estimates under Yule-n-rate and BDS models (unrealistically high λ values). As the mean and standard deviation of parameter estimates are strongly impacted by outliers (Leys et al., 2013), we reported the median and absolute deviation from the median (MAD) of the –Log Likelihood value, models' parameters and Akaike Information Criterion (AIC) scores, for each of the semi-empirical datasets. In order to compare the relative fit of the models, the 95 % confidence interval on the median of the AIC values was computed with the function ci.median of the R package "asbio". The difference in AIC (dAIC) between each model and the best-fitting model (with the lowest AIC) was computed. Minimal and maximal dAIC were calculated considering the AIC values comprised in the 95 % confidence intervals. The amount of statistical confidence for each model is represented by the Akaike weights (wAIC). For each semi-empirical datasets, we computed the deltaAICrc as the difference between the AIC scores of the best-fit rate-constant model and the best-fit rate-variable model. A t-test was performed to determine if the deltaAICrc from these semi-empirical datasets was significantly different than from the null distribution dataset. A Bonferroni correction is applied to account for multiple comparisons.

In order to test rate-variable models that allow for increasing or decreasing rates of speciation, extinctions and declining diversity, we also used the method of Morlon et al. (2011) implemented in the R package RPANDA. The fit of the following models was compared using the AIC: (1) Bcst: constant speciation rate, no extinction (PB); (2) Bvar: exponential variation of speciation rate, no extinction; (3) BvarDcst: exponential variation of speciation rate, constant extinction; (4) BcstDcst: constant speciation and extinction rates (BD); (5) BcstDvar: constant speciation and exponential variation in extinction rate; and (6) BvarDvar: exponential variation in both speciation and extinction rates. These models were tested assuming sampling fractions of 0.1, 0.5 and 0.795.

The BAMM 2.4.0 (Bayesian Analysis of Macroevolutionary Mixtures; Rabosky, 2014) software was used to explore eventual shifts in regimes across the branches of a phylogenetic tree, a regime being a constant or time-varying process of speciation and extinction. These heterogeneous mixtures of macroevolutionary rate regimes are sampled with reversible-jump MCMC. Priors were estimated using the setBAMMpriors command from the R package BAMMtools. MCMC chains were run for 10 million generations, and sampled every thousand generations. We checked for convergence of the MCMC chains and ESS (at least more than 200) using the R package coda (Plummer et al., 2005). The first 10 % of samples were discarded as burn-in. The R package BAMMtools (Rabosky et al., 2014) was then used to calculate the Bayes Factor and the 95 % credibility set for the shift configurations and to plot diversification rates through time (Rabosky, 2014). BAMM analyses were computed assuming different levels of taxon sampling: 10.0, 50.0 and 79.5 %.

RESULTS

DATA OVERVIEW

The concatenated matrices included 2035 bp for the nuclear dataset and 2619 bp for the total evidence dataset. The length of the aligned fragments, number of variable sites for each gene and best models of nucleotide substitution selected by PartitionFinder for each partition are indicated in Table 2.

Partition	Model	Length (bp)	Variable sites
28S	SYM + G	1679	567
COI_pos1	SYM + I + G		
COI_pos2	HKY + I + G	584	308
COI_pos3	GTR + I + G		
H3_pos1	HKY + I + G		
H3_pos2	JC + I	356	123
H3_pos3	GTR + G		

Table 2. Length of the sequenced fragments and number of variable sites, evolutionary model selected by PartitionFinder for the different partitions. The coding genes (COI and H3) are partitioned by codon position.

PHYLOGENETIC TREES

For each dataset, topological discrepancies between the three gene trees affected only unsupported nodes. Differences between the topologies of the two reconstruction methods (ML and BI) were also minimal and, in all cases, only affected unsupported nodes.

BI and ML analyses of the nuclear dataset supported the monophyly of Antarctic iphimediids (PP = 1.00; BV = 93). The monophyly of non-Antarctic iphimediids is supported by BI (PP = 0.98), but not by ML (BV = 66). The monophyly of the genera *Echiniphimedia, Stegopanoploea* and *Labriphimedia* is supported, whereas the genera *Iphimediella* and *Gnathiphimedia* are polyphyletic. The genus

Iphimedia also appears polyphyletic, as the only sampled Antarctic species is not part of the clade of non-Antarctic species. The monophyly of the remaining genera — *Pariphimedia, Anchiphimedia*, *Maxilliphimedia* and *Parapanoploea* — cannot be assessed, as they are represented by only one species (Fig. 1).

The monophyly of most morphospecies was supported, except for *Gnathiphimedia sexdentata* (Fig. 2).

SPECIES DELIMITATIONS

All the ESS values obtained from the BEAST analyses of the COI and 28S individual datasets were above 200. The topologies of the resulting ultrametric trees, used as input for the GMYC analyses, were the same as the topologies of the BI trees obtained with MrBayes, using these individual datasets.

The bPTP analysis of the COI Bayesian phylogeny gave a total of 57 putative species within the Antarctic iphimediid clade. The GMYC analysis of the COI ultrametric tree returned 54 ML entities ("species") (confidence interval 51–58). The log-likelihood ratio test suggested that this model was a better fit for the data than the single-species model (likelihood ratio = 23.9, $p = 6.4\ 10^{-6}$*). Both methods were mostly congruent regarding the delimited putative species and the incongruent delimitations were supported by PP (bPTP) < 0.7. The ABGD method was more conservative in the number of delimited species, which amounted to 40 (Fig. 2).

The bPTP analysis of the 28S Bayesian phylogeny returned a total of 20 putative species. Generally accepted described species were lumped together by this species delimitation method, e.g. the genus *Echiniphimedia* (Fig. 2). The GMYC analysis of the 28S ultrametric tree returned 16 ML entities, with a very large confidence interval of 1–26. However, the log-likelihood ratio test suggested that this model was not a significantly better fit for the data than the single-species model (likelihood ratio = 3.48, $p = 0.13$).

Using the methodology described above, most morphospecies were identified as single putative species, except for *Echiniphimedia echinata* and *Gnathiphimedia sexdentata,* which were each split into two putative species. A total number of 35 putative species were defined (Fig. 2).

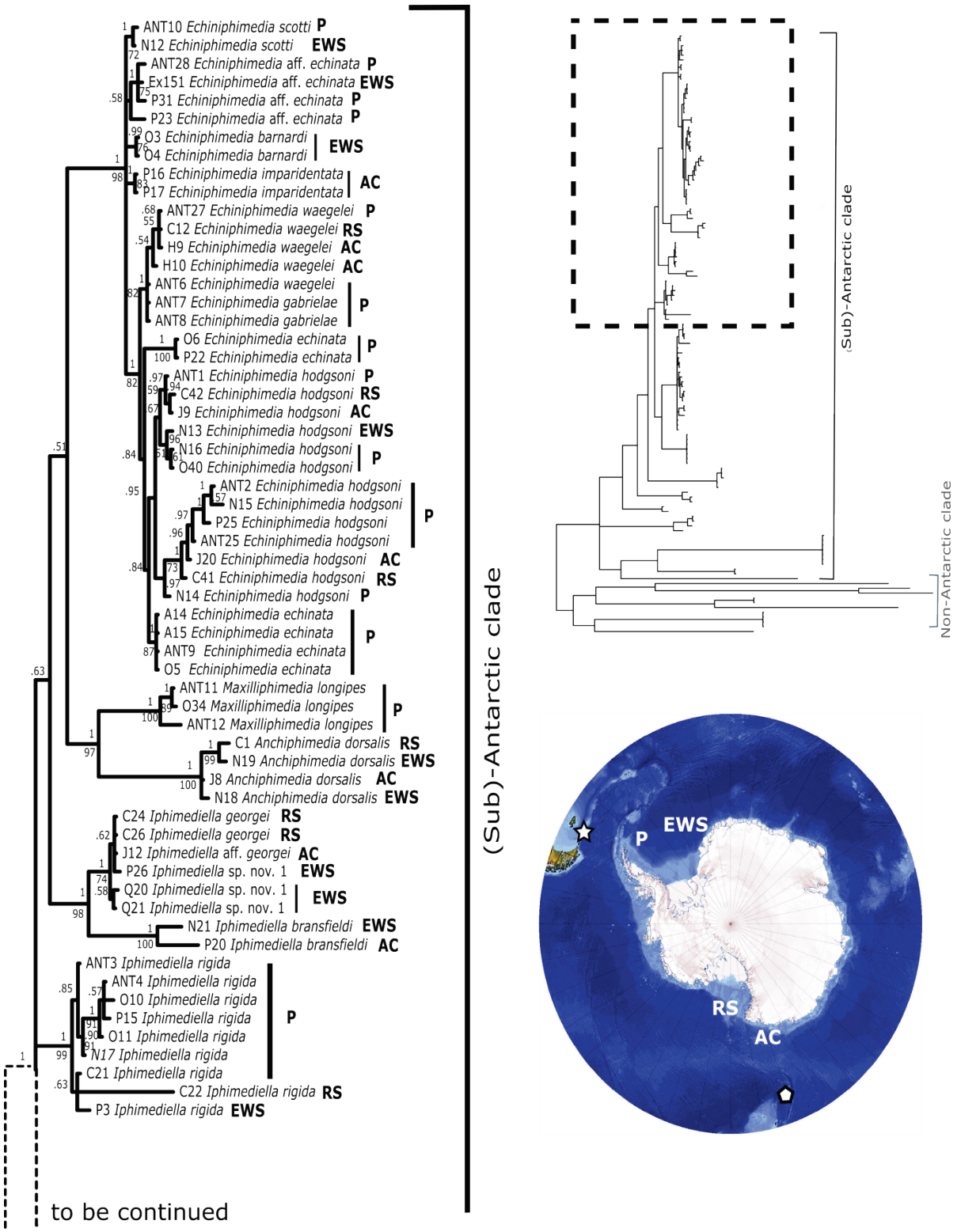

Figure 1. Phylogenetic tree obtained by Bayesian analysis of the concatenated 28S and H3 sequences. Bayesian PP and BV (1000 replicates) from the ML analysis are indicated besides the nodes of interest. Bootstrap values inferior to 50 are not indicated. Geographical origins of the specimens are indicated on the maps and besides the species names. Antarctica: P=Peninsula and Scotia Arc islands; EWS = Eastern Weddell Sea; B = Bouvet Island; RS = Ross Sea; AC = Adélie Coast. Sub-Antarctic region: ☆ = Falkand Islands; ⬠ = Macquarie Ridge. Non-Antarctic localities: SA = South Africa; V = Vanuatu; F = France; I = Italy; N = Norway.

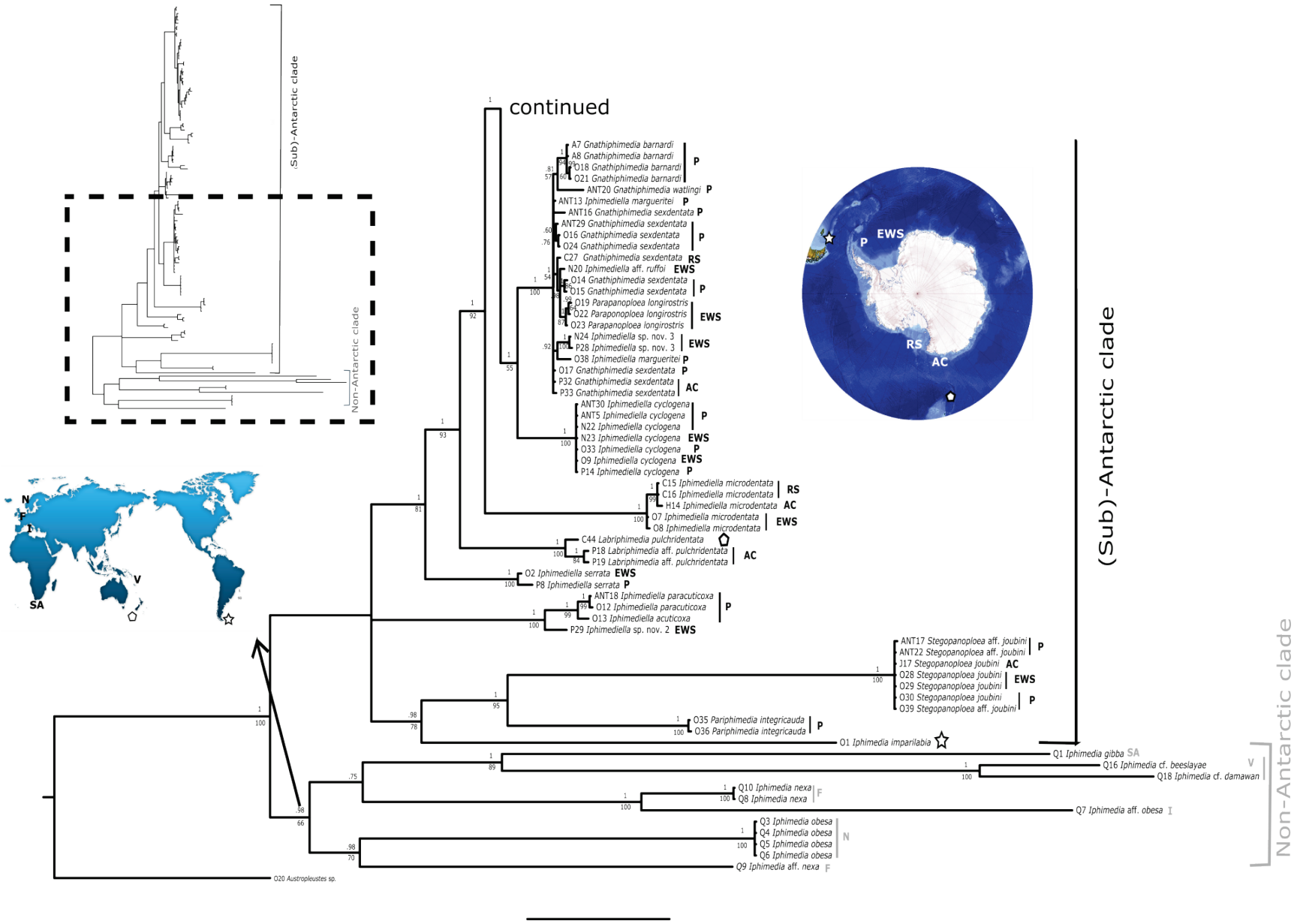
(Sub)-Antarctic clade
Non-Antarctic clade
continued
A7 Gnathiphimedia barnardi
A8 Gnathiphimedia barnardi
O18 Gnathiphimedia barnardi
O21 Gnathiphimedia barnardi
P
ANT20 Gnathiphimedia watlingi P
ANT13 Iphimediella margueritei P
ANT16 Gnathiphimedia sexdentata P
ANT29 Gnathiphimedia sexdentata
O16 Gnathiphimedia sexdentata
O24 Gnathiphimedia sexdentata
P
C27 Gnathiphimedia sexdentata RS
N20 Iphimediella aff. ruffoi EWS
O14 Gnathiphimedia sexdentata
O15 Gnathiphimedia sexdentata
P
O19 Parapanoploea longirostris
O22 Paraponoploea longirostris
O23 Parapanoploea longirostris
EWS
N24 Iphimediella sp. nov. 3
P28 Iphimediella sp. nov. 3
EWS
O38 Iphimediella margueritei P
O17 Gnathiphimedia sexdentata P
P32 Gnathiphimedia sexdentata
P33 Gnathiphimedia sexdentata
AC
ANT30 Iphimediella cyclogena
ANT5 Iphimediella cyclogena
N22 Iphimediella cyclogena
P
N23 Iphimediella cyclogena EWS
O33 Iphimediella cyclogena P
O9 Iphimediella cyclogena EWS
P14 Iphimediella cyclogena P
C15 Iphimediella microdentata
C16 Iphimediella microdentata
RS
H14 Iphimediella microdentata AC
O7 Iphimediella microdentata
O8 Iphimediella microdentata
EWS
C44 Labriphimedia pulchridentata
P18 Labriphimedia aff. pulchridentata
P19 Labriphimedia aff. pulchridentata
AC
O2 Iphimediella serrata EWS
P8 Iphimediella serrata P
ANT18 Iphimediella paracuticoxa
O12 Iphimediella paracuticoxa
P
O13 Iphimediella acuticoxa
P29 Iphimediella sp. nov. 2 EWS
ANT17 Stegopanoploea aff. joubini
ANT22 Stegopanoploea aff. joubini
P
J17 Stegopanoploea joubini AC
O28 Stegopanoploea joubini
O29 Stegopanoploea joubini
EWS
O30 Stegopanoploea joubini
O39 Stegopanoploea aff. joubini
P
O35 Paripimedia integricauda
O36 Paripimedia integricauda
P
O1 Iphimedia imparilabia
Q1 Iphimedia gibba SA
Q16 Iphimedia cf. beeslayae
Q18 Iphimedia cf. damawan
V
Q10 Iphimedia nexa
Q8 Iphimedia nexa
F
Q7 Iphimedia aff. obesa I
Q3 Iphimedia obesa
Q4 Iphimedia obesa
Q5 Iphimedia obesa
Q6 Iphimedia obesa
N
Q9 Iphimedia aff. nexa F
O20 Austropleustes sp.
P
EWS
RS
AC
N
V
SA

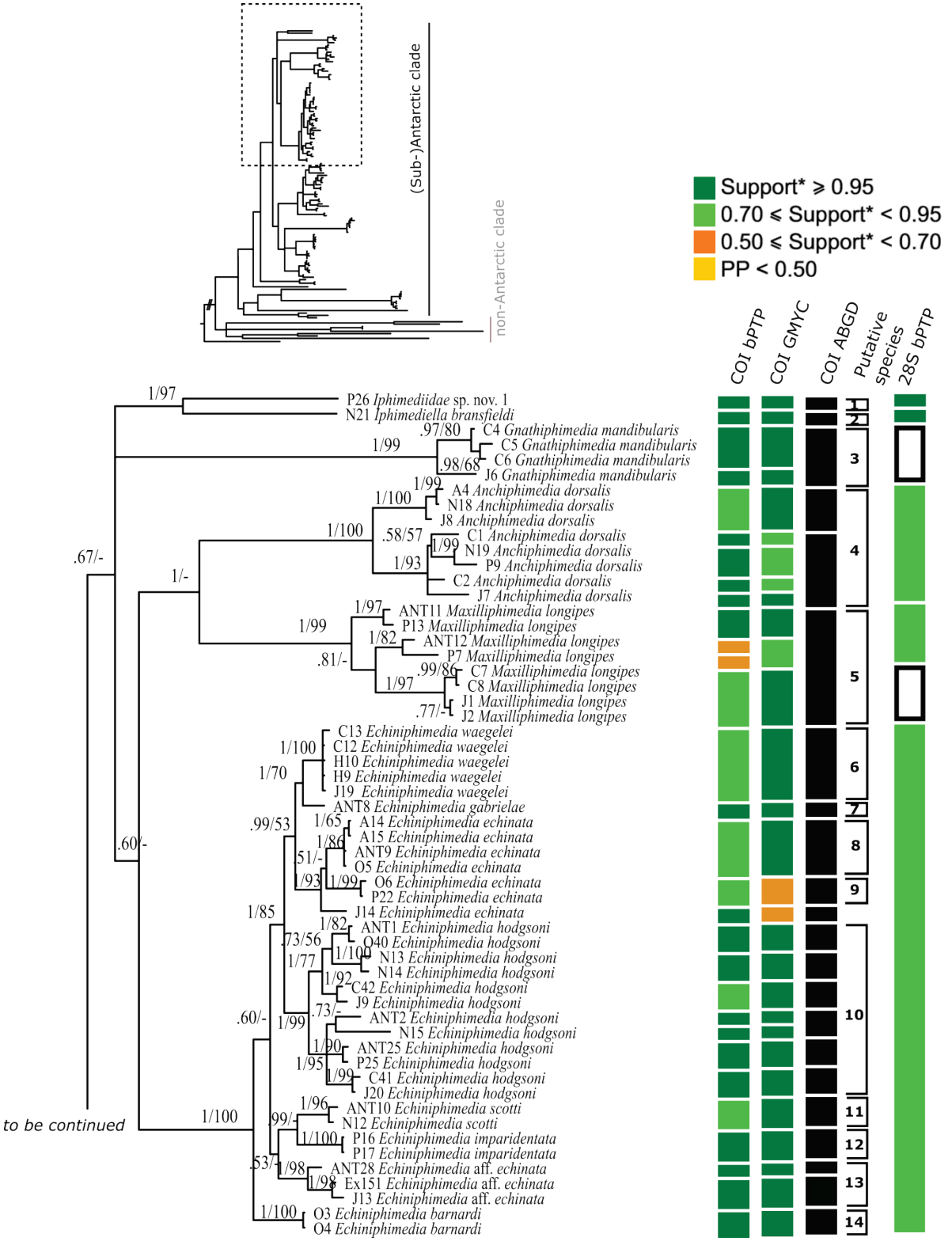

Figure 2. Phylogenetic tree obtained by Bayesian analysis of the concatenated COI, 28S and H3 sequences. Bayesian PP and BV (1000 replicates) from the ML analysis are indicated besides the nodes of interest. Bootstrap values inferior to 50 are not indicated. Species delimitation results of the DNA-based methods (bPTP, GMYC, ABGD) applied separately on COI and 28S (bPTP only) gene trees are indicated besides the concatenated tree. *Boxes are colored according to the posterior probability (bPTP) or the AIC-based GMYC support values (GMYC) of the inferred delimitation.

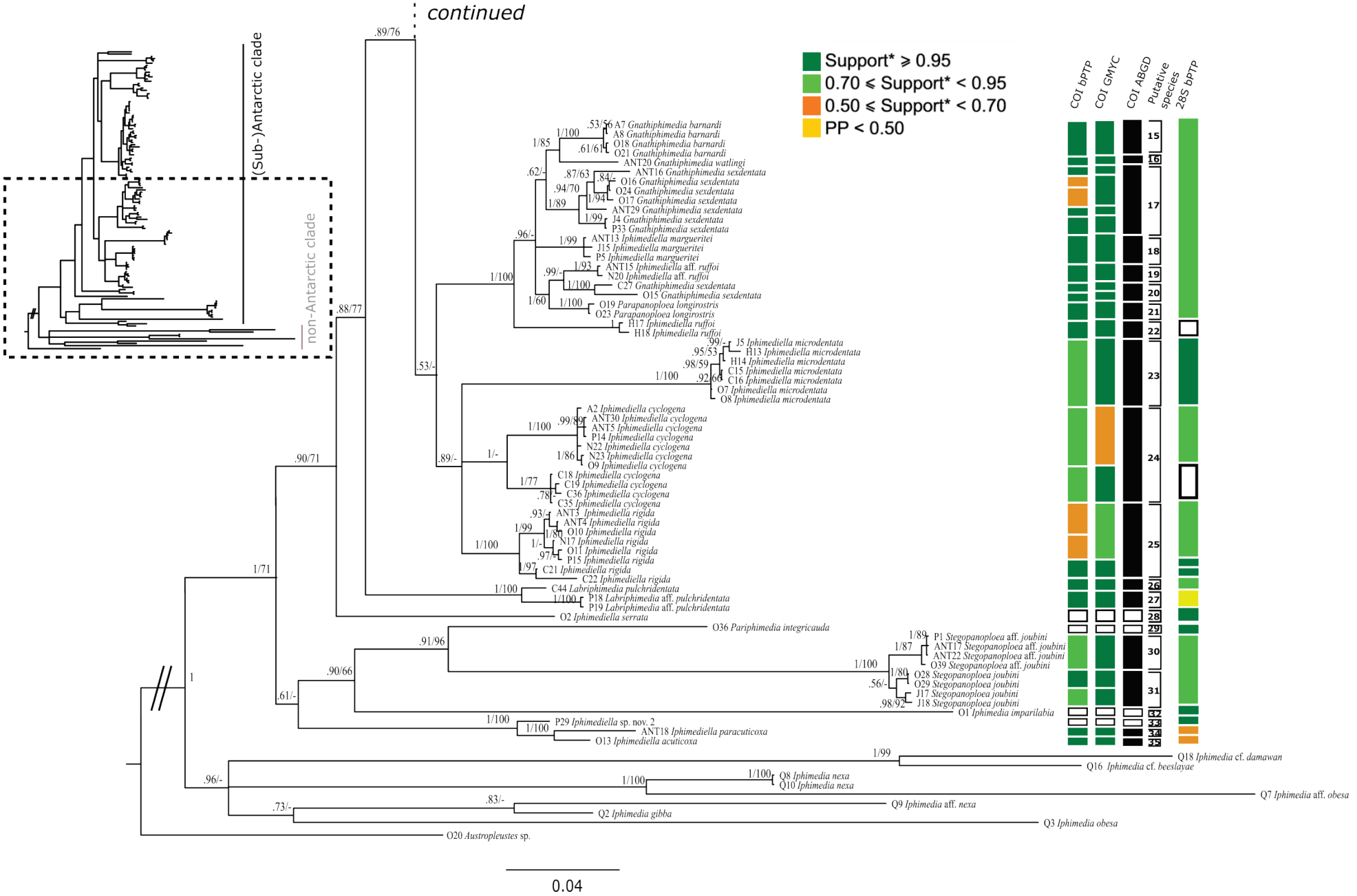
continued
(Sub-)Antarctic clade
non-Antarctic clade
Support* ⩾ 0.95
0.70 ⩽ Support* < 0.95
0.50 ⩽ Support* < 0.70
PP < 0.50
COI bPTP
COI GMYC
COI ABGD
Putative species
28S bPTP
A7 Gnathiphimedia barnardi
A8 Gnathiphimedia barnardi
O18 Gnathiphimedia barnardi
O21 Gnathiphimedia barnardi
ANT20 Gnathiphimedia watlingi
ANT16 Gnathiphimedia sexdentata
O16 Gnathiphimedia sexdentata
O24 Gnathiphimedia sexdentata
O17 Gnathiphimedia sexdentata
ANT29 Gnathiphimedia sexdentata
J4 Gnathiphimedia sexdentata
P33 Gnathiphimedia sexdentata
ANT13 Iphimediella margueritei
J15 Iphimediella margueritei
P5 Iphimediella margueritei
ANT15 Iphimediella aff. ruffoi
N20 Iphimediella aff. ruffoi
C27 Gnathiphimedia sexdentata
O15 Gnathiphimedia sexdentata
O19 Parapanoploea longirostris
O23 Parapanoploea longirostris
H17 Iphimediella ruffoi
H18 Iphimediella ruffoi
J5 Iphimediella microdentata
H13 Iphimediella microdentata
H14 Iphimediella microdentata
C15 Iphimediella microdentata
C16 Iphimediella microdentata
O7 Iphimediella microdentata
O8 Iphimediella microdentata
A2 Iphimediella cyclogena
ANT30 Iphimediella cyclogena
ANT5 Iphimediella cyclogena
P14 Iphimediella cyclogena
N22 Iphimediella cyclogena
N23 Iphimediella cyclogena
O9 Iphimediella cyclogena
C18 Iphimediella cyclogena
C19 Iphimediella cyclogena
C36 Iphimediella cyclogena
C35 Iphimediella cyclogena
ANT3 Iphimediella rigida
ANT4 Iphimediella rigida
O10 Iphimediella rigida
N17 Iphimediella rigida
O11 Iphimediella rigida
P15 Iphimediella rigida
C21 Iphimediella rigida
C22 Iphimediella rigida
C44 Labriphimedia pulchridentata
P18 Labriphimedia aff. pulchridentata
P19 Labriphimedia aff. pulchridentata
O2 Iphimediella serrata
O36 Pariphimedia integricauda
P1 Stegopanoploea aff. joubini
ANT17 Stegopanoploea aff. joubini
ANT22 Stegopanoploea aff. joubini
O39 Stegopanoploea aff. joubini
O28 Stegopanoploea joubini
O29 Stegopanoploea joubini
J17 Stegopanoploea joubini
J18 Stegopanoploea joubini
O1 Iphimedia imparilabia
P29 Iphimediella sp. nov. 2
ANT18 Iphimediella paracuticoxa
O13 Iphimediella acuticoxa
Q18 Iphimedia cf. damawan
Q16 Iphimedia cf. beeslayae
Q8 Iphimedia nexa
Q10 Iphimedia nexa
Q7 Iphimedia aff. obesa
Q9 Iphimedia aff. nexa
Q2 Iphimedia gibba
Q3 Iphimedia obesa
O20 Austropleustes sp.
0.04

DIVERGENCE TIMES

The coefficients of variation were much higher than 0.1 for the three genes (COI: 0.32, 28S: 1.23, H3: 0.75), indicating that the sequences analyzed did not evolve at a constant rate along the branches. Therefore, we proceeded to use a relaxed molecular clock. Results of the path-sampling analysis and calculation of the Bayes Factor are presented in Table 3. The UCLN relaxed clock was favoured over the UCED model. The BD tree model is indicated as a strongly better fit to our data than the Yule model (Table 3).

	MLE	2 lnBF
UCED	-26248.93	-
UCLN	-26235.98	12.95
Birth-Death	-26226.95	21.98
Yule	-26248.93	-

Table 3. Marginal likelihood estimation (MLE) values recovered by path-sampling (PS). Bayes Factors (2 lnBF) were estimated from the MLE to compare two relaxed clock models (UCED and UCLN) and two tree models (Yule and Birth-Death).

The BEAST analysis under a lognormal relaxed clock model and BD tree model recovered mean age of 44.1 Ma (95 % HPD: 58.7–30.9Ma) for the divergence between the Antarctic and non-Antarctic iphimediid clades. The MRCA of the Antarctic iphimediid clade was given a mean age of 35.1 Ma (95 % HPD: 46.4–25.2Ma). The MRCA of the non-Antarctic iphimediid clade was dated at 37.9 Ma (95 % HPD: 50.0–26.9 Ma) (Fig. 3).

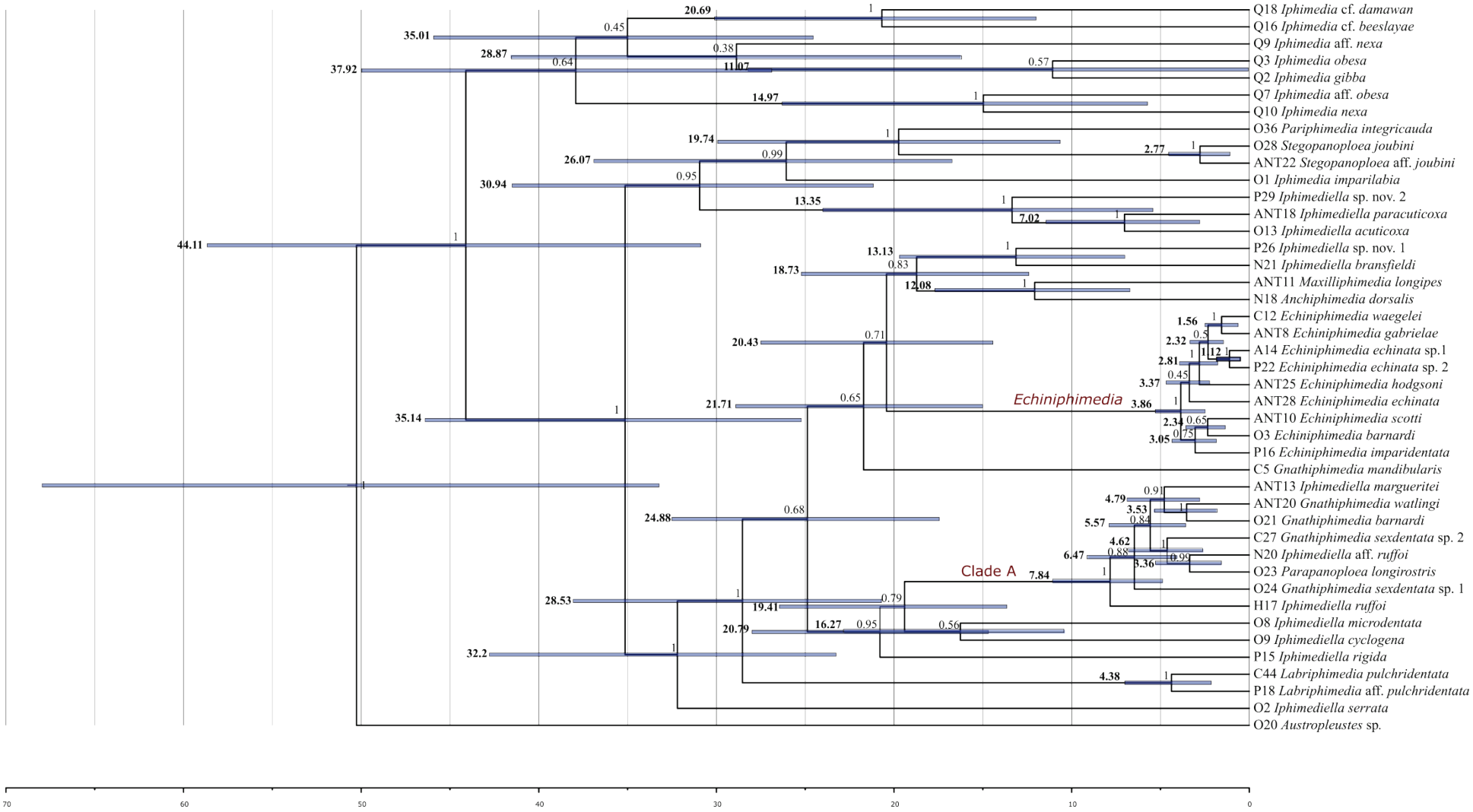

Figure 3. Maximum clade credibility chronophylogenetic tree from the BEAST analysis of the concatenated (COI, 28S, H3) dataset. The timescale is in millions of years. Blue bars on the tree indicate 95 % confidence intervals for estimated node ages. Mean node ages are indicated in front of the bars. Posterior probabilities are indicated above the nodes.

RATES OF DIVERSIFICATION

Based on the γ statistic, we found no evidence of a decelerating lineage accumulation rate towards present time in the origination pattern of the Antarctic iphimediid clade. When incomplete sampling is taken into account, assuming 79.5 or 50.0 % sampling fractions, the γ values are positive, but the null hypothesis of constant rate of speciation is not rejected ($p > 0.01$). Only when a sampling fraction of 10 % is assumed, the γ value is significantly positive ($p < 0.01$), indicating either an increasing rate of speciation, or non-zero extinction (Table 4).

Dataset	γ	p-value (2-tailed)
Semiemp 10.0 %	11.5 (0.77)	0*(0)
Semiemp 50.0 %	1.44 (0.6)	0.21 (0.2)
Semiemp 79.5 %	0.04 (0.44)	0.74 (0.19)
Empirical	-0.36	0.72

Table 4. Results of the CR test applied on the empirical and semi-empirical datasets.

No evident deviation from the null hypotheses of constant-rate models (BD or PB) is visible on the LTT plots, assuming 79.5 % and 50.0 % sampling fractions (Appendix S6). Assuming a sampling fraction of 10 %, the diversification pattern deviates from the null hypothesis of PB, but not of BD (Fig. 4).

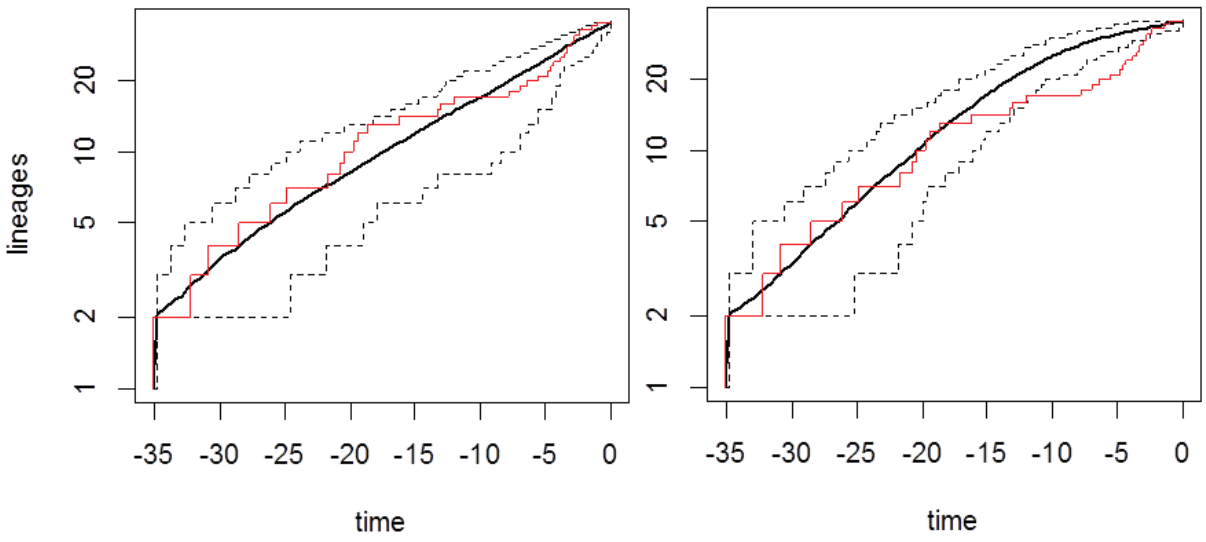

Figure 4. Lineage diversification through time plot of the Antarctic iphimediid clade, generated with the dated tree from the BEAST analysis (in red). Dashed lines represent the 95 % confidence interval of lineage diversification simulated 100 times under a BD (left; λ = 0.67 and μ = 0.60) and a PB (right; λ = 0.16) model and assuming a sampling fraction of 10 %.

The BDS analyses indicate Yule4rate as the best supported model of lineage diversification. This model implies a speciation rate decrease from λ = 0.12 to λ = 0.04 at 18.73 Ma, which increases to λ = 0.17 at 4.78 Ma and decreases again to λ = 0.02 at 2.31 Ma (Fig. 5). The estimated probability that Yule4rate is the best model for our data among the evaluated models (wAIC) is 52 % (Table 5). When incomplete sampling is taken into account, Yule4rate also has the lowest median AIC for each of the evaluated sampling fractions. Assuming a sampling fraction of 79.5 %, Yule4rate has a median wAIC of 37.1 %, while the median wAIC of Yule3rate is 26.8 %. The range of minimal to maximal dAIC values — calculated based on the 95 % confidence interval on the median AIC values — for the Yule3rate model does contain zero, indicating that it is equally fitting to Yule4rate. The result of the t-test showed that the deltaAICrc of the 79.5 % semi-empirical dataset was significantly different (α = 0.05) from that of the null distribution dataset (t = -2.68, df = 364.63, *p = 0.007**). Applying the Bonferroni correction for multiple comparisons, the difference remains significant (α = 0.016). The 95 % confidence interval on the rate shift times and speciation rates parameters for Yule3rate and Yule4rate are indicated on Table 5. Assuming a sampling fraction of 50 %, Yule4rate has a median wAIC of 50.8 % but is also considered as equally fitting to Yule3rate (median wAIC = 31.9 %). The result of the t-test showed that the deltaAICrc of the 50.0 % semi-empirical dataset was not significantly different from that of the null distribution dataset (t = -1.77, df = 236.85, *p = 0.08*). Assuming a sampling fraction of 10 %, the absolute deviation around the median (mad) is larger, and hence, multiple models are equally supported (BD, DDX, Yule3rate, Yule4rate, BD-1shift, BD-2shifts and BD-3shifts), i.e. their dAIC range contains zero (Appendix S7).

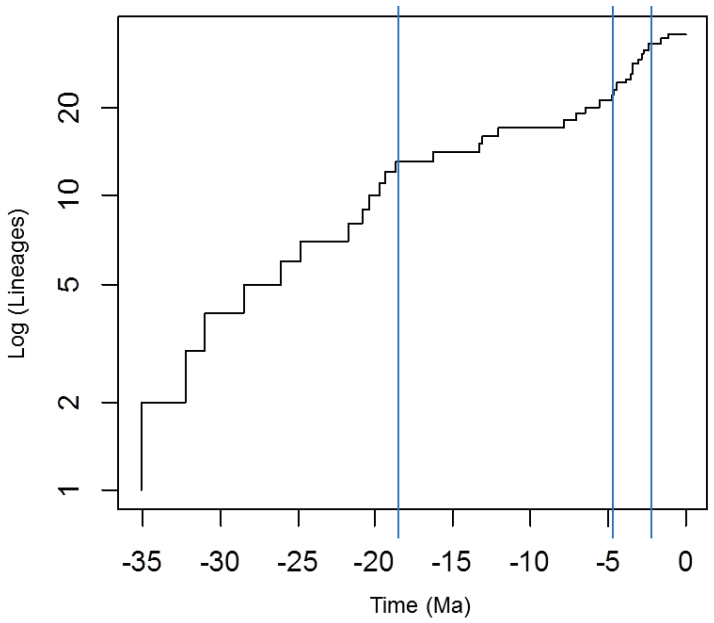

Figure 5. Rate shifts under the Yule4rate model represented on the lineage-through-time plot.

Dataset	Models	shift times	λ	AIC	dAIC	wAIC
Empirical	Yule4rate	18.73 4.78 2.31	0.12 0.04 0.17 0.02	60.90	0.00	0.52
Semi-emp 79.5 %	Yule4rate	18.73 [18.73–18.73] 4.93 [5.57–4.78] 2.32 [2.32–2.32]	0.12 [0.12–0.12] 0.05 [0.04–0.05] 0.16 [0.15–0.16] 0.04 [0.04–0.04]	51.43 [50.87–52.33]	0.00	0.37
	Yule3rate	4.81 [4.78–4.97] 2.32 [2.32–2.32]	0.08 [0.07–0.08] 0.17 [0.16–0.18] 0.04 [0.04–0.05]	52.08 [51.23–52.92]	0.65 (-1.10, 2.05)	0.27
Semi-emp 50.0 %	Yule4rate	12.09 [16.26–10.89] 4.79 [5.57–4.38] 2.32 [3.18–2.28]	0.10 [0.09–0.11] 0.14 [0.07–0.16] 0.34 [0.22–0.74] 0.11 [0.10–0.12]	-15.5 [-17.50–-14.25]	0.00	0.51
	Yule3rate	5.57 [4.90–6.47] 3.99 [3.34–4.78]	0.09 [0.09–0.10] 0.21 [0.17–0.29] 0.12 [0.11–0.13]	-14.57 [-16.46–-13.11]	0.93 (-2.21 ; 4.39)	0.32

Table 5. Parameter estimates and comparison of the fit of different lineage diversification models to the empirical dataset and two semi-empirical datasets, reconstructed assuming sampling fractions of 0.795 and 0.50. Results are shown for the best-scoring models. The shift times (Ma), speciation rates (λ), AIC score, dAIC (difference in AIC from the best-scoring model) and wAIC (Akaike weights) are indicated. The median of the latter parameters and AIC value are reported for each of the semi-empirical datasets, along with their 95 % confidence interval (between brackets). Minimal and maximal values for dAIC were calculated based on the AIC and the 95 % confidence intervals (between parentheses).

The evaluation of Morlon et al.'s (2011) models of lineage diversification with RPANDA yielded the following results. When a 0.795 sampling fraction was assumed, Bcst (PB) was the best fit among the evaluated models (wAIC = 0.49), followed by the two equally-probable models Bvar — implying decreasing speciation rate and no extinction — and BcstDcst (BD; both wAIC = 0.16). The Bcst model was also the best-fitting model when assuming a sampling fraction of 50 % (wAIC = 0.45), followed by BcstDcst (BD; wAIC = 0.23). For the 10 % sampling fraction, BcstDcst (wAIC = 0.43) was the best-fitting model, followed by the two equally-probable models BvarDcst — implying a decreasing speciation rate and a constant extinction rate — and BcstDvar — implying a constant speciation rate and increasing extinction rate (both wAIC = 0.24).

Table 6 shows the results for the best-scoring models only and Appendix S8 for all evaluated models.

Dataset	Model	AIC	dAIC	wAIC	λ	α	μ	β
Sampling 79.5 %	Bcst	241.90	0.00	0.49	0.080	-	-	-
	BcstDcst	244.13	2.23	0.16	0.084	-	0.008	-
	Bvar	244.12	2.22	0.16	0.077	0.004	-	-
Sampling 50 %	Bcst	242.79	0.00	0.45	0.098	-	-	-
	BcstDcst	244.13	1.34	0.23	0.135	-	0.058	-
Sampling 10 %	BcstDcst	244.13	0.00	0.43	0.674	-	0.598	-
	BvarDcst	245.29	1.16	0.24	0.865	0.006	0.868	-
	BcstDvar	245.33	1.20	0.24	0.872	-	0.873	-0.007

Table 6. Parameter estimates and comparison of the fit of Morlon et al.'s (2011) lineage diversification models with RPANDA. Results are shown for the best scoring model and the second best fit, whenever the wAIC of the best-scoring model was < 0.5. For each model, the Akaike Information criterion (AIC) was computed. The best-fitting model with the lowest AIC score is indicated in shaded grey. dAIC is the difference between the AIC score of the evaluated model and the AIC score of the best-fitting model. wAIC are the Akaike weights. λ is the speciation rate; α is the parameter controlling the exponential variation of the speciation rate with time; and β is the parameter controlling the exponential variation of the extinction rate with time.

For the 79.5 % sampling fractions, the 95 % credible set returned by BAMM comprises two shift configurations: the best configuration is a constantly decreasing diversification rate, i.e. no core shift (*p = 0.72*) and the other shows a diversification rate acceleration event in the Pliocene near the MRCA of the *Echiniphimedia* clade (*p = 0.25*) (Fig. 6A). The BF does not favour one of these two configuration models over the other (Table 7). The decelerating diversification rate is due to a decelerating speciation rate, while the extinction rate remains constant. The diversification rate shift at the base of the *Echiniphimedia* clade is the result of both increasing speciation and extinction rates (Appendix S9). The rate through time plot shows a decelerating diversification rate over time which increases from the Pliocene, around 4 Ma (Fig. 7A).

When the assumed sampling fraction is decreased to 50 %, the same two shift configurations are included in the 95 % credible shift set, but the posterior probability of the best one (no core shift) decreases (*p = 0.63*), while the posterior probability of the second best one (one core shift at the base of the *Echiniphimedia* clade) increases (*p = 0.37*) (Fig. 6B). The BF does not favour one of these two configuration models over the other (Table 7). The rate through time plot shows a higher diversification rate increase from the Pliocene, around 4 Ma (Fig. 7B).

The shift at the base of the *Echiniphimedia* clade is also present in 3 out of the 4 distinct shift configurations comprised in the 95 % credible shift set recovered when assuming a 10 % sampling

fraction. This core shift is present in the best configuration (*p = 0.55*), along with another diversification rate acceleration close to the MRCA of clade A (in the Late Miocene to Pliocene) and is also the only core shift in the second best configuration (*p = 0.23*; Fig. 6C). The BF favors the two-shifts configuration relative to the null hypothesis of no rate shift (BF = 12; Table 7). The rate through time plot shows a much higher diversification rate increase from the end of Miocene, around 7 Ma (Fig. 7C).

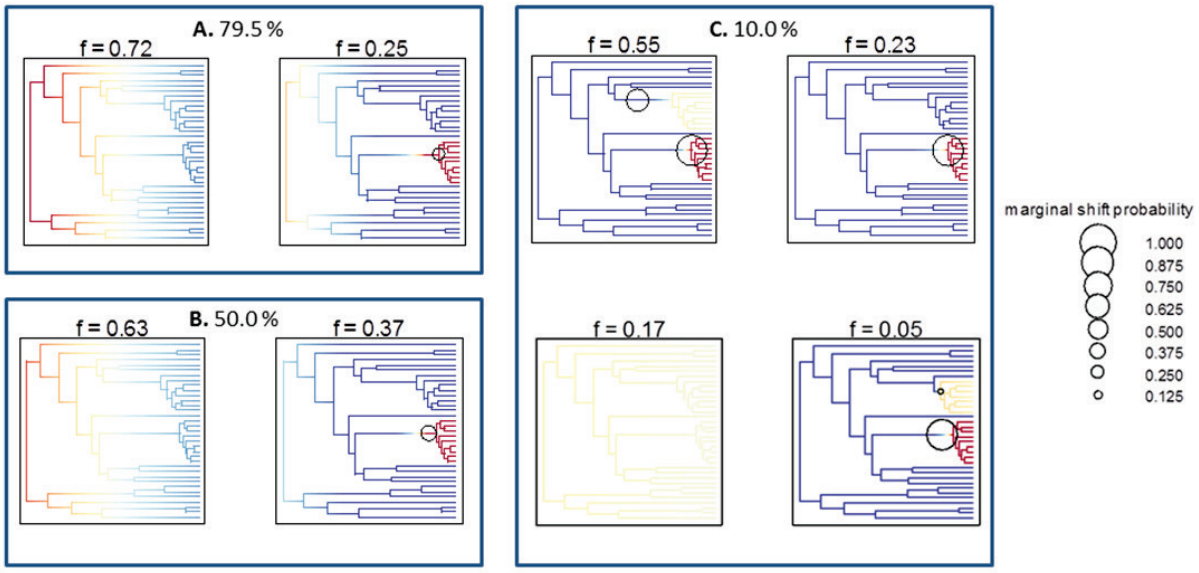

Figure 6. The 95 % credibility set of shift configurations generated by BAMM assuming A. 79.5 %, B. 50 % and C. 10 % taxon sampling fraction. Warm colors indicate high diversification rates, whereas cold colors indicate low diversification rates. Dots indicate a diversification rate shift and are sized according to the marginal probability of the shift. The sampling frequency of each diversification scheme is shown over each plot.

Sampling		1 shift	2 shifts	3 shifts
0 shift	10 %	2.41	11.89	6.60
	50 %	0.91	0.69	0.35
	79.5 %	0.71	0.43	0.21

Table 7. Matrix of pairwise Bayes Factors (BF), where the BF is the ratio of marginal likelihoods between two models, Mi and Mj. Numerator models are given as rows and denominator models as columns. BF > 3 is considered positive support for Mi, while > 20 is a strong support (Kass and Raftery, 1995).

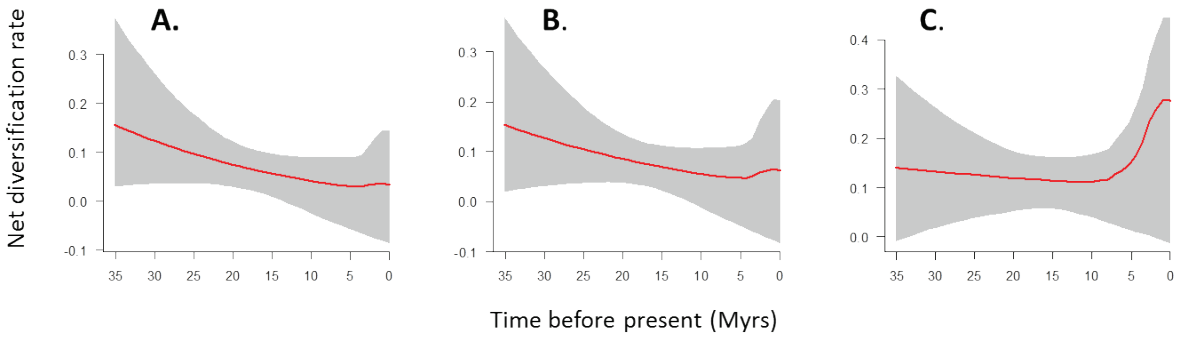

Figure 7. Diversification rate through time plots generated by BAMM assuming A. 79.5 %, B. 50 % and C. 10 % taxon sampling fraction. The shaded area is the 95 % confidence interval.

DISCUSSION

SYSTEMATICS OF IPHIMEDIIDAE

GENUS-LEVEL CLASSIFICATION

The monophyly of the genus *Iphimedia* has been questioned because of the high variability of its diagnostic characters (Watling and Holman, 1980). The present results show that *Iphimedia imparilabia* from the Southern Ocean does not form a clade with the non-Antarctic *Iphimedia.* The genera *Iphimediella* and *Gnathiphimedia* were previously shown to be paraphyletic (Lörz and Held, 2004). In our phylogenies, which include a higher taxon sampling within both genera, they appear polyphyletic (Fig. 1 and 2). Hitherto, the generic subdivision of Iphimediidae is based on the mouthpart morphology, which is highly diverse within the family (Coleman, 2007). For instance, the shape and dentation of the mandible incisor is used to distinguish *Iphimediella* from *Gnathiphimedia*. *Iphimediella* is characterized by an elongate and dentate incisor, orientated to cut in the transverse plane, whereas *Gnathiphimedia* has a broad and blunt incisor, to crush food in the frontal plane (Coleman, 1989a). The structure of the mandible was previously interpreted as a dietary adaptation (Watling, 1993), e.g. *Gnathiphimedia mandibularis* crushes morsels of bryozoans with its stout mandibles (Coleman, 1989a), whereas *Iphimediella cyclogena* uses its mandibles to cut soft holothurian tissues (Dauby et al., 2001b; Nyssen et al., 2002). The polyphyly of both genera shows that similar trophic morphologies evolved several times independently. Characters related to the feeding mode are likely to show convergent evolution, while species adapt to similar trophic niches, as has been shown before for other Antarctic amphipods (Havermans et al., 2011). These results therefore highlight the need for a phylogenetically-informed revision of the generic subdivision of Iphimediidae.

Species delimitation

Among the 35 putative species defined by the methods used here, 6 differ morphologically from any known species (*Iphimediella* sp. nov. 1, *I*. sp. nov. 2, *Stegopanoploea* aff. *joubini*, *Echiniphimedia* aff. *echinata*, *I.* aff. *ruffoi* and *Labriphimedia* aff. *pulchridentata*) and two described species are each split into two putative species (*Gnathiphimedia sexdentata* and *Echiniphimedia echinata*). However, the species diversity within the family is likely still underestimated by this conservative approach. Indeed, the DNA-based species delimitation methods used here recovered 40 (ABGD), 54 (GMYC) or 57 (bPTP) putative species (Fig. 2). These COI-based delimitation results are to be used in combination with additional data — e.g. the application of these delimitation methods on a more variable nuclear gene than 28S and a detailed morphological analysis of the specimens — in order to delimit species within Iphimediidae. “Hidden diversity” has similarly been revealed by molecular tools in a wide range of organisms (e.g. Allcock et al., 2011; Brasier et al., 2016; Grant et al., 2011; Janosik and Halanych, 2010; Linse et al., 2007; Thornhill et al., 2008; Wilson et al., 2007), among which amphipods are no exception (Baird et al., 2011; Havermans et al., 2011; Verheye et al., 2016a).

Historical biogeography of Iphimediidae

Origin of (sub-)Antarctic iphimediids

All sequenced iphimediid species from the Antarctic and sub-Antarctic regions (including the Falkand Islands) form a clade, whereas all sequenced non-Antarctic species — from Europe, South Africa and Vanuatu — form another clade. The divergence between these two clades occurred 44.11 [58.67; 30.88] Ma (Fig. 3). The first hypothesis aiming at determining the temporal and geographical origin of Antarctic iphimediids was presented by Lörz and Held (2004). Ages of between 71.7 and 34.4 Ma were inferred for the MRCA of eight Antarctic iphimediids, based on COI distances and rates estimated respectively for cirripeds (3.1 %/Myr) and for alpheid shrimps (2.4 %/Myr), and assuming a strict molecular clock. Applying a relaxed clock model on a combined dataset (COI, 28S and H3) and including a more extensive taxon sampling (35 Antarctic and sub-Antarctic species), we obtained a mean COI rate estimate of 2.0 %/Myr and an age of 35.14 [46.41; 25.22] Ma for the MRCA of the (sub-)Antarctic iphimediid clade (Fig. 3).

The time spanning the divergence of the (sub-)Antarctic iphimediid clade from the non-Antarctic clade to its initial diversification in the Antarctic region is a critical period in the Antarctic benthos’ evolutionary history. In the early Cenozoic, Antarctica, South America and Australia were connected in an area of cool temperate shallow seas, known as the Weddellian Province (Woodburne and

Zinsmeister, 1984; Zinsmeister, 1979, 1984). The cooling trend started across the early to middle Eocene boundary (ca. 48–49 Ma) and culminated by the onset of continental glaciations at the Eocene/Oligocene boundary (ca. 34 Ma). This period also corresponds to the onset of highly seasonal variations in light regime, temperatures and hence, primary food supply (Thomas and Gooday, 1996). These environmental changes had a marked impact on the Weddellian Province's fauna. The fossil record indicates a replacement of the cool-temperate Middle Eocene fauna by successively colder-adapted faunal assemblages (Aronson and Blake, 2001; Aronson et al., 2007, 2009; Boersma et al., 1987; Jadwiszczak, 2010; Keller et al., 1992; Stilwell and Zinsmeister, 1992). This time period also spans the final stages of Gondwana's breakup, ultimately leading to the physical isolation of Antarctica. The opening of the Drake Passage (between Antarctica and South America) and the Tasmanian Gateway (between Antarctica and Australia) are inferred as important vicariant events in the biogeographical history of Antarctic shelf benthic organisms (Göbbeler and Klussmann-Kolb, 2010; Lee et al., 2004; Matschiner et al., 2011; Near, 2004). It was inferred that a deep seaway between Australia and East Antarctica might have existed as early as 40 Ma. However, the deepening of the Tasmanian Gateway is usually dated in the interval 35–30 Ma (Lawver and Gahagan, 2003; Lawver et al., 2013; Lawver et al., 2014; Stickley et al., 2004). Similarly, the opening of the Drake Passage to deep-water is generally dated in the time period from 34 to 30 Ma (Lagabrielle et al., 2009; Latimer and Filippelli, 2002; Lawver and Gahagan, 2003; Livermore et al., 2005; Scher and Martin, 2004).

Because of the large confidence interval around the origin of the (sub-)Antarctic iphimediid clade, it cannot be inferred from these results if the clade originated in the late Gondwanan Weddelian province or directly following the geographical isolation of Antarctica (Fig. 3). The monophyly of (sub-)Antarctic iphimediids suggests that an isolating factor, whether geographical or environmental, would be at the origin of the clade. Tectonic vicariance and/or adaptation to harsh polar environmental conditions might have promoted the divergence of a late Gondwanan/early Antarctic iphimediid lineage.

Dispersal in/out of the Antarctic shelf

The occurrence of two species in both the high Antarctic region and the sub-Antarctic islands or Tierra del Fuego (*Pariphimedia normani* and *Iphimedia pacifica*, not sampled for this study) suggests that at least some iphimediid species are able to cross the APF and establish viable populations on the other side (Coleman, 2007). Moreover, the distribution of *Labriphimedia pulchridentata* includes Heard Island and the sub-Antarctic Macquarie ridge (Lörz, 2012). In our phylogeny, a sister species (*L*. aff. *pulchridentata*) was sampled on the Adélie Coast, and both species are nested within a high

Antarctic clade (Fig. 1), suggesting dispersal from the high Antarctic region to sub-Antarctic islands, after the geographical isolation of Antarctica (4.38 [7.01; 2.14] Ma) (Fig. 3). Some iphimediid species appear endemic to southern South America (Tierra del Fuego and/or the Falkland Islands), such as *Iphimedia imparilabia*, which is included in the (sub-)Antarctic clade on our phylogeny (Fig. 1). This species diverged from its sister clade 26.07 [36.9; 16.73] Ma and is nested within a high Antarctic clade. Because of this large confidence interval on its timing of origin, it cannot be determined if *I. imparilabia* arose by vicariance when the Drake Passage opened or following dispersal of Antarctic ancestors to the Falkland Islands (Fig. 3).

Dispersal of benthic organisms in/out of the Antarctic shelf can occur in two ways: (1) through the deep-sea and (2) by passive transport on a pelagic organism or floating substrate. Iphimediidae includes almost exclusively shelf species. Only *Gnathiphimedia mandibularis* (Coleman, 2007), *Echiniphimedia hodgsoni* (Verheye, unpublished data) and *Iphimediella* aff. *georgei* (present data) have been recorded on the slope, at ca. 2000 m depth. However, the Drake Passage has an average depth of 3400 m (Smith and Sandwell, 1997). The bathymetric distribution of iphimediid species worldwide suggests that this would be too deep for iphimediids to disperse in and/or out of the Antarctic shelf along the benthos. Iphimediids with a distributional range including the high Antarctic region and at least one low Antarctic or sub-Antarctic island (South Orkneys, South Georgia, South Sandwich, Heard and Kerguelen Islands) and/or the Magellanic region (including the Falkland Islands), usually (but not always) have lower recorded bathymetric ranges than exclusively high Antarctic species (although available records of bathymetric and geographical ranges are surely non exhaustive; Table 8). As macroalgae thrive at these shallow sublittoral depths, floating algal mats might be a means for long-distance dispersal of these iphimediid species. Adults or eggs of benthic organisms lacking a pelagic stage may disperse over long distances and sometimes across the APF by drifting on detached macroalgae, pumices or driftwood (Barnes et al., 2006; Helmuth et al., 1994; Leese et al., 2010; Nikula et al., 2010; Waters, 2008). These floating substrates are transported within the ACC (Barber et al., 1959; Coombs and Landis, 1966; Fraser et al., 2009; Smith, 2002), passing eastward along the western side of the Antarctic Peninsula and connecting remote low Antarctic and sub-Antarctic islands (Rintoul et al., 2001). While the ACC is forced through the relatively narrow Drake Passage, numerous eddies are formed (Glorioso et al., 2005), which would allow a bidirectional transport to and from southern South America (Antezana, 1999; Clarke et al., 2005; Nowlin and Klinck, 1986).

Despite the current and historical ability of at least some iphimediid species to disperse in and/or out of the Antarctic shelf, the (sub-)Antarctic Iphimediidae form an endemic and monophyletic

group, i.e. members of this clade do not appear to have dispersed further north than the sub-Antarctic islands and southern South America at any point of their evolutionary history.

Distribution	Species	Depth range
High Antarctic and Sub-Antarctic	*Echiniphimedia echinata*	0 – 728 m
	Echiniphimedia hodgsoni	20 – 1120 m
	Echiniphimedia scotti	0 – 457 m
	Gnathiphimedia barnardi	26 – 250 m
	Gnathiphimedia fuchsi	5 – 157 m
	Gnathiphimedia macrops	120 – 540 m
	Iphimediella margueritei	10 – 732 m
	Pariphimedia integricauda	0 – 145 m
	Pariphimedia normani	0 – 124 m
	Iphimedia pacifica	36 – 416 m
	Iphimediella georgei	348 – 732 m
	Iphimediella margueritei	10 – 732 m
Exclusively High Antarctic	*Anchiphimedia dorsalis*	200 – 732 m
	Echiniphimedia barnardi	165 – 710 m
	Echiniphimedia gabrielae	130 – 424 m
	Echiniphimedia imparidentata	50 m
	Echiniphimedia waegelei	170 – 254 m
	Gnathiphimedia incerta	60 – 426 m
	Gnathiphimedia mandibularis	45 – 2000 m
	Gnathiphimedia sexdentata	9 – 720 m
	Gnathiphimedia watlingi	388 m
	Iphimediella acuticoxa	146 – 220 m
	Iphimediella bransfieldi	200 – 399 m
	Iphimediella cyclogena	210 – 540 m
	Iphimediella dominici	421 – 429 m
	Iphimediella microdentata	216 – 720 m
	Iphimediella paracuticoxa	68 m
	Iphimediella rigida	256 – 625 m
	Iphimediella ruffoi	242 – 264 m
	Iphimediella serrata	54 – 549 m
	Iphimediella discoveryi	200 – 220 m

Table 8. Bathymetric distributions of iphimediid species from the high Antarctic and sub-Antarctic regions.

This presumably cold-water lineage might not be able to colonize lower latitudes. Moreover, dispersal across the APF might involve only a small number of iphimediid species, potentially those

inhabiting algae-populated habitats. Apart from potentially rare ACC-driven long-distance dispersal, iphimediid dispersal abilities might remain relatively limited. Observations of several species in aquaria indeed showed that, most of the time, these iphimediids sit motionless on their host substrate or walk very slowly, but seldomly swim (De Broyer et al., 2001). The monophyly and endemicity of (sub-)Antarctic iphimediids should however be verified by including a more extensive non-Antarctic taxon sampling, especially from geographically close areas such as northern South America, New Zealand and Australia.

DIVERSIFICATION DYNAMICS

The diversification rate decline inferred by BAMM and the slowdown around 18.43 Ma under a Yule4rate model are not significantly different from a Yule3rate model (without this shift) or constant-rate models when incomplete taxon sampling is taken into account (Table 5; Fig. 5 and 7). The observation of a diversification rate decline over time has often been interpreted as a signature of adaptive radiation, i.e. a burst of diversification in the early history of a clade, followed by a diversity-dependent decrease as available niches fill up (e.g. Glor, 2010; Losos and Mahler, 2010; Phillimore and Price, 2008; Rabosky and Lovette, 2008; Schluter, 2000). The initial diversification of Antarctic iphimediids occurred in a late Gondwanan to early Antarctic cooling environment, under a developing seasonality of light and temperature regimes. Adaptation to such changing conditions and the newly available niche-space left by the extinction of cold-intolerant taxa likely led to the successful diversification of iphimediids on the Antarctic shelf. They are typically found within the rich suspension feeder assemblages (De Broyer et al., 2001), which flourished as a result of the late Gondwanan extinction of durophagous predators (Aronson et al., 2007, 2009). Such ecological opportunity could be expected to drive an early burst of diversification into lineages that are better able to exploit the newly available habitats, by fulfilling a variety of distinct ecological roles (Gavrilets and Losos, 2009; Glor, 2010; Losos, 2010; Schluter, 2000). Among Antarctic amphipods, Iphimediidae appears to present a particularly high diversity of ecological specializations (Coleman, 2007), comprising mostly micropredatory browsers feeding on invertebrates (Coleman, 1989a, b; Coleman, 1991; Nyssen et al., 2002), but also active predators (Nyssen et al., 2005).

The non-significance of the detected slowdown in diversification could mean that competition was higher in the early history of iphimediids than expected under the “early-burst model”. Alternatively, it could result from insufficient data. As the actual diversity of the iphimediid clade is unknown, it is possible that a low taxon sampling in our phylogeny decreases the statistical power of the tests. Indeed, a small tree size compromises the detection of discrete rate shifts and slowdowns in diversification (Laurent et al., 2015). Furthermore, following the MMCT, the ice sheet extended to

the outer shelf during glacial maxima, at least in some places, thereby erasing shelf habitats and their associated biota (e.g. Chow and Bart, 2003; Hambrey and McKelvey, 2000; Passchier et al., 2003). Repeated mass extinctions, which likely occurred within this almost entirely shelf lineage, could have eroded the signals of earlier pulses of diversification (Phillimore and Price, 2008; Rabosky and Lovette, 2008; Ricklefs and Jønsson, 2014; Weir, 2006), as it was also suggested for Antarctic *Epimeria* amphipods (Chapter 4) and notothenioid fishes (Near et al., 2012). However, as the fossil record is completely lacking, we cannot determine whether this turnover rate was sufficiently high compared to the initial speciation rate to erode an early burst signature (Quental and Marshall, 2009).

Yule4rate and Yule3rate models are significantly better-fitting models than constant-rate models when a sampling fraction of 79.5 % is assumed (Table 5). Both these models imply a rate increase at 5.57–4.78 Ma and a rate decrease at 4.78–2.32 Ma (Table 5; Fig. 5). The BAMM analysis shows that the detected rate increase is mostly due to a diversification rate shift at the base of the *Echiniphimedia* clade (Fig. 6), which originated 3.86 [5.29; 2.48] Ma (Fig. 3). The evidence for this shift in BAMM results increases when the assumed species diversity within Iphimediidae is increased. Assuming that our data only represents 10 % of the actual diversity within the Iphimediidae, this shift is present in 83 % of the posterior samples, while 60 % also show a diversification rate increase at the base of clade A (Fig. 6). This increase in diversification of *Echiniphimedia* (and possibly, to a lesser extent, of clade A) should be confirmed when the actual diversity of the Antarctic clade can be estimated more accurately. An increased diversification rate of *Echiniphimedia* would also explain why all species of this genus were lumped together as one "putative species" by the COI-based ABGD method, unless this clade was analysed independently.

The initial diversification of *Echiniphimedia* and clade A both occurred after the MMCT, respectively 3.86 [5.29; 2.48] Ma (Pliocene) and 7.83 [11.08; 4.87] Ma (late Miocene to Pliocene) (Fig. 3). Similarly, pulses of lineage diversification were observed within late Miocene to early Pliocene subclades of nothotenioid fishes and were interpreted as bursts of allopatric speciation events resulting from the repeated isolation of populations in ice-free refugia during glacial maxima (Near et al., 2012). If the elevated diversification rates of *Echiniphimedia*, and to a lesser extent, clade A, are confirmed, such climatically-driven diversification bursts might have occurred within Antarctic Iphimediidae as well.

Alternatively, the potential diversification burst of the genus *Echiniphimedia* might have been driven by key innovations leading to ecological opportunity. Indeed, several *Echiniphimedia* species are among the very few amphipods which feed almost exclusively on sponges (Amsler et al., 2009;

Coleman, 1989b; Dauby et al., 2001b; Graeve et al., 2001; Nyssen, 2005; Nyssen et al., 2005). The unique hedgehog-like morphology of *E. hodgsoni* is an efficient camouflage while sitting among the spicules of its sponge-host (Fig. 8A) (Barnard, 1932). Although ecological data are lacking for some species, the shared, unique, heavy spination of *Echiniphimedia* species could reflect an association with sponges, for shelter and/or food (Fig. 8). Moreover, stable isotope analyses suggest that different *Echiniphimedia* species may specialize on different sponge species (Dauby et al., 2001b; Nyssen, 2005). The Antarctic shelf houses the most extensive sponge grounds known (Barthel and Gutt, 1992; Dayton et al., 1974; Hogg et al., 2010; Klitgaard and Tendal, 2004). Adaptations in mouthpart and foregut-related characters (Coleman, 1989b) possibly enabled *Echiniphimedia*'s ancestor to process such abundant, but hardly palatable, preys (Peters et al., 2009), leading to a diversification burst within numerous newly available trophic niches and under reduced competition.

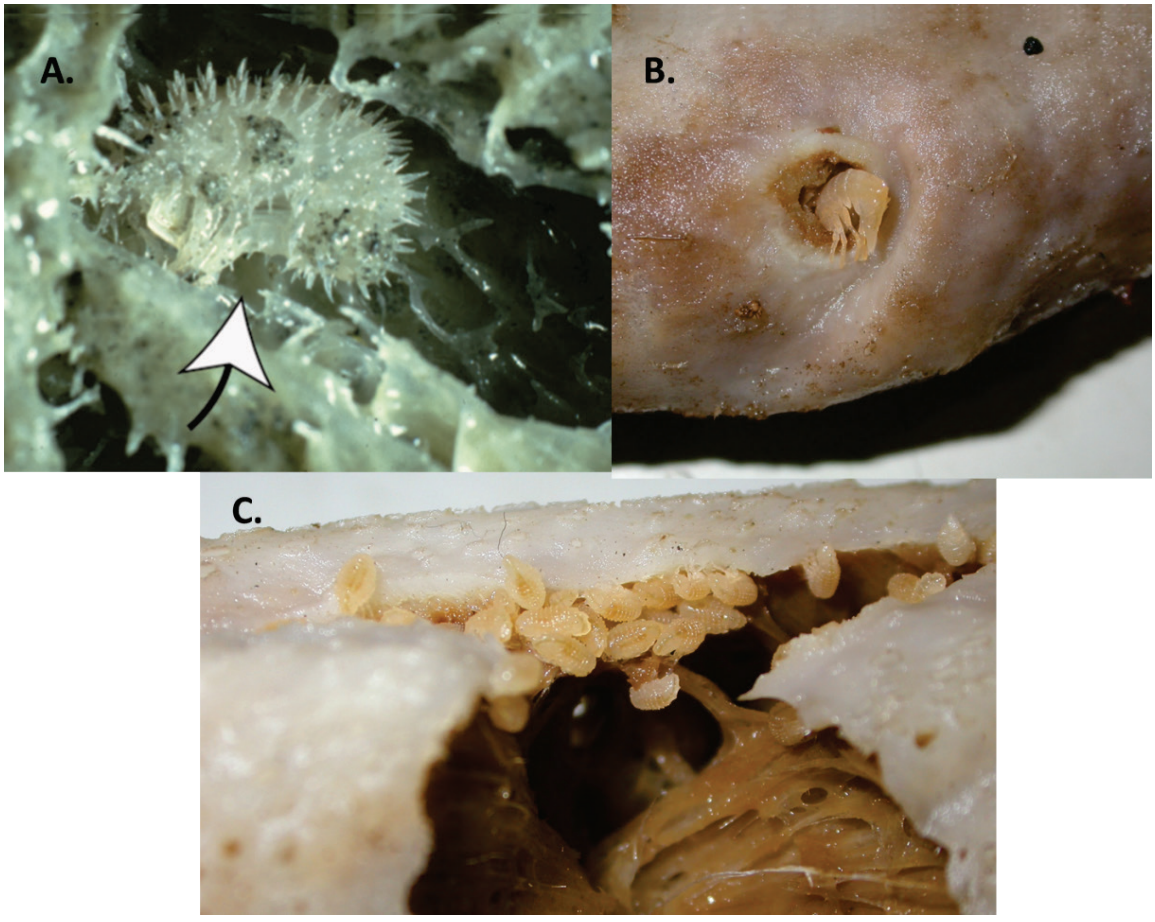

Fig. 8. A. *Echiniphimedia hodgsoni* (arrow) sitting on a sponge host. **B.** *Echiniphimedia* aff. *imparidentata* digging a hole in a candle-like sponge. **C.** Group of juvenile *Echiniphimedia* sp. on a candle-like sponge. Pictures by O. Coleman (A) and C. d'Udekem d'Acoz (B and C).

CONCLUSIONS

This study provides the first time-calibrated molecular phylogeny of the family Iphimediidae. Watling and Thurston's (1989) first inferences on the evolution of this family in the Southern Ocean, based on a morphological cladistic analysis, can be addressed in the light of these new molecular data. Watling and Thurston (1989) introduced the new paradigm of the "Antarctic shelf acting as an evolutionary incubator", supplying colonizing taxa to the world's ocean after climatically-driven radiations in Antarctic waters. Although the precise divergence time of the clade composed of (sub-) Antarctic species remains ambiguous, it likely arose in a late Gondwanan/early Antarctic environment and evolved *in situ*, isolated from northern iphimediids by tectonic vicariance and/or adaptation to high latitude environmental conditions. The clade's diversification would be related to cold waters, as suggested by Watling and Thurston (1989). Whereas our data bear some evidence of diversification bursts within one (or two) subclade(s) after the MMCT — possibly related to allopatric speciation events resulting from the fragmentation of populations in glacial refugia — this should be verified when the actual diversity of the (sub-)Antarctic iphimediid clade is better known. After successfully diversifying in the Antarctic region, historical dispersal event(s) to sub-Antarctic areas have occurred and still occur today, as several species have distributional ranges crossing the APF. However, our data bear no evidence of dispersal further north than sub-Antarctic islands or the tip of South America, at any point of iphimediids' evolutionary history, although this should be further tested with a more extensive non-Antarctic sampling.

ACKOWLEDGEMENTS

This work was supported by a Ph.D. fellowship from F.R.I.A. (F.N.R.S., Belgium). We thank the Alfred-Wegener-Institut, Helmholtz-Zentrumfür Polar- und Meeresforschung (AWI) and the captain, crew and chief scientists of various *R.V. Polarstern* expeditions for their efficiency, as well as present and past colleagues of the staff of the Royal Belgian Institute of Natural Sciences (RBINS) for collecting specimens on board. The travel expenses of the first and last authors during ANT-XXIX/3 were funded by the Fonds Léopold III. The research program led by Guillaume Lecointre, REVOLTA 1124, supported by the Institut polaire français Paul Emile Victor (IPEV) and the Muséum national d'Histoire naturelle (MNHN), and the CAML-CEAMARC cruise of RSV Aurora Australis (IPY project no. 53), supported by the Australian Antarctic Division, the Japanese Science Foundation and the IPEV (project ICOTA), are acknowledged for providing extensive Antarctic material. The specimens from Vanuatu used in this study were collected during the SANTO expedition, conducted respectively by

MNHN and Institut de Recherche pour le Développement (IRD) as part of the Tropical Deep-Sea Benthos programme (http://expeditions.mnhn.fr/program/tropicaldeep-seabenthos). Funders and sponsors include the French Ministry of Foreign Affairs, the Total Foundation, Prince Albert II of Monaco Foundation, Stavros Niarchos Foundation, and Richard Lounsbery Foundation. We thank Laure Corbari (MNHN) for giving us access to this material. We appreciate the kind help of the NIWA Invertebrate Collection staff, Wellington, New Zealand with loan of the material from expeditions TAN402 and TAN802 of the *RV Tangaroa*. Dirk Schories (University Austral de Chile) is thanked for providing additional Antarctic specimens. We are also grateful to Charles Griffiths (University of Cape Town) for the *Iphimedia gibba* samples from South Africa. TB contributed to this manuscript on behalf of the "Joint Experimental Molecular Unit" (RBINS-JEMU) and the FWO Research Community W0.009.11N "Belgian Network for DNA Barcoding" (BeBoL).

GENERAL DISCUSSION

1. SUMMARY OF THE RESULTS

CHAPTER 1: PHYLOGENY AND SYSTEMATICS OF EUSIROIDEA

The phylogenetic analysis of all available families once suspected to belong or to be close to Eusiroidea resulted in the following provisional delimitation of the superfamily: Acanthonotozomatidae, Amathillopsidae, Astyridae, Calliopiidae (excluding *Cleippides* and *Weyprechtia*), Dikwidae, Eusiridae, Epimeriidae, Gammarellidae s.l. (excluding *Gammarellus*), Iphimediidae, Pleustidae, Pontogeneiidae, Stilipedidae and Vicmusiidae. All latter families share a number of putative morphological synapomorphies.

The position of eight long-branched taxa in relation to the "Eusiroidea clade" remained unresolved due to long-branch attraction artefacts. These long-branch taxa belong to the families Amphilochidae, Colomastigidae, Leucothoidae, Oedicerotidae and the suborder Hyperiidea. Their phylogenetic position should be revised with additional DNA sequence data and a more thorough taxon sampling (in order to break up long branches). Furthermore, they do not possess most of the putative synapomorphies of the "Eusiroidea clade". Hence, these families are provisionally excluded from Eusiroidea.

Most of the studied eusiroid families (represented by more than one genus) were found to be polyphyletic on the ML and/or BI phylogenies, i.e. Pleustidae, Calliopiidae, Pontogeneiidae, Gammarellidae, Epimeriidae and Acanthonotozomellidae. Hence, the morphological characters traditionally used in the taxonomy of these families were shown to be highly convergent, e.g. the shape of the telson, the shape of the labium, the body calcification and spination, and the presence/absence of the senticaudate character state.

CHAPTER 2: SPECIES DIVERSITY AND GEOGRAPHICAL DISTRIBUTIONS IN ANTARCTIC *EPIMERIA*

Most of the Antarctic *Epimeria* species from Coleman (2007) available for this study were shown to be complexes of several morphologically similar (pseudocryptic) species, i.e. *E. macrodonta*, *E. similis*, *E. puncticulata*, *E. walkeri*, *E. georgiana*, *E. robusta*, *E. grandirostris* and *E. pulchra*. A total of

25 *Epimeria* lineages were identified as putative new species by morphology and DNA sequence-based methods.

Most of these Antarctic *Epimeria* species and putative species appear to be regionally-restricted, whereas some of them would be able to disperse over large distances. Indeed, *E.* aff. *similis* SI5 and *E.* aff. *walkeri* WA1 are distributed on both sides of the Weddell Sea, *E. macronyx* is found in the Antarctic Peninsula and Adélie Coast and *E. inermis* is circum-Antarctic.

CHAPTER 3: MORPHOLOGICAL DESCRIPTION OF *EPIMERIA* SP. NOV. ROSS FROM THE ROSS SEA

The morphological description of a new *Epimeria* species endemic to the Ross Sea, *E.* sp. nov. Ross, was presented. This species belongs to the *macrodonta–similis* complex from CHAPTER 2. This description extends the taxonomic treatment of all available Antarctic *Epimeria* (d'Udekem d'Acoz and Verheye, *in Press*), which includes the formal morphological descriptions of all species delimited in CHAPTER 2, along with 3 additional species identified on the basis of morphology only (total of 28 new species). Moreover, additional distributional records based on non-sequenced specimens are included in the monograph, which adds to the distributional data of Antarctic *Epimeria* presented in CHAPTER 2.

CHAPTER 4: ORIGIN, DISPERSAL AND DIVERSIFICATION OF ANTARCTIC *EPIMERIA*

The molecular phylogeny of Antarctic and non-Antarctic *Epimeria*, along with taxa putatively related to *Epimeria*, showed that the Antarctic and non-Antarctic components of the genus form two distinct well-supported clades. Moreover, *Epimeria* appears paraphyletic on the BI tree, as the Antarctic clade is a sister clade to two stilipedid species. The time-calibrated phylogeny suggested that the Antarctic *Epimeria* lineage originated from a late Gondwanan ancestor and hence, did not colonize the Antarctic region after the continent broke apart from the other fragments of Gondwana. The monophyly of this Antarctic component suggested that it evolved in isolation since its origin. The initial diversification of the latter clade occurred in a cooling environment, hence adaptation to cold waters, along with the extinction of cold-intolerant taxa and resulting ecological opportunities, likely led to its successful diversification on the Antarctic shelf. However, there was neither evidence of a rapid lineage diversification early in the clade's history, nor of any shifts in diversification rates concomitant to glacial cycles.

CHAPTER 5: ORIGIN, DISPERSAL AND DIVERSIFICATION OF ANTARCTIC IPHIMEDIIDAE

The molecular phylogeny supported the monophyly of all studied (sub-)Antarctic iphimediids, which together appear as a sister clade to non-Antarctic iphimediids. The monophyly of the (sub-)Antarctic

iphimediids and their inferred divergence time suggest that adaptation to harsh polar conditions and/or tectonic vicariance might have promoted their divergence from a non-Antarctic clade, in a Late Gondwanan or early Antarctic environment. The initial diversification of this (sub-)Antarctic clade occurred in a cooling environment and is therefore inferred to be related to cold waters. A diversification burst within one or two subclade(s) might have occurred after the Mid-Miocene Climate Transition, possibly related to glacial cycles. A dispersal event from the High Antarctic to the sub-Antarctic region occurred in the *Labriphimedia pulchridentata* complex. However, based on the present taxon sampling, Antarctic iphimediids do not appear to have dispersed further than sub-Antarctic islands or Tierra del Fuego at any point of their evolutionary history.

2. AMPHIPOD TAXONOMY AND MORPHOLOGICAL CONVERGENCES

2.1. ON THE USE OF MOLECULAR DATA IN AMPHIPODS' TAXONOMY

The higher-level classification within Amphipoda has been very unstable through time (Bousfield and Shih, 1994). Classifications were essentially phenetic until the end of the 20th century (Barnard, 1969; Barnard and Karaman, 1991; Bousfield, 1978; Stebbing, 1906). Subsequently, several authors evaluated these classifications in a cladistic framework, using matrices of morphological characters (Berge et al., 2000; Kim and Kim, 1993; Lowry and Myers, 2013; Myers and Lowry, 2003). However, most subsequent molecular analyses exploring phylogenetic relationships within Amphipoda from the family to the suborder level revealed extensive incongruences with classifications based on morphology (e.g. Browne et al., 2007; Corrigan et al., 2014; Englisch, 2001; Havermans et al., 2011; Hurt et al., 2013; Ito et al., 2008; Macdonald III et al., 2005). The revision of the superfamily Eusiroidea, presented in **CHAPTER 1**, is a striking example of this issue, as almost every previously defined family appeared polyphyletic. Molecular results therefore suggest that many morphological characters traditionally used in amphipod taxonomy might be highly homoplasious, i.e. appeared multiple times independently throughout evolutionary history. Deeper phylogenetic relationships are more likely to be blurred by homoplasies, as longer time periods potentially allow for a higher occurrence of evolutionary convergences. The use of molecular tools for phylogenetic reconstructions therefore appears necessary in higher-level amphipod systematics, in order to discriminate between homologous and homoplasious morphological characters. The identification of the former is essential to infer morphological synapomorphies, which could be used in a phylogenetically-meaningful classification of Amphipoda. On the other hand, the identification of morphological homoplasies participates to the global understanding of the evolutionary origin of such convergences.

2.2. Towards a phylogenetically-meaningful classification of Amphipoda

Traditionally, amphipods have been divided into three to five suborders: Ingolfiellidea Hansen, 1903, Gammaridea Latreille, 1802, Hyperiidea H. Milne Edwards, 1830, Caprellidea Leach, 1814, and Corophiidea Leach, 1814 [see General Introduction 2.2.3.]. The most recent classification unites former caprellidean and corophiidean families (respectively, parvorders Caprellidira and Corophiidira) in one infraorder, Corophiida (Lowry and Myers, 2013). However, a 18S rDNA phylogeny shows polyphyletic Corophiidira and Caprellidira (Ito et al., 2008). Hyperiid species also appear nested within Gammaridea (*sensu* De Broyer et al. 2007) in 18S rDNA phylogenies (**CHAPTER 1**, Fig. 2; Englisch 2001). The latter result should however be further tested with additional DNA data and a more extensive taxon sampling, as the hyperiid and gammaridean species from the families Amphilochidae, Colomastigidae and Leucothoidae, forming a clade on our 18S rDNA phylogeny, are all long-branched taxa (**CHAPTER 1**, Fig. 2). With the aim of clarifying the higher-level classification within Amphipoda, Lowry and Myers (2013) reconstructed a morphology-based phylogeny including most families previously classified in Gammaridea and Corophiidea *sensu* De Broyer et al. (2007). The latter families were grouped together in a new suborder Senticaudata Lowry and Myers, 2013. However, this suborder was erected on the basis of one alleged synapomorphy, i.e. the possession of apical robust setae on the rami of uropods 1–2, without actually testing its monophyly. The senticaudate character was shown to be homoplasious on the 28S and 18S phylogenies of Eusiroidea (**CHAPTER 1**; Fig. 3), thereby refuting the monophyly of the Senticaudata.

As most previously defined suborders would not be valid (monophyletic) entities, re-delimitations of superfamily groupings based on molecular phylogenetic studies, such as the one presented in **CHAPTER 1** for Eusiroidea, would be a first step towards a phylogenetically meaningful revision of the higher-level classification within Amphipoda. Indeed, whereas some of the previously defined superfamilies are generally accepted (presumably monophyletic), e.g. Lysianassoidea and Talitroidea (Corrigan et al., 2014; Havermans et al., 2011; Kim and Kim, 1993; Ritchie et al., 2015; Serejo, 2004), most of them need to be revised in a phylogenetic context (Martin and Davis, 2001).

2.3. Evolutionary origins of convergent morphologies

Convergent evolution has often been interpreted as evidence for adaptation. Multiple unrelated lineages experiencing the same selective environments might develop similar adaptive traits. Natural selection is not, however, the only possible explanation for morphological convergences: similar traits can arise independently from random evolutionary changes or constraints on the range of

phenotypic variation that can be produced by the genotype (caused by e.g. shared patterns of genetic correlations) (Losos, 2011).

As morphological convergences in amphipods were very often observed in presumably functional traits (i.e. traits impacting fitness in a given environment), they were tentatively interpreted as independent adaptations to similar ecological niches (without however testing for selection). As amphipods are very diverse ecologically, occurring in marine, fresh- and brackish water as well as humid terrestrial ecosystems (Barnard and Karaman, 1991; Poltermann et al., 2000; Serejo, 2004; Takhteev, 2000; Van dover et al., 1992; Vinogradov et al., 1996), the widespread occurrence of morphological convergences in this suborder was explained by adaptive radiations in a wide variety of ecological niches (Browne et al., 2007; Macdonald III et al., 2005).

Characters related to the feeding morphology (gnathopods and mouthparts) have extensively been used in amphipod taxonomy (e.g. Bowman and Gruner, 1973; Coleman, 2007; Vinogradov et al., 1996) and were shown to be highly convergent (Havermans et al., 2011; Hurt et al., 2013). The polyphyly of Pleustidae — defined exclusively on the shape of the labium — evidenced in **CHAPTER 1** (Fig. 3) and of the iphimediid genera *Iphimediella* and *Gnathiphimedia* —defined exclusively on mouthpart characters, such as the shape of the mandible incisor — demonstrated in **CHAPTER 4** (Fig. 2) similarly argue against the sole use of trophic ecology-related characters in amphipods' taxonomy. This is especially valid for taxa presenting a wide variety of trophic specializations such as iphimediids — which appear mostly composed of micropredators specializing on different types of prey taxa [see General Introduction 2.2.5., **CHAPTER 4**] — or hyperiids — exhibiting commensal and parasitic associations with a variety of zooplankton groups (Gasca et al., 2007; Harbison et al., 1977; Madin and Harbison, 1977). Characters related to diet might however remain phylogenetically informative in some less inclusive taxa sharing a similar trophic type, such as Eusiridae, erected on synapomorphies associated with carnivory (**CHAPTER 1**).

Traits related to the habitat, such as the modifications of the visual system, streamlined body and elongated appendages of pelagic amphipods (Hurt et al., 2013; Macdonald III et al., 2005) or the short, compact bodies and appendages and numerous setae of fossorial amphipods (Macdonald III et al., 2005) were also shown to be convergent across lineages.

Similarly, the polyphyly of the former Iphimedioid complex (Lowry and Myers, 2000) — which grouped together a range of families with armored body forms (strongly clacified and/or with dorsal and lateral teeth and carinae) — evidenced in **CHAPTER 1**, confirms that such a processiferous morphology is highly convergent, as it was previously shown for Baikalian amphipods (Macdonald III

et al., 2005; Sherbakov et al., 1998, 1999). Notably, the processiferous *Paramphithoe hystrix* (previously classified in Epimeriidae) is phylogenetically nested within smooth or weakly toothed *Halirages* species (Fig. 1A). Similarly, iphimediids are more closely related to smooth or weakly toothed *Oradarea* and *Liouvillea* species (Fig. 1B). This armored form was hypothesized to be adaptative under predation pressure, as it would render these amphipods less palatable. The spines could prick in the mouth of predators and the calcified teguments could be more difficult to digest (Brandt, 1999; Moore, 1981). The very rare occurrence of iphimediid species (which are however common) in fishes' stomach contents tends to confirm this hypothesis (Dauby et al., 2003). A "spiny" morphology also seems to act as a camouflage in some cases, such as for *Paramphithoe hystrix* (Fig. 1A) and *Echiniphimedia hodgsoni* (**CHAPTER 4**; Fig. 8), which are commensal on sponges (Coleman, 1989b; Oshel and Steele, 1985).

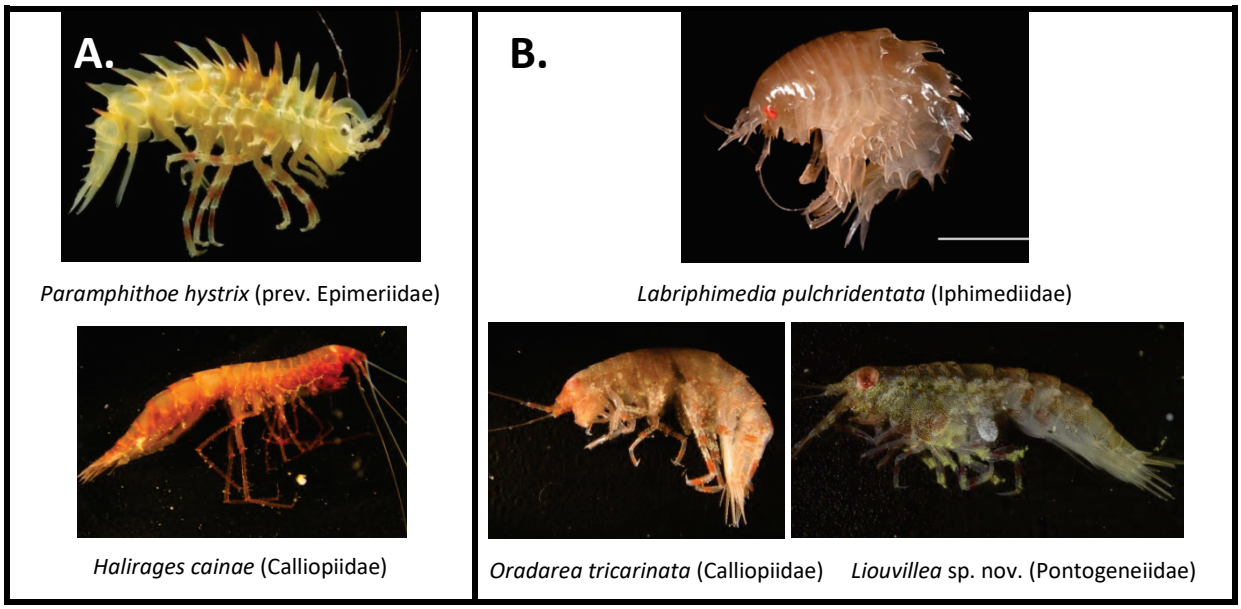

Figure 1. Pictures of some armored/spiny species in regards to their smooth/ weakly toothed relatives.

3. (PSEUDO)CRYPTIC SPECIES IN THE SOUTHERN OCEAN

Cryptic species are species that are or have been classified as a single nominal species because they are, at least superficially, morphologically indistinguishable (Bickford et al., 2007). In **CHAPTER 2**, twenty-five putative new *Epimeria* species, most of them previously confounded with a described species, have been delimited based on a combination of morphological and molecular data. Similarly, such "hidden diversity" has been revealed by molecular studies in a wide variety of Antarctic marine organisms, such as polychaetes (Schüller, 2011), nemerteans (Mahon et al., 2008; Thornhill et al., 2008), molluscs (Allcock et al., 2011; Linse et al., 2007), arthropods (Arango et al., 2011; Baird et al., 2011; Raupach et al., 2007) and echinoderms (Hemery et al., 2012; Janosik and

Halanych, 2010). This has implications on the general estimation of biodiversity in the Southern Ocean, which is consequently grossly underestimated, but also on inferred biogeographical patterns [see section 4 of this discussion; **CHAPTER 2**]

In many cases, however, "cryptic" species are likely to be readily separated by morphological variations that were previously assumed to be intraspecific (Saez and Lozano, 2005). Morphological diagnostic characters could be defined for the *Epimeria* lineages delimited as separate species by DNA-based methods in **CHAPTER 2** and they will be formally described in d'Udekem and Verheye (*in Press*). Informations from other sources (such as ecological, behavioral or genetic data) are needed in such cases to investigate species boundaries and thereby identify species-level morphological differences. Moreover, some important morphological characters for species identification might be destroyed along the preservation process, e.g. the coloration which disappears in alcohol. While some *Epimeria* species were shown to include different color morphs (Lörz et al., 2007, 2009) (Fig. 2A), coloration might be a diagnostic feature for some others (Fig. 2B).

Figure 2. A. Different colour morphs of *Epimeria* aff. *georgiana* GE1 and **B**. Constant coloration of *Epimeria* aff*. macrodonta* MA3 (d'Udekem D'Acoz and Verheye, *in Press*; Verheye et al., 2016a).

(Pseudo)cryptic speciation might occur when (complete or partial) reproductive isolation results from differences in behavioral, ecological or reproduction-related traits which have no (or little) morphological correlates, e.g. habitat preferences, auditory or chemical mate recognition systems, courtship behavior, reduced viability or fertility of the offspring, gametic incompatibilities. For instance, the dominant role of chemical recognition systems for mate choice in the sea might explain the higher occurrence of marine cryptic species (Knowlton, 1993). Although data are not available for all species — especially Antarctic ones, which are rarely kept in aquaria — chemical communication appears to be commonly used by amphipods (Dahl et al., 1970; Kolding, 1986; Krång and Baden, 2004; Lowry, 1986; Stanhope et al., 1992; Sutherland et al., 2010; Thiel, 2011). Notably, some *Epimeria* species possess callynophores, a sensory organ presumably used for chemoreception (Lowry, 1986).

Cryptic species are often regarded as a product of recent speciation, because a supposedly limited time since divergence potentially didn't allow for extensive morphological changes (Saez and Lozano, 2005), although rates of molecular and morphological evolution can also be decoupled (e.g. Rocha-Olivares et al., 2001; Mamos et al., 2014). Plio-Pleistocene glacial cycles were hypothesized to have caused relatively recent allopatric speciations, following the isolation of small populations in glacial

refugia. According to this hypothesis, stochastic genetic processes (genetic drift and mutations) might have played an important role in driving the presumed "diversity pump" [see section 6.3 of this discussion]. Speciation resulting from such non-selective processes could be less often accompanied by appreciable morphological changes than divergences caused by selection, which targets reproductive and/or ecological traits. However, it remains highly uncertain whether the time spent in isolation during glacial maxima was sufficient to actually lead to speciations.

Alternatively, specific environments might also promote morphological stasis over longer periods of time. Notably, widely fluctuating environmental conditions (e.g. changing sea level, substrate, salinity or climate) would impose stabilizing selection on morphology (Lindholm, 2014; Sheldon, 1996). Environmentally plastic lineages, characterized by a high physiological or ecological plasticity are favored in such cases, as they are able to cope with a wide range of environmental conditions, with no further adaptations needed. Glacial-interglacial cycles have been notably inferred to explain the morphological stasis of some lineages (Coope, 2004; Sheldon, 1996).

As biodiversity is incompletely documented, it is not known if the fluctuating and harsh environmental conditions on the Antarctic shelf during Plio-Pleistocene glacial cycles [see General Introduction 4.5.] could have led to an elevated number of cryptic species compared to less impacted lower-latitude environments. In the case of *Epimeria*, notably, complexes of morphologically similar (although distinguishable) species appear similarly present in tropical Indo-Pacific *Epimeria* (Fig. 3; **CHAPTER 3**).

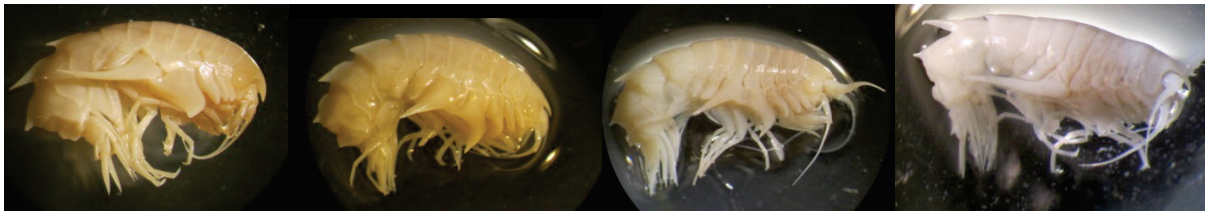

Figure 3. Four species of the *Epimeria norfanzi* complex from the Indo-Pacific region (specimens from MNHN, Paris).

4. Distributional patterns on the Antarctic shelf

4.1. Circum-Antarctic or regionally-restricted?

Following De Broyer and Jażdżewska (2014)'s definition of "circum-Antarctic", i.e. distributed in at least 3 widely separated localities around the continent, in the West Antarctic or/and the Weddell Sea and at least two distant East Antarctic localities, 10 *Epimeria* species on a total of 26 (**38 %**) were previously recorded to have a circum-Antarctic distribution (Coleman, 2007; Lörz, 2009; Lörz et al.,

2007, 2009, 2011): *Epimeria georgiana*, *E. grandirostris*, *E. inermis, E. macrodonta, E. puncticulata, E. macronyx, E. robusta, E. walkeri, E. scabrosa* and *E. similis.* However, most of these *Epimeria* species are complexes of (pseudo-)cryptic species (**CHAPTER 2, 3**; d'Udekem and Verheye, *in Press*). The methods used in **CHAPTER 2** to delimit species within these complexes, along with detailed morphological examinations of all available *Epimeria* material (**CHAPTER 3**; d'Udekem and Verheye, *in Press*) revealed a total of 28 new *Epimeria* species and enabled a complete re-assessment of species' distributional ranges. Based on the distribution record of all known Antarctic *Epimeria* species from d'Udekem and Verheye (*in Press*) (Appendix S10), only five out of the 65 species studied (**7.7 %**) are still recorded as circum-Antarctic: *Epimeria* aff. *macrodonta* MA1*, E.* aff*. similis* SI5, *E. macronyx, E. inermis* and *E. walkeri.* A vast majority of species have a distributional range restricted to one of the operational geographic/hydrographic units defined by De Broyer and Jażdżewska (2014) for amphipods (Fig. 4): 69 % of the species to 75 % when those distributed in only two adjacent units are added.

Such restricted geographical distributions for most Antarctic *Epimeria* species could be due in part to sampling biases, as species from the same complex were likely confounded in previous distributional records and the present records are surely not exhaustive. However, such a generalized pattern among Antarctic *Epimeria* likely translates into a globally limited dispersal potential.

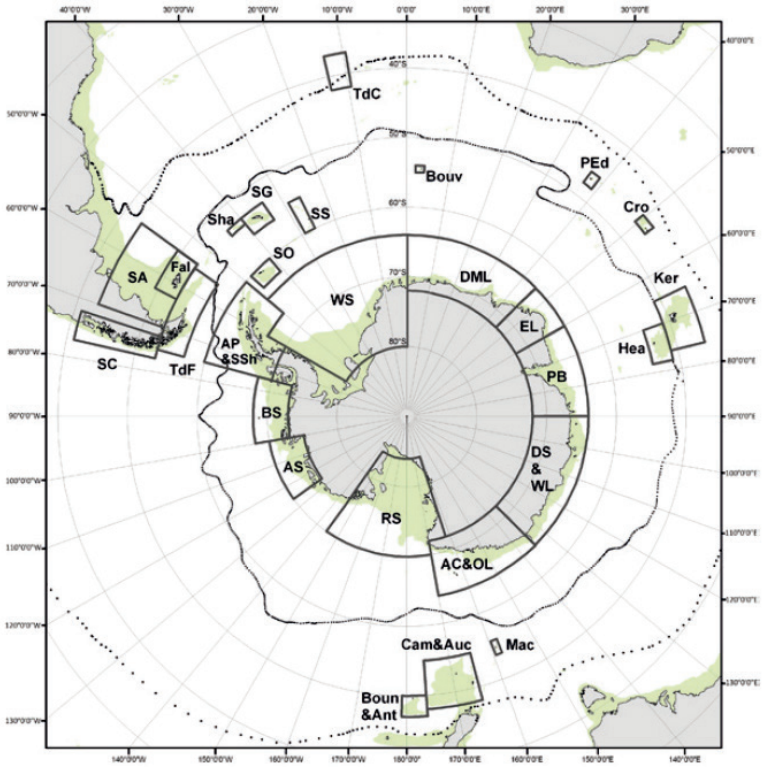

Figure 4. Geo-hydrographic units used for the biogeographical analysis of Antarctic amphipods of De Broyer and Jażdżewska (2014). SC: South Chile. SA: South Argentina. TdF: Tierra del Fuego. Fal: Falkland Islands. Sha: Shag Rocks. SG: South Georgia. TdC: Tristan da Cunha and Gough Islands. PEd: Prince Edward and Marion Islands. Cro: Crozet Islands. Ker: Kerguelen Islands. Hea: Heard and McDonald Islands. Mac: Macquarie Island. Cam&Auc: Campbell and Auckland Islands. Boun&Ant: Bounty and Antipodes Islands. AP&SSh: Antarctic Peninsula and South Shetland Islands. SO: South Orkney Islands. SS: South Sandwich Islands. WS: Weddell Sea. DML: Queen Maud Land. EL: Enderby Land. PB: Prydz Bay. DS&WL: Davis Sea and Wilkes Land. AC&OL: Adélie Coast and Oates Land. RS: Ross Sea. AS: Amundsen Sea. BS: Bellingshausen Sea.

The distributional range of Antarctic shelf taxa depends on a number of co-acting and interdependent factors, related both to the biology of an organism and environmental features. First, the mode of larval development is expected to be important, as species with long-lived pelagic larvae (broadcasters) are likely to disperse over long distances, as opposed to species without any pelagic stages (brooders) (Hoffman et al., 2011). However, some brooders are widely distributed (**CHAPTER 2**) (Nikula et al., 2010), suggesting that other factors are also at play. The mobility of the adults may be determinant as well, as suggested by the wide distribution of some amphipod species (brooders) which are good swimmers as adults (Baird et al., 2011; Havermans et al., 2013). The latter factor is in turn closely related to their trophic ecology. Indeed, suspension-feeders are likely to be less mobile, while active predators and scavengers will be good swimmers (De Broyer et al., 2001; Lörz and Coleman, 2009).

The mobility of the adult in relation to the species' trophic ecology could explain to some extent the contrasting distribution patterns of some *Epimeria* species. *E. macrodonta* and *E. robusta* were inferred to be weakly motile and opportunistic feeders. The latter species indeed have relatively restricted distributions (respectively, RS only and AC & OL+RS on Fig. 4). The presumably weakly motile *E. rubrieques* has the same trophic type, but appears more widely distributed in the East Antarctic region (DML and AC & OL). *E. similis* is a micropredatory browser of (mainly) hydrozoans and is therefore expected to be relatively sedentary. The species is indeed found only in the West Antarctic region (AP & SSh). The poor swimmer *E. georgiana* is a deposit-feeder presumably endemic to South Georgia. In contrast, *E. walkeri* was inferred to be highly motile predator of brittle stars and opportunistic scavenger and is circum-Antarctic (Dauby et al., 2001b; De Broyer et al., 2001; Nyssen et al., 2002).

The only recorded pelagic (therefore presumably more dispersive) Antarctic *Epimeria*, *E. macronyx*, is also found all around the continent. Ocean currents — the ACC, Antarctic coastal current closer to the continent and more regional gyre systems such as the Weddell and Ross gyres [see General Introduction 1.3.] — likely significantly aid long-distance dispersal of pelagic organisms.

The trophic niche also determines suitable micro-habitats for each species. Different types of macrobenthic assemblages have been identified [see General Introduction 2.1.]. The distributions of such communities are very patchy and unpredictable, more influenced by small-scale biological processes and interactions than by larger-scale variables such as depth or sediment grain size (Cummings et al., 2010; Gutt et al., 2013; Raguá-Gil et al., 2004). In addition, shelf areas down to 300 m deep are disturbed by ice scouring with such frequency that only rapid recolonisers (pioneer species) are locally abundant, thereby contributing to small-scale habitat patchiness (Gutt et al., 2013; Gutt and Piepenburg, 2003).

As communities are highly heterogeneous at intermediate and local spatial scales (Gutt et al., 2013), the limited mobility of many *Epimeria* species could prevent dispersal through large stretches of unfavorable habitats. Some continental shelf areas are also permanently covered by floating ice shelves (Weddell and Ross embayments and to a lesser extent, Amundsen and Bellingshausen seas) or perennial pack ice (western Weddell Sea). The sub-ice-shelf ecosystems are largely unknown because of their inaccessibility (Griffiths, 2010). However, in these oligotrophic ecosystems, benthic communities are likely to be impoverished, as it was shown for the area previously covered by the now collapsed Larsen A and B ice shelves — notably very poor in mobile fauna associated with large filter feeders (e.g. amphipods and isopods) (Gutt et al., 2011). These areas are therefore likely to be important barriers to the dispersal of weakly mobile amphipods inhabiting sessile suspension-feeder assemblages, such as many *Epimeria*.

4.2. The East/West biogeographical split

Many biogeographical studies attempted to map Southern Ocean biodiversity patterns, using distribution data from different sets of taxa [summarized in Koubbi *et al.* (2014)]. While the defined biogeographical subdivisions of the Antarctic region somewhat varied, a general consensus emerged on a longitudinal division into a “West Antarctic” part, including the Peninsula and most Scotia arc islands and an “East Antarctic” part, including the rest of continental Antarctica [see General Introduction 2.3.]. However, recent compilations of the distribution records of a variety of organisms (bivalves, bryozoans, pycnogonids, poriferans, ascidians, echinoids and tanaids) did not reveal such an East/West biogeographical split and instead showed the Southern Ocean as a “single functional unit” (Griffiths et al., 2009; Koubbi et al., 2014). Amphipods, gastropods and actinarians were the only taxa displaying a level of differentiation between East and West Antarctica (Koubbi et al., 2014).

43 % (28 species) of Antarctic *Epimeria* are endemic to the East Antarctic region and another 43 % are endemic to the West Antarctic (Appendix S10). Only 14 % of the species are present in both

bioregions (9 species). However, out of the 28 species endemic to the East Antarctic region, the vast majority (20 species) are restricted to only one biogeographic unit (from Fig. 4). The pattern appears similar for amphipods as a whole, as among the East Antarctic endemics, the vast majority is only known from rare records in one or two adjacent units (De Broyer and Jażdżewska, 2014). Therefore, the observed "East/West split" could be largely due to the high number of species endemic to a restricted geographical area. Alternatively, many restricted distributions could be an artefact of undersampling in the large East Antarctic region. Further sampling efforts are therefore needed to clarify amphipod biogeographic patterns and corroborate or reject the existence of an East/West split.

5. How isolated is the Antarctic shelf fauna?

The Antarctic benthic fauna is characterized by a high degree of endemism, generally around 50 % to 80 % of the species, depending on the group (Griffiths et al., 2009) [see General Introduction 2.3.]. Such high endemism levels support an ancient origin and long period of *in situ* evolution for many Antarctic taxa (Clarke and Crame, 2010). A pre-Antarctic origin was indeed inferred for a range of modern Antarctic lineages, using the fossil record or time-calibrated molecular phylogenies — such as the ones reconstructed in **CHAPTERS 4** and **5**. Many lineages originated after major climatic events, associated with drastic faunal turnovers. Origination rates indeed increased in the aftermath of the Cretaceous-Paleogene mass extinction event (~66 Ma), resulting from a significant global warming (Krug et al., 2009; Miller and Sepkoski, 1988; Oleinik and Zinsmeister, 1996; Stilwell, 2003) [see General Introduction 4.2.]. Notably, a comprehensive biostratigraphical analysis of the latest Cretaceous–Early Paleogene molluscan fossil record shows that approximately 18 % of the modern genera can be traced back to this period (Crame et al., 2014). In a similar way, the fossil record from the time spanning the final break-up of Gondwana (opening of the Drake and Tasmanian Passage) — associated with a progressive cooling from the middle Eocene (~49 Ma) to the onset of continental glaciations at the Eocene-Oligocene boundary (34 Ma) — provides evidence of a second major faunal turnover (Aronson and Blake, 2001; Boersma et al., 1987; Jadwiszczak, 2010; Keller et al., 1992; Stilwell and Zinsmeister, 1992) [see General Introduction 4.3]. The molluscan fossil record attests for high degrees of species-level endemism already by the middle Eocene, suggesting that an Antarctic province might have existed before the complete geographical isolation of the continent (Stilwell and Zinsmeister, 2000). Various modern lineages were inferred to have originated by vicariance, either caused by the final breakup of Gondwana and/or by climatic deterioration, among which are molluscs (Beu, 2009; Göbbeler and Klussmann-Kolb, 2010; Williams et al., 2003),

echinoderms (Lee et al., 2004), penguins (Baker et al., 2006), notothenioid fishes (Bargelloni et al., 2000; Near, 2004) and amphipods (**CHAPTERS 4** and **5**).

Since the final breakup of Gondwana, the Antarctic shelf fauna is well isolated from other oceans' shelves by great distances, deep seas and a marked thermal gradient at the APF (Clarke et al., 2005). However, many taxa still managed to disperse in and out of the Southern Ocean (e.g. Brandt et al., 2007; Krabbe et al., 2010; Page and Linse, 2002; Wilson et al., 2009). The ability to overcome these physical barriers mainly depends on the life history strategies (Thatje et al., 2005a). Pelagic adults or long-lived larvae might disperse within eddies transported out of the ACC or through the Antarctic Intermediate water [see General Introduction 5.1.]. The ability of benthic organisms (with short-lived pelagic larvae or brooding their young) to disperse in and/or out of Antarctica appears to be conditioned by their bathymetric range. Indeed, many deep-sea or highly eurybathic species are distributed on both sides of the APF (Havermans et al., 2013; Pawlowski et al., 2007; Raupach et al., 2007; Thornhill et al., 2008) and historical emergences (Schüller, 2011) or submergences (Held, 2000; Strugnell et al., 2008) did occur in the evolutionary history of some benthic lineages. On the other hand, benthic organisms thriving in the euphotic zone (from the coastline to about 70 m) might disperse by rafting on drifting kelp (Castilla and Guinez, 2000; Helmuth et al., 1994), or alternatively, pumices (O'Foighil et al., 1999). Long-distance dispersal on macroalgae might, for instance, explain the distributional range of a few shallow-water iphimediid species extending from the Antarctic to sub-Antarctic regions, as well as an historical dispersal event of *Labriphimedia pulchridentata* complex out of the Southern Ocean (**CHAPTER 5**). As Antarctic *Epimeria* species globally have deeper bathymetric ranges than iphimediids (Coleman, 2007) — although a few species are found in the sublittoral zone, e.g. *E. monodon* — passive rafting might not be an option for most of them. On the other hand, as known Antarctic *Epimeria* species are restricted to shelf and slope depths, their bathymetric range would not extend deep enough to disperse through the deep-sea (**CHAPTER 4**).

Even if dispersal in and/or out of the Antarctic region appears possible — as for some iphimediids (**CHAPTER 5**) — a restricted thermal tolerance is likely to be a limiting factor on the latitudinal range of these amphipods, as for many other cold-adapted Antarctic lineages. The thermal tolerance of epimeriid and iphimediid species has not been investigated. However, the origin and diversification of the (sub-)Antarctic lineages in a cooling environment, along with their presumed endemicity (**CHAPTERS 4** and **5**), suggest that they could be cold-adapted and relatively stenothermal. Amphipods are marine ectotherms, which are generally considered to be among the most stenothermal organisms on earth (Aronson et al., 2007; Peck and Conway, 2000). Living in cold and

oxygenated waters might result in slower physiological rates and growth, as well as a larger size of some Antarctic amphipods (Chapelle and Peck, 1999). Such characteristics would be detrimental in warmer waters, where lower oxygen content results in higher metabolic needs (Peck, 2002). A temperature increase is likely to limit their capacity to perform critical biological functions, such as locomotion and feeding (Pörtner et al., 2007).

6. DIVERSIFICATION PATTERNS

6.1. ANTARCTIC SPECIES FLOCKS?

Species-rich environments which remained isolated for a long period over geological time scales are home to species flocks. Originally, the definition of "species flocks" referred to very speciose clades (compared to non-endemic relatives), endemic to the region of interest (Greenwood, 1984). Under this definition, *in situ* radiations inferred for a wide variety of animal groups in ancient lakes such as lake Tanganyika (9–12 My old) and lake Baikal (~30 My old), but also on the Antarctic shelf (geological isolation since 30–40 My) have been qualified as species flocks (Lecointre et al., 2013; Martens, 1997; Schön and Martens, 2004).

"Species flock" is, however, an ill-defined concept, as depending on the authors, additional criteria were considered relevant or not. Some definitions imply that the observed diversity arose rapidly (Ribbink, 1984). Species flocks were often inferred to result from explosive radiation, i.e. (initial) very high rates of speciation (Fryer, 1991; Fryer et al., 1983; Kontula et al., 2003; Seehausen, 2000, 2002; Sherbakov et al., 1998; Sturmbauer et al., 2003). However, a high diversity can either be the result of one (or more) burst(s) of speciation punctuating a lower background rate or of a more gradual cladogenesis over a long period of time. According to some definitions, species flocks should also be characterized by high morphological and ecological diversity (Eastman and McCune, 2000; Lecointre et al., 2013), although this is often not directly measured but rather grossly evaluated. The latter two criteria, along with an early burst of diversification, were used because of an underlying assumption that species flocks result from adaptive radiations. Strong divergent natural and sexual selection in different environments can indeed result in rapid ecological divergence and speciation (termed ecological speciation) (Rundle and Nosil, 2005; Schluter, 2009).

However, divergences can also occur when distinct mutations arise and are fixed by chance in allopatric populations, adapting to similar selection pressures (Schluter, 2009). In such cases when environments differ only slightly, the process of speciation appears to be slower (Rundell and Price, 2009). However, the simultaneous formation of multiple geographical barriers could result in a

similar pattern of speciation burst (Kozak et al., 2006; Lovette and Bermingham, 1999). All in all, species flocks *sensu* Greenwood (1984) are likely to result from a combination of adaptive and non-adaptive processes (Rundell and Price, 2009; Schön and Martens, 2004).

Antarctic *Epimeria* and iphimediids evolved on the shelf since at least its geological isolation ~34 Ma, and possibly even earlier (**CHAPTERS 4** and **5**). Since Antarctic *Epimeria* species are monophyletic (**CHAPTER 4**), endemic and speciose — including the new Antarctic species from d'Udekem d'Acoz and Verheye (*in Press*) to the count, 66 % of all known *Epimeria* species are from the Southern Ocean — the lineage was qualified as a species flock (Lecointre et al., 2013). If the endemicity criterium is relaxed for secondary dispersals (Eastman and McCune, 2000; Lecointre et al., 2013), Antarctic iphimediids could be as well, as only a few species recently dispersed to sub-Antarctic regions and therefore, the initial radiation did occur on the Antarctic shelf. Based on the current taxonomic knowledge, Antarctic iphimediids represent 36 % of the worldwide species richness within the family. The adaptive and/or non-adaptive processes behind these two radiations and their relative contribution are not known. Some subclades of Antarctic iphimediids could be prone to rapid ecological speciation, regarding their possibly elevated diversification rate and inferred trophic specializations (**CHAPTER 5**). In contrast, *Epimeria* does not appear to present a high ecological specialization (although ecological data are scarce) and no diversification bursts were detected (**CHAPTER 4**). However, these are general remarks rather than inferences on the processes generating diversity, as morphological and ecological diversification patterns were not examined in regards to the lineage diversification patterns analyzed in **CHAPTERS 4** and **5** [see Future Directions].

Whereas the actual processes generating diversity need further investigations, two main events in Antarctica's climatic history could have been major influences:

6.2. Transition to the Icehouse and faunal turnover

The geological isolation of the Antarctic shelf and simultaneous onset of the cooling trend led to different possible outcomes for the Antarctic shelf benthos: migrate north and/or to greater depths, adapt or go extinct. Hence, the Late Gondwanan/early Antarctic environment was the theatre of a major faunal turnover, as visible in the fossil record: while many lineages went extinct, others flourished (Aronson et al., 2009; Berkman et al., 2004; Beu, 2009; Stilwell and Zinsmeister, 1992).

(Pre)adaptations to the new conditions (cold water temperatures and high seasonality in food regimes) were suggested to be at the root of the evolutionary success of amphipods in the Southern Ocean. Their brooding reproduction would be more advantageous to cope with the high seasonality of plankton productivity and its prolonged reduction during glacial maxima [see General Introduction

1.2.] (Brandt, 1999; Poulin et al., 2002). Pelagic larvae are indeed affected by the decreased salinity of surface waters during summer and, for the planktotrophic larvae, the short period of phytoplankton availability. In such food-depleted conditions, marine invertebrates should have a low reproductive output. Therefore, the K-strategy of amphipods (increase in parental investment, fewer offspring, slower growth rate, deferred maturity and greater longevity) would be favored (Brandt, 1999; Poulin and Feral, 1996). As mentioned before [section 5], probable adaptations to cold water likely participated in the evolutionary success of the Antarctic *Epimeria* and iphimediid lineages.

Climate-driven extinctions of durophagous predators allowed abundant populations of sessile epifaunal suspension-feeding organisms to establish (Aronson et al., 1997) [see General Introduction 4.3.]. Such dense assemblages increase microenvironmental heterogeneity and resource patchiness, providing ideal conditions for niche partitioning and specialization (Arntz et al., 1994). The increase in habitat complexity raises the number of species that can stably coexist, thereby potentially intensifying diversification (MacArthur and Levins, 1964; Schoener, 1974). As suspension-feeder assemblages constitute the habitat of a number of Antarctic epimeriids and iphimediids [see General Introduction 2.2.4. and 2.2.5.], their progressive establishment along the cooling trend likely participated in the evolutionary success of the latter amphipod lineages. Moreover, it has been hypothesized that, as amphipods occupy many niches taken by decapod crustaceans in other ecosystems (Dauby et al., 2001a, b; De Broyer et al., 2001; Nyssen et al., 2005), the extinction of many decapods during this transition period (Feldmann and Schweitzer, 2006) reduced the competition for the newly available ecological niches (Brandt, 1999).

Antarctic notothenioids, similarly to Antarctic *Epimeria* and iphimediids (**CHAPTERS 4** and **5**), possibly originated in the period spanning the transition to an Icehouse climate, as the estimates of these fishes' divergence time range from 29.8 to 56.9 Ma (Matschiner et al., 2011; Near, 2004, 2012). Iphimediids are rarely found in nothotenioids' stomachs, although nothotenioid fishes are the main predators of benthic amphipods (Dauby et al., 2003). It was suggested that the iphimediids' spinose and calcified body might offer some protection against heavy predation (Brandt, 1999). *Epimeria* species appear to be more frequently eaten by fishes, although their occurrence in stomach contents remains limited compared to non-armored eusiroids (Dauby et al., 2003). If the armored body form indeed offers some protection against heavy predation, Antarctic *Epimeria* and iphimediids might have been particularly competitive in the face of amphipod predators' radiation.

6.3. GLACIAL CYCLES AS A DIVERSITY PUMP?

After the MMCT, ice sheets repeatedly advanced on the shelf (Chow and Bart, 2003; O'Brien et al., 2004; Pollard and DeConto, 2009), and more extensively so in the Plio-Pleistocene period as the amplitude of glacial/interglacial cycles increased (Lisiecki and Raymo, 2007). During glacial maxima, part of the fauna might have survived *in situ* in ice-free shelf or slope refugia (Thatje et al., 2005b; Thatje et al., 2008) [see General Introduction 4.5.]. Isolation of small populations during long periods in such glacial refugia followed by deglaciation leaves distinct genomic signatures of bottlenecks and subsequent demographic expansions (Allcock and Strugnell, 2012). For less dispersive benthic species (lacking a pelagic stage), a slower post-glaciation recolonization of the shelf would allow for further genetic drift and therefore, possible allopatric speciation (Held, 2003; Held and Wägele, 2005; Thatje et al., 2005b). Range fragmentations during glacial maxima were hypothesized to act as a "diversity pump", enhancing diversification (Clarke and Crame, 1989, 2010; Clarke et al., 1992a).

Species divergences occurring in the Plio-Pleistocene period were often interpreted as climate-driven allopatric speciation (e.g. **CHAPTER 2**; Allcock et al., 2011; Baird et al., 2011; Wilson et al., 2009). However, an actual test of the diversity pump hypothesis would require inferences on past diversification dynamics of a wide range of taxa, aiming to potentially detect a generalized increase in speciation after the MMCT, possibly in the Plio-Pleistocene period. Previous to this study, such analysis had been done only once for an Antarctic organism. Pulses of lineage diversification were observed within Late Miocene to early Pliocene subclades of notothenioid fishes and were interpreted as climate-driven bursts of allopatric speciation (Near et al., 2012). No such post-MMCT diversification increase was detected in Antarctic *Epimeria* amphipods (**CHAPTER 4**). An elevated diversification rate might characterize one or two Antarctic iphimediid subclade(s), which originated in the Late Miocene to Pliocene. However, the amount of evidence for the latter rate shifts is dependent on the (unknown) taxon sampling and these results should therefore be further evaluated when additional data become available (**CHAPTER 5**). Moreover, clade-specific increases in diversification rates could also be driven by ecological opportunity, as suggested in **CHAPTER 5** for *Echiniphimedia*. Such diversification analyses are further complicated by probable repeated mass extinctions resulting from the destruction of benthic habitats during ice sheet advances on the shelf. A high turnover rate could indeed have eroded the signal of earlier diversification pulses (Phillimore and Price, 2008; Rabosky and Lovette, 2008; Ricklefs and Jønsson, 2014; Weir, 2006). In conclusion, "glacial cycles as a diversity pump" remains an often cited, yet untested, hypothesis.

FUTURE DIRECTIONS

PHYLOGENY OF AMPHIPODA

Phylogenetic relationships across species separated by hundreds of millions of years are difficult to infer based on a few genetic markers, as such a long time potentially allowed for multiple parallel substitutions among branches (possibly causing LBA problems such as in **CHAPTER 1**), as well as multiple substitutions at the sites containing the original phylogenetic signal (saturation). Using both an increased taxon sampling and an increased number of conserved loci for phylogenetic reconstruction should help to overcome these issues. Recently developed next-generation sequencing techniques (NGS) enable the production of thousands or millions of sequences in one run (Metzker, 2010). The "targeted enrichment" approach aims to enrich the DNA libraries with specific genomic targets (Mamanova et al., 2010). For deep phylogenies, ultraconserved genomic elements (UCEs) can be targeted to enrich the library with thousands of orthologous loci across very distant species. This method has already enabled the reconstruction of well-resolved deep phylogenies of a variety of inclusive taxa (Faircloth et al., 2012; Lemmon et al., 2012; McCormack et al., 2012; Prum et al., 2015). Alternatively, the extraction of messenger RNA and sequencing of cDNA on an NGS platform (RNA-seq) has been used to produce hundreds of protein alignments that resolved deep phylogenetic relationships in different groups (Smith et al., 2011; Wickett et al., 2014). As widespread morphological convergences misled traditional classifications within Amphipoda, a well-resolved molecular phylogeny of the order (or at a less inclusive level, Eusiroidea) is needed to establish a phylogenetically-informed higher-level classification of amphipods and to better understand the evolution of morphological characters.

HIDDEN DIVERSITY

DNA-based species delimitation methods, used in combination with morphology, enabled a thorough reassessment of the diversity within Antarctic *Epimeria* (**CHAPTER 2** and **3**). DNA-based methods also suggested that cryptic (or pseudocryptic) diversity might be present within Antarctic iphimediids as well. However, these delimitations relied on the COI marker only (**CHAPTER 5**). It is recommended to use multiple complementary data types to delimit species, in an integrative taxonomic framework (Dayrat, 2005; Padial et al., 2010; Schlick-Steiner et al., 2010; Sites and Marshall, 2004). Therefore, in order to investigate the "hidden diversity" within Antarctic iphimediids, a more variable nuclear marker (than 28S) should be sequenced and other data types should be used in combination to these DNA-based delimitation results, e.g. morphological and/or ecological.

CONNECTIVITY ON THE ANTARCTIC SHELF

In the future, an increased taxon sampling within Antarctic *Epimeria* will surely improve the assessment of species' distributional ranges around the continent. Furthermore, as the present study gave a better overview of the species limits within the complexes (**CHAPTER 2**), along with formal morphological descriptions (**CHAPTER 3**; d'Udekem and Verheye, *in Press*), the species can now be readily identified and used in population-level studies. Some of the relatively widespread ones (e.g. *Epimeria* sp. nov. MA1, *E.* sp. nov. SI5*, E. macronyx, E. inermis, E. walkeri*) could be used as models to study the genetic connectivity between shelf locations all around the continent, in relation to potential barriers to gene flow (e.g. ocean currents, topographical constraints, habitat availability). Traditional population genetic markers (e.g. microsatellites, COI, CytB) could be used to infer the intraspecific genetic structure and levels of gene flow between populations, as it was done for other Antarctic amphipod species (Baird et al., 2011; Baird et al., 2012). Furthermore, NGS techniques such as RAD-seq (restriction site-associated DNA sequencing) and GBS (genotyping-by-sequencing) were used to identify and genotype thousands of genetic markers randomly distributed across the entire genome of a species (Davey and Blaxter, 2010; Davey et al., 2011) and could therefore potentially provide a wealth of informative data for population genetic analyses of selected *Epimeria* species.

ADAPTIVE RADIATION?

Numerous species flocks have been interpreted as adaptive radiations (e.g. Clarke and Johnston, 1996; Fryer, 1991; Turner, 2007), i.e. rapid accumulation of morphologically and ecologically distinct lineages resulting from an invasion into new niches. However, whether the observed burst of endemic diversification was accompanied by positive (diversifying) selection was infrequently tested (Naumenko et al., 2017). Methods based on a comparison of non-synonymous (i.e. changing the protein sequence, d_N) and synonymous (i.e. no change at the protein level, d_S) substitution rates of protein-coding genes can be used to this purpose, as adaptive selection is expected to inflate this ratio ($d_N / d_S > 1$) (Murrell et al., 2012, 2015; Smith et al., 2015; Yang, 2007). RNA next-generation sequencing methods can be used to obtain the sequences of a high number of coding genes from whole-transcriptome datasets (Chu and Corey, 2012). It can then be investigated if the frequency of episodes of positive selection is elevated for the radiating lineage compared to non-radiating sister lineages or during a time period of increased diversification rate (Naumenko et al., 2017). If the inferred elevated diversification rates in some iphimediid subclades (**CHAPTER 5**) are confirmed, it could be

investigated if their radiation was accompanied by frequent episodes of positive (diversifying) selection.

An adaptive radiation is the evolution of ecomorphological diversity within a rapidly multiplying lineage (Schluter, 2000). Another way to investigate whether an observed lineage diversification burst is (at least partly) the result of adaptive processes would be to analyze the rates of phenotypic diversification in the rapidly multiplying clade compared to sister clades (e.g. Lee et al., 2016; Rabosky and Adams, 2012; Rabosky et al., 2013). Similarly to the analyses of lineage diversification dynamics performed in **CHAPTERS 4** and **5**, the rate of phenotypic diversification (for continuous traits) can be estimated along the phylogeny and eventual shifts in diversification regimes inferred (Rabosky, 2014). A potential correlation between lineage and phenotypic diversification rates can be tested (Rabosky et al., 2013). A number of continuous and potentially functional traits (related to feeding and/or locomotion) could be selected and measured for Antarctic iphimediid species of Fig. 3 in **CHAPTER 5.** If the inferred elevated lineage diversification rates in some iphimediid subclades are confirmed, it could be investigated if these are correlated with significantly elevated phenotypic diversification rates.

GLACIAL CYCLES

The isolation of populations in refugia during glacial maxima leaves distinct genetic signatures depending on the dispersal ability of the species and whether population(s) survived in one shelf refugium, multiple shelf refugia or the deep-sea (Allcock and Strugnell, 2012). For instance, a "star-like" pattern of the haplotype network is indicative of a bottleneck event followed by population expansion and rapid recolonization of the shelf for a good disperser (Allcock and Strugnell, 2012; Slatkin and Hudson, 1991). The haplotype network of selected markers (e.g. COI, IT2, CytB) could be reconstructed for some epimeriid and/or iphimediid species in order to investigate these patterns. Moreover, historical fluctuations in population size can be examined and their timing estimated, in order to eventually detect a sudden population expansion following deglaciation (Drummond et al., 2005; Rogers and Harpending, 1992; Schneider and Excoffier, 1999).

SUMMARY

The physical isolation of the Antarctic shelf and extreme life conditions contribute to its high degree of endemism. The shelf fauna would, however, be composed of Gondwanan descendants, but also of more recent colonizers. Extreme temperature changes along the climatic history of this region led to the extinction of some lineages, while others flourished. Using molecular phylogenetic methods, this thesis aims to contribute to the general understanding of the evolutionary processes — extinctions, dispersals and *in situ* diversifications — shaping the biodiversity and geographical distributions of Antarctic amphipods of the families Epimeriidae (genus *Epimeria*) and Iphimediidae. The systematics of the superfamily presumably including the latter two model families, Eusiroidea, is first revised. Secondly, species boundaries within *Epimeria* are investigated by using a combination of DNA-based species delimitation methods and morphological descriptions, to ultimately reassess the geographical distribution of species. Finally, the origin of Antarctic lineages, dispersals in/out of the Antarctic shelf and *in situ* diversifications of both *Epimeria* and iphimediids are explored, using time-calibrated phylogenies. The systematic study of Eusiroidea indicates that at least species belonging to 14 families, including Epimeriidae and Iphimediidae, should be included in a phylogenetically meaningful delimitation of the superfamily. The species richness within *Epimeria* is greatly underestimated as most nominal species appear to be complexes of geographically restricted pseudocryptic species. The monophyly of Antarctic *Epimeria* and (sub-)Antarctic iphimediids suggests that both lineages evolved in isolation since their origin. They likely arose from late Gondwanan ancestors and hence, did not colonize Antarctica after it broke apart from other Gondwanan fragments. Moreover, the initial diversification of these two clades would be related to cold waters.

RÉSUMÉ

En raison de l'isolement physique et des conditions environnementales extrêmes du plateau continental antarctique, la faune marine benthique de cette région présente de hauts degrés d'endémisme. Elle serait composée à la fois de descendants d'ancêtres gondwaniens, mais également de colonisateurs plus récents. Les changements extrêmes de température tout au long de l'histoire climatique de la région antarctique ont mené à l'extinction de certaines lignées, tandis que d'autres ont pu s'adapter aux nouvelles conditions et se diversifier. Par l'utilisation de méthodes de phylogénie moléculaire, cette thèse de doctorat vise à contribuer à la compréhension globale des processus évolutifs — extinctions, dispersions et diversifications *in situ* — qui ont façonné la biodiversité et les distributions géographiques actuelles de deux familles d'amphipodes, les Epimeriidae (genre *Epimeria*) et Iphimediidae. Dans un premier temps, la systématique de la superfamille incluant potentiellement ces deux familles modèles, Eusiroidea, est révisée. Ensuite, la diversité spécifique au sein du genre *Epimeria* est réévaluée par une combinaison de méthodes de délimitation d'espèces basées sur l'ADN et de descriptions morphologiques, pour ensuite redéfinir les distributions géographique des espèces. Finalement, l'origine des lignées antarctiques, d'éventuelles dispersions dans et en dehors d'Antarctique et les patterns de diversifications *in situ* au sein des deux familles modèles sont inférés sur base de phylogénies calibrées dans le temps. L'étude systématique des Eusiroidea démontre que des espèces appartenant à au moins 14 familles différentes, y compris les Epimeriidae et Iphimediidae, devraient être inclues dans une superfamille monophylétique. Cette étude démontre que la richesse spécifique au sein d'*Epimeria* est largement sous-estimée. En effet, la plupart des espèces nominales seraient en réalité des complexes d'espèces pseudocryptiques à distribution géographique restreinte. La monophylie des *Epimeria* antarctiques d'une part, et des Iphimediidae (sub-)antarctiques d'autre part, suggère que ces deux lignées ont évolué en isolement depuis leur origine. Elles descendraient directement d'ancêtres gondwaniens et n'auraient donc pas colonisé la région antarctique après sa séparation des autres fragments du Gondwana. De plus, la diversification initiale de ces deux clades serait liée au refroidissement progressif de la région antarctique.

REFERENCES

A

Abouheif, E., Zardoya, R., Meyer, A., 1998. Limitations of metazoan 18S rRNA sequence data: implications for reconstructing a phylogeny of the animal kingdom and inferring the reality of the Cambrian explosion. Journal of Molecular Evolution 47, 394-405.

Allcock, A.L., Barratt, I., Eléaume, M., Linse, K., Norman, M.D., Smith, P.J., Steinke, D., Stevens, D.W., Strugnell, J.M., 2011. Cryptic speciation and the circumpolarity debate: A case study on endemic Southern Ocean octopuses using the COI barcode of life. Deep-Sea Research Part II: Topical Studies in Oceanography 58, 242-249.

Allcock, A.L., Strugnell, J.M., 2012. Southern Ocean diversity: new paradigms from molecular ecology. Trends in Ecology & Evolution 27, 520-528.

Amsler, M.O., McClintock, J.B., Amsler, C.D., Angus, R.A., Baker, B.J., 2009. An evaluation of sponge-associated amphipods from the Antarctic Peninsula. Antarctic Science 21, 579-589.

Anderson, F.E., Swofford, D.L., 2004. Should we be worried about long-branch attraction in real data sets? Investigations using metazoan 18S rDNA. Molecular Phylogenetics and Evolution 33, 440-451.

Anderson, J.B., Shipp, S.S., Lowe, A.L., Wellner, J.S., Mosola, A.B., 2002. The Antarctic ice sheet during the Last Glacial Maximum and its subsequent retreat history: a review. Quaternary Science Reviews 21, 49-70.

Angel, M.V., 1997. Pelagic biodiversity. In: Ormond, R.F.G., Gage, J.D., Angel, M.V. (Eds.), Marine biodiversity: patterns and processes. Cambridge University Press, Gran Bretana, pp. 35-68.

Antezana, T., 1999. Plankton of southern chilean fjords: trends and linkages. Scientia Marina 63, 69-80.

Arango, C.P., Soler-Membrives, A., Miller, K.J., 2011. Genetic differentiation in the circum-Antarctic sea spider *Nymphon australe* (Pycnogonida; Nymphonidae). Deep-Sea Research Part II: Topical Studies in Oceanography 58, 212-219.

Arntz, W., Brey, T., Gallardo, V.A., 1994. Antarctic zoobenthos. Oceanography and Marine Biology 32, 241-304.

Arntz, W., Gutt, J., Klages, M., 1997. Antarctic marine biodiversity: an overview. In: Battaglia, B., Valencia, J., Walton, D. (Eds.), Antarctic communities: proceedings of the 6th SCAR Biology Symposium. Cambridge University Press, Venice, pp. 3-14.

Arntz, W.E., Thatje, S., Gerdes, D., Gili, J.M., Gutt, J., Jacob, U., Montiel, A., Orejas, C., Teixido, N., 2005. The Antarctic-Magellan connection: macrobenthos ecology on the shelf and upper slope, a progress report. Scientia Marina 69, 237-269.

Aronson, R.B., Blake, D.B., 2001. Global climate change and the origin of modern benthic communities in Antarctica. American Zoologist 41, 27-39.

Aronson, R.B., Blake, D.B., Oji, T., 1997. Retrograde community structure in the late Eocene of Antarctica. Geology 25, 903-906.

Aronson, R.B., Moody, R.M., Ivany, L.C., Blake, D.B., Werner, J.E., Glass, A., 2009. Climate change and trophic response of the Antarctic bottom fauna. PloS one 4, e4385.

Aronson, R.B., Thatje, S., Clarke, A., Peck, L.S., Blake, D.B., Wilga, C.D., Seibel, B.A., 2007. Climate change and invasibility of the Antarctic benthos. Annual Review of Ecology, Evolution and Systematics 38, 129-154.

B

Baird, H.P., Miller, K.J., Stark, J.S., 2011. Evidence of hidden biodiversity, ongoing speciation and diverse patterns of genetic structure in giant Antarctic amphipods. Molecular Ecology 20, 3439-3454.

Baird, H.P., Miller, K.J., Stark, J.S., 2012. Genetic population structure in the Antarctic benthos: insights from the widespread amphipod, *Orchomenella franklini*. PloS one 7, e34363.

Baker, A.J., Pereira, S.L., Haddrath, O.P., Edge, K.-A., 2006. Multiple gene evidence for expansion of extant penguins out of Antarctica due to global cooling. Proceedings of the Royal Society of London B: Biological Sciences 273, 11-17.

Barber, H.N., Dadswell, H.E., Ingle, H.D., 1959. Transport of driftwood from South America to Tasmania and Macquarie Island. Nature 184, 203-204.

Bargelloni, L., Marcato, S., Zane, L., Patarnello, T., 2000. Mitochondrial phylogeny of notothenioids: a molecular approach to Antarctic fish evolution and biogeography. Systematic Biology 49, 114-129.

Barker, F.K., Lutzoni, F.M., 2002. The utility of the Incongruence length Difference Test. Systematic Biology 51, 625-637.

Barker, P.F., 2001. Scotia Sea regional tectonic evolution: implications for mantle flow and palaeocirculation. Earth-Science Reviews 55, 1-39.

Barker, P.F., Filippelli, G.M., Florindo, F., Martin, E.E., Scher, H.D., 2007. Onset and role of the Antarctic Circumpolar Current. Deep-Sea Research Part II: Topical Studies in Oceanography 54, 2388-2398.

Barnard, J., 1961. Gammaridean Amphipoda from depths of 400 to 6000 meters. Galathea Report 5, 23-128.

Barnard, J.L., 1964. Revision of some families, genera and species of gammaridean Amphipoda. Crustaceana 7, 49-74.

Barnard, J.L., 1969. The families and genera of marine gammaridean Amphipoda. Smithsonian Institution Press, Washington.

Barnard, J.L., 1989. Rectification of *Halirages regis* and *H. huxleyanus* (Crustacea: Amphipoda), from marine Antarctica, with description of a new genus, *Austroregia.* Proceedings of the Biological Society of Washington 102, 701-715.

Barnard, J.L., Barnard, C.M., 1983. Freshwater Amphipoda of the World. I. Evolutionary Patterns. Hayfield Associates, Mt. Vernon, Virginia.

Barnard, J.L., Karaman, G.S., 1975. The higher classification in amphipods. Crustaceana 28, 304-310.

Barnard, J.L., Karaman, G.S., 1984. Australia as a major evolutionary centre for Amphipoda (Crustacea). In: Lowry, J.K. (Ed.), Papers from the conference on the biology and evolution of Crustacea. Australian Museum Memoir 18. Australian Museum, Sydney, pp. 45-61.

Barnard, J.L., Karaman, G.S., 1991. The families and genera of marine gammaridean Amphipoda (except marine gammaroids). Records of the Australian Museum Suppl.13, 1-866.

Barnard, K.H., 1931. On new genera and species of amphipod Crustacea. Taylor and Francis, London.

Barnard, K.H., 1932. Amphipoda. Discovery Reports. University Press, Cambridge.

Barnes, D.K.A., Hodgson, D.A., Convey, P., Allen, C.S., Clarke, A., 2006. Incursion and excursion of Antarctic biota: past, present and future. Global Ecology and Biogeography 15, 121-142.

Barrett, P.J., 1996. Antarctic palaeoenvironment through Cenozoic times - a review. Terra Antarctica 3, 103-119.

Barthel, D., Gutt, J., 1992. Sponge associations in the eastern Weddell Sea. Antarctic Science 4, 137-150.

Beaman, R.J., Harris, P.T., 2003. Seafloor morphology and acoustic facies of the George V Land shelf. Deep-Sea Research Part II: Topical Studies in Oceanography 50, 1343-1355.

Bellan-Santini, D., 1999. Traité de zoologie: anatomie, systématique, biologie. Crustacés péracarides. Mémoires de l'Institut océanographique, Monaco, pp. 93-176.

Benton, M.J., Emerson, B.C., 2007. How did life become so diverse? The dynamics of diversification according to the fossil record and molecular phylogenetics. Palaeontology 50, 23-40.

Berge, J., Boxshall, G., Vader, W., 2000. Cladistic analysis of the Amphipoda, with special emphasis on the origin of the Stegocephalidae. Polskie Archiwum Hydrobiologii 47, 379-400.

Berge, J., Vader, W., Coleman, O., 1999. A cladistic analysis of the amphipod families Ochlesidae and Odiidae, with description of a new species and genus. In: Carel von Vaupel Klein, J. (Ed.), The Biodiversity Crisis and Crustacea - Proceedings of the Fourth International Crustacean Congress. CRC Press, Leiden, pp. 239-265.

Bergsten, J., 2005. A review of long-branch attraction. Cladistics 21, 163-193.

Berkman, P.A., Cattaneo-Vietti, R., Chiantore, M., Howard-Williams, C., 2004. Polar emergence and the influence of increased sea-ice extent on the Cenozoic biogeography of pectinid molluscs in Antarctic coastal areas. Deep-Sea Research Part II: Topical Studies in Oceanography 51, 1839-1855.

Beu, A.G., 2009. Before the ice: Biogeography of Antarctic Paleogene molluscan faunas. Palaeogeography, Palaeoclimatology, Palaeoecology 284, 191-226.

Bickford, *et al.*, 2007. Cryptic species as a window on diversity and conservation. Trends in Ecology and Evolution 22, 148-155.

Birstein, A.J., Vinogradov, E.M., 1958. Pelagic amphipods (Amphipoda, Gammaridea) of the northwestern part of the Pacific Ocean. Trudy Inst. Okcanol. Akad. Nauk. SSSR 27, 219-257.

Boersma, A., Silva, I.P., Shackleton, N.J., 1987. Atlantic Eocene planktonic foraminiferal paleohydrographic indicators and stable isotope paleoceanography. Paleoceanography 2, 287-331.

Bohaty, S.M., Zachos, J.C., 2003. Significant Southern Ocean warming event in the late middle Eocene. Geology 31, 1017-1020.

Bouckaert, R., *et al*., 2014. BEAST 2: a software platform for Bayesian evolutionary analysis. PLoS Computational Biology 10, e1003537.

Bouckaert, R.R., Drummond, A.J., 2015. bModelTest: Bayesian phylogenetic site model averaging and model comparison. BMC Evolutionary Biology 17, 42.

Bousfield, E.L., 1977. A new look at the systematics of gammaroidean amphipods of the world. Crustaceana Suppl.4, 282-316.

Bousfield, E.L., 1978. A revised classification and phylogeny of amphipod crustaceans. Royal Society of Canada, Ottawa.

Bousfield, E.L., 1983. An updated phyletic classification and paleohistory of the Amphipoda. In: Shram, F.R. (Ed.), Crustacean Phylogeny. Crustacean Issues 1, Balkema, Rotterdam.

Bousfield, E.L., Hendrycks, E.A., 1994a. The amphipod superfamily Leucothoidea on the Pacific coast of North America. Family Pleustidae: Subfamily Pleustinae. Systematics and Biogeography. Amphipacifica 1, 3-69.

Bousfield, E.L., Hendrycks, E.A., 1994b. A revision of the family Pleustidae (Crustacea: Amphipoda: Leucothoidea). Part 1. Systematics and biogeography of component subfamilies. Amphipacifica 1, 17-57.

Bousfield, E.L., Hendrycks, E.A., 1995a. The amphipod family Pleustidae on the Pacific coast of North America. Part III. Subfamilies Parapleustinae, Dactylopleustinae and Pleusirinae: Systematics and Distributional Ecology. Amphipacifica 2, 65-133.

Bousfield, E.L., Hendrycks, E.A., 1995b. The amphipod superfamily Eusiroidea in the North American Pacific region. I. Family Eusiridae: systematics and distributional ecology. Amphipacifica 1, 3-59.

Bousfield, E.L., Shih, C.-t., 1994. The phyletic classification of amphipod crustaceans: problems in resolution. Amphipacifica 1, 76-134.

Bowman, T.E., Gruner, H.E., 1973. The families and genera of Hyperiidea (Crustacea: Amphipoda). Smithsonian Contributions to Zoology 146, 1-64.

Brandt, A., 1992. Origin of Antarctic Isopoda (Crustacea, Malacostraca). Marine Biology 113, 415-423.

Brandt, A., 1999. On the origin and evolution of Antarctic Peracarida (Crustacea, Malacostraca). Scientia Marina 63, 261-274.

Brandt, A., *et al.*, 2007. First insights into the biodiversity and biogeography of the Southern Ocean deep-sea. Nature 447, 307-311.

Brandt, A., Gutt, J., 2011. Biodiversity of a unique environment: the Southern Ocean benthos shaped and threatened by climate change. In: Zachos, F.E., Habel, J.C. (Eds.), Biodiversity Hotspots: distribution and protection of conservation priority area. Springer, Berlin, pp. 503-526.

Brasier, M.J., Wiklund, H., Neal, L., Jeffreys, R., Linse, K., Ruhl, H., Glover, A.G., 2016. DNA barcoding uncovers cryptic diversity in 50% of deep-sea Antarctic polychaetes. Royal Society Open Science 3, 1-21.

Brey, T., Dahm, C., Gorny, M., Klages, M., Stiller, M., Arntz, W.E., 1996. Do Antarctic benthic invertebrates show an extended level of eurybathy? Antarctic Science 8, 3-6.

Briggs, D.E., Kear, A.J., 1994. Decay and mineralization of shrimps. Palaios 9, 431.

Briggs, D.E., Wilby, P.R., 1996. The role of the calcium carbonate-calcium phosphate switch in the mineralization of soft-bodied fossils. Journal of the Geological Society 153, 665-668.

Briggs, J.C., 2003. Marine centres of origin as evolutionary engines. Journal of Biogeography 30, 1-18.

Brown, B., Gaina, C., Dietmar Müller, R., 2006. Circum-Antarctic palaeobathymetry: illustrated examples from Cenozoic to recent times. Palaeogeography, Palaeoclimatology, Palaeoecology 231, 158-168.

Browne, W.E., Haddock, S.H., Martindale, M.Q., 2007. Phylogenetic analysis of lineage relationships among hyperiid amphipods as revealed by examination of the mitochondrial gene, cytochrome oxidase I (COI). Integrative and comparative biology 47, 815-830.

Burnham, K.P., Anderson, D.R., 2002. Model selection and multimodel inference: a practical information theroretical approach, second edition. Springer-Verlag, New York.

C

Carstens, B.C., Pelletier, T.A., Reid, N.M., Satler, J.D., 2013. How to fail at species delimitation. Molecular Ecology 22, 4369-4383.

Castilla, J.C., Guinez, R., 2000. Disjoint geographical distribution of intertidal and nearshore benthic invertebrates in the Southern Hemisphere. Revista chilena de historia natural 73, 585-603.

Cavalieri, D.J., Parkinson, C.L., 2008. Antarctic sea ice variability and trends, 1979–2006. Journal of Geophysical Research: Oceans 113, 1-19.

Chapelle, G., Peck, L.S., 1999. Polar gigantism dictated by oxygen availability. Nature 399, 114-115.

Chow, J.M., Bart, P.J., 2003. West Antarctic Ice Sheet grounding events on the Ross Sea outer continental shelf during the middle Miocene. Palaeogeography, Palaeoclimatology, Palaeoecology 198, 169-186.

Chu, Y., Corey, D.R., 2012. RNA sequencing: platform selection, experimental design, and data interpretation. Nucleic acid therapeutics 22, 271-274.

Clarke, A., 1988. Seasonality in the Antarctic marine environment. Comparative Biochemistry and Physiology Part B: Comparative Biochemistry 90, 461-473.

Clarke, A., 2003. Costs and consequences of evolutionary temperature adaptation. Trends in Ecology & Evolution 18, 573-581.

Clarke, A., 2008. Antarctic marine benthic diversity: patterns and processes. Journal of Experimental Marine Biology and Ecology 366, 48-55.

Clarke, A., Aronson, R.B., Crame, J.A., Gili, J.M., Blake, D.B., 2004. Evolution and diversity of the benthic fauna of the Southern Ocean continental shelf. Antarctic Science 16, 559-568.

Clarke, A., Barnes, D.K.A., Hodgson, D.A., 2005. How isolated is Antarctica? Trends in Ecology & Evolution 20, 1-3.

Clarke, A., Crame, J.A., 1989. The origin of the Southern Ocean marine fauna. In: Crame, J.A. (Ed.), Origin and evolution of the Antarctic biota. Geological Society of London Special Publication, London, pp. 253-268.

Clarke, A., Crame, J.A., 1997. Diversity, latitude and time: patterns in the shallow sea. In: Ormond, R.F.G., Gage, J.D., Angel, M.V. (Eds.), Marine Biodiversity: patterns and processes. Cambridge University Press, Cambridge, pp. 122-147.

Clarke, A., Crame, J.A., 2010. Evolutionary dynamics at high latitudes: speciation and extinction in polar marine faunas. Philosophical Transactions of the Royal Society B: Biological Sciences 365, 3655-3666.

Clarke, A., Crame, J.A., Stromberg, J.-O., Barker, P.F., 1992a. The Southern Ocean benthic fauna and climate change: a historical perspective [and discussion]. Philosophical Transactions of the Royal Society of London. Series B: Biological Sciences 338, 299-309.

Clarke, A., Crame, J.A., Stromberg, J.O., Barker, P.F., 1992b. The Southern Ocean benthic fauna and climate change: a historical perspective [and discussion]. Philosophical Transactions: Biological Sciences 338, 299-309.

Clarke, A., Griffiths, H.J., Barnes, D.K.A., Meredith, M.P., Grant, S.M., 2009. Spatial variation in seabed temperatures in the Southern Ocean: implications for benthic ecology and biogeography. Journal of Geophysical Research: Biogeosciences 114, 1-11.

Clarke, A., Johnston, I.A., 1996. Evolution and adaptive radiation of Antarctic fishes. Trends in Ecology & Evolution 11, 212-218.

Clarke, A., Johnston, N.M., 2003. Antarctic marine benthic diversity. In: Gibson, R.N., Atkinson, R.J.A. (Eds.), Oceanography and marine biology: an annual review. Taylor & Francis, London, pp. 47-114.

Clarke, A., Leakey, R.J.G., 1996. The seasonal cycle of phytoplankton, macronutrients and the microbial community in a nearshore Antarctic marine ecosystem. Limnology and Oceanography 41, 1281-1294.

Cochrane, G.R., De Santis, L., Cooper, A.K., 1995. Seismic velocity expression of glacial sedimentary rocks beneath the Ross Sea from sonobuoy seismic-refraction data. Geology and Seismic Stratigraphy of the Antarctic Margin 68, 261-270.

Coleman, C.O., 1989a. *Gnathiphimedia mandibularis* KH Barnard, 1930, an Antarctic amphipod (Acanthonotozomatidae, Crustacea) feeding on Bryozoa. Antarctic Science 1, 343-344.

Coleman, C.O., 1989b. On the nutrition of two Antarctic Acanthonotozomatidae (Crustacea: Amphipoda). Polar Biology 9, 287-294.

Coleman, C.O., 1991. Comparative fore-gut morphology of Antarctic Amphipoda (Crustacea) adapted to different food sources. Hydrobiologia 223, 1-9.

Coleman, C.O., 1994. A new *Epimeria* species (Crustacea: Amphipoda: Epimeriidae) and redescriptions of three other species in the genus from the Antarctic Ocean. Journal of Natural History 28, 555-576.

Coleman, C.O., 2003. “Digital inking”: how to make perfect line drawings on computers. Organisms Diversity & Evolution 3, 303-304.

Coleman, C.O., 2004. Aquatic amphipods (Crustacea: Amphipoda: Crangonyctidae) in three pieces of Baltic amber. Organisms Diversity & Evolution Electr. Suppl. 3, 1-7.

Coleman, C.O., 2009. Drawing setae the digital way. Zoosystematics and Evolution 85, 305-310.

Coleman, C.O., Barnard, J.L., 1991. Revision of Iphimediidae and similar families (Amphipoda: Gammaridea). Proceedings of the Biological Society of Washington 104, 253-268.

Coleman, C.O., Lowry, J.K., 2006. Revision of the Ochlesidae sensu stricto, inlcuding five new Australian species (Crustacea: Amphipoda). Organisms Diversity & Evolution 6, 1-57.

Coleman, C.O., Myers, A.A., 2000. New Amphipoda from Baltic amber. Polskie Archiwum Hydrobiologii 47, 457-464.

Coleman, C.O., Ruffo, S., 2002. Another discovery of a niphargid amphipod (Crustacea) in Baltic amber. Geologisch-Paläontologischen Institut der Universität Hamburg 86, 239-244.

Coleman, O., 2006. An amphipod of the genus *Synurella* Wrzesniowski, 1877 (Crustacea, Amphipoda, Crangonyctidae) found in Baltic amber. Organisms Diversity & Evolution 6, 103-108.

Coleman, O.C., 2007. Synopsis of the Amphipoda of the Southern Ocean. Bulletin de l'Institut Royal des Sciences Naturelles de Belgique 77 Suppl.2, 1-134.

Colgan, D.J., McLauchlan, A., Wilson, G.D.F., Livingston, S.P., Edgecombe, G.D., 1998. Histone H3 and U2 snRNA DNA sequences and arthropod molecular evolution. Australian Journal of Zoology 46, 419-437.

Condamine, F.L., Rolland, J., Morlon, H., 2013. Macroevolutionary perspectives to environmental change. Ecology Letters 16, 72-85.

Convey, P., Stevens, M.I., Hodgson, D.A., Smellie, J.L., Hillenbrand, C.-D., Barnes, D.K.A., Clarke, A., Pugh, P.J.A., Linse, K., Cary, S.C., 2009. Exploring biological constraints on the glacial history of Antarctica. Quaternary Science Reviews 28, 3035-3048.

Coombs, D.S., Landis, C.A., 1966. Pumice from the South Sandwich eruption of March 1962 reaches New Zealand. Nature 209, 289-290.

Coope, G.R., 2004. Several million years of stability among insect species because of, or in spite of, Ice Age climatic instability? Philosophical Transactions of the Royal Society of London.Series B, Biological sciences 359, 209-214.

Cooper, A.K., Barrett, P.J., Hinz, K., Traube, V., Letichenkov, G., Stagg, H.M.J., 1991. Cenozoic prograding sequences of the Antarctic continental margin: a record of glacio-eustatic and tectonic events. Marine Geology 102, 175-213.

Cooper, A.K.,*et al*., 2008. Chapter 5: Cenozoic climate history from seismic reflection and drilling studies on the Antarctic continental margin. In: Fabio, F., Martin, S. (Eds.), Developments in Earth and Environmental Sciences. Elsevier, The Netherlands, pp. 115-234.

Corrigan, L.J., Horton, T., Fotherby, H., White, T.A., Hoelzel, A.R., 2014. Adaptive evolution of deep-sea amphipods from the superfamily Lysiassanoidea in the North Atlantic. Evolutionary Biology 41, 154-165.

Costa, A., 1851. Fauna del Regno di Napoli (and) Catalogo de' Crostacei del Regno di Napoli. Catalogo dei Crostacei Italiani e di Molti Altri del Mediterraneo per Fr. Gugl. Hope. F. Azzolino, Napoli, pp. 1-48.

Coyer, J.A., Smith, G.J., Andersen, R.A., 2001. Evolution of *Macrocystis* spp. (Phaeophyceae) as determined by ITS1 and ITS2 sequences. Journal of Phycology 37, 574-585.

Crame, J.A., 1997. An evolutionary framework for the polar regions. Journal of Biogeography 24, 1-9.

Crame, J.A., 1999. An evolutionary perspective on marine faunal connections between southernmost South America and Antarctica. Scientia Marina 63, 1-14.

Crame, J.A., 2013. Early Cenozoic differentiation of polar marine faunas. PloS one 8, e54139.

Crame, J.A., Beu, A.G., Ineson, J.R., Francis, J.E., Whittle, R.J., Bowman, V.C., 2014. The early origin of the Antarctic marine fauna and its evolutionary implications. PloS one 9, e114743.

Cummings, M.P., Handley, S.A., Myers, D.S., Reed, D.L., Rokas, A., Winka, K., 2003. Comparing bootstrap and posterior probability values in the four-taxon case. Systematic Biology 52, 477-487.

Cummings, V.J., Thrush, S.F., Chiantore, M., Hewitt, J.E., Cattaneo-Vietti, R., 2010. Macrobenthic communities of the north-western Ross Sea shelf: links to depth, sediment characteristics and latitude. Antarctic Science 22, 793-804.

Cusimano, N., Stadler, T., Renner, S.S., 2012. A new method for handling missing species in diversification analysis applicable to randomly or nonrandomly sampled phylogenies. Systematic Biology 61, 785-792.

D

d'Udekem D'Acoz, C., Robert, H., 2008. The Expedition ANTARKTIS-XXIII/8 of the Research Vessel "Polarstern" in 2006/2007. In: Gutt, J. (Ed.), Berichte zur Polar- und Meeresforschung. Alfred Wegener Institute for Polar and Marine Research, Bremerhaven, pp. 48-56.

d'Udekem d'Acoz, C., Vader, W., 2004. Occurrence of *Paramphithoe buchholzi* Stebbing, 1888 in the Barents Sea (Crustacea, Amphipoda, Epimeriidae). Sarsia 89, 292-295.

d'Udekem D'Acoz, C., Verheye, M.L., *in press*. *Epimeria* of the Southern Ocean with notes on their relatives (Crustacea, Amphipoda, Eusiroidea). European Journal of Taxonomy.

Dahl, E., Emanuelsson, H., von Mecklenburg, C., 1970. Pheromone transport and reception in an amphipod. Science 170, 739-740.

Dalziel, I.W.D., Lawver, L.A., Norton, I.O., Gahagan, L.M., 2013a. The Scotia Arc: genesis, evolution, global significance. Annual Review of Earth and Planetary Sciences 41, 767-793.

Dalziel, I.W.D.,*et al.*, 2013b. A potential barrier to deep Antarctic circumpolar flow until the late Miocene? Geology 41, 947-950.

Darlu, P., Lecointre, G., 2002. When Does the Incongruence Length Difference Test Fail? Molecular Biology and Evolution 19, 432-437.

Darriba, D., Taboada, G.L., Doallo, R., Posada, D., 2012. jModelTest 2: more models, new heuristics and parallel computing. Nature Methods 9, 772.

Dauby, P., Nyssen, F., De Broyer, C., 2003. Amphipods as food sources for higher trophic levels in the Southern Ocean: a synthesis. In: Huiskes, A.H.L. (Ed.), Antarctic biology in a global context. Backhuys, Amsterdam, pp. 129-134.

Dauby, P., Scailteur, Y., Chapelle, G., De Broyer, C., 2001a. Potential impact of the main benthic amphipods on the eastern Weddell Sea shelf ecosystem (Antarctica). Polar Biology 24, 657-662.

Dauby, P., Scailteur, Y., De Broyer, C., 2001b. Trophic diversity within the eastern Weddell Sea amphipod community. Hydrobiologia 443, 69-86.

Davey, J.W., Blaxter, M.L., 2010. RADSeq: next-generation population genetics. Briefings in functional genomics 9, 416-423.

Davey, J.W., Hohenlohe, P.A., Etter, P.D., Boone, J.Q., Catchen, J.M., Blaxter, M.L., 2011. Genome-wide genetic marker discovery and genotyping using next-generation sequencing. Nature Reviews Genetics 12, 499-510.

David, B., Saucède, T., 2015. Biodiversity of the Southern Ocean. ISTE Press Ltd, London.

Dayrat, B., 2005. Towards integrative taxonomy. Biological Journal of the Linnean Society 85, 407-415.

Dayton, P.K., 1990. Polar benthos. In: Smith, W.J. (Ed.), Polar Oceanography, Part B: Chemistry, Biology and Geology. Academic Press, London, pp. 631-685.

Dayton, P.K., Robilliard, G.A., Paine, R.T., Dayton, L.B., 1974. Biological accommodation in the benthic community at McMurdo Sound, Antarctica. Ecological Monographs 44, 105-128.

De Broyer, C., Jażdżewska, A., 2014. Chapter 5.17. Biogeographic patterns of Southern Ocean benthic amphipods. In: De Broyer C., Koubbi P., Griffiths H., Raymond B., d'Udekem d'Acoz C. *et al.*(Eds.), Biogeographic Atlas of the Southern Ocean. Scientific Committee on Antarctic Research, Cambridge, pp. 155-165.

De Broyer, C., Jażdżewski, K., 1993. A checklist of the Amphipoda (Crustacea) of the Southern Ocean. Institut Royal des Sciences Naturelles de Belgique, Brussels.

De Broyer, C., Koubbi, P., 2014. Chapter 1.1. The biogeography of the Southern Ocean. In: De Broyer C., Koubbi P., Griffiths H., Raymond B., d'Udekem d'Acoz C. *et al.*(Eds.), Biogeographic atlas of the Southern Ocean. Committee on Antarctic Research, Cambridge, pp. 2-9.

De Broyer, C., Lowry, J.K., Jażdżewski, K., Robert, H., 2007. Synopsis of the Amphipoda of the Southern Ocean. Part 1. Catalogue of the Gammaridean and Corophiidean Amphipoda

(Crustacea) of the Southern Ocean with distribution and ecological data. Bulletin de l'Institut Royal des Sciences Naturelles de Belgique 77 Suppl.1, 1-325.

De Broyer, C., Nyssen, F., Dauby, P., 2004. The crustacean scavenger guild in Antarctic shelf, bathyal and abyssal communities. Deep-Sea Research Part II: Topical Studies in Oceanography 51, 1733-1752.

De Broyer, C., Scailteur, Y., Chapelle, G., Rauschert, M., 2001. Diversity of epibenthic habitats of gammaridean amphipods in the eastern Weddell Sea. Polar Biology 24, 744-753.

Deacon, G.E.R., 1982. Physical and biological zonation in the Southern Ocean. Deep-Sea Research Part A. Oceanographic Research Papers 29, 1-15.

DeConto, R.M., Pollard, D., 2003a. A coupled climate–ice sheet modeling approach to the early Cenozoic history of the Antarctic ice sheet. Palaeogeography, Palaeoclimatology, Palaeoecology 198, 39-52.

DeConto, R.M., Pollard, D., 2003b. Rapid Cenozoic glaciation of Antarctica induced by declining atmospheric CO_2. Nature 421, 245-249.

Dell, R.K., 1972. Antarctic benthos. Advanced Marine Biology 10, 1-216.

Denton, G.H., Hughes, T.J., 2002. Reconstructing the Antarctic ice sheet at the Last Glacial Maximum. Quaternary Science Reviews 21, 193-202.

Díaz, A., Féral, J.P., David, B., Saucède, T., Poulin, E., 2011. Evolutionary pathways among shallow and deep-sea echinoids of the genus *Sterechinus* in the Southern Ocean. Deep-Sea Research Part II: Topical Studies in Oceanography 58, 205-211.

Diekmann, B., Kuhn, G., Gersonde, R., Mackensen, A., 2004. Middle Eocene to early Miocene environmental changes in the sub-Antarctic Southern Ocean: evidence from biogenic and terrigenous depositional patterns at ODP Site 1090. Global and Planetary Change 40, 295-313.

Diester-Haass, L., Zahn, R., 1996. Eocene-Oligocene transition in the Southern Ocean: history of water mass circulation and biological productivity. Geology 24, 163-166.

Dietz, L., Arango, C.P., Dömel, J.S., Halanych, K.M., Harder, A.M., Held, C., Mahon, A.R., Mayer, C., Melzer, R.R., Rouse, G.W., Weis, A., Wilson, N.G., Leese, F., 2015. Regional differentiation and extensive hybridization between mitochondrial clades of the Southern Ocean giant sea spider *Colossendeis megalonyx*. Royal Society Open Science 2, 1-15.

Dolphin, K., Belshaw, R., Orme, C.D.L., Quicke, D.L.J., 2000. Noise and incongruence: interpreting results of the Incongruence Length Difference Test. Molecular Phylogenetics and Evolution 17, 401-406.

Domack, E., O'Brien, P., Harris, P., Taylor, F., Quilty, P.G., De Santis, L., Raker, B., 1998. Late Quaternary sediment facies in Prydz Bay, East Antarctica and their relationship to glacial advance onto the continental shelf. Antarctic Science 10, 236-246.

Dömel, J.S., Convey, P., Leese, F., 2015. Genetic data support independent glacial refugia and open ocean barriers to dispersal for the Southern Ocean sea spider *Austropallene cornigera* (Möbius, 1902). Journal of Crustacean Biology 35, 480-490.

Douglass, L.L., *et al.*, 2014. A hierarchical classification of benthic biodiversity and assessment of protected areas in the Southern Ocean. PloS one 9, e100551.

Drummond, A.J., Bouckaert, R.R., 2015. Bayesian evolutionary analysis wit BEAST. Cambridge University Press, Cambridge.

Drummond, A.J., Rambaut, A., Shapiro, B., Pybus, O.G., 2005. Bayesian coalescent inference of past population dynamics from molecular sequences. Molecular Biology and Evolution 22, 1185-1192.

E

Eagles, G., Livermore, R., Morris, P., 2006. Small basins in the Scotia Sea: the Eocene Drake Passage gateway. Earth and Planetary Science Letters 242, 343-353.

Eastman, J.T., Clarke, A., 1998. A comparison of adaptive radiations of Antarctic fish with those of non-Antarctic fish. In: di Prisco, G., Pisano, E., Clarke, A. (Eds.), Fishes of Antarctica: a biological overview. Springer-Verlag, Milan, pp. 3-26.

Eastman, J.T., McCune, A.R., 2000. Fishes on the Antarctic continental shelf: evolution of amarine species flock? Journal of Fish Biology 57, 84-102.

Edgar, G.J., Burton, H.R., 2000. The biogeography of shallow-water macrofauna at Heard Island. Papers and Proceedings of the Royal Society of Tasmania 133, 23-26.

Eldredge, L.G., Miller, S.E., 1994. How many species are there in Hawaii ? Bishop Museum Occasional Paper 41, 3-18.

Ence, D.D., Carstens, B.C., 2011. SpedeSTEM: a rapid and accurate method for species delimitation. Molecular Ecology Resources 11, 473-480.

Englisch, U., 2001. Analyse der Phylogenie der Amphipoda (Crustacea, Malacostraca) mit Hilfe von Sequenzen des Gens der RNA der kleinen ribosomalen Untereinheit. Ph.D. Dissertation. Fakultät für Biologie. Ruhr–Universität Bochum, Bochum, pp. 1-158.

Erixon, P., Svennblad, B., Britton, T., Oxelman, B., 2003. Reliability of Bayesian posterior probabilities and bootstrap frequencies in phylogenetics. Systematic Biology 52, 665-673.

Erwin, D.H., 2001. Lessons from the past: biotic recoveries from mass extinctions. Proceedings of the National Academy of Sciences 98, 5399-5403.

Erwin, D.H., 2008. Extinction as the loss of evolutionary history. Proceedings of the National Academy of Sciences 105, 11520-11527.

Exon, N., *et al.*, 2000. The opening of the Tasmanian Gateway drove global Cenozoic paleoclimatic and paleoceanographic changes; results of Leg 189. Affiliation (analytic): Australian Geological Survey Organisation, Canberra, A.C.T. 26, 11.

Ezard, T., Fujisawa, T., Barraclough, T.G., 2009. Splits: SPecies' LImits by Threshold Statistics. R package version 1.0-14/r31. http://R-Forge.R-project.org/projects/splits/.

F

Faircloth, B.C., McCormack, J.E., Crawford, N.G., Harvey, M.G., Brumfield, R.T., Glenn, T.C., 2012. Ultraconserved elements anchor thousands of genetic markers spanning multiple evolutionary timescales. Systematic biology 61, 717-726.

Farris, J.S., Källersjö, M., Kluge, A.G., Bult, C., 1995. Testing significance of incongruence. Cladistics 10, 315-319.

Feldmann, R.M., Schweitzer, C.E., 2006. Paleobiogeography of southern hemisphere decapod Crustacea. Journal of Paleontology 80, 83-103.

Fielding, *et al*., 2011. Sequence stratigraphy of the ANDRILL AND-2A drillcore, Antarctica: a long-term, ice-proximal record of Early to Mid-Miocene climate, sea-level and glacial dynamism. Palaeogeography, Palaeoclimatology, Palaeoecology 305, 337-351.

Flores, H., 2009. Frozen Desert Alive. The role of sea ice for pelagic macrofauna and its predators: implications for the Antarctic pack-ice food web. University of Groningen, Groningen.

Florindo, F., Roberts, A.P., 2005. Eocene-Oligocene magnetobiochronology of ODP Sites 689 and 690, Maud Rise, Weddell Sea, Antarctica. Geological Society of America Bulletin 117, 46-66.

Florindo, F., Siegert, M., 2008. Antarctic Climate Evolution. In: Fabio, F., Martin, S. (Eds.), Developments in Earth and Environmental Sciences. Elsevier B.V., The Netherlands, pp. 1-11.

Francis, J.E., *et al.*, 2008. Chapter 8: From Greenhouse to Icehouse – The Eocene/Oligocene in Antarctica. In: Fabio, F., Martin, S. (Eds.), Developments in Earth and Environmental Sciences. Elsevier B.V., The Netherlands, pp. 309-368.

Fraser, C.I., Nikula, R., Spencer, H.G., Waters, J.M., 2009. Kelp genes reveal effects of subantarctic sea ice during the Last Glacial Maximum. Proceedings of the National Academy of Sciences 106, 3249-3253.

Freckleton, R.P., Harvey, P.H., 2006. Detecting non-Brownian trait evolution in adaptive radiations. PLoS Biol 4, e373.

Frey, F.A., Weis, D., 1995. Temporal evolution of the Kerguelen plume: geochemical evidence from 38 to 82 Ma lavas forming the Ninetyeast Ridge. Contributions to Mineralogy and Petrology 121, 12-28.

Friedrich, M., Tautz, D., 1997. An episodic change of rDNA nucleotide substitution rate has occurred during the emergence of the insect order Diptera. Molecular Biology and Evolution 14, 644-653.

Fryer, G., 1991. Comparative aspects of adaptive radiation and speciation in Lake Baikal and the great rift lakes of Africa. Hydrobiologia 211, 137-146.

Fryer, G., Greenwood, P.H., Peake, J.F., 1983. Punctuated equilibria, morphological stasis and the palaeontological documentation of speciation: a biological appraisal of a case history in an African lake. Biological Journal of the Linnean Society 20, 195-205.

Fujisawa, T., Barraclough, T.G., 2013. Delimiting species using single-locus data and the Generalized Mixed Yule Coalescent approach: a revised method and evaluation on simulated data sets. Systematic Biology 62, 707-724.

Fujita, M.K., Leaché, A.D., Burbrink, F.T., McGuire, J.A., Moritz, C., 2012. Coalescent-based species delimitation in an integrative taxonomy. Trends in Ecology & Evolution 27, 480-488.

Funk, D.J., Omland, K.E., 2003. Species-level paraphyly and polyphyly: frequency, causes and consequences, with insights from animal mitochondrial DNA. Annual Review of Ecology, Evolution and Systematics 34, 397-423.

G

Gasca, R., Suárez-Morales, E., Haddock, S.H.D., 2007. Symbiotic associations between crustaceans and gelatinous zooplankton in deep and surface waters off California. Marine Biology 151, 233-242.

Gasson, E., DeConto, R.M., Pollard, D., Levy, R.H., 2016. Dynamic Antarctic ice sheet during the early to mid-Miocene. Proceedings of the National Academy of Sciences 113, 3459-3464.

Gavrilets, S., Losos, J.B., 2009. Adaptive radiation: contrasting theory with data. Science 323, 732-737.

Gibbons, A.D., Whittaker, J.M., Müller, R.D., 2013. The breakup of East Gondwana: assimilating constraints from Cretaceous ocean basins around India into a best-fit tectonic model. Journal of Geophysical Research: Solid Earth 118, 808-822.

Gili, J.-M., *et al.*, 2006. A unique assemblage of epibenthic sessile suspension feeders with archaic features in the high-Antarctic. Deep-Sea Research Part II: Topical Studies in Oceanography 53, 1029-1052.

Gill, A.E., Bryan, K., 1971. Effects of geometry on the circulation of a three-dimensional southern-hemisphere ocean model. Deep-Sea Research 18, 685-721.

Glor, R., 2010. Phylogenetic insights on adaptive radiation. Annual Review of Ecology, Evolution and Systematics 41, 251-270.

Glorioso, P., Piola, A.R., Leben, R.R., 2005. Mesoscale eddies in the Subantarctic Front - Southwest Atlantic. In: Arntz, W.E., Lovrich, G.A., Thatje, S. (Eds.), The Magellan-Antarctic connection: links and frontiers at high southern latitudes. Scientia Marina. Institut de Ciencies del Mar, CMIMA-CSIC, Barcelona, pp. 7-15.

Göbbeler, K., Klussmann-Kolb, A., 2010. Out of Antarctica? New insights into the phylogeny and biogeography of the Pleurobranchomorpha (Mollusca, Gastropoda). Molecular Phylogenetics and Evolution 55, 996-1007.

Graeve, M., Dauby, P., Scailteur, Y., 2001. Combined lipid, fatty acid and digestive tract content analyses: a penetrating approach to estimate feeding modes of Antarctic amphipods. Polar Biology 24, 853-862.

Grant, R.A., Griffiths, H.J., Steinke, D., Wadley, V., Linse, K., 2011. Antarctic DNA barcoding: a drop in the ocean? Polar Biology 34, 775-780.

Greenwood, P.H., 1984. What is a species flock? In: A. A. Echelle, I. Kornfield (Eds.), Evolution of fish species flocks. Orono Press, University of Maine, USA, pp. 13-19.

Griffiths, H.J., 2010. Antarctic marine biodiversity–what do we know about the distribution of life in the Southern Ocean? PloS one 5, e11683.

Griffiths, H.J., Barnes, D.K.A., Linse, K., 2009. Towards a generalized biogeography of the Southern Ocean benthos. Journal of Biogeography 36, 162-177.

Gutt, J., 2007. Antarctic macro-zoobenthic communities: a review and an ecological classification. Antarctic Science 19, 165-182.

Gutt, J., *et al.,* 2011. Biodiversity change after climate-induced ice-shelf collapse in the Antarctic. Deep-Sea Research Part II: Topical Studies in Oceanography 58, 74-83.

Gutt, J., Griffiths, H.J., Jones, C.D., 2013. Circumpolar overview and spatial heterogeneity of Antarctic macrobenthic communities. Marine Biodiversity 43, 481-487.

Gutt, J., Piepenburg, D., 2003. Scale-dependent impact on diversity of Antarctic benthos caused by grounding of icebergs. Marine Ecology Progress Series 253, 77-83.

Gutt, J., Schickan, T., 1998. Epibiotic relationships in the Antarctic benthos. Antarctic Science 10, 398-405.

Gutt, J., Sirenko, B.I., Smirnov, I.S., Arntz, W.E., 2004. How many macrozoobenthic species might inhabit the Antarctic shelf? Antarctic Science 16, 11-16.

H

Hall, R., Cottam, M.A., Wilson, M.E.J., 2011. The SE Asian gateway: history and tectonics of the Australia–Asia collision. Geological Society, London, Special Publications 355, 1-6.

Hambrey, M.J., Ehrmann, W.U., Larsen, B., 1991. Cenozoic glacial record of the Prydz Bay continental shelf, East Antarctica. In: Barron, J., Larsen, B. *et al.* (Eds.), Proceedings of the Ocean Drilling Program, Scientific results. Ocean Drilling Program, College Station, pp. 77-132.

Hambrey, M.J., McKelvey, B., 2000. Major Neogene fluctuations of the East Antarctic ice sheet: stratigraphic evidence from the Lambert Glacier region. Geology 28, 887-890.

Hamon, N., Sepulchre, P., Lefebvre, V., Ramstein, G., 2013. The role of eastern Tethys seaway closure in the Middle Miocene Climatic Transition (ca. 14 Ma). Climate of the Past 9, 2687-2702.

Hara, U., 2001. Bryozoans from the Eocene of Seymour Island Antarctic Peninsula. In: Gazdzicki, A. (Ed.), Palaeontological results of the polish Antarctic expeditions. Part III. Paleontologia Polonica, Poland, pp. 33-156.

Harbison, G.R., Biggs, D.C., Madin, L.P., 1977. The associations of Amphipoda Hyperiidea with gelatinous zooplankton—II. Associations with Cnidaria, Ctenophora and Radiolaria. Deep-Sea Research 24, 465-488.

Hauptvogel, D.W., 2015. The state of the Oligocene icehouse world: sedimentology, provenance, and stable isotopes of marine sediments from the Antarctic continental margin. CUNY Academic Works. City University of New York, New York, p. 217.

Hauptvogel, D.W., Passchier, S., 2012. Early–Middle Miocene (17–14 Ma) Antarctic ice dynamics reconstructed from the heavy mineral provenance in the AND-2A drill core, Ross Sea, Antarctica. Global and Planetary Change 82, 38-50.

Havermans, C., Nagy, Z.T., Sonet, G., De Broyer, C., Martin, P., 2011. DNA barcoding reveals new insights into the diversity of Antarctic species of *Orchomene*sensu lato (Crustacea: Amphipoda: Lysianassoidea). Deep-Sea Research Part II: Topical Studies in Oceanography 58, 230-241.

Havermans, C., *et al*., 2013. Genetic and morphological divergences in the cosmopolitan deep-sea amphipod *Eurythenes gryllus* reveal a diverse abyss and a bipolar Species. PloS one 8, e74218.

Hayward, P.J., Ryland, J.S., 1995. Handbook of the marine fauna of North-West Europe. Oxford University Press, Oxford, New York.

Heads, M., 2016. Biogeography and Evolution in New Zealand. CRC Press, Boca Raton.

Held, C., 2000. Phylogeny and biogeography of serolid isopods (Crustacea, Isopoda, Serolidae) and the use of ribosomal expansion segments in molecular systematics. Molecular Phylogenetics and Evolution 15, 165-178.

Held, C., 2003. Molecular evidence for cryptic speciation within the widespread Antarctic crustacean *Ceratoserolis trilobitoides* (Crustacea, Isopoda). In: A.H. Huiskes, W.W. Gieskes, R.M. Rozema, S.M. Schorno, S.M.Van der Viesand W.J. Wolff (Eds.), Antarctic biology in a global context. Proceedings of the VIIIth SCAR International Biology Symposium 2001. Backhuys Publishers, Amsterdam, pp. 135-139.

Held, C., 2014. Chapter 10.5. Phylogeography. In: De Broyer C., Koubbi P., Griffiths H., Raymond B., d'Udekem d'Acoz C., *et al.*(Eds.), Biogeographic atlas of the Southern Ocean. Scientific Committee on Antarctic Research, Cambridge, pp. 437-440.

Held, C., Wägele, J.-W., 2005. Cryptic speciation in the giant Antarctic isopod *Glyptonotus antarcticus* (Isopoda: Valvifera: Chaetiliidae). Scientia Marina 69, 175-181.

Helmuth, B., Veit, R.R., Holberton, R., 1994. Long-distance dispersal of a subantarctic brooding bivalve (*Gaimardia trapesina*) by kelp-rafting. Marine Biology 120, 421-426.

Hemery, L.G., *et al.*, 2012. Comprehensive sampling reveals circumpolarity and sympatry in seven mitochondrial lineages of the Southern Ocean crinoid species *Promachocrinus kerguelensis* (Echinodermata). Molecular Ecology 21, 2502-2518.

Heroy, D.C., Anderson, J.B., 2005. Ice-sheet extent of the Antarctic Peninsula region during the Last Glacial Maximum (LGM)—Insights from glacial geomorphology. Geological Society of America Bulletin 117, 1497-1512.

Hipp, A.L., Hall, J.C., Sytsma, K.J., 2004. Congruence versus phylogenetic accuracy: revisiting the Incongruence Length Difference test. Systematic Biology 53, 81-89.

Ho, S.Y.W., Saarma, U., Barnett, R., Haile, J., Shapiro, B., 2008. The effect of inappropriate calibration: three case studies in molecular ecology. PloS one 3, e1615.

Hodgson, D., Vyverman, W., Peters, T.A., 1997. Diatoms of meromictic lakes adjacent to the Gordon River, and of the Gordon River estuary in south-west Tasmania. Bibliotheca Diatomologica 35, 1-172.

Hoffman, J.I., Clarke, A., Linse, K., Peck, L.S., 2011. Effects of brooding and broadcasting reproductive modes on the population genetic structure of two Antarctic gastropod molluscs. Marine Biology 158, 287-296.

Hogg, M.M., *et al.*, 2010. Deep-seas sponge grounds: reservoirs of biodiversity. UNEP-WCMC, Cambridge.

Holman, H., Watling, L., 1983. A revision of the Stilipedidae (Amphipoda). Crustaceana 44, 27-53.

Horton, T., de Broyer, C., Costello, M., Bellan-Santini, D., 2013a. Epimeriidae Boeck, 1871. World Amphipoda Database. Horton, T. *et al*., World Register of Marine Species at http://www.marinespecies.org/aphia.php?p=taxdetails&id=101379.

Horton, T., de Broyer, C., Costello, M., Bellan-Santini, D., 2013b. Iphimediidae Boeck, 1871 World Amphipoda Database. Horton, T. *et al*., World Register of Marine Species at http://www.marinespecies.org/aphia.php?p=taxdetails&id=101379.

Hou, Z., Fu, J., Li, S., 2007. A molecular phylogeny of the genus *Gammarus* (Crustacea: Amphipoda) based on mitochondrial and nuclear gene sequences. Molecular Phylogenetics and Evolution 45, 596-611.

Hou, Z., Sket, B., Fišer, C., Li, S., 2011. Eocene habitat shift from saline to freshwater promoted Tethyan amphipod diversification. Proceedings of the National Academy of Sciences 108, 14533-14538.

Howson, C.M., Picton, B.E., 1997. The species directory of the marine fauna and flora of the British Isles and surrounding seas. The Marine Conservation Society, Belfast and Ross-on-Wye, Belfast, Ulser Museum.

Hunter, R.L., Halanych, K.M., 2008. Evaluating connectivity in the brooding brittle star *Astrotoma agassizii* across the Drake Passage in the Southern Ocean. Journal of Heredity 99, 137-148.

Hurt, C., Haddock, S.H.D., Browne, W.E., 2013. Molecular phylogenetic evidence for the reorganization of the Hyperiid amphipods, a diverse group of pelagic crustaceans. Molecular Phylogenetics and Evolution 67, 28-37.

Huybrechts, P., 2002. Sea-level changes at the LGM from ice-dynamic reconstructions of the Greenland and Antarctic ice sheets during the glacial cycles. Quaternary Science Reviews 21, 203-231.

I

Ito, A., Wada, H., Aoki, M.N., 2008. Phylogenetic analysis of caprellid and corophioid amphipods (Crustacea) based on the 18S rRNA gene, with special emphasis on the phylogenetic position of Phtisicidae. The Biological Bulletin 214, 176-183.

J

Jadwiszczak, P., 2010. Penguin response to the Eocene climate and ecosystem change in the northern Antarctic Peninsula region. Polar Science 4, 229-235.

Janosik, A.M., Halanych, K.M., 2010. Unrecognized Antarctic biodiversity: a case study of the genus *Odontaster* (Odontasteridae; Asteroidea). Integrative and Comparative Biology 50, 981-992.

Janosik, A.M., Mahon, A., Halanych, K., 2011. Evolutionary history of Southern Ocean *Odontaster* sea star species (Odontasteridae; Asteroidea). Polar Biology 34, 575-586.

Jażdżewski, K., Grabowski, M., Kupryjanowicz, J., 2014. Further records of Amphipoda from Baltic Eocene amber with first evidence of prae-copulatory behaviour in a fossil amphipod and remarks on the taxonomic position of *Palaeogammarus* Zaddach, 1864. Zootaxa 3765, 401-417.

Jażdżewski, K., Kulicka, R., 2000a. Ein neuer Flohkrebs (Crustacea) in Baltischem Bernstein. Fossilien 1, 24-26.

Jażdżewski, K., Kulicka, R., 2000b. A note on amphipod crustaceans in a piece of Baltic amber. Annals of Zoology 50, 99-100.

Jażdżewski, K., Kulicka, R., 2002. New fossil amphipod, *Palaeogammarus polonicus* sp. nov. from the Baltic amber. Acta Geologica Polonica 52, 379-383.

Jażdżewski, K., Kupryjanowicz, J., 2010. One more fossil niphargid (Malacostraca: Amphipoda) from Baltic amber. Journal of Crustacean Biology 30, 413-416.

Jokat, W., Boebel, T., König, M., Meyer, U., 2003. Timing and geometry of early Gondwana breakup. Journal of Geophysical Research: Solid Earth 108, 1-15.

Just, J., 1990. *Vicmusia duplocoxa*, gen. et sp. nov. (Crustacea : Amphipoda : Gammaridea) of the new family Vicmusiidae from Australian upper bathyal waters. Invertebrate Taxonomy 3, 925-940.

K

Kaiser, S., *et al.*, 2013. Patterns, processes and vulnerability of Southern Ocean benthos: a decadal leap in knowledge and understanding. Marine Biology 160, 2295-2317.

Kass, R.E., Raftery, A.E., 1995. Bayes factors. Journal of the American Statistical Association 90, 773-795.

Katoh, K., Standley, D.M., 2013. MAFFT multiple sequence alignment software version 7: improvements in performance and usability. Molecular Biology and Evolution 30, 772-780.

Keller, G., MacLeod, N., Barrera, E., 1992. Eocene-Oligocene faunal turnover in planktic Foraminifera and Antarctic glaciation. In: Prothero, D.R., Berggren, W.A. (Eds.), Eocene-Oligocene Climatic and Biotic Evolution. Princeton University Press, Princeton, USA, pp. 218-244.

Kennett, J.P., 1977. Cenozoic evolution of Antarctic glaciation, the circum-Antarctic Ocean, and their impact on global paleoceanography. Journal of geophysical research 82, 3843-3860.

Kennett, J.P., *et al.*, 1975. Cenozoic paleoceanography in the southwest Pacific Ocean, Antarctic glaciation and the development of the Circum-Antarctic Current. Initial reports of the deep-sea drilling project 29, 1155-1169.

Kim, C.B., Kim, W., 1993. Phylogenetic relationships among gammaridean families and amphipod suborders. Journal of Natural History 27, 933-946.

Klages, M., Gutt, J., 1990. Comparative studies on the feeding behaviour of high Antarctic amphipods (Crustacea) in laboratory. Polar Biology 11, 73-79.

Klaus, S., Schubart, C.D., Streit, B., Pfenninger, M., 2010. When Indian crabs were not yet Asian — biogeographic evidence for Eocene proximity of India and southeast Asia. BMC Evolutionary Biology 10, 1-9.

Klitgaard, A.B., Tendal, O.S., 2004. Distribution and species composition of mass occurrences of large-sized sponges in the northeast Atlantic. Progress in Oceanography 61, 57-98.

Knowlton, N., 1993. Sibling Species in the Sea. Annual Review of Ecology and Systematics 24, 189-216.

Knox, G.A., 2006. Biology of the Southern Ocean, Second Edition. CRC Press, Boca Raton.

Knox, G.A., Lowry, J.K., 1977. A comparison between the benthos of the Southern Ocean and the North Polar Ocean with special reference to the Amphipoda and Polychaeta. In: Dunbar, M.J. (Ed.), Polar oceans. Proceedings of the Polar Ocean Conference, Calgary, pp. 432-462.

Kolaczkowski, B., Thornton, J.W., 2009. Long-branch attraction bias and inconsistency in Bayesian phylogenetics. PloS one 4, e7891.

Kolding, S., 1986. Interspecific competition for mates and habitat selection in five species of *Gammarus* (Amphipoda: Crustacea). Marine Biology 91, 491-495.

Kontula, T., Kirilchik, S.V., Väinölä, R., 2003. Endemic diversification of the monophyletic cottoid fish species flock in Lake Baikal explored with mtDNA sequencing. Molecular Phylogenetics and Evolution 27, 143-155.

Koubbi, P., *et al.*, 2014. PART 12. Conclusions: present and future of Southern Ocean biogeography. In: De Broyer C., Koubbi P., Griffiths H., Raymond B., d'Udekem d'Acoz C. *et al*. (Eds.), Biogeography of the Southern Ocean. Scientific Commitee on Antarctic Research, Cambridge, pp. 469-476.

Kozak, K.H., Weisrock, D.W., Larson, A., 2006. Rapid lineage accumulation in a non-adaptive radiation: phylogenetic analysis of diversification rates in eastern North American woodland salamanders (Plethodontidae: *Plethodon*). Proceedings of the Royal Society B: Biological Sciences 273, 539-546.

Krabbe, K., Leese, F., Mayer, C., Tollrian, R., Held, C., 2010. Cryptic mitochondrial lineages in the widespread pycnogonid *Colossendeis megalonyx* Hoek, 1881 from Antarctic and Subantarctic waters. Polar Biology 33, 281-292.

Krång, A.-S., Baden, S.P., 2004. The ability of the amphipod *Corophium volutator* (Pallas) to follow chemical signals from conspecifics. Journal of Experimental Marine Biology and Ecology 310, 195-206.

Krapp, R.H., Berge, J., Flores, H., Gulliksen, B., Werner, I., 2008. Sympagic occurrence of Eusirid and Lysianassoid amphipods under Antarctic pack ice. Deep-Sea Research Part II: Topical Studies in Oceanography 55, 1015-1023.

Krug, A.Z., Jablonski, D., Valentine, J.W., 2009. Signature of the end-Cretaceous mass extinction in the modern biota. Science 323, 767-771.

Kück, P., Mayer, C., Wägele, J.-W., Misof, B., 2012. Long branch effects distort maximum likelihood phylogenies in simulations despite selection of the correct model. PloS one 7, e36593.

L

Lagabrielle, Y., Goddéris, Y., Donnadieu, Y., Malavieille, J., Suarez, M., 2009. The tectonic history of Drake Passage and its possible impacts on global climate. Earth and Planetary Science Letters 279, 197-211.

Lanfear, R., Calcott, B., Ho, S.Y., Guindon, S., 2012. Partitionfinder: combined selection of partitioning schemes and substitution models for phylogenetic analyses. Molecular Biology and Evolution 29, 1695-1701.

Lartillot, N., Philippe, H., 2006. Computing Bayes factors using thermodynamic integration. Systematic Biology 55, 195-207.

Latimer, J.C., Filippelli, G.M., 2002. Eocene to Miocene terrigenous inputs and export production: geochemical evidence from ODP Leg 177, Site 1090. Palaeogeography, Palaeoclimatology, Palaeoecology 182, 151-164.

Laurent, S., Robinson-Rechavi, M., Salamin, N., 2015. Detecting patterns of species diversification in the presence of both rate shifts and mass extinctions. BMC Evolutionary Biology 15, 15-157.

Lawver, L.A., Gahagan, L.M., 2003. Evolution of Cenozoic seaways in the circum-Antarctic region. Palaeogeography, Palaeoclimatology, Palaeoecology 198, 11-37.

Lawver, L.A., Gahagan, L.M., Coffin, F., 1992. The development of paleoseaways around Antarctica. In: Kennett, J.P., Warnke, D.A. (Eds.), The Antarctic Palaeoenvironment: a perspective on global change. AGU, Washington D.C., pp. 7-30.

Lawver, L.A., Gahagan, L.M., Dalziel, I., 2013. A Different Look at Gateways: Drake Passage and Australia/Antarctica. In: Anderson, J.B., Wellner, J.S. (Eds.), Tectonic, climatic, and cryospheric evolution of the Antarctic Peninsula. American Geophysical Union, Washington DC, pp. 5-33.

Lawver, L.A., Gahagan, L.M., Dalziel, I., 2014. Chapter 3.2. Reconstruction of the Southern Ocean and Antarctic regions. In: De Broyer C., Koubbi P., Griffiths H., Raymond B., d'Udekem d'Acoz C. *et al*. (Eds.), Biogeographic Atlas of the Southern Ocean. Scientific Committee on Antarctic Research, Cambridge, pp. 36-42.

Leaché, A.D., Fujita, M.K., 2010. Bayesian species delimitation in West African forest geckos (*Hemidactylus fasciatus*). Proceedings of the Royal Society of London B: Biological Sciences 277, 3071-3077.

Lear, C.H., Elderfield, H., Wilson, P.A., 2000. Cenozoic deep-sea temperatures and global ice volumes from Mg/Ca in benthic foraminiferal calcite. Science 287, 269-272.

Lear, C.H., Rosenthal, Y., Coxall, H.K., Wilson, P., 2004. Late Eocene to early Miocene ice sheet dynamics and the global carbon cycle. Paleoceanography 19, 1-11.

Lecointre, G., *et al.* , 2013. Is the species flock concept operational? The Antarctic shelf case. PloS one 8, e68787.

Lee, M.S., Sanders, K.L., King, B., Palci, A., 2016. Diversification rates and phenotypic evolution in venomous snakes (Elapidae). Royal Society Open Science 3, 150277.

Lee, Y.-H., Song, M., Lee, S., Leon, R., Godoy, S.O., Canete, I., 2004. Molecular phylogeny and divergence time of the Antarctic sea urchin (*Sterechinus neumayeri*) in relation to the South American sea urchins. Antarctic Science 16, 29-36.

Leese, F., Agrawal, S., Held, C., 2010. Long-distance island hopping without dispersal stages: transportation across major zoogeographic barriers in a Southern Ocean isopod. Naturwissenschaften 97, 583-594.

Lemmon, A.R., Emme, S.A., Lemmon, E.M., 2012. Anchored hybrid enrichment for massively high-throughput phylogenomics. Systematic Biology 61, 727-744.

Letsch, H.O., Kück, P., Stocsits, R.R., Misof, B., 2010. The impact of rRNA secondary structure consideration in alignment and tree reconstruction: simulated data and a case study on the phylogeny of hexapods. Molecular Biology and Evolution 27, 2507-2521.

Lewis, A.R., *et al.*, 2008. Mid-Miocene cooling and the extinction of tundra in continental Antarctica. Proceedings of the National Academy of Sciences 105, 10676-10680.

Leys, C., Ley, C., Klein, O., Bernard, P., Licata, L., 2013. Detecting outliers: do not use standard deviation around the mean, use absolute deviation around the median. Journal of Experimental Social Psychology 49, 764-766.

Li, S., Cordero, E.C., Karoly, D.J., 2002. Transport out of the Antarctic polar vortex from a three-dimensional transport model. Journal of Geophysical Research: Atmospheres 107, ACL 8-1-ACL 8-8.

Licht, K.J., Jennings, A.E., Andrews, J.T., Williams, K.M., 1996. Chronology of late Wisconsin ice retreat from the western Ross Sea, Antarctica. Geology 24, 223-226.

Lincoln, R.J., 1979. British marine Amphipoda: Gammaridea. British Museum (Natural History), London.

Lincoln, R.J., Hurley, D.E., 1981. The calceolus, a sensory structure of gammaridean amphipods (Amphipoda, Gammaridea). Bulletin of the British Museum of Natural History (Zoology) 40, 103-116.

Lindholm, M., 2014. Morphologically conservative but physiologically diverse: the mode of stasis in Anostraca (Crustacea: Branchiopoda). Evolutionary Biology 41, 503-507.

Linse, K., Cope, T., Lörz, A.-N., Sands, C., 2007. Is the Scotia Sea a centre of Antarctic marine diversification? Some evidence of cryptic speciation in the circum-Antarctic bivalve *Lissarca notorcadensis* (Arcoidea: Philobryidae). Polar Biology 30, 1059-1068.

Liow, L.H., Quental, T.B., Marshall, C.R., 2010. When can decreasing diversification rates be detected with molecular phylogenies and the fossil record? Systematic Biology 59, 646-659.

Lipps, J.H., Hickman, C.S., 1982. Origin, age and evolution of Antarctic and deep-sea faunas. In: Ernst, W., Morin, J. (Eds.), The environment of the deep-sea. Pr.-Hall P., New Jersey, pp. 324-357.

Lisiecki, L.E., Raymo, M.E., 2007. Plio–Pleistocene climate evolution: trends and transitions in glacial cycle dynamics. Quaternary Science Reviews 26, 56-69.

Livermore, R., Nankivell, A., Eagles, G., Morris, P., 2005. Paleogene opening of Drake Passage. Earth and Planetary Science Letters 236, 459-470.

Lörz, A.-N., 2009. Synopsis of Amphipoda from two recent Ross Sea voyages with description of a new species of *Epimeria* (Epimeriidae, Amphipoda, Crustacea). Zootaxa 2167, 59-68.

Lörz, A.-N., 2012. First records of Epimeriidae and Iphimediidae (Crustacea, Amphipoda) from Macquarie Ridge, with description of a new species and its juveniles. Zootaxa 3200, 49-60.

Lörz, A.-N., Coleman, C., 2009. Living gems: jewel-like creatures from the deep. Water & Atmosphere 17, 16-17.

Lörz, A.-N., Held, C., 2004. A preliminary molecular and morphological phylogeny of the Antarctic Epimeriidae and Iphimediidae (Crustacea, Amphipoda). Molecular Phylogenetics and Evolution 31, 4-15.

Lörz, A.-N., Maas, E.W., Linse, K., Coleman, C.O., 2009. Do circum-Antarctic species exist in peracarid Amphipoda? A case study in the genus *Epimeria* Costa, 1851 (Crustacea, Peracarida, Epimeriidae). Zookeys 18, 91-128.

Lörz, A.-N., Maas, E.W., Linse, K., Fenwick, G.D., 2007. *Epimeria schiaparelli* sp. nov., an amphipod crustacean (family Epimeriidae) from the Ross Sea, Antarctica, with molecular characterisation of the species complex. Zootaxa 1402, 23-27.

Lörz, A.-N., Smith, P., Linse, K., Steinke, D., 2011. High genetic diversity within *Epimeria georgiana* (Amphipoda) from the southern Scotia Arc. Marine Biodiversity 42, 137-159.

Losos, J.B., 2010. Adaptive radiation, ecological opportunity, and evolutionary determinism. American Naturalist 175, 623-639.

Losos, J.B., 2011. Convergence, adaptation and constraint. Evolution 65, 1827-1840.

Losos, J.B., Mahler, D.L., 2010. Adaptive radiation: the interaction of ecological opportunity, adaptation, and speciation. In: Bell, M.A., Futuyma, D.J., Eanes, W.F., Levinton, J.S. (Eds.), Evolution since Darwin: the first 150 years. Sinauer Associates, Sunderland, pp. 381-420.

Lovette, I.J., Bermingham, E., 1999. Explosive speciation in the New World *Dendroica* warblers. Proceedings of the Royal Society B: Biological Sciences 266, 1629-1629.

Lowry, J.K., 1986. The callynophore, a eucaridan/peracaridan sensory organ prevalent among the Amphipoda (Crustacea). Zoologica Scripta 15, 333-349.

Lowry, J.K., Myers, A., 2000. A family level phylogeny of iphimedioid amphipods (Crustacea, Amphipoda). Xth International Colloquium on Amphipoda Heraklion, Creta, p. 30.

Lowry, J.K., Myers, A.A., 2013. A Phylogeny and classification of the Senticaudata subord. nov. (Crustacea: Amphipoda). Zootaxa 3610, 1-80.

Lyle, M., Gibbs, S., Moore, T.C., K, R.D., 2007. Late Oligocene initiation of the Antarctic Circumpolar Current: evidence from the South Pacific. Geology 35, 691-694.

M

MacArthur, R., Levins, R., 1964. Competition, habitat selection, and character displacement in a patchy environment. Proceedings of the National Academy of Sciences 51, 1207-1210.

Macdonald III, K.S., Yampolsky, L., Duffy, J.E., 2005. Molecular and morphological evolution of the amphipod radiation of Lake Baikal. Molecular Phylogenetics and Evolution 35, 323-343.

Mackensen, A., 2004. Changing Southern Ocean palaeocirculation and effects on global climate. Antarctic Science 16, 369-386.

Mackintosh, A.N., *et al*., 2014. Retreat history of the East Antarctic Ice Sheet since the Last Glacial Maximum. Quaternary Science Reviews 100, 10-30.

Madin, L.P., Harbison, G.R., 1977. The associations of Amphipoda Hyperiidea with gelatinous zooplankton—I. Associations with Salpidae. Deep-Sea Research 24, 449-463.

Mahon, A.R., Arango, C.P., Halanych, K.M., 2008. Genetic diversity of *Nymphon* (Arthropoda: Pycnogonida: Nymphonidae) along the Antarctic Peninsula with a focus on *Nymphon australe* Hodgson 1902. Marine Biology 155, 315-323.

Mamanova, L., *et al*., 2010. Target-enrichment strategies for next-generation sequencing. Nature Methods 7, 111-118.

Mamos, T., Wattier, R., Majda, A., Sket, B., Grabowski, M., 2014. Morphological vs molecular delineation of taxa across montane regions in Europe: the case study of *Gammarus balcanicus*Schäferna (Crustacea, Amphipoda). Journal of Zoological Systematics and evolutionary Research 52, 237-248.

Mamos, T., Wattier, R., Burzynski, A., Grabowski, M., 2016. The legacy of a vanished sea: a high level of diversification within a European freshwater amphipod species complex driven by 15 My of Paratethys regression. Molecular Ecology 25, 795-810.

Martens, K., 1997. Speciation in ancient lakes. Trends in Ecology & Evolution 12, 177-182.

Martin, J.W., Davis, G.E., 2001. An updated classification of the recent Crustacea. Natural History Museum of Los Angeles County, Los Angeles.

Matschiner, M., Hanel, R., Salzburger, W., 2011. On the origin and trigger of the notothenioid adaptive radiation. PloS one 6, e18911.

McCormack, J.E., Faircloth, B.C., Crawford, N.G., Gowaty, P.A., Brumfield, R.T., Glenn, T.C., 2012. Ultraconserved elements are novel phylogenomic markers that resolve placental mammal phylogeny when combined with species-tree analysis. Genome Research 22, 746-754.

McInnes, L., Orme, C.D.L., Purvis, A., 2011. Detecting shifts in diversity limits from molecular phylogenies: what can we know? Proceedings of the Royal Society B: Biological Sciences 278, 3294-3302.

McKay, R., *et al.*, 2012. Pleistocene variability of Antarctic ice sheet extent in the Ross embayment. Quaternary Science Reviews 34, 93-112.

Menzies, R.J., George, R.Y., Rowe, G.T., 1979. Abyssal environment and ecology of the world oceans. Wiley-Interscience, New York.

Metzker, M.L., 2010. Sequencing technologies— the next generation. Nature Reviews Genetics 11, 31-46.

Miller, A.I., Sepkoski, J.J., Jr., 1988. Modeling bivalve diversification: the effect of interaction on a macroevolutionary system. Paleobiology 14, 364-369.

Miller, K.G., *et al*., 2008a. Eocene-Oligocene global climate and sea-level changes: St. Stephens Quarry, Alabama. Geological Society of America Bulletin 120, 34-53.

Miller, K.G., *et al.*, 2008b. A view of Antarctic ice-sheet evolution from sea-level and deep-sea isotope changes during the Late Cretaceous-Cenozoic. In: Cooper, A.K., Barret, P.J., Stagg, H., Storey, B., Stump, E., Wise, W., and the 10th ISAES editorial team (Eds.), Antarctica: a keystone in a changing world. Proceedings of the 10th International Symposium on Antarctic Earth Sciences. The National Academies Press, Washington DC, pp. 55-70.

Miller, K.G., Wright, J.D., Fairbanks, R.G., 1991. Unlocking the Ice House: Oligocene-Miocene oxygen isotopes, eustasy, and margin erosion. Journal of Geophysical Research: Solid Earth 96, 6829-6848.

Miller, M.A., Pfeiffer, W., Schwartz, T., 2010. Creating the CIPRES science gateway for inference of large phylogenetic trees. Proceedings of the Gateway Computing Environments Workshop (GCE), 1-8.

Miralles, A., Vences, M., 2013. New metrics for comparison of taxonomies reveal striking discrepancies among species delimitation methods in *Madascincus* lizards. PloS one 8, e68242.

Misof, B., Misof, K., 2009. A Monte Carlo approach successfully identifies randomness in multiple sequence alignments: a more objective means of data exclusion. Systematic Biology 58, 21-34.

Monaghan, M.T., *et al.*, 2009. Accelerated species inventory on Madagascar using coalescent-based models of species delineation. Systematic Biology 58, 298-311.

Moore, P.G., 1981. A functional interpretation of coxal morphology in *Epimeria cornigera* (Crustacea: Amphipoda: Paramphithoidae). Journal of the Marine Biological Association U.K. 61, 749-757.

Morlon, H., Parsons, T.L., Plotkin, J.B., 2011. Reconciling molecular phylogenies with the fossil record. Proceedings of the National Academy of Science USA 108, 16327-16332.

Murrell, B., *et al.,* 2015. Gene-wide identification of episodic selection. Molecular Biology and Evolution 32, 1365-1371.

Murrell, B., Wertheim, J.O., Moola, S., Weighill, T., Scheffler, K., Kosakovsky Pond, S.L., 2012. Detecting individual sites subject to episodic diversifying selection. PLOS Genetics 8, e1002764.

Myers, A.A., Lowry, J.K., 2003. A Phylogeny and a new classification of the Corophiidea Leach, 1814 (Amphipoda). Journal of Crustacean Biology 23, 443-485.

N

Nahavandi, N., Ketmaier, V., Plath, M., Tiedemann, R., 2013. Diversification of Ponto-Caspian aquatic fauna: morphology and molecules retrieve congruent evolutionary relationships in *Pontogammarus maeoticus* (Amphipoda: Pontogammaridae). Molecular Phylogenetics and Evolution 69, 1063-1076.

Naish, T., *et al.*, 2009. Obliquity-paced Pliocene West Antarctic ice sheet oscillations. Nature 458, 322-328.

Naumenko, S.A., *et al.*, 2017. Transcriptome-based phylogeny of endemic Lake Baikal amphipod species flock: fast speciation accompanied by frequent episodes of positive selection. Molecular Ecology 26, 536-553.

Near, T.J., 2004. Estimating divergence times of notothenioid fishes using a fossil-calibrated molecular clock. Antarctic Science 16, 37-44.

Near, T.J., *et al.*, 2012. Ancient climate change, antifreeze, and the evolutionary diversification of Antarctic fishes. Proceedings of the National Academy of Sciences USA 109, 3434-3439.

Nee, S., 2006. Birth-Death models in macroevolution. Annual Review of Ecology, Evolution and Systematics 37, 1-17.

Nikula, R., Fraser, C.I., Spencer, H.G., Waters, J.M., 2010. Circumpolar dispersal by rafting in two subantarctic kelp-dwelling crustaceans. Marine Ecology Progress Series 405, 221-230.

Nowlin, W.D., Klinck, J.M., 1986. The physics of the Antarctic Circumpolar Current. Reviews of Geophysics 24, 469-491.

Nyssen, F., 2005. Role of benthic amphipods in Antarctic trophodynamics: a multidisciplinary study. Faculté des Sciences. Département des Sciences et Gestion de l'Environnement. Systématique et Diversité animale. Université de Liège, Liège, p. 271.

Nyssen, F., Brey, T., Dauby, P., Graeve, M., 2005. Trophic position of Antarctic amphipods: enhanced analysis by a 2-dimensional biomarker assay. Marine Ecology Progress Series 300, 135-145.

Nyssen, F., Brey, T., Lepoint, G., Bouquegneau, J.-M., De Broyer, C., Dauby, P., 2002. A stable isotope approach to the eastern Weddell Sea trophic web: focus on benthic amphipods. Polar Biology 25, 280-287.

O

O'Brien, P., De Santis, L., Harris, P., Domack, E., Quilty, P., 1999. Ice shelf grounding zone features of western Prydz Bay, Antarctica: sedimentary processes from seismic and sidescan images. Antarctic Science 11, 78-91.

O'Brien, P., *et al.*, 2004. Prydz Channel Fan and the history of extreme ice advances in Prydz Bay. Proceedings of the Ocean Drilling Program: Scientific Results, pp. 1-32.

O'Foighil, D.O., Marshall, B.A., Hilbish, T.J., Pino, M.A., 1999. Trans-Pacific range extension by rafting is inferred for the flat oyster *Ostrea chilensis*. The Biological Bulletin 196, 122-126.

Ó Cofaigh, C., *et al.*, 2005. Flow of the West Antarctic Ice Sheet on the continental margin of the Bellingshausen Sea at the Last Glacial Maximum. Journal of Geophysical Research: Solid Earth 110, 1-13.

O'Loughlin, P.M., Paulay, G., Davey, N., Michonneau, F., 2011. The Antarctic region as a marine biodiversity hotspot for echinoderms: diversity and diversification of sea cucumbers. Deep-Sea Research Part II: Topical Studies in Oceanography 58, 264-275.

Oleinik, A.E., Zinsmeister, W.J., 1996. Paleocene diversification of bucciniform gastropods on Seymour Island, Antarctica. Journal of Paleontology 70, 923-934.

Omilian, A.R., Taylor, D.J., 2001. Rate acceleration and long-branch attraction in a conserved gene of cryptic daphniid (Crustacea) species. Molecular Biology and Evolution 18, 2201-2212.

Orsi, A.H., Whitworth, T., Sparrow, M., Chapman, P., Gould, J., 2005. Hydrographic atlas of the world ocean circulation experiment (WOCE) Vol 1: Southern Ocean. WOCE International Project Office, Southhampton.

Oshel, P.E., Steele, D.H., 1985. Amphipod *Paramphithoe hystrix:* a micropredator on the sponge *Haliclona ventilabrum*. Marine Ecology Progress Series 23, 307-309.

Otto, J.C., Wilson, K.J., 2001. Assessment of the usefulness of ribosomal 18S and mitochondrial COI sequences in Prostigmata phylogeny. CSIRO Publishing, Collingwood, Victoria.

P

Padial, J.M., Miralles, A., De la Riva, I., Vences, M., 2010. The integrative future of taxonomy. Frontiers in Zoology 7, 1-14.

Page, T.J., Linse, K., 2002. More evidence of speciation and dispersal across the Antarctic Polar Front through molecular systematics of Southern Ocean *Limatula* (Bivalvia: Limidae). Polar Biology 25, 818-826.

Paradis, E., Claude, J., Strimmer, K., 2004. APE: analyses of phylogenetics and evolution in R language. Bioinformatics 20, 289-290.

Parkinson, C.L., 2014. Global sea ice coverage from satellite data: annual cycle and 35-yr trends. Journal of Climate 27, 9377-9382.

Parks, S.L., Goldman, N., 2014. Maximum likelihood inference of small trees in the presence of long branches. Systematic biology 63, 798-811.

Passchier, S., *et al.*, 2011. Early and middle Miocene Antarctic glacial history from the sedimentary facies distribution in the AND-2A drill hole, Ross Sea, Antarctica. Geological Society of America Bulletin 123, 2352-2365.

Passchier, S., O'Brien, P.E., Damuth, J.E., Januszczak, N., Handwerger, D.A., Whitehead, J.M., 2003. Pliocene–Pleistocene glaciomarine sedimentation in eastern Prydz Bay and development of the Prydz trough-mouth fan, ODP Sites 1166 and 1167, East Antarctica. Marine Geology 199, 279-305.

Patarnello, T., Bargelloni, L., Varotto, V., Battaglia, B., 1996. Krill evolution and the Antarctic ocean currents: evidence of vicariant speciation as inferred by molecular data. Marine Biology 126, 603-608.

Pawlowski, J., *et al.*, 2007. Bipolar gene flow in deep-sea benthic Foraminifera. Molecular Ecology 16, 4089-4096.

Pearse, J.S., Mooi, R., Lockhart, S.J., Brandt, A., 2008. Brooding and species diversity in the Southern Ocean: selection for brooders or speciation within brooding clades? In: Krupnik, I., Land, M., A., Miller, S.E. (Eds.), Smithsonian at the Poles. Contributions to International Polar Year Science. Smithsonian Institution Scholarly Press, Washington D.C., pp. 181-196.

Pearson, P.N., Palmer, M.R., 2000. Atmospheric carbon dioxide concentrations over the past 60 million years. Nature 406, 695-699.

Peck, L.S., 2002. Ecophysiology of Antarctic marine ectotherms: limits to life. In: Arntz, W.E., Clarke, A. (Eds.), Ecological Studies in the Antarctic Sea Ice Zone: Results of EASIZ Midterm Symposium. Springer Berlin Heidelberg, Berlin, pp. 221-230.

Peck, L.S., 2005. Prospects for survival in the Southern Ocean: vulnerability of benthic species to temperature change. Antarctic Science 17, 497-507.

Peck, L.S., Conway, L.Z., 2000. The myth of metabolic cold adaptation: oxygen consumption in stenothermal Antarctic bivalves. Geological Society, London, Special Publications 177, 441-450.

Pekar, S.F., DeConto, R.M., 2006. High-resolution ice-volume estimates for the early Miocene: evidence for a dynamic ice sheet in Antarctica. Palaeogeography, Palaeoclimatology, Palaeoecology 231, 101-109.

Peters, K.J., Amsler, C.D., McClintock, J.B., Soest, R., Baker, B.J., 2009. Palatability and chemical defenses of sponges from the western Antarctic Peninsula. Marine Ecology Progress Series 385, 77-85.

Petersen, S.V., Dutton, A., Lohmann, K.C., 2016. End-Cretaceous extinction in Antarctica linked to both Deccan volcanism and meteorite impact via climate change. Nature Communications 7, 1-9.

Pfühl, H.A., McCave, I.N., 2005. Evidence for late Oligocene establishment of the Antarctic Circumpolar Current. Earth and Planetary Science Letters 235, 715-728.

Philippe, H., Germot, A., 2000. Phylogeny of eukaryotes based on ribosomal RNA: Long-Branch Attraction and models of sequence evolution. Molecular Biology and Evolution 17, 830-834.

Phillimore, A.B., Price, T.D., 2008. Density-dependent cladogenesis in birds. PLOS Biology 6, e71.

Phillimore, A.B., Price, T.D., 2009. Ecological influences on the temporal pattern of speciation. In: Butlin, R., Bridle, J., Schluter, D. (Eds.), Speciation and patterns of diversity. Cambridge University Press, Cambridge, pp. 240-256.

Pierrat, B., Saucède, T., Brayard, A., David, B., 2013. Comparative biogeography of echinoids, bivalves and gastropods from the Southern Ocean. Journal of Biogeography 40, 1374-1385.

Pilar Cabezas, M., Cabezas, P., Machordom, A., Guerra-García, J.M., 2013. Hidden diversity and cryptic speciation refute cosmopolitan distribution in *Caprella penantis* (Crustacea: Amphipoda: Caprellidae). Journal of Zoological Systematics and Evolutionary Research 51, 85-99.

Plummer, M., Best, N., Cowles, K., Vines, K., 2006. CODA: convergence diagnosis and output analysis for MCMC. R News 6, 7-11.

Pollard, D., DeConto, R.M., 2009. Modelling West Antarctic ice sheet growth and collapse through the past five million years. Nature 458, 329-332.

Poltermann, M., Hop, H., Falk-Petersen, S., 2000. Life under Arctic sea ice — reproduction strategies of two sympagic (ice-associated) amphipod species, *Gammarus wilkitzkii* and *Apherusa glacialis*. Marine Biology 136, 913-920.

Pons, J., *et al.*, 2006. Sequence-based species delimitation for the DNA taxonomy of undescribed insects. Systematic Biology 55, 595-609.

Pörtner, H.O., Peck, L., Somero, G., 2007. Thermal limits and adaptation in marine Antarctic ectotherms: an integrative view. Philosophical Transactions of the Royal Society B: Biological Sciences 362, 2233-2258.

Post, A., *et al.*, 2014. Chaper 4. Environmental Settings. In: De Broyer C., Koubbi P., Griffiths H., Raymond B., d'Udekem d'Acoz C. *et al*. (Eds.), Biogeographical atlas of the Southern Ocean. Scientific Committee on Antarctic Research, Cambridge, pp. 45-64.

Poulin, E., Feral, J.-P., 1996. Why are there so many species of brooding Antarctic echinoids? Evolution, 820-830.

Poulin, E., González-Wevar, C., Díaz, A., Gérard, K., Hüne, M., 2014. Divergence between Antarctic and South American marine invertebrates: what molecular biology tells us about Scotia Arc geodynamics and the intensification of the Antarctic Circumpolar Current. Global and Planetary Change 123, 392-399.

Poulin, E., Palma, A.T., Féral, J.-P., 2002. Evolutionary versus ecological success in Antarctic benthic invertebrates. Trends in Ecology & Evolution 17, 218-222.

Powell, J.R., 2012. Accounting for uncertainty in species delineation during the analysis of environmental DNA sequence data. Methods in Ecology and Evolution 3, 1-11.

Prebble, J.G., Hannah, M.J., Barrett, P.J., 2006. Changing Oligocene climate recorded by palynomorphs from two glacio-eustatic sedimentary cycles, Cape Roberts Project,

Victoria Land Basin, Antarctica. Palaeogeography, Palaeoclimatology, Palaeoecology 231, 58-70.

Prum, R.O., Berv, J.S., Dornburg, A., Field, D.J., Townsend, J.P., Lemmon, E.M., Lemmon, A.R., 2015. A comprehensive phylogeny of birds (Aves) using targeted next-generation DNA sequencing. Nature 526, 569-573.

Puillandre, N., Lambert, A., Brouillet, S., Achaz, G., 2012. ABGD, Automatic Barcode Gap Discovery for primary species delimitation. Molecular Ecology 21, 1864-1877.

Purvis, A., 2008. Phylogenetic approaches to the study of extinction. Annual Review of Ecology, Evolution and Systematics 39, 301-319.

Pybus, O.G., Harvey, P.H., 2000. Testing macro-evolutionary models using incomplete molecular phylogenies. Proceedings of the Royal Society B: Biological Sciences 267, 2267-2272.

Q

Quental, T.B., Marshall, C.R., 2009. Extinction during evolutionary radiations: reconciling the fossil record with molecular phylogenies. Evolution 63, 3158-3167.

Quental, T.B., Marshall, C.R., 2010. Diversity dynamics: molecular phylogenies need the fossil record. Trends in Ecology & Evolution 25, 434-441.

R

Rabosky, D.L., 2006a. LASER: a Maximum Likelihood toolkit for detecting temporal shifts in diversification rates from molecular phylogenies. Evolutionary Bioinformatics Online 2, 247-250.

Rabosky, D.L., 2006b. Likelihood methods for detecting temporal shifts in diversification rates. Evolution 60, 1152-1164.

Rabosky, D.L., 2010. Extinction rates should not be estimated from molecular phylogenies. Evolution 64, 1816-1824.

Rabosky, D.L., 2014. Automatic detection of key innovations, rate shifts and diversity-dependence on phylogenetic trees. PloS one 9, e89543.

Rabosky, D.L., Adams, D.C., 2012. Rates of morphological evolution are correlated with species richness in salamanders. Evolution 66, 1807-1818.

Rabosky, D.L., *et al*., 2014. BAMMtools: an R package for the analysis of evolutionary dynamics on phylogenetic trees. Methods in Ecology and Evolution 5, 701-707.

Rabosky, D.L., Lovette, I.J., 2008. Density-dependent diversification in North American wood warblers. Proceedings of the Royal Society B: Biological Sciences 275, 2363-2371.

Rabosky, D.L., Santini, F., Eastman, J., Smith, S.A., Sidlauskas, B., Chang, J., Alfaro, M.E., 2013. Rates of speciation and morphological evolution are correlated across the largest vertebrate radiation. Nature Communications 4, 1-8.

Raguá-Gil, J.M., Gutt, J., Clarke, A., Arntz, W.E., 2004. Antarctic shallow-water mega-epibenthos: shaped by circumpolar dispersion or local conditions? Marine Biology 144, 829-839.

Rambaut, A., Drummond, A., 2005. Tracer, a program for analyzing results from Bayesian MCMC programs such as BEAST & MrBayes, version 1.3. Oxford. Available from http://evolve/zoo.ox.ac.uk/software.html?id=tracer/.

Rambaut, A., Suchard, M.A., Xie, D., Drummond, A.J., 2014. Tracer v1.6. Available from http://beast.bio.ed.ac.uk/Tracer.

Rannala, B., Yang, Z., 2013. Improved reversible-jump algorithms for Bayesian species delimitation. Genetics 194, 245-253.

Raupach, M.J., Malyutina, M., Brandt, A., Wägele, J.-W., 2007. Molecular data reveal a highly diverse species flock within the munnopsoid deep-sea isopod *Betamorpha fusiformis* (Barnard,

1920) (Crustacea: Isopoda: Asellota) in the Southern Ocean. Deep-Sea Research Part II: Topical Studies in Oceanography 54, 1820-1830.

Raupach, M.J., Mayer, C., Malyutina, M., Wägele, J.-W., 2009. Multiple origins of deep-sea *Asellota* (Crustacea: Isopoda) from shallow waters revealed by molecular data. Proceedings of the Royal Society B: Biological Sciences 276, 799-808.

Raupach, M.J., Thatje, S., Dambach, J., Rehm, P., Misof, B., Leese, F., 2010. Genetic homogeneity and circum-Antarctic distribution of two benthic shrimp species of the Southern Ocean, *Chorismus antarcticus* and *Nematocarcinus lanceopes*. Marine Biology 157, 1783-1797.

Raupach, M.J., Wägele, J.-W., 2006. Distinguishing cryptic species in Antarctic *Asellota* (Crustacea: Isopoda) — a preliminary study of mitochondrial DNA in *Acanthaspidia drygalskii*. Antarctic Science 18, 191-198.

Rauschert, M., Arntz, W.E., 2015. Antarctic Macrobenthos. A field guide of the invertebrates living at the Antarctic seafloor. Arntz & Rauschert Selbstverlag, Bremen.

Ribbink, A.J., 1984. Is the species flock concept tenable? . In: A. A. Echelle, I. Kornfield (Eds.), Evolution of Fish Species Flocks. Orono Press, University of Maine, USA, pp. 21–25.

Ricklefs, R.E., 2007. Estimating diversification rates from phylogenetic information. Trends in Ecology & Evolution 22, 601-610.

Ricklefs, R.E., Jønsson, K.A., 2014. Clade extinction appears to balance species diversification in sister lineages of Afro-Oriental passerine birds. Proceedings of the National Academy of Sciences 111, 11756-11761.

Riesgo, A., Taboada, S., Avila, C., 2015. Evolutionary patterns in Antarctic marine invertebrates: an update on molecular studies. Marine Genomics 23, 1-13.

Rintoul, S.R., Hugues, C., Olbers, D., 2001. The Antarctic Circumpolar Current system. In: G. Siedler, G., Church, J., Gould, J. (Eds.), Ocean circulation and climate. Academic Press, London, pp. 271-302.

Ritchie, H., Jamieson, A.J., Piertney, S.B., 2015. Phylogenetic relationships among hadal amphipods of the Superfamily Lysianassoidea: implications for taxonomy and biogeography. Deep-Sea Research Part I: Oceanographic Research Papers 105, 119-131.

Rocha-Olivares, A., Fleeger, J.W., Foltz, D., 2001. Decoupling of molecular and morphological evolution in deep lineages of a meiobenthic harpacticoid copepod. Molecular Biology and Evolution 18, 1088-1102.

Roberts, A.P., Bicknell, S.J., Byatt, J., Bohaty, S.M., Florindo, F., Harwood, D.M., 2003a. Magnetostratigraphic calibration of Southern Ocean diatom datums from the Eocene–Oligocene of Kerguelen Plateau (Ocean Drilling Program Sites 744 and 748). Palaeogeography, Palaeoclimatology, Palaeoecology 198, 145-168.

Roberts, A.P., Wilson, G.S., Harwood, D.M., Verosub, K.L., 2003b. Glaciation across the Oligocene–Miocene boundary in southern McMurdo Sound, Antarctica: new chronology from the CIROS-1 drill hole. Palaeogeography, Palaeoclimatology, Palaeoecology 198, 113-130.

Rodríguez, E., López-González, P.J., Gili, J.M., 2007. Biogeography of Antarctic sea anemones (Anthozoa, Actiniaria): what do they tell us about the origin of the Antarctic benthic fauna? Deep Sea Research Part II: Topical Studies in Oceanography 54, 1876-1904.

Rogers, A.D., 2000. The role of the oceanic oxygen minima in generating biodiversity in the deep-sea. Deep-Sea Research Part II: Topical Studies in Oceanography 47, 119-148.

Rogers, A.D., 2007. Evolution and biodiversity of Antarctic organisms: a molecular perspective. Philosophical Transactions of the Royal Society of London B: Biological Sciences 362, 2191-2214.

Rogers, A.R., Harpending, H., 1992. Population growth makes waves in the distribution of pairwise genetic differences. Molecular Biology and Evolution 9, 552-569.

Ronquist, F., Huelsenbeck, J.P., 2003. MrBayes 3: Bayesian phylogenetic inference under mixed models. Bioinformatics 19, 1572-1574.

Rundell, R.J., Price, T.D., 2009. Adaptive radiation, nonadaptive radiation, ecological speciation and nonecological speciation. Trends in Ecology & Evolution 24, 394-399.
Rundle, H.D., Nosil, P., 2005. Ecological speciation. Ecology Letters 8, 336-352.

S

Saez, A.G., Lozano, E., 2005. Body doubles. Nature 433, 111.
Sanger, F., Nicklen, S., Coulson, A.R., 1977. DNA sequencing with chain-terminating inhibitors. Proceedings of the National Academy of Science USA 74, 5463-5467.
Satler, J.D., Carstens, B.C., Hedin, M., 2013. Multilocus species delimitation in a complex of morphologically conserved trapdoor spiders (Mygalomorphae, Antrodiaetidae, *Aliatypus*). Systematic Biology 62, 805-823.
Scher, H.D., Martin, E.E., 2004. Circulation in the Southern Ocean during the Paleogene inferred from neodymium isotopes. Earth and Planetary Science Letters 228, 391-405.
Schlick-Steiner, B.C., Steiner, F.M., Seifert, B., Stauffer, C., Christian, E., Crozier, R.H., 2010. Integrative taxonomy: a multisource approach to exploring biodiversity. Annual Review of Entomology 55, 421-438.
Schluter, D., 2000. The ecology of adaptive radiation. Oxford University Press, Oxford.
Schluter, D., 2009. Evidence for ecological speciation and its alternative. Science 323, 737-741.
Schneider, S., Excoffier, L., 1999. Estimation of past demographic parameters from the distribution of pairwise differences when the mutation rates vary among sites: application to human mitochondrial DNA. Genetics 152, 1079-1089.
Schoener, T.W., 1974. Resource partitioning in ecological communities. Science 185, 27-39.
Schön, I., Martens, K., 2004. Adaptive, pre-adaptive and non-adaptive components of radiations in ancient lakes: a review. Organisms Diversity & Evolution 4, 137-156.
Schüller, M., 2011. Evidence for a role of bathymetry and emergence in speciation in the genus *Glycera* (Glyceridae, Polychaeta) from the deep Eastern Weddell Sea. Polar Biology 34, 549-564.
Seehausen, O., 2000. Explosive speciation rates and unusual species richness in haplochromine cichlid fishes: effects of sexual selection. Advances in Ecological Research 31, 237-274.
Seehausen, O., 2002. Patterns in fish radiation are compatible with Pleistocene desiccation of Lake Victoria and 14 600 year history for its cichlid species flock. Proceedings of the Royal Society of London B: Biological Sciences 269, 491-497.
Sepkoski, J., 1996. Patterns of Phanerozoic extinction: a perspective from global data bases. In: Walliser, O.H. (Ed.), Global events and event stratigraphy in the Phanerozoic. Springer-Verlag, Berlin, pp. 35-51.
Serejo, C.S., 2004. Cladistic revision of talitroidean amphipods (Crustacea, Gammaridea), with a proposal of a new classification. Zoologica Scripta 33, 551-586.
Shaw, P.W., Arkhipkin, A.I., Al-Khairulla, H., 2004. Genetic structuring of Patagonian toothfish populations in the Southwest Atlantic Ocean: the effect of the Antarctic Polar Front and deep-water troughs as barriers to genetic exchange. Molecular Ecology 13, 3293-3303.
Sheldon, P.R., 1996. Plus ça change — a model for stasis and evolution in different environments. Palaeogeography, Palaeoclimatology, Palaeoecology 127, 209-227.
Sherbakov, D.Y., Kamaltynov, R.M., Ogarkov, O.B., Vaïnölä, R., Vainio, J.K., Verheyen, E., 1999. On the phylogeny of Lake Baikal amphipods in the light of mitochondrial and nuclear DNA sequence data. Crustaceana 72, 911-919.
Sherbakov, D.Y., Kamaltynov, R.M., Ogarkov, O.B., Verheyen, E., 1998. Patterns of evolutionary change in baikalian gammarids inferred from DNA sequences (Crustacea, Amphipoda). Molecular Phylogenetics and Evolution 10, 160-167.

Shevenell, A.E., Kennett, J.P., Lea, D.W., 2004. Middle Miocene Southern Ocean cooling and Antarctic cryosphere expansion. Science 305, 1766.

Shimomura, M., Tomikawa, K., 2016. *Epimeria abyssalis* sp. n. from the Kuril-Kamchatka Trench (Crustacea, Amphipoda, Epimeriidae). Zookeys 638, 125-142.

Ship, S., Anderson, J., Domack, E., 1999. Late Pleistocene–Holocene retreat of the West Antarctic Ice-Sheet system in the Ross Sea: part 1—geophysical results. Geological Society of America Bulletin 111, 1486-1516.

Sites, J.W., Marshall, J.C., 2004. Operational criteria for delimiting species. Annual Review of Ecology, Evolution & Systematics 35, 199-227.

Slatkin, M., Hudson, R.R., 1991. Pairwise comparisons of mitochondrial DNA sequences in stable and exponentially growing populations. Genetics 129, 555-562.

Smith, J.A., Hillenbrand, C.-D., Pudsey, C.J., Allen, C.S., Graham, A.G.C., 2010. The presence of polynyas in the Weddell Sea during the Last Glacial Period with implications for the reconstruction of sea-ice limits and ice sheet history. Earth and Planetary Science Letters 296, 287-298.

Smith, M.D., Wertheim, J.O., Weaver, S., Murrell, B., Scheffler, K., Kosakovsky Pond, S.L., 2015. Less is more: an adaptive branch-site random effects model for efficient detection of episodic diversifying selection. Molecular Biology and Evolution 32, 1342-1353.

Smith, S.A., *et al.*, 2011. Resolving the evolutionary relationships of molluscs with phylogenomic tools. Nature 480, 364-367.

Smith, S.D.A., 2002. Kelp rafts in the Southern Ocean. Global Ecology and Biogeography 11, 67-69.

Smith, W.H.F., Sandwell, D.T., 1997. Global sea floor topography from satellite altimetry and ship depth soundings. Science 277, 1956.

Sokolov, S., Rintoul, S.R., 2009. Circumpolar structure and distribution of the Antarctic Circumpolar Current fronts: 1. Mean circumpolar paths. Journal of Geophysical Research: Oceans 114, 1-19.

Som, A., 2015. Causes, consequences and solutions of phylogenetic incongruence. Briefings in Bioinformatics 16, 536-548.

Sorlien, C.C., Luyendyk, B.P., Wilson, D.S., Decesari, R.C., Bartek, L.R., Diebold, J.B., 2007. Oligocene development of the West Antarctic Ice Sheet recorded in eastern Ross Sea strata. Geology 35, 467-470.

Stadler, T., 2011. Mammalian phylogeny reveals recent diversification rate shifts. Proceedings of the National Academy of Sciences USA 108, 6187-6192.

Stanhope, M.J., Connelly, M.M., Hartwick, B., 1992. Evolution of a crustacean chemical communication channel: Behavioral and ecological genetic evidence for a habitat-modified, race-specific pheromone. Journal of Chemistry and Ecology 18, 1871-1887.

Stebbing, T.R.R., 1906. Amphipoda. I. Gammaridea. R. Friedländer und Sohn, Berlin.

Steele, V.J., Steele, D.H., 1993. Presence of two types of calceoli on *Gammarellus angulosus* (Amphipoda: Gammaridea). Journal of Crustacean Biology 13, 538-543.

Stickley, C.E., *et al.*, 2004. Timing and nature of the deepening of the Tasmanian Gateway. Paleoceanography 19, 1-18.

Stilwell, J.D., 2003. Patterns of biodiversity and faunal rebound following the K-T boundary extinction event in Austral Palaeocene molluscan faunas. Palaeogeography, Palaeoclimatology, Palaeoecology 195, 319-356.

Stilwell, J.D., Zinsmeister, W.J., 1992. Molluscan systematics and biostratigraphy: lower Tertiary La Meseta formation, Seymour Island, Antarctic Peninsula. American Geophysical Union, Washington D.C.

Stilwell, J.D., Zinsmeister, W.J., 2000. Paleobiogeographic synthesis of the Eocene macrofauna from McMurdo Sound, Antarctica. In: Stilwell, J.D., Feldmann, R. M. (Eds.), Paleobiology and paleoenvironments of Eocene rocks, McMurdo Sound, East Antarctica. American Geophysical Union Antarctic Research Series, Washington D.C., pp. 365-372.

Stilwell, J.D., Zinsmeister, W.J., Oleinik, A.E., 2004. Early Paleocene molluscs of Antarctica: systematics, paleoecology, and paleobiogeographic significance. Bulletin of American Paleontology 367, 1-89.

Stolldorf, T., Schenke, H.-W., Anderson, J.B., 2012. LGM ice sheet extent in the Weddell Sea: evidence for diachronous behavior of Antarctic Ice Sheets. Quaternary Science Reviews 48, 20-31.

Struck, T.H., 2014. TreSpEx — Detection of misleading signal in phylogenetic reconstructions based on tree information. Evolutionary Bioinformatics 10, 51-67.

Struck, T.H., Purschke, G., Halanych, K.M., 2006. Phylogeny of Eunicida (Annelida) and exploring data congruence using a Partition Addition Bootstrap Alteration (PABA) approach. Systematic Biology 55, 1-20.

Strugnell, J.M., *et al.*, 2011. The Southern Ocean: source and sink? Deep-Sea Research Part II: Topical Studies in Oceanography 58, 196-204.

Strugnell, J.M., Rogers, A.D., Prodöhl, P.A., Collins, M.A., Allcock, A.L., 2008. The thermohaline expressway: the Southern Ocean as a centre of origin for deep-sea octopuses. Cladistics 24, 853-860.

Sturmbauer, C., Hainz, U., Baric, S., Verheyen, E., Salzburger, W., 2003. Evolution of the tribe Tropheini from Lake Tanganyika: synchronized explosive speciation producing multiple evolutionary parallelism. Aquatic Biodiversity. Springer, pp. 51-64.

Susko, E., 2015. Bayesian long branch attraction bias and corrections. Systematic biology 64, 243-255.

Sutherland, D.L., Hogg, I.D., Waas, J.R., 2010. Phylogeography and species discrimination in the *Paracalliope fluviatilis* species complex (Crustacea: Amphipoda): can morphologically similar heterospecifics identify compatible mates? Biological Journal of the Linnean Society 99, 196-205.

Swofford, D.L., 2003. PAUP*. Phylogenetic analysis using parsimony (*and other methods). Version 4. Sinauer Associates, Sunderland.

T

Takezaki, N., Rzhetsky, A., Nei, M., 1995. Phylogenetic test of the molecular clock and linearized trees. Molecular Biology and Evolution 12, 823-833.

Takhteev, V.V., 2000. Trends in the evolution of Baikal amphipods and evolutionary parallels with some marine malacostracan faunas. Advances in Ecological Research. Academic Press, pp. 197-220.

Talarico, F.M., Kleinschmidt, G., 2009. Chapter 7. The Antarctic continent in Gondwanaland: a tectonic review and potential research targets for future investigations. In: Florindo, F., Siegert, M. (Eds.), Developments in Earth and Environmental Sciences. Elsevier, Amsterdam, pp. 257–308.

Tamura, K., Stecher, G., Peterson, D., Filipski, A., Kumar, S., 2013. MEGA6: molecular evolutionary genetics analysis version 6.0. Molecular Biology and Evolution 30, 2725-2729.

Taylor, B.J., 1972. An urdid isopod from the Lower Cretaceous of South-East Alexander Island. British Antarctic Survey Bulletin 27, 97-103.

Thatje, S., 2012. Effects of capability for dispersal on the evolution of diversity in Antarctic benthos. Integrative and comparative biology 52, 470-482.

Thatje, S., Anger, K., Calcagno, J.A., Lovrich, G.A., Pörtner, H.-O., Arntz, W.E., 2005a. Challenging the cold: crabs reconquer the Antarctic. Ecology 86, 619-625.

Thatje, S., Fuentes, V., 2003. First record of anomuran and brachyuran larvae (Crustacea: Decapoda) from Antarctic waters. Polar Biology 26, 279-282.

Thatje, S., Hillenbrand, C.-D., Larter, R., 2005b. On the origin of Antarctic marine benthic community structure. Trends in Ecology & Evolution 20, 534-540.

Thatje, S., Hillenbrand, C.-D., Mackensen, A., Larter, R., 2008. Life hung by a thread: endurance of Antarctic fauna in glacial periods. Ecology 89, 682-692.

Thiel, H., Pörtner, H.-O., Arntz, W., 1996. Marine life at low temperatures — a comparison of polar and deep-sea characteristics. In: Uiblein, F., Ott, J., Stachowitsch, M. (Eds.), Deep-sea and extreme shallow-water habitats affinities and adaptations. Biosystematics and Ecology Series. Austrian Academy of Science Press, Vienna, pp. 183-219.

Thiel, M., 1999. Duration of extended parental care in marine amphipods. Journal of Crustacean Biology 19, 60-71.

Thiel, M., 2011. Chemical communication in peracarid crustaceans. In: Breithaupt, T., Thiel, M. (Eds.), Chemical Communication in Crustaceans. Springer New York, New York, pp. 199-218.

Thomas, D.N., *et al.*, 2008. The biology of polar regions. Oxford University Press, New York.

Thomas, E., Gooday, A.J., 1996. Cenozoic deep-sea benthic foraminifers: tracers for changes in oceanic productivity? Geology 24, 355-358.

Thornhill, D.J., Mahon, A.R., Norenburg, J.L., Halanych, K.M., 2008. Open-ocean barriers to dispersal: a test case with the Antarctic Polar Front and the ribbon worm *Parborlasia corrugatus* (Nemertea: Lineidae). Molecular Ecology 17, 5104-5117.

Toews, D.P.L., Brelsford, A., 2012. The biogeography of mitochondrial and nuclear discordance in animals. Molecular Ecology 21, 3907-3930.

Tripati, A.K., Roberts, C.D., Eagle, R.A., 2009. Coupling of CO_2 and ice sheet stability over major climate transitions of the last 20 million years. Science 326, 1394-1397.

Turner, G.F., 2007. Adaptive radiation of cichlid fish. Current Biology 17, R827-R831.

V

Vaidya, G., Lohman, D.J., Meier, R., 2011. SequenceMatrix: concatenation software for the fast assembly of multi-gene datasets with character set and codon information. Cladistics 27, 171-180.

Väinölä, R., Witt, J.D.S., Grabowski, M., Bradbury, J.H., Jażdżewski, K., Sket, B., 2008. Global diversity of amphipod (Amphipoda; Crustacea). Hydrobiologia 595, 241-255.

Valdes, P.J., Sellwood, B.W., Price, G.D., 1996. The concept of Cretaceous climate equability. Palaeoclimates 1, 139-158.

Van dover, C.L., Kaartvedt, S., Bollens, S.M., Wiebe, P.H., Martin, J.W., France, S.C., 1992. Deep-sea amphipod swarms. Nature 358, 25-26.

Verheye, M.L., 2011. Systématique et diversité génétique des *Eusirus* de l'Ocean Austral (Crustacea, Amphipoda, Eusiridae). Laboratoire de Biologie Marine. Université Catholique de Louvain-la-Neuve, Louvain-la-Neuve, p. 127.

Verheye, M.L., Backeljau, T., d'Udekem d'Acoz, C., 2016a. Looking beneath the tip of the iceberg: diversification of the genus *Epimeria* on the Antarctic shelf (Crustacea, Amphipoda). Polar Biology 39, 925-945.

Verheye, M.L., Martin, P., Backeljau, T., d'Udekem D'Acoz, C., 2016b. DNA analyses reveal abundant homoplasy in taxonomically important morphological characters of Eusiroidea (Crustacea, Amphipoda). Zoologica Scripta 45, 300-321.

Verheye, M.L., Backeljau, T., d'Udekem d'Acoz, C.,2017.Locked in the icehouse: evolution of an endemic *Epimeria* (Amphipoda, Crustacea) species flock on the Antarctic shelf. Molecular Phylogenetics and Evolution 114, 14-33.

Vinogradov, M.E., Volkov, A.F., Semenova, T.N., 1996. Hyperiid amphipods (Amphipoda, Hyperiidea) of the world oceans. Smithsonian Institution Libraries, Washington DC.

W

Wägele, J.W., Mayer, C., 2007. Visualizing differences in phylogenetic information content of alignments and distinction of three classes of long-branch effects. BMC Evolutionary Biology 7, 147.

Walker, A.O., 1906. Preliminary descriptions of new species of Amphipoda from the "Discovery" Antarctic Expedition 1902-1904. Annals and Magazine of Natural History 7, 13-18.

Walker, T.D., Valentine, J.W., 1984. Equilibrium models of evolutionary species diversity and the number of empty niches. The American Naturalist 124, 887-899.

Warrant, E.J., Locket, N.A., 2004. Vision in the deep-sea. Biological reviews of the Cambridge Philosophical Society 79, 671-712.

Waters, J.M., 2008. Driven by the West Wind Drift? A synthesis of southern temperate marine biogeography, with new directions for dispersalism. Journal of Biogeography 35, 417-427.

Waters, J.M., McCulloch, G.A., Eason, J.A., 2007. Marine biogeographical structure in two highly dispersive gastropods: implications for trans-Tasman dispersal. Journal of Biogeography 34, 678-687.

Watling, L., 1993. Functional morphology of the amphipod mandible. Journal of Natural History 27, 837-849.

Watling, L., Holman, H., 1980. New Amphipoda from the Southern Ocean, with partial revisions of the Acanthonotozomatidae and Paramphithoidae. Proceedings of the Biological Society of Washington 93, 609-654.

Watling, L., Thurston, M., 1989. Antarctica as an evolutionary incubator: evidence from the cladistic biogeography of the amphipod family Iphimediidae. In: Crame, J.A. (Ed.), Origin and evolution of Antarctic biota. Geological Society Special Publications, London, pp. 297-313.

Weir, J.T., 2006. Divergent timing and patterns of species accumulation in lowland and highland neotropical birds. Evolution 60, 842-855.

Weitschat, W., Brandt, A., Coleman, C.O., Moller-Andersen, N., Myers, A.A., Wichard, W., 2002. Taphocoenosis of an extraordinary arthropod community in Baltic amber. Mitteilungen des Geologischen-Palaontologischen Instituts, Universitat Hamburg 86, 189-210.

Whitworth, T., 1980. Zonation and geostrophic flow of the Antarctic circumpolar current at Drake Passage. Deep-Sea Research Part A. Oceanographic Research Papers 27, 497-507.

Wickett, N.J., *et al.*, 2014. Phylotranscriptomic analysis of the origin and early diversification of land plants. Proceedings of the National Academy of Sciences 111, E4859-E4868.

Williams, S.T., Reid, D.G., Littlewood, D.T., 2003. A molecular phylogeny of the Littorininae (Gastropoda: Littorinidae): unequal evolutionary rates, morphological parallelism, and biogeography of the Southern Ocean. Molecular Phylogenetics and Evolution 28, 60-86.

Wilson, D.S., Pollard, D., DeConto, R.M., Jamieson, S.S.R., Luyendyk, B.P., 2013. Initiation of the West Antarctic Ice Sheet and estimates of total Antarctic ice volume in the earliest Oligocene. Geophysical Research Letters 40, 4305-4309.

Wilson, N.G., Hunter, R.L., Lockhart, S.J., Halanych, K.M., 2007. Multiple lineages and absence of panmixia in the “circumpolar” crinoid *Promachocrinus kerguelensis* from the Atlantic sector of Antarctica. Marine Biology 152, 895-904.

Wilson, N.G., Schrodl, M., Halanych, K.M., 2009. Ocean barriers and glaciation: evidence for explosive radiation of mitochondrial lineages in the Antarctic sea slug *Doris kerguelenensis* (Mollusca, Nudibranchia). Molecular Ecology 18, 965-984.

Witt, J.D.S., Threloff, D.L., Hebert, P.D.N., 2006. DNA barcoding reveals extraordinary cryptic diversity in an amphipod genus: implications for desert spring conservation. Molecular Ecology 15, 3073-3082.

Witts, J.D., *et al.*, 2016. Macrofossil evidence for a rapid and severe Cretaceous-Paleogene mass extinction in Antarctica. Nature Communications 7, 1-9.

Woodburne, M.O., Zinsmeister, W.J., 1984. The first land mammal from Antarctica and its biogeographic implications. Journal of Paleontology 58, 913.

Worby, A.P., Jeffries, M.O., Weeks, W.F., Morris, K., Jana, R., 1996. The thickness distribution of sea ice and snow cover during late winter in the Bellingshausen and Amundsen Seas, Antarctica. Journal of Geophysical Research: oceans 101, 28441-28455.

X

Xia, X., 2013. DAMBE5: a comprehensive software package for data analysis in molecular biology and evolution. Molecular Biology and Evolution 30, 1720-1728.

Xia, X., Xie, Z., Salemi, M., Chen, L., Wang, Y., 2003. An index of substitution saturation and its application. Molecular Phylogenetics and Evolution 26, 1-7.

Y

Yang, Z., 2007. PAML 4: phylogenetic analysis by Maximum Likelihood. Molecular Biology and Evolution 24, 1586-1591.

Yang, Z., 2015. The BPP program for species tree estimation and species delimitation. Current Zoology 61, 854–865.

Yang, Z., Rannala, B., 2010. Bayesian species delimitation using multilocus sequence data. Proceedings of the National Academy of Sciences 107, 9264-9269.

Yang, Z., Rannala, B., 2014. Unguided species delimitation using DNA sequence data from multiple loci. Molecular Biology and Evolution 31, 3125-3135.

Yoder, A.D., Irwin, J.A., Payseur, B.A., 2001. Failure of the ILD to determine data combinability for slow loris phylogeny. Systematic Biology 50, 408-424.

Yoder, J.B., *et al.*, 2010. Ecological opportunity and the origin of adaptive radiations. Journal of Evolutionary Biology 23, 1581-1596.

Z

Zachos, J.C., Dickens, G.R., Zeebe, R.E., 2008. An early Cenozoic perspective on greenhouse warming and carbon-cycle dynamics. Nature 451, 279-283.

Zachos, J.C., Quinn, T.M., Salamy, K.A., 1996. High-resolution (104 years) deep-sea foraminiferal stable isotope records of the Eocene–Oligocene climate transition. Paleoceanography 11, 251-266.

Zelaya, D.G., 2005. The bivalves from the Scotia Arc islands: species richness and faunistic affinities. Scientia Marina 69, 113-122.

Zhang, J., Kapli, P., Pavlidis, P., Stamatakis, A., 2013. A general species delimitation method with applications to phylogenetic placements. Bioinformatics 29, 2869-2876.

Zinsmeister, W.J., 1979. Biogeographic significance of the late Mesozoic and early Tertiary molluscan faunas of Seymour Island (Antarctic Peninsula) to the final breakup of Gondwanaland. In: Gray, J., Boucot, A.J. (Eds.), Historical biogeography, plate tectonics, and the changing environment. Oregon State University Press, Corvallis, pp. 349-355.

Zinsmeister, W.J., 1982. Late Cretaceous-early Tertiary molluscan biogeography of the southern circum-Pacific. Journal of Paleontology 56, 84-102.

Zinsmeister, W.J., 1984. Late Eocene bivalves (Mollusca) from the La Meseta Formation, collected during the 1974-1975 joint Argentine-American expedition to Seymour Island, Antarctic Peninsula. Journal of Paleontology 58, 1497-1527.

Zinsmeister, W.J., Feldmann, R.M., 1984. Cenozoic high latitude heterochroneity of Southern Hemisphere marine faunas. Science 224, 281-283.

Zwickl, D.J., 2006. Genetic algorithm approaches for the phylogenetic analysis of large biological sequence datasets under the maximum likelihood criterion. Ph.D. dissertation. University of Texas, Austin.

Appendix

APPENDIX S1. Diagnosis of the superfamily Eusiroidea.

Superfamily Eusiroidea.

Body often carinate or processiferous. Rostrum often well developed. Eye subquadrate, reniform or rounded, never merged dorsally. Antennae not sexually dimorphic in size, or very weakly so. Articles of peduncle of antenna 1 (especially the first one) can bear processes or teeth, of variable development. Flagella of antennae long with many articles. Accessory flagellum of antenna 1 vestigial or absent; if present 1- or 2-articulated. Calceoli present or absent, if present of eusirid, pontogeneiid or gammarellid type (cfr Lincoln & Hurley, 1981). Upper lip very variable in shape, symmetrical or not. Mandibular palp always present and 3-articulated. Lacinia mobilis, if present, uniplated. Maxilla 1 usually with a 2-articulated palp, if 1-articulated, smaller than the outer plate. Inner plate of the maxilla 1 marginally setose. Maxilla 2 always with separated lobes. Maxilliped with well-developed and separated inner plates. Gnathopods and pereiopods weakly setose and normal spination. Gnathopods often but not always weak, subcheliform, cheliform or simple, but not carpochelate. Gnathopod 1 ≤ gnathopod 2; gnathopods 1 and 2 morphologically usually similar or subsimilar. Gnathopod 2 not sexually dimorphic, or very weakly so, with palm smooth or minutely denticulate, rarely dentate or excavate, with dactylus often deeply dentate. Oostegites broad and large. Coxal gills simple, never double-pleated, rarely with basal process, usually present on pereiopod 7; transverse folding absent or very weak. Coxae usually medium-sized to large, very variable in shape. Coxa 4 always excavate. Coxa 5–6 posteriorly lobate. Coxa 5 not very deep when basal in shape. Pereiopods 5–7 homopodous, usually gradually increasing in size posteriorly. Dactylus of pereiopod 7 curved, without strong spines or long setae. Pleonites with spines never disposed in transverse rows. Pleopods strong, with long stalk. Urosome segments never fused, without dorsal clusters of spines. Uropods well developed. Uropods 1 almost always without ventrolateral spines, rami without ventral setae, lanceolate, senticaudate or not; outer ramus subequal or shorter than inner ramus. Rami of uropod 3 lanceolate and much longer than the peduncle; outer ramus one-segmented, shorter or subequal to inner ramus. Telson cleft or entire, not fleshy; if spinose the spines are weak, neither dorsal nor forming clusters.

Composition: Bateidae (not sequenced), Acanthonotozomatidae, Acanthonotozomellidae, Amathillopsidae, Astyridae, Calliopiidae excluding *Cleippides* and *Weyprechtia*, Dikwidae, Epimeriidae, Eusiridae, Gammarellidae excluding *Gammarellus*, Iphimediidae, Laphystiopsidae (not sequenced), Pleustidae, Pontogeneiidae, Sanchoidae (not sequenced), Stilipedidae, Thurstonellidae and Vicmusiidae.

APPENDIX S2. Important morphological character differences between Eusiroidea and the remaining families of clade A: Colomastigidae, Amphilochidae, Hyperiidea, Leucothoidae and Oedicerotidae.

		EUSIROIDEA
OEDICEROTIDAE	The rostrum is usually large and hood-like, bearing the eyes; the eyes are usually dorsally fused, or absent.	The eyes are on the sides of the head, never fused. When the rostrum is present, it is narrow or fairly narrow.
	The antennae bear numerous setae. The antenna 2 is usually longer in the male than in the female. The peduncles of the antennae are often elongated.	The antennae do not bear numerous setae. The sexual dimorphism of the size of the antennae is absent or very weak. The peduncles of the antennae are never strongly elongated.
	The gnathopods are generally dissimilar.	The gnathopods are generally subsimilar.
	The pereiopods are strongly setose. The pereiopods 3–4 have a thick dactylus, with a minute unguis encapsulated in a unguial hood. The pereiopod 7 is considerably larger and of different shape than the pereiopods 5–6 (which are subequal). Its dactylus is straight and very long, adorned with strong spines and long setae.	The pereiopods are not strongly setose. The dactyli of pereiopods 3–4 are thinner; when the unguis is present, it is not reduced and encapsulated in an unguial hood. The pereiopods are homopodous. The dactyli are curved and not adorned with spines and long setae (the dactyli of some stilipedids can bear minute setules).
	The coxae are marginally setose. The coxa 4 is usually non excavated.	The coxae are not setose. The coxa 4 is always excavated.
	The uropod 3 has an elongated peduncle, usually slightly shorter than the rami, sometimes subequal or longer.	The peduncle of uropod 3 is not elongated, much shorter than the rami.
LEUCOTHOIDAE	The flagella of the antennae is short. The peduncles of the antennae are often elongated or inflated.	The flagellae of the antennae are usually long, with many articles. The peduncles of the antennae are never strongly elongated, nor inflated.
	The gnathopods are strong and very dissimilar, with gnathopod 1 carpochelate and gnathopod 2 subcheliform. The palm of the second gnathopod is sometimes toothed or strongly denticulated. The gnathopod 2 of some leucothoids exhibits strong sexual dimorphism.	The gnathopods are usually feeble and subsimilar, when they are dissimilar (Iphimediidae), the first one is simple and the second chelate, and both feeble. The palm of the second gnathopod is usually smooth or finely denticulated, very rarely toothed. The gnathopods of eusiroids are non sexually dimorphic, or very weakly so.
	The maxillipeds have very small outer plates and partially fused inner plates.	The maxillipeds have medium to large outer plates and separated inner plates.
	The uropod 2 is shortened. The uropod 3 has an elongated peduncle, longer than the rami.	The uropod 2 is not shortened. The peduncle of uropod 3 is not elongated, much shorter than the rami.

AMPHILOCHIDAE	The first antenna bears long setae. The flagellae of the antennae are short. The first antenna larger in males than in females.	The first antenna does not bear long setae. The flagellae of the antennae are usually long, with many articles. The sexual dimorphism of the size of the antennae is absent or very weak.
	The gnathopods are dissimilar, with gnathopod 2 often incompletely carpochelate. The palm is usually toothed or strongly denticulated.	The gnathopods are usually similar, the gnathopod 2 is never carpochelate. The palm is usually smooth or finely denticulated, rarely toothed.
	The anterior coxae (coxae 2, 3 and 4 or just 3 and 4) are enlarged, can be hypertrophied.	Some eusiroids can be deeper-plated (Pleustidae) but the anterior coxa are never hypertrophied.
	The uropod 2 is shortened. The uropod 3 has an elongated peduncle, longer than the rami.	The uropod 2 is not shortened. The peduncle of the uropod 3 is not elongated, much shorter than the rami.
	The telson is very long and acutely pointed.	The telson is very variable in shape, but never so long, and never acutely pointed.
COLOMASTIGIDAE	The peduncles of both antennae are enlarged and/or inflated. The flagellae are reduced to a few articles and terminally bear long setae.	The peduncles of the antennae are never strongly elongated, nor inflated. The flagellae of the antennae are usually long, with many articles, never reduced and never strongly setose.
	The gnathopods are very dissimilar. The gnathopod 1 is usually armed with apical spines or setae forming a brush (sometimes not present in males). The gnathopod 2 of many colomastigids exhibits strong sexual dimorphism.	The gnathopods are usually similar. The gnathopod 1 do not bear apical setae or spines. The gnathopods are non sexually dimorphic or very weakly so.
	The coxae are very short.	The coxae are medium to deep.
	The maxilla 1 has a 1-articulated palp, larger than the outer plate. The lobes of the maxilla 2 are partially coalesced. The mandibular palp is absent. The inner plates of the maxillipeds are very small, fully or partially coalesced.	The maxilla 1 usually has a 2-articulated palp, if it is 1-articulated, it is smaller than the outer plate. The lobes of the maxilla 2 are separated. The mandibular palp is always present and 3-articulated. The inner plates of the maxillipeds are well-developed and separated.
	The urosomites 2 and 3 are coalesced. The rami of uropod 3 or the outer ramus only are/is not much longer than the peduncle, sometimes smaller.	The urosomites 2–3 are never fused. The rami of uropod 3 are both much longer than the peduncle.
HYPERIIDAE	The head is globular.	The head is not globular.
	Both antennae are usually reduced in the female, especially antenna 2 which may be rudimentary or absent. The peduncles are shortened. The peduncle of antenna 1 is often less than 3-articulated. The peduncle of antenna 2 is always less than 5-articulated. The flagella are often reduced to a few articles (sometimes not in males).	The sexual dimorphism of the size of the antennae is absent or very weak, the antennae are never reduced. The peduncle is never shortened. The peduncle of antenna 1 is 3-articulated and the peduncle of antenna 2 is 5-articulated. The flagellae of the antennae are usually long, with many articles.
	The gnathopods are usually dissimilar. The prehension is usually effected by the closure of the propodus against the expanded carpus.	The gnathopods are usually similar. The prehension is effected by the closure of the dactylus against an expanded propodus
	The coxae are reduced and do not overlap.	The coxae are medium to deep and overlap.
	The palp of the maxilliped is rudimentary (1 segment) or absent.	The palp of the maxilliped is almost always present and 3 or 4-segmented.
	The urosomites 2–3 are fused.	The urosomites 2–3 are never fused.
	The rami of the uropods are moderately to very broad, rarely quite narrow and never styliform. The uropod 3 often has an elongated peduncle, longer than the rami.	The rami of the uropods are long and narrow. The peduncle of the uropod 3 is not elongated, much shorter than the rami.

APPENDIX S3. Summary of the morphological differences observed between specimens from different clades within the species complexes.

Unique or rare character states for the lineages (possible autapomorphies) are indicated in bold.

CLADE A *similis/ macrodonta* complex	**MA1**	**MA2**	**MA3**	**MA4**	**SI1**	**SI2**	**SI3**	**SI4**	**SI5**	**SP1**	**SP2**
# specimens examined	20+	20+	20+	10+	3	20+	20+	20+	20+	1	5
Dentition of peduncle of antenna 1	strong	strong	strong	strong	strong	strong	strong	strong	strong	**weak**	**weak**
Pereio-, pleonites with styliform mid-dorsal tooth	pleonite 3	pleonite 3	pleonite 3	pleonite 3	none	none	none	none	none	**pereionite 1 to pleonite 3**	none
Pereionite 1 mid-dorsal tooth	small	absent to small	medium	medium	absent	absent	absent to small	absent	absent	**large**	absent
Pereionite 2 mid-dorsal tooth	absent	absent	absent	absent	small	absent	small	small or reduced to a bump	absent	**large**	absent
Pereionite 3 mid-dorsal tooth	medium, broad, blunt	medium, broad, subacute or fairly small and blunt	medium, broad, blunt	medium, broad, blunt	medium, broad and blunt	**small, subacute, not broad**	medium, very broad and blunt	medium, broad, subacute	**small (sometimes reduced to bump), not broad**	**long, styliform**	**absent**
Shape of mid-dorsal teeth on pereionite 7 to pleonite 2	not angulate,	scarcely angulate	**anteriorly very angulate**	scarcely angulate	not angulate	not angulate	not angulate	not angulate	not angulate	not angulate (teeth styliform)	not angulate
Size of mid-dorsal teeth on pereonites 3 to 6 >< pereonite 7 to pleonite 2	size of teeth gradually increasing towards posterior segments	size of teeth gradually increasing towards posterior segments	size of teeth gradually increasing towards posterior segments	size of teeth gradually increasing towards posterior segments	size of teeth gradually increasing towards posterior segments	size of teeth gradually increasing towards posterior segments	size of teeth gradually increasing towards posterior segments	size of teeth gradually increasing towards posterior segments	**teeth of per. 7 and pleonites 1–2 distinctly longer than teeth of per. 3–6**	size of teeth gradually increasing towards posterior segments	**teeth of per. 7 and pleonites 1–2 distinctly longer than teeth of per. 3–6**
Dorsolateral teeth carinate	no	no	no	no	no	no	no	no	**yes**	no	no
Pleonite 1, number of pairs of dorsolateral teeth	1	1	1	1	1	1	1	1	**2**	1	**2**
Coxa 4 lateral tooth	small, pointing obliquely	small, **pointing backwards**	large, pointing obliquely	large, pointing very obliquely	absent	absent	small, pointing obliquely	small, pointing obliquely	**reduced to a blunt angle**	**large, pointing laterally**	absent

Coxa 7, posteroventral angle	bluntly angulate	sharply angulate	sharply angulate	bluntly angulate	produced into a small tooth	produced into a small tooth	**produced into a strong tooth**	produced into a small tooth	sharply angulate	bluntly angulate	bluntly angulate
Posterodistal tooth of basis of P7	**extremely long**	long	long	long	small	small	small	small	small	**very small**	**very small**
Notch of carina of pleonite 3	scarcely distinct	scarcely distinct	absent	absent	**strong**	weak	**strong**	weak	weak	absent	scarcely distinct
Urosomite 1 dorsal process	narrowly triangular, pointing upwards	narrowly triangular, pointing upwards	narrowly triangular, pointing upwards	narrowly triangular, pointing upwards	fairly narrow, triangular, pointing upwards	broadly triangular, pointing upwards	broadly triangular, pointing upwards	broadly triangular, pointing upwards	broadly triangular, pointing upwards	**styliform, slightly pointing backwards**	**triangular, strongly arching backwards**
Urosomite 2 with pair of teeth	yes	yes	yes	yes	yes	yes	no	no	no	no	no

Appendix S3A. *similis*/*macrodonta* complex

CLADE B *puncticulata* **complex**	**PUN1**	**PUN2**	**PUN3**	**PUN4**
# specimens	4	1	1	3
Rostrum in frontal view	fairly broad	**narrow**	medium	medium
Coxa 4 anterior border	with angular discontinuity	**without angular discontinuity**	with angular discontinuity	with angular discontinuity
Ornamentation of pereionite 7 to pleonite 2	pleonite 1 smooth or with bump, pleonite 2 with tooth, pereionite 7 smooth	pleonite 1 with bump, pleonite 2 with tooth, pereionite 7 smooth	pleonite 1 with bump, pleonite 2 with tooth, pereionite 7 smooth	**pereionite 7 with small tooth, pleonites 1–2 with strong tooth**
Pleonite 3 posterodorsal profile	broadly rounded	broadly rounded	**narrowly rounded (subtriangular)**	**squared angle**
Anterior and posterior borders of basis of pereiopod 6	nearly parallel	**strongly diverging**	nearly parallel	slightly diverging
Posterodistal corner of basis of pereiopod 7	bluntly angulate	produced into a tooth	produced into a tooth	bluntly angulate

Appendix S3B. *puncticulata* complex

CLADE C *walkeri* **complex**	**WA1**	**WA2***	**WA3**	**WA4**
# specimens	15	1 (incomplete juvenile)	6	4
Eyes	huge	huge	huge	**medium**
Rostrum in dorsal and lateral view	**Narrow and short, reaching 1/2 article 1 peduncle A1**	Broad and short, reaching 1/2 article 1 peduncle A1	**Narrow and long, reaching 2/3 article 1 peduncle A1**	Broad and short, reaching 1/2 article 1 peduncle A1

Coxa 4	broad	narrow	**very narrow**	broad
Posterodistal corner of basis of pereiopods 6	angulate	rounded	angulate	rounded
Posterodistal corner of basis of pereiopod 7	produced into a triangular tooth, followed by concavity	rounded, not followed by concavity	rounded, not followed by concavity	produced into a rounded process, followed by concavity

Appendix S3C. *walkeri* complex*.* *As the only specimen of WA2 available is an incomplete juvenile, the character states of adults might differ.

CLADE E ***georgiana-rimicarinata-rubriequies* complex**	**GE1**	**GE2**	**GE3**	**GE4**	**GE5**	**RI**	**RU**
# specimens	30+	5	1	3	14	2	5
Rostrum in lateral view	weakly curved on anterior border, straight on posterior border, **tip broad**; medium-sized, reaching mid art. 2 of peduncle of A1	distinctly curved on anterior border, straight on posterior border, tip narrow; long, reaching tip art. 2 of peduncle of A1	distinctly curved on anterior border, straight on posterior border, tip narrow; medium-sized, reaching mid art. 2 of peduncle of A1	weakly curved on anterior border, straight on posterior border, tip narrow; long, reaching tip art. 2 of peduncle of A1	curved on both sides, tip narrow; **short, reaching tip art. 1 of peduncle of A1**	curved on both sides, tip narrow; medium-sized, reaching 0.3 of art. 2 of peduncle of A1	curved on both sides, tip narrow; **very long, reaching 0.7 of art. 2 of peduncle of A1**
Rostrum in frontal view	**broad until the tip, borders weakly convergent**	narrow, especially distally, borders distinctly convergent	**proximally broad, but narrower distally,** borders distinctly convergent	narrow, especially distally, borders strongly convergent	narrow, especially distally, borders distinctly convergent	narrow, especially on tip, borders strongly convergent	**extremely narrow, with border straight**
Eye	broadly elliptic	broadly elliptic	broadly elliptic	**Reniform**	**Reniform**	broadly elliptic	broadly elliptic
Mid-dorsal ornamentation of pereionites and pleonites	low blunt, weakly laterally compressed, **carinae from pereionite 3 to pleonite 3**	low blunt, weakly laterally compressed, **carinae from pereionite 4 to pleonite 3**	low blunt, weakly laterally compressed, carinae from pereionite 5 to pleonite 3	low blunt**, distinctly laterally compressed**, carinae from pereionite 5 to pleonite 3	low blunt, **carinae from pereionite 2 to pleonite 3; the posterior ones are strongly compressed**	**low tridimensionnally sculpted carinae from pereionite 2 to pleonite 3**	**huge styliform teeth on all segments**
Coxa 4, anterior corner	blunt acute (nearly squared) angle	blunt acute (nearly squared) angle	**very broadly rounded angle**	blunt obtuse angle	**very broad asymmetrical angle**	blunt squared angle	blunt obtuse (nearly squared) angle
Coxa 4, anteroventral border	weakly concave	weakly concave	weakly concave	straight	straight	very weakly concave	straight
Coxa 4, ventral corner	sharp, squared angle	sharp, squared angle	sharp, squared angle	**acute angle**	**broadly rounded squared angle**	**acute angle**	**produced into a tooth**
Coxa 4, posteroventral area	low carina present, **at its deepest point very distant from border;** border distinctly	low carina present, at its deepest point close to border; border distinctly concave	low carina present, at its deepest point close to border; border distinctly concave	no carina; border distinctly concave	no carina; border distinctly concave	**strong carina, at its deepest point very distant from border; border strongly**	low carina present, at its deepest point moderately distant from border; border

	concave					**concave**	distinctly concave
Coxa 5 in dorsal view: posterior projection	very rounded, obtuse (nearly squared) angle	rounded squared angle	extremely rounded, obtuse angle	**small tooth pointing laterally**	blunt ,obtuse (nearly squared) angle	**small rounded tooth pointing backwards**	**huge styliform tooth pointing obliquely backwards**
Posterodistal notch of basis of P7 (adults)	acute to squared angle	acute angle	acute angle	**reduced to very weak, obtuse concavity**	obtuse (nearly squared) angle	obtuse (nearly squared) angle	**Very obtuse angle**

Appendix S3D. *georgiana-rimicarinata-rubrieques* complex

CLADE G *robustoides/robusta* **complex**	**RO1**	**RO2**	**RO3**
# specimens			
Rostrum: anterior border in lateral view	**strongly curved**	weakly curved	weakly curved
Pleonites 1-2 posterodorsal corner	produced into a posteriorly directed tooth	produced into a posteriorly directed tooth	**not produced into a posteriorly directed tooth**
Urosomite 3 dorsolateral margins	very weakly concave	**strongly concave**	weakly concave
Posterodistal corner of basis of pereiopods 5–7	produced into a sharp tooth	**produced into a fairly blunt tooth**	produced into a sharp tooth

Appendix S3E. *robusta-robustoides* complex

CLADE H *grandirostris-pulchra-oxicarinata* **complex**	**GR1**	**GR2**	**PUL2**	**OX**
# specimens	7	3	2	20+
Rostrum	anterior border weakly curved, only on distal half	**anterior border very curved on all its length**	anterior border weakly curved, only on distal half	**anterior border very curved on its distal 0.75**
Mid-dorsal carinae of pereionites 1 to pleonite 2 height and sharpness	low, broad and blunt	low, broad and blunt	**Medium-sized, broad and subacute**	**high, styliform**
Size of mid dorsal carina in pereionite 2 >< per. 1	about same height	about same height	a bit shorter	**Considerably shorter**
Lateral symmetry of mid-dorsal carina of pereionites 4–6	posterior border nearly as broad as anterior border	**posterior border distinctly narrower than anterior border**	posterior border nearly as broad as anterior border	posterior border nearly as broad as anterior border
Coxa 4	laterally weakly expanded; very broadly rounded	laterally moderately expanded; broadly rounded	laterally very expanded; broadly rounded	laterally very expanded; **narrowly and sharply triangular**

Coxa 5	laterally moderately expanded and bluntly triangular	laterally weakly expanded; broadly and bluntly triangular	**laterally extremely expanded; narrowly and sharply triangular**	**laterally very expanded, styliform**
Basis of P5, posteroproximal process	triangular and sharp	**rounded**	triangular and sharp	triangular and sharp
Basis of P7 median angle of posterior border	obtuse, **broadly rounded**	obtuse, nearly squared	obtuse, nearly squared	acute, nearly squared

Appendix S3F. *grandirostris-pulchra-oxicarinata* complex

APPENDIX S4. Comparison of the fit of different lineage diversification models to the empirical and semi-empirical Antarctic *Epimeria* datasets.

Dataset	Model	LH	Rate shift times	λ	μ	x	K	AIC	dAIC	wAIC
Semi-emp 10 %	PB	1010 (17.79)	-	0.34 (0.02)	-	-	-	-2018 (35.58) [-2022.93 ;-2013.07]	128.13 (117.25 ; 139.01)	$9\ 10^{-29}$
	BD	1075.07 (21.46)	-	0.83 (0.07)	0.74 (0.08)	-	-	-2146.13 (42.92) [-2152.08 ; -2140.18]	0.00	0.62
	DDL	1008.87 (19.75)	-	0.34 (0.02)	-	-	6085859 (1026968)	-2013.74 (39.5) [-2019.21 ; -2008.27]	132.39 (120.97 ; 143.81)	$1\ 10^{-29}$
	DDX	1073.7 (21.54)	-	0.02 (0.01)	-	-0.58 (0.05)	-	-2143.4 (43.08) [-2149.37 ; -2137.43]	2.73 (-9.19 ; 14.65)	0.16
	Yule2rate	1063.62 (20.5)	0.01 (0.01)	0.34 (0.02) 0.81 (0.61)	-	-	-	-2121.25 (41) [-2126.93 ; -2115.57]	24.88 (13.95 ; 25.85)	$2\ 10^{-6}$
	BD- 1 shift	1077.7 (21.39)	19.45 (4.86)	0.16 (0.04) 0.8 (0.08)	0.01 (0.04) 0.68 (0.11)	-	-	-2142.26 (43.08) [-2148.23 ; -2136.29]	3.87 (-8.05; 15.79)	0.09
	BD- 2 shifts	1077.92 (21.45)	19.23 (6.04) 7.63 (5.13)	0.13 (0.06) 0.7 (0.75) 0.78 (0.09)	0 (0.01) 0.52 (0.75) 0.61 (0.17)	-	-	-2139.83 (42.89) [-2145.77 ; -2133.89]	6.3 (-5.59 ; 18.19)	0.03
	BD- 3 shifts	1079.28 (21.5)	21.69 (5.18) 12.79 (7.04) 6.5 (5.59)	0.12 (0.06) 0.38 (0.02) 0.62 (0.5) 0.78 (0.09)	0 (0.01) 0.14 0.45 (0.54) 0.6 (0.2)	-	-	-2142.57 (43) [-2148.53 ; -2136.61]	3.56 (-8.35 ; 15.47)	0.10
Semi-emp 50 %	PB	14.58 (3.36)	-	0.12 (0.01)	-	-	-	-27.16 (6.73) [-28.09 ; -26.23]	0.97 (-0.99 ; 2.93)	0.17
	BD	15.88 (3.89)	-	0.16 (0.02)	0.08 (0.03)	-	-	-27.76 (7.77) [-28.84 ; -26.68]	0.37 (-1.74 ; 2.48)	0.22
	DDL	14.57 (3.38)	-	0.12 (0.01)	-	-	1202874 (229958.4)	-25.14 (6.75) [-26.07 ; -24.20]	4.88 (1.03 ; 4.96)	0.06
	DDX	15.86 (3.83)	-	0.06 (0.01)	-	-0.21 (0.07)	-	-27.73 (7.67) [-28.79 ; -26.67]	2.29 (-1.69 ; 2.49)	0.22
	Yule2rate	17.06 (3.72)	0.35 (0.21)	0.12 (0.01) 0.12 (0.1)	-	-	-	-28.13 (7.43) [-29.16 ; -27.10]	0.00	0.27

	BD- 1 shift	17.36 (3.79)	15.35 (4.61)	0.07 (0.03) 0.14 (0.02)	0.01 (0.02) 0.02 (0.03)	-	-	-24.73 (7.57) [-25.78 ; -23.68]	3.4 (1.32 ; 5.48)	0.05
	BD- 2 shifts	18.6 (3.71)	17.69 (4.64) 10.31 (6.95)	0.07 (0.02) 0.13 (0.14) 0.13 (0.03)	0 (0) 0.05 (0.14) 0.02 (0.05)	-	-	-21.19 (7.41) [-22.22 ; -20.16]	6.94 (4.88 ; 9)	$8\ 10^{-3}$
	BD- 3 shifts	19.59 (3.71)	8.09 (6.63) 14.13 (6.33) 20.43 (5.94)	0.07 (0.03) 0.16 (0.28) 0.14 (0.19) 0.13 (0.04)	0 (0) 0.06 (0.26) 0.09 (0.5) 0.03 (0.1)	-	-	-17.19 (7.42) [-18.22 ; -16.16]	10.94 (8.88 ; 13)	$1\ 10^{-3}$
Semi-emp 72 %	PB	-16.9 (1.93)	-	0.09 (0)	-	-	-	35.79 (3.85) [35.26 ; 36.32]	0.00	0.33
	BD	-16.71 (2.07)	-	0.11 (0.01)	0.02 (0.02)	-	-	37.43 (4.14) [36.86 ; 38.00]	1.64 (0.54 ; 2.74)	0.15
	DDL	-16.87 (1.9)	-	0.1 (0.01)	-	-	506016 (454041.2)	37.74 (3.8) [37.21 ; 38.27]	1.95 (0.89 ; 3.01)	0.13
	DDX	-16.71 (2.06)	-	0.07 (0.01)	-	-0.09 (0.06)	-	37.42 (4.13) [36.85 ; 37.99]	1.63 (0.53 ; 2.73)	0.15
	Yule2rate	-15.41 (1.94)	0.9 (0.3)	0.1 (0) 0.06 (0.04)	-	-	-	36.82 (3.88) [36.28 ; 37.36]	1.03 (-0.04 ; 2.1)	0.20
	BD- 1 shift	-15.32 (2.05)	4.73 (4.67)	0.07 (0.03) 0.09 (0.03)	0 (0.01) 0 (0)	-	-	40.64 (4.1) [40.07 ; 41.21]	4.85 (3.75 ; 5.95)	0.03
	BD- 2 shifts	-14.02 (2.01)	19.01 (4.48) 8.65 (7.99)	0.06 (0.02) 0.09 (0.08) 0.07 (0.03)	0 (0) 0.01 (0.03) 0 (0.01)	-	-	44.04 (4.01) [43.48 ; 44.59]	8.25 (7.16 ; 9.33)	$5\ 10^{-3}$
	BD- 3 shifts	-13.19 (1.93)	21.39 (5.46) 17.23 (5.96) 7.41 (7.57)	0.06 (0.03) 0.06 (0.09) 0.11 (0.08) 0.07 (0.03)	0 (0) 0.01 (0.03) 0.01 (0.07) 0 (0.01)	-	-	48.39 (3.86) [47.85 ; 48.92]	12.6 (11.53 ; 13.66)	$6\ 10^{-4}$
Empirical	PB	-28.47	-	0.078	-	-	-	58.94	0.00	0.31
	BD	-28.47	-	0.078	0.000	-	-	60.94	2.00	0.12
	DDL	-28.31	-	0.093	-	-	120.040	60.62	1.68	0.14
	DDX	-28.47	-	0.082	-	0.016	-	60.94	2.00	0.12
	Yule2rate	-26.62	2.09	0.088 0.027	-	-	-	59.24	0.30	0.27

	BD- 1 shift	-26.79	2.00	0.088 0.029	0.001 0.000	-	-	63.58	4.64	0.03
	BD- 2 shifts	-25.51	17.00 2.00	0.049 0.102 0.028	0.000 0.000 0.000	-	-	67.02	8.08	0.005
	BD- 3 shifts	-24.77	19.00 17.00 2.00	0.058 0.000 0.103 0.029	0.000 0.000 0.001 0.000	-	-	71.54	12.60	0.001

Appendix S4. Mean parameter estimates (with standard deviations) and comparison of the fit of different lineage diversification models to the empirical and semi-empirical datasets (assuming 10 %, 50 % and 72 % sampling). LH is the log-likelihood value of the model; the shift times (Ma) are indicated for the models implying discrete shifts in diversification rates; λ is the speciation rate for the constant-rate models and the initial speciation rate for the rate-variable models; μ is the extinction rate; x is the rate change parameter of the density-dependent exponential (DDX) model; K is the carrying capacity parameter of the density-dependent linear (DDL) model. For each model, the Akaike Information Criterion (AIC) was computed. The best-fitting model with the lowest AIC score is highlighted in dark grey. The 95 % confidence intervals of the AIC values are indicated. dAIC is the difference between the AIC score of the model and the AIC score of the best fitting model. Minimal and maximal values for dAIC were calculated based on the AIC 95 % confidence intervals. The best-fitting model with the lowest mean AIC score is highlighted in dark grey. The evaluated models for which the dAIC range contains zero are highlighted in light grey. wAIC are the Akaike weights.

APPENDIX S5. Comparison of the fit of the lineage diversification models from Morlon et al. (2011) to the empirical Antarctic *Epimeria* dataset.

Dataset	Model	AIC	dAIC	wAIC	λ	α	μ	β
Sampling 72 %	BcstDcst	245.55	2.11	0.16	0.10	-	0.02	-
	BvarDcst	247.26	3.82	0.07	0.11	-0.015	0.00	-
	BcstDvar	247.08	3.64	0.07	0.10	-	0.007	0.08
	BvarDvar	249.62	6.18	0.02	0.10	0.002	0.008	0.08
	Bcst	243.44	0.00	0.45	0.093	-	-	-
	Bvar	244.88	1.44	0.22	0.11	-0.015	-	-
Sampling 50 %	BcstDcst	245.55	1.37	0.16	0.15	-	0.07	-
	BvarDcst	246.57	2.39	0.10	0.14	-0.03	0.00	-
	BcstDvar	246.65	2.47	0.09	0.14	-	0.02	0.06
	BvarDvar	249.07	4.89	0.03	0.14	-0.02	0.004	0.07
	Bcst	244.34	0.16	0.30	0.11	-	-	-
	Bvar	244.18	0.00	0.32	0.14	-0.03	-	-
Sampling 10 %	BcstDcst	245.55	2.83	0.13	0.75	-	0.66	-
	BvarDcst	245.11	2.39	0.16	0.37	-0.07	0.00	-
	BcstDvar	245.93	3.21	0.11	0.55	-	0.39	0.01
	BvarDvar	247.59	4.87	0.05	0.42	-0.06	0.09	-0.05
	Bcst	259.60	16.88	0.00	0.19	-	-	-
	Bvar	242.72	0.00	0.54	0.37	-0.07	-	-

Appendix S5. Parameter estimates and comparison of the fit of the lineage diversification models from Morlon et al. (2011) to the empirical dataset, assuming sampling fractions of 0.72, 0.5 and 0.1. λ is the speciation rate (when constant) or the initial speciation rate (when variable); α is the rate change parameter for the exponential variation of the speciation rate; μ is the extinction rate (when constant) or the initial extinction rate (when variable) ; β is the rate change parameter for the exponential variation of the extinction rate. For each model, the Akaike Information Criterion (AIC) was computed. dAIC is the difference between the AIC score of the evaluated model and the AIC score of the best-fitting model. wAIC is the Akaike weight. The best-fitting model with the lowest AIC score is highlighted in dark grey. When the wAIC of the best model < 0.5, the second best-fit is highlighted in light grey.

APPENDIX S6. Lineage diversification through time plot of the Antarctic iphimediid clade.

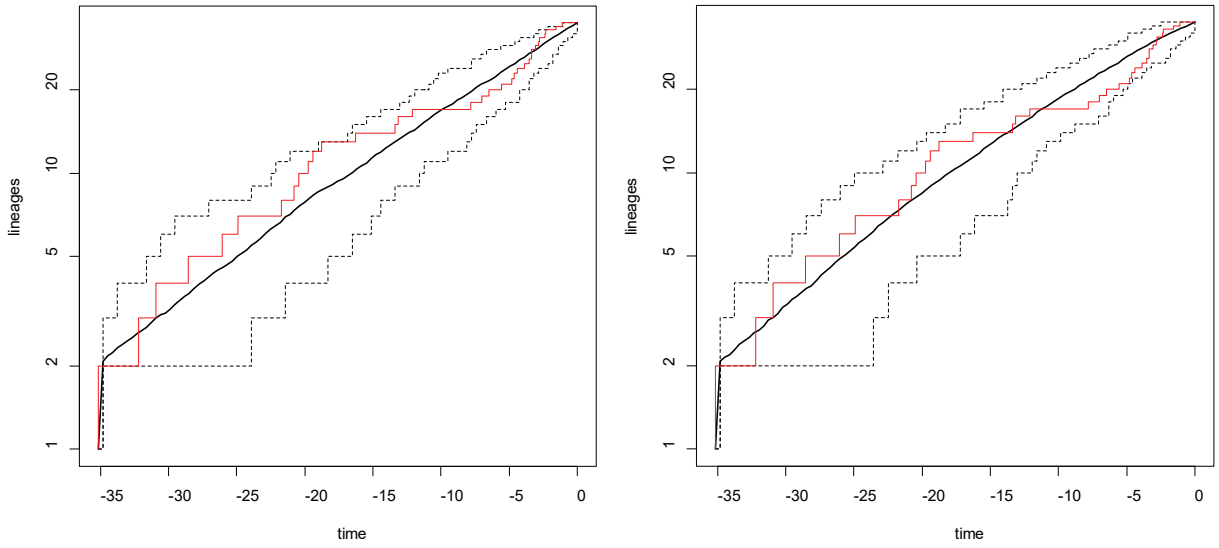

Appendix S6 -A. Lineage diversification through time plot of the Antarctic iphimediid clade, generated with the dated tree from the BEAST analysis (in red). Dashed lines represent the 95 % confidence interval of lineage diversification simulated 100 times under a BD (left; λ = 0.135 and μ = 0.06) and a PB (right; λ = 0.098) model, and assuming a sampling fraction of 50 %.

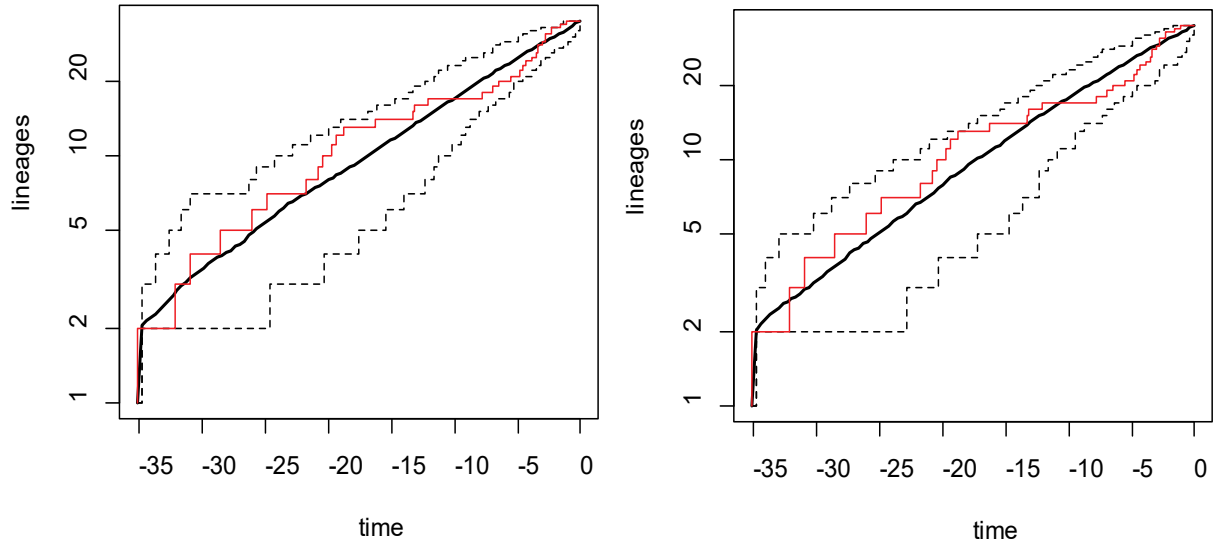

Appendix S6 -B. Lineage diversification through time plot of the Antarctic iphimediid clade, generated with the dated tree from the BEAST analysis (in red). Dashed lines represent the 95 % confidence interval of lineage diversification simulated 100 times under a BD (left; λ = 0.085 and μ = 0.008) and a PB (right; λ = 0.08) model, and assuming a sampling fraction of 79 %.

APPENDIX S7. Comparison of the fit of different lineage diversification models to the empirical and semi-empirical Antarctic iphimediid datasets.

Dataset	Model	LH	Rate shift times	λ	μ	x	K	AIC	dAIC	wAIC
Semi-emp 10 %	PB	939.50 (18.10)	-	0.31 (0.02)	-	-	-	-1877.00 (36.2) [-1886.39 ; -1871.15]	144.86 (130.94, 162.69)	$2.4\ 10^{-32}$
	BD	1010.32 (21.73)	-	0.78 (0.07)	0.71 (0.07)	-	-	-2016.65 (43.46) [-2025.75 ; -2008.76]	5.21 (-8.42, 25.08)	0.051
	DDL	938.2 (18.15)	-	0.31 (0.02)	-	-	6101472 (202079.2)	-1872.4 (36.3) [-1882.41 ; -1865.74]	149.46 (134.92, 168.10)	$2.4\ 10^{-33}$
	DDX	1007.89 (22.42)	-	0.02 (0)	-	-0.63 (0.05)	-	-2011.78 (44.84) [-2017.78 ; -2000.80]	10.08 (-0.45, 33.04)	0.004
	Yule2rate	1003.15 (22.11)	0.01 (0.01)	0.31 (0.02) 0.56 (0.34)	-	-	-	-2000.29 (44.22) [-2007.54 ; -1992.22]	21.57 (9.79, 41.62)	$1.4\ 10^{-5}$
	Yule3rate	1013.71 (24.1)	4.94 (1.15) 1.17 (0.66)	0.10 (0.01) 0.33 (0.06) 0.61 (0.08)	-	-	-	-2017.42 (48.20) [-2025.07 ; -2009.52]	4.44 (-7.74, 24.32)	0.074
	Yule4rate	1017.93 (22.75)	5.17 (1.92) 1.91 (1.45) 0.88 (0.57)	0.1 (0.02) 0.32 (0.11) 0.47 (0.37) 0.61 (0.08)	-	-	-	-2021.86 (45.49) [-2033.84 ; -2017.33]	0.00	0.686
	BD- 1 shift	1014.32 (23.14)	8 (2.97)	0.17 (0.04) 0.72 (0.07)	0 (0) 0.58 (0.12)	-	-	-2018.64 (46.28) [-2028,75 ; -2011.35]	3.22 (-11.42, 22.49)	0.137
	BD- 2 shifts	1016.74 (23.33)	9 (2.97) 5 (2.97)	0.14 (0.03) 0.37 (0.14) 0.70 (0.08)	0 (0) 0.21 (0.21) 0.51 (0.17)	-	-	-2016.19 (46.66) [-2027.90 ; -2008.81]	5.67 (-10.57, 25.03)	0.040
	BD- 3 shifts	1017.35 (22.80)	14 (7.41) 9 (4.45) 4 (2.97)	0.14 (0.03) 0.25 (0.25) 0.39 (0.22) 0.70 (0.08)	0 (0) 0.02 (0.04) 0.23 (0.32) 0.14 (0.03)	-	-	-2012.69 (45.6) [-2024.47 ; -2005.60]	9.67 (-7.14, 28.24)	0.007
Semi-emp 50 %	PB	5.87 (3.06)	-	0.11 (0)	-	-	-	-9.75 (6.11) [-10.63 ; -8.79]	5.75 (3.62, 8.71)	0.029

	BD	6.97 (3.87)	-	0.14 (0.02)	0.07 (0.03)	-	-	-9.94 (7.74) [-11.06 ; -8.63]	5.56 (3.19, 8.87)	0.031
	DDL	5.61 (3.07)	-	0.11 (0.01)	-	-	1188730 (62867.81)	-7.22 (6.15) [-8.46 ; -6.29]	8.28 (5.79, 11.21)	0.008
	DDX	6.22 (3.37)	-	0.07 (0.02)	-	-0.13 (0.09)	-	-8.44 (6.75) [-9.42 ; -7.19]	7.06 (4.83, 10.31)	0.149
	Yule2rate	8.64 (4.2)	0.33 (0.17)	0.11 (0.01) 0.09 (0.05)	-	-	-	-11.28 (8.41) [-13.56 ; -10.27]	4.22 (0.69, 7.23)	0.061
	Yule3rate	12.28 (4.19)	5.57 (4.07) 3.99 (3.47)	0.09 (0.02) 0.21 (0.27) 0.12 (0.03)	-	-	-	-14.57 (8.38) [-16.46 ; -13.11]	0.93 (-2.21, 4.39)	0.319
	Yule4rate	14.75 (5.04)	12.09 (9.85) [16.26 ; 10.89] 4.79 (3.50) [5.57 ; 4.38] 2.32 (2.09) [3.18 ; 2.28]	0.10 (0.03) [0.09-0.11] 0.14 (0.13) [0.07-0.16] 0.34 (0.44) [0.22-0.74] 0.11 (0.05) [0.10-0.12]	-	-	-	-15.5 (10.09) [-17.50 ; -14.25]	0.00	0.508
	BD- 1 shift	9.38 (4.74)	8 (1.48)	0.09 (0.01) 0.16 (0.03)	0 (0) 0.05 (0.06)	-	-	-8.76 (9.47) [-10.07 ; -7.19]	6.74 (4.18, 10.31)	0.017
	BD- 2 shifts	11.87 (5)	11 (7.41) 5 (4.45)	0.11 (0.02) 0.07 (0.01) 0.13 (0.04)	0 (0) 0 (0.01) 0.01 (0.02)	-	-	-7.56 [-9.75 ; -6.28]	7.94 (4.50, 11.22)	0.009
	BD- 3 shifts	12.93 (4.73)	18 [15 ; 18] 8 [8 ; 9] 3 [2 ; 4]	0.12 (0.02) [0.11 ; 0.12] 0.07 (0.08) [0.06 ; 0.07] 0.15 (0.13) [0.14 ; 0.17] 0.12 (0.04) [0.11 ; 0.13]	0 (0) 0 (0) 0.01 (0.01) 0.01 (0.02)	-	-	-3.87 (9.45) [-6.05 ; -2.39]	11.63 (8.20, 15.11)	0.001
Semi-emp 79.5 %	PB	-25.86 (1.63)	-	0.08 (0)	-	-	-	53.72 (3.26) [53.21 ; 54.70]	2.29 (0.88, 3.83)	0.118
	BD	-25.83 (1.77)	-	0.08 (0.01)	0.01 (0.01)	-	-	55.65 (3.54) [55.13 ; 56.66]	4.22 (2.80, 5.79)	0.045
	DDL	-25.83 (1.58)	-	0.09 (0)	-	-	372.25 (367.98)	55.66 (3.15) [55.15 ; 56.56]	4.23 (2.82, 5.69)	0.044

	DDX	-25.67 (1.45)	-	0.12 (0.03)	-	0.14 (0.09)	-	55.34 (2.9) [54.89 ; 56.19]	3.91 (3.86, 5.32)	0.052
	Yule2rate	-24.34 (1.39)	1.27 (0.43)	0.09 (0) 0.04 (0.01)	-	-	-	54.69 (2.77) [53.90 ; 55.22]	3.26 (2.89, 4.35)	0.072
	Yule3rate	-21.04 (2.13)	4.81 (1.89) 2.32 (1.13)	0.08 (0.01) 0.17 (0.17) 0.04 (0.03)	-	-	-	52.08 (4.26) [51.23 ; 52.92]	0.65 (-1.10, 2.05)	0.268
	Yule4rate	-18.72 (2.29)	18.73 (0) 4.93 (0) 2.32 (0.95)	0.12 (0.01) 0.05 (0.01) 0.16 (0.03) 0.04 (0.02)	-	-	-	51.43 (4.57) [50.87 ; 52.33]	0.00	0.371
	BD- 1 shift	-23.85	5	0.09 0.09	0 0	-	-	57.71 (3.4) [56.94 ; 58.44]	6.28 (4.61, 7.57)	0.016
	BD- 2 shifts	-21.51	12 2	0.12 0.13 0.05	0 0.01 0	-	-	59.02 (4.41) [58.18 ; 59.79]	7.59 (5.85, 8.92)	0.008
	BD- 3 shifts	-19.62 (2.47)	18 (2.97) 8 (4.45) 2 (1.48)	0.12 (0.02) 0.05 (0.03) 0.14 (0.05) 0.04 (0.05)	0 (0) 0 (0) 0.01 (0.02) 0 (0)	-	-	61.24 (4.95) [60.44 ; 61.99]	9.81 (8.11, 11.12)	0.002
Empirical	PB	-31.32	-	0.072	-	-	-	64.63	3.72	0.080
	BD	-31.32	-	0.072	0.000	-	-	66.63	5.73	0.029
	DDL	-31.10	-	0.088	-	-	101.903	66.20	5.30	0.036
	DDX	-30.77	-	0.156	-	0.283	-	65.53	4.63	0.051
	Yule2rate	-29.48	2.32	0.081 0.025	-	-	-	64.95	4.05	0.068
	Yule3rate	-26.48	4.78 2.31	0.063 0.169 0.025	-	-	-	62.95	2.05	0.185
	Yule4rate	-23.45	18.73 4.78 2.31	0.12 0.04	-	-	-	60.90	0.00	0.517

				0.17 0.02						
	BD- 1 shift	-28.70	1.00	1.00 10-4 1.11 10^{-4}	3.96 10^{-11} 1.19 10^{-5}	-	-	67.41	6.51	0.020
	BD- 2 shifts	-26.49	10 1	0.14 0.17 2 10^{-3}	3.42 10^{-4} 0.22 2.14 10^{-3}	-	-	68.98	8.08	0.009
	BD- 3 shifts	-24.63	10 8 1	0.12 2.37 10^{-4} 0.16 2.10 10^{-3}	1.11 10^{-8} 0.56 0.21 2.00 10^{-3}	-	-	71.26	10.36	0.003

Appendix S7. Comparison of the fit of different lineage diversification models to the empirical and semi-empirical datasets (assuming 10 %, 50 % and 72 % sampling). Because the mean and standard deviation of parameter estimates are strongly impacted by outliers (Leys et al. 2013), the median (and absolute deviation around the median) were reported here. LH is the log-likelihood value of the model; the shift times (Ma) are indicated for the models implying discrete shifts in diversification rates; λ is the speciation rate for the constant-rate models and the initial speciation rate for the rate-variable models; μ is the extinction rate; x is the rate change parameter of the density-dependent exponential (DDX) model; K is the carrying capacity parameter of the density-dependent linear (DDL) model. For each model, the Akaike Information Criterion (AIC) was computed. The best fitting model with the lowest AIC score is highlighted in dark grey. The 95 % confidence intervals of the AIC values are indicated. dAIC is the difference between the AIC score of the model and the AIC score of the best fitting model. Minimal and maximal values for dAIC were calculated based on the AIC 95 % confidence intervals. The evaluated models for which the dAIC range contains zero are highlighted in light grey. wAIC are the Akaike weights.

APPENDIX S8. Comparison of the fit of the lineage diversification models from Morlon et al. (2011) to the empirical Antarctic iphimediid dataset.

Dataset	Model	AIC	dAIC	wAIC	λ	α	μ	β
Sampling 79.5 %	BcstDcst	244.13	2.23	0.16	0.084	-	0.008	-
	BvarDcst	245.25	3.35	0.09	0.106	0.031	0.124	-
	BcstDvar	245.95	4.05	0.06	0.115	-	0.121	-0.085
	BvarDvar	247.81	5.91	0.02	0.105	0.036	0.122	0.010
	Bcst	241.90	0.00	0.49	0.080	-	-	-
	Bvar	244.12	2.22	0.16	0.077	0.004	-	-
Sampling 50 %	BcstDcst	244.13	1.34	0.23	0.135	-	0.058	-
	BcstDvar	245.57	2.78	0.11	0.178	-	0.187	-0.047
	BvarDvar	247.81	5.02	0.04	0.168	0.031	0.181	0.014
	Bcst	242.79	0.00	0.45	0.098	-	-	-
	Bvar	244.77	1.98	0.17	0.111	-0.010	-	-
Sampling 10 %	BcstDcst	244.13	0.00	0.43	0.674	-	0.598	-
	BvarDcst	245.29	1.16	0.24	0.865	0.006	0.868	-
	BcstDvar(exp)	245.33	1.20	0.24	0.872	-	0.873	-0.007
	Bvar(exp)Dvar(exp)	247.80	3.67	0.07	0.840	0.025	0.847	0.022
	Bcst	256.58	12.45	8.10^{-4}	0.161	-	-	-
	Bvar(exp)	249.96	5.83	0.02	0.298	-0.056	-	-

Appendix S8. Parameter estimates and comparison of the fit of the lineage diversification models from Morlon et al. (2011) to the empirical dataset, assuming sampling fractions of 0.72, 0.5 and 0.1. λ is the speciation rate (when constant) or the initial speciation rate (when variable); α is the rate change parameter for the exponential variation of speciation rate; μ is the extinction rate (when constant)or the initial extinction rate (when variable) ; β is the rate change parameter for the exponential variation of the extinction rate. For each model, the Akaike Information Criterion (AIC) was computed. dAIC is the difference between the AIC score of the evaluated model and the AIC score of the best-fitting model. wAICis the Akaike weight. The best-fitting model with the lowest AIC score is highlighted in dark grey. When the wAIC of the best model < 0.5, the second best-fit is highlighted in light grey.

APPENDIX S9. Rate through time plots generated for the Antarctic iphimediid clade.

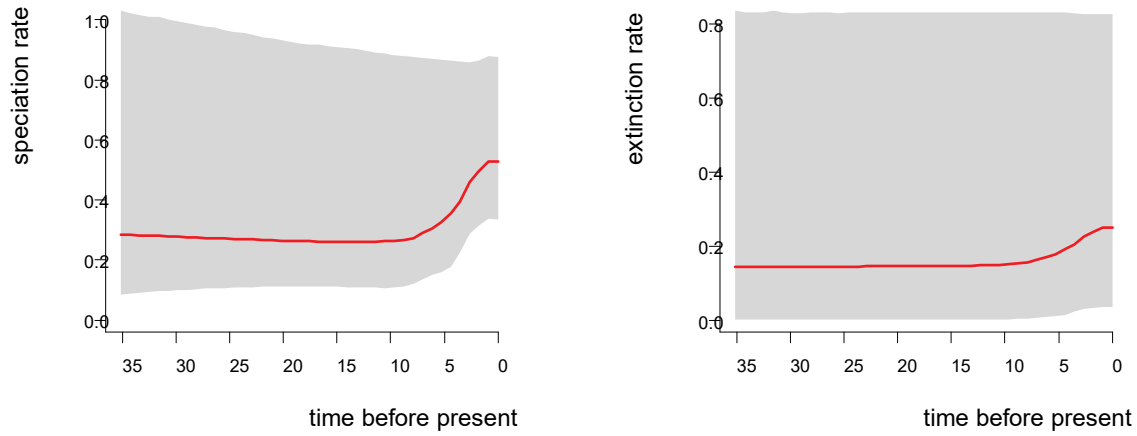

Appendix S9 -A. Speciation (left) and extinction (right) rate through time plots generated by BAMM assuming 10 % taxon sampling fraction. The shaded area is the 95 % confidence interval.

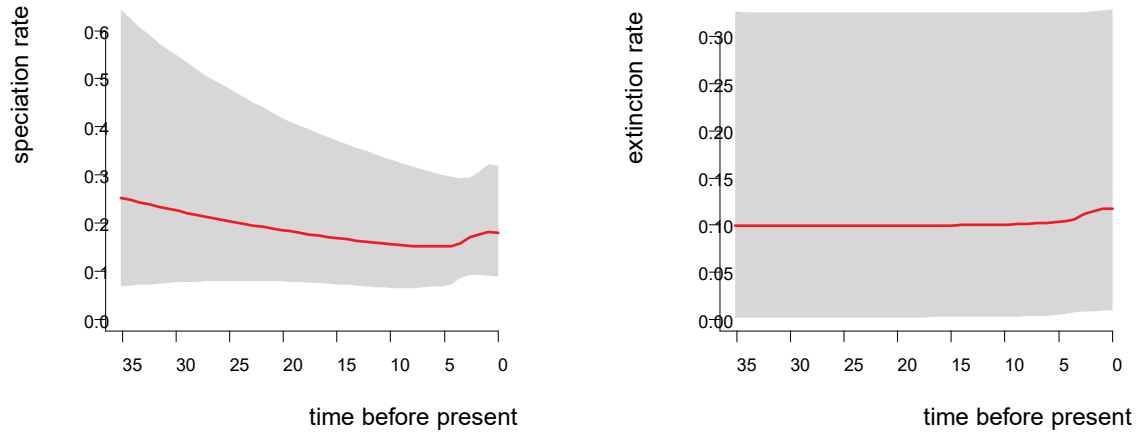

Appendix S9 -B. Speciation (left) and extinction (right) rate through time plots generated by BAMM assuming 50 % taxon sampling fraction. The shaded area is the 95 % confidence interval.

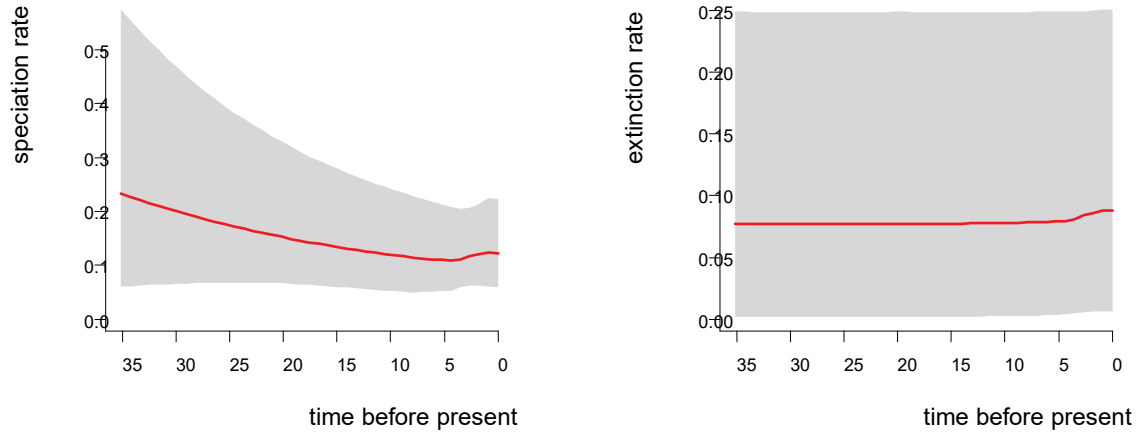

Appendix S9 -C. Speciation (left) and extinction (right) rate through time plots generated by BAMM assuming 79.5 % taxon sampling fraction. The shaded area is the 95 % confidence interval.

APPENDIX S10. Distribution of *Epimeria* species and subgenera in the Southern Ocean [from d'Udekem and Verheye *(in Press)*].

Distribution and bathymetry	depth (m)	Magellan	New Zealand Sub-Antarctic Islands and Macquarie Island	South Georgia and Shag Rocks	Bruce Ridge	South Orkney Islands	Elephant and Clarence Island	South Shetland Islands (excl. Elephant Island), tip and West of Antarctic Peninsula	Larsen Area (western Weddell Sea excl. northern tip)	eastern shelf of the Weddell Sea	Princess Ragnhild Coast	Davis Sea	Adélie Coast and Oates Land	western Ross Sea
DRAKEPIMERIA														
***acanthochelon* (SI3)**	204–791									+	+		+	
***anguloce* (MA1)**	189–431							+	+	+	+	+		
***colemani* (SI5)**	397–828							+		+	+	+	+	+
***corbariae* (MA2)**	33–827												+	
***cyrano* (SP1)**	867–955									+				
***havermansiana* (SI1)**	189–573									+	+	+	+	
leukhoplites	131–298						+	+						
***loerzae* (MA3)**	102–298					+	+	+		+				
macrodonta	915													+
***pandora* (SI2)**	90–483						+	+						
***pyrodrakon* (MA4)**	170–490							+		+	+			
reoproi	48							+						
***robertiana* (SP2)**	1724–2190									+				
schiaparelli	130–350													+
***similis* (SI4)**	90–483						+	+						
vaderi	332						+							
variolata	218–307						+							
sp. 1	151–300													+
sp. 2	0–145						+							
EPIMERIELLA														
atalanta	189–405								+	+				
macronyx	0–1200					+		+		+		+	+	+
scabrosa	329–366												+	
truncata	100–622							+		+				
HOPLEPIMERIA														
***angelikae* (GE5)**	781–1194									+			+	

***cyphorachis* (GE3)**	413–990						+	+						
***gargantua* (RO1)**	404–580							+						
georgiana	75–310			+										
heldi	230–235						+							
inermis	33–791						+	+		+		+	+	+
***larsi* (GE4)**	1954–2154												+	+
***linseae* (GE2)**	100–1014					+								
***quasimodo* (GE1)**	131–407						+	+						
rimicarinata	337–540											+		+
***robusta* (RO3)**	85–814												+	+
***robustoides* RO2)**	274–605									+				
rubrieques	254–1030									+		+		
xesta	457–574									+				
sp.	362–371				+									
LAEVEPIMERIA														
***anodon* (WA4)**	525–791												+	
***cinderella* (WA3)**	106–270						+	+					+	
***walkeri* (WA1)**	170–889						+	+		+			+	+
sp.	258–273							+						
METEPIMERIA														
acanthurus	27–494	+												
ashleyi	676–750		+											
***intermedia* f. A**	75			+										
***intermedia* f. B**	88–273			+										
PSEUDEPIMERIA														
***amoenitas* (PUL1)**	461–573												+	
***callista* (GR2)**	97–573												+	
debroyeri	499–515									+				
cf. *debroyeri*	248–298						+	+						
***grandirostris* (GR1)**	146–342						+	+						
kharieis	330–450									+				
oxicarinata	127–267						+	+						
pulchra	50–190					+								
SUBEPIMERIA														
***adeliae* (PUN4)**	750–788												+	
geodesiae	115–135												+	
***iota* (PUN1)**	121–265						+	+						

puncticulata	175													+
***teres* (PUN2)**	196–202								+					
***urvillei* (PUN3)**	52–54												+	
sp. 1	60–270			+										
sp. 2	765–840									+				
UREPIMERIA														
annabellae	159–459									+				
extensa	230–260							+						
monodon	0–15					+		+						
Number of taxa		1	1	4	1	5	16	23	3	19		6	17	11